

TABLE OF CONTENTS

Prize Lectures	2
Symposia	8
Oral Communications	87
Poster Communications	195

Experiments on animals and animal tissues

It is a requirement of The Society that all vertebrates (and *Octopus vulgaris*) used in experiments are humanely treated and, where relevant, humanely killed.

To this end authors must tick the appropriate box to confirm that:

For work conducted in the UK, all procedures accorded with current UK legislation.

For work conducted elsewhere, all procedures accorded with current national legislation/guidelines or, in their absence, with current local guidelines.

Experiments on humans or human tissue

Authors must tick the appropriate box to confirm that:

All procedures accorded with the ethical standards of the relevant national, institutional or other body responsible for human research and experimentation, and with the principles of the World Medical Association's Declaration of Helsinki.

Guidelines on the Submission and Presentation of Abstracts

Please note, to constitute an acceptable abstract, The Society requires the following ethical criteria to be met. To be acceptable for publication, experiments on living vertebrates and *Octopus vulgaris* must conform with the ethical requirements of The Society regarding relevant authorisation, as indicated in Step 2 of submission.

Abstracts of Communications or Demonstrations must state the type of animal used (common name or genus, including man. Where applicable, abstracts must specify the anaesthetics used, and their doses and route of administration, for all experimental procedures (including preparative surgery, e.g. ovariectomy, decerebration, etc.).

For experiments involving neuromuscular blockade, the abstract must give the type and dose, plus the methods used to monitor the adequacy of anaesthesia during blockade (or refer to a paper with these details). For the preparation of isolated tissues, including primary cultures and brain slices, the method of killing (e.g. terminal anaesthesia) is required only if scientifically relevant. In experiments where genes are expressed in *Xenopus* oocytes, full details of the oocyte collection are not necessary. All procedures on human subjects or human tissue must accord with the ethical requirements of The Society regarding relevant authorisation, as indicated in Step 2 of submission; authors must tick the appropriate box to indicate compliance

PL01

Gordon Holmes and The Irish Spirit of Adventure; Lessons for Modern Thinkers

Sean Roe¹

¹*Queens University Belfast, School of Medicine, Dentistry and Biomedical Science, Belfast, United Kingdom*

On the Western Front of the First World War, Gordon Holmes transformed neurology. There, between 1915 and 1918, existed a coincidence of factors. These, combined with Holmes' voracious curiosity, adventurous nature and eclectic skillset produced a profound, lasting legacy.

His early life was spent in Castlebellingham, Ireland. Initial schooling may explain this adventurous spirit; The Dundalk Educational Institution produced three VC Awardees along with the most outstanding Irish fighter pilot of the First World War (McCrea and Patterson, 2014). He studied Medicine in Trinity College, Dublin, then spent two years at the Senckenberg Institute in Frankfurt, under Ludwig Edinger and Carl Wiegert (Fine *et al*, 2011). Thus, Holmes' training saw him grounded thoroughly in the German Neuroanatomy tradition which saw his stunning hand-drawn diagrams of Golz' famous "dog without a forebrain" published in the Journal of Physiology (Holmes, 1901). To this may be added his subsequent rigorous inculcation in clinical observation under Hughlings Jackson at Queen Square, London. In Holmes was a unique mix of artist, anatomist, physiologist and clinician, waiting for the right set of circumstances.

This mix of circumstances arrived in 1914 when Holmes was appointed as consultant neurologist to the British Armies in France. Harvey Cushing describes his tireless work thus; "*There are 900 acutely ill soldiers, convoys of 300 wounded might arrive in a day, and there were only 10 Doctors; in less than 9 months Holmes had amassed a lifes work*" (Lepore, 1994).

Here, a confluence of events led to some of the most important neurologic advances of the 20th Century. The Brodie helmet used on the Western front was designed to be cheaply produced from a single stamping of metal and provided good protection from airburst shells but not from rounds that burst closer to ground level, leaving the occipital cortex and cerebellum vulnerable (Shadrake and Pugh, 2014). The introduction of new rifles in the late 1800's imparted enough velocity to allow a projectile enter the skull and cause limited (and measurable) damage, but not so much velocity as to produce the lethal damage that modern weapons do.

Holmes' training in anatomy, physiology and clinical observation uniquely disposed him to the characterisation and mapping of visual field loss due to lesions of the occipital lobe. His extensive pre-war experience in measuring functional loss due to cerebellar tumours (Stewart and Holmes, 1904) was also invaluable when studying the large cerebellar lesions consequent to shrapnel and bullet wounds.

Holmes' maps of visual field localisation (Holmes, 1918) survived unaltered for 73 years (Horton and Hoyt, 1991). His description of the clinical signs of cerebellar damage (Holmes, 1917), provide neurologic tools in current use.

Ireland, The UK and Europe have cause to be proud of his legacy which has extended globally with warm tributes from notables such as Wilder Penfield (Penfield, 1967). His achievements resulted from his interdisciplinarity and refusal to think in narrow silos. The right person with the appropriate talents came forward to do their duty a time of unique challenge (and ironically) unique creativity.

Fine EJ, Mehta B, Lohr LA (2011). Neurognostics Answer. *Journal of the History of the Neurosciences* 20,170–176. <https://doi.org/10.1080/0964704X.2011.560826> Holmes GM (1901). The nervous system of the dog without a forebrain. *Journal of Physiology* 27 (1-2), 1-25. <https://doi.org/10.1113/jphysiol.1901.sp000855> Holmes G (1917) The symptoms of acute cerebellar injuries due to gunshot injuries. *Brain* 40 (4), 461–535. <https://doi.org/10.1093/brain/40.4.461> Holmes G (1918). Disturbances of vision by cerebral lesions. *British Journal of Ophthalmology* 2 (7), 353-384. <https://doi.org/10.1136/bjo.2.7.353> Horton JC, Hoyt WF (1991). The Representation of the Visual Field in Human Striate Cortex: A Revision of the Classic Holmes Map. *Archives of Ophthalmology* 109 (6), 816–824. <https://doi.org/10.1001/archopht.1991.01080060080030> Lepore FE (1994). Harvey Cushing, Gordon Holmes, and the Neurological Lessons of World War I. *Archives of Neurology* 51(7), 711–722. <https://doi.org/10.1001/archneur.1994.00540190095022> McCrea CT, Patterson T (2014) Dundalk Grammar School, The first 275 Years 1739-2014 Dundalk, Dundalk Grammar School. Penfield W (1967). Sir Gordon Morgan Holmes 1876-1965. *Journal of Neurological Science* 5, 185-192. [https://doi.org/10.1016/0022-510x\(67\)90016-0](https://doi.org/10.1016/0022-510x(67)90016-0) Shadrake, D, Evans-Pughe, C (2014). "Putting a lid on it [First World War Equipment Design]. *Engineering & Technology* 9 (6), 44-47. <https://doi.org/10.1049/et.2014.0603> Stewart TG, Holmes G (1904). Symptomology of cerebellar tumours. *Brain* 27, 522-592 <https://doi.org/10.1093/brain/27.4.522>

PL02

GABAergic signaling as a coordinating factor in brain development and disease: Focusing on postsynaptic ionic mechanisms

Kai Kaila¹

¹*University of Helsinki, Helsinki, Finland*

The cornerstones of research on postsynaptic inhibition were laid by Charles Sherrington, who deduced its hyperpolarizing nature and, notably, emphasized “*Inhibition as a coordinative factor*” in the CNS (Nobel lecture, 1932). The prescient ideas of Sherrington have not only materialized in work on neuronal information processing in the mature CNS: it has become obvious that major milestones of brain development are associated with remarkable qualitative changes in the responses generated by postsynaptic GABA_A receptors. These, in turn, are attributable to coordinated alterations in the spatiotemporal expression patterns of plasmalemmal chloride transporters - such as the Na-K-2Cl cotransporter NKCC1 and the neuron-specific K-Cl cotransporter, KCC2 – and other ion-regulatory proteins, including carbonic anhydrases (CAs), whereof isoform CA7 is neuron-specific.

The default state of mammalian cells, including immature CNS neurons, is a high NKCC1-dependent intracellular Cl⁻ concentration ([Cl⁻]_i) which leads to a depolarizing action of GABA. Thus, the adult neurons with their low [Cl⁻]_i and hyperpolarizing GABA responses are an “aberrant” type of cells. As shown in our early work, upregulation of KCC2 expression accounts for the developmental hyperpolarizing shift in GABA action. This shift follows the distinct time courses of maturation in various neuronal populations and animal species, with striking differences in GABA actions during the perinatal period between altricial and precocial mammals. Current data indicate that in the full-term healthy human baby, GABA is hyperpolarizing in the cortex and, by implication, elsewhere in the brain.

A subsequent developmental shift or “switch” is caused by the abrupt emergence of the neuron-specific CA isoform 7 (CA7) at a developmental stage by which KCC2 has reached a near-maximum functionality. GABA_ARs have a significant permeability to HCO₃⁻, and because of its rather positive equilibrium (at around -10 mV), the HCO₃⁻ current component is depolarizing. In the cortex, intense activity of GABAergic interneurons results in fast collapse of the chloride gradient in principal neurons, giving rise to depolarizing and excitatory GABA actions. Indeed, selective interneuronal stimulation in the healthy brain can promote seizure activity, accentuated by an increase in extracellular [K⁺].

Soon after identifying the causal role of KCC2 in the ontogeny of hyperpolarizing postsynaptic GABA_AR responses, we found that kindling-induced seizures in adult mice led, within a few hours, to down-regulation of KCC2. This observation has since been replicated in virtually all models of cortico-hippocampal neuronal trauma (e.g. stroke, mechanical damage, and neuroinflammation). KCC2 down-regulation, paralleled by neuronal NKCC1 upregulation, may well be one aspect of neuronal dedifferentiation required for re-wiring of functional circuits in CNS disorders. Maintaining a low [Cl⁻]_i imposes a high burden on neuronal energy metabolism, especially during an energy crisis. Therefore, it is not immediately clear whether the depolarizing GABA responses have a

disease-promoting (maladaptive) or an adaptive/compensatory role. NKCC1-dependent depolarizing GABA signaling is likely to promote interictal activity - but not seizures - in the epileptic brain. The presence of NKCC1 in virtually all kinds of cells within and outside the brain has led to lots of confusion regarding the pharmacological actions of bumetanide and other NKCC1 blockers, especially in vivo.

In addition to their roles in modulating the efficacy of GABAergic inhibition, some ion-regulatory proteins act as morphogenic factors. For instance, the large C-terminus of KCC2 interacts with cytoskeletal elements influencing dendritic spinogenesis in cortical neurons, suggesting a role for KCC2 in coordinating the development of GABAergic and glutamatergic synapses. Such cytoskeletal effects are also likely to affect the neurological phenotype of disease mutations of KCC2, which is known to have a very high genic intolerance.

PL03

Endogenous physiological mechanisms as basis for treatment of obesity and type 2 diabetes

Jens Juul Holst¹

¹NNF Center for Basic Metabolic Research and Department of Medical Sciences, University of Copenhagen, Copenhagen, Denmark

Since their discovery there has been an interest in the translational aspects of the gut hormones, starting in 1906 with attempts to treat diabetes with gut extracts, continuing with search for inhibitors of acid secretion to treat duodenal ulcer disease as well as inhibitors of appetite and food intake to treat obesity. For diabetes therapy the interest focused around the incretins, and GIP (glucose-dependent insulintropic polypeptide) was found to potently stimulate insulin secretion, but had no effect in T2DM. Further research resulted in discovery of another incretin, glucagon-like peptide-1, a product of the enteroendocrine L-cells. This peptide was soon demonstrated to also inhibit glucagon secretion, gastrointestinal secretion and motility, and to inhibit appetite and food intake. Importantly, it retained activity in T2D. Most recently, GLP-1 receptor agonists for weekly or even oral administration, given either alone or as the main component of compounds with additional receptor activities (GIP, glucagon) have demonstrated weight losses of up to 25 % within 1.5-2 years in obese individuals and normalization of average glucose levels in T2DM patients (> 50 % reaching < 5.7 % glycated hemoglobin). Therapy is also associated with a reduced risk of stroke, cognitive impairment, occurrence of dementia and occurrence of or aggravation of diabetic kidney disease. But most importantly, therapy of individuals at risk, both with and without T2DM, has been shown to reduce risk of major adverse cardiovascular events, including mortality, by 14-20 %. The underlying mechanisms have not been clearly elucidated but seem to include anti-atherosclerotic and anti-inflammatory actions. The new GLP-1RAs are now changing our approach to therapy of both T2DM and obesity.

PL04

Having Fun Teaching Physiology

Frances MacMillan¹

¹*University of Bristol, Bristol, UK*

Learning should be fun! Or at least engaging. Undergraduate students seem to have become more and more focussed solely on results. Who hasn't been asked 'How do I get a first?' This isn't surprising; the financial pressure of attending university means that students are focussed on the metrics of their degree outcome without stopping to think about how their degree can lead to attainment of skills that will support them into their first job and beyond. So how can we enhance the student learning experience, encouraging them to engage in their university journey starting at the very beginning with their transition to university? I will describe the varied activities we have developed for students on our Physiology, Pharmacology and Neuroscience programmes to support them in the transition to university and to improve the student experience by trying to make their skills development engaging.

A series of 'Programme Enhancement Activities' support students in the transition to university and encourage them to develop the necessary skills needed for learning. The sessions include 'Survive and Thrive at University' and 'Reliability of information & Investigating a scientific myth'.

I strive to incorporate gaming elements into my teaching to support students' learning. Activities include self-directed quizzes for numeracy skills development, a 'Pub quiz' style revision session and a histology card game. I have also developed an interactive workshop to develop scientific writing skills in first year students, many of whom will not have previously written essays at school. We have recently converted this to a standalone interactive online resource which has had excellent student feedback and is being trialled in another institution. I will also describe an innovative cross faculty final year research project we created with a colleague in Classics.

I am keenly aware that developing successful teaching comes through teamwork and all the activities I will describe have been created in collaboration with others. Many of my ideas have developed from hearing about things that others have done so hopefully there will be something in my talk that inspires you.

SA01

Muscle mitochondrial dysfunction in astronauts during spaceflight. What we can learn from and about the space environment.

Marta Murgia^{1,2}, Joern Rittweger³, Carlo Reggiani¹, Roberto Bottinelli⁴, Matthias Mann⁵, Stefano Schiaffino⁶, Marco Narici¹

¹Department of Biomedical Sciences, University of Padova, Padua, Italy, ²Department of Proteomics and Signal Transduction, Max-Planck-Institute of Biochemistry, Martinsried, Germany, ³Institute of Aerospace Medicine, German Aerospace Center, Cologne, Germany, ⁴Department of Molecular Medicine, University of Pavia, Pavia, Italy, ⁵Department of Proteomics and Signal Transduction, Max-Planck-Institute of Biochemistry, Martinsried, Germany, ⁶Veneto Institute of Molecular Medicine, Padua, Italy

We analyzed the muscle biopsies of two astronauts who spent six months on the International Space Station (ISS) using mass spectrometry-based proteomics, with the aim of assessing how spaceflight modifies the structure and function of human skeletal muscle. We quantified on average 3800 proteins per sample, and a total of over 7000 proteins, spanning seven orders of magnitude in intensity. The two astronauts trained onboard using a treadmill and an Advanced Resistive Exercise Device (aRED) to simulate the use of free weights in the absence of gravity. The astronaut A trained more intensively and could preserve 80% of his muscle fiber cross-sectional area, compared to only 50% of astronaut B. Comparing the biopsies taken pre-mission to those from the day of landing we revealed in both astronauts a dramatic decrease in the expression of mitochondrial proteins located in all main compartments of the organelle, particularly the inner mitochondrial membrane and the matrix. The correlation of the mitochondrial protein loss to the relative amount of physical exercise was less straightforward than for the preservation of muscle mass. Our results are in line with the emerging consensus that mitochondria are a hub of the impact of spaceflight in humans as well as in various model organisms that were stationed on the ISS. Our data show that the relationship between exercise, muscle growth and mitochondrial biogenesis works differently in the space environment. My talk will discuss reactive oxygen species as a possible direct cause of mitochondrial damage and propose a role of physical exercise in the induction of an antioxidant response which can partially safeguard skeletal muscle structure and function.

SA02

Extreme postprandial muscle growth in a sedentary ectotherm: Gut-derived humoral signals trigger a rapid postprandial anabolic response in the digesting Burmese python.

Emil Rindom¹, Katja Bundgaard Last¹, Niels Jessen², Frank Vincenzo de Paoli³, Tobias Wang¹

¹*Zoophysiology, Department of Biology, Aarhus University, Aarhus, Denmark*, ²*Steno Diabetes Centre Aarhus, Institute for Clinical Medicine, Aarhus University, Aarhus, Denmark*, ³*Department of Biomedicine, Aarhus University, Aarhus, Denmark*

While physical inactivity poses significant health risks for humans, certain animal species have evolved remarkable adaptations to thrive despite sedentary lifestyles. Among these, the Burmese python (*Python bivittatus*), a sit-and-wait predator renowned for their capacity to devour massive prey items, stands out for its ability to undergo extreme postprandial muscle growth, even in the absence of physical activity.

Recent findings from our laboratory reveals an unexpected increase in metabolism and protein synthesis in skeletal muscles already within the first few hours after feeding, even before the prey has been digested in the stomach. Using chemical inhibitors targeting the protein degradation systems, we elucidated that this early anabolic response occurs through increased breakdown of endogenous proteins, compensating for the absence of exogenous nutrients.

Our current investigation delves into the mechanisms underlying this metabolic transition. Through blood transfusion experiments, we demonstrate that fasting snakes receiving blood plasma from digesting counterparts, sampled in the pre-absorptive phase of digestion, exhibit elevated skeletal muscle protein synthesis. Furthermore, by sequentially obstructing and/or circumventing different segments of the gastrointestinal tract, we ascertain the pivotal role of the small intestines in the initial stimulation of muscle growth following feeding.

Collectively, our observations suggest that during early digestion, humoral signalling originating from the small intestines triggers the rapid increase in postprandial protein synthesis in the skeletal muscle tissue of the Burmese python. Our findings not only uncover fascinating insights into the Burmese python's unique adaptations but also hold promise for future clinical applications. By revealing the role of humoral signaling from the small intestines in stimulating muscle growth, our research suggests potential avenues for developing therapies to combat muscle wasting disorders in humans, offering hope for patients with conditions such as sarcopenia or cachexia.

SA03

Harnessing the gut microbiota to facilitate muscle protein synthesis during fasting hibernation.

Matthew Regan¹, Garret Suen², Fariba Assadi-Porter³, Hannah Carey²

¹University of Montreal, Montreal, Canada, ²University of Wisconsin-Madison, Madison, United States, ³University of Wisconsin-Madison, Madison, United States

Hibernation is a mammalian adaptation to wintertime food scarcity. It is the net manifestation of multiple underlying traits, and the most important of these is torpor, a regulated depression of metabolism that reduces wintertime metabolic rate – and thus energy use – by up to 98% relative to basal summertime rates. This allows hibernators to forego eating and rely entirely on stored fat for multiple months at a time, effectively solving the food scarcity problem. However, in the process, hibernation presents the animal with an array of “collateral” challenges to which they have needed to evolve resilience. One of these challenges is the risk of muscle atrophy, which arises from the combined effects of fasting and inactivity that typify the hibernation season. It has been known for over 20 years that hibernating mammals are resistant to muscle atrophy, but the mechanisms underlying this resistance, including the cellular mechanisms of protein balance and the continued supply of nitrogen despite the lack of exogenous source, are still being resolved. Recently, we have shown that hibernating ground squirrels obtain nitrogen during the winter fast by salvaging the nitrogen atoms present in urea using a gut microbe-dependent process called urea nitrogen salvage (UNS). The microbially liberated urea nitrogen is subsequently absorbed and incorporated into the protein content of liver and skeletal muscle, a process that progressively increases from the summer active season to early winter, and then peaks in late winter just prior to spring emergence. We are now in the process of characterizing which proteins in the skeletal muscle and heart are synthesized with the aid of UNS. We are conducting this project in the context of possible countermeasure development for spaceflight-induced disuse atrophy, as it is known that humans are capable of using UNS under certain conditions. This suggests that the necessary machinery for UNS is in present in humans, and so the mechanisms by which hibernators optimize their machinery to maximize UNS late in the hibernation season may provide insight into how our own UNS machinery may be optimized. This could potentially benefit humans under a variety of muscle atrophying conditions, particularly those in which limited nitrogen supply is a factor.

Regan, M.D., Chiang, E., Liu, Y., Tonelli, M., Verdoorn, K.M., Gugel, S.R., Suen, G., Carey, H.V. and Assadi-Porter, F.M., 2022. Nitrogen recycling via gut symbionts increases in ground squirrels over the hibernation season. *Science*, 375(6579), pp.460-463.

SA06

Retroviral transposable elements and the pregnancy remodelling functions of human trophoblast

Jennifer Frost^{1,2}, Miguel Branco³, Samuel Amante², Hiroaki Okae⁴, Eleri Jones², Jane Cleal⁵, Rohan Lewis⁵, Matthew Caley², Takahiro Arima⁶, Rachel Tribe⁷, Lucilla Poston⁷, Michael Simpson¹

¹Medical and Molecular Genetics, King's College London, Guy's Campus, Great Maze Pond, SE1 1UL, London, United Kingdom, ²Genomics and Child Health, The Blizard Institute, Queen Mary University of London, 4 Newark Street, E1 2AT, London, United Kingdom, ³Genomics and Child Health, The Blizard Institute, Queen Mary University of London, 4 Newark Street, E1 2AT, London, United Kingdom, ⁴Department of Trophoblast Research, Institute of Molecular Embryology and Genetics, Kumamoto University, Kumamoto, Japan, ⁵School of Human Development and Health, Faculty of Medicine, University of Southampton, Southampton, United Kingdom, ⁶Department of Informative Genetics, Environment and Genome Research Center, Tohoku University Graduate School of Medicine, Sendai, Japan, ⁷Women and Children's Health, King's College London, St Thomas' Hospital, Westminster Bridge Road, London, United Kingdom

Complications of pregnancy, such as recurrent pregnancy loss, pre-eclampsia, fetal growth restriction, and spontaneous preterm birth, affect ~20 % of human pregnancies, causing maternal and fetal morbidity and mortality. Although the molecular aetiology of these disorders is not well understood, they are thought to share a common pathogenesis, in insufficient uterine invasion by the placenta. Transposable elements (TEs) comprise 50 % of our genome and are increasingly recognised as important in human physiology and disease, contributing to genetic variation and species-specific gene expression patterns. Previously, we found that a subset of transposable elements that have been co-opted following previous viral infections, known as endogenous retroviruses (ERVs), exhibit regulatory potential in the human placenta. These ERVs feature active chromatin marks specifically in placenta, and were bound by transcription factors with key roles in placental development. These elements were almost all primate-specific, and altered placental gene expression. To test their function in more depth, we used CRISPR-Cas9 excisions to show that several ERVs act as enhancers for key genes in the human placenta, such as CSF1R, ENG and PSG5. Research is now underway to explore whether human genetic and epigenetic variation at ERVs may contribute to pregnancy complications, using samples of placenta from normal and complicated pregnancies, and human trophoblast organoids.

SA07

Multi-omic mapping of human myometrium and decidua to decipher spontaneous labour.

Pei Lai¹, Alessia Visconti^{2,3}, Florence Burté⁴, Brendan Browne¹, Nik Matthews¹, Victoria Male¹, Mario Falchi³, Raffaele Calogero², Michael Taggart⁴, Mark Johnson¹, Rachel Tribe³

¹Imperial College London, London, United Kingdom, ²University of Turin, Turin, Italy, ³King's College London, London, United Kingdom, ⁴Newcastle University, Newcastle, United Kingdom

Greater understanding of physiological mechanisms driving parturition is needed if we are to develop more effective therapies for managing preterm and post-term birth. The problem of preterm birth (defined as birth before completion of 37 weeks gestation) exemplifies why action needs to be taken; it affects ~10% of all live births worldwide, acts as the leading cause of mortality for children under 5 years old, and presents a substantial risk of serious ill-health for surviving babies throughout the lifecourse [1-2]. Preterm birth can occur either spontaneously or by clinical intervention; spontaneous preterm labour (sPTL) typically accounts for almost half of all preterm births [3]. There are currently no reliable therapies available for preventing sPTL [4] due to notable gaps in our understanding of maternal-fetal interactions involved in coordinating the onset of spontaneous labour (for both preterm and term pregnancies). There is consensus that the myometrial and decidual tissue layers of the uterus are important contributors to labour. Myometrium predominantly comprises smooth muscle, which produces the uterine contractions that are characteristic of labour. Decidua is the mucosal lining between the myometrium and placenta/fetal membranes, which is integral to maternal-fetal immunomodulation and inflammatory events during parturition.

This talk presents the feasibility phase of the Borne Uterine Mapping Project (BUMP), which utilises a collaborative multidisciplinary approach to establish robust experimental protocols using innovative molecular mapping technologies, with the aim to explore multi- cellular and tissue processes that underpin the process of human labour. We applied bulk approaches for RNA-seq and proteomics to profile five distinct uterine sites (Figure 1) using biopsies acquired from term pregnancies undergoing Caesarean section while either not in labour or in early/established labour (LREC # 10/H0801/45; n=8 per group); single cell (sc) RNA-seq, single nucleus (sn) RNA-seq, spatial transcriptomics and sc proteomics were also used for biopsies from a separate cohort of not in labour and established labour Caesarean sections (n=4 per group).

Data from bulk approaches to RNA-seq and proteomics demonstrated regional differences between the five uterine sites of interest, which has important implications for understanding co-ordination of uterine contractile function. However, far less differences in gene and protein expression were significantly detected for labour status, especially for early labour. This supported the need to utilise scRNA-seq, snRNA-seq, spatial transcriptomics and sc proteomics, which delineate changes in mRNA or protein abundance between different cell types that exist in heterogenous tissues. Comparisons of scRNA-seq and snRNA-seq data for the same tissue type (decidua parietalis) will be made, and we will examine how well snRNA-seq can identify different cell types and their labour-related transcriptomic changes for three uterine regions according to our findings so far. Preliminary spatial transcriptomics data from upper segment (sub-parietalis) biopsies will also be presented to highlight the value of visualising changes in intact tissues for exploring how neighbouring cell types coordinate to mediate labour. Finally, contributions of these

data to our understanding of how the timing of birth is regulated will be discussed, and we will present plans to proceed with the analysis of samples from preterm pregnancies.

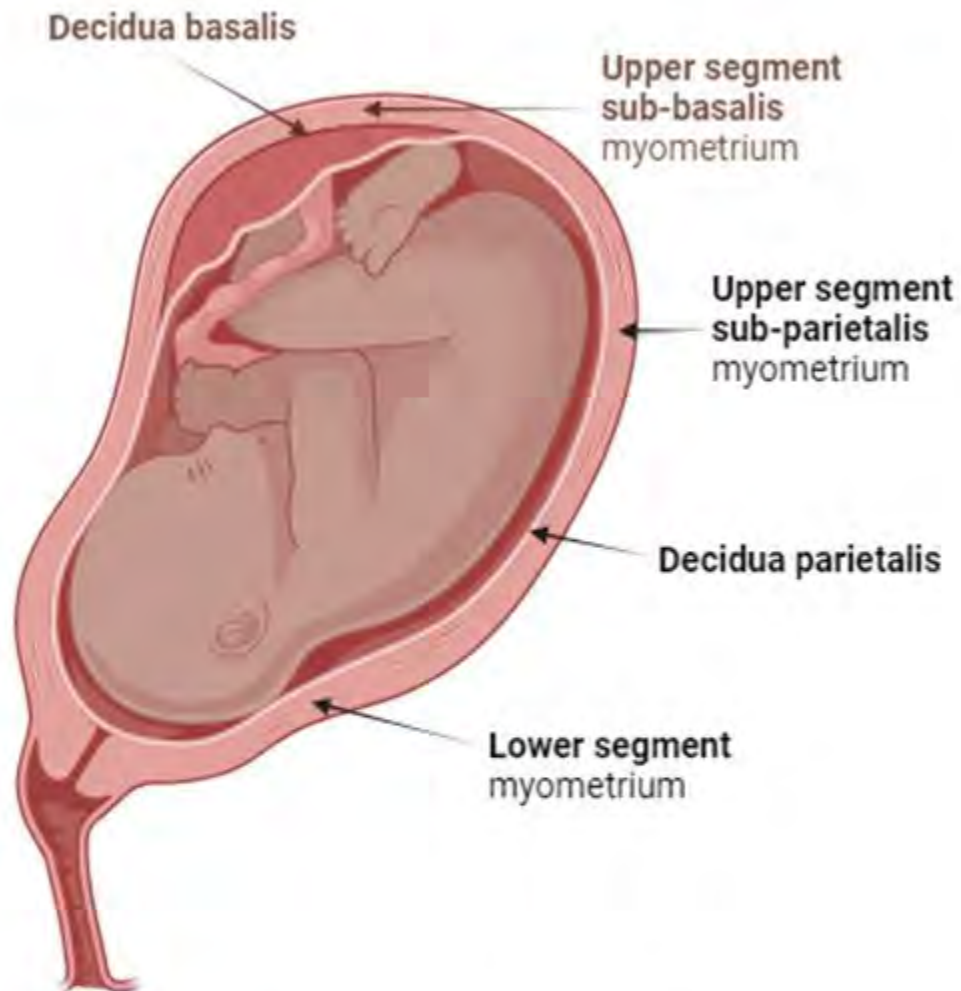


Figure 1. Uterine regions of interest for the Borne Uterine Mapping Project (BUMP). Created in Biorender.com

1. Understanding pregnancy: Accelerating the development of new therapies for pregnancy-specific conditions, in Academy of Medical Sciences' FORUM workshop. 2024, The Academy of Medical Sciences. p. 1-38. 2. Taggart, M.J. & Tribe, R.M. (2022) Physiological resilience across the

lifecourse: in utero and beyond. *Experimental Physiology* 107: 395-397. 3. Goldenberg, R.L., et al., Preterm birth 1 - Epidemiology and causes of preterm birth. *Lancet*, 2008. 371(9606): p. 75-84. 4. Campbell, F., et al., Interventions for the prevention of spontaneous preterm birth: a scoping review of systematic reviews. *BMJ Open*, 2022. 12(5): p. 12.

SA08

The importance of developing a sense of student belonging for success and progression at university

Teresa Thomas¹, Wendy Leadbeater¹

¹School of Biomedical Sciences, University of Birmingham, Birmingham, United Kingdom

The graduate attributes and skills that we try to foster in our biomedical science and physiology-based programmes provide a set of skills, behaviours and values that we hope students will develop by connecting with the culture, curriculum and community of the university at which they study. The development of these attributes will rely to some extent on them feeling like they belong to a community and having a strong sense of belonging.

We will present and discuss the findings from student surveys on transition and sense of belonging that we have carried out for several years at the University of Birmingham. Data from our Biomedical Science students indicates that their sense of belonging increased as students progressed through the programme. This sense of belonging became less dependent on staff-student engagement as students progressed through their studies and alternative support structures such as having meaningful and strong networks became more important.

In year 1 students there was a high correlation between having a strong sense of belonging and having 1 or 2 close friends, students engaging with extra-curricular activities and having at least one staff member knowing their name. Students indicated that merely mixing students in large group meetings was not sufficient to develop a sense of belonging, but the opportunity to connect with like-minded students as a result of those meetings or through extracurricular engagement was reported to be more effective. This indicates the importance of meaningful interactions between students. If these opportunities are to be programme-based then staff need to engage with students through co-creation of activities.

First year students transitioning into the university showed a high level of interest in engaging with extracurricular activities. However, their active involvement did not match this desire to engage. Focus group discussions indicated the greatest barrier to engagement with extracurricular activities was student perception that they did not have enough time given the expectations and requirements of an academically challenging programme. There are, however, likely to be other contributing factors such as cost and part-time working. These results may link in some way to awarding and employability gaps.

We will facilitate an open discussion inviting ideas and examples of best practice on how to address the following questions:

How can we increase opportunities and communicate the importance of extracurricular activities for the development of graduate attributes in students?

How can we provide more opportunities for students to increase their networks and sense of community through meaningful activities?

Our data indicated that a high sense of belonging correlated well with students feeling more motivated to study, being more likely to form study groups, and being more likely to prepare for and participate in teaching sessions. This supports the literature which indicates an association between a sense of belonging and academic success, motivation, and self-belief (Freeman, Anderman and Jensen, 2007).

Freeman, T. M., Anderman, L. H., & Jensen, J. M. (2007). Sense of belonging in college freshmen at the classroom and campus levels. *Journal of Experimental Education*, 75(3), 203–220.
<https://doi.org/10.3200/JEXE.75.3.203-220>

SA09

Enhancing belonging with programme-level synoptic assessment

Clare Tweedy¹, Alexandra Holmes¹, Dan Donnelly¹, Charlotte Haigh¹

¹School of Biomedical Sciences, University of Leeds, Leeds, United Kingdom

Students across several programmes at the University of Leeds (Biomedical Sciences, Neuroscience, and Pharmacology) share a substantial amount of teaching during first year. Focus groups were carried out with current students and the importance of belonging at the programme-level was highlighted, which was largely felt to be missing due to large-cohort shared teaching. As part of a period of educational transformation at Leeds, synoptic assessment was introduced within the school at Year 1. This was done in part to encourage students to transition from a modular view of learning to a more integrated approach, but also to encourage students to see the relevance of content to their programme within large-cohort shared modules.

In Semester 1, students complete synoptic assessment pieces in their broad discipline area. During Semester 2, all students engage with the same teaching material and formative problem-based application of knowledge short answer questions (SAQ's) during active learning workshops, followed by summative individual SAQ's. Each assessment piece contains "core knowledge" questions for students on all programmes, followed by programme-specific questions. To support programme-level assessment, programme meetings and community events were also implemented.

Reflections will be presented on some of the opportunities and challenges that have been encountered in implementing programme-level synoptic assessment across multiple modules of teaching, one of which is delivered outside of the school. The impact of this type of assessment is currently being assessed and initial findings will be shared as to whether it plays a role in encouraging student belonging to a programme of study.

SA10

The 'what' and 'why' of undergraduate physiology - student motivations for specialising in the science of life

Harley Stevenson-Cocks¹, Martyna Fugiel¹, Anna Toon¹

¹Newcastle University, Newcastle upon Tyne, United Kingdom

A students' sense of belonging is known to influence academic engagement, achievement and retention. At Newcastle, our large Biomedical and Biomolecular Sciences (BBS) cohort is split across five subjects but dominated yearly by Biomedical Sciences (BMS, ~200-250/360 students), with far fewer students opting to study Physiological Sciences. Teaching group size is known to influence students' ability to build meaningful relationships with peers and staff, influencing their sense of belonging, so the purpose of this project was to investigate BBS students' sense of belonging and whether it was influenced by or determined subject choice.

A survey sent to registered BBS students received 256 responses (25% response rate). The respondent population was 70% female, 85% aged 18-21, 77% Caucasian and 88% Home/EU students which broadly reflects the overall BBS student body. The data revealed little difference in overall sense of belonging (using a 10-point scale) by gender identity and fee status, but a decrease in sense of belonging as students advance through their BSc degree (6.6 vs 6.0 in year 1 vs year 3) and notable differences between degree programme with the large BMS cohort scoring lowest (6.1) and Physiological Sciences highest (6.6). Interestingly, 4th year MSci (7.1) and placement year/study abroad students (7.5) reported the highest overall sense of belonging.

Focus groups and further analyses of survey data are ongoing and the preliminary findings of these will be presented with a view to identify approaches to target and improve student engagement and sense of belonging across diverse student cohorts, and elicit ways to enhance student understanding of degree choice.

SA11

Focusing on belonging in curriculum design

Charlotte Haigh¹, Alexandra Holmes², Clare Tweedy³

¹*Univeristy of Leeds, Leeds, United Kingdom*, ²*University of Leeds, Leeds, United Kingdom*,

³*Univeristy of Leeds, Leeds, United Kingdom*

Community and student engagement is a global sector wide problem. There is a growing area of research within student education about sense of belonging and increased motivation for learning. Sense of belonging is one of the most significant factors in students' success and retention in higher education. It is something highly valued but rather hard to quantify. Despite its clear importance, many students report not feeling part of a community, in the UK, is reflected in low National Student Survey (NSS) scores for questions related to belonging sector wide.

At Leeds, recently the year 1 UG curriculum has been re-designed with the sense of belonging as a focus. This includes enhanced contact time, but still utilising a flipped classroom approach to teaching. A scaffolded approach to training students to engage with team work along with activities with autonomy of choice of the topic area studied within the team. This has been shown to support the building of a community within peers on their course.

A synoptic programme level assessment approach was also adapted which included reflective writing about both academic on course experiences but also extra curricula activities and part time work. This enabled students to link their whole university journey together to identify the skills they have identified and practiced throughout their first year of study.

Data will be discussed to support whether different activities within the undergraduate curriculum can support students to feel part of a community and therefore engaging more with their studies leading to higher student success rates.

SA12

Bidirectional metabokine and lipokine-mediated adipose tissue – skeletal muscle crosstalk during browning of adipose tissue

Lee Roberts¹

¹*Leeds Institute of Cardiovascular and Metabolic Medicine, University of Leeds, Leeds, United Kingdom*

Brown adipose tissue (BAT) regulates body temperature through non-shivering thermogenesis. Browning, the induction of a brown adipose-like phenotype in white adipose tissue (WAT), increases β -oxidation, mitochondrial biogenesis and thermogenesis(1). Brown adipocyte-like cells (beige adipocytes) are interspersed within WAT, and alter systemic energy balance with anti-obesity effects. In humans, BAT quantity correlates with decreased risk of diabetes and cardiovascular disease. However, BAT and beige adipose tissue can affect systemic energy balance independently of thermogenesis. Brown and beige adipose tissue thermogenesis leads to propagation of thermogenesis in surrounding and distal WAT and increases fat oxidation in skeletal muscle. This suggests brown/beige adipocytes influence systemic metabolism through interorgan signals in the adipocyte secretome. The nature of these signals is incompletely defined.

Metabolites were considered intermediates or end-products of metabolism, passive participants changed by metabolic processes. There is emerging evidence of metabolites, which function to mediate cellular signalling and interorgan crosstalk, regulating local metabolism and systemic physiology. These signals have been termed metabokines. Developing contemporaneously with the new appreciation of the complexity of tissue-crosstalk mediated by metabolites is an understanding that bioactive lipids also have a key role in the communication between cells, organs and tissues. These bioactive lipids have been termed lipokines. There is impetus to uncover novel metabokine signalling axes to understand how these are perturbed in metabolic diseases and determine their utility as therapeutic targets.

Our research has defined discrete brown/beige adipose tissue-derived metabokine and lipokine-mediated signalling axes that drive enhanced fatty acid oxidation in skeletal muscle. Reciprocally, we have identified an exercise-induced skeletal muscle-derived metabokine that drives adipose tissue browning. Here we will provide an overview of our research identifying novel metabokine signals:

- 1) Monocarboxylic acids secreted from thermogenic adipose tissue, which induce a thermogenic phenotype in white adipose tissue and oxidative energy metabolism in skeletal muscle to reduce adiposity, increase energy expenditure and improve glucose and insulin homeostasis in models of obesity and diabetes.
- 2) A lysophosphatidylcholine that functions as a BAT/beige adipocyte interorgan lipokine increasing fat oxidation in muscle and adipose tissue to increase systemic energy expenditure with anti-obesity effects

3) A bioactive non-protein β -aminoacid secreted from skeletal muscle during exercise, which induces adipose tissue thermogenesis and liver β -oxidation.

Our discoveries further our understanding of metabokine and lipokine mediated adipose tissue – skeletal muscle crosstalk, and the potential therapeutic role that these metabokines/lipokines may have to treat obesity and related cardiometabolic diseases.

SA13

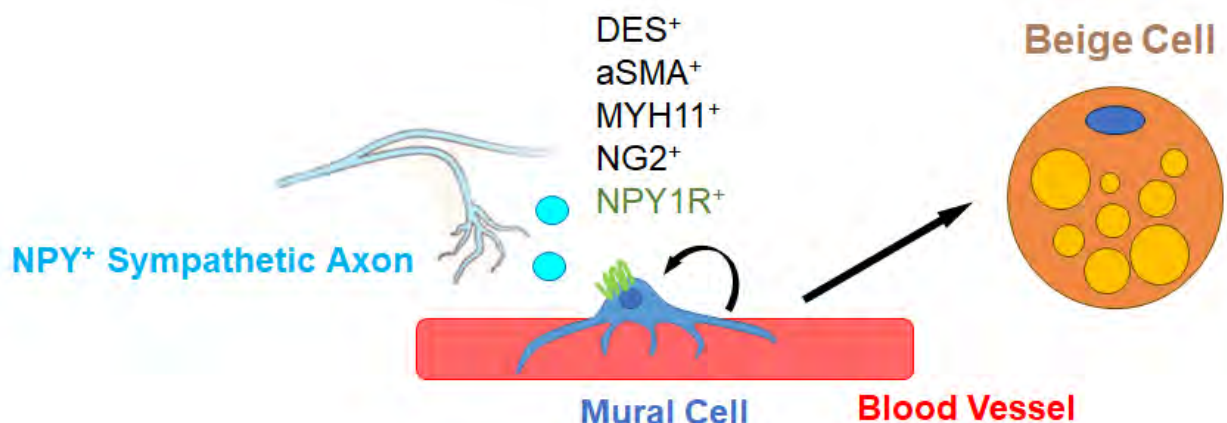
Sympathetic neuron-derived NPY protects from obesity by sustaining the mural progenitors of thermogenic adipocytes.

Yitao Zhu¹, Lu Yao¹, Ana Domingos¹, Shingo Kajimura², Ichitaro Abe³, Ana Gallo-Ferraz⁴, Bruna Bombassaro⁴, Marcela Simoes⁴, Licio Velloso⁴

¹Department of Physiology, Anatomy and Genetics, University of Oxford, Oxford, United Kingdom,

²Beth Israel Deaconess Medical Center, Division of Endocrinology, Diabetes & Metabolism, Harvard Medical School, Boston, United States, ³Department of Cardiology and Clinical Examination, Oita University, Faculty of Medicine, Oita, Japan, ⁴Laboratory of Cell Signaling, Obesity and Comorbidities Research Center, University of Campinas, Brazil, Campinas, Brazil

Neuropeptide Y (NPY) is secreted by sympathetic nerves, but its direct impact on thermogenic adipocytes is unknown. Here we uncover the mechanism by which peripheral NPY protects from obesity. Our imaging of cleared murine brown and white adipose tissue (BAT and WAT) established that NPY+ sympathetic axons are only a minority that mostly maps to the peri-vasculature; our analysis of single-cell RNA-sequencing datasets identifies mural cells as the main NPY-responsive cells in adipose tissues. We show that NPY sustains mural cells, which are known to be a source of beige cells in both BAT and WAT and that NPY facilitates the differentiation to thermogenic adipocytes. We found that diet-induced obesity leads to neuropathy of NPY+ axons and concomitant depletion of the mural cell pool of beige fat progenitors. This defect is replicated in conditional knockout (cKO) mice with NPY specifically abrogated from sympathetic neurons. These cKO mice have whitened BAT with reduced thermogenic ability and lower energy expenditure even before the onset of obesity; they develop adult-onset obesity on a regular chow diet and are more susceptible to diet-induced obesity without increasing food consumption. Our results indicate that relative to central NPY, peripheral NPY produced by the sympathetic nerves has the opposite effect on body weight homeostasis by sustaining the proliferation of the mural cell progenitors of thermogenic adipocytes.



SA14

CIRCADIAN TRANSCRIPTOME OSCILLATIONS IN HUMAN ADIPOSE TISSUE DEPEND ON NAPPING STATUS AND LINK TO METABOLIC AND INFLAMMATORY PATHWAYS

María Rodríguez Martín^{1,3}, Fernando Pérez-Sanz², Carolina Zambrano^{1,2}, Juan Luján⁴, Mikael Ryden⁵, Frank A.J.L. Scheer^{6,7,8}, Marta Garaulet^{1,2,6,7}

¹Department of Physiology, Regional Campus of International Excellence, University of Murcia, Murcia, Spain, ²Biomedical Research Institute of Murcia, Instituto Murciano de Investigación Biosanitaria (IMIB)-Arrixaca-Universidad de Murcia (UMU), University Clinical Hospital, Murcia, Spain, ³Biomedical Research Institute of Murcia, Instituto Murciano de Investigación Biosanitaria (IMIB)-Arrixaca-Universidad de Murcia (UMU), University Clinical Hospital, Murcia, Spain, ⁴General Surgery Service, Hospital Quirón salud, Murcia, Spain, ⁵Endocrinology Unit, Department of Medicine Huddinge (H7), Karolinska Institutet, Karolinska University Hospital, Stockholm, Sweden, ⁶Medical Chronobiology Program, Division of Sleep and Circadian Disorders, Brigham and Women's Hospital, Boston, United States, ⁷Division of Sleep Medicine, Harvard Medical School, Boston, United States, ⁸Broad Institute of Massachusetts Institute of Technology (MIT) and Harvard, Cambridge, United States

Intro. Napping is a common habit in many countries, but the impact of napping on general health is still unclear. Studies about the chronic effects of napping on obesity are contradictory, and the molecular link between napping and metabolic alterations has yet to be studied. Studies in animals and humans have shown that several genes expressed in adipose tissue (AT) follow a circadian rhythmic pattern, and disruption of circadian rhythms leads to obesity and metabolic disorders.

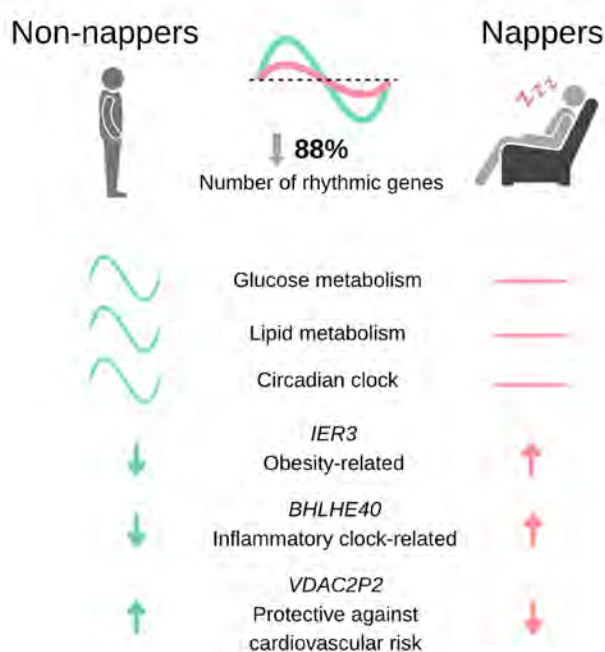
Aim. We aim to identify molecular mechanisms in AT that may connect napping and abdominal obesity. We propose that napping may induce, in AT, changes in the rhythmicity in those genes involved in energy metabolism, inflammation, and adipogenesis.

Method. We analyzed the circadian rhythmicity and global expression of genes expressed in 24-h cultured AT explants in 17 subjects with severe obesity, to assess differences between nappers (n=8) (long nappers, nap duration=1.18±0.7, mean±SD) and non-nappers (n=9). We extracted the RNA repeatedly across 24h from cultured AT explants of habitual nappers and non-nappers and performed RNA sequencing. Circadian rhythms were analyzed using 6 consecutive time points during 24 hours. Biostatistical and bioinformatic analyses were carried out in R. This work is in accordance with The Code of Ethics of the World Medical Association (Declaration of Helsinki) and procured in line with World Health Organization Guiding Principles on Human Cell, Tissue and Organ Transplantation.

Results. RNAseq analysis showed that 28.31% of the total genes analyzed in the total population displayed significant rhythms both by cosinor and non-parametric analyses. We further divided the total population into nappers and non-nappers to answer our main aim. In nappers, there was a loss of rhythmicity in 88% of genes that showed circadian rhythmicity among non-nappers (among non-nappers, 2666 genes were rhythmic, while among nappers, only 321 genes showed circadian rhythmicity). We observed a reduction in rhythm amplitudes of 29% in nappers and identified cholecystokinin (CCK) as the gene with the strongest decrease in amplitude in nappers. We also

found significant phase differences from a coherent unimodal acrophase in non-nappers towards a scattered and bimodal acrophase in nappers. *CTNNAL1* and *CHUK* were two relevant genes with significant delay in acrophase. Further pathway enrichment analysis showed that those genes that lost rhythmicity with napping were mainly involved in pathways of glucose and lipid metabolism, as well as of the circadian clock. Additionally, we found differential global gene expression between nappers and non-nappers, with 34 genes down- and 32 genes up-regulated in nappers. The top-up-regulated gene (*IER3*), another gene highly up-regulated (*BHLHE40*, a clock-related gene), and top-down-regulated pseudogene (*VDAC2P2*) in nappers have been previously shown to be involved in inflammation.

Conclusion. These findings not only resolve conflicting evidence on napping's chronic effects on obesity but also offer crucial insights into molecular mechanisms, shaping our understanding of napping's role in metabolic disorders. Since napping during the day, especially long napping, may alter the AT circadian rhythm and this may influence obesity, we would recommend not taking long naps, based on our previous results.



References 1. Faraut B, Andrillon T, Vecchierini MF, Leger D. Napping: A public health issue. From epidemiological to laboratory studies. *Sleep Med Rev.* 2017; 35: 85-100. 2. Vizmanos B, Cascales AI, Rodriguez-Martin M, et al. Lifestyle mediators of associations among siestas, obesity, and metabolic health. *Obesity (Silver Spring).* 2023; 31 (5): 1227-1239. 3. Lopez-Minguez J, Morosoli JJ, Madrid JA, Garaulet M, Ordonana JR. Heritability of siesta and night-time sleep as continuously assessed by a circadian-related integrated measure. *Sci Rep.* 2017; 7 (1): 12340. 4. Dashti HS, Daghlasi I, Lane JM, et al. Genetic determinants of daytime napping and effects on cardiometabolic health. *Nature communications.* 2021; 12 (1): 900. 5. Garaulet M, Madrid JA. Chronobiological aspects of nutrition, metabolic syndrome and obesity. *Adv Drug Deliv Rev.* 2010; 62 (9-10): 967-978. 6. Froy O, Garaulet M. The Circadian Clock in White and Brown Adipose Tissue: Mechanistic, Endocrine, and Clinical Aspects. *Endocr Rev.* 2018; 39 (3): 261-273. 7. Ando H, Yanagihara H, Hayashi Y, et al. Rhythmic messenger ribonucleic acid expression of clock genes and

adipocytokines in mouse visceral adipose tissue. *Endocrinology*. 2005; 146 (12): 5631-5636. 8. Zambrano C, Kulyte A, Lujan J, et al. Habitual nappers and non-nappers differ in circadian rhythms of LIPE expression in abdominal adipose tissue explants. *Front Endocrinol (Lausanne)*. 2023; 14: 1166961. 9. Garaulet M, Hernández-Morante JJ, Tébar FJ, Zamora S. Anthropometric indexes for visceral fat estimation in overweight/obese women attending to age and menopausal status. *J Physiol Biochem*. 2006; 62 (4): 245-252. 10. Zimmet P, Magliano D, Matsuzawa Y, Alberti G, Shaw J. The metabolic syndrome: a global public health problem and a new definition. *J Atheroscler Thromb*. 2005; 12 (6): 295-300. 11. Rodríguez-Martín M, Pérez-Sanz F, Zambrano C, et al. **Differential global gene expression in adipose tissue of nappers and non-nappers**. In: figshare; 2024. 12. Carlucci M, Kriščiūnas A, Li H, et al. DiscoRhythm: an easy-to-use web application and R package for discovering rhythmicity. *Bioinformatics*. 2019; 36 (6): 1952-1954. 13. Refinetti R, Lissen GC, Halberg F. Procedures for numerical analysis of circadian rhythms. *Biol Rhythm Res*. 2007; 38 (4): 275-325. 14. Bingham C, Arbogast B, Guillaume GC, Lee JK, Halberg F. Inferential statistical methods for estimating and comparing cosinor parameters. *Chronobiologia*. 1982; 9 (4): 397-439. 15. Cornelissen G. Cosinor-based rhythmometry. *Theor Biol Med Model*. 2014; 11: 16. 16. Storey JD, Tibshirani R. Statistical significance for genomewide studies. *Proc Natl Acad Sci U S A*. 2003; 100 (16): 9440-9445. 17. Fabregat A, Jupe S, Matthews L, et al. The Reactome Pathway Knowledgebase. *Nucleic Acids Res*. 2018; 46 (D1): D649-D655. 18. Love MI, Huber W, Anders S. Moderated estimation of fold change and dispersion for RNA-seq data with DESeq2. *Genome Biol*. 2014; 15 (12): 550. 19. Benjamini Y, Hochberg Y. Controlling the False Discovery Rate: A Practical and Powerful Approach to Multiple Testing. 1995; 57 (1): 289-300. 20. Kreiseder B, Holper-Schichl YM, Muellauer B, et al. Alpha-catulin contributes to drug-resistance of melanoma by activating NF-kappaB and AP-1. *PLoS One*. 2015; 10 (3): e0119402. 21. Liu XH, Zhang Y, Chang L, et al. Apolipoprotein A-IV reduced metabolic inflammation in white adipose tissue by inhibiting IKK and JNK signaling in adipocytes. *Mol Cell Endocrinol*. 2023; 559: 111813. 22. Hayashi N, Yasuo S, Ebihara S, Yoshimura T. Expression of IKKalpha mRNA in the suprachiasmatic nucleus and circadian rhythms of mice lacking IKKalpha. *Brain Res*. 2003; 993 (1-2): 217-221. 23. Plaza A, Merino B, Ruiz-Gayo M. Cholecystokinin promotes functional expression of the aquaglycerol channel aquaporin 7 in adipocytes. *Br J Pharmacol*. 2022; 179 (16): 4092-4106. 24. Barnea M, Chapnik N, Genzer Y, Froy O. The circadian clock machinery controls adiponectin expression. *Molecular and cellular endocrinology*. 2015; 399: 284-287. 25. Chen L, Yang G. PPARs Integrate the Mammalian Clock and Energy Metabolism. *PPAR Res*. 2014; 2014: 653017. 26. Schibler U, Ripperger J, Brown SA. Peripheral circadian oscillators in mammals: time and food. *J Biol Rhythms*. 2003; 18 (3): 250-260. 27. Civelek E, Ozturk Civelek D, Akyel YK, Kaleli Durman D, Okyar A. Circadian Dysfunction in Adipose Tissue: Chronotherapy in Metabolic Diseases. *Biology (Basel)*. 2023; 12 (8). 28. Hepler C, Bass J. Circadian mechanisms in adipose tissue bioenergetics and plasticity. *Genes Dev*. 2023. 29. Takahashi JS. Transcriptional architecture of the mammalian circadian clock. *Nat Rev Genet*. 2017; 18 (3): 164-179. 30. Corbalan-Tutau MD, Madrid JA, Ordovas JM, Smith CE, Nicolas F, Garaulet M. Differences in daily rhythms of wrist temperature between obese and normal-weight women: associations with metabolic syndrome features. *Chronobiol Int*. 2011; 28 (5): 425-433. 31. Devine JK, Wolf JM. Determinants of cortisol awakening responses to naps and nighttime sleep. *Psychoneuroendocrinology*. 2016; 63: 128-134. 32. Mohd Azmi NAS, Juliana N, Azmani S, et al. Cortisol on Circadian Rhythm and Its Effect on Cardiovascular System. *Int J Environ Res Public Health*. 2021; 18 (2). 33. Vujovic N, Piron MJ, Qian J, et al. Late isocaloric eating increases hunger, decreases energy expenditure, and modifies metabolic pathways in adults with overweight and obesity. *Cell Metab*. 2022; 34 (10): 1486-1498 e1487. 34. Tse LA, Wang C, Rangarajan S, et al. Timing and Length of Nocturnal Sleep and Daytime Napping and Associations With Obesity Types in High-, Middle-, and Low-Income Countries. *JAMA Netw Open*.

2021; 4 (6): e2113775. 35. Ravaud C, Esteve D, Villageois P, Bouloumie A, Dani C, Ladoux A. IER3 Promotes Expansion of Adipose Progenitor Cells in Response to Changes in Distinct Microenvironmental Effectors. *Stem Cells*. 2015; 33 (8): 2564-2573. 36. Jakubowski KP, Boylan JM, Cundiff JM, Matthews KA. Poor sleep moderates the relationship between daytime napping and inflammation in Black and White men. *Sleep Health*. 2017; 3 (5): 328-335. 37. Zafar A, Ng HP, Kim GD, Chan ER, Mahabeleshwar GH. BHLHE40 promotes macrophage pro-inflammatory gene expression and functions. *FASEB J*. 2021; 35 (10): e21940. 38. Wang JM, Cheng YQ, Shi L, et al. KLRG1 negatively regulates natural killer cell functions through the Akt pathway in individuals with chronic hepatitis C virus infection. *J Virol*. 2013; 87 (21): 11626-11636. 39. Wu N, Li J, Chen X, et al. Identification of Long Non-Coding RNA and Circular RNA Expression Profiles in Atrial Fibrillation. *Heart Lung Circ*. 2020; 29 (7): e157-e167. 40. Lockley SW, Skene DJ, Arendt J. Comparison between subjective and actigraphic measurement of sleep and sleep rhythms. *J Sleep Res*. 1999; 8 (3): 175-183.

SA15

Esr1+ hypothalamic-habenula neurons shape aversive states

Daniela Calvigioni¹

¹Karolinska Institutet, Stockholm, Sweden

Excitatory projections from the lateral hypothalamic area (LHA) to the lateral habenula (LHb) drive aversive responses. We used patch-sequencing (Patch-seq) guided multimodal classification to define the structural and functional heterogeneity of the LHA-LHb pathway. Our classification identified six glutamatergic neuron types with unique electrophysiological properties, molecular profiles and projection patterns. We found that genetically defined LHA-LHb neurons signal distinct aspects of emotional or naturalistic behaviors, such as estrogen receptor 1-expressing (Esr1⁺) LHA-LHb neurons induce aversion, whereas neuropeptide Y-expressing (Npy⁺) LHA-LHb neurons control rearing behavior. Repeated optogenetic drive of Esr1⁺ LHA-LHb neurons induces a behaviorally persistent aversive state, and large-scale recordings showed a region-specific neural representation of the aversive signals in the prelimbic region of the prefrontal cortex. We further found that exposure to unpredictable mild shocks induced a sex-specific sensitivity to develop a stress state in female mice, which was associated with a specific shift in the intrinsic properties of bursting-type Esr1⁺ LHA-LHb neurons. In summary, we describe the diversity of LHA-LHb neuron types and provide evidence for the role of Esr1⁺ neurons in aversion and sexually dimorphic stress sensitivity.

SA16

The Forgotten Circulation: Reduced mesenteric venous capacitance in hypertensive rats is improved by decreasing sympathetic activity

Tonja Emans¹, Davi Moraes², Alona Ben-Tal^{1,4}, Carolyn Barrett¹, Julian Paton¹, Fiona McBryde¹

¹Manaaki Manawa – The Centre for Heart Research, Department of Physiology, Faculty of Medical and Health Sciences, University of Auckland, Auckland, New Zealand, ²Department of Physiology and Biophysics, Biomedical Sciences Institute, University of São Paulo, São Paulo, Brazil, ³Manaaki Manawa – The Centre for Heart Research, Department of Physiology, Faculty of Medical and Health Sciences, University of Auckland, Auckland, New Zealand, ⁴Insightful Modelling Limited, Auckland, New Zealand

The mesenteric venous reservoir plays a vital role in mediating blood volume and/or pressure changes and is richly innervated by sympathetic nerves; however, the precise nature of venous sympathetic regulation and its role during hypertension remains unclear. We hypothesized that sympathetic drive to mesenteric veins in spontaneously hypertensive (SH) rats is raised, increasing mean circulatory filling pressure (MCFP), and impairing mesenteric capacitance.

Arterial pressure, central venous pressure, mesenteric arterial and venous blood flow were measured simultaneously in conscious male Wistar and SH rats. MCFP was assessed using an intra-atrial balloon. Hemodynamic responses to volume changes ($\pm 20\%$) were measured before and after ganglionic blockade and carotid body denervation (CBD). Sympathetic venoconstrictor activity was measured in situ.

MCFP in vivo (10.8 ± 1.6 vs 8.0 ± 2.1 mmHg; $P=0.0005$) and sympathetic venoconstrictor drive in situ (18 ± 1 vs 10 ± 2 μ V; $P<0.0001$) were higher in SH rats; MCFP decreased in SH rats after hexamethonium and CBD (7.6 ± 1.4 ; $P<0.0001$ and 8.5 ± 1.0 mmHg; $P=0.0045$). During volume changes, arterial pressure remained stable. With blood loss, net efflux of blood from the mesenteric bed was measured in both strains. However, during volume infusion, we observed net influx in Wistar ($+2.3 \pm 2.6$ ml/min) but efflux in SH rats (-1.0 ± 1.0 ml/min; $P=0.0032$); this counterintuitive efflux was abolished by hexamethonium and CBD ($+0.3 \pm 1.7$ and 0.5 ± 1.6 ml/min, respectively).

In SH rats, excessive sympathetic venoconstriction elevates MCFP and reduces capacitance, impairing volume buffering by mesenteric veins. We propose selective targeting of mesenteric veins through sympathetic drive reduction as a novel therapeutic opportunity for hypertension.

SA17

The elusive but large role of the venous system in vasovagal syncope and orthostatic hypotension

J. Gert van Dijk¹

¹Dept. of Neurology, Leiden University Medical Centre, Leiden, Netherlands

Vasovagal syncope (VVS) and classical orthostatic hypotension (cOH) are very common causes of syncope and orthostatic intolerance. VVS causes syncope at least once in one third of all people and cOH occurs with or without syncope in 25-30% of the elderly.

Both can be evoked with a 'tilt test' (TT). Applying continuous non-invasive blood pressure recordings and analysis software ('Modelflow') yield estimates of the three determinants of Mean Arterial Pressure (MAP), i.e., heart rate (HR), stroke volume (SV) and total peripheral resistance (TPR).

VVS is most often triggered by pain, fear ('emotional VVS') or just standing ('orthostatic VVS'); TT studies of the latter type of VVS showed that the first abnormality is a gradual decrease of SV, explained through by gradual venous pooling in the splanchnic and probably muscle venous beds. This causes a moderate decrease of MAP, which, if not countered by sitting or lying, can in turn evoke a sudden calamitous decrease of HR causing an ever faster decrease of MAP, ending in syncope. It is unclear how and why standing occasionally causes venous pooling that sets the VVS cascade in motion, functioning normally on other occasions.

cOH is by definition triggered by standing. The best understood mechanism is autonomic damage causing a triple defect. First, a failure of TPR to increase when upright causes an 'arterial leak'; second, a simultaneous decrease of SV again suggests venous pooling, presumably because of deficient venous vasoconstriction; third, a failure of HR to increase can cause very low upright MAP. The contribution of low SV, i.e., venous pooling to cOH is probably underestimated.

In VVS as well as cOH, the role of the venous system is implied by alterations on the arterial side of the circulation. Understanding the pathophysiology of VVS and cOH could benefit from tools that measure fluid distribution over venous beds and assess venous vasoconstriction.

SA18

Use it or lose it: the importance of contractile activity for maintenance of skeletal muscle mass and function in older age.

Bethan Phillips¹

¹*University of Nottingham, Derby, United Kingdom*

Beyond their most commonly recognised roles in locomotion and postural support, skeletal muscles also serve as the central node for whole-body metabolic health, acting as, for example, the largest amino acid (AA) reservoir and glucose disposal site in the body. Alongside AA nutrition, muscle contraction in the form of exercise and/ or physical activity is well established to improve metabolic health and induce both favourable physiological adaptations (e.g., muscle mass gains, mitochondrial biogenesis) and secondary health benefits (e.g., improved insulin sensitivity). Indeed, nutrition x contractile interaction is the fundamental basis of muscle mass maintenance across the life course. In stark contrast, the absence of muscle contraction in the form of “disuse” (e.g. through simple inactivity, casting, immobilization, or bed rest) has the opposite effect causing muscle atrophy, functional declines, and metabolic impairment (e.g., muscle insulin resistance). In older adults, events leading to periods of disuse or reduced physical activity are relatively commonplace (i.e., after falls, surgery, or during illness), with the additional complication of an existent background of sarcopenia progression in these individuals. Despite it being largely accepted that the regulatory processes underpinning muscle mass and functional declines with both advancing age and as a result of disuse are complex and multifactorial, we are still some way from complete understanding; with phenomenon such as atrophy resistant versus atrophy susceptible (aRaS) muscles posing novel questions. This presentation will i) outline the importance and underlying mechanisms of skeletal muscle mass maintenance for older adults, ii) highlight the rapidity of skeletal muscle disuse atrophy in both healthy and clinical cohorts, iii) address the observation of aRaS muscles, and iv) finally, provide early-data from studies looking to develop intervention strategies to mitigate losses of muscle mass and function in older surgical patients.

SA19

Fusion of myofibre branches is a physiological feature of healthy human skeletal muscle regeneration

Grith Højfeldt^{1,2}, Trent Sorenson¹, Alana Gonzales¹, Michael Kjaer^{1,3}, Jesper L. Andersen^{1,3}, Abigail Mackey^{1,3}

¹Department of Orthopaedic Surgery, Institute of Sports Medicine Copenhagen, Copenhagen University Hospital - Bispebjerg and Frederiksberg, Copenhagen, Denmark, ²Department of Biomedical Sciences, Faculty of Health and Medical Sciences, University of Copenhagen, Copenhagen, Denmark, ³Department of Clinical Medicine, Faculty of Health and Medical Sciences, University of Copenhagen, Copenhagen, Denmark

Background: The occurrence of hyperplasia, through myofibre splitting, remains a widely debated phenomenon. Structural alterations and fibre typing of skeletal muscle fibres, as seen during regeneration and in certain muscle diseases, can be challenging to interpret. Neuromuscular electrical stimulation can induce myofibre necrosis followed by changes in spatial and temporal cellular processes. Thirty days following electrical stimulation, remnants of regeneration can be seen in the myofibre and its basement membrane as the presence of small myofibres and encroachment of sarcolemma and basement membrane (suggestive of myofibre branching/splitting). The purpose of this study was to investigate myofibre branching and fibre type in a systematic manner in human skeletal muscle undergoing adult regenerative myogenesis.

Methods: Electrical stimulation was used to induce myofibre necrosis to the vastus lateralis muscle of one leg in 5 young healthy males. Muscle tissue samples were collected from the stimulated leg 30 days later and from the control leg for comparison. Biopsies were sectioned and stained for dystrophin and laminin to label the sarcolemma and basement membrane, respectively, as well as ATPase, and antibodies against types I and II myosin, and embryonic and neonatal myosin. Myofibre branches were followed through 22 serial Sects. (264 µm). Single fibres and tissue blocks were examined by confocal and electron microscopy, respectively.

Results: Regular branching of small myofibre segments was observed (median length 144 µm), most of which were observed to fuse further along the parent fibre. Central nuclei were frequently observed at the point of branching/ fusion. The branch commonly presented with a more immature profile (nestin + , neonatal myosin + , disorganised myofilaments) than the parent myofibre, together suggesting fusion of the branch, rather than splitting. Of the 210 regenerating muscle fibres evaluated, 99.5% were type II fibres, indicating preferential damage to type II fibres with our protocol. Furthermore, these fibres demonstrated 7 different stages of “fibre-type” profiles.

Conclusions: By studying the regenerating tissue 30 days later with a range of microscopy techniques, we find that so-called myofibre branching or splitting is more likely to be fusion of myotubes and is therefore explained by incomplete regeneration after a necrosis-inducing event.

SA20

Acute effects of exercise on brain metabolites and cognition in older adults

Naiara Demnitz¹, Michal Povazan¹, Jasmin Merhout¹, Nathalie Just¹, Alena Svatkova¹, Petr Bednarik¹, Michael Kjaer^{2,3}, Hartwig Siebner^{1,3}, Carl-Johan Boraxbekk^{2,3}

¹Danish Research Centre for Magnetic Resonance, Copenhagen, Denmark, ²Institute of Sports Medicine Copenhagen, Copenhagen, Denmark, ³University of Copenhagen, Copenhagen, Denmark

The health benefits of physical activity are widespread across the human body – including the brain. Particularly in older adults, physical activity has been shown to promote cognitive function, protect brain structure against expected age-related declines, and potentially even reduce the risk, or delay the onset, of dementia. Using *in vivo* neuroimaging methods, the last decade has seen significant developments in our understanding of the mechanisms behind these effects. Using proton Magnetic Resonance Spectroscopy (1H-MRS), metabolites which are more commonly found in glia than in neurons, such as myo-inositol (mIns), total creatine (tCr) and total choline (tCho), have been shown to be increased in older adults. Overactive glial cells - as observed in some brain diseases - can result in chronic neuroinflammation. Importantly, the same metabolites have been reported to negatively correlate with performance on a working memory task, suggesting a potential mechanistic link between age-related changes in brain metabolites and cognitive function. The current study will test whether exercise modulates these markers of neuroinflammation in older adults and, crucially, if these changes explain exercise-induced cognitive improvements. To examine the effects of a single exercise session on brain metabolite concentrations and working memory function, forty-eight older adults (65 – 75 years old; 50% women) will undergo a working memory test and 1H-MRS imaging at 7 Tesla before and after a cycling exercise. Exercise protocols are individualized to each participant, based on their performance on a VO2 max fitness test. In addition, participants will attend a control session, where they will undergo the same working memory test and brain scans before and after remaining seated. Data collection is currently underway. If exercise-induced metabolite changes are associated with cognitive changes, then these findings will contribute to our understanding of the underlying neural mechanisms of exercise-induced brain benefits in ageing.

SA21

Mind the Brain: Powering your brain through exercise and diet

Carl-Johan Boraxbekk¹

¹Institute of Sports Medicine Copenhagen, Copenhagen, Denmark

Lifestyle factors, including exercise and diet, is offering a promising solution for age-related negative effects on brain health, with a potential to postpone the onset of neurodegenerative diseases. The results, however, are muffled with large individual difference in the effects, and it appears as if one-size does not fit all. In this talk I will provide an overview about our current understanding about the link between exercise- and dietary-induced brain plasticity in aging. I will also discuss potential reasons why some individuals gain from these lifestyle interventions and why some individuals appear to have little room for brain plasticity. I believe that understanding these factors is the necessary next step to harvest the full potential of lifestyle factors for brain health.

SA22

Contribution(s) of the permeability transition pore to the pathophysiology of Vici syndrome, a severe multisystem disorder of childhood.

Michael Duchen¹, Kritarth Singh¹, Heinz Jungbluth^{3,4}, Manolis Fanto³

¹1. Dept of Cell and Developmental Biology and UCL Consortium for Mitochondrial Research, UCL, Gower street, London WC1E 6BT, London, United Kingdom, ²1. Dept of Cell and Developmental Biology and UCL Consortium for Mitochondrial Research, UCL, London WC1E 6BT, United Kingdom, ³2. Randall Centre for Cell and Molecular Biophysics, Muscle Signalling Section, Faculty of Life Sciences and Medicine (FoLSM), King's College London, London, United Kingdom, ⁴3. Department of Paediatric Neurology – Neuromuscular Service, Evelina London Children's Hospital, Guy's & St Thomas' NHS Foundation Trust, London, UK, London, United Kingdom

The mitochondrial permeability transition pore (mPTP) seems to be a critical final common path to cell injury and death in multiple disease states. Discovered in the 1970's by Hunter and Haworth, the critical trigger for pore opening is an excess of calcium in the mitochondrial matrix, while oxidative or nitrosative stress lower the threshold for calcium induced pore opening. Once the large conductance pore in the inner mitochondrial membrane has opened, the membrane potential will collapse causing depletion of ATP, mitochondria swell and – if the whole population of mitochondria in a cell undergo permeability transition – cell death. Critically, pore opening can be limited pharmacologically, making the pore a potential therapeutic target for multiple diseases (for a recent review, see (1)).

I will talk about a disease in which a pathophysiological cascade seems to involve opening of the mPTP probably in a subset of mitochondria with more complex but critical consequences. Vici syndrome is an apparently rare devastating early onset multisystem disorder caused by mutations of a protein known as EPG5, which plays a key role in autophagy, mediating fusion specificity of the autophagosome and lysosome. Almost every system is involved in Vici syndrome but in addition to multiple developmental defects, neurological and neuromuscular features are most prominent. Affected children suffer from a progressive neurodegeneration that, in combination with severe cardiorespiratory involvement, is usually fatal by the age of 10 at the severe end of the disease spectrum.

In fibroblasts from children with EPG5 mutations, mitophagy is significantly impaired². We have found that, as a consequence, mitochondria are profoundly dysfunctional, with impaired respiration and reduced mitochondrial membrane potential. In exploring the impact of a calcium signal on mitochondrial function in these cells, we were surprised to find that mitochondrial calcium uptake was paradoxically significantly increased. This was attributable to downregulation of MICU1, the Ca²⁺ dependent gatekeeper of mitochondrial calcium uptake. As a consequence, mitochondria from these cells show an increased vulnerability to mPTP opening in response to normally innocuous calcium signals. This is followed by release of mtDNA into the cytosol which

activates the cGAS/STING pathway, initiating the innate inflammatory response. It seems probable that this response plays a significant role in shaping the disease presentation and progression, especially in relation to the neurodegenerative disorder. These data point to multiple steps at which therapeutic intervention might prove beneficial – pharmacological stimulation of mitophagy, reducing mitochondrial calcium overload, inhibition of the mPTP or inhibition of the cGAS/STING pathway.

1. Briston T, Selwood DL, Szabadkai G, Duchen MR. Mitochondrial Permeability Transition: A Molecular Lesion with Multiple Drug Targets. *Trends Pharmacol Sci.* 2019 Jan;40(1):50-70. 2. Cullup T, Kho AL, Dionisi-Vici C, Brandmeier B, Smith F, Urry Z, Simpson MA, Yau S, Bertini E, McClelland V, Al-Owain M, Koelker S, Koerner C, Hoffmann GF, Wijburg FA, ten Hoedt AE, Rogers RC, Manchester D, Miyata R, Hayashi M, Said E, Soler D, Kroisel PM, Windpassinger C, Filloux FM, Al-Kaabi S, Hertecant J, Del Campo M, Buk S, Bodi I, Goebel HH, Sewry CA, Abbs S, Mohammed S, Josifova D, Gautel M, Jungbluth H. Recessive mutations in EPG5 cause Vici syndrome, a multisystem disorder with defective autophagy. *Nat Genet.* 2013 Jan;45(1):83-7.

SA23

Electrophysiological Properties of the Inner Mitochondrial Membrane: Diversity of Mechanisms of Mitochondrial Dysfunction

Zoya Niatsetsckaya¹, Sergey Sosunov¹, Sally Morris², Vadim Ten¹, Maria Neginskaya³

¹*Rutgers University, New Brunswick, United States*, ²*New York University, New York, United States*,

³*Albert Einstein College of Medicine, New York, United States*

Mitochondrial permeability transition (mPT) is a phenomenon of a sudden increase in the permeability of the inner mitochondrial membrane (IMM). Patch-clamp experiments on isolated mitochondria identified the mPT mechanism as the Ca²⁺- and ROS-stimulated opening of a large, unspecific pore in the IMM, known as the permeability transition pore (mPTP). The opening of the mPTP disrupts normal mitochondrial function and has been implicated as the hallmark of mitochondria-driven cell death in many diseases, including ischemia-reperfusion injuries of organs.

Here, we applied advanced whole-mitoplast patch-clamp and *ex vivo* patch clamp approaches to investigate the still-understood mechanism of mitochondrial dysfunction associated with mPTP. The whole-mitoplast configuration allows us to observe mPTP currents at the level of the whole mitochondrion (Neginskaya & Pavlov, 2023), and *ex vivo* patch clamp detects the changes in IMM permeability induced by *in vivo* stress, contrasting with the stress applied to mitochondrial membranes after isolation (Niatsetsckaya et al., 2020). Patch-clamp findings were supported by holographic imaging (HI) in cultured MEF cells. HI detects changes in the refractive indexes of mitochondria upon mPTP opening, enabling the observation of mPTP within the living cell, independently of mitochondrial depolarization (Neginskaya, Morris, & Pavlov, 2022).

Whole-mitoplast recordings from isolated cardiac mitochondria demonstrated that Ca²⁺-induced currents were partially blocked by CSA (42%, n=12) and by ADP (100%, n=2), but not sensitive to bongkreikic acid (BA), an inhibitor of the Adenine Nucleotide Translocator. In contrast, the ROS-stimulated whole-mitoplast current was transiently blocked by BA (n=1), suggesting that the mechanisms of IMM permeability might vary depending on stress conditions.

Ex vivo patch-clamping of brain mitochondria isolated from neonatal (p10) mice exposed to hypoxia-ischemia brain injury detected elevated IMM permeability after 30 min of reperfusion (420±40 pS, n=54 vs. 250±40 pS in control, n=18; p=0.05, Kruskal-Wallis). This elevated IMM permeability did not exhibit the classic CSA-sensitive mPTP current behavior. Neuroprotective hypothermia applied during reperfusion attenuated the infarct volume of brain (n=15, 36.7±6.0% to 19.2±5.0%) and normalized the associated elevation of IMM permeability (420±40 pS, n=54 to 290±50 pS, n=30, p=0.03, Kruskal-Wallis). These results suggest the existence of a non-mPTP mechanism of mitochondrial damage contributing to the injury. Interestingly, hyperoxia during reperfusion resulted in the activation of the classical CSA-sensitive mPTP (80% of CSA-sensitive channels (n=10) vs. 14% (n=14) in normoxia, p=0.01, χ^2 test) and exacerbated post-ischemic injury.

Finally, HI demonstrated that mitochondrial Ca²⁺ overload induced by the ionophore ferutinin stimulates classic CSA-sensitive mPTP activation (Neginskaya et al., 2022), while ionomycin-

induced Ca^{2+} dysregulation triggered mitochondrial depolarization and swelling but not the mPTP opening (n=4). CSA did not inhibit ionomycin-induced mitochondrial depolarization and swelling (n=3), or subsequent cell death (n=2), but it abolished the effect of ferutinin.

Therefore, we have demonstrated the existence of at least two mechanisms: mPTP and non-mPTP mitochondrial dysfunction that might contribute to acute ischemia-reperfusion injuries, with each pathway's impact determined by the unique stress conditions.

Neginskaya, M. A., Morris, S. E., & Pavlov, E. V. (2022). Both ANT and ATPase are essential for mitochondrial permeability transition but not depolarization. *iScience*, 25(11), 105447. doi: 10.1016/j.isci.2022.105447 Neginskaya, M. A., & Pavlov, E. V. (2023). Investigation of Properties of the Mitochondrial Permeability Transition Pore Using Whole-Mitoplast Patch-Clamp Technique. *DNA Cell Biol.* doi: 10.1089/dna.2023.0171 Niatsetskaya, Z., Sosunov, S., Stepanova, A., Goldman, J., Galkin, A., Neginskaya, M., . . . Ten, V. (2020). Cyclophilin D-dependent oligodendrocyte mitochondrial ion leak contributes to neonatal white matter injury. *J Clin Invest*, 130(10), 5536-5550. doi: 10.1172/JCI133082

SA24

The interplay between mitochondrial calcium, permeability transition, and cell death in cardiac maladaptation to chronic stress

Joanne Garbincius¹

¹*Aging + Cardiovascular Discovery Center, Lewis Katz School of Medicine, Temple University, Philadelphia, United States*

The acute uptake of calcium (Ca^{2+}) into the mitochondrial matrix via the mitochondrial calcium uniporter is a key signal that enhances mitochondrial ATP production in parallel with stimuli that increase cytosolic Ca^{2+} signaling and cellular energy demand. This physiologic mitochondrial Ca^{2+} (mCa^{2+}) accumulation is critical for the heart to rapidly increase its workrate in response to sympathetic stimulation during exercise or fight-or flight responses. In excess, though, acute mCa^{2+} loading triggers mitochondrial permeability transition (mPT) and necrotic cell death. Such mCa^{2+} -dependent mPT drives initial tissue injury and subsequent organ-level dysfunction in response to acute ischemic insults including myocardial infarction and stroke. However, the contribution of mCa^{2+} overload and mPT to more gradually-developing dysfunction in cardiovascular diseases featuring a sustained increase in cytosolic Ca^{2+} concentration remains poorly defined. This question is particularly relevant for forms of non-ischemic heart failure that develop over time following chronic elevations in cardiac afterload and neurohormonal stimulation. These pathologies feature progressive cardiomyocyte death that can compromise the contractile function of the heart. Understanding the relationship between mCa^{2+} accumulation, mPT, and cardiomyocyte dropout in the context of such chronic heart disease is complicated by the proposed homeostatic role of the mitochondrial permeability transition pore (mPTP) as a route for physiologic mCa^{2+} efflux that limits deleterious mCa^{2+} overload. This talk will highlight recent *in vivo* findings from genetic mouse models featuring manipulation of the mitochondrial calcium uniporter or the mCa^{2+} efflux machinery to modulate mCa^{2+} accumulation in experimental models of non-ischemic heart failure. It will also address the complex interplay between altered mCa^{2+} homeostasis, the proposed constituents of the mPTP, and cell death in the chronically-stressed heart.

SA25

Emerging Role of mPT in Driving Atrophy, Mitochondrial Dysfunction and Denervation in Skeletal Muscle with Aging and Disease

Russell Hepple¹, Vita Sonjak², Sally Spendiff², Tanja Taivassalo¹, Maya Semel¹, Cole Lukasiewicz¹

¹University of Florida, Gainesville, United States, ²McGill University, Montreal, Canada

Statement of the Problem: In contrast to the established role of mitochondrial permeability transition (mPT) in cardiac ischemia-reperfusion injury, neurodegeneration, and other tissue pathology, the role of mPT in skeletal muscle is less clear, notwithstanding some work in muscular dystrophies.

Methods: To address this gap, we used approaches in adult mouse single muscle fibers and isolated skeletal muscle mitochondria to establish the consequences of mPT in skeletal muscle. We induced mPT using Bz423, an agent that binds to the same site as cyclophilin D (CypD) on the oligomycin sensitivity conferring protein of the ATP synthase. We used inhibitors of mPT that worked through CypD (Alisporivir) or were CypD-independent (TR002, Isox63). We assessed mitochondrial ROS (mROS) generation using mitoSox, and inhibited mROS using mitoTEMPO. We assessed caspase 3 (Casp3) activation using a Casp3 FLICA assay, and inhibited Casp3 using a novel inhibitor (Ac-ATS0101-KE). We assessed mitochondrial respiration in isolated mouse skeletal muscle mitochondria. We evaluated the integrity of the acetylcholine receptor cluster (AChR) on single mouse muscle fibers by labeling with Alexa 488-conjugated α -bungarotoxin (α BG). To provide context to mPT in skeletal muscle, we performed a calcium retention capacity (CRC) in muscle bundles from elderly men and women, in mouse muscle fiber bundles incubated in pancreatic tumor-conditioned media, and in mice inoculated with pancreatic tumor cells. All animal and human experimentation were done in compliance with institutional regulations, including IACUC approval (protocol 202011171 at UF), IRB approval (BMC-06-015, A08-M66-12B), and written informed consent.

Results: Inducing mPT in single mouse muscle fibers using 300 nM Bz423 increased mROS and this was prevented by either an mPT inhibitor (1 mM TR002) or 5 mM mitoTEMPO. Similarly, Bz423 increased Casp3 activity and this was prevented by co-treating with TR002 or Ac-ATS010-KE. Incubating single mouse muscle fibers with 300 nM Bz423 for 24 h reduced muscle fiber diameter by ~20% and this was prevented by inhibiting mPT (TR002), inhibiting mROS, or inhibiting Casp3 (Fig 1). Treatment of isolated mouse skeletal muscle mitochondria with 25-50 mM Bz423 caused a complex I-specific respiratory impairment (Fig 2). Bz423 treatment of single mouse muscle fibers also reduced AChR content and fragmented the AChR cluster at the muscle endplate and this was prevented by inhibiting mPT or Casp3 (Fig 3). We found that the time to mPT in the CRC assay was reduced in muscle bundles from the vastus lateralis of elderly men and women (Fig 4). CRC was also reduced following an acute 60 min incubation of mouse muscle bundles in pancreatic tumor-conditioned media and in mice inoculated with pancreatic tumor cells (Fig 5).

Conclusions: Collectively, our results show that inducing mPT in skeletal muscle causes muscle atrophy, AChR cluster dismantling, and a complex I-specific respiratory impairment, which are common muscle phenotypes seen with aging and a variety of disease conditions. Consistent with mPT being relevant to muscle pathology with aging and disease, we also show that mitochondria are sensitized to mPT in aging and in response to tumor-host factors in cancer cachexia.

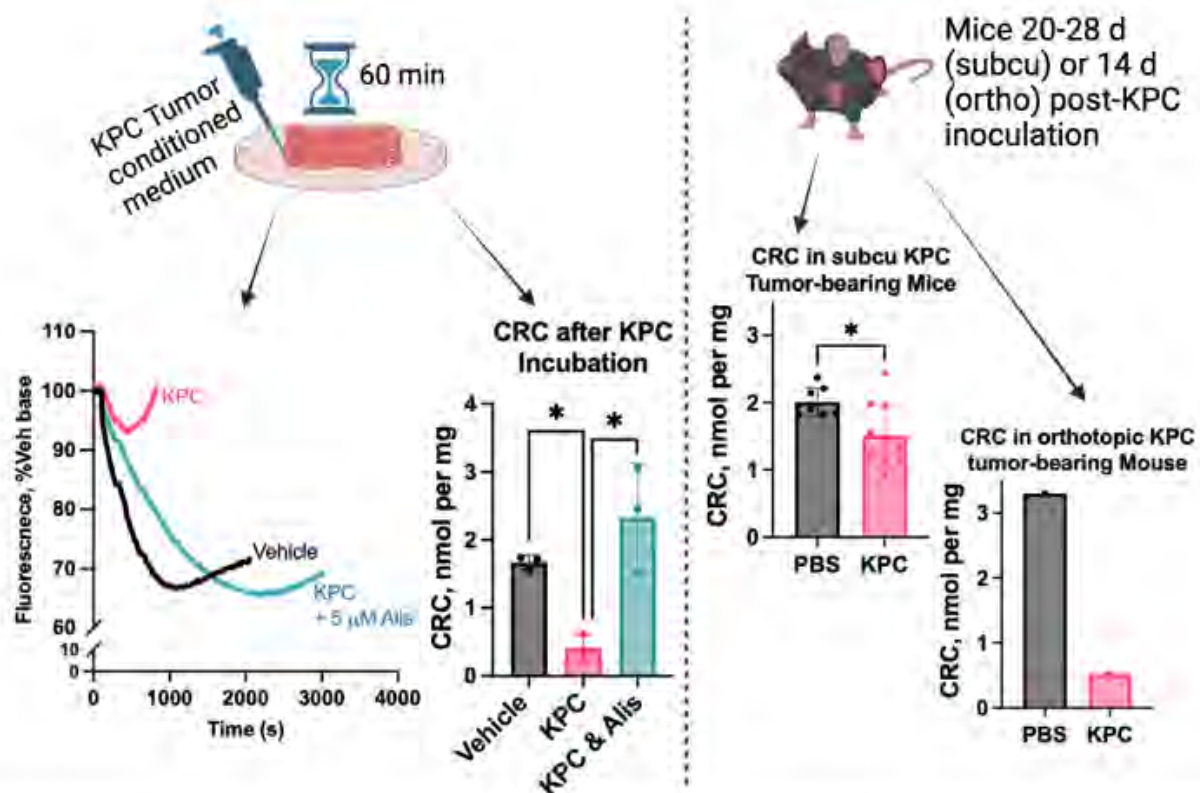


Figure 5. Tumor-host factors reduce the Ca^{2+} threshold for mPT. We incubated tibialis anterior myosin-depleted (ghost) muscle fiber bundles in KPC pancreatic tumor conditioned medium (50% diluted in DMEM) or Vehicle for 60 min at 4C. We then ran the muscle bundles through a Calcium Retention Capacity (CRC) assay. The KPC conditioned medium reduced CRC versus Vehicle and this was prevented by an mPT-inhibitor (5 μ M of the CypD-inhibitor Alisporivir [Alis]) (n=3 mice per treatment) (ANOVA). Similarly, mice bearing KPC tumors (n=10 KPC male mice for subcutaneous model; n=1 KPC female mouse for orthotopic model) had a reduced CRC versus PBS injected mice (n=8 male mice PBS for subcu, n=1 female mouse for orthotopic PBS) (compared by t-test). *P<0.05.

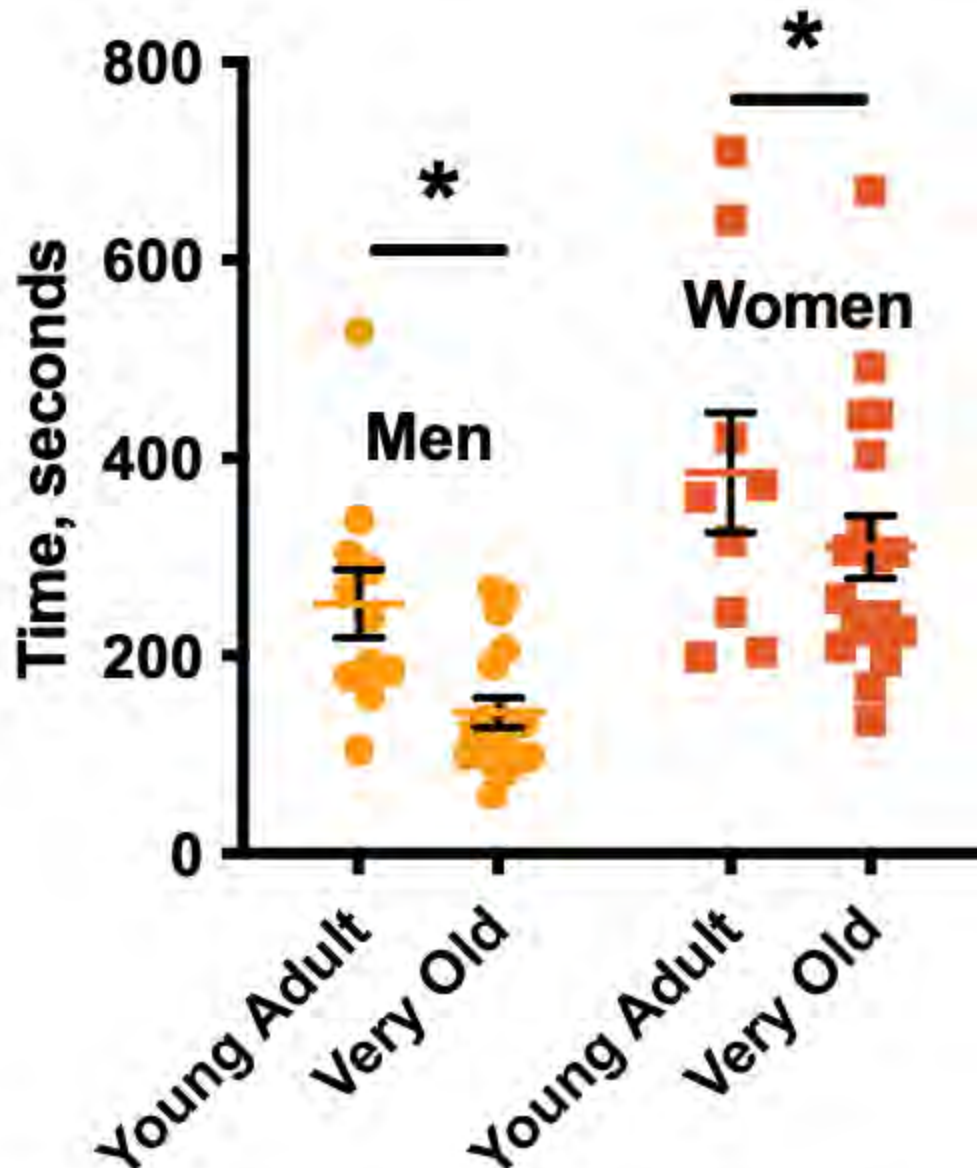


Figure 4. Bergstrom needle biopsies from the vastus lateralis muscle were obtained from young adult (20-30 y) and very old (76-89 y old) men and women. Saponin-permeabilized muscle bundles that had been depleted of myosin (so-called ghost bundles) were used in a Calcium Retention Capacity (CRC) assay using Ca^{2+} Green 5N. There was a main effect with no sex interaction for a longer time to reversal of the Ca^{2+} trace on the CRC assay in very old men and women versus their young adult counterparts. * $P < 0.01$ vs Day 0 (two-way ANOVA).

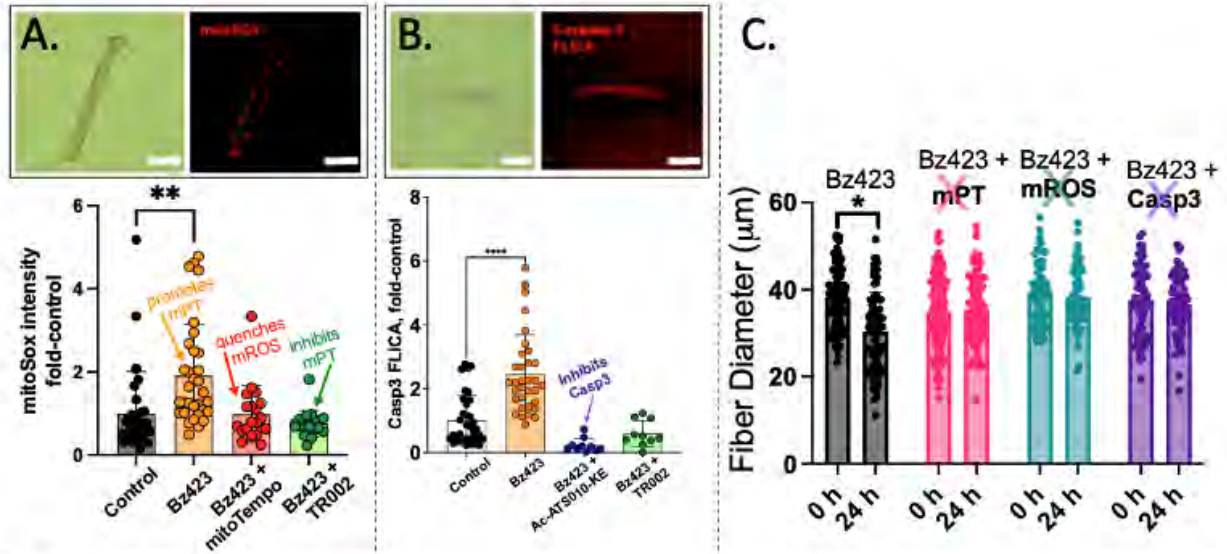


Fig 1. To determine if mPT causes atrophy in skeletal muscle fibers and its dependence upon mROS and Casp3, single mouse FDB muscle fibers were treated for 24h with 300 nM Bz423 (mPT-inducer), 300 nM Bz423 + 1 μM TR002 (mPT-inhibitor), 300 nM Bz423 + mitoTEMPO (mROS scavenger) or 300 nM Bz423 + 20 μM Ac-ATS010-KE (Casp3 inhibitor). mPT increased (A) mROS & (B) Casp3 activity, and induced atrophy that required both mROS and Casp3 activation (C). Biological replicates = 2-4. *** $P < 0.001$ and **** $P < 0.0001$ versus Day 0 (nested one-way ANOVA).

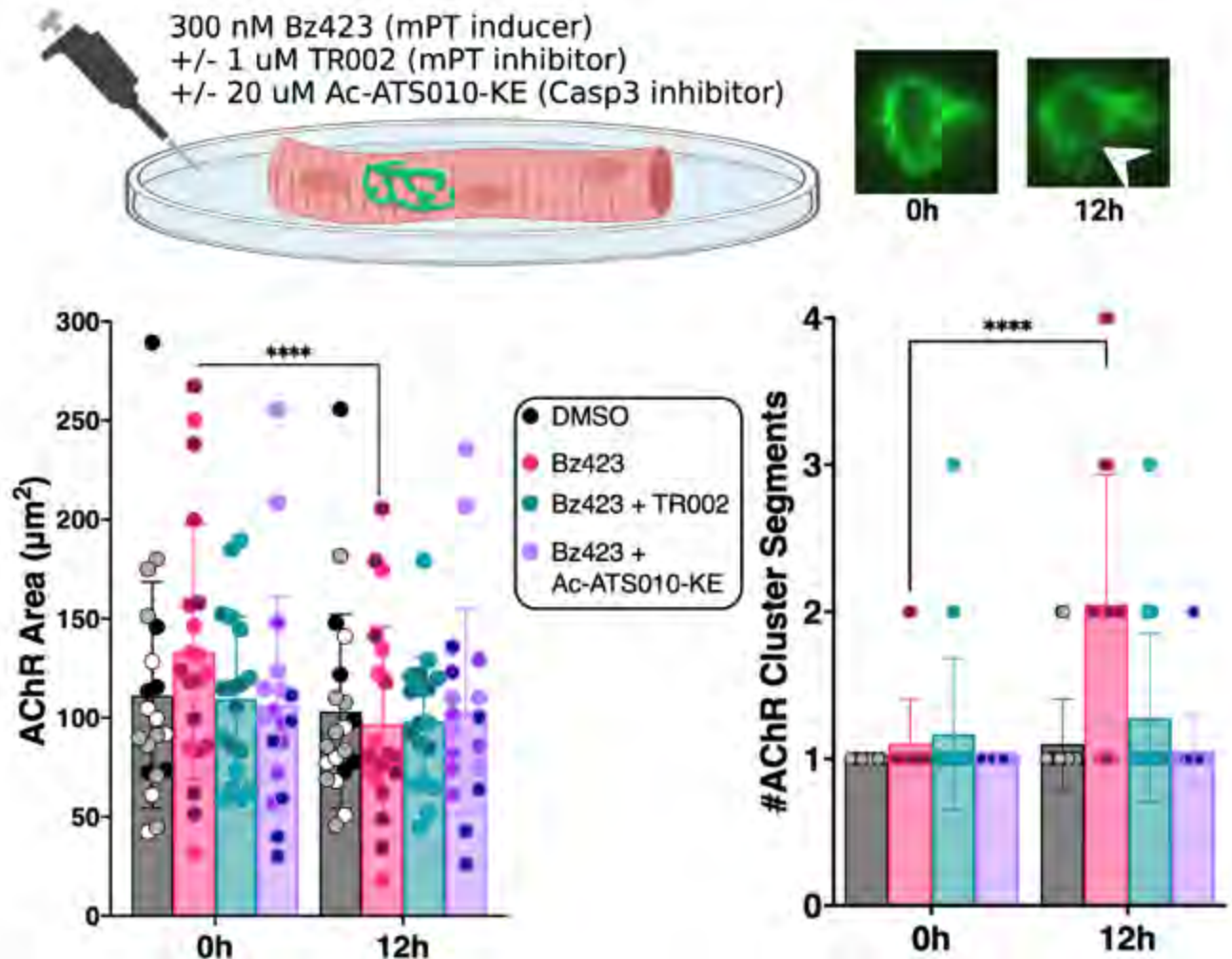


Figure 3. mPT causes AChR dismantling at the muscle endplate. AChRs on flexor digitorum brevis muscle fibers were labeled with AF488-bungarotoxin, treated with 300 nM Bz423 (mPT-inducer) +/- 1 μ M TR002 (mPT inhibitor), and imaged for 12 h. Images in upper right show a single endplate at time 0 and 12 h following treatment with Bz423. The white arrowhead shows an area of the AChR cluster that has fragmented and has reduced AChR intensity vs time 0. Graphs based on n=3 biological replicates (5 fibers/replicate) show that mPT reduced AChR area and induced AChR cluster fragmentation. **** P <0.0001 vs Day 0 (nested one-way ANOVA).

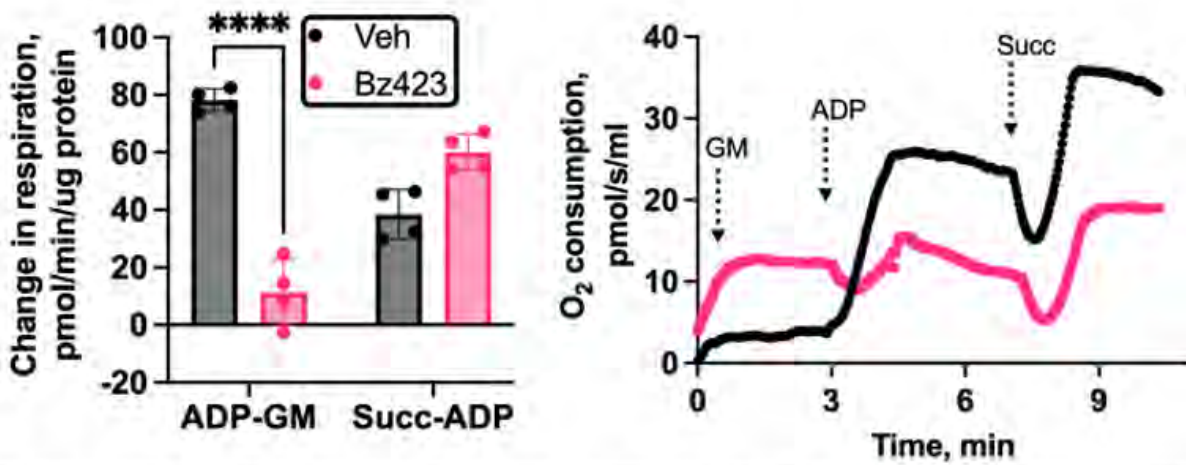


Fig 2. Treatment of skeletal muscle mitochondria with 50 μ M of the mPT-inducer Bz423 causes a complex I-specific respiratory defect. GM = 10 mM glutamate, 2.5 mM malate; +ADP = 2 mM adenosine diphosphate; +10 mM Succ = succinate. ****P<0.0001 versus Vehicle (one-way ANOVA).

SA26

Using the gut brain axis to improve obesity treatment

Carel le Roux¹

¹University College Dublin, Dublin, Ireland

Obesity is now being recognised as a neurological disease that is associated with serious morbidity and increased mortality. Understanding gastro intestinal signalling to the subcortical areas of the brain offer a view on a therapeutic window for obesity which promises better clinical benefits as well as lower side effects.

Bariatric surgery is a good model to investigate gut brain signalling in humans and rodents, because it provides major changes in appetite with subsequent weight loss maintenance. Following gastric bypass, pleiotrophic responses from the gastro intestinal tract may contribute to improved appetite reduction, long-term lowering of body weight, glycaemic control and improvements in end organ damage.

The new third-generation medications based on optimising gut brain signalling are however now facilitating a revolution. These medications appear to address many of the diseases leading to obesity at their origins. Treating obesity as a chronic disease with effective therapies allows the disease to come under control and remain under control as long as the therapies continue. The impact of effectively treating obesity will reduce the symptoms of obesity such as excessive appetitive behaviour, but it will also reduce the complications of obesity which will have far-reaching benefits for the individual, healthcare systems, and wider society.

SA27

TGR5-dependent host-microbiome interactions reestablish epithelial intestinal homeostasis following colon injury.

Antoine Jalil³, Alessia Perino¹, Yuan Dong², Jérôme Imbach¹, Colin Volet⁴, Eduard Vico-Oton⁴, Hadrien Demagny¹, Rizlan Bernier-Latmani⁴, Siegfried Hapfelmeier², Kristina Schoonjans¹

¹Laboratory of Metabolic Signaling, Institute of Bioengineering, School of Life Sciences, École Polytechnique Fédérale de Lausanne, Lausanne, Switzerland, ²Institute for Infectious Diseases, University of Bern, Bern, Switzerland, ³Laboratory of Metabolic Signaling, Institute of Bioengineering, School of Life Sciences, École Polytechnique Fédérale de Lausanne, Lausanne, Switzerland, ⁴Environmental Microbiology Laboratory, School of Architecture, Civil and Environmental Engineering, École Polytechnique Fédérale de Lausanne, Lausanne, Switzerland

Introduction: Inflammatory bowel disease (IBD), which includes Crohn's disease (CD) and ulcerative colitis (UC), is a chronic relapsing disorder characterized by inflammation of the gastrointestinal tract. Ulceration of the intestinal epithelium is a central factor in IBD, and preservation of its homeostasis appears crucial to prevent disease progression. A well-established feature of IBD is gut microbiome dysbiosis, which is characterized by a shift in microbial composition, leading to alterations in bacterial metabolites. Among these metabolites are secondary bile acids (BAs), pivotal in regulating intestinal and host physiology. BAs, initially synthesized in the liver as primary BAs and released into the intestine postprandially for lipid solubilization, undergo reabsorption and recycling in the small intestine. However, a fraction reaches the colon, where resident bacteria catalyze primary BA conversion into a variety of secondary BAs with different biological activities. Of particular importance are BA 7 α -dehydroxylating bacteria which convert the primary BAs cholic acid and chenodeoxycholic acid into deoxycholic acid and lithocholic acid, respectively, which are potent agonists of the BA-responsive membrane receptor Takeda G-coupled receptor 5 (TGR5). TGR5 activation drives multiple host processes, including gut hormone secretion, immunomodulation and stem cell-induced intestinal renewal. Since secondary BA production is diminished in IBD patients, we hypothesized that restoring 7 α -dehydroxylated BA levels may enhance the regenerative capacity of the colonic epithelium in mouse models and human patients with impaired or delayed intestinal repair capacity.

Aims and objectives: In this study, we investigated whether restoration of 7 α -dehydroxylated BA levels through colonization with the most characterized human-derived 7 α -dehydroxylating bacterium, *Clostridium scindens* (*C. scindens*), could re-establish epithelial intestinal homeostasis following colon injury. In addition, we analyzed omics datasets from UC patients and non-IBD individuals to translate our results to humans.

Methods: We colonized gnotobiotic Oligo-MM¹² and conventional C57BL/6J specific-pathogen free (SPF) mice with *C. scindens* and quantified fecal BAs. In both mouse models, colonic lesions were induced by administration of dextran sulfate sodium (DSS) and disease severity was assessed. SPF TGR5 knock-out mice and wild-type controls were also subjected to chemically-induced experimental colitis to evaluate the impact of the BA receptor TGR5. In addition, we reanalyzed public multi-omics datasets from a cohort of UC patients and controls to increase the relevance of our preclinical results.

Results and conclusion: Our study revealed that the amendment of *C scindens* confers protection to DSS-induced colitis in both a prophylactic and therapeutic manner. Mechanistically, *C. scindens* improved the integrity of intestinal epithelium by promoting TGR5-mediated tissue regeneration. Finally, we observed that UC patients displayed dampened intestinal cell renewal and differentiation, and genes involved in those pathways showed a robust positive correlation with 7 α -dehydroxylated BAs levels. Our study reports *C. scindens* administration as a promising biotherapeutic strategy to foster epithelial regeneration and healing following colon injury by restoring the secondary to primary BA ratio.

SA28

Exploring fructose kinetics in Type 2 Diabetes: preliminary data from the ERIE trial

Florine Westerbeke¹, Ilias Attaye¹, Melany Rios-Morales¹, Max Nieuwdorp^{1,2}

¹*Department of Internal and Experimental Vascular Medicine, Amsterdam University Medical Center, location AMC, Amsterdam, Netherlands,* ²*Diabeter Center Amsterdam, Amsterdam, Netherlands*

Background and aims

Dietary fructose consumption has increased substantially in recent decades and is associated with higher incidence of obesity, type 2 diabetes (T2D) and other non-communicable diseases. However, causality and underlying mechanisms remain to be elucidated. Therefore, the 'Effect of dietary fructose on fructose kinetics in type 2 diabetes' (ERIE) trial is being performed. The trial aims to investigate fructose metabolism, including microbial fermentation, and its effects in T2D individuals, through examining oral fructose handling in T2D subjects receiving a high- or low-fructose diet.

Materials and methods

The ERIE trial, a double-blinded, isocaloric randomized controlled trial, aims to recruit 40 non-insulin dependent T2D participants on stable metformin therapy. Participants are randomly assigned to group A or B, receiving either a high- (100g/day) or a low-fructose (30g/day) diet for 4 weeks. Primary endpoints include changes in oral fructose handling, assessed through a fructose challenge test (FCT) by ingesting 1g/kg bodyweight unlabeled fructose and 120mg ¹³C₆-labeled fructose, in relation to metabolic markers such as HOMA-IR. Preliminary data from up to 18 participants were analyzed using multiple non-parametric tests, comparing deltas (Δ) of pre- and post-intervention results between both groups.

Results

In groups A and B, 45.5% and 28.6% of participants were female, respectively. Median age [IQR] was 65 years [56-68] in group A and 60 years [59-66] in group B. Median BMI [IQR] was 29.3 kg/m² [27.1-33.8] in group A and 29.9 kg/m² [27.9-32.2] in group B. Group B exhibited a significantly faster peripheral appearance of ¹³C₆-fructose and reached higher concentrations after 30 minutes with a median Δ [IQR] of 0.93 μ M [0.89-1.45], compared to 0.02 μ M [-0.46-0.45] in group A ($p=0.012$). Concurrently, group B showed a trend towards increased peripheral appearance of unlabeled fructose with a median Δ [IQR] of 207.70 μ M [144.26-271.14] after 30 minutes, compared to 1.14 μ M [-25.19-72.78] in group A ($p=0.178$). Uric acid levels in group B exhibited a significant rise throughout the FCT, with a median Δ [IQR] of 49.0 μ M/L [41.5-69.5] after 150 minutes, compared to -8.0 μ M/L [-14.0-23.0] in group A ($p<0.001$). No changes in glucose levels were observed in either group, with current inclusion numbers.

Conclusion

The accelerated and heightened peripheral appearance of fructose in group B, compared to group A, following ingestion of an equivalent oral fructose dose pre- and post-intervention, suggests altered fructose absorption in group B. This aligns with a significant increase in uric acid levels in group B, indicating enhanced hepatic fructose metabolism. These results show that varying levels

of fructose consumption affect acute fructose metabolism. Prolonged exposure to high fructose levels in the intestine may induce an upregulation of intestinal GLUT-5, facilitating increased fructose absorption. This can have negative metabolic effects by elevating fructose levels reaching the liver, thereby augmenting hepatic fructose metabolism. This can lead to increased uric acid production and fatty acid synthesis. Despite the trial's blinding, preliminary data suggest that group B adhered to the high fructose diet. These results provide novel insights into fructose metabolism in individuals with T2D, highlighting potential deleterious metabolic consequences likely associated with increased fructose consumption.

SA29

The gut-brain GLP-1 axis: role in limiting nutrient uptake and countering obesity

Fiona Gribble¹

¹Institute of Metabolic Science, University of Cambridge, Cambridge, United Kingdom

The gut endocrine system comprises a collection of enteroendocrine cells scattered throughout the intestinal epithelium, producing hormones that signal locally within the gut and distantly at tissues such as the brain and pancreas. In the field of diabetes and obesity, therapies based on GLP-1 are now in widespread clinical use, and dual/triple agonists such as GLP1/GIP and GLP1/GIP/glucagon are showing even greater efficacy.

The study of GLP-1 secretion can now be performed using human intestinal organoids, engineered by CRISPR-Cas9 to label specific enteroendocrine cell populations or to knock out genes of interest. Application of live cell imaging, electrophysiology and transcriptomics to these organoid model has identified signalling pathways of particular interest including those activated by glucose, bile acids and free fatty acids. Whereas glucose stimulates enteroendocrine cells as a consequence of its electrogenic uptake via SGLT1, bile acids and free fatty acids target specific G-protein coupled receptors on the cell membrane, most notably GPBAR1 and FFAR1.

Understanding signalling in the gut brain axis provides a foundation for identifying new drugs for type 2 diabetes and obesity that act by targeting gut endocrine cells, thus mimicking the gut endocrine consequences of bariatric surgery.

SA30

Time-Of-Day Dependent Metabolic Response to Exercise

Juleen Zierath^{1,2}

¹Karolinska Institutet, Stockholm, Sweden, ²CBMR, University of Copenhagen, Copenhagen, Denmark

Exercise is a potent energetic stressor and a major counter measure against metabolic disease. Timing of energetic stressors over the day may specify close alignment between tissue clocks and promote coherent and efficient temporal gating of metabolic processes. My team have integrated emerging omics technologies to interrogate biorhythms and physiological responses to energetic stressors. This led to an atlas of exercise metabolism, in which we mapped global metabolite responses of multiple tissues after exercise. Thus, we have made the surprising discovery that the therapeutic response to exercise is time-dependent. In fact, we have also shown that timing of exercise or meals throughout the day affects metabolism in people with obesity or type 2 diabetes, but the mechanism(s) are unknown. My team is advancing the notion of “chrono-exercise”. We integrate omics approaches with physiological phenotyping and downstream mechanistic analyses, to optimize metabolism by timing energetic stressors to the peak times of metabolic rhythms to positively impact cardiometabolic health. In lecture, I will present emerging evidence that timing may optimize the adaptive response to exercise and improve health outcomes. Chrono-exercise may optimize metabolism by timing energetic stress during the day to improve insulin sensitivity and glycemia, and thereby positively impact metabolic health.

SA31

Optimising concomitant metformin and exercise treatment by precision timing to improve glycaemic regulation in people with Type 2 Diabetes

Brenda Pena Carrillo^{1,3}, Rasmus Kjøbsted², Jonas Møller Kristensen², Jørgen Wojtaszewski²,
Brendan Gabriel^{1,3,4}

¹Aberdeen Cardiovascular and Diabetes Centre, Institute of Medical Sciences, School of Medicine, Medical Sciences & Nutrition, University of Aberdeen, Aberdeen, United Kingdom, ²August Krogh section for molecular physiology, University of Copenhagen, Copenhagen, Denmark, ³The Rowett Institute, School of Medicine, Medical Sciences & Nutrition University of Aberdeen, Aberdeen, United Kingdom, ⁴Department of Physiology and Pharmacology, Integrative Physiology, Karolinska Institute, Stockholm, Sweden

Exercise is beneficial for several organ systems in the body and increases insulin sensitivity [1]. However, previous evidence suggests that the timing of exercise in people with Type 2 Diabetes may have opposing outcomes on glycaemia [2]. This may be particularly relevant in people also being prescribed metformin [3], the most prescribed anti-hyperglycaemic medication for people with Type 2 Diabetes and often recommended concomitantly along exercise. Although exercise improves glycaemia, this effect is inhibited when undertaken alongside metformin ingestion [4,5]. Metformin intake also appears further inhibit the beneficial response to exercise, including ablating improvements in insulin sensitivity and skeletal muscle mitochondrial protein synthesis and respiration [6,7]. Therefore, we hypothesise that the skeletal muscle signalling response to exercise is disrupted by metformin and that it may be possible to optimise recommendations for when to take metformin together with exercise. To test this, we performed a remote crossover study, 9 male and 9 females with T2D undergoing metformin monotherapy completed 2-week baseline, six weeks randomly assigned to morning (7-10am) or evening (4-7pm) exercise (30 mins), with a two-week wash-out period. Acute AUC glucose was significantly lower ($p=0.01$) in participants taking metformin before breakfast ($152.5\pm29.95\text{mmol/L}$) compared with participants taking metformin after breakfast ($227.2\pm61.51\text{mmol/L}$) only during the morning exercise arm. Our data indicates that morning moderate exercise lower glucose levels in people with T2D on metformin, especially when metformin is taken before breakfast. We also analysed skeletal muscle biopsies from seven healthy lean men that completed one bout of single-leg exercise with a contralateral control-leg after acute metformin/placebo supplementation [8]. After fasting overnight, participants had biopsies taken from the vastus lateralis in both legs and then received either 1.5g of metformin or a placebo with breakfast. They then rested for 4½ hours and had biopsies taken from both legs. Then, they did a 40-minute knee extensor exercise at 80%PWL followed by another biopsy. RNA sequencing analysis revealed that metformin supplementation inhibited the transcriptomic response to exercise by reducing the total number of differentially expressed genes in response to exercise. After exercise, 53 genes were upregulated in the placebo trial, while only 17 genes were upregulated in the Metformin trial. Importantly, the transcription factor NR4A3 was upregulated in response to exercise during the placebo trial (adj. $p=0.011$), but not when participants consumed metformin (adj. $p=0.234$). In Human skeletal muscle myotubes (HSM), metformin (10µM) did not change NR4A3 expression (RT-qPCR, 1.2-fold-change, $p=0.536$) compared to the control. As expected, exercise mimetic Ionomycin (8µM) significantly increased NR4A3 expression (4.3-fold-change, $p<0.001$), however concomitant metformin incubation significantly reduced the NR4A3 response (2.4-fold-change, $p=0.002$). In summary, our preliminary

data suggest that taking metformin before breakfast when combined with morning moderate intensity exercise lowers blood sugar compared to other treatment timings. Our mechanistic investigations reveal that *NR4A3* response to exercise in skeletal muscle is inhibited by metformin, which is likely underlying the apparent inhibition of exercise-induced skeletal muscle glucose uptake with concomitant metformin. Our data suggest that it may be possible to optimised exercise timing alongside concomitant metformin to augment skeletal muscle glucose uptake.

1. Gabriel, BM, et al. (2017). The Limits of Exercise Physiology: From Performance to Health. *Cell metabolism*, 25(5), 1000–1011. <https://doi.org/10.1016/j.cmet.2017.04.018>. 2. Savikj, M, et al. (2019). Afternoon exercise is more efficacious than morning exercise at improving blood glucose levels in individuals with type 2 diabetes: a randomised crossover trial. *Diabetologia*, 62(2), 233–237. <https://doi.org/10.1007/s00125-018-4767-z>. 3. Gabriel BM & Zierath JR (2021). Zeitgebers of skeletal muscle and implications for metabolic health. *The Journal of Physiology*; 600(5):1027–1036. <https://doi.org/10.1113/JP280884>. 4. Boulé NG, et al. (2011) Metformin and exercise in type 2 diabetes: examining treatment modality interactions. *Diabetes Care* 34(7):1469–1474. <https://doi.org/10.2337/DC10-2207>. 5. Peña Carrillo, BJ, et al. (2024). Morning exercise and pre-breakfast metformin interact to reduce glycaemia in people with Type 2 Diabetes: a randomized crossover trial. *MedRxiv* 2023-09. <https://doi.org/10.1101/2023.09.07.23295059>. 6. Das S, et al. (2018) Effect of metformin on exercise capacity: A meta-analysis. *Diabetes Res Clin Pr* 144:270–278. <https://doi.org/10.1016/j.diabres.2018.08.022>. 7. Konopka AR, et al. (2019) Metformin inhibits mitochondrial adaptations to aerobic exercise training in older adults. *Aging Cell* 18(1):e12880. <https://doi.org/10.1111/accel.12880>. 8. Kristensen JM, et al. (2019) Metformin does not compromise energy status in human skeletal muscle at rest or during acute exercise: A randomised, crossover trial. *Physiol Rep* 7(23). <https://doi.org/10.14814/phy2.14307>.

SA32

The complexities of characterising shift work, diet and blood glucose variability in a real-world setting

Rachel Gibson, Nick Oliver, Nicola Guess, Fabiana Lorencatto, Luigi Palla, Barbara McGowan, Maria D'annibale

undefined

The night-time economy contributes £93.7bn annually to the UK economy(1) and relies on extensive employment of night workers. The association between night work and adverse cardiometabolic health is of increasing concern. Shift workers, compared to day workers, are more likely to be diagnosed with type 2 diabetes (T2D)(2) and shift workers living with T2D are reported to have higher glycated haemoglobin compared to day workers(3). Simulated shift work studies have significantly contributed to understanding how eating at night impacts physiology however, real world research is needed among shift workers. The Shift-Diabetes study (ISTCTN 11764942) is a mixed methods study with the aim to characterise current management of T2D in shift workers.

An observational study was conducted in 40 shift workers (working a combination of night and day shifts) living with T2D. Across 10-days, data was collected on blood glucose (continuous glucose monitor), diet (self-report diary), sleep and physical activity (actigraphy). The monitoring period covered night shifts, day shifts and rest days. Within person mean glucose concentration (MG), coefficient of variation (CV), mean absolute glucose (MAG), mean amplitude of glycaemic excursion (MAGE) and dietary intake (food choices, nutrient intake) were compared between 'behavioural day' types. A 'behavioural day' was defined as the period between two main sleep periods (sleep off set to sleep off set)(4) Figure 1. Behavioural day types were categorised as: night shift, day shift, rest after night shift and day off. A parallel qualitative study was conducted in 15 shift workers using semi-structured interviews to explore barriers and enablers to dietary behaviour during shift work(5).

The study sample was predominantly female (89.2%) and employed as a nurse or midwife (62.2%). The behavioural day duration was significantly longer when a night shift was worked (26.9 SD2.5hrs) compared to a day off (23.5 SD1.0hrs, $p < 0.001$). A rest after night shift day was shorter than all other day types (17.2 SD2.7hrs, $p < 0.001$). Energy intake (%) from confectionary was higher on a night shift compared to a rest after night shift (13.4 SD12.0% vs. 7.8 SD11.8%, $p = 0.013$). Caffeine intake was significantly different across all day types, except between day off and day shifts, with intake highest on night shifts (164.8 SD175.5mg/day). There were differences in the number of eating occasions, with night shifts having the highest occasions (7.0 SD2.2) and rest after night the lowest (3.4 SD1.6). No differences were observed for MG, MAGE or CV. MAG was higher for night shift compared to rest after night shift (3.4 SD1.0 vs. 2.9 SD1.6, $p = 0.029$). The qualitative study found shift workers wanted to make healthier food choices during night work but were inhibited due to limited access to food and a lack of confidence in adjusting diet intake to shift schedules(5).

Physiology in Focus 2024

Northumbria University, Newcastle, UK | 2 – 4 July 2024

The duration of behavioural day when dictated by type of shift can vary significantly and may impact dietary intake and blood glucose. Further research to understand how changes in behavioural day duration impact shift worker behaviours and health are needed.

King's College London BDM Research Ethics Subcommittee (HR-19/20-14630)

1) Night Time Industries Association (2023) Night Time Economy Report. 2) Health and Social Care Information Centre (2013) Health Survey for England 3) Manodpitipong A et al.(2017) J Sleep Res. 26:764–72. 4) Kosmadopoulos A et al (2020) Nutrients. 12:999 5) Gibson R et al. (2023). Diabet Med.41: e15179

SA33

Examining the Contribution of NR1D1 to Adaptive Metabolic Response

David Bechtold¹

¹University of Manchester, Manchester, United Kingdom

The circadian system is essential to normal regulation of energy balance and metabolic health. Local circadian mechanisms shape rhythmic transcriptional and translational events in the brain and key peripheral tissues to cope with the daily switch between fed and fasted states. Importantly, clock function and individual components of the circadian clock contribute to homeostatic mechanisms which dictate physiological response to acute and chronic shifts in energy state and can mitigate response to metabolic perturbation, such as mistimed food intake. Here I will discuss some of our work examining the role of Rev-erba (Nr1d1) in adaptive metabolic response to both acute energy deficit and chronic surplus in mice.

SA34

Reversing pericyte-mediated capillary constriction: a therapeutic target for restoring cerebral blood flow in dementia-causing conditions.

David Attwell¹

¹*Dept Neuroscience, Physiology & Pharmacology, UCL and BHF/UK-DRI Centre for Vascular Dementia Research, London, United Kingdom*

Although the generation of amyloid beta oligomers and plaques, and of hyperphosphorylated tau, are hallmarks of Alzheimer's disease (AD), it has been shown that an earlier change in AD is a decrease of cerebral blood flow (CBF) by ~50% in affected brain areas. Cerebral blood flow can also decrease in vascular dementia.

By imaging capillary diameter in neuropathological biopsy sections from the right prefrontal cortex of humans developing AD we previously showed that capillaries in humans with AD are constricted as a result of pericyte contraction (Nortley et al., 2019). A similar pericyte-mediated constriction of capillaries in vivo was seen using 2-photon imaging through a cranial window in anaesthetised AD mice (APP^{NL-G-F} mice) expressing dsRed in pericytes controlled by the NG2 promoter. In the mice we also showed that there was no constriction of arterioles or venules, and that the capillary constriction leads to a stalling of neutrophils near pericyte locations and to tissue hypoxia.

In rodent brain slices we found that applying exogenous oligomerised amyloid beta (EC₅₀~6 nM) led to a pericyte-mediated constriction of capillaries, that was generated by endothelin-1 (ET) release and activation of ET_A receptors (Nortley et al., 2019). This reflected reactive oxygen species generation, since it was reduced by NOX4 and NOX2 blockers (Nortley et al., 2019). ET-evoked pericyte contraction is amplified by a rise of [Ca²⁺]_i activating TMEM16A chloride channels, which generate a depolarisation that activates voltage-gated Ca²⁺ channels (Korte et al., 2022).

To attempt to use a re-purposed drug to reverse the capillary constriction in AD, we employed the voltage-gated calcium channel blocker nimodipine, which is licensed for human use in sub-arachnoid haemorrhage. Giving nimodipine, either intravenously, or in the drinking water from 1.5 to 4 months of age, led to a relaxation of pericytes and arteriolar smooth muscle cells, an increase of cerebral blood flow, a block of the stalling of neutrophils in capillaries, and a partial reversal of the tissue hypoxia.

Other possible therapeutic targets for reversing or preventing a decrease of cerebral blood flow in AD or in some types of vascular dementia would include the mechanisms leading to endothelin

release in AD, ET_A receptors, TMEM16A channels, and the concentration of cyclic nucleotides in contractile mural cells where a rise of cGMP and cAMP concentration (for example in response to a guanylate cyclase receptor agonist: Nortley et al., 2019) leads to vasorelaxation. Agents that increase cerebral blood flow are likely to be useful as adjunct therapies with other dementia-targeting drugs.

Nortley, R. et al. (2019) Amyloid β oligomers constrict human capillaries in Alzheimer's disease via signaling to pericytes. *Science*. 365, eaav9518. Korte, N. et al. (2022) The Ca²⁺-gated channel TMEM16A amplifies capillary pericyte contraction and reduces cerebral blood flow after ischemia. *J Clin Invest* 132, e154118.

SA35

Lasting, low amplitude responses characterize the remodeled neurovascular coupling and Ca²⁺ signaling in the aged awake mouse brain

Changsi Cai¹

¹Department of Neuroscience, University of Copenhagen, Copenhagen, Denmark

Brain aging is associated with reduced vascular reactivity, exacerbated brain energy deficits and cognitive decline. However, it is still unclear how normal aging impacts neurovascular function and its underlying mechanism, especially in the awake brains. It is also unknown whether arteries and capillaries undergo different age-related structural and functional remodeling. Using laser speckle contrast imaging and two-photon imaging in awake, behaving young adult and aged mice, we show that neurovascular coupling (NVC) responses in the aged brain are prolonged, with reduced amplitudes, and this is more pronounced at the capillaries than at the arteries. Compared with anesthetized state, the total flow change of NVC at both arteries and capillaries are preserved in the awake aged brains. Furthermore, the NVC response is mediated by Ca²⁺ signaling in vascular mural cells, i.e. vascular smooth muscle cells and pericytes. We revealed a different Ca²⁺ kinetics of vascular mural cells in young adult and aged mice. The rate of calcium transport and the calcium sensitivity of vascular mural cells are reduced in aged mice, which explains the reduced and prolonged vasodilation. Structurally, we further revealed the retraction of transitional point from contractile to non-contractile mural cells at aged capillaries. Lastly, the vascular and Ca²⁺ responses triggered by spontaneous behavior such as locomotion also exhibits consistent prolonged characteristics. In all, our data suggests that the altered NVC responses in the aged awake brain is associated with remodeling of Ca²⁺ signals and vascular coverage of contractile mural cells. Novel interventions to delay age-related brain pathology could be based on fully harnessing the power of the vascular remodeling mechanisms with age.

SA36

Capturing rapid changes in cerebral blood flow.

Dmitry Postnov¹

¹Center of Functionally Integrative Neuroscience, Department of Clinical Medicine, Aarhus University,, Aarhus, Denmark

Adequate neurovascular dynamics, hemodynamic resistance, and microvascular stiffness are key to maintaining healthy brain function, whereas associated abnormalities play a crucial role in developing neurodegenerative or cardiovascular diseases. Characterising these features is pivotal for research and diagnostics and can generally be achieved by measuring perfusion and diameter changes associated with indigenous, e.g. cardiac or neurovascular activity, or exogenous factors, e.g. pharmacological stimulation. Such changes, however, often propagate rapidly over short microvascular segments and, therefore, require high-speed, high-resolution imaging to characterise them in detail. To address this challenge, our group has developed High-Speed Laser Speckle Contrast Imaging [1,2] (HS-LSCI) – a dynamic light scattering imaging technique that allows full-field microvascular perfusion imaging at >5000 frames per second. Here, we will explain the theoretical and technical foundations of high-speed blood flow imaging, discuss potential applications and show some of the first results acquired from the mouse cortex. Specifically, we will present the analysis of cardiac-cycle associated perfusion changes in ageing mice and approach the topic of the spatiotemporal dynamics of neurovascular response caused by air-puff stimulation of the mouse whiskers. All experimental protocols in the relevant studies were approved by the Danish National Animals Experiments Inspectorate and conducted according to their guidelines and guidelines from Directive 2010/63/EU of the European Parliament on the protection of animals used for scientific purposes.

[1] Olmos AG, Postnov DD. High-speed laser speckle contrast imaging. Patent pending, application number EP 22173808. 2022 [2] Postnov DD, Tang J, Erdener SE, Kılıç K, Boas DA. Dynamic light scattering imaging. Science advances. 2020 Nov 6;6(45):eabc4628

SA37

Neurovascular Impulse Response Function, Neuromodulation and Behavior

Anna Devor¹, Bradley C. Rauscher¹

¹Boston University, Boston, United States

Ascending neuromodulatory projections from deep brain nuclei generate internal brain states that differentially engage specific neuronal cell types. Because neurovascular coupling is cell-type specific and neuromodulatory transmitters have vasoactive properties, we hypothesized that the impulse response function (IRF) linking spontaneous neuronal activity with hemodynamics would depend on brain state.

To test this hypothesis, we used optical imaging to measure (1) release of neuromodulatory transmitters norepinephrine (NE) or acetylcholine (ACh), (2) Ca^{2+} activity of local cortical neurons, and (3) changes in hemoglobin concentration and oxygenation across the dorsal surface of cerebral cortex during spontaneous neuronal activity in awake mice.

Fluctuations in total hemoglobin (HbT), reflective of dilation dynamics, were well predicted by a weighted sum of positive Ca^{2+} and negative NE contributions, while ACh signals were largely redundant with Ca^{2+} . IRF varied in time and depended on the arousal (dilation of the eye pupil, whisking) captured by NE but not ACh. During high arousal, the dynamic nature of IRF resulted in the loss of hemodynamic coherence between cortical regions (known as “functional connectivity” in BOLD fMRI studies) despite coherent behavior of the underlying neuronal Ca^{2+} activity.

We conclude that neurovascular coupling is a dynamic phenomenon that reflects NE neuromodulation and behavior. Dynamics of IRF challenges the metric of functional connectivity because the loss of hemodynamic coherence can be falsely interpreted as neuronal desynchronizations.

SA38

Direct activation of renal, Ghrelin-family GPR39 receptors reduces urinary concentration capacity

Lingzhi Lui^{1,4}, Mackenzie Kui², Lena L Rosenbaek³, Samuel L Svendsen³, Annemette Overgaard Brethvad^{1,4}, Alexander Jakobsen^{1,4}, Mattias Skov³, Jacob R Therkildsen³, Jesper Kingo Andresen⁵, Anna Laitakari⁴, Thomas Michael Frimurer⁴, Boye Lagerbon Jensen⁵, Jennifer Pluznick², Robert A Fenton³, Birgitte Holst^{1,4}, Helle Praetorius³

¹Laboratory for Molecular Pharmacology, Department of Biomedical Sciences, University of Copenhagen, Copenhagen, Denmark, ²Department of Physiology, Johns Hopkins University School of Medicine, Baltimore, United States, ³Department of Biomedicine, Aarhus University, Aarhus, Denmark, ⁴Section of Metabolic Receptology, Novo Nordisk Foundation Center for Basic Metabolic Research, University of Copenhagen, Copenhagen, Denmark, ⁵The Faculty of Health Sciences, Department of Molecular Medicine, Cardiovascular and Renal Research, University of Southern Denmark, Odense, Denmark

Fasting results in significant changes in the distribution of body fluids, leading to a decrease in blood pressure and circulatory volume. Lately, several primary gastrointestinal hormones and orphan receptors in taste and olfaction have been implicated in the regulation of renal function¹⁻⁵, and hence, one can speculate that appetite-regulating signalling might be responsible for the circulatory volume contraction observed in response to anorectic states. Activation of the orphan receptor GPR39 of the ghrelin receptor family in the gastrointestinal tract results in local GLP-1 release and a following decrease in food intake and weight reduction in mice⁶. In the current study, oral gavage of a selective GPR39 agonist (Cpd1324) increases the water intake in C57BL/6J mice. The effect is dose-dependent fashion, and results in over two-fold increase in 24-hour water intake relative to vehicle controls, an effect that was completely absent in global GPR39 deficient mice. Cpd1324 markedly reduced the urinary concentrate capacity in C57BL/6J mice after eight hours of water restriction (1927.0 ± 129.3 mosmol/kg, $n=5$) compared to vehicle controls (3196.0 ± 139.9 mosmol/kg, $n=5$, $p<0.001$). In *ex vivo* perfused cortical collecting ducts, GPR39 ($10\mu\text{M}$) directly counteracted the AVP-induced water permeability, corresponding to a Cpd1324-induced around 50% reduction in phosphorylated AQP2 (S256) abundance assessed by immunoblotting of renal tubule suspension. GPR39 activation also reduced the amount of phosphorylated NCC in distal convoluted tubules, with a parallel increase in urinary K^+ excretion. These data suggest that the Cpd1324-induced drinking behaviour is secondary to a urinary concentration deficiency caused by opposing AVP-induced water reabsorption in the collecting duct. Moreover, we propose that a GPR39-dependent urine concentration defect and reduced NaCl reabsorption in the distal convoluted tubule might explain the circulatory volume contraction observed during fasting.

1. Berg P, Svendsen SL, Sorensen MV, et al. Impaired Renal HCO_3^- Excretion in Cystic Fibrosis. *J Am Soc Nephrol.* 2020;31(8):1711-1727. 2. Rajkumar P, Cha B, Yin J, et al. Identifying the localization and exploring a functional role for Gprc5c in the kidney. *FASEB J.* 2018;32(4):2046-2059. 3. Shepard BD, Koepsell H, Pluznick JL. Renal olfactory receptor 1393 contributes to the progression of type 2 diabetes in a diet-induced obesity model. *Am J Physiol Renal Physiol.* 2019;316(2):F372-F381. 4. Pluznick JL, Protzko RJ, Gevorgyan H, et al. Olfactory receptor responding to gut microbiota-derived signals plays a role in renin secretion and blood pressure regulation. *Proc Natl Acad Sci U S A.* 2013;110(11):4410-4415. 5. Cuffe JE, Bielfeld-Ackermann A,

Thomas J, Leipziger J, Korbmacher C. ATP stimulates Cl⁻ secretion and reduces amiloride-sensitive Na⁺ absorption in M-1 mouse cortical collecting duct cells. *J Physiol.* 2000;524:77-90. 6. Grunddal KV, Diep TA, Petersen N, et al. Selective release of gastrointestinal hormones induced by an orally active GPR39 agonist. *Mol Metab.* 2021;49:101207.

SA39

Transcriptomics and Proteomics Data from Micro-dissected Renal Tubules Identifies the Distributions of All GPCRs Along the Renal Tubule

Mark Knepper^{1,2}, Mark Knepper^{1,3}

¹National Heart, Lung and Blood Institute, NIH, Bethesda, United States, ²National Heart, Lung and Blood Institute, Bethesda, United States, ³National Heart, Lung and Blood Institute, Bethesda, United States

A broad objective in systems biology is to identify every gene expressed in every cell type in the body. In kidney, we have used RNA-seq and protein mass spectrometry in microdissected kidney tubule segments to map expression of all genes in all renal tubular epithelia. Because collecting ducts (CDs) contain a mixture of principal cells (PCs) and intercalated cells (ICs), we have resolved separate transcriptomes in these cell types using single-cell RNA-seq. Data have been provided to the kidney research community through web-based sharing of curated data sets (<https://esbl.nhlbi.nih.gov/Databases/KSBP2/>). These data sets can be browsed, searched or downloaded, allowing them to be ‘mined’ to tie gene expression patterns to physiological functions of different renal epithelial cells.

Because signaling through GPCRs is vital to control of transport and metabolism in the kidney, we have used the data to curate all GPCRs present in mammalian genomes amounting to 790 genes (<https://esbl.nhlbi.nih.gov/Databases/GPCRs/>) and mapped them to each of 14 renal tubule segments and to PCs and ICs of the CD (<https://esbl.nhlbi.nih.gov/Databases/GPCRs/TubuleTPM.html>). One area of interest is regulation of aquaporin-2 (AQP2) in principal cells. Although it is well known that regulation of AQP2 trafficking and transcription are dependent on increased cAMP secondary to the G_s-coupled vasopressin V2 receptor (Avpr2), two other G_s-coupled receptors were identified in PCs. These are the prostaglandin EP4 receptor (Ptger4) and the calcitonin-related receptor-like receptor (Calcrl), which binds adrenomedullin in collecting duct PCs. Ligand interactions with both receptors have been shown to increase cAMP and water permeability in collecting ducts, pointing to alternative treatment modalities in X-linked nephrogenic diabetes insipidus due to mutations in Avpr2. In addition, some G_s-coupled receptors expressed in collecting duct are intercalated-cell-specific (namely, the secretin receptor [Sctr] and β adrenergic receptors [Adrb1 and Adrb2]), which have been shown to regulate acid-base transport. In addition to the vasopressin V2 receptor, another vasopressin receptor is also expressed in the collecting duct (viz. the V1a receptor), and is found only in intercalated cells.

Aside from the renal collecting duct, the epithelial cells of the nephron, including the subsegments of the proximal tubule, the thin and thick limbs of Henle’s loop, macula densa and distal convoluted tubule all have been found to express combinations of GPCRs that are indicative of intricate regulation of transport and metabolism (Poll et al. Am J Physiol 2021; 321: F50-F68), much of which remains to be investigated.

SA40

Secretin: a key regulator of urine production and acid/base excretion

Peder Berg¹

¹Department of Biomedicine, Aarhus University, Aarhus, Denmark

In 1902 Bayliss and Starling discovered the first peptide hormone, secretin. Secretin is released in response to food intake and the postprandial effects of secretin in the gastrointestinal system are well explained and understood. Here, its effects are well-understood: it activates pancreatic and bile duct bicarbonate secretion and inhibits gastric acid secretion. Beyond the gastrointestinal system, the secretin receptor is also expressed in the kidney, where it has been implicated in water conservation, although the mechanism remained uncertain.

We have discovered that secretin via its receptor controls renal base excretion by activation of the base secretion in beta-intercalated cells of the kidney collecting duct. Notably, secretin-release is augmented during acute metabolic alkalosis. Consequently, loss of the secretin receptor impairs the kidneys' ability to increase renal base excretion and compensate an acutely imposed metabolic alkalosis.

Additionally, we have uncovered that secretin also strongly modulates the glomerular filtration rate by selective vasodilation of the vas efferens, thereby controls urine production. Both effects - decreased renal acid excretion and decreased urine production - can be viewed as beneficial in the postprandial state by normalizing the postprandial blood alkalinity and redistribute more volume to the gastrointestinal system for digestive secretions.

Physiological quantification of GI hormones and their mechanisms of release

Katrine D. Galsgaard^{1,2}, Ida M. Modvig¹, Jens J. Holst^{1,3}

¹Department of Biomedical Sciences, Faculty of Health and Medical Sciences, University of Copenhagen, Copenhagen, Denmark, ²BRIDGE-Translational Excellence Programme, Faculty of Health and Medical Sciences, University of Copenhagen, Copenhagen, Denmark, ³Novo Nordisk Foundation Center for Basic Metabolic Research, Faculty of Health and Medical Sciences, University of Copenhagen, Copenhagen, Denmark, Copenhagen, Denmark

The gastrointestinal tract is a central organ for regulation of appetite and metabolism being part of the gut-brain axis and due to its production of hormones regulating digestion, gastrointestinal motility and secretion, food intake and glucose homeostasis. The gut hormones affecting appetite and glucose metabolism are of particular interest due to their pharmacological potential. Thus, agents based on glucagon-like peptide 1 (GLP-1) and glucose-dependent insulintropic polypeptide (GIP) have proven effective in the treatment of type 2 diabetes mellitus and obesity. However, side effects of GLP-1 analog treatment (nausea, vomiting, and diarrhea) affect some patients. These side effects might be avoided by targeting endogenous hormone secretion reflecting normal physiology more closely. Identifying mechanisms that can be engaged to increase endogenous gut-derived hormone secretion is thus an important area of research.

Gut hormones are secreted from enteroendocrine cells scattered throughout the gastrointestinal tract. Knowledge about how the enteroendocrine cells sense and react to the different nutritional components is essential but is still limited and we have only recently begun to understand how macronutrients and their digestive products stimulate the secretion. The nutrient sensing mechanisms range from electrogenic transporters, ion channels and nutrient-activated G-protein coupled receptors activating a variety of intracellular signaling pathways which all represent relevant targets.

Using the perfused intestinal rat model, it is possible to obtain detailed knowledge of these mechanisms by evaluating nutrient handling and absorption, the effect of blocking or stimulating specific transporters and receptors, and the resulting hormone secretion in different sections of the intestine. Using this highly physiological relevant model, we now have strong indications for a role for both Sodium-Glucose Transporter 1 (SGLT1) and the K⁺_{ATP} channel activity in carbohydrate-induced GLP-1 secretion. Lipid-induced GLP-1 secretion has been linked to the G-protein-coupled receptors; GPR40 and GPR119, and protein-induced GLP-1 secretion is believed to depend on Peptide Transporter 1 (Pept1) mediated absorption and activation of the Calcium-Sensing Receptor (CaSR). Expression analysis and stimulation experiments indicated that numerous additional mechanisms may be at play, so more work is clearly needed.

SA42

The effects of glucagon on the kidney distal convoluted tubule and blood pressure

Robert Fenton¹

¹*Department of Biomedicine, Aarhus University, Denmark, Aarhus, Denmark*

Introduction. The NaCl cotransporter (NCC) is expressed in the kidney distal convoluted tubule (DCT) and is a widely used pharmacological target for hypertension treatment. NCC is also important for plasma potassium (K⁺) homeostasis, as changes in NCC activity can influence the degree of electrogenic K⁺ secretion in the latter portions of the renal tubule. Changes in NCC phosphorylation track with NCC activity, with greater NCC phosphorylation correlating with higher NCC activity. Phosphorylation of NCC is increased in response to various stimuli, including changes in the extracellular K⁺ concentration, or after alterations in intracellular cAMP following vasopressin or adrenergic hormone stimulation of GPCRs. Database searching indicated that the GαS coupled glucagon receptor (GluR), which also signals via cAMP, was abundantly expressed in the DCT. We hypothesized that glucagon was a potent modulator of NCC activity, Na⁺ and K⁺ balance and ultimately blood pressure.

Methods. *Ex vivo* effects of glucagon on NCC phosphorylation status were assessed in mouse and human tissue. Involvement of selective signaling pathways downstream of the GluR were determined using pharmacological tools. *In vivo* effects of short-term or long-term glucagon administration on blood pressure, and Na⁺ and K⁺ balance was examined in mice.

Results. In mice, 30-min glucagon exposure increased NCC phosphorylation. In *ex vivo* kidney tubule suspensions glucagon increased NCC phosphorylation in a time and dose-dependent manner, an effect prevented by a GluR inhibitor. Glucagon increased NCC phosphorylation in human kidney slices. Selective pharmacological inhibition of adenylyl cyclase, protein kinase A, with no lysine kinases (WNK) and inward-rectifier potassium channels 4.1/5.1 or intracellular Ca²⁺ chelation antagonized the effects of glucagon on NCC phosphorylation. Glucagon effects were absent in tubules isolated from protein phosphatase 1 inhibitor-1 KO mice. In mice administered glucagon by osmotic mini-pump for 14 days, plasma glucagon was significantly higher and NCC phosphorylation 2-fold greater than the vehicle group. Plasma Na⁺ and K⁺ levels were not significantly different between groups. Despite the increase in NCC phosphorylation, preliminary studies suggest that glucagon prevents the ability of a high NaCl intake to increase blood pressure.

Conclusion. Glucagon is a potent stimulator of NCC phosphorylation and activity. The actions of glucagon in modulating electrolyte balance and blood pressure may be underappreciated and play an important role in human physiology/pathophysiology.

SA43

Aldo/MR therapeutic targeting, epigenetics and transcriptional regulation

Achim Lothar¹

¹*University of Freiburg, Freiburg, Germany*

The mineralocorticoid receptor (MR) is a ligand-activated transcription factor from the nuclear receptor family. The physiological function of MR is the control of water and electrolyte balance, primarily via the regulation of sodium channels such as ENaC in epithelial cells of the kidney and colon. In addition, MR has strong inflammatory and pro-fibrotic properties and thus unfavorable impact on heart and kidney function. MR antagonists are widely established in the treatment of chronic heart failure and renal insufficiency. However, currently available compounds are associated with an increased risk of adverse effects such as hyperkalemia, which considerably limits their clinical applicability [1]. During the past two decades, mouse models with cell type-specific deletion of MR demonstrated that the pathological effect of MR is primarily mediated via cardiomyocytes, endothelial cells, and immune cells [2]. Selective blockade of the MR signaling pathway in these cell types could therefore separate the pathological inflammatory effects from the physiological function of MR.

Endothelial cells are considered a central hub of cell-cell communication in the heart. They form capillaries that are crucial to maintain the high oxygen and energy demand of cardiomyocytes. As endothelial cells represent the inner layer of the vasculature, they have an important barrier function, control the migration of immune cells from the bloodstream, and regulate tissue homeostasis [3]. Gene expression is controlled by transcription factors binding to enhancers and promoters. We created a comprehensive atlas of chromatin accessibility, histone modifications, and 3D chromatin organization and determined enhancer-promoter interactions in cardiac endothelial cells and confirmed the functional relevance of enhancer-promoter interactions by CRISPRi-mediated enhancer silencing. A systematic comparison of mouse models representing different cardiovascular risk factors identified MR as common regulator of pathological gene expression in cardiac endothelial cells and predicted direct MR target genes [4]. We conclude that epigenetic modulation may be a promising strategy towards selective targeting of MR-dependent pathological gene expression.

[1] Clarisse D, Deng L, de Bosscher K, Lothar A. Approaches towards tissue-selective pharmacology of the mineralocorticoid receptor. *Br J Pharmacol*. 2022 Jul;179(13):3235-3249 [2] Bauersachs J, Lothar A. Mineralocorticoid receptor activation and antagonism in cardiovascular disease: cellular and molecular mechanisms. *Kidney Int Suppl* (2011). 2022 Apr;12(1):19-26. [3] Lothar A, Kohl P. The heterocellular heart: identities, interactions, and implications for cardiology. *Basic Res Cardiol*. 2023 Jul 26;118(1):30. [4] Deng L, Pollmeier L, Bednarz R, Cao C, Laurette P, Wirth L, Mamazhakypov A, Bode C, Hein L, Gilsbach R, Lothar A. Atlas of cardiac endothelial cell enhancer elements linking the mineralocorticoid receptor to pathological gene expression. *Sci Adv*. 2024 Mar 8;10(10):eadj5101.

SA44

Expression of functional mineralocorticoid receptor (MR) and G-protein coupled estrogen receptor (GPER) in human T lymphocytes

Maria Piazza¹, Riccardo Scarpa², Brasilina Caroccia³, Samuela Carraro¹, Teresa Maria Seccia¹, Gian Paolo Rossi¹

¹University of Padova, Padova, Italy, ²Internal Medicine I, Ca' Foncello Hospital, Treviso, Italy,

³University of Padova, Padova, Italy

Introduction

Aldosterone plays a key role in controlling blood pressure values by maintaining salt, water, and body fluid homeostasis. It exerts genomic effects that are mediated by activation of the mineralocorticoid receptor (MR) and 'rapid' or 'non genomic' effects that involve additional receptors as the G-protein coupled estrogen receptor (GPER). Excessive production of aldosterone generates an inflammatory state that is associated with cardiovascular and metabolic diseases that can be promoted by the involvement of innate and adaptive immunity. However, it is unknown if cells of the innate and adaptive immunity are endowed with aldosterone receptor(s) and are implicated in the inflammatory action of aldosterone.

Aims

Therefore, we sought for aldosterone receptors on human T lymphocytes and investigate whether aldosterone affects T cells activation.

Method

The expression of MR and GPER on human T cells was tested by measuring mRNA copy number by droplet digital PCR and immunoblotting from 7 healthy donors (HD). Peripheral blood mononuclear cells (PBMCs) from HD were exposed to different concentrations of aldosterone (from 10^{-10} M to 10^{-8} M) with or without MR antagonist (canrenone) and GPER antagonist (G36) under chronic and acute stimulation. We evaluated the effect of aldosterone CD8⁺ T cells by measuring IFN γ release with flow cytometry. We also sought for the expression of the cortisol inactivating enzyme 11 β -Hydroxysteroid Dehydrogenase Type 2 (11 β HSD2) in CD4⁺ and CD8⁺ lymphocytes.

Results

We detected the MR and GPER both at mRNA and protein level in CD8⁺ and CD4⁺ T cells. MR mRNA copy number (CD4⁺= 3061 \pm 4037 copies/50 ng of mRNA and CD8⁺= 3379 \pm 3112 copies/50 ng of mRNA) was at least 40-fold high that of the GPER (CD4⁺= 65 \pm 71.7 copies/50 ng of mRNA and CD8⁺=86.4 \pm 68.9 copies/50 ng of mRNA). At the protein level, the rank expression was GPER>MR in both CD4⁺ and CD8⁺ lymphocytes. Aldosterone significantly increased IFN γ release in CD8⁺ T-cell both under chronic and acute stimulation. Chronic exposure to aldosterone increased IFN γ production in a dose-dependent manner in CD8⁺ T cells by acting via the MR, as it was prevented by canrenone ($p < 0.0001$), while the rapid aldosterone action was slight reduced by G36 and

mimicked by G1. However, we found only a bare expression of mRNA for 11bHSD2 in CD4⁺ (4.2±8.3 copies/50ng mRNA) and CD8⁺ (3.6±6.3 copies/50ng mRNA) lymphocytes of HD subjects. Therefore, as the physiological concentration of cortisol in plasma is 10²-10³ fold higher than aldosterone, it could be that some effect elicited in vitro by aldosterone are in fact driven by cortisol.

Conclusions

In conclusion we found compelling evidence for the presence of MR and GPER receptors in human T lymphocytes and suggested that aldosterone and cortisol affect IFN γ release in human CD8⁺ lymphocytes.

SA45

Cardiometabolic consequences of adrenal gland dysfunction

Linghui Kong¹, Coralie Frimat³, Nicolo Faedda², Bakhta Fedlaoui², Isabelle Giscos-Douriez², Fabio L Fernandes-Rosa², Maria-Christina Zennaro^{2,4}, Bruno Fève^{5,6,7}, Antoine Ouvrard-Pascaud³, Sheerazed Boulkroun²

¹Université Paris Cité, Inserm, PARCC, Paris, France, ²Université Paris Cité, Inserm, PARCC, Paris, France, ³Inserm U1096, UFR santé, Rouen, France, ⁴Service de Génétique, Assistance Publique Hôpitaux de Paris (AP-HP), Hôpital Européen Georges Pompidou, Paris, France, ⁵Sorbonne Université-Inserm, Centre de Recherche Saint-Antoine UMR_S938, Paris, France, ⁶Institut hospitalo-universitaire de cardio-métabolisme et nutrition (ICAN), Paris, France, ⁷Service d'endocrinologie-diabétologie, centre de référence des maladies rares de l'insulino-sécrétion et de l'insulino-sensibilité (PRISIS), Hôpital Saint-Antoine, Assistance publique-Hôpitaux de Paris, Paris, France

Overweight and obesity are major public health issues. Central obesity is associated with the risk of developing a metabolic syndrome. However, less than 20% of overweight people achieve sustainable weight loss, leading to repeated cycles of weight loss and regain, which are particularly associated with an increased risk of developing metabolic syndrome. Moreover, in postmenopausal women, estrogen deficiency promotes metabolic and endothelial dysfunction, further predisposing them to metabolic syndrome and its cardiovascular complications. Furthermore, leptin, an adipokine whose levels are higher in obese patients, especially in women, directly stimulates aldosterone production, suggesting that the adrenal glands could be a comorbidity factor in metabolic diseases. During estrogen deficiency, such as in menopause, there is an increase in Luteinizing Hormone (LH), due to the loss of negative feedback by sex steroid. In experimental studies, menopause increases aldosterone levels, an effect alleviated by estrogen treatment, while other studies have shown a decrease in aldosterone levels in postmenopausal women.

All these observations support a strong physiological and/or pathological link between the sex steroids' status (pre- or post-menopausal) and aldosterone synthesis and secretion. In turn, excess aldosterone could lead to cardiovascular and metabolic alterations

Our objective is to assess the role of the adrenal gland in postmenopausal cardiometabolic complications associated with cyclic weight variations.

For this purpose, female mice, both ovariectomized and non-ovariectomized, were subjected to three cycles of a high-fat diet/standard diet (yo-yo diet) or to a standard diet for 33 weeks. Functional and molecular explorations were performed at the end of each phase.

The yo-yo diet induced greater weight gain in ovariectomized mice compared to non-ovariectomized mice. Post-ovariectomy, the mice exhibited higher fasting blood glucose levels and circulating leptin levels, an effect that was more pronounced when the mice were subjected to the yo-yo diet. Ovariectomized mice on the yo-yo diet developed heart failure with preserved ejection fraction, which was prevented by the use of a mineralocorticoid receptor antagonist. Interestingly,

ovariectomized mice on the yo-yo diet showed an increase in adrenal gland weight, accompanied by significant morphological and functional remodeling of the adrenal cortex.

The absence of estrogens leads to cardiometabolic disorders that are worsened by a yo-yo diet but also to adrenal dysfunction, which could in turn contribute to the worsening of cardiometabolic functions.

SA46

Mineralocorticoid Receptors in Metabolic Syndrome

Massimiliano Caprio¹, Andrea Armani², Alessandra Feraco¹, Caterina Mammi³, Stefania Gorini¹

¹*San Raffaele Roma University, Rome, Italy*, ²*San Raffaele Roma University, Rome, Italy*, ³*IRCCS San Raffaele Roma,, Rome, Italy*

The pathophysiology of cardio-metabolic diseases involves a delicate interplay between biological and environmental factors regulating energy homeostasis, water and electrolyte balance, as well as inflammation and oxidative stress in critical organs for cardio-metabolic health.

In this context, several studies clearly demonstrated a specific role of extra-renal mineralocorticoid receptors (MR) in controlling endothelial function, vascular tone, adipose tissue differentiation and inflammation, and heart physiology. In preclinical models, abnormal activation of MR in the vascular endothelial cells and in adipocyte favors the occurrence of several components of the metabolic syndrome, such as hypertension, obesity, and glucose intolerance. Moreover, it is well known that high circulating levels of aldosterone are associated with obesity and metabolic syndrome in humans, suggesting that altered activation of the MR in extra-renal tissues leads to important metabolic alterations. In this context, MR antagonists represent a promising approach to tackle cardiovascular and metabolic disorders occurring in the metabolic syndrome, even if there is still an important gap of knowledge about the metabolic effects of MR antagonists in clinical settings. This talk will discuss the complex interplay between the mineralocorticoid system, adipose tissue and endothelial cells and its role in the pathophysiology of cardio-metabolic diseases.

SA47

Hypoxia-inducible factors and brain metabolism: adaptation and pathology

Andrew Murray

undefined

Tissue hypoxia arises when there is a mismatch between oxygen delivery and tissue metabolic demand. As such, hypoxia can result from exposure to environmental hypoxia e.g. hypobaric hypoxia at high altitude, or under pathological circumstances when convective oxygen supply to the tissues is perturbed. In highly oxidative tissues, such as the brain, this can challenge energetic and redox homeostasis, but is associated with metabolic responses that might mitigate this challenge. The hypoxia-inducible factor (HIF) pathway acts as a major regulator of the tissue response to hypoxia, controlling the expression of thousands of genes, including many genes involved in metabolic function. The characteristic metabolic response of tissues includes the suppression of mitochondrial respiratory function and increased glycolytic flux. Components of the HIF pathway including *EPAS1* (encoding HIF2 α) have undergone natural selection in populations native to high-altitude regions including the Tibetan Plateau and the Andean Altiplano. The brain metabolic response to hypoxia, and the role of the HIF-pathway, can therefore be understood, in part, through studies of lowlanders and adapted highlander populations undergoing acute exposure to hypoxia. Conversely, emerging evidence suggests that metabolic disease might influence brain oxygenation and metabolic function. Hypersecretion of the pancreatic hormone, amylin, is a feature of type 2 diabetes. Amylin aggregation has been associated with cerebrovascular dysfunction and brain accumulation of HIF1 α and HIF2 α in patients with Alzheimer's Disease, with possible consequences for mitochondrial respiratory function and tissue energetics. This talk will consider the inter-relation of hypoxia, oxygen-sensing pathways and energy metabolism in the brain from these differing perspectives.

SA48

A study of hypoxia and innate immune mechanisms in experimental autoimmune optic neuritis

Zhiyuan Yang¹, Cristina Marcoci², Eleni Giama¹, Ayse Gertrude Yenicecik¹, Christopher Linington³, Roshni Desai¹, Kenneth Smith²

¹Department of Neuroinflammation, UCL Queen Square Institute of Neurology, London, United Kingdom, ²Department of Neuroinflammation, UCL Queen Square Institute of Neurology, London, United Kingdom, ³Institute of Infection, Immunity, and Inflammation, College of Medical, Veterinary, and Life Sciences, Glasgow Biomedical Research Centre, Glasgow, United Kingdom

Introduction: Optic neuritis is an inflammatory demyelinating (i.e. loss of insulation around nerve fibres) disease of the optic nerve, and it is a common presenting symptom in patients with multiple sclerosis (MS). The visual deficits caused by acute optic neuritis, which can include blindness, often appear to resolve over time, but permanent residual deficits typically remain due to unresolved demyelination and to axonal degeneration. The acute deficits are typically attributed to the demyelination, but more recent evidence raises the possibility that the deficits could be due to inflammatory hypoxia. Thus the optic nerve may have insufficient oxygen to support the mitochondrial function essential for impulse activity and to prevent axonal degeneration. We have therefore examined whether the inflamed optic nerve is hypoxic, using an animal model of MS, experimental autoimmune encephalomyelitis (EAE).

Method: EAE was induced in female Dark Agouti rats by immunization with recombinant myelin oligodendrocyte glycoprotein and adjuvant. Control animals were “immunized” with adjuvant only. Tissue hypoxia was assessed using an immunohistochemical probe, pimonidazole, injected intravenously, and by labelling for endogenous hypoxia-inducible factor-1a (HIF1a). Oxidative and nitrative stress was assessed by labelling for inducible nitric oxide synthase (iNOS) and 3-nitrotyrosine (3NT), as well as by the fluorescence products of dihydroethidium (DHE) previously injected intravenously. Vascular density and diameter were also examined histologically.

Results: Out of 57 nerves collected from animals with EAE, 48 exhibited optic neuritis and were identified as EAE with optic neuritis (EAE-ON), while only 9 showed no sign of inflammation and were designated EAE-NON. The inflamed optic nerves (EAE-ON) were found to be hypoxic, with significantly higher labelling for HIF1a ($p=0.002$) and pimonidazole ($p=0.001$) compared with nerves from control animals (IFA, $n=29$ nerves). Hypoxia is known to trigger oxidative and nitrative stress, revealed in our study by significantly higher labelling for iNOS ($p<0.001$) and 3NT ($p=0.003$), and fluorescence due to DHE ($p=0.055$) in the EAE-ON nerves compared with nerves from IFA animals. EAE-ON nerves also showed significant dilation of capillaries compared with IFA ($p<0.001$).

Conclusion: We conclude that the inflamed optic nerve is hypoxic, associated with oxidative and nitrative stress and damage, as well as alterations in the vasculature. This finding has implications for the treatment of optic neuritis, and provides insights on the early detection and treatment of MS.

SA49

Exploring the effect of hypoxia (1% O₂) on the neuroinflammatory activity of mouse primary microglial cells and microglial cell line (BV-2 cells) under Lipopolysaccharide (LPS) induced inflammatory stimulation.

John Bennett¹, Ruoli Chen²

¹Keele Univeristy, Stoke on Trent, United Kingdom, ²University of Keele, Stoke on Trent, United Kingdom

Cerebral hypoxia is a feature for several neurological diseases. The low concentration of oxygen and existing inflammation in the brain in these diseases forms a vicious circle that damages brain cells and inhibits the brain regeneration. Neuroinflammation is thought to potentially play both a positive and negative role in hypoxic injury since, depending on severity and duration of the pro-inflammatory stimuli, with prolonged stimulation being associated with activation of cell death pathways and the promotion of damaging oedema and systemic immune invasion. As such, better understanding the ways in which hypoxic stimulation alters the inflammatory activity of microglial cells (the specialised form of immune cells unique to the CNS) is vital to understanding and exploiting endogenous neuroinflammation during hypoxic injury.

To investigate the role of hypoxia in neuroinflammation we established a model of microglial inflammatory stimulation, using a dosage curve of Lipopolysaccharide (LPS) from 1ng/mL to 10,000ng/mL, which were applied to both mouse primary microglial cells and a microglial cell line - BV-2 cells in either normoxia (21% O₂) and hypoxia (1% O₂) oxygen exposures, for 24h. Responses were measured in terms of cell viability, cellular death, TNF- α production, and inflammatory gene expression, as well as phagocytosis through immunofluorescence imaging. Further exploration of the role of established cellular hypoxic response pathways, specifically the role of the Hypoxia Inducible Factors (HIF) 1 and 2, was then conducted by observing how the established cellular responses altered by co-exposure of the cells to 100uM of a clinically approved 100uM PHD2 inhibitor, namely FG4592 (Roxadustat).

We found that BV-2 cells generally showed decreased inflammatory signalling, i.e. TNF- α production in response to hypoxia regardless of LPS dosage, but also that hypoxia did not induce inflammatory signalling in the absence of the LPS (Figure 1). No consistent effect for FG4592 on TNF- α production was identified during hypoxia, however, it did both non-significantly reduce TNF- α expression for all LPS dosages in normoxia and ameliorate hypoxia induced cell death (Figure 2). Mouse Primary microglia displayed a more varied response. Hypoxia generated an apparent increase in cell death provided LPS stimulation was present (Figure 3), unlike in BV-2 cells where hypoxic death was not dependent on LPS stimulation, and it only appeared to promote existing inflammatory signalling at low levels of LPS stimulation (10ng/mL + 1ng/mL), which may suggest hypoxia limits the inflammatory activity of already stimulated/activated microglia but acts as an inflammatory promotor itself when such activation would otherwise be limited (Figure 4). Our phagocytosis assay results were inconclusive.

Our findings suggest that hypoxia limits inflammatory activity by BV-2 cells but may promote it in primary microglia when total inflammatory stimulation is limited. Additionally, inflammatory

stimulation seemingly makes primary microglia, though not BV-2s, more susceptible to hypoxic cell death. FG4592 was effective in ameliorating hypoxic cell death and metabolism loss, seemingly through inflammation independent mechanisms in BV-2 cells (Figure 5.)

Figure 3: Bar chart displaying MTT activity for BV-2 cells under hypoxic and LPS stimulation. Results are displayed as % of normoxic controls \pm SD. Significances are displayed above bars for differing FG4592 dosage of same oxygenation (21% Oxygen = *, 1% Oxygen = #) (* = $p < .05$, ** = $p < .005$, *** = $p \leq .001$)

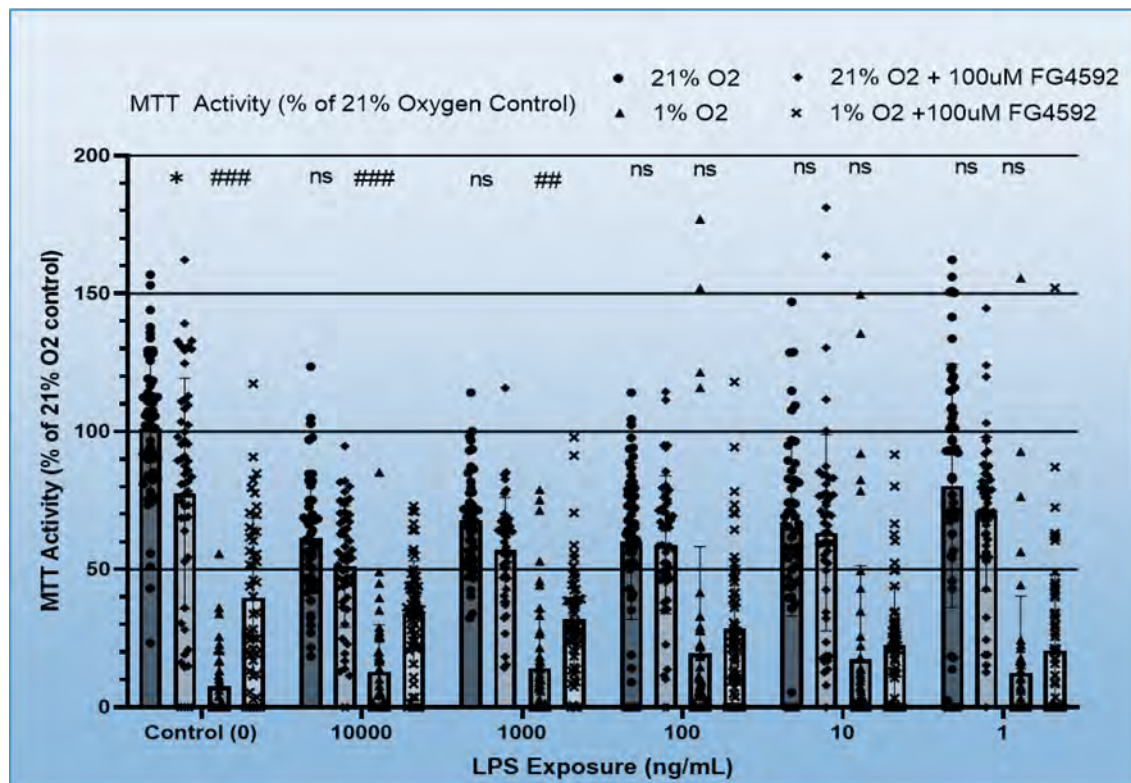


Figure 4: Bar chart displaying TNF- α expression for Mouse Primary Microglia under hypoxic and LPS stimulation. Results are displayed as pg/mL of TNF- α \pm SD.

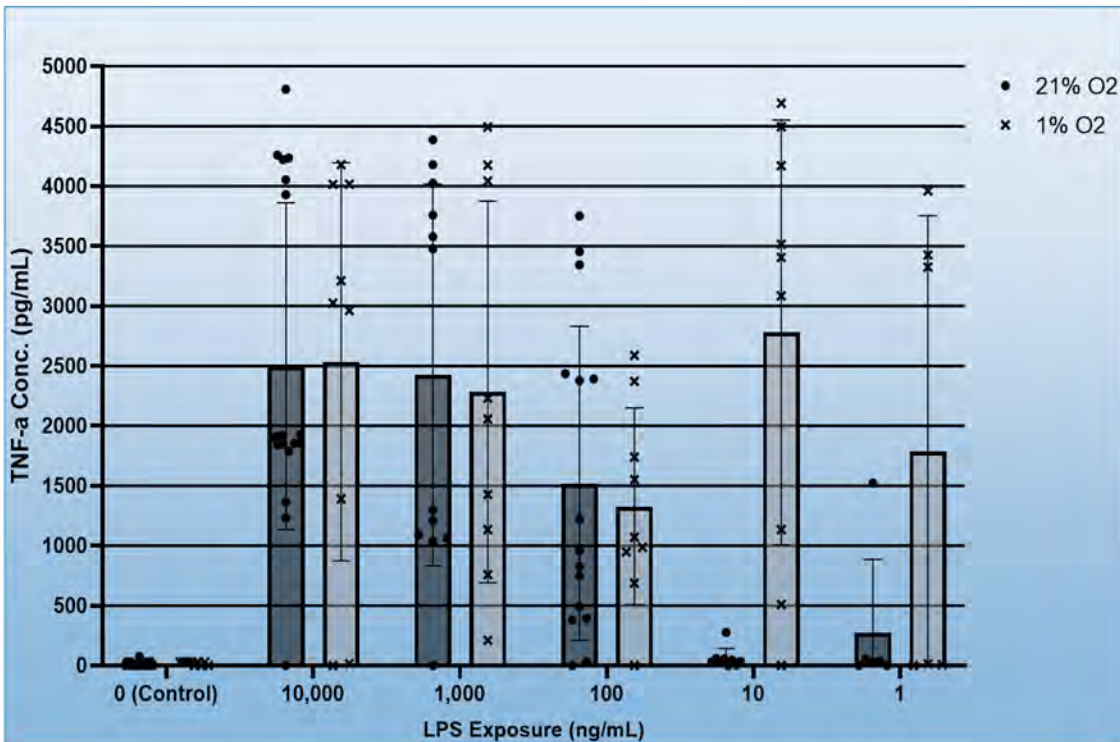


Figure 1: Bar chart displaying TNF- α expression for BV-2 cells under hypoxic and LPS stimulation. Results are displayed as pg/mL of TNF- α \pm SD. Significance is displayed above bars for differing FG4592 dosage of Same oxygenation and LPS dosage (21% Oxygen = * , 1% Oxygen = #) (* = $p < .05$, ** = $p < .005$, *** = $p \leq .001$)

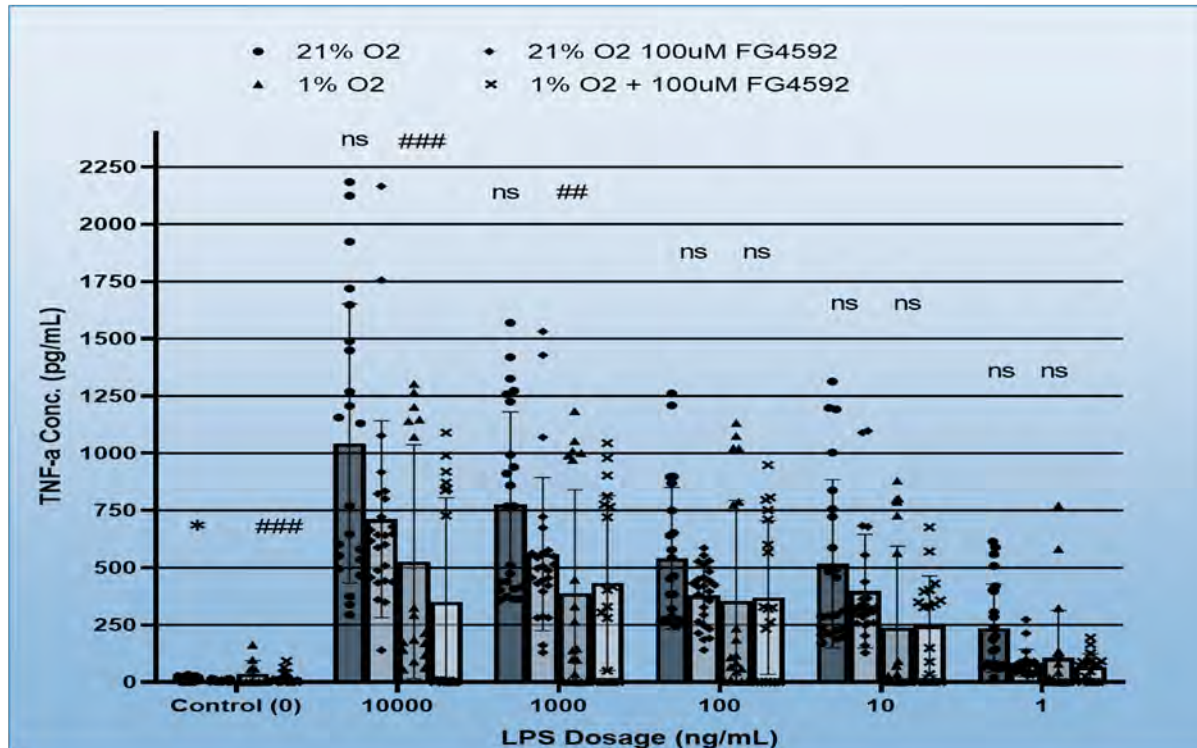


Figure 5: Bar chart displaying LDH concentrations for Mouse primary microglia under hypoxic and LPS stimulation. Results are displayed as % of normoxic maximum release \pm SD

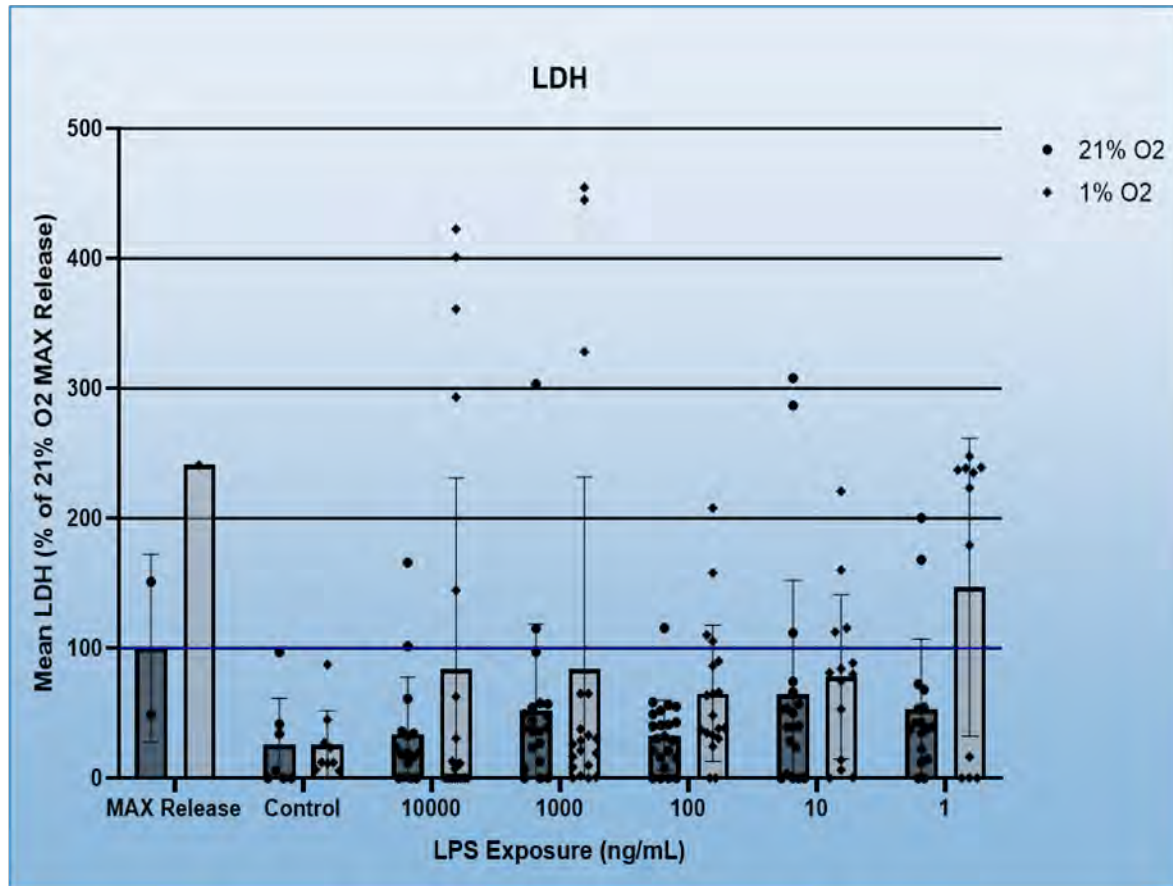
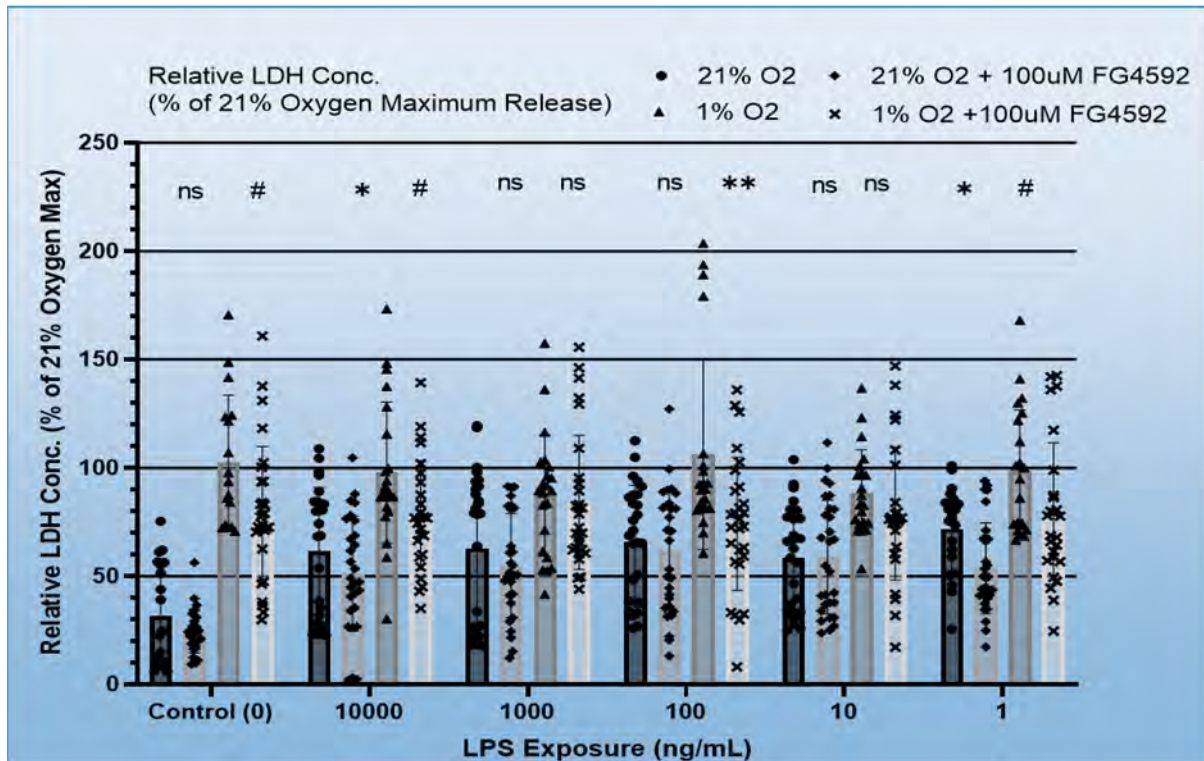


Figure 2: Bar chart displaying LDH concentrations for BV-2 cells under hypoxic and LPS stimulation. Results are displayed as % of normoxic maximum release \pm SD. Significances are displayed above bars for differing FG4592 dosage of same oxygenation (21% Oxygen = *, 1% Oxygen = #) (* = $p < .05$, ** = $p < .005$, *** = $p \leq .001$)



SA50

Hypoxia signalling in vascular dementia.

Tracy Farr¹

¹*University of Nottingham, Nottingham, United Kingdom*

Introduction: Vascular cognitive impairment (VCI) refers to cognitive decline attributed to vascular risk factors. Vascular dysfunction produces cerebral hypoperfusion and the brain uses the hypoxia inducible factor (HIF) pathway to compensate and restore oxygen availability. White matter is vulnerable to hypoxia, and an emerging area of interest aims to understand whether epigenetic processes contribute to this. A handful of reports showed that manipulating small, non-coding microRNAs (miRNAs) may provide new therapeutic strategies in animal models of VCI. The aim of this study was to use a hypothesis free approach to profile miRNA changes in the white matter of a mouse model.

Methods: Twenty male C57BL6 mice were randomised to undergo bilateral carotid artery stenosis (BCAS) or sham surgery. This involved wrapping microcoils with 180 or 500µm diameters, respectively, around both carotid arteries. Subsequently, RNA was harvested from the white matter, hippocampus, and cortex at either 7 or 30d post-surgery and electrophysiology was performed on the optic nerves. RNA was sequenced and bioinformatics analysis was performed (Genewiz, UK). A false discovery rate of <0.05 was applied to the bioinformatics analysis to confirm differentially expressed miRNAs (DEMs). Electrophysiology data, compound action potentials (CAPs) are presented as mean ± standard error and unpaired t-tests or mixed two-way repeated measures ANOVAs were used.

Results: At 7 and 30d post surgery, all the sham optic nerves consistently displayed a third peak in the recorded CAP, but most of the BCAS nerves did not. There was also differential expression of several miRNAs following BCAS in the hippocampus and white matter at both timepoints. The greatest number of DEMs (76) were observed in the hippocampus, and 45 survived multiple comparisons. There were 10 and 29 DEMs in the white matter at 7 and 30d, respectively, and mmu-let-7K, miR-30d-5p, and mmu8-miR-362-5p all survived multiple comparisons. Pathway analysis suggests the genes regulated by these DEMs are associated with cell signalling and axon guidance.

Conclusions: The variability in the optic nerve function after BCAS suggests that hypoperfusion may impact white matter most via disruption to the smallest diameters axons. Our data driven approach identified several miRNAs that are differentially regulated in the white matter following hypoxia. While further investigation is required to characterise the roles of these miRNAs, these results suggest epigenetic processes are involved, and we hope this could eventually lead to new therapeutic targets in the future.

SA51

The Role of ATP-Sensitive Potassium Channels in Migraine Pathogenesis

Messoud Ashina¹

¹Professor of Neurology, Lundbeck Foundation Professor, Director of the Human Migraine Research Unit, Chief Consultant, Department of Neurology & Danish Headache Center, Rigshospitalet, Valdemar Hansens Vej 5, DK-2600 Glostrup; Department of Clinical Medicine, Faculty of Health and Medical Sciences, University of Copenhagen., Copenhagen, Denmark

Migraine, a prevalent and debilitating neurological disorder, remains a puzzle with elusive pathophysiological mechanisms. Recent investigations have shed light on the involvement of intracellular cyclic adenosine monophosphate (cAMP) in migraine pathogenesis, implicating cAMP-dependent signaling pathways in migraine attacks. These studies revealed that oral administration of cilostazol, a cAMP degradation blocker, induced migraine attacks in individuals with migraine, suggesting a pivotal role of cAMP accumulation in migraine onset.

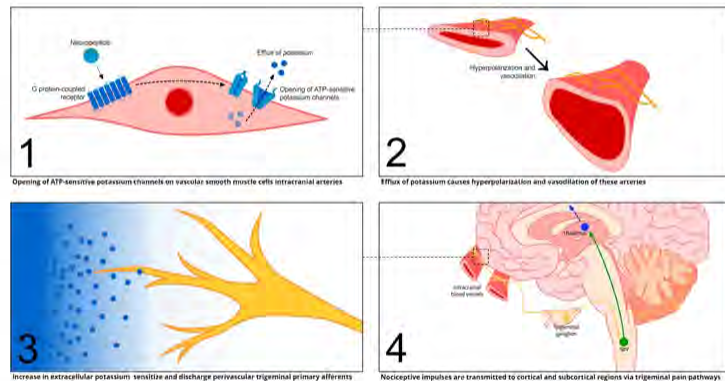
Further exploration led to the hypothesis that downstream effects of cAMP-mediated migraine attacks involve the opening of potassium channels. Provocation studies conducted in our laboratory demonstrated that openers of adenosine-triphosphate (ATP)-sensitive potassium channels and large conductance calcium-activated potassium channels triggered migraine attacks in individuals with migraine.

This lecture presents an overview of our research, emphasizing the pivotal role of ATP-sensitive potassium channels in migraine pathogenesis. Understanding the involvement of these channels offers promising avenues for targeted therapeutic interventions and deeper insights into the complex mechanisms underlying migraine.

A Proposed Trigemino-vascular Ion Channel Hypothesis of Migraine Pathogenesis

A plausible explanation of migraine pathogenesis suggests the following sequence of events within the framework of the trigemino-vascular system: 1) various signaling molecules (e.g. nitric oxide, calcitonin gene-related peptide, pituitary adenylate cyclase activating peptide) initiate a cascade of intracellular processes that result in opening of ATP-sensitive potassium channels on vascular smooth muscle cells within the intracranial arteries 2) efflux of potassium causes hyperpolarization and vasodilation of these arteries 3) increase in extracellular potassium provides the requisite electrochemical gradient to sensitize and discharge perivascular trigeminal primary afferents in the walls of intracranial arteries, 4) nociceptive impulses are transmitted to and processed by cortical and subcortical regions via ascending trigeminal pain pathways, ultimately resulting in the perception of migraine pain. Of note, this line of reasoning emphasizes that elevations in extracellular levels of positively charged ions, not potassium exclusively, may be the principal drivers needed to activate and sensitize trigeminal primary afferents in the walls of intracranial arteries.

• Supplement to: Ashina M. Migraine. *N Engl J Med* 2020;383:1866-76. DOI: 10.1056/NEJMra1915327



<https://bit.ly/49GUVo1>

Key references: 1: Ashina M. Migraine. *N Engl J Med*. 2020 Nov 5;383(19):1866-1876. <https://doi.org/10.1056/nejmra1915327> 2: Ashina M, Hansen JM, Do TP, Melo-Carrillo A, Burstein R, Moskowitz MA. Migraine and the trigemino-vascular system-40 years and counting. *Lancet Neurol*. 2019 Aug;18(8):795-804. [https://doi.org/10.1016/s1474-4422\(19\)30185-1](https://doi.org/10.1016/s1474-4422(19)30185-1)

SA52

New insights to KATP cardiovascular and skeletal muscle channelopathies

Conor McClenaghan¹

¹*Center for Advanced Biotechnology and Medicine, and Departments of Pharmacology and Medicine, Robert Wood Johnson Medical School, Rutgers University, Piscataway, NJ, United States*

ATP-sensitive potassium (KATP) channels are expressed throughout the body and serve to couple cellular metabolism to membrane excitability. The channels are composed of pore-forming Kir6 subunits co-assembled with obligate regulatory SUR subunits and are critically regulated by the intracellular nucleotides ATP and ADP - activating in response to metabolic compromise. Mutations of the *KCNJ11* and *ABCC8* genes, which encode the predominant Kir6.2 and SUR1 subunits expressed in pancreatic beta-cells, have long been associated with insulin secretion disorders. The effects of mutations of the paralogous *KCNJ8* and *ABCC9* genes (encoding Kir6.1 and SUR2), remained less clear, until discoveries over the last decade which have now associated congenital gain-of-function with the rare heritable disorder Cantu Syndrome, and loss-of-function with *ABCC9*-related intellectual disability and myopathy syndrome (AIMS). Here we report a summary of recent works dissecting the mechanisms of cardiovascular remodeling in Cantu Syndrome using knock-in mouse models of the disease, which reveal that KATP overactivity in vascular smooth muscle (VSM) drives low systemic vascular resistance, and secondary cardiac remodeling to high-output heart failure (HOHF). Inspired by these findings, we will report preliminary data testing the generality of this pathophysiological cascade, derived from the conditional deletion of other ion channels in mice, which tests whether VSM hypo-excitability inevitably drives HOHF. In addition, we will summarize recent advances in understanding of the human consequences of LoF mutations in *ABCC9* in AIMS, alongside dissection of skeletal muscle and cardiac pathology, and preliminary data on novel gene-therapy approaches to counter myopathy.

SA53

Impaired electro-metabolic signaling in capillary pericytes disrupts hemodynamic control in aging and Alzheimer's disease

Ashwini Hariharan¹, Thomas Longden¹

¹*University of Maryland, Baltimore, Baltimore, United States*

Disruptions to the mechanisms governing the metabolic supply-and-demand relationship that are integral to brain energy homeostasis can have deleterious consequences on brain health, making it vulnerable to the development of age-related disorders like Alzheimer's disease (AD). Energy supply is dynamically and precisely controlled by mechanisms inherent to the cerebral vasculature, and here, capillary thin-strand pericytes are quickly emerging as key players. A K_{ATP} channel signalling complex imbues pericytes with the ability to detect subtle changes in local glucose and rapidly couples decreases in this key substrate to robust increases in blood flow. Blocking glucose import into the brain with a glucose transporter-1 blocker (1 μ M BAY-876) activates pericyte K_{ATP} channels to increase brain blood flow in young (2-4 months) mice. Remarkably, this effect is completely lost in older (12-15 months) mice, and even earlier (6-8 months) in mice with familial AD mutations. Our emerging data suggest that a key interaction between membrane cholesterol and K_{ATP} channels underlies this dysfunction, and disrupting cholesterol in older mice reinstates the ability of pericyte K_{ATP} channels to sense decreases in local glucose. Perturbations in pericyte membrane cholesterol due to aging or AD may disrupt the delicate macromolecular organization of K_{ATP} channels, causing a breakdown of energy sensing mechanisms and progressive loss of hemodynamic control by pericytes.

C01

Hepatocyte-specific deletion of HIF2 α is associated with basal dysfunction, but protection against Western diet induced sympathetic dominance in the mouse heart

Lorenz Holzner¹, Youguo Niu¹, Paula Darwin¹, Dino Giussani¹, Andrew Murray¹

¹*Department of Physiology, Development and Neuroscience, University of Cambridge, Cambridge, United Kingdom*

Introduction: Non-alcoholic fatty liver disease (NAFLD) is an independent risk factor for heart disease (1). Hepatic HIF2 α deletion, is protective against NAFLD in some rodent models (2), but the effects on basal or stimulated cardiac function are unknown.

Objective: To determine cardiac function *ex vivo* in Western diet-induced NAFLD and the impact of hepatocyte-specific HIF2 α deletion in mice.

Methods: HIF2 α was deleted in hepatocytes using Cre-recombinase under control of the albumin promoter in male HIF2 $\alpha^{fl/fl}$ mice. These mice (hHIF2 $\alpha^{-/-}$), and related male, Cre-negative (WT) mice were fed a high fat, fructose and cholesterol Western diet (WD, Research Diets D09100310), or chow for 28 weeks (n = 4-5 per group). Cardiac basal systolic and diastolic function, and responsiveness to the acetylcholine receptor agonist carbachol (range: 10⁻⁸-10⁻⁶ M) and the β -adrenergic receptor agonist isoprenaline (range: 10⁻⁹-10⁻⁷ M) were assessed in isolated, Langendorff-perfused hearts. Sympathetic dominance was calculated as the ratio of left ventricular (LV) developed pressure (LVDP) responses to maximum doses of isoprenaline and carbachol. Data were analysed by two-way ANOVA with Tukey's *post hoc* test for significant genotype:diet interactions, and presented as mean \pm standard deviation.

Animal procedures were approved by the University of Cambridge Animal Welfare and Ethical Research Board and conducted according to UK Home Office regulations under the Animals in Scientific Procedures Act (1986).

Results: Three indices of basal cardiac dysfunction occurred in hHIF2 $\alpha^{-/-}$ mice relative to WT mice. The minimum first derivative of LV pressure (dP/dt_{min}), a measure of diastolic function, was 34% lower in hHIF2 $\alpha^{-/-}$ mice than WT mice (p = 0.0007; 1006 \pm 93 mmHg.s⁻¹ in chow-fed WT mice, 720 \pm 228 mmHg.s⁻¹ in WD-fed WT mice, 552 \pm 126 mmHg.s⁻¹ in chow-fed hHIF2 $\alpha^{-/-}$ mice, 561 \pm 63 mmHg.s⁻¹ in WD-fed hHIF2 $\alpha^{-/-}$ mice) (Fig. 1A). Similarly, the maximum first derivative of LV pressure (dP/dt_{max}), a measure of systolic function, was 32% lower in hHIF2 $\alpha^{-/-}$ mice (p = 0.0035; 1338 \pm 172 mmHg.s⁻¹ in chow-fed WT mice, 1097 \pm 381 mmHg.s⁻¹ in WD-fed WT mice, 830 \pm 151 mmHg.s⁻¹ in chow-fed hHIF2 $\alpha^{-/-}$ mice, 808 \pm 119 mmHg.s⁻¹ in WD-fed hHIF2 $\alpha^{-/-}$ mice) (Fig. 1B). LVDP, another measure of systolic function, was 25% lower in WD-fed mice (p = 0.0278) and 24% lower in hHIF2 $\alpha^{-/-}$ mice (p = 0.0384; 48 \pm 9 mmHg in chow-fed WT mice, 32 \pm 8 mmHg in WD-fed WT mice, 33 \pm 13 in chow-fed hHIF2 $\alpha^{-/-}$ mice, 27 \pm 8 mmHg in WD-fed hHIF2 $\alpha^{-/-}$ mice) (Fig. 1C). In contrast, relative to chow-fed WT mice (ratio = 1.0 \pm 0.3), the sympathetic dominance ratio, a measure of cardiac stimulated function, was 5.3-fold higher (5.3 \pm 2.4) in WD-fed WT mice but normalised in WD-fed hHIF2 $\alpha^{-/-}$ mice (Fig. 2).

Conclusion: The data provide novel insight into liver-heart crosstalk. Hepatocyte-specific deletion of HIF2 α was associated with basal cardiac dysfunction, but protection against cardiac sympathetic dominance in the mouse heart. Since cardiac sympathetic dominance has been linked to cardiac arrhythmia and heart failure (3), further investigation of hepatic HIF2 α deletion may suggest strategies for cardiac therapy in NAFLD.

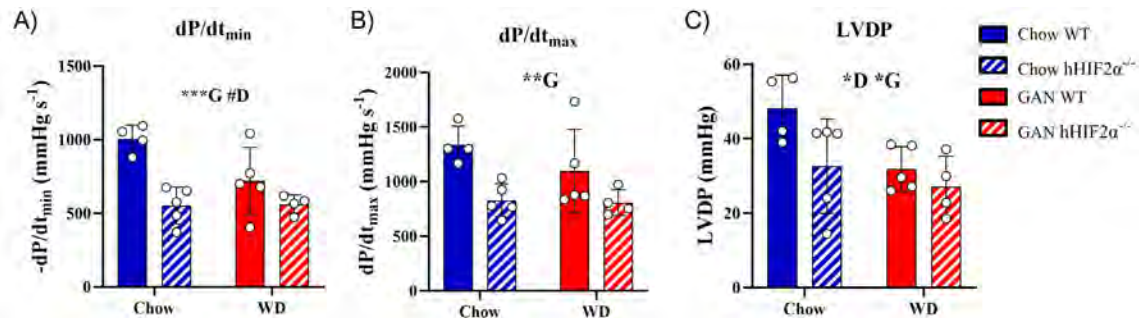


Figure 1: Diastolic and systolic function in chow and WD-fed WT and hHIF2 $\alpha^{-/-}$ mice. A) The minimal first derivative of left ventricular pressure dP/dt_{min} , a measure of diastolic function. B) The maximal first derivative of left ventricular pressure dP/dt_{max} , a measure of systolic function. C) Left ventricular developed pressure (LVDP). D = diet effect, G = genotype effect in two-way ANOVA. # $p < 0.1$, * $p < 0.05$, ** $p < 0.01$, *** $p < 0.0001$. Data are presented as mean \pm standard deviation, $n = 4-5$ per group.

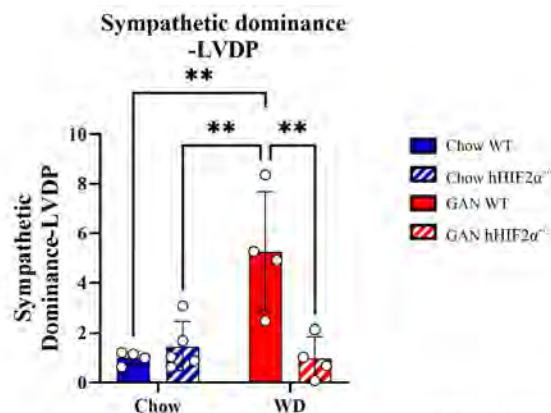


Figure 2: Cardiac sympathetic dominance in chow and WD-fed WT and hHIF2 $\alpha^{-/-}$ mice. The left ventricular developed pressure (LVDP) response to the maximal isoprenaline dose was divided by the response to the maximal carbachol dose to calculate the sympathetic dominance ratio. Due to a significant genotype:diet effect in two-way ANOVA results of Tukey's *post hoc* test are shown. ** $p < 0.01$. Data are presented as mean \pm standard deviation, $n = 4-5$ per group.

1. Anstee QM, Mantovani A, Tilg H, Targher G: Risk of cardiomyopathy and cardiac arrhythmias in patients with nonalcoholic fatty liver disease. *Nat Rev Gastroenterol Hepatol.*(2018);15. p. 425-39. doi: 10.1038/s41575-018-0010-0.
2. Morello E, Sutti S, Foglia B, Novo E, Cannito S, Bocca C, et al.: Hypoxia-inducible factor 2alpha drives nonalcoholic fatty liver progression by triggering hepatocyte release of histidine-rich glycoprotein. *Hepatology.*(2018);67. p. 2196-214. doi: 10.1002/hep.29754.
3. Shen MJ, Zipes DP: Role of the autonomic nervous system in modulating cardiac arrhythmias. *Circ Res.*(2014);114. p. 1004-21. doi: 10.1161/CIRCRESAHA.113.302549.

C02

Thrombocytes constitutes an efficient clearance system for uropathogenic *Escherichia coli* in a murine urosepsis model

Nanna Johnsen¹, Emil Lambertsen¹, Mette Christensen¹, Thomas Corydon¹, Helle Praetorius¹

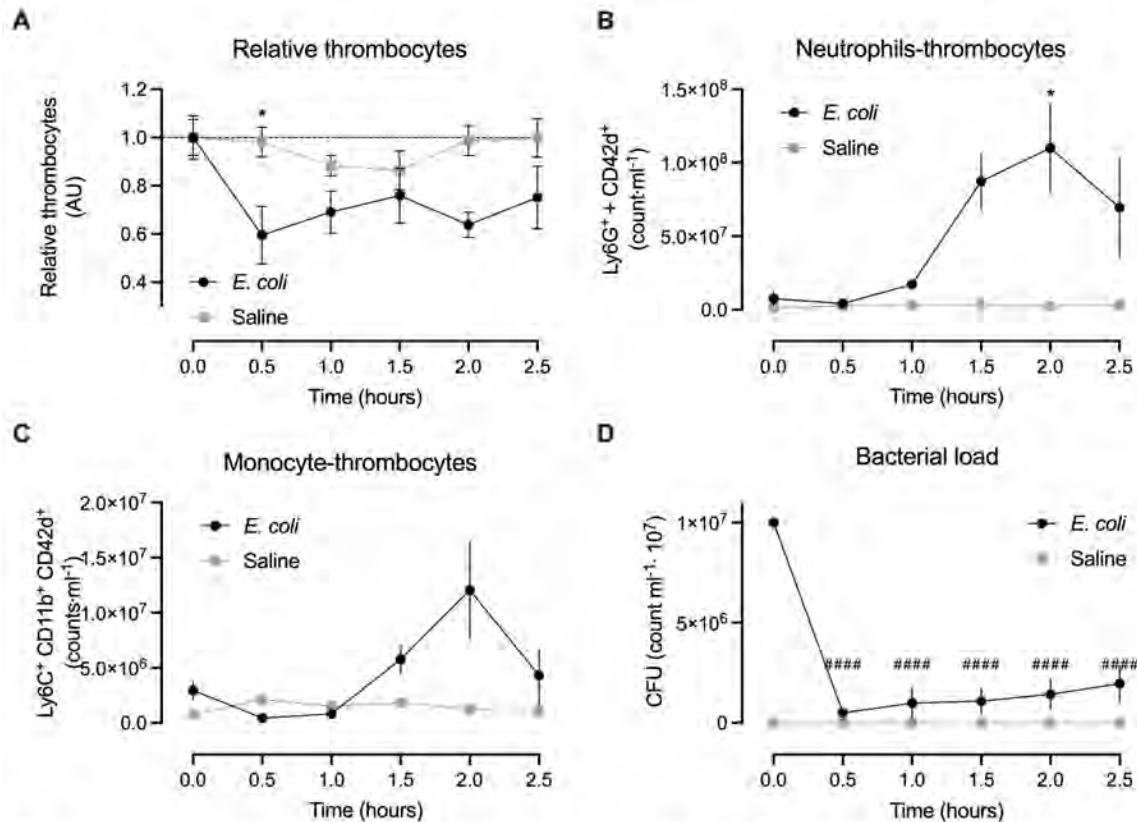
¹Aarhus University, Department of Biomedicine, Aarhus, Denmark

Sepsis is a life-threatening host reaction to circulating pathogens associated with reduced microperfusion and tissue hypoxaemia. Thrombocytopenia, one of the central diagnostic criteria for sepsis, is a distinct negative prognostic marker for survival (1, 2). Thrombocytes capability has transcended, solely within the coagulation system, to encompass a modulatory role in the immune response and a direct mediator of pathogen killing. Studies has shown a binding capability among others to monocytes, neutrophils and pathogens (3-5). Interestingly, our preliminary data in a murine model of sepsis reveal that the thrombocyte number falls prior to intravascular coagulation. Here we investigate the fate of circulating thrombocytes during sepsis.

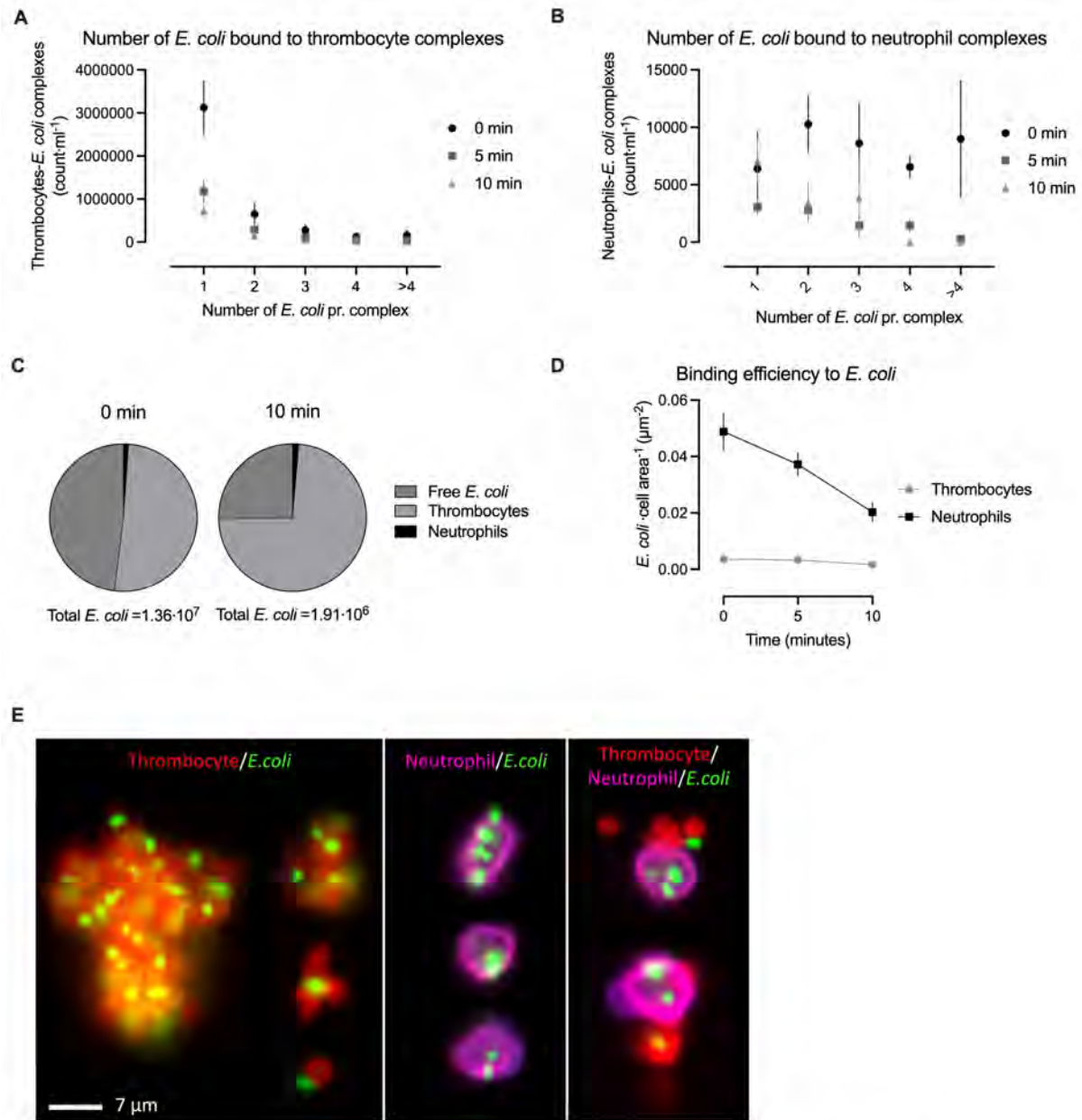
All experiments were carried out in male Balb/cJrJ mice (8-10 weeks, 24.8 ± 0.2 g). Mice were anaesthetised for the entire experiment with ketamine/xylazine ($100/10$ mg kg⁻¹) sc. A bolus of $330 \cdot 10^6$ *E. coli* (O6:K13:H1) with or without eGFP-pBAD plasmid was administered through the tail vein. The number of circulating thrombocytes (CD42⁺), neutrophils (Ly6G⁺) and monocytes (Ly6C⁺/CD11b⁺) were determined by flow cytometry. Bacterial load was quantified as CFU on LB-agar plates or by flow cytometry (EGFP). The results are given as mean \pm S.E.M., and statistical significance was tested by two-way ANOVA in GraphPad Prism v10.2.1 Experiments were approved by the National Animal Experiment Inspectorate, Denmark (2020-15-0201-00422).

In this model, sepsis-induced thrombocytopenia develops in a biphasic manner. We detected an early reduction of about 38.6%, already 30 min after *E. coli* injection ($48.9 \cdot 10^7 \pm 97.8 \cdot 10^6$ thrombocytes/ml, n=6) compared to mice receiving vehicle ($77.4 \cdot 10^7 \pm 48.2 \cdot 10^6$ thrombocytes/ml, n=6 p<0.06). Thrombocytes are known to form complexes with neutrophils or monocytes. However, the number of thrombocytes in complex with neutrophils or monocytes remained constant during the early fall in thrombocyte number and, thus, cannot explain the early drop in circulating thrombocytes. Interestingly, we found that the number of bacteria in the blood fell in parallel with the thrombocytes from $1.0 \cdot 10^7 \pm 0.10^7$ CFU (n=4) immediately after injection to $5.1 \cdot 10^5 \pm 0.9 \cdot 10^5$ CFU (n=7) 30 minutes after injection. By image-enhanced flow cytometry, we were able to show that the EGFP-expressing uropathogenic *E. coli* instantly and primarily is scavenged by circulating thrombocytes and that these complexes are acutely removed from the circulation. Preliminary *in vitro* data support the theory of thrombocytes acting primary as a scavenger system during sepsis. Data indicates that thrombocytes possess the ability to induce bacterial death, albeit gradually, but not sufficiently pronounced to achieve a 94.9% reduction in bacterial load within 30 min.

The data strongly suggest that circulating thrombocytes constitute the most important cell type for fast scavenging and clearance of invading bacteria during urosepsis.



Sepsis induces a parallel rapid and persistent drop in thrombocytes and *E. coli* (A) Relative number of circulating thrombocytes at different time points after injection with either saline (150 μ l) or 3.3×10^8 *E. coli*. (n=4-7) (B) Counts of neutrophils in complex with thrombocytes whole blood from mice at different timepoints with or without sepsis (n=4-7) (C) Counts of monocytes in complex with thrombocytes in whole blood at different timepoints after induction of sepsis or saline (n=4-7) (D) Colony forming units (CFU) in blood from mice with or without sepsis (n=4-7). Data were tested for normal distribution. Normally distributed data were tested by two-way ANOVA Šidák's multiple comparisons test, and data, which were not normally distributed, were analysed with Mann-Whitney test to compare sepsis and non-sepsis (indicated with asterisk). CFU was only tested with a two-way ANOVA within the sepsis-group (indicated with hashtags). Data are shown as mean \pm SEM. * indicates $p < 0.05$, ##### indicates $p < 0.001$.



Thrombocytes have the biggest binding capacity. Blood was collected after different incubation periods (0, 5 or 10 minutes) of bacteremia induced with *iv*-injection of $330 \cdot 10^6$ ARD-6/EGFP-pBAD in male mice and stained for thrombocytes (CD42d) and neutrophils (CD11b/Ly6G). For estimation of the number of GFP bound to each **A**) thrombocyte or **B**) neutrophil a GFP-mask was used. **C**) Pie charts of the total amount of *E. coli* bound to thrombocytes, neutrophils, or none of these at each time point. **D**) *E. coli* per cell area (neutrophil or thrombocyte) based on area masks and GFP-mask. **E**) Illustrative images of *E. coli* complex formation: CD42d-APC (thrombocytes, red), ARD-6/EGFP-pBAD(*E. coli*, green), CD11b-PE-cy7/ Ly6G-BV421(neutrophils, pink/purple) stained blood collected seconds after injection of *E. coli*. $n=3-4$ for each group. Data are given as mean \pm SEM.

1. Singer M, Deutschman CS, Seymour CW, Shankar-Hari M, Annane D, Bauer M, et al. The Third International Consensus Definitions for Sepsis and Septic Shock (Sepsis-3). *Jama*.

2016;315(8):801-10. 2. Wang D, Wang S, Wu H, Gao J, Huang K, Xu D, et al. Association Between Platelet Levels and 28-Day Mortality in Patients With Sepsis: A Retrospective Analysis of a Large Clinical Database MIMIC-IV. *Frontiers in Medicine*. 2022;9. 3. Hurley SM, Lutay N, Holmqvist B, Shannon O. The Dynamics of Platelet Activation during the Progression of Streptococcal Sepsis. *PLOS ONE*. 2016;11(9):e0163531-e. 4. Gawaz M, Fateh-Moghadam S, Pilz G, Gurland HJ, Werdan K. Platelet activation and interaction with leucocytes in patients with sepsis or multiple organ failure. *European Journal of Clinical Investigation* 1995. p. 843-51. 5. Palankar R, Kohler TP, Krauel K, Wesche J, Hammerschmidt S, Greinacher A. Platelets kill bacteria by bridging innate and adaptive immunity via platelet factor 4 and FcγRIIA. *Journal of Thrombosis and Haemostasis*. 2018;16(6):1187-97.

C03

High-fat diet blunts the carotid body mediated-ventilatory effects of TNF- α

Gonçalo M. Melo¹, Joana F. Sacramento¹, Kryspin Andrzejewski², Adriana M. Capucho¹, Katarzyna Kaczyńska², Sílvia V. Conde¹

¹NOVA Medical School|Faculdade de Ciências Médicas, Universidade NOVA de Lisboa, Lisboa, Portugal, ²Department of Respiration Physiology, Mossakowski Medical Research Center, Polish Academy of Sciences, Pawińskiego, Poland

Metabolic diseases pose a significant global health challenge, with profound impact on mortality and morbidity rates. The carotid bodies (CBs), traditionally recognized as an oxygen-sensitive organ, is a metabolic sensor implicated in these diseases [1-3]. In dysmetabolic states the CB is dysfunctional and the abolishment of its activity improves metabolic function [1-3]. Contributing to CB dysfunction is hyperinsulinemia and hyperleptinemia and probably inflammatory cytokines [4], whose presence, along with their receptors, has been evidenced within the CB [1,5]. By exploring the effects of TNF- α in the cardioventilatory responses and on CB inflammation this study aims to investigate the contribution of TNF- α to CB dysfunction in metabolic diseases. Moreover, the sexual dimorphism on TNF- α action was also explored.

Methods: Two groups of Wistar rats (male and female) were used - a control group (CTL) submitted to a standard diet and a group fed with high-fat diet (HF, 60% energy from fat) for 3 weeks. Animals were anesthetized with pentobarbital (60 mg/kg i.p.), and ventilation, blood pressure, and autonomic activity (heart rate variability) were assessed before and after the administration of TNF- α (0.5 and 5 ng/ml) in CTL and HF groups with and without resection of the carotid sinus nerve (CSN). Blood levels of TNF- α and the levels of TNF- α and its receptors in the CBs of CTL and HF animals were evaluated. For statistical analysis, ANOVA with Dunnett's comparison test and t-Student test were used. Ethical approval was obtained from the Animal Welfare Committee, from the NMS Ethics Committee and from The Portuguese Authorities (DGAV).

Results: In male CTL rats, TNF- α increased minute ventilation (MV) by 26.5% and 52.0% ($p < 0.001$) in response to 0.5 and 5 ng/ml TNF- α , respectively. Resection of the CSN attenuated MV response to TNF- α . In male HF animals, ventilatory response to TNF- α was blunted, increasing only 8%. In male CTL rats 0.5 and 5 ng/ml TNF- α reduced mean arterial pressure by 8.0% and 13.7% ($p < 0.01$), an effect not altered by CSN resection. CTL and HF females exhibit lower basal ventilation parameters, but similar responses to TNF- α . The CBs of HF rats showed a 46% increase in TNF- α compared to CTLs ($p < 0.01$).

Conclusion: TNF- α increases ventilation, and effect that is mediated by the CB and blunted in high-fat animals. It seems that there is no sexual dimorphism in TNF- α ventilatory responses mediated by the CB. The effect of TNF- α in the CB might contribute to its dysfunction in dysmetabolic states.

References: [1] Conde SV et al. J. Physiol. 2017; 595: 31-41; [2] Sacramento JF et al. Diabetologia. 2018; 61: 700-710; [3] Ribeiro MJ et al. Diabetes. 2013; 62: 2905-2916; [4] Sacramento JF et al. Int.

Physiology in Focus 2024

Northumbria University, Newcastle, UK | 2 – 4 July 2024

J. Mol. Sci. 2020; 21(15): 1-22; [5] Conde and Monteiro 2004, J Neurochem. 89:1148-56; [6] de Toda et al. Mechanisms of Ageing and Development. 2023; 211(1).

C04

The effects of water temperature and immersion depth on shear stress, arterial dilation, and Flow-Mediated Dilation following heating

Campbell Menzies², Charles Steward², Neil Clarke³, Doug Thake², Chris Pugh¹, Tom Cullen²

¹Cardiff Metropolitan University, Cardiff, United Kingdom, ²Coventry University, Coventry, United Kingdom, ³Birmingham City University, Birmingham, United Kingdom

Repeated exposure to hot water immersion improves arterial function [1,2]. However, there is a lack of evidence supporting specific protocol selection. Acute elevations in shear rate and flow-mediated dilation (FMD) positively correlate to subsequent chronic adaptations with exercise [3] and therefore may provide evidence with hot water immersion to support a particular immersion protocol. Core and skin temperature have distinct contributions to acute vascular responses [4] meaning, different immersion protocols may lead to divergent responses. Accordingly, this study aimed to compare the effects of (i) immersion depth, (ii) water temperature, and (iii) rectal temperature on acute changes in brachial artery diameter, shear rate, and subsequent FMD. It was hypothesised that shear stress and arterial diameter would differ between conditions and that greater increases in diameter post-heating would result in larger reductions in FMD.

Twenty-two healthy young adults completed three thirty-minute bouts of hot water immersion in a randomised order consisting of (i) Shoulder-deep immersion in 40 °C water (40-Shoulder), (ii) Waist-deep immersion in 40 °C water (40-Waist), and (iii) Waist-deep immersion in 42 °C water (42-Waist). Rectal temperature and vascular responses in the brachial artery (arterial diameter, blood flow, shear rate, FMD) were measured. Data were analysed using two-way repeated-measures ANOVAs, with the exception of FMD, which was allometrically scaled according to baseline diameter [5] and analysed using a generalised estimation equation. Significance was accepted at $p < 0.05$. Ethical approval was provided by the Coventry University (P146084) and conformed to the Declaration of Helsinki.

Rectal temperature increased less in the 40-Waist ($\Delta 0.5 \pm 0.1$ °C) condition than either the 40-Shoulder ($\Delta 0.9 \pm 0.3$ °C. $p < 0.001$), or 42-Waist condition ($\Delta 0.9 \pm 0.3$ °C. $p < 0.001$), which were similar ($p = 1.0$). Shear rate differed between all conditions ($p < 0.001$. 40-Shoulder: $\Delta 225 \pm 131$ 1/s. 42-Waist: $\Delta 105 \pm 117$ 1/s 40-Waist: $\Delta -22 \pm 66$ 1/s), whilst a greater increase in diameter was observed in the 40-Shoulder condition ($\Delta 0.43 \pm 0.22$ mm), than either the 42-Waist ($\Delta 0.11 \pm 0.33$ mm $p < 0.001$) or 40-Waist ($\Delta -0.02 \pm 0.33$ mm. $p < 0.001$) condition, which were similar ($p = 0.14$). Similarly, the 40-Shoulder condition demonstrated a larger decrease in FMD ($\Delta -3.9 \pm 3.8\%$) than either the 42-Waist ($\Delta -1.7 \pm 6.2\%$. $p = 0.01$) or 40-Waist ($\Delta 0.2 \pm 5.4\%$. $p < 0.001$) condition, which were similar ($p = 0.14$).

This study demonstrates that in response to a 30-minute hot water immersion bout, immersion depth has a larger influence than water temperature, or rectal temperature on arterial dilation, shear rate, and subsequent FMD. These findings provide novel evidence for the importance of heating larger body surface areas, over increases in rectal temperature, in the prescription of heating stimuli to elicit larger vasoactive and haemodynamic responses. In line with the stated hypothesis, larger reductions in FMD were observed in conditions that elicited greater brachial

vasodilation. Future work is required to examine the physiological meaningfulness of this in terms of changes to endothelial function and potential inference for effects on subsequent adaptation.

[1] Brunt et al. (2016). *J Physiol*, 594(18), 5329-5342. [2] Bailey et al. (2016). *Int J Sports Med*, 757-765. [3] Dawson et al. (2018). *Eur J Appl Physiol*, 118, 523-530. [4] Coombs et al. (2021). *J Appl Physiol*, 130(1), 149-159. [5] Atkinson et al. (2013). *J Hypertens*, 31(2), 287-291.

C05

Cerebral pulsatility index in a mouse model of acute ischemic stroke

Christina Shen-Zhuang Nielsen¹, Dmitry Postnov², Christian Aalkjaer¹, Vladimir Matchkov¹

¹Department of Biomedicine, Faculty of Health, Aarhus University, Aarhus, Denmark, ²Center of Functionally Integrative Neuroscience, Department of Clinical Medicine, Faculty of Health, Aarhus University, Aarhus, Denmark

Background: Cerebral pulsatility index (PI) is used as a proxy for downstream vascular resistance in acute ischemic stroke in clinical studies, with PI measurements from the contralateral hemisphere serving as reference value¹. We hypothesize that PI and cerebral blood flow changes occur in both hemispheres during acute ischemic stroke and aim to investigate these changes in a mouse model of transient acute ischemic stroke.

Methodology: Cerebral blood flow and PI before, during and after stroke-induction were measured using laser speckle contrast imaging in both brain hemispheres through bilateral cranial windows in five C57BL/6Jrj male mice (age: 15-16 weeks). All animals received 10-13 training sessions for both handling^{2,3} and for head fixation to allow for cerebral blood flow imaging in awake mice, as anaesthesia with isoflurane affects cerebral arteries⁴. All surgeries were performed under inhalation of isoflurane (induction: 4 %, 100% O₂, flow: 0.6 L/min; maintenance: 1.5%, 100% O₂, flow: 0.4 L/min).

The middle cerebral artery (MCA) was accessed through a 2-3 mm craniotomy in the right temporal bone, and the MCA was gently compressed for 1 hour with two micropipettes⁵. Decrease in MCA blood flow was assessed in real-time to validate MCA-occlusion (MCA-O). Cerebral blood flow and PI were measured repeatedly at baseline (awake and anaesthetized mouse), during MCA-O and immediately after pipette retraction (anaesthetized mouse), and on daily follow-ups for seven days (awake mouse).

Data are presented as mean \pm SD, and changes between the two MCA were analysed with paired t-test. Longitudinal changes in PI and cerebral blood flow were analysed with two-way repeated measures ANOVA and corrected for multiple comparisons with post-hoc Bonferroni test. Significant effects are defined as $p < 0.05$.

Results: There were no differences in PI between both MCA at baseline, during MCA-O and follow-up. There were no significant changes in PI for both MCAs over time during MCA-O. Changes in PI for the right MCA were observed during follow-up at 48h (0.15 ± 0.04 vs 0.21 ± 0.03 , $p=0.0004$) and 96h (0.16 ± 0.03 vs 0.21 ± 0.03 , $p=0.0125$) as compared to baseline.

Changes in PI for the left MCA were identified during follow-up at 48h (0.15 ± 0.02 vs 0.22 ± 0.01 , $p<0.0001$) and 96h (0.17 ± 0.03 vs 0.22 ± 0.01 , $p=0.0053$) as compared to baseline.

Blood flow index did not change between both MCA at baseline and during follow-up. There were no changes in blood flow index over time at baseline and follow-up (awake). Blood flow index between the right and left MCA (107.4 ± 45.6 vs 455.2 ± 215.3 , $p < 0.003$) was significantly different

during MCA-O. Significant changes in blood flow index over time were observed in the right MCA between baseline (anaesthetized) and during MCA-O (360 ± 148.9 vs 107.4 ± 45.6 , $p < 0.0007$).

Conclusion: There were no differences between PI in both MCA before, during and after MCA-O. PI from both MCA were reduced during follow-up, as compared to baseline. Blood flow index did not differ between the two MCAs at baseline and during follow-up, except during MCA-O.

1. Ng, F. C. et al. *Stroke* 49, 2512-2515, doi:10.1161/STROKEAHA.118.021631 (2018). 2 Hurst, J. L. & West, R. S. *Nat Methods* 7, 825-826, doi:10.1038/nmeth.1500 (2010). 3 Marcotte, M. et al. *J Vis Exp*, doi:10.3791/62593 (2021). 4 Sullender, C. T et al. *J Neurosci Methods* 366, 109434, doi:10.1016/j.jneumeth.2021.109434 (2022). 5 Erdener, Ş. E. et al. *Journal of Cerebral Blood Flow & Metabolism* 41, 236-252, doi:10.1177/0271678X20914179 (2020).

C06

Novel Dbh+ Catecholaminergic Cardiomyocytes Contributing to the Structure and Function of the Cardiac Conduction System in Murine Heart

Tianyi Sun¹, Alexander Grassam-Rowe², Weinian Shou³, Nicola Smart⁴, Xiaoqiu Tan⁵, Ming Lei¹

¹*Department of Pharmacology, University of Oxford, Oxford, United Kingdom,* ²*Department of Pharmacology, University of Oxford, Oxford, United Kingdom,* ³*Herman B Wells Centre for Pediatric Research, Department of Pediatrics, Indiana University School of Medicine, Indianapolis, United States,* ⁴*Department of Physiology, Anatomy & Genetics, University of Oxford, Oxford, United Kingdom,* ⁵*Department of Cardiology, the Affiliated Hospital of Southwest Medical University, Luzhou, China*

Research rationale

The heterogeneity of functional cardiomyocytes arises during heart development, which is essential to the complex and highly coordinated cardiac physiological function¹. Yet the biological and physiological identities and the origin of the specialized cardiomyocyte populations have not been fully clarified.

Methodology

Single-cell RNA-seq and spatial transcriptomic technologies are applied to investigate cardiogenesis and the genetic profile of the cells of interest. The genetic mouse model DbhCre/Td-ChR2 was generated for lineage tracing and cell fate mapping. Transmission electron microscopy was applied for structural and functional study.

Results

Using single-cell RNA sequencing (scRNA-Seq), we mapped the transcriptional landscape of CCS (Cardiac Conduction System) formation and maturation in the murine heart. This led to the identification of an unreported cardiomyocyte population expressing *Dbh* gene encoding Dopamine-beta-hydroxylase which is key enzyme for biosynthesis of neurotransmitter Noradrenaline. We determined how these myocytes are distributed across the heart by utilising advanced single-cell and spatial transcriptomic analyses, genetic fate mapping and molecular imaging with computational reconstruction. From E14.5 to adulthood, Dbh+ CMs were abundant in the CCS regions where sympathetic innervation is enriched, as detected by immunostaining with anti-Th antibody, particularly in the adult heart, revealing their close relationship with sympathetic innervation. Immuno-Electron Microscopy further unveiled the presence of high electron-density vesicles in adult Dbh+ cardiomyocytes, which strongly indicates the secretory function of Dbh+ cardiomyocytes.

Conclusions

We discovered a uniquely distributed group of unreported catecholaminergic cardiomyocytes with key regulatory roles in cardiac excitation conduction, providing new insights into neuron-endocrine

function of cardiomyocytes. The physiological and pathophysiological implications of such function need to be further explored in the future.

We discovered a uniquely distributed group of unreported catecholaminergic cardiomyocytes with key regulatory roles in cardiac excitation conduction. We also revealed their close relationship with sympathetic innervation during cardiac conduction system (CCS) formation.

Our study thus provides new insights into the development and heterogeneity of the mammalian cardiac conduction system by revealing a new cardiomyocyte population with potential catecholaminergic endocrine function.

Ethics declarations

Competing interests: The chip, procedure, and application of Stereo-seq are covered in pending patents. The remaining authors declare no other competing interests.

Animals and ethical approval

All animal experiments were performed on mice neonatal or adult mice (both genders) in accordance with the United Kingdom Animals (Scientific Procedures) Act 1986 and were approved by the University of Oxford Pharmacology ethical committee (approval ref. PPL: PP8557407) or Animal Care and Use Committee of the Southwest Medical University, Sichuan (China) (No: 20160930) in conformity with the national guidelines under which the institution operates.

Statistics

For the spatial transcriptomics, we had at least $n = 3$ sections for hearts from *Dbh^{Cre}/Rosa26-tdTomato* mice at E12.5, E14.5, P3, and P56, respectively.

Whole embryos (E8.5, E9.5, E10.5, E12.5, E14.5, $n = 5$ embryos per stage) or isolated hearts (E12.5, E13.5, E14.5, E16.5, P3, P56, $n = 5$ hearts per stage) were analyzed by using multiplex nucleic acid in situ hybridization (RNAscope), immunohistological staining, confocal microscopic imaging and EM.

Reference 1. Lescroart, F. et al. Defining the earliest step of cardiovascular lineage segregation by single-cell RNA-seq. <https://www.science.org>.

C07

P2X3 antagonists as a novel anti-arrhythmic

Carol T Bussey¹, Rexson Tse², Martin K Stiles³, David J Paterson⁴, Julian FR Paton⁵

¹Manaaki Manawa Centre for Heart Research, Department of Physiology, Faculty of Medical & Health Sciences, University of Auckland, Auckland, New Zealand, ²Gold Coast Hospital and Health Service, Queensland Health, Gold Coast, Australia, ³Waikato Clinical School, Faculty of Medical & Health Sciences, University of Auckland, Hamilton, New Zealand, ⁴Burdon Sanderson Cardiac Science Centre, Department of Physiology, Anatomy and Genetics, Medical Sciences Division, University of Oxford, Oxford, United Kingdom, ⁵Manaaki Manawa Centre for Heart Research, Department of Physiology, Faculty of Medical & Health Sciences, University of Auckland, Auckland, New Zealand

Introduction: Cardiovascular diseases are characterised by elevated sympathetic nerve activity, which contributes to end-organ damage, morbidity and mortality. Surgical removal of the stellate ganglion to short-circuit sympathetic nerve overactivity can eradicate arrhythmias, however this is a highly invasive approach with significant side-effects, necessitating discovery of novel non-invasive druggable targets. Recent transcriptomic data shows upregulation of P2X3 purinergic receptors in the stellate ganglia of Spontaneously Hypertensive (SHR) compared to Wistar rats (Bardsley EN *et al.* 2018. Sci Rep 8, 8633). We hypothesise that these purinergic receptors within cardiac stellate ganglia contribute to sympathetic overactivity and the development of cardiovascular diseases such as hypertension and arrhythmias.

Objectives: Confirm expression of P2X3 receptor in stellate ganglia, investigate cardiac responses to stellate ganglia P2X3 receptor stimulation/inhibition, and examine effect of P2X3 receptor antagonism on cardiac arrhythmias.

Methods: Stellate ganglia from Wistar and SH rats (n=6) and humans (n=2) were immunofluorescently stained for P2X3 receptor and tyrosine hydroxylase, and P2X3 receptor expression in rat stellate ganglia was quantified using qPCR. Cardiac responses to stellate ganglion P2X3 receptors were investigated in the decerebrated working heart-brainstem preparation of Wistar and SH rats (4-5 week old), following anaesthesia with 5% isoflurane in oxygen. Arrhythmias were triggered in SHR, which exhibit increased arrhythmogenicity, with a combination of atropine (30µM) and caffeine (100µM) delivered in the perfusate, followed by electrical stimulation of the stellate ganglion.

Results: We have confirmed in both rat and human stellate ganglia that P2X3 receptors are co-localised with tyrosine hydroxylase-expressing sympathetic cells. P2X3 receptor expression is upregulated in SHR stellate ganglia (Wistar 1.03 ± 0.10 , SHR 3.77 ± 0.78 fold, mean \pm SEM, n=7-8, p<0.01 students t-test). Microinjection of stable ATP analogue $\alpha\beta$ methylene-ATP (100µg) directly into the stellate ganglion causes tachycardia (Wistar 45.6 ± 8.3 ; SHR 62.5 ± 14.1 Δ bpm, n=7), which is attenuated by P2X3 inhibition with AF353 (Wistar 25.0 ± 7.5 ; SHR 19.5 ± 7.5 Δ bpm; n=4-5, p<0.05 mixed effects model). Arrhythmias were triggered in the ECG of 61% of experiments (n=13), particularly AV block (n=3), and fragmented QRS complexes (n=4), with bundle block and

bradyarrhythmia also observed. Of these arrhythmias, 70% were attenuated or abolished following blockade of P2X3 receptors (n=9).

Conclusions: Stellate ganglion P2X3 purinergic receptors regulate cardiac function, and P2X3 overexpression likely contributes to sympathetic overactivity in cardiovascular disease. P2X3 inhibition rapidly and profoundly recovers arrhythmic heart rhythms, and reverses electrical instability.

C08

The Na,K-ATPase-dependent Ca²⁺-sensitization by cSrc kinase in murine middle cerebral arteries is partially independent of the Rho kinase pathway

Ask Carit Andersen¹, Christian Staehr¹, Vladimir Matchkov¹

¹Aarhus University, Aarhus, Denmark

Aims: In the vascular wall of cerebral arteries, micromolar ouabain inhibits the $\alpha 2$ Na,K-ATPase and activates cSrc kinase, which was shown to increase Ca²⁺-sensitivity of the smooth muscle cell contractile machinery. It has been proposed, that this cSrc-dependent Ca²⁺-sensitization depends on the phosphorylation of myosin phosphatase target subunit 1 (MYPT1) by Rho kinase signaling, as the conventional pathway for Ca²⁺-sensitization of vascular smooth muscle cells. However, this Src-Rho-MYPT1 signaling remains to be shown and validated in cerebral arteries. Familial hemiplegic migraine type 2 is associated with mutations in the $\alpha 2$ Na,K-ATPase, including the G301R missense mutation, associated with reduced abundance of the Na,K-ATPase in cerebrovascular smooth muscle cells, resulting in increased cSrc activation. We aimed to test whether cSrc potentiates Ca²⁺-sensitivity via Rho-kinase-dependent MYPT1 phosphorylation in middle cerebral arteries and to compare this signaling in mice bearing the G301R mutation (ATP1A2^{+/G301R}) and wild types.

Methods: Middle cerebral artery contractility to thromboxane A₂ analog, U46619, was assessed ex-vivo in isometric myograph. The effects of pre-incubation with Rho kinase inhibitor, Y27632 (3·10⁻⁶M) and ouabain (10⁻⁵M) were studied. Arteries from ATP1A2^{+/G301R} and wild type mice were compared.

To assess cSrc and MYPT1 phosphorylation and its dependence on Rho kinase, U46619-stimulated middle cerebral arteries from wild type and ATP1A2^{+/G301R} mice were studied with Western blot upon pre-incubation with Y27632, ouabain or both.

Results: Ouabain potentiated the U46619-induced contraction of middle cerebral arteries from wild type mice (n=5), while Y27632 inhibited it (n=4). In the presence of Y27632, ouabain still potentiated the contraction of wild type arteries (n=5). In contrast, ouabain did not significantly affect the contraction of ATP1A2^{+/G301R} mice (n=5), neither under control conditions nor after Rho kinase inhibition, while Y27632 still suppressed the contraction (n=3). Western blot data indicates a positive correlation between cSrc kinase and MYPT1 phosphorylation, which is only partially prevented by Rho kinase inhibition (24 mice divided into 6 groups exposed to 4 different interventions).

Conclusion: We suggest, that cSrc kinase increases Ca²⁺-sensitivity in vascular smooth muscle cells via MYPT1 phosphorylation. Our results suggest that this arterial tonus regulating pathway is partially independent of Rho kinase signaling.

Staehr, C., et al., Smooth muscle Ca²⁺ sensitization causes hypercontractility of middle cerebral arteries in mice bearing the familial hemiplegic migraine type 2 associated mutation. *Journal of Cerebral Blood Flow & Metabolism*, 2018. 39(8): p. 1570-1587.

C09

The differential pro-contractile effect of ouabain depends on agonist and smooth muscle activation state.

Anna Giné Martínez^{1,2}, Daniel Løgstrup Nielsen², Josef Khalid², Elizaveta Melnikova², Vladimir Matchkov²

¹*Facultat de Medicina i Ciències de la Salut, Universitat Internacional de Catalunya, Barcelona, Spain,* ²*Department of Biomedicine, Health, Aarhus University, Aarhus, Denmark*

The Na,K-ATPase modulates arterial tone by means of ionic gradients, and via the Na,K-ATPase-dependent signal transduction, including the Src kinase signaling pathway. Inhibition of the Na,K-ATPase leads to accumulation of intracellular Na⁺, which modifies the Na,Ca-exchanger activity leading to elevation of intracellular Ca²⁺ and smooth muscle contraction. Src kinase activates upon interaction with the Na,K-ATPase inhibitor, i.e., cardiotonic steroid ouabain, which leads to sensitization of smooth muscle cell contractile machinery and potentiation of arterial contraction. It has been proposed that both Na,K-ATPase-dependent mechanisms potentiate the contraction in response to different pro-contractile stimuli, however, their contribution depends on contractile agonist.

This study aims to analyze the agonist-dependence (methoxamine, U46619, and noradrenaline) of the pro-contractile action of ouabain, and its effect at different activation states in the vascular wall.

Male Wistar Hannover rats were obtained from Janvier-Labs (France) and sacrificed with CO₂ inhalation. Mesenteric arteries (2nd – 3rd order branches) were dissected and used in isometric myography, where the contraction was induced by either U46619 (thromboxane A₂ mimetic), methoxamine (alpha1-adrenergic receptor agonist), or noradrenaline (unspecific adrenoreceptor agonist). The arterial segments were compared under control conditions and in the presence of either ouabain, or iberiotoxin (IbTX), the inhibitor of big conductance Ca²⁺-activated potassium channels, or in the combination of these drugs. Intracellular Ca²⁺ was measured with Ca²⁺-sensitive dye, FURA-2/AM simultaneously with contractile responses in myograph. Western blot with arterial segment lysates was performed to assess the phosphorylation of Src kinase and MYPT protein responsible for Ca²⁺ sensitization. The comparison of concentration-response curves was done with two-way ANOVA. Data presented as mean±standard deviation.

Ouabain (10 µM) significantly potentiated the contraction in response to U46619 (pEC₅₀ changes from 6.2±0.5 to 6.8±0.7, *n*=7, *P*=0.016). IbTX also potentiated the U46619-induced contraction in comparison with the control (pEC₅₀: 7.5±3, *n*=7, *P*<0.0001). Pro-contractile effects of IbTX and ouabain were not additive (pEC₅₀: 7.1±0.7, *n*=5, *P*=0.0003). In contrast, ouabain showed no clear potentiation of methoxamine-induced constriction (pEC₅₀: 5.2±0.7 and 5.5±0.3, *n*=7, *P*=0.92). However, the pro-contractile effect of IbTX was still seen (pEC₅₀: 5.8±0.3, *n*=7, *P*=0.03) but this was not affected by a combination of IbTX and ouabain (pEC₅₀: 5.7±0.2, *n*=7, *P*=0.13). Finally, no potentiation of vessel contractility by ouabain was observed in the stimulation with noradrenaline (pEC₅₀: 5.9±0.2 and 6.0±0.1, *n*=6, *P*=0.20), neither with IbTX (pEC₅₀: 6.1±0.2, *n*=6, *P*=0.28), but this effect was strengthened in the presence of both IbTX and ouabain (pEC₅₀: 6.2±0.2, *n*=6, *P*=0.03).

Further analyses demonstrated that a major part of ouabain pro-contractile action is not associated with elevation of intracellular Ca^{2+} but with Ca^{2+} sensitization. In contrast, IbTX strongly elevates intracellular Ca^{2+} in smooth muscle cells.

This study demonstrates the agonist-dependent character of the pro-contractile action of ouabain, where agonists whose action is primarily mediated by Ca^{2+} -sensitization are most sensitive to inhibition of the Na,K-ATPase. Importantly, this ouabain action can further be potentiated by the elevation of intracellular Ca^{2+} with IbTX. This study suggests that caution should be taken when comparing the pro-contractile ouabain action for different agonists and at different activation states of the vascular wall.

Staehr, C., Aalkjaer, C., & Matchkov, V. V. (2023). The vascular Na,K-ATPase: clinical implications in stroke, migraine, and hypertension. *Clinical science (London, England : 1979)*, 137(20), 1595–1618. Blaustein, M. P., & Hamlyn, J. M. (2024). Sensational site: the sodium pump ouabain-binding site and its ligands. *American journal of physiology. Cell physiology*, 326(4), C1120–C1177. Hangaard, L., Jessen, P. B., Kamaev, D., Aalkjaer, C., & Matchkov, V. V. (2015). Extracellular Calcium-Dependent Modulation of Endothelium Relaxation in Rat Mesenteric Small Artery: The Role of Potassium Signaling. *BioMed research international*, 2015, 758346. Zhang, L., Aalkjaer, C., & Matchkov, V. V. (2018). The Na,K-ATPase-Dependent Src Kinase Signaling Changes with Mesenteric Artery Diameter. *International journal of molecular sciences*, 19(9), 2489. Bouzinova, E. V., Hangaard, L., Staehr, C., Mazur, A., Ferreira, A., Chibalin, A. V., Sandow, S. L., Xie, Z., Aalkjaer, C., & Matchkov, V. V. (2018). The $\alpha 2$ isoform Na,K-ATPase modulates contraction of rat mesenteric small artery via cSrc-dependent Ca^{2+} sensitization. *Acta physiologica (Oxford, England)*, 224(1), e13059.

C10

Evaluating the impact of succinate on cardiac electrical integrity in the mouse

Sean Benson^{1,2}, Andrew Coney^{1,2}, Andrew Holmes^{1,2}

¹*School of Biomedical Sciences, Institute of Clinical Sciences, University of Birmingham, Birmingham, United Kingdom*, ²*Institute of Cardiovascular Sciences, University of Birmingham, Birmingham, United Kingdom*, ³*School of Biomedical Sciences, Institute of Clinical Sciences, University of Birmingham, Birmingham, United Kingdom*

Introduction. During cardiac ischaemia-reperfusion, high levels of succinate accumulation and metabolism promote reactive oxygen species mediated cell death and dysfunction [1]. There is also a high risk of both atrial and ventricular arrhythmias following exposure to ischaemia/reperfusion. However, the impact of succinate on cardiac electrical function remains largely uncharacterised and it is unclear if elevated succinate metabolism may have a role in promoting cardiac arrhythmia.

Aims/Objectives. This study analysed the effects of succinate on murine ECGs to identify potential proarrhythmic electrical changes in the atria and ventricles.

Methods. ECGs were recorded from male and female adult FVB mice (n=15) under alfaxalone anaesthesia (Alfaxan®; Vetoquinol UK Ltd), at 20-25 mg kg⁻¹ h⁻¹, i.v., with 0.02 ml boluses as necessary. The left jugular vein was cannulated to allow for infusion of diethyl succinate (DESucc) a cell permeable form of succinate [2]. ECG recordings were measured at baseline (Pre-infusion), throughout 15-20 minutes infusion of Vehicle (n=3) or low dose DESucc (8 mg kg⁻¹ min⁻¹ (n=3)) or high dose DESucc (80 mg kg⁻¹ min⁻¹ (n=9)), and again 10 minutes post-infusion. Analysis was performed in ECG and HRV modules in LabChart v8 (AD Instruments, Oxford, UK). Signal averaged ECGs were used for waveform analysis. The arrhythmia index (number of premature or delayed R-waves per minute) was recorded across the whole experiment. Following the experiment, animals were killed by a schedule 1 method. Values are expressed as mean±SEM. Statistical analysis was performed using a one-way repeated measures Analysis of Variance with Bonferroni post hoc analysis (Prism9, GraphPad, Cal, USA). Significance was taken as P<0.05.

Results. High dose DESucc infusion did not significantly modify heart rate (Pre-infusion: 476±9; high DESucc: 494±25; Post-infusion: 517±41 beats per minute, n=9). However, high dose DESucc infusion produced an elevation in irregularly spaced R-R intervals and delayed beats as evidenced by an increase in arrhythmia index (Pre-infusion: 0.8±0.3; high DESucc: 4.1±0.9; Post-infusion: 1.9±0.8 abnormal beats per minute, n=9, P<0.05). Similarly, high dose DESucc infusion increased the standard deviation of the R-R interval (SDRR) (Pre-infusion: 5.7±0.5; high DESucc: 20±3; Post-infusion: 7±3 ms, n=9, P<0.05). Analysis of ECG waveforms showed that high dose DESucc significantly prolonged the P-R interval, the QRS duration and the Q-T interval. However, the most striking effect was to cause irreversible prolongation the P-wave duration (Pre-infusion: 9±0.4; high DESucc: 13±1; Post-infusion: 13±1 ms, n=9, P<0.05). Arrhythmia index, SDRR, P-wave duration, P-R interval, QRS duration and Q-T interval were not significantly modified by Vehicle (n=3) or low dose DESucc (n=3) infusion.

Conclusion. High dose DESucc infusion causes acute cardiac arrhythmia and changes in ECG waveforms which are consistent with major conduction disturbances in both the atria and ventricles. More work is required to determine if these actions are dependent on direct modifications in ion channel function, such as $\text{Na}_v1.5$, which may be preventable by targeted treatment.

1. Chouchani ET, Pell VR, Gaude E, Aksentijević D, Sundier SY, Robb EL, Logan A, Nadtochiy SM, Ord ENJ, Smith AC, Eyassu F, Shirley R, Hu CH, Dare AJ, James AM, Rogatti S, Hartley RC, Eaton S, Costa ASH, Brookes PS, Davidson SM, Duchon MR, Saeb-Parsy K, Shattock MJ, Robinson AJ, Work LM, Frezza C, Krieg T, Murphy MP. Ischaemic accumulation of succinate controls reperfusion injury through mitochondrial ROS. *Nature* 515:431-435. 2. Swiderska A, Coney AM, Alzahrani AA, Aldossary HS, Batis N, Ray CJ, Kumar P & Holmes AP. (2021). Mitochondrial Succinate Metabolism and Reactive Oxygen Species Are Important but Not Essential for Eliciting Carotid Body and Ventilatory Responses to Hypoxia in the Rat. *Antioxidants* 10(6):840.

C11

The effect of interrupting prolonged sitting with light movement on central and peripheral haemodynamics in Long COVID

Nicholas Hudson¹, Scott Hannah¹, Simon Fryer², Mark Rickenbach³, Margaret Husted¹, Helen Ryan Stewart⁴, James Faulkner¹

¹University of Winchester, Winchester, United Kingdom, ²University of Gloucestershire, Gloucester, United Kingdom, ³Park and St Francis Surgery, Eastleigh, United Kingdom, ⁴Eastern Institute of Technology, Napier, New Zealand

Long COVID-19 is defined as signs, symptoms and conditions that develop after initial SARS-CoV-2 infection and persist for over four weeks. Nearly 2 million people in the UK are currently experiencing self-reported long COVID, of which 61% of these people have been living with symptoms for more than a year. (*Office for National Statistics, 2023*).

Long COVID presents with over fifty different symptoms, which can vary significantly from person to person. People with long COVID demonstrate significantly greater levels of sedentary behaviour (Delbressine *et al.*, 2021), partially explained by fatigue being one of the most common symptoms. Sedentary time is known to have an adverse effect on vascular function and can increase the risk of cardiovascular disease. Acute sitting periods as short as one hour can worsen vascular function (Taylor *et al.*, 2022), however, interrupting these periods with short bouts of movement has been shown to mitigate the negative effect on vascular health (Paterson *et al.*, 2020). Arterial stiffness is a measure of vascular dysfunction through changes in the structure and function of blood vessels. Carotid-femoral pulse wave velocity (cfPWV) is the gold standard tool to non-invasively measure arterial stiffness.

This study aimed to investigate whether prolonged sitting for 2 hours induces a vascular response in people with long COVID and if interrupting sitting periods has a beneficial effect on arterial stiffness. Participants were tasked with sitting still for two hours. Interruption includes three bouts of five sit-to-stands, five calf raises, and three minutes of self-paced walking to mimic activities of daily living. Measures of central and peripheral blood pressure, arterial stiffness (SphygmCor XCEL), executive function (TrailMaking Tasks), and cerebral oxygenation (Near Infrared Spectroscopy) were recorded at baseline and following two hours of interrupted or uninterrupted sitting. Ethical approval was obtained by Health and Care Research Wales (IRAS: 309606 22/SC/0120).

Thirty participants (52.84 ± 13.19 years, symptoms lasting >12 months) completed both experimental visits and were used in the analysis. Repeated measures ANOVA demonstrated a significant increase in central systolic blood pressure (cSBP) ($P=0.005$, $\eta_p^2 = 0.258$), central diastolic blood pressure (cDBP) ($P<0.001$, $\eta_p^2 = 0.519$), brachial systolic blood pressure (SBP) ($P<0.001$, $\eta_p^2 = 0.348$) and mean arterial pressure (MAP) ($P<0.001$, $\eta_p^2 = 0.391$) following prolonged sitting regardless of interruptions. There was no significant change in cfPWV ($P=0.541$). Mental fatigue significantly increased in both conditions ($P=0.019$, $\eta_p^2 = 0.194$).

This research demonstrates that sitting for 2 hours instigates changes in central and peripheral blood pressure, which is thought to be driven by blood pooling in the lower limbs resulting in a decrease in venous return and cardiac output causing compensations through the sympathetic nervous system including increased peripheral vascular resistance (Adams *et al.*, 2023). Although interrupting sitting did not affect cfPWV, it is unclear whether the intensity of interruption or the duration of sitting time was sufficient to induce changes in arterial stiffness. Additionally, understanding the effect of chronic periods of sedentary behaviour through prolonged sitting on arterial stiffness is important to understand the clinical relevance of increased sedentary behaviour in long COVID.

Adams, N. *et al.* (2023) 'The Effect of Sitting Duration on Peripheral Blood Pressure Responses to Prolonged Sitting, With and Without Interruption: A Systematic Review and Meta-Analysis', *Sports Medicine*, 54. Available at: <https://doi.org/10.1007/s40279-023-01915-z>. Delbressine, J.M. *et al.* (2021) 'The Impact of Post-COVID-19 Syndrome on Self-Reported Physical Activity', *International Journal of Environmental Research and Public Health*, 18(11), p. 6017. Available at: <https://doi.org/10.3390/ijerph18116017>. Paterson, C. *et al.* (2020) 'The Effects of Acute Exposure to Prolonged Sitting, With and Without Interruption, on Vascular Function Among Adults: A Meta-analysis', *Sports Medicine*, 50(11), pp. 1929–1942. Available at: <https://doi.org/10.1007/s40279-020-01325-5>. Prevalence of ongoing symptoms following coronavirus (COVID-19) infection in the UK - Office for National Statistics (no date). Available at: <https://www.ons.gov.uk/peoplepopulationandcommunity/healthandsocialcare/conditionsanddiseases/bulletins/prevalenceofongoingsymptomsfollowingcoronaviruscovid19infectionintheuk/2february2023> (Accessed: 17 March 2023). Taylor, F.C. *et al.* (2022) 'The Acute Effects of Prolonged Uninterrupted Sitting on Vascular Function: A Systematic Review and Meta-analysis', *Medicine & Science in Sports & Exercise*, 54(1), p. 67. Available at: <https://doi.org/10.1249/MSS.0000000000002763>.

C12

Raising the Bar on Health: Can one year of endurance exercise training enhance vascular function in healthy individuals?

Marcos Paulo Rocha Alves¹, Casper Sejersen¹, Mads Fischer¹, Andrea Tamirezz-Ellemann¹, Lasse Gliemann¹

¹*The August Krogh Section for Human Physiology, Department of Nutrition, Exercise and Sports, University of Copenhagen, Copenhagen, Denmark., Copenhagen, Denmark*

Introduction: Endurance exercise training improves aerobic capacity and endothelial function in people with an elevated risk of cardiovascular disease by augmenting nitric oxide synthesis through the shear stress mechanism. However, whether long-term endurance exercise enhances vascular function concomitant with aerobic capacity in healthy individuals is unclear. We hypothesized that long-term endurance exercise training improves aerobic capacity and enhances global vascular function in healthy individuals. **Aim:** To determine the impact of one year of supervised endurance exercise training on healthy individuals' vascular function and aerobic capacity. **Materials and Methods:** Over one year, seven health subjects (4 males and 3 females; 25 ± 5.2 yrs, 74.8 ± 14.6 kg) engaged in regular supervised cycling training three times per week, 60 minutes for each session. Aerobic capacity ($\dot{V}O_2\text{max}$) was assessed at entry (Baseline) and after 1, 2, 6, and 12 months; forearm vascular function was assessed at Baseline, 1, 4, 6, and 12 months. Catheters (20-gauge arterial cannula; BD) were placed in the brachial artery to measure arterial pressure and for drug infusion. Endothelium-dependent and -independent vasodilation were estimated by a cumulative increase in infusion rates of acetylcholine (10, 25, and 100 $\mu\text{g/L/min}$) and sodium nitroprusside (1.5, 3, and 6 $\mu\text{g/L/min}$). Mean arterial pressure (MAP), brachial artery diameter (BA), and blood velocity (BV) were simultaneously quantified (Doppler ultrasound) at the last 30 sec of each infusion rate. Blood flow (BF) was calculated as $\text{BF} = \text{BV} \cdot \pi \cdot (\text{BA}/2)^2 \cdot 60$. **Statistical analysis:** Data were analyzed using one-way repeated measures ANOVA. The area under the curve (AUC) was used to calculate the total BF response for each drug infusion. The AUC was calculated as the sum of the three infusion rates over the last 30-second period above the baseline values representing the total BF ($100/\text{mL} \cdot \text{min}^{-1}$). Data are expressed as mean \pm SD, with statistical significance accepted at $p < 0.05$. **Ethical:** The local institutional review board approved the study, and the subjects gave written informed consent. **Results:** Six months after the commencement of cycling training, a significant improvement in aerobic capacity was evident, with an increase in $\dot{V}O_2\text{max}$ from $40.1 \text{ mL} \cdot \text{min}^{-1} \cdot \text{kg}^{-1}$ to $50.8 \text{ mL} \cdot \text{min}^{-1} \cdot \text{kg}^{-1}$; $p = 0.02$. This enhancement continued over a year, resulting in an increase in $\dot{V}O_2\text{max}$ by 28 % (Baseline $40.1 \text{ mL} \cdot \text{min}^{-1} \cdot \text{kg}^{-1}$ vs. 12 months, $51.3 \text{ mL} \cdot \text{min}^{-1} \cdot \text{kg}^{-1}$; $p = 0.04$). The MAP remained stable during pharmacological challenges at all infusion rates and visits. The BF response curve (AUC) to acetylcholine and sodium nitroprusside across different visits was not different from baseline at any timepoint ($p > 0.05$). **Conclusion:** The preliminary results confirm that a year-long supervised endurance exercise training significantly increases aerobic capacity in healthy individuals. Contrary to our hypothesis, increased aerobic capacity was not followed by increased vascular function, suggesting that vascular health is already at its optimum in those who are untrained yet healthy subjects.

1. Hellsten Y, Nyberg M, Jensen LG, Mortensen SP. Vasodilator interactions in skeletal muscle blood flow regulation. *J Physiol* 590: 6297–6305, 2012. PMID: 22988140 2. Green DJ. Exercise

training as vascular medicine: direct impacts on the vasculature in humans. *Exerc Sport Sci Rev.* 2009 Oct;37(4):196-202 PMID: 19955869. 3. Maiorana A, O'Driscoll G, Dembo L, Goodman C, Taylor R, Green D. Exercise training, vascular function, and functional capacity in middle-aged subjects. *Med Sci Sports Exerc.* 2001 Dec;33(12):2022-8 PMID: 11740294. 4. Møller S, Hansen CC, Ehlers TS, Tamariz-Ellemann A, Tolborg SÁR, Kurell ME, Pérez-Gómez J, Patrzalek SS, Maulitz C, Hellsten Y, Gliemann L. Exercise Training Lowers Arterial Blood Pressure Independently of Pannexin 1 in Men with Essential Hypertension. *Med Sci Sports Exerc.* 2022 Sep 1;54(9):1417-1427. Epub 2022 Apr 12. PMID: 35420578. 5. Padilla J, Simmons GH, Vianna LC, Davis MJ, Laughlin MH, Fadel PJ. Brachial artery vasodilatation during prolonged lower limb exercise: role of shear rate. *Exp Physiol.* 2011 Oct;96(10):1019-27. Epub 2011 Jul 22. PMID: 21784788;

C13

Teamwork, proposal writing, and application-style assignments prepare undergraduates for research and science-related careers.

Michelle French¹, Helen Miliotis¹, Stavroula Andreopoulos⁴, Rebecca Laposa⁴, Christina Zakala⁵, Michelle Arnot³

¹Department of Physiology, University of Toronto, Toronto, Canada, ²Department of Physiology, Toronto, Canada, ³Department of Pharmacology and Toxicology, University of Toronto, Toronto, Canada, ⁴Department of Pharmacology and Toxicology, University of Toronto, Toronto, Canada, ⁵University of Toronto, Toronto, Canada

Undergraduate education serves to both broaden and deepen knowledge of a specific discipline while also aiming to develop transferrable skills. In terms of physiology majors, published transferable skills encompass four broad areas: critical thinking, communication, professional behaviours, and laboratory proficiency^{1,2}. While these skills are often developed through laboratory and independent research project courses, opportunities can be limited due to funding and space constraints. In addition, the size and need to cover content limits opportunities in lecture-based courses. More broadly, we observed that undergraduates were under-prepared for independent research courses and were unaware of the diverse range of science-related careers. To address this gap and help build transferrable skills, we created *Research Readiness and Advancing Biomedical Discoveries*, a third-year course for life science students. Central to the course is a scaffolded research proposal assignment aimed at solving real-world problems. Online pre-class modules and in-class group work cover topics such as project management and good laboratory practice (see <https://experientialmodules.utoronto.ca/research-readiness/>). To assess the usefulness of the course in the long term, we surveyed former students one to four years post course completion (Univ. Toronto REB#18345). Survey questions included statements rated on a five-point Likert scale and open-ended prompts. For the latter, two research assistants independently identified and grouped the responses into themes. Of the 63 former students who completed the survey (a 29% response rate), the majority (n = 52) had taken the course three or four years before. Almost two thirds were pursuing advanced degrees: the most common being in research-based graduate programs (41%). Most of the remainder were employed in science-related positions. Responses to the quantitative questions were favourable with students agreeing or strongly agreeing that the course improved their skill set to achieve future goals (4.14 +/- 0.10, mean +/- SEM, 4 = agree, 5 = strongly agree); consider flexible career paths (4.16 +/- 0.10) and in helping them prepare for research opportunities (4.00 +/- 0.12). The most common themes that emerged from the open-ended prompt: “*What aspects of the course helped with your current career pursuits*” were: working in teams (68% of respondents), developing and writing an original research proposal (68% of respondents) and applying your knowledge (59% of respondents). While this study was for a single course, we believe that our results are broadly applicable and encourage educators to incorporate teamwork, proposal writing, and assignments requiring the application of knowledge into the curriculum. Our results also illustrate the value of surveying former students to learn the aspects of a course that are most useful for graduates.

1. French MB et al. (2020) Adv Physiol Educ 44, 653-657. 2. Zubek J et al. (2023) Adv Physiol Educ 47, 117-123.

C14

Cheating or Not Cheating? A workflow for including critical appraisal when writing paragraphs using a large language model.

Matthew Hardy¹

¹*University of Bradford, Bradford, United Kingdom*

Since OpenAI made ChatGPT publicly available in November 2022, the use of large language models (LLMs) within academia and higher education has been widely scrutinised. Some points of view are critical of their use: using LLMs to generate written work has been considered akin to plagiarism, while software that can be used to identify work written using generative artificial intelligence (AI) is fallible. This suggests that the impact of LLM use may include restructuring of assessments and, in some cases, reverting to pen and paper-based submissions (Milano *et al.*, 2023). Alternatively, the accessibility and widespread use of LLMs suggests that they are tools that will become common in many future careers and thus there is a responsibility of academics to teach students how to use them ethically and effectively (Hardy, 2023). Indeed, Russel Group Universities have released a statement to this effect (Russel Group, 2023).

In response to this dilemma, this project aimed to develop a workflow utilising an LLM to include critical appraisal in paragraphs suitable for written academic work. This was to be done in a manner that would facilitate writing production, without reducing the need for understanding of the scientific content.

ChatGPT 4 was provided with a sequence of prompts that utilised a combination of Generate Knowledge Prompting (Liu *et al.*, 2021) and Prompt Chaining (Anthropic, 2024). The LLM was instructed that it would be provided with knowledge and it should then write a paragraph according to the following structure: Claim, Justification, Evidence, Conclusion. Constraints were provided that defined content and a range for the number of sentences for each part of the paragraph. Knowledge was provided that included appraisal from two journal articles, as well as providing a hierarchy regarding the importance of details. The resultant paragraph was refined by providing additional prompts for ease of reading, academic format, and to remove statements that could not be confirmed with the knowledge that had been provided. While ChatGPT 4 successfully produced a comprehensible paragraph, the text produced was identified as being generated by AI using the Turnitin AI-checker.

This workflow demonstrates that using LLMs can be a valid approach to producing written work and can be done without encouraging cognitive dissonance from the scientific content incorporated. Furthermore, using LLMs may provide more inclusive writing practices for authors who may have barriers to producing written content, for example, those for whom English is a second language. However, using such approaches provides content that will be identified as being generated by AI, which will impact future approaches to identifying and defining academic misconduct within written work.

Anthropic. <https://docs.anthropic.com/claude/docs/chain-prompts> /accessed 03 April 2024 Hardy M.E. (2023) The Impact of Artificial Intelligence on Teaching Writing Skills to Life Science Students.

Physiology News. 132, pp. 38-9. Liu, J., Liu, A., Lu, X., Welleck, S., West, P., Bras, R.L., Choi, Y. and Hajishirzi, H. (2021) Generated knowledge prompting for commonsense reasoning. arXiv preprint arXiv:2110.08387. Milano, S., McGrane, J.A. and Leonelli, S. (2023) Large language models challenge the future of higher education. Nature Machine Intelligence, 5(4), pp.333-334. Russell Group. (2023) New principles on use of AI in education. <https://russellgroup.ac.uk/news/new-principles-on-use-of-ai-in-education/> accessed 13 October 2023

C15

Ten Years of Worms: Development of an ‘Earthworm Action Potentials’ Practical Class

Matthew Mason¹

¹*University of Cambridge, Department of Physiology, Development & Neuroscience, Cambridge, United Kingdom*

Michael Foster, who introduced experimental physiology to Cambridge, used a frog sciatic nerve-muscle preparation in his practical classes. A very similar preparation was used to teach generations of medical, veterinary and natural science students over a period of around 140 years. However, obtaining frogs became increasingly difficult, and there was a desire to reduce the use of vertebrates in our classes. As a result, in 2014 we moved to the use of earthworms (*Lumbricus terrestris*) instead. We report here on the ‘Earthworm Action Potentials’ practical class which we have developed and refined over the last ten years, with a view to inspiring the development of similar introductory neurobiology classes in other physiology departments.

Worms, readily obtained from a fishing-bait supplier, are anaesthetized by immersion in a 15% ethanol solution for 7 minutes, and are then decapitated. Standard dressmakers’ pins are inserted at different positions along the length of the worm. Stimulating and recording electrodes attached to AD Instruments’ PowerLab system are connected to these pins and can be used to initiate action potentials in the worm’s median and lateral giant fibres. Because these are essentially single-fibre action potentials, the all-or-none law can be easily demonstrated. Experiments that students then perform within our three-hour class include measuring conduction velocity, refractory period, bidirectionality and effects of temperature. Following dissection to expose the nerve cord, students also investigate the effects of reducing sodium levels in the worm’s extracellular fluid. Unexpected findings from this class have led to final-year honours research projects using the same preparation, described separately in a cognate submission (Knight & Fraser).

A small minority of first-year students are uncomfortable with the use of worms in a practical class, and so we have developed an interactive, online tutorial for those who do not wish to participate. However, responses from students have generally been positive and the class has been welcomed by our neurobiology staff members, who see it as an excellent introduction to their field. This very simple preparation helps to meet many of the same learning objectives that were covered in the traditional frog sciatic nerve preparation, plus some new ones, but with minimal consumable cost and a much higher level of reliability.

[This submission forms one of a pair of submissions together with the abstract of Knight and Fraser. We are hoping that, if accepted, they could please be allocated adjacent slots within a teaching-focused podium session]

C16

Investigating action potential conduction velocity supernormality in Earthworm giant fibres as a student project.

James Fraser¹, Rosie Knight¹

¹*University of Cambridge, Cambridge, United Kingdom*

Introduction

In the 'Earthworm Action Potentials' practical class described in the companion abstract (Mason), it was clear that the simple preparation provides a stable platform with which to investigate some fundamental questions of nerve conduction. In comparison to amphibian and mammalian nerve preparations, benefits of the earthworm median fibre include single fibre recording, long length and relatively slow conduction, which together permit accurate measurement of conduction velocity. In particular, visual inspection of student recordings showed that the preparation demonstrated strong conduction velocity supernormality, a phenomenon whereby when one action potential immediately follows another, the second shows faster conduction.

Aims

The aetiology of conduction velocity supernormality has received considerable attention over the years but there is no unifying hypothesis that fully describes it. The earthworm nerve preparation offered an opportunity to further investigate the supernormality phenomenon as a final-years Honours research project.

Methods

Earthworms were prepared as described by Mason. They were placed within a chamber and each end was passed through holes in opposite sides that were then sealed with adhesive putty. This allowed the long central length of the worm to be exposed to worm Ringer at different temperatures, while keeping short end lengths of the worm sufficiently dry in the regions of the extracellular stimulation and recording electrodes.

Results

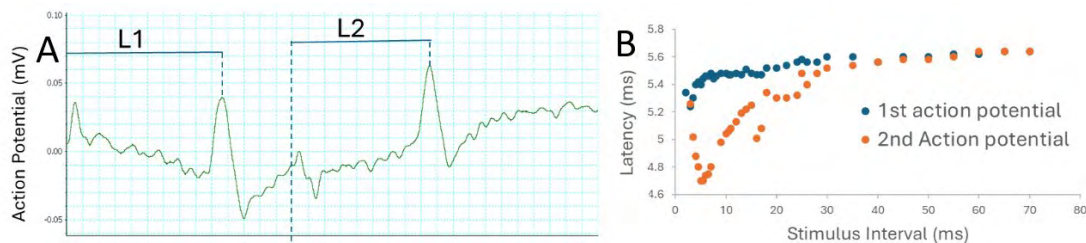
Figure 1A shows an example of two stimuli delivered with a 7 ms interval and the resultant extracellular action potential traces. The measurements of latency from each stimulus to each action potential peak is shown (marked L1 and L2). Pairs of stimuli were delivered with stimulus intervals ranging from less than the refractory period to the point where the first action potential had no influence on the latency of the second. *Figure 1B* shows the influence of stimulus interval on the latency of the first and second action potentials in each pair. As has been described previously in a range of different preparations, the second action potential of each pair shows a reduction in latency, representing an increase in conduction velocity, over a range of stimulus intervals. Note that even very small changes in latency (<<5%) are consistently detectable in this simple preparation. Exposure of the earthworm median giant fibre allowed an investigation into the

effects of changes in temperature and extracellular ion concentrations on the supernormality phenomenon.

Conclusions

The earthworm nerve preparation is quick and easy for a student to set up without the need for continuous academic supervision. As an invertebrate model, research students are able to conduct original experiments on live nerve fibres without any requirement for a Home Office licence. As a robust single-fibre preparation, it lends itself to experiments investigating the effects of extracellular ion concentrations, pH, temperature, osmolality or pharmacological agents for both teaching and research purposes.

Note This submission forms one of a pair of submissions together with the abstract of M. Mason. We are hoping that, if accepted, they could be allocated adjacent slots within a teaching-focused podium session.



C17

Decolonising the curriculum: healthcare inequalities faced by Gypsy, Traveller, Roma, Showmen and Boater Communities

Emílie Puttová¹, Iain Rowe¹, Marie Bowers¹

¹*University of Aberdeen, Aberdeen, United Kingdom*

Decolonising the curriculum is an ongoing process in our Universities as we identify areas where we can challenge the bias that has meant that marginalised communities are excluded from our traditional teaching approaches (1). To support this we need our students to be partners and agents of change, helping to improve and invigorate our physiology and medical science teaching. In this case study a final year Honours project focuses on contextualising healthcare inequalities faced by Gypsy, Traveller, Roma, Showmen and Boaters (GTRSB) communities to collate relevant information and consider how it could be best utilised in future teaching and outreach events.

A narrative review of Ovid and PubMed databases revealed a lack of peer-reviewed research publications, therefore a grey literature search of governmental, parliamentary and charity publications was performed to fill knowledge gaps (2,3). This produced 12 peer-reviewed papers and 28 grey literature sources which were synthesised to describe: who GTRSB communities are; moments of their history which may impact on current healthcare inequalities with a focus on the Tinker Experiments in Scotland and forced sterilisations of Roma women in the Czech Republic; present-day disparities in healthcare outcomes of GTRSB communities compared to mainstream society; proposed drivers of current healthcare inequalities; and proposed routes for improvement through education. Examples of the inequalities include: 6-7x higher suicide rates; reduced life expectancy by 10-15 years; 20x higher premature death of an offspring; 2-4x times higher risk of death/hospitalisation following COVID-19 diagnosis; all data compared to the wider population. A poster session within the Honours project timeline allowed some of the data to be presented to staff and students within Medical Sciences at the University of Aberdeen. This revealed a significant lack of knowledge of the GTRSB communities, their history, and current healthcare inequalities.

This work offers a unique Scottish and Central/Eastern European perspective on the topics of health inequalities and GTRSB communities. It has revealed that decolonising our curriculum can highlight bias and racism in our current approaches to communities that are often unseen in medical science teaching. Based on the lack of awareness of these issues within our own University community, and the scale of the healthcare inequalities identified, the next steps will focus on working with the diverse GTRSB communities to create inclusive teaching resources. We will use a community-informed activist-based model to improve our teaching and outreach.

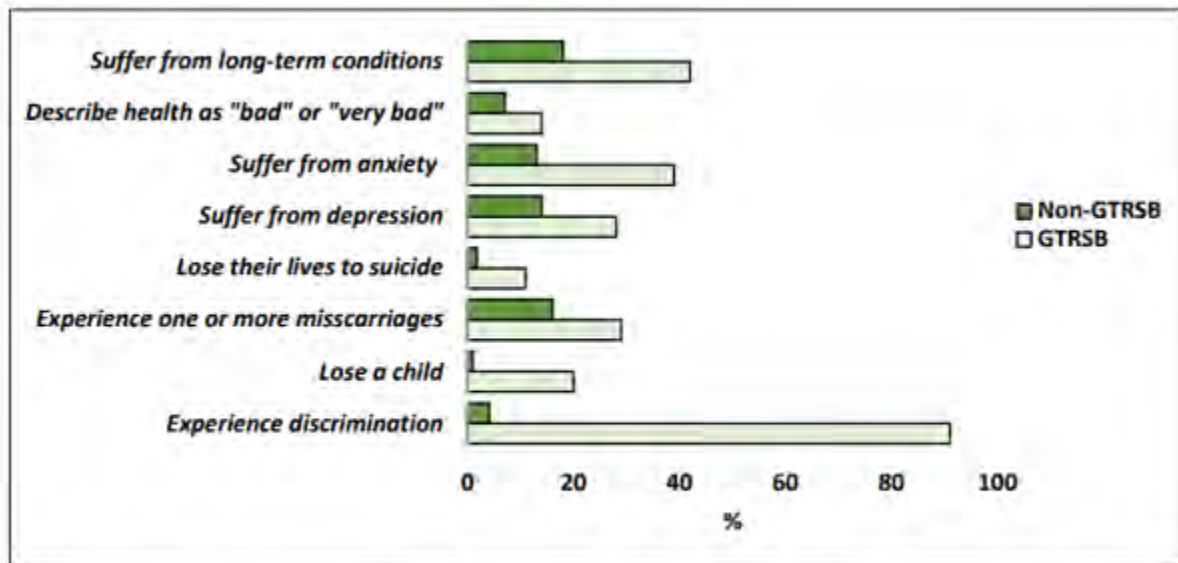


Figure 1. Health outcomes of GTRSB communities compared to non-GTRSB, where the x-axis shows the percentage of population affected and y-axis shows the health outcome in question.

(1) Lu et al. (2023) A framework for decolonising and diversifying biomedical sciences curricula: rediscovery, representation and readiness. bioRxiv. (2) All Ireland Traveller Health Study Team (2010). All Ireland Traveller Health Study: Summary of Findings. University College Dublin, pp.91–95. (3) Women and Equalities Committee (2019). Tackling inequalities faced by Gypsy, Roma and Traveller communities - Women and Equalities Committee Parliament. U.K

C18

The Importance of Re-establishing group work in post-Covid Physiology Laboratory Team Activities.

Elizabeth Sheader¹, Michelle Keown²

¹Faculty of Biology, Medicine and Health. The University of Manchester., Manchester, United Kingdom, ²Faculty of Biology, Medicine and Health. The University of Manchester., Manchester, United Kingdom, Manchester, United Kingdom

Society and learning approaches have changed over the last 5 years, particularly due to the Covid-19 pandemic with a notable shift towards independent and online learning approaches being observed. We have noticed an increased reluctance of some students to volunteer for roles within group settings and to engage with teamwork, as well as a decline in student confidence when working in teams. We feel laboratory practicals remain key in fostering interpersonal skills, promoting collaboration, improving self-esteem and reconnecting students by encouraging team-work opportunities.

This small study aims to evaluate student perceptions of in person face to-face team-based activity post pandemic in our 2nd year human volunteer exercise physiology projects.

Comprising two teams of 15, students were tasked with designing and implementing their projects, organising tasks, designing protocols and allocating roles to all team members.

The effectiveness of this approach was evaluated by questionnaire (n=26). 88% of students reported that the pandemic affected their experiences with group work. Initial data shows a positive experience with the face-to-face project format. 100% of students enjoyed the team format and the same number confirmed that the format motivated them to actively participate in the project. Furthermore, 23 out of the 26 students reported that the practical environment was inclusive and conducive to collaboration. When asked to rank factors that most positively influenced team-work and collaboration, the highest ranking factor was “face to face interaction” (Mode of 1) All students ranked “The pandemic has no effect on my experience of teamwork and collaboration” as the lowest factor.

Qualitative feedback, given in free text comments, supported the numerical values reported above, students repeatedly reported: (1) making friends more easily, (2) getting to know people better and (3) being more engaging than online interactions as important outcomes from this project format.

The initial findings of this study highlights, the pivotal role and benefit of teamwork in our physiology practical sessions and the importance of allowing students face-to-face activities to support their interpersonal skills development and overall learning. It suggests that face-to -face interaction can help to rebuild the social bonds that were weakened during the pandemic. By working in teams in the physiology laboratory, students may regain their confidence in their abilities to contribute effectively to a group setting. Group work allows students to learn from each other, benefit from diverse perspectives and appreciate the value of collaborative effort. It is also vital

Physiology in Focus 2024

Northumbria University, Newcastle, UK | 2 – 4 July 2024

preparation for professional opportunities as face- to-face group work in the curriculum could better prepare students for future employment.

C20

A students as partners approach to developing online interactive physiology content

Israth Miskin Sahibu¹, Sowda Dhaqane¹, Iain Rowe¹, Catriona Jane Cunningham¹

¹School of Medicine, Medical Sciences & Nutrition, University of Aberdeen, Aberdeen, United Kingdom

Physiology is widely considered to be a challenging subject by students on medicine and medical science degrees [1,2]. To increase student engagement and understanding of complex content, many educators have adopted active learning approaches. While active learning has been shown to be effective in improving exam performance across STEM subjects [3] there are challenges. This includes negative perceptions among students and lack of guidance for educators [4]. Personally, we have found active learning approaches can be more difficult to integrate with large class sizes.

Here, we share our experiences of student-led online interactive content creation. Our two resources were targeted at year 2 undergraduate medical sciences students (n=220) and year 1 undergraduate medical students (n=330) to supplement respective cardiovascular physiology teaching. Content was created using H5P (HTML5 Package) and hosted on a WordPress website.

The first resource developed was “Escape the Pharaoh’s Tomb” digital escape room. This consisted of a series of 6 interactive puzzles including a cipher and crossword. Correctly solving each puzzle revealed a code to “unlock” the door and allow the participant to progress to the next room. To simulate the physical escape room experience, a countdown timer which carried across pages was integrated into the design. Secondly, we developed a clinical case study about a patient presenting to his GP with atrial fibrillation and hypertension. The interactive elements included multiple choice questions, fill in the blanks and labelling a diagram.

The resources were shared with both cohorts of students via email and a QR code displayed during an in-person lecture. Anonymous feedback was collected using surveys (Microsoft Forms), including both Likert scales and free text questions. To assess interaction with the content, the H5PxAPlkatchu plugin was used to collect data including puzzle scores. Google Analytics was used to quantify number of page views and average time spent on each page.

The feedback for both resources was overwhelmingly positive. Over 90% of respondents (n=14) strongly agreed that the escape room was enjoyable and helped them apply their cardiovascular physiology knowledge. In the free-text comments, most students (n=7) found it engaging but some (n=3) reported difficulties with the ECG puzzle and found the clues confusing. This was reflected in

the analytics data which showed students spent more than twice as long on this puzzle than any other (557 vs. ≤ 224 s). All respondents (n=14) reported the case study was clear and 92.3% strongly agreed it was a good supplement to their lectures. Several positively commented that the case study covered a range of lecture content and it was useful for revision (n=5).

In conclusion, involving students as co-designers is a successful approach for developing new online interactive physiology content.

1. Bordes SJ, Manyevitch R, Huntley JD, Li Y, Murray IVJ. Medical student misconceptions in cardiovascular physiology. *Advances in Physiology Education*. 2021 Jun 1;45(2):241–9. 2. Michael J. What makes physiology hard for students to learn? Results of a faculty survey. *Advances in Physiology Education*. 2007 Jan;31(1):34–40. 3. Freeman S, Eddy SL, McDonough M, Smith MK, Okoroafor N, Jordt H, et al. Active learning increases student performance in science, engineering, and mathematics. *Proceedings of the National Academy of Sciences*. 2014 May 12;111(23):8410–5. 4. Rhodes A. Lowering barriers to active learning: a novel approach for online instructional environments. *Advances in Physiology Education*. 2021 Sep 1;45(3):547–53.

C21

Evaluating the implementation of online exam proctoring on physiology module attainment and student experience

Matthew Jones¹, Pika Miklavc²

¹Biomedical Research Centre, School of Science, Engineering and Environment, University of Salford, Salford, United Kingdom, ²Biomedical Research Centre, School of Science, Engineering and Environment, University of Salford, Salford, United Kingdom

Introduction

Online examination is a widely utilised strategy for higher education assessment due to its numerous benefits for universities, academic staff, and students. Exemplar benefits of online assessment include increased student flexibility to complete the exam and automated marking, decreasing academic workload (Huber et al., 2024). However, within the wider sector, online examinations have been shown to inflate grades due to students completing exams in groups or as open-book exams, meaning knowledge acquisition is inadequately tested (Newton & Essex, 2023). A phenomenon which became prominent during the rapid shift to online assessment during the COVID-19 pandemic.

To mitigate this, invigilation of online assessments using approaches known as proctoring has been suggested. Proctoring software utilises recording or artificial intelligence-based approaches to monitor student information associated with potential academic misconduct, thus ensuring online examinations are conducted under comparable conditions to in-person examinations (Nigam et al., 2021). With knowledge acquisition one of the key intended learning outcomes of physiology-based modules, developing a detailed understanding of proctored online examinations may benefit students and staff. This study aims to evaluate the impact of implementing online examination proctoring on student academic attainment, experience, and wellbeing.

Methods

Physiology-aligned module grade analysis was conducted using exam board data from 2022/23 (Unproctored) and 2023/24 (Proctored) academic years following ratification by internal and external moderation. The student experience was evaluated by the completion of an anonymous survey following the completion of proctored examinations. All questions used a 5-point Likert scale containing negative, neutral, and positive options. Survey questions related to student experience, academic integrity, and wellbeing. This study was approved by the University of Salford's ethical review board (Ethics ID: 11889).

Results

Evaluation of student attainment following proctoring implementation revealed a leftward shift in grade distributions following the addition of proctoring to online exams. This resulted from average exam grades significantly decreasing from $65.8 \pm 12.4\%$ ($n=307$) to $57.8 \pm 15.9\%$ ($n=274$) following the addition of proctoring ($P < 0.0001$). When compared to students' coursework grades achieved in the

same academic year, the disparity in attainment between assessment styles significantly increased from $7.7 \pm 14.5\%$ to $12.4 \pm 18.2\%$ following the implementation of exam proctoring ($n=273-300$; $P=0.0006$). Irrespective of proctoring status, there was a positive correlation between coursework attainment and exam attainment (Unproctored: $R=0.33$, $P<0.0001$, $n=300$; Proctored: $R=0.32$, $P<0.0001$, $n=270$).

A total of 36 students completed the student experience and wellbeing survey following proctored exams. Students stated that they believed proctoring negatively impacted their attainment (41.7% of respondents) but decreased academic misconduct (55.6%) and ensured exam conditions (72.2%). Only a third of respondents had positive experiences using proctoring with 38.9% stating they had a negative experience. Students revealed they were more nervous before proctored exams compared to unproctored ones (77.8%). The majority of students surveyed (72.2%) found proctoring easier and less stressful in subsequent proctored exams.

Conclusion

These data show that exam proctoring is an effective tool to combat grade inflation whilst simultaneously ensuring academic conduct and rigour in online examinations. However, its implementation may adversely impact student experience, which should be accounted for before its implementation.

Huber, E., Harris, L., Wright, S., White, A., Radulescu, C., Zeivots, S., Cram, A., & Brodzeli, A. (2024). Towards a framework for designing and evaluating online assessments in business education. *Assessment & Evaluation in Higher Education*, 49(1), 102-116. Newton, P. M., & Essex, K. (2023). How Common is Cheating in Online Exams and did it Increase During the COVID-19 Pandemic? A Systematic Review. *Journal of Academic Ethics*. <https://doi.org/10.1007/s10805-023-09485-5> Nigam, A., Pasricha, R., Singh, T., & Churi, P. (2021). A systematic review on AI-based proctoring systems: Past, present and future. *Education and Information Technologies*, 26(5), 6421-6445.

C22

The use of ‘hospital ward’ clinical simulations and escape games to enhance career development for physiology students studying Life Sciences courses

Sara Namvar¹

¹*University of Salford, Salford, United Kingdom*

Sara Namvar, Komal Amar, Matthew Jones, Nathan Connell, Danielle Mayo, Lee Forde and Niroshini Nirmalan

Introduction

There is an increasing focus in higher education on graduate employment outcomes, but we know that success is not only shaped by the quality of traditional classroom and laboratory-based teaching. Extensive evidence suggests that prior learning experiences, socioeconomic status, and the multiple forms of ‘graduate capital’ shape sense of belonging and confidence to reach one’s full potential. Physiology educators are under increasing pressure to think more creatively about how university experiences prepare all students, irrespective of prior learning or privileges for the world of work. The use of clinical scenarios is popular in healthcare programmes, but there is little training in this area for students undertaking Life Sciences courses, despite many such students intending to pursue postgraduate clinical careers.

Aim

The University of Salford runs a highly popular and successful mentorship programme for Life Sciences students hoping to pursue postgraduate clinical careers. We set out to introduce the use of clinical simulations and escape game-based learning that could provide students with insight into clinical decision making and enhance the existing preparation we offer for clinical interviews.

Methods

We designed four clinical scenarios that were then played out in the University of Salford cutting-edge hospital ward simulations facilities. Scenarios included a patient requiring cancer investigations, safeguarding issues surrounding a domestic violence case, ethical dilemmas around liver transplants and clinical observations under pressure in an immersive escape game. Each case unfolded in a separate ‘hospital room’ appropriately dressed to bring realism and excitement to the scenario, with academic actors as well as ‘talking’ and moving mannequins. Students rotated between each room every 15min, followed by a debriefing session at the end.

Results

A total of 65 students from several programmes took part in this extracurricular opportunity, many from BAME backgrounds and low participation neighbourhoods. Most students indicated a strong interest in pursuing a postgraduate Medicine or Physician Associate career, with 100% reporting they enjoyed the experience and would like to see such experiences embedded into programmes.

Over 90% of students felt the experience helped develop their confidence and communication skills, whilst 87% felt it improved their employability. Examples of feedback included *'It was such a wonderful experience and I hope there will be more sessions like this...'* and *'I enjoyed having alumni back ... along with the simulations which enabled us to have a real understanding of what to expect'*.

Conclusion

Collectively we present evidence of the value that clinical simulations and escape games add to the development of transferable employability skills in a fun and engaging manner for Life Sciences students. Co-creating such experiences with alumni and working across Schools is an important approach to developing Life Sciences graduates that are better prepared for the world of work.

C23

Comparison of undergraduate science student evaluation of skills confidence before and after Objective Structured Practical Examinations (OSPEs)

Alison Jenkinson¹, Derek Scott¹

¹*University of Aberdeen, Aberdeen, United Kingdom*

Introduction: Increasing student numbers and diversity of academic backgrounds, combined with the need to effectively evidence practical and employability skills has challenged traditional delivery of core practical skills (Lakshmipathy, 2015; Hultgren et al., 2023). We have been pioneering the use of Objective Structured Practical Examinations (OSPEs) in medical science teaching and have reported successful delivery of theoretical, practical and problem-solving skills at multiple stations to formally examine a wide range of communication and science laboratory practical skills (Scott et al., 2018). Feedback from students has indicated that they find this assessment approach challenging but, overall, a positive experience. However, we lack information regarding student perceptions of their skills and whether they felt the OSPE experience helped them improve these.

Aims: We aimed to assess students' evaluations of their own confidence in practical and transferable skills before and after the OSPE.

Methods: Prior to attending a practice session, students were encouraged to consider their level of confidence in the skills assessed during the OSPE - general laboratory skills, time management (both organising time and dealing with time pressures), communication skills, and awareness of both ethics and laboratory health and safety. An audit of questionnaire data collected during this process demonstrated that 83% of final year undergraduate students from anatomy, physiology, pharmacology and sport science degrees completed the pre-OSPE skills evaluation questionnaire (n = 76) and 48% (n= 44) the post-OSPE questionnaire. Students also considered whether the OSPE would improve awareness of skill levels and the post-OSPE questionnaire issued after the assessment session encouraged exploration of skill strengths and weaknesses.

Results: Pre-OSPE students were least confident in general laboratory skills and aspects of time management. After the OSPE assessment levels of confidence were generally improved in all areas with the proportion of students expressing good or high levels of confidence increasing in several areas e.g. Extreme and Somewhat Confidence in Lab skills pre-and post-OSPE increased from 63.2% to 90.9% (P=0.0009, Z score test), Lab Health & Safety 84.2% to 97.8% (P=0.02). There was no significant difference in communication skills (Pre 85.6%, Post 84.1%). The OSPE was considered to be helpful with identifying strengths and weaknesses and improving awareness of skill levels.

Conclusions: These results suggest that confidence in and awareness of both practical laboratory and key employability skills may be positively influenced by practical assessment approaches. The OSPE may encourage students to consider their strengths and weaknesses. However, although confidence in these skills generally improved following preparation, practice and delivery of the assessment, some aspects (e.g. one to one communication skills and managing time under

pressure) were particularly highlighted as areas where students recognised that further skill development was required. This has given staff a better awareness of skills gaps and the inclusion of this assessment at the beginning of the Honours year allows students time to develop skills they felt needed enhancement. Our hope is that this approach will help students enhance their employability.

Lakshmipathy, K (2015) MBBS student perceptions about physiology subject teaching and objective structured practical examination based formative assessment for improving competencies. *Adv Physiol Educ* 39(3), 198-204 <https://doi.org/10.1152/advan.00073.2014>
Hultgren C, Lindkvist A, Curbo S, Heverin M (2023) Students' performance of and perspective on an objective structured practical examination for the assessment of preclinical and practical skills in biomedical laboratory science students in Sweden: a 5-year longitudinal study. *J Educ Eval Health Prof* (20), 13 DOI: <https://doi.org/10.3352/jeehp.2023.20.13>
Scott DA, Kirkman J, Malcolm CJ, Jenkinson AM (2018) Use of student-created video resources to enhance practical training in Objective Structured Practical Examinations (OSPE's). *Proc Physiol Soc* 41, PCB083

C24

Rubric-based assessment of Flipped Classroom Presentations – A Marker's Perspective

Marta Woloszynowska-Fraser¹, Ella Maysami¹, Simon Trent¹

¹*Keele University, Newcastle-under-Lyme, United Kingdom*

This study explores the use of rubric in the flipped classroom presentations assessment in the final year neuroscience module Behavioural Neuroscience at Keele University (from 2020 to current 2024 cohort). Students are tasked with delivering presentations in a flipped classroom format, where they take ownership of their learning by preparing and delivering content. Staff employ a predefined rubric to evaluate student performance across various four domains including verbal skills, visual aids, content, organisation, and teamwork, with a total of 17 specific criteria (adapted from Peeters et al., 2010). Presentations, each lasting 45 minutes, are recorded for assessment, with one marker present during the presentation and a second marker assessing the presentation from the recording. By engaging students in active learning through presentation preparation, the flipped classroom model promotes deeper comprehension and retention of course material. Meanwhile, the use of a rubric for assessment ensures clarity and consistency in grading, guiding markers in evaluating presentations based on predefined criteria. Additionally, the rubric is explained during a tutorial and readily available afterwards, thereby providing students with clear expectations, enabling them to focus on key aspects of their presentations and align their efforts with assessment criteria. Moreover, the integration of rubric-based assessment enhances the comprehensiveness of evaluation in the final year module. By encompassing various dimensions of presentation quality, including verbal communication, visual aids, content coherence, organisation, and collaborative skills, the rubric offers a holistic assessment of student performance. This comprehensive evaluation approach provides valuable insights into students' abilities beyond mere content knowledge, such as their communication proficiency and teamwork skills, which are essential for success in academia and beyond. Nevertheless, there are some challenges with this approach, such as ensuring consistency in the application of the rubric across different markers and presentations requires clear guidelines. Additionally, technical issues related to recording quality and accessibility may arise, impacting the reliability of assessment data. In conclusion, the integration of rubric-based assessment into flipped classroom presentations offers a promising avenue for enhancing final year module evaluation. By combining the active learning benefits of flipped classroom pedagogy with the clarity and comprehensiveness of rubric-based assessment, educators can foster student engagement and provide meaningful feedback on presentation skills. However, addressing logistical challenges and ensuring robust assessment procedures are essential for the successful implementation of this approach.

Peeters, M. J., Sahloff, E. G., & Stone, G. E. (2010). A Standardized Rubric to Evaluate Student Presentations. *American Journal of Pharmaceutical Education*, 74(9), 171.
<https://doi.org/10.5688/aj7409171>

C25

Regulation of the NaCl cotransporter NCC and blood pressure by the ubiquitin E3 ligase CHIP

Mariavittoria D'Acierno¹, Robert Little¹, Jonathan C Schisler², Vladimir Matchkov¹, Robert A Fenton¹

¹*Department of Biomedicine, Aarhus University, Aarhus, Denmark,* ²*Department of Pharmacology, University of North Carolina, Chapel Hill, United States*

The activity of the thiazide-sensitive sodium-chloride cotransporter NCC within the kidney distal convoluted tubule (DCT) is crucial for modulating blood pressure (BP). Emerging evidence also suggests that alterations in NCC activity play a pivotal role in the effects of dietary potassium (K⁺) on BP. Greater dietary K⁺ intake lowers NCC abundance and activity, which is often associated with reduced BP. Our previous studies have demonstrated that during high K⁺ intake there is greater ubiquitin-dependent NCC degradation, a process that involves an interaction between heat shock protein 70 (Hsp70) and NCC, and is potentially orchestrated by the ubiquitin E3 ligase CHIP (carboxy-terminus of Hsc70-interacting protein) (1). To validate this mechanism, we investigated the role of CHIP in modulating NCC activity *in vivo* and its implications for BP control.

Methods: CHIP knockout (KO) and wildtype (WT) control mice were fed diets with variable K⁺ content; low (0% K⁺), normal (1%), or high (5%) for 5 days. BP measurements on the various diets or after treatment with the NCC inhibitor hydrochlorothiazide (HCTZ) (37.5 mg/kg BW) or the epithelial sodium channel (ENaC) inhibitor amiloride (5 mg/kg BW) were obtained using telemetry (24 h readings) or tail cuff plethysmography (early evening). To examine NCC half-life, *ex vivo* kidney tubule suspensions from KO and control mice were incubated in control media (4.0 mM K⁺) containing cycloheximide and actinomycin for various time points and NCC expression was evaluated by immunoblotting.

Results: On a normal K⁺ diet, CHIP KO mice had elevated NCC protein levels (n = 5/ group; p<0.0001), but NCC mRNA levels were not significantly different between the genotypes. CHIP KO mice had higher BP compared to WT controls (n = 8/group; p<0.001) on a normal diet. Inhibition of NCC activity using hydrochlorothiazide normalized BP in the CHIP KO mice to similar levels as WT mice (n = 4-5/group; p<0.001), emphasizing NCC's predominant role in the observed higher BP phenotype. Inhibition of ENaC activity with amiloride had a similar effect to lower BP in WT and CHIP KO mice (n = 4-5/group; p<0.05). The ability of a high K⁺ diet to reduce NCC abundance was attenuated in CHIP KO mice (n = 4-5/group; p<0.0001). In *ex vivo* tubule suspensions from CHIP KO mice, NCC half-life was prolonged compared to WT controls (n = 3/group with 3 technical replicates; p <0.05), suggesting a role for CHIP in NCC degradation.

Conclusions: Our findings highlight the critical involvement of CHIP-mediated NCC ubiquitylation for regulating NCC abundance and BP. Preliminary studies also suggest a role for CHIP in mediating the effects of higher dietary potassium intake on NCC. Understanding the molecular mechanisms governing NCC regulation may offer valuable insights into hypertension pathophysiology and facilitate the development of targeted therapeutic interventions.

(1) Kortenoeven, MLA. et al., J Biol Chem 297, (2):100915 (2021)

C26

Interstitial cell of Cajal-like cells (ICC-LC) exhibit dynamic spontaneous activity but are not functionally innervated in mouse urethra

Neha Gupta¹, Salah Baker², Kenton Sanders², Caoimhin Griffin¹, Mark Hollywood¹, Gerard Sergeant¹, Bernard Drumm¹

¹Dundalk Institute of Technology, Dundalk, Ireland, ²University of Nevada, Reno School of Medicine, Reno, United States

Urethral smooth muscle cells (USMC) sustain tonic contractions to occlude the internal urethral sphincter during bladder filling. Interstitial cells also exist in urethral tissues and are hypothesized to influence USMC behaviours and neural responses. These cells are similar to Kit⁺ interstitial cells of Cajal (ICC), gastrointestinal pacemakers and neuroeffectors. Isolated cell studies of urethral ICC-like cells (ICC-LC) exhibit spontaneous intracellular Ca²⁺ signalling behaviours linked to proposed roles as USMC pacemakers and neuromodulators similar to ICC in the gut, although observation and direct stimulation of ICC-LC within intact urethral tissues is lacking. Using a mouse line with cell-specific expression of the Ca²⁺ indicator GCaMP6f, driven off the Kit promoter (Kit-GCaMP6f mice), we unequivocally identified ICC-LC within *in situ* urethra preparations and characterized their activity. Across 54 cells imaged from 13 animals, ICC-LC fired spontaneous Ca²⁺ waves that propagated on average 40.1 ± 0.7 mm, with varying amplitudes (0.08 - 1.96 DF/F₀), which originated from multiple firing sites per cell (average 3.1 ± 0.2). ICC-LC imaged from Kit-GCaMP6f urethra did not form interconnected networks. ICC-LC activity was uncoordinated across multiple cells with no obvious entrainment of ICC-LC. ICC-LC Ca²⁺ event frequency was unaffected by the L-type Ca²⁺ channel inhibitor nifedipine (P=0.25, n=5) but was abolished by cyclopiazonic acid (P=0.0005, n=6) and decreased by an inhibitor of store-operated Orai Ca²⁺ channels (GSK-7975A, P<0.0001, n=6). While the α-adrenoceptor agonist phenylephrine increased Ca²⁺ wave frequency (P=0.0007), amplitude (P=0.04) and spread (P=0.14) (n=6), the nitric oxide (NO) donor DEA-NONate had no effect (n=7). Electrical field stimulation (EFS, 10 Hz) of intrinsic nerves under excitatory (n=6) or inhibitory conditions (n=7) failed to elicit responses in ICC-LC. In contrast, EFS of ICC from Kit-GCaMP6f colon yielded consistent excitatory (cholinergic, n=3) and inhibitory (nitroergic, n=5) postjunctional responses. We conclude urethral ICC-LC are spontaneously active but are not functionally innervated.

C27

Maternal, paternal and combined parental obesity impact fetal growth via parent-specific and combined effects on placental morphology and transport function.

Sachi Gwalani¹, Jonas Zaugg², Edina Gulacsi¹, Jorge Lopez-Tello¹, Amanda Sferruzzi-Perri¹

¹Centre for Trophoblast Research, Department of Physiology, Development and Neuroscience, University of Cambridge, UK, Cambridge, United Kingdom, ²Centre for Trophoblast Research, Department of Physiology, Development and Neuroscience, University of Cambridge, UK, Cambridge, United Kingdom

Introduction

Concerningly, 20% of women and 14% of men are estimated to be obese by 2030¹. The reproductive effects of maternal and paternal obesity have been investigated independently and include subfertility, fetal growth abnormalities, gestational disorders and adverse offspring health^{2,3,4}. We hypothesise that two obese parents have divergent and compounded effects on male and female fetal growth associated with unique effects on placental morphology, transport and imprinted gene expression.

Aim

To assess the individual and combined role of parental obesity on fetal development, placental morphology and transport.

Methods

Female and male mice were fed a chow diet (11% fat, 7% sugar) or obesity-inducing high-fat/high-sugar diet (38% fat, 33% sugar). They were time-mated 5 weeks later, creating 4 pregnancy groups and females continued on the diet they consumed prior to mating. Stereological analyses on placentas (embryonic day 18.5; 4-6 fetuses/group) of gross morphology (point counting), interhaemal membrane thickness (length measurements), surface area for exchange (SA; cycloid arc intersections) and glycogen deposition (ImageJ analysis) were conducted following Haematoxylin and Eosin staining, Periodic acid-Schiff staining and double-label immunohistochemistry (4-6 replicates/group)⁵, respectively. Relative mRNA expression of imprinted genes and nutrient transporters was measured by RT-qPCR (6-8 fetuses/group; 1-2 fetuses/litter). To assess *in vivo* transplacental transport (>11 fetuses/group; 1-2 fetuses/litter), anaesthesia was induced in dams on embryonic day 18 by 90.9mg/kg Ketamine + 4.55mg/kg Xylazine via intraperitoneal injection (0.01mL/g body weight), followed by injection of radiolabelled glucose/amino acid analogues into the jugular vein.

Results (data quoted as mean±SEM)

Male and female fetuses: Combined parental obesity reduced fetal weight relative to controls (734.0±8.202mg vs 777.8±10.54mg; p=0.0459; one-way ANOVA). Paternal obesity increased trophoblast volume (14.16±0.7277mm³ vs 9.274±1.126mm³; p=0.0031; one-way ANOVA) and

maternal obesity increased interhaemal membrane thickness ($5.177 \pm 0.06273 \mu\text{m}$ vs $4.378 \pm 0.1919 \mu\text{m}$; $p=0.0230$; Kruskal-Wallis test) relative to controls. Combined parental obesity increased glycogen deposition relative to controls ($2.731 \pm 0.6736\%$ vs $0.8152 \pm 0.2813\%$; $p=0.0242$; one-way ANOVA) and reduced theoretical diffusion capacity relative to paternal obesity ($0.008240 \pm 0.0003738 \text{cm}^2 \cdot \text{min}^{-1} \cdot \text{kPa}^{-1}$ vs $0.01047 \pm 0.0003094 \text{cm}^2 \cdot \text{min}^{-1} \cdot \text{kPa}^{-1}$; $p=0.0452$; Kruskal-Wallis test).

Male fetuses: Combined parental obesity reduced fetal weight ($744.0 \pm 10.40 \text{mg}$ vs $800.7 \pm 9.069 \text{mg}$; $p=0.0225$; one-way ANOVA), increased relative brain weight (0.07795 ± 0.001488 vs 0.06748 ± 0.003793 ; $p=0.0214$; Kruskal-Wallis test) compared to controls and decreased relative liver weight compared to paternal obesity (0.04370 ± 0.0005922 vs 0.04917 ± 0.001412 ; $p=0.0470$; one-way ANOVA), indicating asymmetric growth restriction. Maternal blood space SA was reduced in combined parental obesity ($15.20 \pm 0.5187 \text{cm}^2$ vs $23.95 \pm 1.668 \text{cm}^2$; $p=0.0282$; one-way ANOVA) relative to paternal obesity. Combined parental obesity reduced relative *H19* (-0.7055 ± 0.1045 vs 0 ; $p=0.0002$; one-way ANOVA), *Igf2* (-0.2911 ± 0.06285 vs 0 ; $p=0.0373$; one-way ANOVA) and *Slc2a1/GLUT1* (-0.2771 ± 0.04968 vs 0 ; $p=0.0158$; one-way ANOVA) expression compared to controls. Reductions in glucose and amino acid placental transfer in maternal and combined parental obesity, respectively, were normalised by average SA.

Female fetuses: Fetal and placental weight/morphology were unaltered by parental obesity. *H19* expression was reduced in combined parental obesity relative to maternal obesity (-0.4861 ± 0.1163 vs 0.1954 ± 0.2225 ; $p=0.0089$; one-way ANOVA).

Conclusion

Singular and combined parental obesity compromise fetal growth via sex-specific, parent-specific and combined effects on placental morphology, nutrient transporter and imprinted gene expression. Such changes would disturb transplacental transfer and highlight the reproductive ramifications of obesity/calorie-dense diets in both parents.

References 1 One billion people globally estimated to be living with obesity by 2030 (no date) World Obesity Federation. Available at: <https://www.worldobesity.org/news/one-billion-people-globally-estimated-to-be-living-with-obesity-by-2030> (Accessed: 19 February 2024). 2 Lean, S.C. et al. (2022) 'Obesogenic diet in mice compromises maternal metabolic physiology and lactation ability leading to reductions in neonatal viability', *Acta Physiologica*, 236(2), p. e13861. Available at: <https://doi.org/10.1111/apha.13861> (Accessed: 2 January 2024). 3 Lin, J., Gu, W. and Huang, H. (2022) 'Effects of Paternal Obesity on Fetal Development and Pregnancy Complications: A Prospective Clinical Cohort Study', *Frontiers in Endocrinology*, 13. Available at: <https://www.frontiersin.org/articles/10.3389/fendo.2022.826665> (Accessed: 3 January 2024). 4 McPherson, N.O. et al. (2015) 'When two obese parents are worse than one! Impacts on embryo and fetal development', *American Journal of Physiology-Endocrinology and Metabolism*, 309(6), pp. E568–E581. Available at: <https://doi.org/10.1152/ajpendo.00230.2015> (Accessed: 6 January 2024). 5 De Clercq, K. et al. (2020) 'Double-label immunohistochemistry to assess labyrinth structure of the mouse placenta with stereology', *Placenta*, 94, pp. 44–47. Available at: <https://doi.org/10.1016/j.placenta.2020.03.014> (Accessed: 17 October 2023).

C28

E. coli Nissle improves short-chain fatty acid absorption, microbial composition, and gut barrier function in the inflamed cecum of *slc26a3*^{-/-} mice

Zhenghao Ye¹, Qinghai Tan^{1,2}, Sabrina Woltemate¹, Xinjie Tan^{1,3}, Dorothee Römermann¹, Guntram Grassl¹, Marius Vital¹, Ursula Seidler¹, Archana Kini¹

¹Hannover Medical School, Hannover, Germany, ²Tongji Medical School, Wuhan, China, ³Zhejiang University Medical School, Hangzhou, China

Background

Defects in *SLC26A3*, the major colonic Cl⁻/HCO₃⁻ exchanger, result in chloride-rich diarrhea, a reduction in short-chain fatty acids (SCFA) producing bacteria, and a high incidence of inflammatory bowel disease (IBD) in humans and in mice. *Slc26a3*^{-/-} mice are therefore an interesting animal model for spontaneous but mild colonic inflammation, and for testing strategies to reverse or prevent the inflammation. This study investigates the effect of *E. coli* Nissle (EcN) application on the microbiome, SCFA production, barrier integrity and mucosal inflammation in *slc26a3*^{-/-} mice.

Methods

In vivo fluid absorption and bicarbonate secretion were assessed in the gut of *slc26a3*^{+/+} and *slc26a3*^{-/-} mice before and during luminal perfusion with 100mM sodium acetate. Age-matched *slc26a3*^{+/+} and *slc26a3*^{-/-} mice (13 wt and 12 ko) were intragastrically gavaged twice daily with 2×10⁸ CFU/100μL of EcN for 21 days. Body weight and stool water content were assessed daily, stool and tissues were collected for further analysis. The data was analysed using Graphpad Prism Version 8.0.2. The unpaired Student's *t* test was used for parametric data with normal distribution or non-parametric Mann-Whitney U test for the comparisons within genotypes and/or between control and EcN-treated groups. For the microbial 16s rRNA gene analysis, the analysis, alpha-diversities, and non-metric multidimensional scaling (NMDS) based on relative abundance data were conducted using the phyloseq package (McMurdie & Holmes, PlosOne 2013).

Results

Luminal addition of sodium acetate significantly increased both fluid absorption and luminal alkalization in the *slc26a3*^{-/-} mice. Gavage with EcN resulted in significantly improving overall SCFA levels and the expression of its transporters primarily in the *slc26a3*^{-/-} cecum, the predominant habitat of EcN in mice (n=12-13, p<0.05). This was accompanied by an increase in mucus producing goblet cells, a decrease in the expression of inflammatory markers as well as of host defense anti-microbial peptides. EcN did not improve the overall diversity of the luminal microbiome, but resulted in a significant increase in SCFA producers *Lachnospiraceae* and *Ruminococcaceae* in the *slc26a3*^{-/-} feces (n=7 for *slc26a3*^{+/+} and *slc26a3*^{-/-} w/o EcN: n=12 for *slc26a3*^{+/+} and n=13 for *slc26a3*^{-/-}, p<0.05).

Conclusions: These findings suggest that EcN is able to proliferate in the inflamed cecum of the *slc26a3*^{-/-} mice, resulting in increased microbial SCFA production, decreased inflammation, and improved gut barrier properties. In sufficient dosage, probiotics may thus be an effective anti-inflammatory strategy in the diseased gut.

C29

The antimicrobial peptide cathelicidin gates the bacterial survival in urine from newly renal transplanted recipients

Laura Vang Sparsø², Aimi Danielle Klostergaard Hamilton², Lene Ugilt Pagter Ludvigsen^{1,3}, Bente Jespersen^{1,3}, Mathias Skov², Helle Prætorius²

¹*Department of Clinical Medicine, Aarhus University, Aarhus, Denmark,* ²*Department of Biomedicine, Aarhus University, Aarhus, Denmark,* ³*Department of Renal Medicine, Aarhus University Hospital, Aarhus, Denmark*

Introduction:

Urinary tract infections (UTIs) are one of the most common types of infections in humans. Renal transplant recipients are known to be especially prone to these infections, which can lead to renal damage and graft dysfunction. Normally, the urinary tract is sterile, and antimicrobial peptides (AMPs) play an important role in this as part of the innate immune system. AMPs are generally released into the urine in response to inflammation¹. Here, we hypothesise that urine concentration of cathelicidin determines the survival of uropathogenic *E. coli* in the urinary tract of newly renal transplanted recipients.

Methods:

Urine was collected on day 4 after renal transplantation at Aarhus University Hospital (n=50) and from healthy gender and age-matched controls (n=50). Growth and damage (propidium iodide (PI) assay) of uropathogenic *E. coli* strain RAR0001 (resistant to sulfamethoxazole and trimethoprim) in the human urine samples was determined by flowcytometry. Urine concentrations of cathelicidin (LL-37), Human b-defensin 1 (HBD-1), lipocalin-2 and uromodulin were determined by ELISA. Direct effect of purified cathelicidin on bacterial damage and lysis was addressed by adding increasing concentrations of cathelicidin measuring damage with a PI-assay and by Green Fluorescence Protein (GFP) release from GFP-producing *E. coli*.

Results:

The current study represents preliminary data from 14-36 transplant patients and matched controls, depending on the assay. Urine from renal transplant recipients had a statistically significantly higher mean concentration of the AMPs cathelicidin, HBD-1 and Lipocalin-2 compared to controls (table 1), even though the urine was more dilute as indicated by a lower osmolality and creatinine concentration compared to controls (table 1). Notably, urine uromodulin concentrations were reduced markedly more in renal transplant recipients compared to controls than what could

be explained by dilution. Corresponding to the high urinary AMP levels, RAR0001 had a mean of 19.9 ± 2.2 % PI-positive bacteria after one hour of incubation in urine from renal transplanted patients (n=33). In contrast, there were only 7.4 ± 0.95 % PI-positive RAR0001 in urine from controls (n=33) after one hour of incubation (Figure 1, $p < 0.0001$, Mann-Whitney test). Moreover, we confirm that cathelicidin is bactericidal in the used *E. coli*, since cathelicidin concentration-dependently (0-10 μ M) increased the lysis of GFP-producing *E. coli* (n=3), and cathelicidin (10 μ M for four hours) caused 91.5 ± 1.2 % RAR0001 *E. coli* to become PI positive (n=3).

Conclusion:

Recently renal transplanted recipients have significantly higher levels of the antimicrobial peptides cathelicidin, HBD-1 and Lipocalin-2, and our *in vitro* studies confirm bactericidal properties of cathelicidin in uropathogenic *E. coli*. *E. coli* is markedly more damaged in urine from these patients compared to urine from healthy controls. We speculate this to be caused by inflammation-induced cathelicidin secretion to the pre-urine caused by the transplantation and propose that higher levels of antimicrobial peptides in the urine can be protective against UTIs in the acute phase after transplantation.

	Renal transplant patients (Mean \pm SEM)	Controls (Mean \pm SEM)	P-value (Mann-Whitney test)
Cathelicidin (ng/ml), n=23	16.7 ± 2.8	2.7 ± 0.3	P<0.0001
HBD-1 (ng/ml), n=27	3.9 ± 0.3	2.1 ± 0.3	P<0.0001
Lipocalin-2 (ng/ml), n=27	14.8 ± 4.2	1.5 ± 0.3	P<0.0001
Uromodulin (ng/ml), n=14	1906 ± 333	10978 ± 1934	P<0.0001
Creatinine (mM), n=36	7.4 ± 0.6	11.0 ± 0.9	P=0.0032
Osmolality (mOsmol/kg), n= 33	409 ± 19.5	633 ± 43.9	P=0.0004

Table 1. Concentration of the AMPs Cathelicidin, HBD-1, Lipocalin-2 and Uromodulin and osmolality and creatinine concentration of urine samples from recently renal transplanted patients and healthy age and gender-matched controls. Data are presented as mean \pm SEM. Statistical analysis was performed with a Mann-Whitney test.

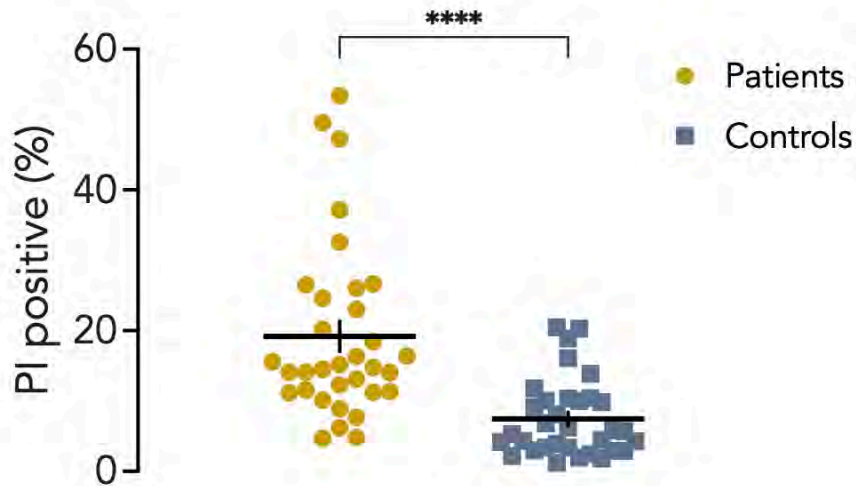


Figure 1. Propidium iodide (PI) positive percentage after one hour of incubation in urine from recently renal transplanted patients and healthy age and gender-matched controls (n=33). Data are presented as mean \pm SEM. Statistical analysis was performed with a Mann-Whitney test. $P < 0.0001$.

1. Lindblad A, Wu R, Persson K, et al. The Role of NLRP3 in Regulation of Antimicrobial Peptides and Estrogen Signaling in UPEC-Infected Bladder Epithelial Cells. *Cells* 2023;12(18) doi: 10.3390/cells12182298 [published Online First: 20230918]

C30

The role of Aquaporin-2 in cyst progression in Autosomal Dominant Polycystic Kidney Disease

Vishalini Venkatesan¹, Robert A. Fenton², Emma Tina Bisgaard Olesen¹

¹*Department of Biomedical Sciences, University of Copenhagen, Copenhagen N, Denmark,*

²*Department of Biomedicine, Aarhus University, Aarhus C, Denmark*

Introduction: Cystogenesis in Autosomal Dominant Polycystic Kidney Disease (ADPKD) is caused by a mutation in the genes encoding polycystin-1 or 2 (Pkd1/Pkd2), and involves dysregulated fluid transport in the kidney tubules. ADPKD patients present with a urinary concentrating defect, even prior to decreased glomerular filtration rate despite higher plasma vasopressin levels. Hence, we investigated whether vasopressin-mediated aquaporin-2 (AQP2) trafficking and water balance are dysregulated in ADPKD and lead to cyst expansion.

Methods: Doxycycline-inducible, kidney-tubule-specific Pkd1 knock-out (KO) mice (Pax8; tetO-Cre; Pkd1^{flox/flox}) and control littermates (Pax8; tetO-Cre; Pkd1^{wt/wt}) were treated with doxycycline on postnatal (PN) day 10, 11 and 12. On PN day 21, dDAVP (0.1 µg/kg), a synthetic analog of vasopressin, was administered as a single intraperitoneal (IP) injection and mice were euthanized after 6 hours (acute studies). For long term studies, dDAVP (0.1 µg/kg) was administered IP for 5 days (PN day 17 to 21). Urine samples were collected for osmolality measurements, and kidneys were harvested for western blotting and immunohistochemistry (IHC). A novel polycystin-1 deficient mouse cortical collecting duct cell line (mpkCCD-Pkd1^{-/-}) was developed using the CRISPR/Cas9 technique, and validated through PCR, western blotting, 3D cell morphogenesis, and cAMP assays.

Results: At 3 weeks of age, KO mice (n=3) had lower urine osmolality at baseline compared with control mice (n=5) (481.7 versus 1874 mOsm/Kg; p≤ 0.01). Urine osmolality increased with dDAVP administration in the control mice (p≤ 0.001), whereas no response was noted in the KO mice. In long-term studies, AQP2 expression increased and was apically targeted with dDAVP treatment in the renal cortex and inner medulla of both control (n=4) and KO mice (n=4). However, AQP2 expression was lower in the inner medulla of both saline (p<0.01) and dDAVP-treated (p<0.01) KO mice compared to controls. IHC indicated that NKCC2 and NHE3 protein expression were reduced in the whole kidneys of KO mice. Large cysts were observed in the cortex of KO mice. When grown in a basement membrane matrix (cultrex), mpkCCD-Pkd1^{-/-} cells grew as cysts while the control-transduced mpkCCD cells grew as tubules, providing a phenotypical confirmation of the cell lines. mpkCCD-Pkd1^{-/-} cells exhibited significantly lower dDAVP-induced AQP2 protein expression (n=3, p≤ 0.05) when compared to control cells, although both mpkCCD-Pkd1^{-/-} and control cells displayed dDAVP-induced cAMP production.

Conclusion: ADPKD mice have a urine concentrating defect, which may be explained by the downregulation of AQP2 in the inner renal medulla, and sodium transporters important for countercurrent multiplication such as NKCC2 and NHE3. In mpkCCD-Pkd1^{-/-} cells, AQP2 is downregulated despite dDAVP-induced cAMP elevation, suggesting AQP2 dysregulation. Further investigations are required to understand AQP2 trafficking in these models.

Physiology in Focus 2024

Northumbria University, Newcastle, UK | 2 – 4 July 2024

Ethical approval: All protocols of the animal studies were approved by the Animal Experiments Inspectorate of the Ministry of Food, Agriculture and Fisheries in Denmark.

C31

Adenine-Induced Kidney Disease: An Animal Model to Study Uremic Toxins

Søren Elsborg³, Jasmine Atay³, Johan Palmfeldt^{3,4}, Henricus Mutsaers³, Rikke Nørregaard^{3,5}

¹Aarhus University, Aarhus, Denmark, ²Aarhus University, Aarhus, Denmark, ³Department of Clinical Medicine, Aarhus University, Aarhus, Denmark, ⁴Research Unit for Molecular Medicine, Aarhus University, Aarhus, Denmark, ⁵Department of Renal Medicine, Aarhus University Hospital, Aarhus, Denmark

Chronic kidney disease (CKD) increases the risk of cardiovascular disease (CVD) development. However, conventional treatments for CVD shows limited efficacy in patients with concurrent CKD, suggesting a different CVD mechanism. To better treat these patients, an improved understanding of how uremic toxins accumulate in the plasma during CKD is needed. Therefore, we aimed to characterise the plasma and urinary metabolic profiles of adenine-treated mice, with a focus on key renal drug transports, across various stages of renal injury to evaluate the fidelity of this model to study uremic toxicity.

8-week-old C57BL/6J male mice were exposed to a diet supplemented with 0.2% adenine to induce renal injury and divided into five groups: 1) control group (n=11), 2) two weeks of adenine diet (n=8), 3) four weeks of adenine diet (n=8), 4) four weeks of adenine diet and one week without (n=8), and 5) four weeks of adenine diet and two weeks without (n=7). The latter two groups allowed us to study recovery of the kidney disease. 24-h urine samples were collected the day before termination and blood and kidneys were harvested at termination. At termination, mice were anaesthetised with 4% sevoflurane and the kidneys were harvested and a blood sample was collected from the heart. The mice were euthanased using cervical dislocation. LC-MS/MS was employed for urinary and plasma metabolic profiling. Compound identification was performed using the mzLogic Data Analysis Algorithm (Compound Discover, Thermo Fischer), and untargeted data analysis was conducted using MetaboAnalyst 5.0. Gene expression of renal transporters in cortical kidney tissue was determined by qPCR.

Targeted metabolomics revealed a significant increase in mean plasma levels of the uremic toxins indoxyl sulfate, hippuric acid, and kynurenic acid after 2 and 4 weeks of adenine-feeding, which normalized after the 2-week washout period ($p < 0.05$). This was accompanied by significantly reduced levels of urinary kynurenic acid, hippuric acid and indole-3-acetic. Importantly, these levels normalized after the washout period. Untargeted metabolomics demonstrated elevated plasma and reduced urinary levels of specifically uremic toxins after 2 weeks of adenine treatment. After 4 weeks, nucleic acids became the predominant metabolites in both plasma and urine. Notably, we found two previously unidentified metabolites among the top 20 upregulated metabolites in adenine-fed mice. mRNA expression analysis revealed a significant decrease of the proximal tubule influx transporters *Slc22a6*, *Slc22a8*, *Slco4c1*, *Slc22a2* after 2 weeks, while only *Slc22a6* and *Slc22a2* was significantly reduced after 4 weeks. On the contrary, the proximal tubule efflux transporter *Slc47a1* was significantly increased after 2 weeks, while the *Abcg2* levels were decreased after both 2 and 4 weeks. This dysregulation of the proximal tubule drug transporters suggested proximal tubular stress.

In summary, adenine-feeding in mice induced a state of uremia characterised by increased levels of plasma uremic toxins and reduced levels in the urine probably due to proximal tubule transporter dysregulation. After 2 weeks of washout, renal transporter levels fully recovered, partially restoring the uremic state. We show that the adenine-model in mice is fit to investigate uremic toxicity.

C32

Species differences in renal response to the bile acid lithocholic acid

Sandra M. Hansen¹, Rianne V. Dekken¹, Rikke Nørregaard¹, Henricus A.M. Mutsaers¹

¹*Department of Clinical Medicine, Aarhus University, Aarhus, Denmark*

Background: Hydrophobic bile acids (BA) have long been known to be cytotoxic. Because of this, growing attention has centered on their role in the development of renal injury. So far research has predominantly relied on mouse models to study BA toxicity. This is despite the fact that humans and mice have substantially different BA pool compositions, with hydrophobic BAs being much more predominant in humans than in mice. To address this disparity, this study utilizes Precision-Cut Kidney Slices (PCKS) to conduct a comparative analysis of the impact of Lithocholic acid (LCA), the most hydrophobic BA, on human and mouse kidney tissue.

Methods: Using an Alabama R&D Tissue Slicer (formerly Krumdieck Tissue Slicer), human PCKS (hPCKS) (n=3) were prepared from macroscopically healthy kidney tissue obtained from tumor nephrectomies. Mice PCKS (mPCKS) (n=5) were prepared from kidneys harvested from C57BL/6 mice. Mice were anesthetized with 5% sevoflurane and sacrificed by cervical dislocation. Both hPCKS and mPCKS were cultured for 24H, 48H, and 72H with and without 100 μ M LCA. The inflammatory and fibrotic responses in the PCKS were characterized by qPCR of the inflammatory genes *IL-6* and *IL-1 β* and the fibrotic genes *fibronectin* and *collagen 1A1*. Gene expression levels were compared with two-tailed unpaired T-test. The use of human tissue for the hPCKS was approved by the Central Denmark Region Committees on Biomedical Research Ethics and the Danish Data Protection Agency.

Results: Exposure to LCA for 24H induced a strong inflammatory response in the mPCKS, seen by a large increase in *Il6* (p: 0.0034) and in *Il1b* (p: 0.0088). This was accompanied by an increase in the fibrotic genes *Fn* (p: 0.0430) and *Col1a1* (p: 0.0170). Only the increase in *Fn* persisted after 48H of exposure (p: 0.0263), and this was likewise no longer evident after 72H of exposure. However, mPCKS exposed to LCA for 48H and 72H exhibited markedly low RNA concentrations, which might indicate low viability. Further viability measures will be done.

hPCKS exhibited no alteration in *IL6* and *IL1B* levels after 24H, 48H, and 72H of LCA exposure. The non-exposed hPCKS exhibited culture-induced fibrosis at 48H and 72H compared to the 24H (p<0.041), a response normally seen in PCKS. This phenomenon was absent in LCA-exposed hPCKS, where *FN* and *COL1A1* levels remained stable throughout all time points.

Conclusion: This study demonstrated that mouse and human kidney tissue differ in their response to LCA. As anticipated, LCA had harmful effects on mPCKS, evidenced by heightened expression of inflammatory and fibrotic genes. Surprisingly the opposite was observed in hPCKS, where LCA protected against culture-induced fibrosis. This species difference in response to BAs emphasizes the importance of incorporating human models in research on the nephrotoxicity of BAs.

C33

Acute thrombocyte-dependent clearance of *Escherichia coli* requires D-mannose-sites for bacterial adherence

Emil Herrig Lambertsen¹, Nanna Johnsen¹, Thomas Corydon¹, Helle Praetorius¹

¹*Department of Biomedicine, Aarhus University, Aarhus C, Denmark*

EH Lambertsen, N. Johnsen, T. Corydon, H. Prætorius¹

Aarhus University, Department of Biomedicine, 8000 Aarhus, Denmark

Background:

Uropathogenic *E. coli* (UPEC) is the leading cause of urinary tract infections (UTIs). UPEC causing severe disease express various virulence factors that allow the UPEC to colonise the bladder, ascend to the kidney and disseminate to urosepsis^{1,2}. Our preliminary data show that thrombocytes are important for acute clearing of UPEC from the blood in a murine model of urosepsis. UPEC are known to adhere to epithelia via type 1 fimbriae, recognising D-mannose-rich structures^{3,4}. Here, we investigate if thrombocyte/*E. coli* complexes are prevented by pre-incubating UPEC with DM or preincubating thrombocytes with concanavalin A, a soluble lectin that binds D-mannose.

Methods:

Here, we use an *in vitro* assay of GFP-expressing UPEC ($165 \cdot 10^6$ ml⁻¹) added to whole blood samples or isolated thrombocytes from humane healthy volunteers (Danish Research Ethics Committees: 1-10-72-202-17). Complex formation between UPEC and thrombocytes (using CD42b as a thrombocyte marker) was determined at various time points by flow cytometry (Accuri 6plus, BD Biosciences). Data are analysed using one-way ANOVA and given as mean±SEM.

Results:

In our assay, we could easily confirm the instant formation of UPEC-thrombocyte complexes similar to what we observe in a mouse model of urosepsis. The complexes also readily form after thrombocytes have been fixed with 0.4% paraformaldehyde. Although thrombocytes have previously been suggested to be able to adhere *E. coli* via surface lipopolysaccharide (LPS) binding to thrombocyte TLR4, we could not prevent complex formation by either preincubation with TLR4 antagonists, TLR4 antibodies or pre-incubating thrombocytes with LPS. Moreover, we have not been able to prevent complex formation with antibodies directed against FcγRII or CD41/CD61.

Both D-mannose and concanavalin A cause a concentration-dependent reduction in UPEC/thrombocyte complexes. D-mannose reduced UPEC-thrombocyte complex formation from $6.71 \cdot 10^6 \pm 0.78 \cdot 10^6$ counts/ml to $2.69 \cdot 10^6 \pm 0.56 \cdot 10^6$ counts/ml equal to a ~60% decrease (n=8, p=0.023). Concanavalin A reduced complex formation from $3.21 \cdot 10^5 \pm 0.34 \cdot 10^5$ counts/ml to $1.57 \cdot 10^5 \pm 0.91 \cdot 10^5$ counts/ml equal to a ~51% decrease (n=7, p=0.004).

Conclusions:

We show that pre-treatment of UPEC with DM, and pre-treatment of thrombocytes with Concanavalin A reduced complex formation *in vitro*. These data suggest that type 1 fimbriae and not LPS are important for E. coli-thrombocyte interaction, and currently, we are gaining further evidence for this notion. Once confirmed, the relevant mannose-bearing interaction partners on thrombocytes will be determined by proteomics.

1) Medina M, Castillo-Pino E. An introduction to the epidemiology and burden of urinary tract infections. *Ther Adv Urol*, 2019 May 2;11:1756287219832172. 2) Whelan S, Lucey, B, Finn K. Uropathogenic Escherichia coli (UPEC)-Associated Urinary Tract Infections: The Molecular Basis for Challenges to Effective Treatment. *Microorganisms*, 2023 Aug 28;11(9):2169 3) Lane MC, Mobley, HLT. Role of P-fimbrial-mediated adherence in pyelonephritis and persistence of uropathogenic Escherichia coli (UPEC) in the mammalian kidney. *Kidney Int*, 2007 Jul;72(1):19-25 4) Sheikh A, Rashu R, Begum YA, Kuhlman FM, Ciorba MA, Hultgren SJ, Qadri F, Fleckenstein JM. Highly conserved type 1 pili promote enterotoxigenic E. coli pathogen-host interactions *PLoS Negl Trop Dis*, 2017 May 22;11(5):e0005586

C34

The SGLT-2 inhibitor empagliflozin reduces intrarenal complement activation in patients with diabetes and chronic kidney disease

Mia Jensen¹, Steffen Flindt Nielsen^{2,3}, Steffen Thiel⁴, Søren W.K. Hansen⁵, Yaseelan Palarasah⁵, Per Svenningsen¹, Jesper N. Bech^{2,3}, Frank H. Mose^{2,3}, Boye L. Jensen¹

¹Unit of Cardiovascular and Renal Research, Department of Molecular Medicine, University of Southern Denmark, Odense, Denmark, ²University Clinic in Nephrology and Hypertension, Gødstrup Hospital, Herning, Denmark, ³Department of Clinical Medicine, Aarhus University, Aarhus, Denmark, ⁴Department of Biomedicine, Aarhus University, Aarhus, Denmark, ⁵Unit of Cancer and Inflammation Research, Department of Molecular Medicine, University of Southern Denmark, Odense, Denmark

Background and hypothesis: Sodium-glucose cotransporter 2 (SGLT-2) inhibitors (SGLT2i) improve kidney and cardiovascular outcomes in patients with diabetes and chronic kidney disease (CKD). Since complement system precursors are aberrantly filtered and activated in conditions with albuminuria, it was hypothesized that SGLT2i lower plasma collectins and attenuate intratubular complement activation and deposition in patients with CKD.

Methods: Patient plasma and urine samples were analyzed from three randomized, blinded, cross-over intervention studies where patients with type 2 diabetes mellitus (DM) and CKD (DM-CKD, n=17), DM without CKD (DM, n=16), and CKD without DM (CKD, n=16) were given empagliflozin (10 mg/day) and placebo for four weeks with a washout of at least two weeks in-between. ELISA was used to determine concentrations of collectin kidney 1 (CL-K1), collectin liver 1 (CL-L1), mannose-binding lectin (MBL), MBL-associated serine protease (MASP-2), anaphylatoxins C3a and C5a, stable C3 split product C3dg and the membrane attack complex (sC5b-9) in urine and plasma. Apical deposition of membrane-bound C5b-9 was determined in isolated extracellular vesicles (EVs) from urine by western blotting (n=5). A paired two-tailed t-test was used to determine statistical significance between the treatments in each group. Non-normal distributed values were reported as median [interquartile range]. The studies were approved by the Ethical Committee of the Central Jutland Region and the Danish Health and Medicine Authority. The collection of samples was performed in accordance with the Helsinki Declaration, the EU Directive on Good Clinical Practice (GCP), and International Conference of Harmonization (ICH-GCP) guidelines and all participants gave written informed consent before inclusions.

Results: Empagliflozin induced no change in plasma levels of CL-K1, CL-L1, MBL, MASP-2, C3a, C5a, and C5b-9 while C3dg levels increased (18%, 114.1 [91-139] vs. 131.9 [98-157] units/mL, p=0.03) in DM-CKD. Collectins were not detectable in protease-inhibited spot urine or in ex vivo up-concentrated urine. Empagliflozin decreased urine C3a/creatinine ratio in the DM (32.5%, 5.7 [2.6-15] vs. 4.1 [1.8-6.4] ng/μmol, p=0.01) and DM-CKD groups (58.3%, 5.1 [3.6-238] vs. 4.7 [2.0-105] units/μmol, p=0.012), whereas urine C5a- and C3dg/creatinine ratio did not change. Urine sC5b-9/creatinine decreased significantly (45%, 0.9 [0.1-17] vs. 0.4 [0.1-12] units/μmol, p=0.02) after empagliflozin but only in the DM-CKD group. This was recapitulated in urine EVs by immunoblotting for C5b-9. Empagliflozin reduced the urine albumin/creatinine ratio in the DM-CKD group (24.5%, 201 [62-1130] vs. 164 [44-719] mg/g, p=0.02).

Conclusion: While SGLT2i do not lower plasma concentrations of collectins and complement activation products, they significantly reduce indices of intrarenal complement activation and membrane deposition in patients with DM and DM-CKD. Thus, SGLT2 inhibitors may protect kidneys in diabetic patients with CKD by reducing complement-induced tubular injury.

C35

The Secondary Bile acid, Lithocholic Acid, Exerts Anti-secretory Actions in Colonic Epithelial Cells in Vitro

Caitriona Curley¹, Magdalena Mroz¹, Stephen Keely¹

¹*Royal College of Surgeons in Ireland, Dublin, Ireland*

Introduction: Bile acids, classically known for their roles in facilitating lipid digestion, are now also appreciated as a family of enterocrine hormones that modulate many aspects of intestinal and metabolic function. We have previously shown lithocholic acid (LCA), a secondary bile acid formed in the colon, to be protective against colonic inflammation. Here, we sought to investigate if LCA might also regulate colonic epithelial fluid and electrolyte transport.

Methods: T₈₄ cell monolayers were mounted in Ussing chambers for measurements of Cl⁻ secretion, the primary driving force for colonic fluid secretion. qRT-PCR and Western blotting were used to analyze mRNA and protein expression. To assess the effects of LCA on CFTR promoter activity, we used a luciferase promoter/reporter system in HEK293. Results were expressed as mean ± SEM and data were analyzed by one way ANOVA and Tukey's post hoc test or by mixed-effects analysis and Dunnett's post hoc test.

Results: Pretreatment of T₈₄ cell monolayers with LCA inhibited subsequent Cl⁻ secretory responses to the cAMP-dependent agonist, forskolin (FSK; 10 mM), in a concentration (1 – 10 μM) and time-dependent (3 - 24 hrs) manner. Maximal effects of LCA were observed at a concentration of 10 μM after treatment for 24 hrs, when responses to FSK were reduced to 50.9 ± 8.5% of those in controls (n = 6; p < 0.01). LCA (10 μM; 24 hrs) also inhibited responses to the Ca²⁺-dependent secretagogues, thapsigargin (2 μM) and histamine (100 μM), by 59.4 ± 2.4% (n = 4; p < 0.001) and 52.2 ± 1.9% (n = 5; p < 0.001), respectively. In further experiments, using nystatin-permeabilized T₈₄ monolayers to isolate apical Cl⁻ conductances, LCA (10 μM; 24 hrs) reduced FSK-stimulated responses to 72.7 ± 6.6% (n = 17; p < 0.001) of those in control cells. Analysis of CFTR expression, the primary exit pathway for Cl⁻ in colonic epithelial cells, revealed that LCA treatment reduced mRNA and protein expression of the channel to 0.65 ± 0.05 (n = 7; p < 0.01) and 0.43 ± 0.06 (n = 6; p < 0.001) fold of controls, respectively. In CFTR promoter assays, LCA (10 μM) reduced CFTR promoter activity to 0.7 ± 0.02 fold of that in control cells (n = 5; p < 0.01), with expression of FXR being required for this effect to be observed. Finally, while LCA activated both FXR and the vitamin D receptor (VDR) in T₈₄ cells, its effects in downregulating CFTR expression and Cl⁻ conductances were mimicked by the FXR agonist, GW4064, but not by the VDR agonist, calcitriol.

Conclusion: LCA, at physiologically-relevant concentrations, inhibits Cl⁻ secretion across colonic epithelial cells, likely through a mechanism involving FXR activation and inhibition of CFTR expression. These data add to the growing pool of knowledge regarding regulatory actions of LCA in the colon and its potential role as a target for the treatment of intestinal disorders.

C36

Induction of ATF4-Regulated Atrogenes Is Uncoupled from Muscle Atrophy during Disuse in Halofuginone-Treated Mice and in Hibernating Brown Bears

Lydie Combaret¹, Laura Cussonneau², Cécile Coudy-Gandilhon³, Guillemette Gauquelin-Koch⁴, Fabrice Bertile⁵, Etienne Lefai¹, Pierre Fafournoux¹, Anne-Catherine Maurin¹

¹Université Clermont Auvergne, INRAE, Unité de Nutrition Humaine, UMR 1019, Clermont-Ferrand, France, ²Université Clermont Auvergne, INRAE, Unité de Nutrition Humaine, UMR 1019, Clermont-Ferrand, France, ³Université Clermont Auvergne, INRAE, Unité de Nutrition Humaine, UMR 1019, Clermont-Ferrand, France, ⁴Centre National d'Etudes Spatiales, CNES, Paris, France, ⁵Université de Strasbourg, CNRS, IPHC UMR 7178, Strasbourg, France

Introduction: Muscle atrophy observed in several physio-pathological situations has harmful consequences for the patients and results from an imbalance between protein synthesis and proteolysis. With no proven treatment of muscle atrophy, there is still a need to develop efficient strategies. Activation of the transcription factor 4 (ATF4) is involved in muscle atrophy through the overexpression of some atrogenes, i.e. genes whose mRNA levels are regulated during muscle atrophy. However, ATF4 also controls the transcription of genes involved in muscle homeostasis maintenance (1), and a controlled activation of the eIF2alpha/ATF4 pathway before a stressful event preserved organ function (2).

Aim: Here, we explored whether such a controlled activation of ATF4 before induction of atrophy may preserve muscle function.

Method: For that purpose, mice were treated with the pharmacological molecule halofuginone (0.25mg/kg, 3 times a week) for 3 weeks, before inducing muscle atrophy by hindlimb suspension for 3 or 7 days. Data were analyzed by ANOVA and were considered statistically different between groups for p-values below 0.05.

Results: Firstly, we reported that periodic activation of ATF4-regulated atrogenes (Gadd45a, Cdkn1a, and Eif4ebp1) by halofuginone was not associated with muscle atrophy in untreated and treated healthy mice (6 mice/group). Secondly, the atrophy induced by hindlimb suspension was reduced in halofuginone-treated mice compared to untreated ones, although the induction of the ATF4 pathway by hindlimb suspension was identical in halofuginone treated and untreated mice (8-19 mice/group). We further showed that transforming growth factor- β (TGF- β) signaling was inhibited, while bone morphogenetic protein (BMP) signaling was promoted in halofuginone-treated healthy mice compared to untreated ones (5-8 mice/group). In addition, halofuginone treatment also slightly preserved protein synthesis during hindlimb suspension (5-8 mice/group). Finally, ATF4-regulated atrogenes were also induced in the atrophy-resistant muscles of hibernating compared to active brown bears (6 bears/group), in which we previously also reported concurrent TGF- β inhibition and BMP maintenance during hibernation (3).

Conclusions: Overall, we show that ATF4-induced atrogenes can be uncoupled from muscle atrophy. Our data also indicate that halofuginone can control the TGF- β /BMP balance toward muscle mass maintenance. Whether halofuginone-induced BMP signaling can counteract

the effect of ATF4-induced atrogenes needs to be further investigated and may open a new avenue to fight muscle atrophy. Finally, our study opens the way for further studies to identify well-tolerated chemical compounds in humans that enable fine-tuning of the TGF- β /BMP balance and could be used to preserve muscle mass during catabolic situations.

(1) Kasai et al. Role of the ISR-ATF4 Pathway and Its Cross Talk with Nrf2 in Mitochondrial Quality Control. *J. Clin. Biochem. Nutr.* 2019;64:1–12. doi: 10.3164/jcbn.18-37. (2) Peng et al. Surgical Stress Resistance Induced by Single Amino Acid Deprivation Requires Gcn2 in Mice. *Sci. Transl. Med.* 2012;4:118ra11. doi: 10.1126/scitranslmed.3002629. (3) Cussonneau et al. Concurrent BMP Signaling Maintenance and TGF- β Signaling Inhibition Is a Hallmark of Natural Resistance to Muscle Atrophy in the Hibernating Bear. *Cells*. 2021. 10(8):1873. doi: 10.3390/cells10081873.

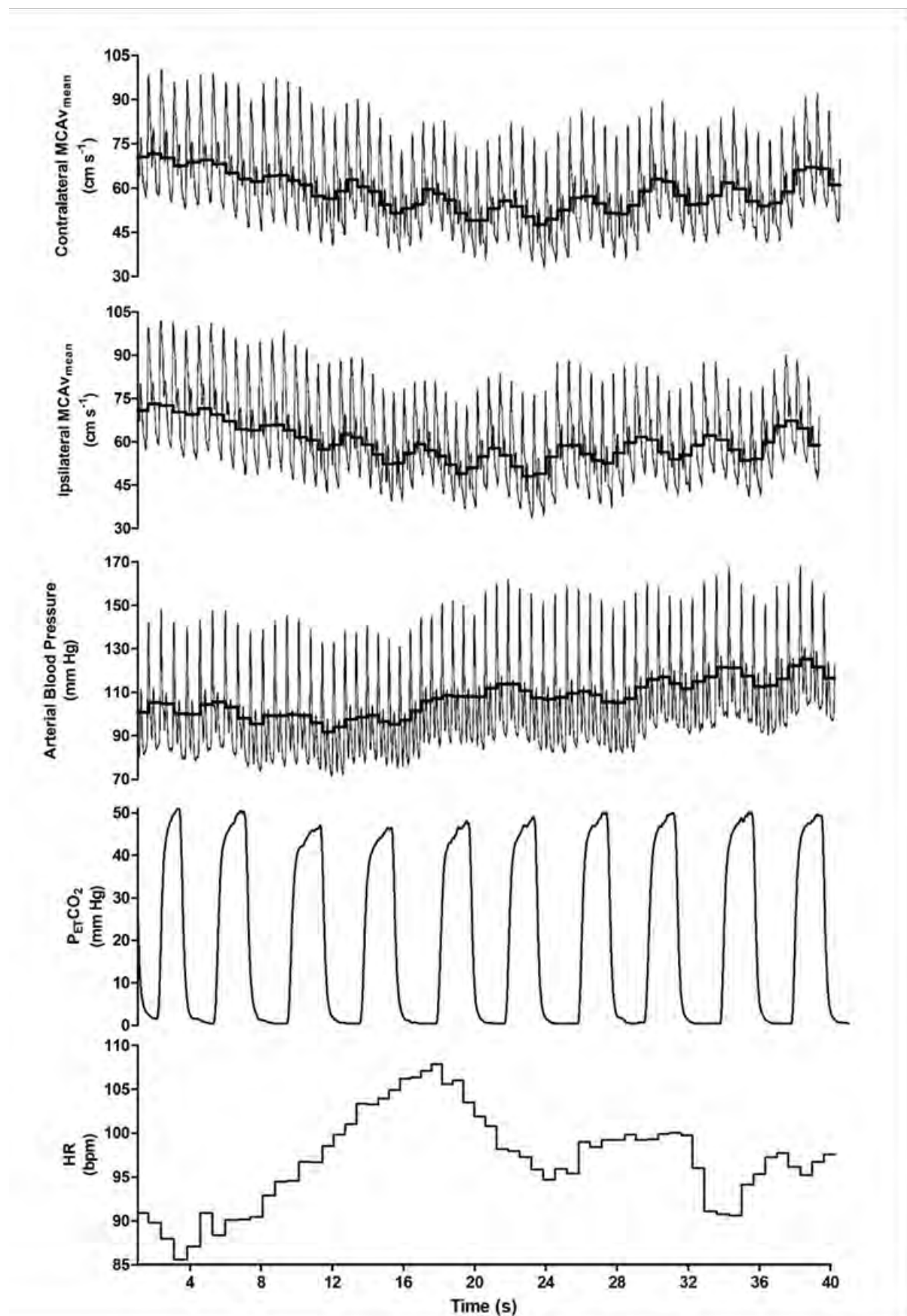
C37

Neurovascular coupling during dynamic upper body resistance exercise in healthy individuals

Stephanie Korad¹, Toby Mundel^{2,3}, Blake Perry¹

¹*School of Health Sciences, Massey University, Wellington, New Zealand,* ²*School of Sport, Exercise and Nutrition, Massey University, Palmerston North, New Zealand,* ³*Department of Kinesiology, Brock University, St Catharines, Canada*

During dynamic exercise many of the regulators of cerebral blood flow (CBF) are concomitantly perturbed. These regulators include neurovascular coupling (NVC), arterial carbon dioxide content, arterial blood pressure, sympathetic nerve activity, and cerebral autoregulation (CA). Neurovascular coupling refers to the matching of local CBF to neuronal activity. That is, when neuronal activity increases, so does local blood flow. During unilateral static handgrip exercise blood velocity in the middle cerebral artery (MCAv) contralateral to the exercising limb increases, indicative of NVC. However, it is unknown whether this persists during dynamic resistance exercise (RE). This study aimed to examine the cerebral haemodynamic response to unilateral dynamic upper body RE in healthy individuals. We hypothesised that during unilateral dynamic upper body RE, there will be no differences between contralateral and ipsilateral MCAv due the overriding influence of arterial carbon dioxide concentration and blood pressure. The current study could provide valuable insights for the safe prescription of dynamic RE to those who have suffered cerebrovascular injury. Thirty (female = 16, mean \pm SD: age, 26 ± 6 years, height 175 ± 10 cm, weight 74 ± 15 kg, BMI 24 ± 5 kg/m²) healthy individuals completed 4 sets of 10 paced repetitions (15-beats-per-minute) of unilateral bicep curl exercise at 60% of predicted 1 repetition maximum (60% of 1RM 7 ± 3 kg). Beat-to-beat blood pressure, bi-lateral MCAv, and the partial pressure of end-tidal carbon dioxide ($P_{ET}CO_2$ – as a proxy for arterial CO_2) were measured throughout. One-way ANOVA was used to analyse cardiovascular variables, and two-way ANOVA was used to analyse dependent cerebrovascular variables (side \times sets, 2×4). Typical cerebrovascular and cardiovascular responses during RE are shown in Figure 1. Within exercise bilateral MCAv, cerebral conductance index, and pulse velocity decreased across the exercise sets (all $P < 0.001$), but no significant interaction effect was observed (all $P > 0.221$) for any dependent variables. Despite the recruitment of a small muscle mass during the bicep curl, we observed sinusoidal fluctuations in MAP typical of dynamic RE. Furthermore, although not significant (all $P > 0.316$), average $P_{ET}CO_2$ was ~ 2 mmHg lower during exercise. The current data indicates no differences between contralateral and ipsilateral MCAv during unilateral dynamic RE, consistent with our hypothesis, but contradicting findings of static RE studies. The effects of NVC were not discernible in the MCAv data, possibly obfuscated by the small reduction in $P_{ET}CO_2$ and the fluctuating MAP. Future studies are required to attempt to discern the underlying physiology of local and global CBF during dynamic RE.



C38

Comparison of ectopic fat deposition between children with and without obesity: Influence of sex and physical activity level

Ryan G. Larsen¹, Charlotte N. Eggertsen^{2,3,4}, Jonas Gelardi¹, Jan C. Brønd⁶, Aase Handberg^{4,5}, Esben T. Vestergaard^{7,8}, Jens B. Frøkjær⁹, Søren Hagstrøm^{2,3,4}

¹ExerciseTech, Department of Health Science and Technology, Aalborg University, Aalborg, Denmark, ²Department of Pediatrics and Adolescent Medicine, Aalborg University Hospital, Aalborg, Denmark, ³Steno Diabetes Center North Denmark, Aalborg University Hospital, Aalborg, Denmark, ⁴Department of Clinical Medicine, Aalborg University Hospital, Aalborg, Denmark, ⁵Department of Clinical Biochemistry, Aalborg University Hospital, Aalborg, Denmark, ⁶Department of Sport Science and Clinical Biomechanics, University of Southern Denmark, Odense, Denmark, ⁷Department of Pediatrics and Adolescent Medicine, Aarhus University Hospital, Aarhus, Denmark, ⁸Department of Clinical Medicine, Aarhus University, Aarhus, Denmark, ⁹Department of Radiology, Aalborg University Hospital, Aalborg, Denmark

Introduction: According to the theory of lipotoxicity, ectopic fat deposition (i.e., storage of triglycerides in non-adipose tissues, such as muscle, liver, pancreas) can lead to inflammation, insulin resistance and beta-cell dysfunction (1, 2). A previous study reported greater fat deposition in skeletal muscle and liver in children with obesity compared to their lean counterparts (3). However, the role of weight status (obesity vs. normal weight) on pancreatic fat deposition in children is yet unclear. In addition, little is known about the roles of sex and physical activity level in modulating ectopic fat deposition in children. We tested the hypotheses that children with obesity exhibit greater fat deposition in psoas muscle, liver, and pancreas compared to children with normal weight, matched for age and sex. We also investigated if sex and physical activity level modulate fat deposition in these organs.

Methods: 3T MR scanning with multi-echo Dixon imaging was used to acquire proton density fat fraction (PDFF) maps in 48 children (9-16 years; 33 boys, 15 girls) with obesity (body mass index, BMI > 90 percentile for age and sex) and in 30 age-matched children with normal weight (18 boys, 12 girls). From the PDFF maps, liver, psoas muscle and pancreas were outlined to obtain fat fraction in each specific organ. To assess physical activity level, participants wore a 3-axis accelerometer on the thigh for seven consecutive days. Daily minutes spent in sedentary, light, moderate and vigorous intensity were quantified. Fat fractions and physical activity categories were analyzed using 2-way (group, sex) repeated measures ANOVA. Associations between physical activity level and fat fractions were explored using Pearson's correlation.

Results: Compared to normal weight, children with obesity showed higher fat fraction in liver ($6.3 \pm 6.9\%$ vs. 1.7 ± 0.7 ; $p < 0.001$), psoas ($2.8 \pm 1.6\%$ vs. $1.1 \pm 0.6\%$; $p < 0.001$) and pancreas ($4.9 \pm 2.8\%$ vs. $1.7 \pm 0.7\%$; $p < 0.001$) with no effects or interactions of sex. Daily minutes spent in moderate (29.0 ± 13.7 vs. 43.1 ± 19.5 ; $p < 0.001$) and vigorous (8.2 ± 7.6 vs. 21.9 ± 13.2 ; $p < 0.001$) intensity were lower in children with obesity compared with normal weight, with no effects or interactions of sex. Daily minutes of moderate-to-vigorous intensity was inversely associated with fat fraction in liver ($r = -0.27$, $p < 0.05$), psoas ($r = -0.34$, $p < 0.01$), and pancreas ($r = -0.50$, $p < 0.01$).

Conclusion: Children with obesity exhibited greater fat deposition in liver, psoas muscle and pancreas compared to their lean counterparts. While sex did not play a role in modulating fat deposition, time spent in moderate-to-vigorous intensity activities were inversely associated with fat fraction in each organ. Future studies are required to 1) elucidate biomarkers that can identify children who display a critical amount of ectopic fat deposition, and 2) explore interventions effective in reducing ectopic fat deposition in children with obesity.

1) Plötz T and Lenzen S. Mechanisms of lipotoxicity-induced dysfunction and death of human pancreatic beta cells under obesity and type 2 diabetes conditions, *Obesity reviews*, 2024, online ahead of print 2) Rada P et al. Understanding lipotoxicity in NAFLD pathogenesis: is CD36 a key driver? *Cell Death & Disease*, 2020, 11(9):802 3) Fonvig CE et al. 1H-MRS Measured Ectopic Fat in Liver and Muscle in Danish Lean and Obese Children and Adolescents, *Plos One*, 2015, 10(8): e0135018

C39

High-intensity continuous exercise elevates I-FABP2 levels equally across 30 and 60-minute durations in healthy males.

Lewis R Mattin¹, Victoria J McIver², Adora MW Yau³, Gethin H Evans³

¹*School of Life Sciences, University of Westminster, London, UK, London, United Kingdom,*

²*Department of Sport, Exercise and Rehabilitation, Northumbria University, Newcastle, UK,*

³*Department of Life Sciences, Manchester Metropolitan University, Manchester, UK, Manchester, United Kingdom*

Introduction: Intestinal fatty acid binding protein two (I-FABP₂) is a small 15 KDa cytosolic protein expressed in epithelial cells of the mucosal layer of the small and large intestines [1]. When damage occurs, I-FABP₂ is released, and plasma concentrations increase [2]. Notably, I-FABP₂ is not expressed in any other tissues. Therefore, I-FABP₂ is used to evaluate gut wall integrity and intestinal injury, contributing to gastrointestinal complications and delayed nutrient delivery [1-4]. However, in trained participants, mucosal damage increases in response to exercise > 70% $\dot{V}O_{2Max}$ for durations of ~60 minutes [2, 4, 5]. Therefore, this study aimed to investigate the effect of high-intensity continuous exercise at two different durations, 30 and 60 minutes, on I-FABP₂ responses in healthy male participants. **Method:** Fourteen healthy males (Mean \pm SD; age 27 \pm 6 years; height 179 \pm 9 cm; body mass 79 \pm 10 kg; body fat 18.5 \pm 4.1 %; BMI 24.9 \pm 2 kg/m²; $\dot{V}O_{2peak}$ 42 \pm 9 ml/kg/min). Completed two ~4-h trials in a randomised order. Diet was standardised 24-h before experimental trials. Participants arrived at the laboratory following an overnight fast before completing a 60-min continuous cycle (EX-60) or a split 30-min morning and 30-min afternoon cycle (EX-30) at the same intended intensity of ~70% $\dot{V}O_{2Max}$. Participants then received breakfast at 75-min (Semi-skimmed milk), which amounted to 30% of the estimated trial energy expenditure (ETEE), with the total volume standardised to 500ml with water. Participants then recovered for 2-h (90-210 min) followed by the second 30-min exercise bout from 210-240-min (EX-30 second bout). Heart rate (HR) was recorded every 5-min, and REP every 10-min during all exercise periods. I-FABP₂ was measured at baseline (0), Pre-breakfast (75-min), and Post-second EX (270-min). **Results:** There were no differences in Pre-trial energy intake between EX-60 and EX-30 (2571 \pm 1173 Kcal Vs 2547 \pm 1311 Kcal; p = 0.779). There was no main effect for I-FABP₂ AUC for EX-60 vs EX-30, respectively (p = 0.400). No main effect for trial (p = 0.252) nor trial x time interaction (p = 0.780) was observed. However, an effect for time (p < 0.001) was identified for I-FABP₂. Post-hoc tests revealed I-FABP₂ increased from baseline to Post-EX (75-min) respectively EX-60 (485 \pm 301 vs 1334 \pm 626 pg.ml⁻¹; p < 0.001) and EX-30 (572 \pm 325 vs 1454 \pm 792 pg.ml⁻¹) and baseline to post-second EX (270 min) highly significant in both trials (p < 0.001). REP was significantly different across all measurements during exercise (p < 0.001). There were no differences in HR averaged over 60-min EX-60 and EX-30 (156 \pm 14 vs 154 \pm 14 bpm; p = 0.534). **Conclusion:** The results of this study demonstrate that 30 min of high-intensity exercise was sufficient to cause an increased intestinal cellular injury, which caused cell membrane integrity to be compromised following strenuous exercise to the same extent as 60 min when a health population is used. Therefore, the effect of I-FABP₂ may depend upon training status, and an individualised approach should be warranted.

1. Agellon LB et al. (2007). *Molecular and Cell Biology of Lipids*, 1771 (10). 2. Pugh JN et al. (2017). *Appl Physiol Nutr Metab*, 42 (9). 3. Lau E et al. (2016). *Nutr Metab (Lond)*, 13 (31). 4. van Wijck K et al. (2011). *PLoS One*, 6 (7). 5. Van Wijck K et al. (2012). *Med Sci Sports Exerc*, 44 (12).

C41

Characterising the Cellular Physiology of a Novel Phospholipase Target in Skeletal Muscle within the Aetiologies of Obesity and Diabetes

Rashmi Sivasengh¹, Iris Pruñonosa Cervera², Nicholas M. Morton³, Brendan M. Gabriel¹

¹University of Aberdeen, Aberdeen, United Kingdom, ²University of Edinburgh, Edinburgh, United Kingdom, ³School of Science and Technology, Nottingham Trent University, Nottingham, United Kingdom

Obesity increases the risk for diabetes and cardiovascular disease. Genetic predisposition exacerbates environmental drivers of obesity such as energy-dense diets and a sedentary lifestyle. We have used divergently selected Fat (23% fat) and Lean (4% fat) lines of mice to identify the genes underlying adiposity. A stratified approach using quantitative trait loci (QTL; heritable genetic intervals segregating with adiposity in Fat x Lean F2 populations), transcriptomics, and comparative cross-species bioinformatics identified candidate obesity genes (Morton et al., 2016). A specific phospholipase A2 isoform (we name here PlaX), positioned in obesity (Fob)-1 QTL, exhibited ~5-fold elevated mRNA levels in the skeletal muscle of Fat mice compared to Lean mice. PlaX has been previously linked to the regulation of intracellular membrane vesicle trafficking and generation of lipid signalling mediators (Prunonosa Cervera et al., 2021). Overexpression of PlaX in C2C12 myotubes impaired cellular energetics and increased levels of the active form of AMP-activated protein kinase (AMPK). This led us to hypothesize that skeletal muscle PlaX overexpression may drive obesity by compromising myocyte energetics. To characterize the role of PlaX in skeletal muscle, we have overexpressed PlaX in L6 myotubes (n=3) using lentiviral transduction and performed RNA-sequencing on the Illumina NextSeq 2000 platform. As expected, PlaX was most significantly overexpressed with a +6.1886-fold change (Adj.p= 5.84e-14) in overexpressed cells (differential gene expression analysis). Several genes with differential expression in PlaX overexpression cells were linked to mitochondrial respiration and metabolism. These included Pdk4, which was down regulated with -1.02327 fold-change (adj.p value 0.0012); and Mitochondrial calcium uptake gene (Micu1) which was down regulated with a -0.328-fold change (Adj.P= 1.16e⁻¹¹). It is known that Mitochondrial calcium uptake 1 (Micu1) negatively regulates thermogenesis and deletion of Micu1 in adiposity impairs thermogenesis and may lead to increased risk of obesity and metabolic dysfunction. Anti-Flag magnetic beads were used to perform Immunoprecipitant (IP) pull down to identify PlaX binding partners. As expected, PlaX was overexpressed in IP eluant >1*10⁸. We performed Gene ontology on proteins detected in PlaX eluant (which were not detected in GFP and not treated controls) and found mitochondrial cellular compartments were overexpressed (Differentially expressed protein analysis, n=3, FDR-adjusted (adj.) p<0.02). Our IP and RNA-Sequencing data indicate the PlaX has a regulatory role on mitochondrial metabolism, and this may be a mechanism driving increased adiposity. In summary, our genetic strategy has identified a novel potential skeletal muscle driver of obesity that could be a tractable target for therapeutic development.

1. Azevedo PG de, Miranda LR, Nicolau ES, Alves RB, Bicalho MAC, Couto PP, Ramos AV, Souza RP de, Longhi R, Friedman E, Marco L De & Bastos-Rodrigues L (2021). Genetic association of the PERIOD3 (PER3) Clock gene with extreme obesity. *Obesity Research & Clinical Practice* 15, 334–338. 2. Cervera IP, Gabriel BM, Aldiss P & Morton NM (2021). The phospholipase A2 family's role in metabolic diseases: Focus on skeletal muscle. *Physiological Reports*; DOI: 10.14814/PHY2.14662.

3. Massart J, Sjögren RJO, Egan B, Garde C, Lindgren M, Gu W, Ferreira DMS, Katayama M, Ruas JL, Barrès R, O’Gorman DJ, Zierath JR & Krook A (2021). Endurance exercise training-responsive miR-19b-3p improves skeletal muscle glucose metabolism. *Nature Communications* 2021 12:1 12, 1–13.
4. Morton NM et al. (2016). Genetic identification of thiosulfate sulfurtransferase as an adipocyte-expressed anti-diabetic target in mice selected for leanness. *Nat Med* 22, 771–779.

C42

Iron-catalysed free radical formation underpins the systemic vasculopathic complications in chronic mountain sickness

Damian Miles Bailey¹, Marcel Culcasi², Teresa Filipponi¹, Julien Brugniaux³, Benjamin Stacey¹, Christopher Marley¹, Rodrigo Soria⁴, Stefano Rimoldi⁴, David Cerny⁴, Emrush Rexhaj⁴, Lorenza Pratali⁵, Carlos Salinas Salmòn⁶, Carla Murillo Jáuregui⁶, Mercedes Villena⁶, Francisco Villafuerte⁷, Antal Rockenbauer⁸, Sylvia Pietri², Urs Scherrer⁴, Claudio Sartori⁹

¹University of South Wales, Glamorgan, United Kingdom, ²Aix Marseille University, Marseille, France, ³Grenoble Alpes University, Grenoble, France, ⁴University Hospital Bern, Bern, Switzerland, ⁵Institute of Clinical Physiology, Pisa, Italy, ⁶Instituto Boliviano de Biología de Altura, La Paz, Bolivia, Plurinational State of, ⁷Universidad Peruana Cayetano Heredia, Lima, Peru, ⁸Research Center for Natural Sciences, Budapest, Hungary, ⁹University Hospital, Lausanne, Switzerland

Background: Chronic mountain sickness (CMS) is a high-altitude maladaptation syndrome that affects between 5-10 % of the world's estimated 140 million highlanders who permanently reside >2,500 meters above sea-level (Leon-Velarde et al. 2005). It is characterised by excessive erythrocytosis, severe hypoxaemia and elevated systemic oxidative-nitrosative stress (OXNOS) subsequent to a free radical-mediated reduction in vascular nitric oxide (NO) bioavailability (Bailey et al. 2013; Bailey et al. 2019). To better define underlying molecular mechanisms, dietary risk factors and vascular consequences, we compared healthy male lowlanders (80 m, n = 10) against age/sex-matched highlanders born and bred in La Paz, Bolivia (3,600 m) with (CMS+, n = 10) and without (CMS-, n = 10) clinically diagnosed CMS.

Methods: Ethical approval protocol was obtained from the Institutional Review Boards for Human Investigation at the University of San Andres, La Paz, Bolivia (CNB #52/04), Universidad Peruana Cayetano Heredia, Lima, Perú (#101686), University of Lausanne, Lausanne, Switzerland (#89/06, #94/10), and University of South Wales, Glamorgan, UK (#4/07), prior to registration in a clinical trials database (NCT01182792). Cephalic venous blood was assayed for systemic OXNOS using electron paramagnetic resonance spectroscopy and reductive ozone-based chemiluminescence (Bailey et al. 2019). Nutritional intake was assessed via dietary recall. Systemic vascular function and structure were assessed via flow-mediated dilatation, aortic pulse wave velocity and carotid intima-media thickness using duplex ultrasound and applanation tonometry. Following confirmation of distribution normality (Shapiro-Wilk *W* tests), data were analysed using one-way ANOVAs with post-hoc Bonferroni-corrected independent samples *t*-tests. Relationships between variables were assessed using Pearson Product Moment Correlations.

Results: Basal systemic OXNOS was permanently elevated in highlanders ($P = <0.001$ vs. lowlanders) and further exaggerated in CMS+, reflected by increased hydroxyl radical spin adduct formation ($P = <0.001$ vs. CMS-) subsequent to liberation of free 'catalytic' iron consistent with a Fenton and/or nucleophilic addition mechanism(s). This was accompanied by elevated global protein carbonylation ($P = 0.046$ vs. CMS-) and corresponding reduction in plasma nitrite ($P = <0.001$ vs. lowlanders). Dietary intake of vitamins C and E, carotene, magnesium and retinol were lower in highlanders and especially deficient in CMS+ due to reduced consumption of fruit and vegetables ($P = <0.001$ to 0.028 vs. lowlanders/CMS-). Systemic vascular function and structure

were also impaired in highlanders ($P = <0.001$ to 0.040 vs. lowlanders) with more marked dysfunction observed in CMS+ ($P = 0.035$ to 0.043 vs. CMS-) in direct proportion to systemic OXNOS ($r = -0.692$ to 0.595 , $P = <0.001$ to 0.045).

Conclusions: Collectively, these findings suggest that lifelong exposure to iron-catalysed systemic OXNOS, compounded by a dietary deficiency of antioxidant micronutrients, likely contributes to the systemic vasculopathic complications and increased morbidity/mortality in CMS+.

Leon-Velarde F et al. (2005). High Alt Med Biol 6, 147-157. Bailey DM et al. (2013). Chest 143, 444-451. Bailey DM et al. (2019). J Physiol 597, 611-629.

C43

The role of neural input and microvascular blood flow as mediators of neuromuscular control

Eleanor Jones¹, Yuxiao Guo¹, Philip Atherton¹, Bethan Phillips¹, Mathew Piasecki¹

¹*Centre of Metabolism and Ageing Physiology (COMAP), University of Nottingham, Derby, United Kingdom*

Introduction

Force steadiness (FS), the ability to maintain a constant level of force output is known to progressively decrease during prolonged isometric contractions [1,2] which is partly mediated by the level of common synaptic input to motor units (MU). Ischemia, in which occlusion of the limb microvasculature reduces the delivery of oxygen and nutrients may also contribute to performance fatigue and reduced FS. However, the extent of the influence of each remains undefined. The aim of this study was to determine the effects of vastus lateralis (VL) neural input and microvascular blood flow on FS during a knee extensor fatiguing contraction.

Methods

Ten young volunteers (3 females; 30 ± 6 years) completed a 3-minute isometric leg extension at 30% maximum voluntary contraction (MVC), with data collected during the first and final 30-seconds (s) of the contraction. High-density surface electromyography (HD-sEMG) was used to identify individual MU potentials (MUPs) from the VL. FS was defined as the coefficient of variation (CoV) of force and compared between the first and final 30s of the contraction. Estimates of common synaptic inputs were made using the magnitude-squared coherence in the delta bandwidth (0–5 Hz) [3]. Microvascular blood volume (MBV) was determined from the plateau phase of a non-linear regression of echo acoustic intensity (AI) simultaneously recorded using contrast enhanced ultrasound (CEUS)[4]. Between time point data for all parameters was compared using paired t-tests with significance assumed as $p < 0.05$.

Results

10.4 ± 8.5 (Mean \pm SD) MUs per person were identified in the first 30s and 10.3 ± 8.1 in the last 30s. CoV force increased from the first to the last 30s of the fatiguing contraction (CoV: 3.13 ± 0.74 vs. $4.97 \pm 1.72\%$; $p = 0.005$) as did MBV (AI: 6.66 ± 0.72 vs. 7.72 ± 1.50 au; $p = 0.004$) but delta coherence (Z-score: 3.40 ± 1.83 vs. 3.40 ± 1.56 ; $p = 0.996$) did not change.

Conclusion

As expected, FS decreased during an isometric contraction of the knee extensors with an increase in MBV also observed. However, no changes were observed in the common synaptic input to MUs. These findings suggest that during an isometric contraction muscle blood flow may have a greater influence on FS at the onset of fatigue than neural properties. These findings can translate into

understanding ways to improve athletic performance as well as ameliorating functional impairment in clinical populations therefore, further investigation is needed into the neurophysiological factors involved in maintaining force control during fatigue.

1. Enoka RM, Farina D. Force steadiness: From motor units to voluntary actions. *Physiology*. 2021;36: 114–130. doi:10.1152/physiol.00027.2020
2. Martinez-Valdes E, Negro F, Falla D, Dideriksen JL, Heckman CJ, Farina D. Inability to increase the neural drive to muscle is associated with task failure during submaximal contractions. *J Neurophysiol*. 2020;124: 1110–1121. doi:10.1152/jn.00447.2020
3. Alix-Fages C, Jiménez-Martínez P, de Oliveira DS, Möck S, Balsalobre-Fernández C, Del Vecchio A. Mental fatigue impairs physical performance but not the neural drive to the muscle: a preliminary analysis. *Eur J Appl Physiol*. 2023; 508212. doi:10.1007/s00421-023-05189-1
4. Mitchell WK, Phillips BE, Williams JP, Rankin D, Smith K, Lund JN, et al. Development of a new sonovueTM contrast-enhanced ultrasound approach reveals temporal and age-related features of muscle microvascular responses to feeding. *Physiol Rep*. 2013;1. doi:10.1002/phy2.119

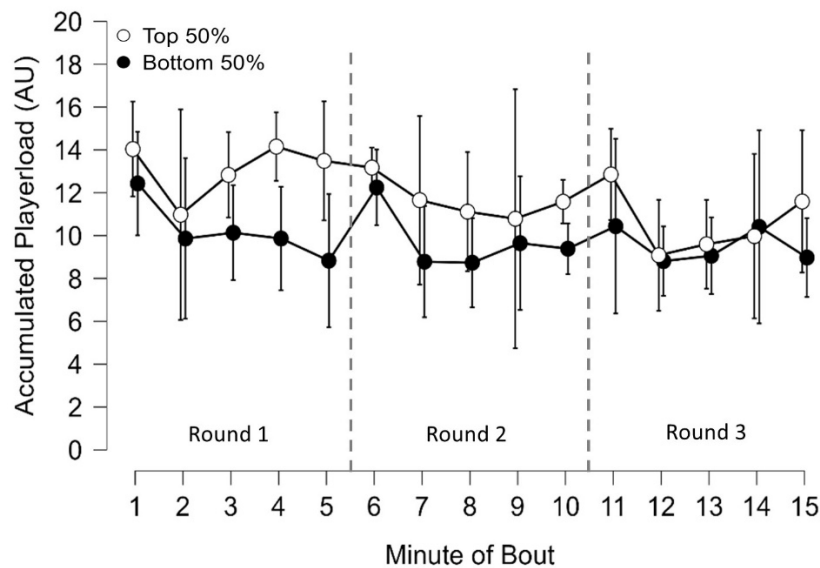
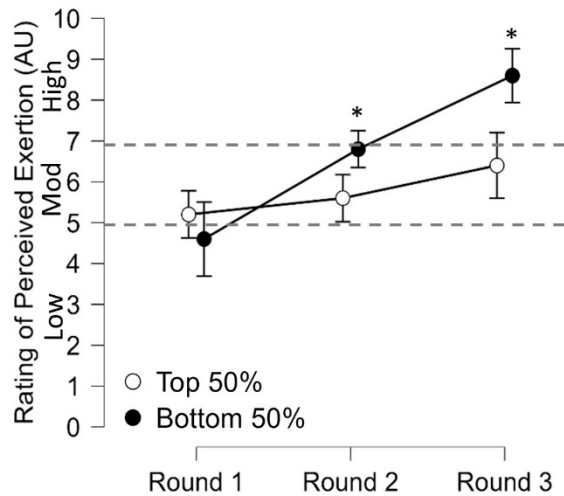
C44

Influence of cardiorespiratory fitness on RPE and Playerload in simulated mixed martial arts bouts

Christopher Kirk¹, David Clark², Carl Langan-Evans³

¹Sheffield Hallam University, Sheffield, United Kingdom, ²Robert Gordon University, Aberdeen, United Kingdom, ³Liverpool John Moores University, Liverpool, United Kingdom

Mixed martial arts (MMA) may potentially be classified as a high intensity aerobic endurance event (1). The influence of aerobic capacity ($\dot{V}O_2\text{max}$) on MMA performance is, however, currently unknown. The aim of this study was to compare the laboratory measured aerobic capacities of MMA participants to the external load, internal intensity and external intensity of MMA sparring bouts to examine the influence of aerobic fitness on performance. A cohort of $n=10$ male MMA participants (age = 24 ± 2.8 years; mass = 74.3 ± 8.2 kg; stature = 176.8 ± 7.9 cm) completed a treadmill based graded exercise test (GXT) to measure their absolute ($\text{L} \cdot \text{min}^{-1}$) and relative ($\text{ml} \cdot \text{kg} \cdot \text{min}^{-1}$) $\dot{V}O_2\text{max}$. Participants also took part in a 3x5mins MMA sparring bout whilst equipped with a Catapult Optimeye S5 accelerometer which recorded Playerload (PLd_{ACC}) as external load and Playerload per minute ($\text{PLd}_{\text{ACC}} \cdot \text{min}^{-1}$) as external intensity(2) throughout. Sessional rating of perceive exertion (sRPE) was recorded as internal intensity at the end of each round(3). sRPE of each round was classified as low intensity ($\leq 4\text{AU}$); moderate intensity ($5 - 6\text{AU}$); high intensity ($\geq 7\text{AU}$) as applied previously(4). All data were collected following institutional ethical approval and informed consent. The cohort's mean $\dot{V}O_2\text{max} = 53.1 \pm 5.9 \text{ ml} \cdot \text{kg} \cdot \text{min}^{-1}$. The cohort's median $\dot{V}O_2\text{max}$ ($53.3 \text{ ml} \cdot \text{kg} \cdot \text{min}^{-1}$) was used to split the cohort into top 50% and bottom 50% groups. Top 50% group $\dot{V}O_2\text{max} = 57.7 \pm 3.6 \text{ ml} \cdot \text{kg} \cdot \text{min}^{-1}$; $4.1 \pm 0.5 \text{ L} \cdot \text{min}^{-1}$. Bottom 50% group $\dot{V}O_2\text{max} = 48.5 \pm 3.6 \text{ ml} \cdot \text{kg} \cdot \text{min}^{-1}$; $3.8 \pm 0.4 \text{ L} \cdot \text{min}^{-1}$. Bayesian repeated measures ANOVA ($\text{BF}_{10} \geq 3$) were used to determine any differences in external/internal intensity between groups, between rounds, and between minutes(5). All analyses were completed using JASP 0.18.3 (JASP Team, NETHERLANDS). Round*group differences in sRPE were found to be decisive with a large effect ($\text{BF}_{10} = 143$, $\omega^2 = 0.15$) (Figure 1). The top 50% group were found to maintain moderate sRPE throughout sparring (round 1 = $5.2 \pm 1.3\text{AU}$; round 2 = $5.6 \pm 1.3\text{AU}$; round 3 = $6.4 \pm 1.9\text{AU}$). The bottom 50% group's sRPE moved from moderate in round 1 ($4.6 \pm 1.1\text{AU}$) and round 2 ($6.8 \pm 1.3\text{AU}$) to high in round 3 ($8.6 \pm 1.1\text{AU}$). Whilst the top 50% group recorded greater PLd_{ACC} and $\text{PLd}_{\text{ACC}} \cdot \text{min}^{-1}$ than the bottom 50% group in each round, these differences were not statistically relevant between groups or rounds. When analysing PLd_{ACC} there was a moderate minute*group difference with a medium effect ($\text{BF}_{10} = 3$, $\omega^2 = .11$). Resulting post hoc between groups differences were decisive with a medium effect ($\text{BF}_{10} = 380$, $\omega^2 = .12$) with the top 50% group recording greater PLd_{ACC} for most of rounds 1 and 2, and displaying an 'end spurt' in round 3 (Figure 2). These results indicate having a $\dot{V}O_2\text{max} < 53 \text{ ml} \cdot \text{kg} \cdot \text{min}^{-1}$ is related to increased internal intensity in MMA sparring. Participants with $\dot{V}O_2\text{max}$ above this appeared capable of maintaining greater and qualitatively more consistent external intensity throughout the first and second rounds of sparring. These data support the aerobic nature of MMA and may provide minimum aerobic fitness levels to aim for during competition preparation.



1. Draper N, Marshall H. High-intensity aerobic endurance sports. In: Draper, Nick and Marshall, Helen, editor. *Exercise Physiology for Health and Sports Performance*. New York: Routledge; 2013. p. 322 – 350.
2. McLean BD, Cummins C, Conlan G, Duthie G, Coutts AJ. The fit matters: influence of accelerometer fitting and training drill demands on load measures in rugby league players. *Int J Sports Physiol Perform*. Human Kinetics; 2018;13(8):1083–9.
3. Kirk C, Langan-Evans C, Clark D, Morton J. The relationships between external and internal training loads in mixed martial arts. *Int J Sports Physiol Perform*. 2024;
4. Kirk C, Langan-Evans C, Clark D, Morton J. Quantification of training load distribution in mixed martial arts athletes: A lack of periodisation and load management. *PLoS One*. 2021;16(5).
5. Van Doorn J, van den Bergh D, Bohm U, Dablander F, Derks K, Draws T, et al. The JASP Guidelines for Conducting and Reporting a Bayesian Analysis. *PsyArXiv*; 2019;

C45

Metformin inhibits glucose-uptake regulating transcription factor NR4A3 expression after exercise.

Brenda J. Peña Carrillo¹, Rasmus Kjøbsted², Jonas M Kristensen², Jørgen F.P. Wojtaszewski²,
Brendan M. Gabriel¹

¹University of Aberdeen, Aberdeen, United Kingdom, ²August Krogh section for molecular physiology, Institute for Nutrition, Exercise and Sports, University of Copenhagen, Copenhagen, Denmark

Metformin is the most prescribed initial anti-hyperglycaemic medication for people with Type 2 Diabetes. Exercise also has many beneficial health effects and is often recommended concomitantly. Although exercise also improves glycaemia, this effect is inhibited when undertaken alongside metformin ingestion [1,2]. Metformin intake also appears to further inhibit the beneficial response to exercise, including ablating improvements in insulin sensitivity and skeletal muscle mitochondrial protein synthesis and respiration [3,4]. Therefore, we propose that the skeletal muscle transcriptional response to exercise is disrupted by metformin. In this study, we hypothesise that metformin alters the transcriptomic response to exercise, and that this plays a role in the metformin inhibition of the beneficial exercise response. To test this, we analysed skeletal muscle biopsies from a previous study [5]. In this study, seven healthy lean male participants completed one bout of single-leg exercise with a contralateral non-exercising control-leg after acute metformin/placebo supplementation in a crossover design. After an overnight fast, muscle biopsies from the vastus lateralis were obtained in both legs after 1 hr of rest. Thereafter, 1.5 g metformin/placebo was ingested together with a standardized breakfast, the following 4½ hr were spent lying on a bed, after 2 hr a second metformin dose of 1.5 g metformin/placebo was ingested, at 4½ hr a second needle biopsy in both legs was taken. Immediately after this, the participant performed one-legged knee extensor exercise for 40 min with an intensity of 80% PWL (peak work-load) and a third biopsy was taken from both legs. RNA sequencing analysis was performed on biopsy samples from the rest and exercised leg from metformin/placebo groups, after 1 hr of rest, after 4½ hr (after metformin/placebo supplementation), and after exercise. This analysis revealed that metformin supplementation inhibited the transcriptomic response to exercise by reducing the total number of differentially expressed genes in response to exercise. After exercise, 81 genes were upregulated in response to exercise in both the metformin and placebo trials. 53 genes were uniquely upregulated in the placebo trial, while only 17 genes were uniquely upregulated in the Metformin trial. Importantly, the transcription factor NR4A3 was upregulated in response to exercise during the placebo trial (adj.p=0.011), but not when participants consumed metformin (adj.p=0.234). In HSMM (Human skeletal muscle myotubes), metformin (10µM) did not change NR4A3 expression (RT-qPCR, 1.2-fold-change, p=0.536) compared to the control. As expected, the exercise mimetic Ionomycin (8µM) significantly increased NR4A3 expression (4.3-fold-change, p<0.001), while concomitant metformin incubation significantly reduced the relative NR4A3 response (2.4-fold-change, p=0.002). In summary, we propose that the NR4A3 response to exercise is inhibited by metformin and that this may be a mechanism inhibiting exercise training-induced adaptations and skeletal muscle insulin sensitisation during metformin treatment.

1. Boulé NG, et al. (2011) Metformin and exercise in type 2 diabetes: examining treatment modality interactions. *Diabetes Care* 34(7):1469–1474. <https://doi.org/10.2337/DC10-2207>.
2. Peña Carrillo, BJ, et al. (2024). Morning exercise and pre-breakfast metformin interact to reduce glycaemia in people with Type 2 Diabetes: a randomized crossover trial. *MedRxiv* 2023-09. <https://doi.org/10.1101/2023.09.07.23295059>.
3. Das S, et al. (2018) Effect of metformin on exercise capacity: A meta-analysis. *Diabetes Res Clin Pr* 144:270–278. <https://doi.org/10.1016/j.diabres.2018.08.022>.
4. Konopka AR, et al. (2019) Metformin inhibits mitochondrial adaptations to aerobic exercise training in older adults. *Aging Cell* 18(1):e12880. <https://doi.org/10.1111/accel.12880>.
5. Kristensen JM, et al. (2019) Metformin does not compromise energy status in human skeletal muscle at rest or during acute exercise: A randomised, crossover trial. *Physiol Rep* 7(23). <https://doi.org/10.14814/phy2.14307>.

C46

Insights into the Transforming Growth Factor superfamily specific modulation: unravelling the impact of hibernating bear serum in primary human muscle cells

Chloé Richard¹, Guillaume Fourneaux¹, Alexandre Geffroy², Gwendal Cueff¹, Christophe Tatout³, Alina L Evans⁴, Jonas Kindberg⁵, Guillemette Gauquelin-Koch⁶, Etienne Lefai¹, Fabrice Bertile², Lydie Combaret¹

¹Université Clermont Auvergne, INRAE, Unité de Nutrition Humaine, UMR 1019, Clermont-Ferrand, France, ²Université de Strasbourg, CNRS, IPHC UMR 7178, Strasbourg, France, ³Université Clermont Auvergne, CNRS, Inserm, iGReD, Clermont-Ferrand, France, ⁴Department of Forestry and Wildlife Management, Inland Norway University of Applied Sciences, Campus Evenstad, NO-2480, Koppang, Norway, ⁵Norwegian Institute for Nature Research (NINA), Trondheim, Norway, ⁶Centre National d'Etudes Spatiales, CNES, 75001, Paris, France

Muscle atrophy observed in several physio-pathological situations has harmful consequences for the patients and results from an imbalance between protein synthesis and proteolysis. Despite a thorough understanding of molecular events involved in muscle atrophy, primarily through using rodent and human models, no proven effective treatment exists to date (1). In our group, we use the brown bear model, which does not display muscle atrophy during hibernation, although prolonged fasting and physical inactivity. This muscle atrophy resistance is correlated with inhibition of the pro-atrophic TGF- β (Transforming Growth Factor) signalling and maintenance of the hypertrophic BMP (Bone Morphogenetic Protein) signalling (2). We also showed that winter-hibernating bear serum (WBS) induces hypertrophy in human myotubes (3).

The study aimed to further investigate WBS effects on human myotubes by analysing transcriptome changes (mRNA sequencing) after 48h cultivation with 5% SBS (summer-active bear serum) or WBS (n=3, DESEQ2 analysis). Subsequently, we selected some differentially expressed genes (DEGs) identified above within the BMP pathway and analysed their protein levels (n=8-9, ratio paired t-test). Finally, we investigated the impact of bear serum on human myotubes response (n=6) to increasing doses of BMP7 (0 to 2 μ g/ml) or TGF- β 3(0 to 100ng/ml) for 30 min. We thus analyzed SMAD3 or SMAD1/5 phosphorylation, indicative of TGF- β or BMP pathway activation, respectively (2-way ANOVA). Data are means +/-SEM and statistical significance threshold was set at 0.05.

We identified 352 DEGs in human myotubes cultivated with WBS versus SBS. Gene Ontology analysis revealed enrichment in pathways related to muscle function, extracellular matrix remodelling and regulation of BMP signalling. Specifically, mRNA levels for several BMP signalling inhibitors (*SMAD6*, *CHRD*, *GREM1/2*) and activators (*ENG*, *SCUBE3*) decreased by 20-58% in WBS compared to SBS conditions. In addition, several BMP-regulated genes were also downregulated by 40-70% in WBS (*ID1*, *ID3*, *SMAD6*, *SAMD11*). We further report here that ENG and GREM1 protein levels were also downregulated by 18-37% in WBS versus SBS conditions. We showed that BMP7 treatment induces dose-dependent SMAD1/5 phosphorylation in human myotubes, beginning at 0.1 μ g/ml in SBS conditions and 0.5 μ g/ml in WBS. The maximal induction was nevertheless identical in both conditions. Similarly, the response of human myotubes to TGF- β 3 treatment was also lower in WBS conditions compared to SBS conditions. SMAD3

phosphorylation showed a dose-dependent increase, starting at 1 ng/ml in SBS and 10 ng/ml in WBS. By contrast to the BMP challenge, the induction remained consistently lower across all concentrations, including the higher one (100 ng/ml).

Overall, we show a transcriptomic reprogramming of human myotubes cultivated with WBS, including BMP signalling pathway regulation. The reduced responsiveness of both TGF β and BMP pathways to their ligands in the presence of WBS aligns with the hypometabolism previously reported in these myotubes (3) or hibernating brown bear muscle (4). Conversely, the lower induction of TGF β signalling for all concentrations, contrasted with the consistent plateau of BMP induction at high doses, suggests that WBS may modulate the TGF β /BMP balance towards the BMP pathway. These data are consistent with the specific TGF- β /BMP balance depicted in atrophy-resistant muscles from the hibernating brown bear (2).

(1) Peris-Moreno et al. Ubiquitin Ligases at the Heart of Skeletal Muscle Atrophy Control. *Molecules*. 2021 Jan 14;26(2):407. doi: 10.3390/molecules26020407. (2) Cussonneau et al. Concurrent BMP Signaling Maintenance and TGF- β Signaling Inhibition Is a Hallmark of Natural Resistance to Muscle Atrophy in the Hibernating Bear. *Cells*. 2021. 10(8):1873. doi: 10.3390/cells10081873. (3) Chanon et al. Proteolysis inhibition by hibernating bear serum leads to increased protein content in human muscle cells. *Sci Rep*. 2018. 8(1):5525. doi: 10.1038/s41598-018-23891-5. (4) Chazarin et al. Metabolic reprogramming involving glycolysis in the hibernating brown bear skeletal muscle. *Front Zool*. 2019 May 6;16:12. doi: 10.1186/s12983-019-0312-2.

C47

The Role of Extracellular Matrix Components in Determining Skeletal Muscle Fiber Types: An Investigation with C2C12 Myoblasts

Yhusi Karina Riskawati^{1,3}, Hsi Chang², Chuang-Yu Lin⁴

¹International PhD Program for Cell Therapy and Regenerative Medicine, College of Medicine, Taipei Medical University, Taipei, Taiwan, Province of China, ²Department of Pediatrics, School of Medicine, College of Medicine, Taipei Medical University, Taipei, Taiwan, Province of China,

³Physiology Department, Faculty of Medicine, Universitas Brawijaya, Malang, Indonesia,

⁴Department of Biomedical Science and Environmental Biology, Kaohsiung Medical University, Kaohsiung, Taiwan, Province of China

Introduction Muscle functionality and adaptability depend on the precise specification of muscle fiber types, a process that directly influences contraction dynamics and overall performance. While the critical role of extracellular matrix (ECM) components in muscle development is recognized, the specific mechanisms through which ECM influences the differentiation of myoblasts into distinct muscle fiber types remain inadequately explored. This gap in knowledge, particularly regarding how different ECM cues guide the activation of myogenic regulatory factors (MRFs) and mediate fiber type-specific transitions, limits our understanding of muscle physiology and the development of targeted therapeutic interventions. Addressing this gap, our study delves into the modulation of C2C12 myoblast differentiation by ECM components present in Matrigel™, aiming to elucidate the intricate processes of muscle contraction regulation and fiber type specification. Through this investigation, we seek to contribute to the broader comprehension of muscle tissue engineering and the potential for ECM-based strategies in regenerative medicine.

Method C2C12-GFP myoblasts were differentiated on a Matrigel™ substrate, enabling the assessment of myotube formation. The expression patterns of key MRFs were evaluated via quantitative PCR (qPCR), while the expression of myosin heavy chain (MyHC) genes and proteins, indicative of fast and slow skeletal muscle fibers, was analyzed using Western blotting and immunocytochemistry. RNA sequencing was employed to dissect the signaling pathways and gene expression profiles underlying muscle fiber type differentiation in response to ECM cues.

Results Observations from Day 7 post-differentiation highlighted a pronounced shift towards fast-type myotube predominance, with decreased Pax7 and increased Myogenin expressions reflecting advanced differentiation stages. This trend was validated through Western blot and immunofluorescence analyses, revealing an altered expression ratio favoring fast-type over slow-type myotube proteins. qPCR analysis corroborated these findings, demonstrating upregulation of the MYH4 gene and downregulation of MYH7, alongside modulations in HIF-1α and PGC-1α levels. RNA sequencing analysis utilizing Gene Ontology (GO) and the Kyoto Encyclopedia of Genes and Genomes (KEGG) databases to analyze differentially expressed genes (DEGs), revealed a gene expression profile distinct from controls, with pathway analyses emphasizing activity within specific pathways such as C5 isoprenoid biosynthesis and inositol phosphate metabolism. Central genes to these pathways, including Cenpf, Brca1, and Nek2, were pinpointed as potential targets for modulating muscle fiber type differentiation.

Conclusions The ECM components in Matrigel™ play a significant role in steering C2C12 myoblast differentiation towards specific muscle fiber types, with significant implications for muscle contraction and overall muscle health. Our study enhances the understanding of the molecular landscape governing muscle fiber specificity and opens avenues for targeted strategies in muscle repair and regeneration. By elucidating the mechanisms through which ECM influences muscle cell fate, we contribute to the broader knowledge base in muscle physiology, offering insights into optimizing muscle function and combating muscle-related diseases.

1. Hoppeler, H., Molecular networks in skeletal muscle plasticity. *Journal of Experimental Biology*, 2016. 219(2): p. 205-213. 2. Oskolkov, N., et al., High-throughput muscle fiber typing from RNA sequencing data. *Skeletal Muscle*, 2022. 12(1): p. 16. 3. Zhang, W., Y. Liu, and H. Zhang, Extracellular matrix: an important regulator of cell functions and skeletal muscle development. *Cell & Bioscience*, 2021. 11(1): p. 65. 4. Yasuda, T., et al., Mitochondrial dynamics define muscle fiber type by modulating cellular metabolic pathways. *Cell Reports*, 2023. 42(5): p. 112434. 5. Grefte, S., et al., Matrigel, but not collagen I, maintains the differentiation capacity of muscle derived cells in vitro. *Biomedical Materials*, 2012. 7(5): p. 055004.

C48

Retinal cone-driven responses to flickering stimuli recorded from over 2000 adults: associations with age, sex and ethnicity

Muhammad Hamza Ahmed¹, Xiaofan Jiang^{1,2,3}, Isabelle Chow^{2,3}, Diana Kozareva^{2,3}, Pirro Hysi^{2,3}, Christopher Hammond^{2,3}, Omar Mahroo^{1,2,3}

¹*Institute of Ophthalmology, University College London, London, United Kingdom*, ²*Department of Twin Research and Genetic Epidemiology, King's College London, London, United Kingdom*, ³*Section of Ophthalmology, King's College London, St Thomas' Hospital Campus, London, United Kingdom*

Purpose

The peak time of the electroretinogram (ERG) response to flicker is a sensitive measure of human panretinal cone system function in health and disease. Here, we analysed responses in over 2000 healthy adult twins, with the aim of exploring associations with age, sex and ethnicity.

Methods

Participants were recruited from the TwinsUK cohort and underwent non-mydriatic light-adapted ERG recordings using a portable device (RETeval system, LKC Technologies) in conjunction with specialised skin electrodes. The study had Research Ethics Committee approval and conformed to the tenets of the Declaration of Helsinki. The device delivered white full-field flickering stimuli (28.3 Hz) on a white background. Pupil diameter was automatically measured and adjusted for, such that the retinal illuminance of stimuli (85 Td.s) and background (850 Td) were equivalent to that delivered by international standard stimuli through a dilated pupil. Flicker ERG peak times were averaged across both eyes for each participant. Participants were excluded where reliable recordings were unavailable from either eye or if the interocular difference in peak time exceeded 2 ms. When both members of a twin pair were included, peak times were averaged for both twins (to avoid confounding due to intrapair correlation). Correlation with age was quantified and comparisons (age-adjusted where appropriate) were made between sexes and ethnicities.

Results

Recordings were analysed from 2395 participants (83% female, 94% of white ethnicity), including 852 full twin pairs. Mean (SD) age was 55.7 (16.3) years; median age was 60. Mean (SD) flicker ERG peak time was 25.6 (1.2) ms; the median was 25.4 ms. Peak times showed a highly significant ($p < 0.0001$) positive correlation with age; the Spearman correlation coefficient was 0.52. The relationship with age was non-linear, such that the increase in peak time per year was greater for older age groups. Male and female participants had similar mean ages, and the difference between averaged peak times across sexes was not significant ($p = 0.059$). Where ethnicity was recorded,

806 pairs identified as white, 14 pairs as black, and 12 pairs as Asian. Age-adjusted comparisons revealed the following significant differences: compared with black participants mean peak time was shorter for white participants ($p=0.000086$) and shorter for Asian participants ($p=0.0097$). Other comparisons did not reach significance.

Conclusions

The highly significant association between ERG flicker peak times and age suggests possible slowing of retinal processing with age. The relationship was not linear. We also found a difference between ethnicities that invites further investigation, and suggests potential importance of development of ethnicity-specific reference ranges.

C49

The impact of fatiguing exercise on corticospinal function in relapse-remitting multiple sclerosis

Gemma Brownbill¹, Jeanne Dekerle², Mara Cercignani³, James Stone¹

¹Brighton and Sussex Medical School, Brighton, United Kingdom, ²Brighton University, Brighton, United Kingdom, ³Cardiff University, Cardiff, United Kingdom

Background: Multiple sclerosis (MS) is an autoimmune demyelinating disease that disrupts corticospinal functioning. Transcranial magnetic stimulation (TMS) of the motor cortex allows assessment of both corticospinal excitability, inhibition, and conduction time via recordings of motor evoked potentials (MEPs) and silent periods (SPs), respectively. A change indicates a central origin of neuromuscular fatigue. Research has shown that corticospinal integrity is impaired at rest in MS. This study investigated how sustained isometric exercises of the wrist extensors affects corticospinal responses in people with relapsing-remitting MS compared to healthy controls.

Methods: 22 people with relapse-remitting MS (3 males; Expanded Disability Status Scale < 3.5) and 22 healthy matched controls (CG) performed an all-out 3-minute effort, and 8 minutes later, a 5-minute submaximal effort (17.2 ± 6.6 % Maximal Voluntary Contraction (MVC)). Active motor threshold (AMT) was quantified as the minimum stimulator output to evoke 3/6 MEP > 0.5mV at 20% MVC. Ten single-pulse TMS (120% AMT) were delivered to the primary motor cortex during a 10% MVC, before the 3-minute all-out effort, immediately after, and 9 minutes following the 5-minute submaximal exercise bout. Surface electromyography was recorded from the extensor carpi radialis longus (ECRL) and extensor carpi radialis brevis (ECRB) muscles. MEP amplitude, latency, and silent period (SP) were measured for each MEP. Student t-tests and linear mixed models were used to assess group, time, and interaction effects. Critical p value was set at 0.05. Ethical approval was obtained by the Health Research Authority (IRAS: 260176).

Results: AMT was significantly higher in the MS group (MS: 55 ± 10 % of maximum stimulator output (MSO); CG: 47 ± 8 % of MSO ($t_{(21)} = -3.66$, $p = .001$). Averages and standard deviations for both groups at each time point for all variables can be viewed in Table 1. A significant effect of time was found for ECRB SP only ($F_{(2, 70.7)} = 3.77$, $p = .02$). MEP latency and SP were overall longer and absolute ECRB MEP amplitude smaller for the MS group (ECRL latency: $F_{(1, 29.3)} = 8.51$, $p = .007$; ECRL SP: $F_{(1, 20.3)} = 4.67$, $p = .04$; ECRB latency: $F_{(1, 37.6)} = 6.79$, $p = .01$; ECRB SP: $F_{(1, 24.2)} = 7.08$, $p = .01$; ECRB MEP amplitude: $F_{(1, 36.7)} = 7.82$, $p = .01$). No group x time interactions were observed ($p > .05$).

Conclusion: These findings support the notion of impaired corticospinal function in MS, as evidenced by the higher AMT, longer SP, delayed MEP latencies and smaller MEP amplitudes in the MS group both at rest and following exercise of the wrist extensors. Exercise did not induce changes in corticospinal excitability or inhibition exclusive to the MS group.

Table 1. Mean \pm standard deviation for motor evoked potential (MEP) amplitude, silent period (SP) and latency for the extensor capri radialis longus (ECRL) and extensor capri radialis brevis (ECRB).

Dependent variable	Muscle	Group	Pre-exercise	Post-exercise	Post-recovery
MEP amplitude (mV)	ECRL	CG (n = 22)	1.48 \pm 1.02	1.56 \pm 1.07	1.49 \pm 1.04
		MS (n = 20)	0.95 \pm 0.57	1.16 \pm 0.71	1.16 \pm 0.54
	ECRB	CG (n = 22)	1.87 \pm 1.07	2.14 \pm 1.21	1.99 \pm 0.98
		MS (n = 20)	1.12 \pm 0.53	1.32 \pm 0.64	1.46 \pm 0.70
MEP SP (ms)	ECRL	CG (n = 20)	139 \pm 17.4	136 \pm 21.9	131 \pm 21.6
		MS (n = 16)	159 \pm 43.5	161 \pm 48.7	154 \pm 30.0
	ECRB	CG (n = 21)	137 \pm 20.0	136 \pm 20.6	129 \pm 21.4
		MS (n = 18)	163 \pm 37.1	164 \pm 51.9	157 \pm 32.0
MEP latency (ms)	ECRL	CG (n = 22)	14.1 \pm 1.2	14.3 \pm 1.3	14.1 \pm 1.3
		MS (n = 22)	16.2 \pm 2.7	16.1 \pm 3.0	15.8 \pm 2.6
	ECRB	CG (n = 22)	14.5 \pm 1.7	14.6 \pm 1.8	14.5 \pm 2.0
		MS (n = 21)	16.3 \pm 2.3	16.3 \pm 2.7	16.3 \pm 2.7

C50

The Human Taste Code

Göran Hellekant^{5,6}

¹University of Wisconsin-Madison School of Veterinary Medicine Department of Biomedical Sciences 1656 Linden Drive Madison, WI 53706, USA Retired Professor University of Minnesota Duluth Campus School of Medicine Department of Biomedical Sciences 1035 University Drive Duluth, MN 55812, USA Guest Senior Professor Swedish University of Agricultural Sciences School of Veterinary Medicine Department of Animal Breeding and Genetics Uppsala, Sweden, Madison WI, United States, ²Swedish University of Agricultural Sciences School of Veterinary Medicine Department of Animal Breeding and Genetics Uppsala, Sweden Guest Senior Professor Swedish University of Agricultural Sciences School of Veterinary Medicine Department of Animal Breeding and Genetics Uppsala, Sweden, Uppsala, Sweden, ³University of Wisconsin-Madison, Madison, United States, ⁴Swedish University of Agricultural Sciences, Uppsala, Sweden, ⁵University of Wisconsin-Madison, Madison, United States, ⁶Swedish University of Agricultural Sciences, Uppsala, Sweden

Background: Since antiquity human taste has been divided into 4-5 taste qualities. However, responses in taste fibers of other animal species have only partly clustered according to human qualities. We realized taste qualities vary according to phylogeny, where species closer to humans show higher fidelity to human taste qualities.

Methods/Results: We compared psychophysical data and taste nerve recording from humans to behavioral tests and single taste fiber recordings in chimpanzee, rhesus and marmoset. Our data show how, with phylogenetic closeness to humans, taste fibers responded more exclusively to taste stimuli within each human taste quality. We then used the human sweet taste modifiers, miraculin and gymnemic acid. In human, miraculin adds sweet to sour taste and doubles nerve responses to acids. After miraculin nonhuman primates also doubled acid intake while both acid-specific and sweet-specific single taste fibers responded to acids. In human gymnemic acid eliminates sweet quality. In chimpanzee gymnemic acid abolished taste fiber responses to sweet without affecting responses to other tastes.

Analytical and statistical tools: Clusters of taste fibers in both CT and NG were identified with hierarchical cluster analysis. Responses to all stimuli were taken into consideration and the analysis considers each stimulus as an independent variable and a Pearson correlation coefficient is calculated between the responses. The results of hierarchical cluster analysis were presented as a Dendrogram. Multidimensional Scaling presented the single fiber results in a multidimensional space for further analyses.

The animal research was conducted in accordance with the principle and guidelines established by the Association for the Assessment and Accreditation of Laboratory Animal Care International (AAALAC) and procedures were approved by the local Institutional Animal Care and Use Committee (IACUC) from the University of Wisconsin-Madison, WI, USA (marmoset and rhesus monkey) and Laboratory for Experimental Medicine and Surgery in Primates, New York Medical Center, NY, USA. (chimpanzee).

Conclusions: Information from each type of taste receptor cell reaches a specific cortical taste area where it gives rise to taste qualities; taste is created in the cortical region where taste fibers deliver action potentials, thus satisfying the criteria of labeled-line coding which follows Mueller's law of specific nerve energy for pain, touch, and temperature where sensation is created in the cortex after conveyance by sensory fibers. In humans these cortical areas give rise to the taste qualities, sweet, sour, bitter, salt and umami. It is likely that this principle applies to other mammals, but their taste qualities differ due to species differences in taste receptor structure.

Hellekant G, Ninomiya Y, Danilova V: Taste in chimpanzees II: single chorda tympani fibers. *Physiol Behav* 1997, 61(6):829-841. Hellekant G, Ninomiya Y, Danilova V: Taste in chimpanzees III: Labeled line coding in sweet taste. *Physiol Behav* 1998, 65(2):191-200. Lee H, Macpherson LJ, Parada CA, Zuker CS, Ryba NJP: Rewiring the taste system. *Nature* 2017, 548(7667):330-333.

C51

Chronic vagus nerve stimulation reduces muscle sympathetic nerve activity in drug-resistant epilepsy

Mikaela Patros¹, Shobi Sivathamboo¹, Hugh Simpson¹, Terence J O'Brien¹, Vaughan G Macefield¹

¹*Department of Neuroscience, School of Translational Medicine, Monash University, Melbourne, Australia*

Background:

Vagus Nerve Stimulation (VNS), delivered via surgically implanted cuff electrodes on the left cervical vagus, is used to treat drug-resistant epilepsy (DRE). VNS is believed to act on the brain to reduce seizures by chronic neuromodulation, but it is not known what effects it has on other systems, including the sympathetic nervous system. Here we tested the hypothesis that chronic VNS reduces muscle sympathetic nerve activity (MSNA).

Methods:

Nineteen patients between the ages of 18-66 years with a diagnosis of DRE were recruited from the Alfred Health epilepsy clinics. Spontaneous bursts of MSNA were recorded via a tungsten microelectrode inserted percutaneously into a muscle fascicle of the common peroneal nerve. MSNA recordings were obtained from 11 DRE patients with implanted VNS devices who had been stimulated chronically (>6 months stimulation) and 8 DRE patients yet to receive a VNS implant. Baseline recordings were obtained in existing VNS patients, lying supine with their VNS device stimulating at their clinically set parameters (1.125-3.5 mA, 20 Hz, 250µs, duty cycle 10%-35%).

Results:

Patients without VNS (n=8) had a mean of 26.6 ± 9.5 (SD) bursts/min at rest, while those treated with VNS (n=11) had a mean of 13.1 ± 7.9 SD bursts/min, measured between trains of VNS. Although VNS did not appear to affect MSNA acutely, MSNA was significantly lower in patients following chronic VNS ($p=0.0017$).

Conclusions:

While VNS appeared to have no acute effects on MSNA at rest, nor during manoeuvres that increase MSNA, such as passive head-up tilt, MSNA was reduced in patients with chronic VNS treatment compared to those without. Chronic VNS treatment may have a protective effect on cardiovascular risk by reducing sympathetic activity. This may contribute to the mechanism behind risk-reduction for sudden unexplained death in epilepsy (SUDEP) in VNS-treated patients (Ryvlin et al., 2018).

Ryvlin P, So EL, Gordon CM, Hesdorffer DC, Sperling MR, Devinsky O, Bunker MT, Olin B, Friedman D. Long-term surveillance of SUDEP in drug-resistant epilepsy patients treated with VNS therapy. *Epilepsia*. 2018; 59: 562-572.

C52

The loss of Ca²⁺-activated Cl⁻ channel, TMEM16A worsens the ischemic stroke-reperfusion outcome

Elizaveta Melnikova¹, Ida Damsgaard Larsen¹, Line Mathilde Brostrup Hansen¹, Dmitry Postnov², Christian Aalkjær¹, Vladimir Matchkov¹

¹Aarhus University, Aarhus, Denmark, ²Department of Clinical Medicine - Center of Functionally Integrative Neuroscience (CFIN), Aarhus, Denmark

The brain is the most active and highly metabolically demanding organ (1). Oxygen delivery is carried out through strictly controlled cerebral perfusion via local redistribution of blood flow under variations in neuronal activity. There is an intimate relationship between cerebral vasculature and neuronal tissue, where changes in local perfusion affect supplied cells and vice versa, glia and neurons influence adjacent blood flow (2). Anoctamin-1 (TMEM16A) belongs to the family of Ca²⁺-activated Cl⁻ channels (3) and is suggested to act as a central regulator of neuromodulation. Tmem16A is activated by intracellular Ca²⁺ ions, leading to Cl⁻ influx and subsequent depolarization of smooth muscle cells (3). This enables an amplification loop for voltage-dependent Ca²⁺-influx and cerebrovascular contraction. This reinforces the idea of TMEM16A implication for ischemic stroke outcome. Ischemic Stroke is caused by a rapid loss of blood supply to a part of the brain due to thromboembolic occlusion in cerebral circulation (4). Understanding the mechanisms contributing to the harmful action of stroke reperfusion is of great importance for new treatment paradigms to improve stroke survival and outcome.

We aim to evaluate the importance of cerebrovascular TMEM16A for neuroprotection during ischemic stroke.

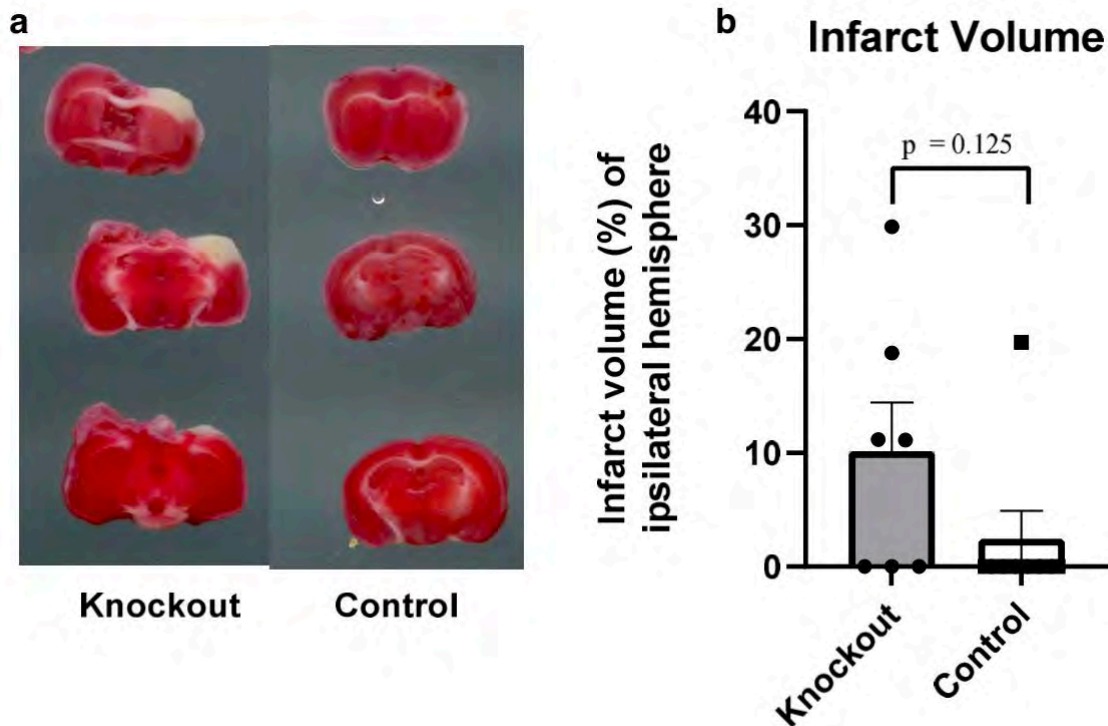
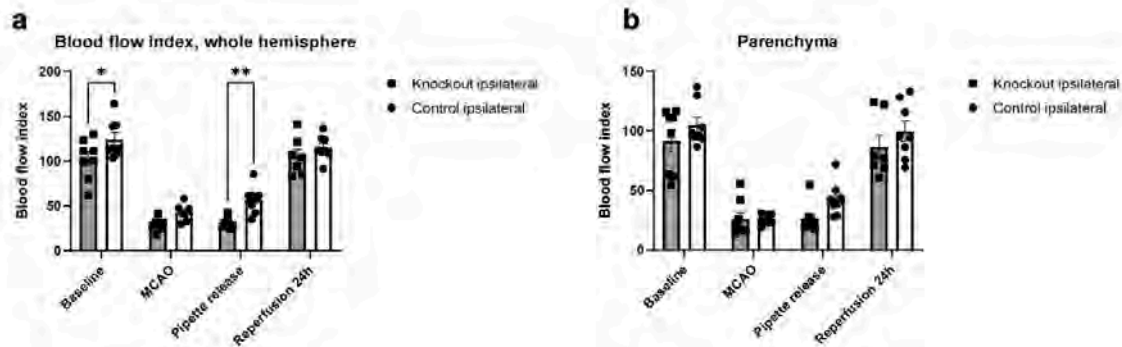
Procedures were performed according to the guidelines from Directive 2010/63/EU of the European Parliament on the protection of animals used for scientific purposes and approved by the Animal Experiments Inspectorate of the Danish Ministry of Environment and Food.

We used 3.5-6 months old, smooth-muscle-specific conditional TMEM16A knockout (KO) male mice. Mice expressed TMEM16A gene floxed around exon7 and Cre recombinase with estrogen receptor type 2 under control of smooth muscle myosin heavy chain promoter. Age-matched male mice expressing Cre only were used as a control. All mice were treated with tamoxifen injections to induce smooth-muscle-specific knockout. Cerebral blood flow was assessed with Laser Speckle Contrast Imaging. Ischemic stroke was induced with a transient middle cerebral artery occlusion (tMCAO) for 60 min in mice anesthetized with isoflurane. Stroke severity was analyzed with post-mortal 2,3,5-triphenyltetrazolium (TTC) staining.

tMCAO reduced blood flow in the ipsilateral hemisphere for both KO (n=7-8) and controls (n=8; $p < 0.05$; *fig. 1a*), with TMEM16A KO mice having an attenuated flow reduction ($< 80\%$ compared to the controls ($p > 0.01$; *fig. 1a*). No difference between KO and control mice in brain perfusion was observed 24 hours after reperfusion ($p < 0.05$; *fig. 1a*). When blood flow changes during MCA occlusion were analyzed in detail, a larger area of severe blood flow drop ($< 80\%$) was

seen in TMEM16A KO mice over the occlusion period ($p > 0.01$)(fig.1a). TTC staining suggested a larger infarct volume in KO ($n=7$) than in control mice ($n=7-8$; $p=0.125$; fig.2).

We found that smooth muscle-specific knockout of TMEM16A worsens ischemic stroke-reperfusion outcomes in mice. We suggest this occurs due to diminished cerebral blood flow control in TMEM16A knockout mice and their abnormal vascular tone. This proposes that under ischemic conditions, when there is an imbalance in ion concentrations, TMEM16A is an important component for vascular tone optimization. Our results indicate that TMEM16A may be a potential pharmacological target in improving stroke outcomes.



- 1) Mireille Bélanger et. al. Volume 14, Issue 6, December 2011, Pages 724-738.
- 2) Costantino Iadecola. Neuron. 2017 Sep 27; 96(1): 17–42.
- 3) Weiliang Bai et. al. J Adv Res. 2021 Nov; 33: 53–68.
- 4) Eng H. Lo et. Al. Nature Reviews Neuroscience, volume 4, pages 399–414 (2003).

C53

G155D mutation associated with Autosomal Dominant Nocturnal Frontal Lobe Epilepsy alters the structure-function relationship of Calcium Binding Protein 4.

Vanessa Morris², Dan Rigden², Caroline Dart², Nordine Helassa²

¹University of Liverpool, Liverpool, United Kingdom, ²Department of Biochemistry, Cell and Systems Biology, Institute of Systems, Molecular and Integrative Biology, University of Liverpool, Liverpool, United Kingdom

Introduction – Autosomal dominant frontal lobe epilepsy (ANDFLE) is a form of partial epilepsy disorder characterised by frequent focal seizures with usual onset at around 10 years of age. Currently, 30 % of ANDFLE patients do not respond to treatment. Calcium Binding Protein 4 (CaBP4) regulates the activity of voltage-dependent calcium channels including Cav1.3 and Cav1.4. Cav1.4 is predominantly expressed in photoreceptor synaptic terminals and plays a crucial role in maximal glutamate release under low light conditions. The point mutation G155D in CaBP4 has been associated with ANDFLE, yet its impact on the structure-function relationship of CaBP4 is still unknown.

Methods – Computational biology tools (AlphaFold and DynaMut) alongside circular dichroism (CD) were utilised to examine the G155D induced modifications to secondary and tertiary structure. Predicted changes to protein stability were also considered using computational tools (DynaMut). Susceptibility to protease digestion (SDS-PAGE) and thermostability (CD) were also used to investigate the impact of G155D on protein stability. The impact of the G155D mutation on CaBP4's calcium affinity was evaluated through intrinsic fluorescence spectroscopy (tyrosine). Isothermal titration calorimetry (ITC) assessed whether G155D caused changes to CaBP4's affinity for the IQ domains of voltage-dependent calcium channels (Cav1.2, Cav1.3, Cav1.4).

Results and Conclusions – Under both calcium-bound (n = 5) and calcium-free conditions (n = 5), the G155D variant exhibited a decrease of $10 \pm 1\%$ in alpha-helical content and a $5 \pm 1\%$ increase in unordered structure. DynaMut predictions revealed a notable increase in flexibility within the region of the G155D mutation and an elevated number of intra-molecular interactions. Susceptibility to protease digestion showed that the G155D mutation destabilised the protein in both calcium-bound (n = 7) and calcium-free conditions (n = 5). The G155D variant also displayed a significant reduction in thermostability with V_{50} values dropping from 44.0 ± 0.8 °C to 37.9 ± 0.5 °C in calcium-free conditions (n = 6) and from 82.5 ± 1.3 °C to 76.2 ± 1.2 °C when calcium-bound (n = 6). Equilibrium calcium titrations showed a 2-fold reduction in Ca^{2+} affinity (n = 3) for the G155D variant. There was also reduced affinity seen between the G155D protein and all the voltage-dependent calcium channels' IQ domains. For the Cav1.2 IQ domain there was a 3.6-fold reduction in affinity from $K_d \text{ CaBP4} = 1.85$ M (n = 2) to $K_d \text{ G155D} = 6.59$ M (n = 4). Meanwhile for both Cav1.3 and Cav1.4 there was a 4.7 fold reduction in affinity from $K_d \text{ CaBP4} = 1.85$ M (n = 5) to $K_d \text{ G155D} = 8.67$ M (n = 7) and from $K_d \text{ CaBP4} = 1.59$ M (n = 5) to $K_d \text{ G155D} = 7.41$ M (n = 6) respectively. To summarize, our findings indicate that the ANDFLE-associated mutant G155D has a significant impact on the structure, stability and binding affinity of CaBP4. This study marks the beginning of understanding the mechanism in which the G155D point mutation in CaBP4 leads to ANDFLE.

C54

The influence of the menopause and hormone replacement therapy on cortical neuroplasticity

Paul Ansdell¹, Padraig Spillane¹, Mollie O'Hanlon², Elisa Nédélec², Thomas Inns², Markus Hausmann³, Stuart Goodall¹, Katy Vincent⁴, Charlotte Stagg⁴, Jessica Piasecki²

¹Northumbria University, Newcastle Upon Tyne, United Kingdom, ²Nottingham Trent University, Nottingham, United Kingdom, ³Durham University, Durham, United Kingdom, ⁴University of Oxford, Oxford, United Kingdom

Rationale: Previous research has demonstrated the neuroactive effects of ovarian hormones across the menstrual cycle [1], however it remains less clear how the cessation of hormone production across the menopause influences motor cortical properties. Additionally, it is currently unknown how nervous system adaptation (neuroplasticity) is mediated by endogenous and exogenous hormones across the human lifespan.

Methods: Participants' menopausal status was classified according to NICE guidelines on the diagnosis and management of menopause, with 12 pre-menopausal (age: 29 ± 7 years), 7 peri-menopausal (49 ± 4 years), 5 post-menopausal females (54 ± 5 years), and 7 females using HRT (54 ± 4 years) taking part in the study. Participants underwent a baseline neurophysiological assessment, including electrical stimulation of the median nerve and transcranial magnetic stimulation of the motor cortex to assess corticospinal excitability and intracortical inhibition and facilitation (SICI and ICF). Then, a paired associative stimulation (PAS) protocol was performed with electrical stimulation at 300% perceptual threshold delivered 25 ms prior to TMS at 120% motor threshold. 200 paired stimuli were delivered at 0.2 Hz, which were then followed with repeated neurophysiological assessments immediately, 10-, 20- and 30-minutes after PAS.

Results: No differences between groups were observed at baseline for corticospinal excitability ($p = 0.322$), SICI ($p = 0.570$) or ICF ($p = 0.961$). In response to the PAS protocol, only the pre-menopausal group experienced a significant increase in corticospinal excitability (+69%, $p < 0.001$), compared to peri- (+38%, $p = 0.136$) and post-menopausal females (+4%, $p = 0.868$). HRT users experienced a +53% increase in corticospinal excitability, however, this did not reach statistical significance ($p = 0.084$).

Conclusions: Motor cortical neuroplasticity was only evident in pre-menopausal females, implying that the cessation of ovarian hormone production impairs the nervous system's ability to adapt to novel stimuli. HRT could present an exogenous method of attenuating this menopause-related effect, which has implications for functional capacity in health and disease.

[1] Piasecki et al. (2024) *Exerc Sports Sci Rev* 52(2): p54-62

Expiratory muscle activation pattern during exposure to hypoxia and hypercapnia

Letícia Mendes¹, Beatriz Vieira¹, Isabela Leirão¹, Daniel Zoccal¹

¹*Department of Physiology and Pathology, School of Dentistry of Araraquara, São Paulo State University, Araraquara, Brazil*

The coordination of respiratory muscle activity is essential to move air in and out of the lungs. At rest, inspiration is an active process with contractions of diaphragmatic (DIA) and external intercostal muscles (eIC), while the expiratory airflow is generated by elastic recoil forces of the thorax and lungs. Exposure to reduced oxygen (hypoxia) or elevated carbon dioxide levels (hypercapnia) transforms expiration into an active process, with the recruitment of abdominal (ABD) and internal intercostal muscles (iIC) that increase the expiratory flow. It remains unclear how the ABD and iIC muscles are coordinated during active expiration and how their entrainment modifies the expiratory flow to improve pulmonary ventilation. In the present study, we examined the ABD and iIC muscle activity patterns and the corresponding alterations in the expiratory flow during conditions of hypoxia and hypercapnia. Electrodes were implanted in the DIA, eIC, iIC, and ABD muscles of anesthetized (urethane, 1.2 mg/kg, i.v.) adult male Holtzman rats (n=8, 250-300 g). These animals also received a snout mask that allowed exposure to gas mixtures while monitoring nasal airflow. Experiments were performed under anesthesia. Physiological parameters were recorded under resting conditions and during 10-min exposure to hypoxia (7% O₂) and hypercapnia (7% CO₂). All procedures were approved by the institutional Ethics Committee (#17/2020). Values are expressed as mean±SD and compared using one-way ANOVA followed by Bonferroni or Friedman post-tests. Under resting conditions, DIA and eIC showed synchronized bursts during the inspiratory phase, ABD and iIC were silent, and the expiratory flow peaked during the first expiration stage. Hypoxia caused an initial increase in the respiratory frequency (fR) (resting: 88±11 vs 2nd-min: 113±19 bpm, P<0.01), elicited a sustained increase in DIA (Δ: 25-41%) and eIC (Δ: 37-58%) burst amplitudes (P<0.05), and brought about phase-locked ABD (Δ: 60-120%) and iIC (Δ: 116-325%) expiratory bursts (P<0.05) during the initial six minutes of exposure. These hypoxia-induced respiratory motor changes were accompanied by increased airflow during the second stage of expiration. Under hypercapnic conditions, fR increased during the last 2 min of exposure (resting: 85±12 vs 10th-min: 97±14 bpm, P=0.0299), DIA (Δ: 45-56%) and eIC (Δ: 111-128%) burst amplitudes were higher throughout the exposure time (P<0.05), and ABD (Δ: 105-144%) and iIC (Δ: 219-255%) expiratory activities were higher during the last four minutes of exposure (P<0.02). The respiratory motor responses to hypercapnia did not change the airflow pattern, peaking during the first stage of expiration as noted during resting conditions. Our data indicate that hypoxia and hypercapnia exposures evoke entrained ABD and iIC bursts during the expiratory phase. However, their recruitment timing differs between gas conditions, occurring earlier under hypoxia than in hypercapnia. Moreover, their impact on the expiratory airflow is different, indicating that the adjustments of active expiration on the pulmonary mechanics involve stimulus-dependent recruitment of additional respiratory muscles.

C56

Unveiling the unseen: an in-depth exploration of fetal brain metabolism with magnetic resonance spectroscopy

Jordan Minns^{1,2}, Jack Darby^{1,2}, Stacey Holman^{1,2}, Brahmdeep Saini^{3,4,5}, Georgia Williams⁶, Mike Seed^{3,4,5}, Steven Miller^{5,8}, Christopher Macgowan^{3,4}, Jessie Guo⁵, Janna Morrison^{1,2}

¹Early Origins of Adult Health Research Group, Adelaide, Australia, ²Health and Biomedical Innovation: Clinical and Health Sciences, University of South Australia, Adelaide, Australia, ³Translational Medicine, Hospital for Sick Children, Toronto, Canada, ⁴Department of Medical Biophysics, University of Toronto, Toronto, Canada, ⁵Department of Paediatrics, University of Toronto, Toronto, Canada, ⁶Preclinical, Imaging and Research Laboratories, South Australian Health and Medical Research Institute, Adelaide, Australia, ⁷British Columbia Women's Hospital Ambulatory Care Centre, Vancouver, Canada, ⁸Department of Paediatrics, University of British Columbia & BC Children's Hospital Research Institute, Vancouver, Canada

Background: Magnetic Resonance Spectroscopy (MRS) is a non-invasive advanced imaging technique for assessing the brain's biochemical and metabolic states. For normal brain development, the fetal circulation preferentially delivers oxygen and nutrient-rich blood to the brain through unique adaptations within the fetal circulation. If these adaptations fail, poor neurodevelopment may ensue. With the overall goal of detecting altered neurodevelopment earlier in pregnancy, we aimed to develop an MRS method that overcomes the imaging complexities introduced by maternal respiration and fetal movement, to understand how variations in cerebral oxygen delivery can affect cerebral metabolism.

Methods: At 105–110 days gestation (term, 150 days), pregnant ewes (n=5) underwent fetal surgery where catheters were implanted in the fetal femoral artery and vein, and the amniotic cavity under aseptic conditions. Anaesthesia was induced with intravenous diazepam (0.3 mg/kg) and ketamine (5 mg/kg) and maintained with isoflurane (1.5%–2.5% in 100% oxygen). All ewes received an analgesic, meloxicam (0.5 mg kg⁻¹, subcutaneously) on the day before and the day of surgery. MRI scans were performed on a 3T Siemens clinical system (Magnetom Skyraa, Siemens Healthineers, Erlangen) while the ewe was ventilated. Proton MRS was performed using PRESS at an intermediate echo time (135ms) and a voxel size 15x15x15, gated to maternal respiration. To measure blood flow and oxygenation within the major fetal vessels, phase-contrast MRI and T2 oximetry were performed as previously described (Darby *et al.*, 2020; Saini *et al.*, 2020). Measures were performed during a normoxemic (Nx) and a hyperoxemic (Hyx) fetal state, achieved by maternal hyperoxygenation and confirmed with blood gas analysis (PO₂; Siemens RAPIDPOINT). After MRI, ewes and their fetuses were humanely killed with an overdose of sodium pentobarbitone, and fetal brains were collected. Data is presented as mean±SD and analysed using a Students' t-test; $P < 0.05$ is considered statistically significant.

Results: During MRI, maternal Hyx (22.933±1.712) increased fetal PO₂ compared to Nx (17.983±3.058; $P=0.0061$). Cerebral blood flow ($P=0.6534$) as well as oxygen delivery ($P=0.8236$) and consumption ($P=0.1604$) were the same in Nx and Hyx. MRS detected total choline, creatine and N-acetyl aspartate peaks, key molecules for brain metabolism and development, that were quantified utilising Tarquin. There was no significant difference in total choline, creatine or N-acetyl aspartate concentrations between Nx (2.561±0.589; 2.528±1.274; 4.142±0.875) and Hyx

(2.411 ± 0.587 ; 2.438 ± 0.773 ; 2.639 ± 1.839 ; all $P > 0.05$). However, Hyx (0.896 ± 0.404) lowered the N-acetyl aspartate to choline ratio when compared to Nx (1.528 ± 0.404 ; $P = 0.0442$).

Conclusions: This study demonstrated that acute maternal hyperoxygenation elevated fetal oxygenation without affecting blood flow in the fetal circulatory system. Despite the lack of change in cerebral oxygen delivery or consumption, we showed for the first time that MRS in fetal sheep is feasible for measuring metabolic biochemicals that have a crucial role in neuronal density and function, myelin integrity and overall fetal brain metabolism. Further validation of this technique may lead to the development of a novel tool for assessing the early biochemical changes in the fetal brain of complicated pregnancies.

Darby JRT, Schrauben EM, Saini BS, Holman SL, Rajan Perumal S, Seed M, MacGowan CK & Morrison JL. (2020). Umbilical vein infusion of Prostaglandin I₂ increases ductus venosus shunting of oxygen rich blood but does not increase cerebral oxygen delivery in the fetal sheep. *The Journal of Physiology* 598, 4957-4967. Saini BS, Darby JRT, Portnoy S, Sun L, Amerom J, Lock MC, Soo JY, Holman SL, Perumal SR, Kingdom JC, Sled JG, Macgowan CK, Morrison JL & Seed M. (2020). Normal human and sheep fetal vessel oxygen saturations by T2 magnetic resonance imaging. *J Physiol* 598, 3259-3281.

C57

Vastus medialis activation and knee extensor neuromuscular function across the menstrual cycle

Elisa Nédélec¹, Mollie O'Hanlon¹, Tom Inns¹, Angus Hunter¹, Mathew Piasecki², Jessica Piasecki¹

¹Nottingham Trent University, Nottingham, United Kingdom, ²University of Nottingham, Nottingham, United Kingdom

Introduction

Estrogen and progesterone are the primary female endogenous reproductive hormones and have neuroactive excitatory and inhibitory effects, respectively [1]. However, research on the influence of fluctuating concentrations across the menstrual cycle on neuromuscular function and performance has led to conflicting findings ([2]ref). Increases in muscle force production are mediated by recruitment of progressively larger MUs and an increase in MU discharge rate. The ability to control force production is tightly connected with functional outcomes such as walking, risk of falls, and dexterity in humans; thus, being of clinical relevance in prevention of sports injuries, such as non-contact anterior cruciate ligament (ACL) injuries [3]. There are currently no data quantifying vastus medialis (VM) MU adaptation combined with menstrual cycle tracking across the human menstrual cycle. Therefore, the purpose of the study herein was to assess knee-extensor strength, force steadiness and VM activation using high density electromyography (HD-EMG) across the menstrual cycle.

Methods

Eight recreationally active eumenorrheic participants (age: 28 ± 7 years;; BMI: 23.9 ± 3.07) had their menstrual cycles tracked (mean cycle length: 29 ± 3 days; luteinizing hormone surge occurring on day 14 ± 2) prior to participation in the study. All attended for repeated identical assessments at the early follicular phase (EF), 24 to 48h pre-ovulation (Ov) and mid-luteal (ML) phases of the menstrual cycle. Maximum voluntary contraction (MVC) of the knee-extensors was recorded, and neuromuscular control was assessed through isometric trapezoid contractions (5s ramp up, 12s hold, 5s ramp down) peaking at 40% MVC, with real-time visual target feedback. During contractions, a 64 channel HD-EMG electrode was placed over the VM and RMS EMG was calculated as the highest amplitude within a 50ms window, and reported as a ratio of maximum RMS EMG. One way ANOVA was used to determine differences across timepoints with statistical significance accepted as $p < 0.05$.

Results

No statistical differences across the menstrual cycle were observed for knee extensor strength (EF:433N, Ov:418N, ML:442, $p=0.500$). Normalised RMS EMG did not differ across the cycle (EF:60.8, Ov:47.0, ML:56.5, $p=0.139$). Similarly, no statistical differences were observed in

neuromuscular control during sustained phase at 40% MVC ($p=0.661$), during the ascent phase ($p=0.292$), or the descent phase ($p=0.940$).

Conclusion

The current pilot data highlight minimal effect of the hormonal fluctuations of the menstrual cycle in VM activation of neuromuscular performance of the knee extensors. However, additional factors of neuromuscular performance, such as individual MU features at a range of contraction levels, should be investigated to help understand the vast discrepancy of ACL injuries incidence between men and women.

References [1] S. S. Smith and C. S. Woolley, 'Cellular and molecular effects of steroid hormones on CNS excitability', *Cleve Clin J Med*, vol. 71 Suppl 2, pp. S4-10, Feb. 2004, doi: 10.3949/ccjm.71.suppl_2.s4. [2] J. Piasecki et al., 'Menstrual Cycle Associated Alteration of Vastus Lateralis Motor Unit Function', *Sports Medicine - Open*, vol. 9, no. 1, p. 97, Oct. 2023, doi: 10.1186/s40798-023-00639-8. [3] R. J. Schmitz, K. R. Ford, B. Pietrosimone, S. J. Shultz, and J. B. Taylor, 'ACL Research Retreat IX Summary Statement: The Pediatric Athlete, March 17–19, 2022; High Point, North Carolina', *Journal of Athletic Training*, vol. 57, no. 9–10, pp. 990–995, Jan. 2023, doi: 10.4085/1062-6050-0219.22.

C58

Identification of novel APOE4-induced impairments to action potential firing in murine CA1 pyramidal neurons and associated rescue with clinically relevant NMDAR antagonists

Oliver G. Steele¹, Bradley Payne¹, Nicoleta Stegarescu¹, Alex Stuart-Kelly², Sarah King³, Ruth Murrel-Lagnado², Lewis Taylor², Andrew Penn²

¹Department of Clinical Neuroscience, Brighton and Sussex Medical School, Falmer, United Kingdom, ²School of Life Sciences, University of Sussex, Falmer, United Kingdom, ³School of Psychology, University of Sussex, Falmer, United Kingdom

Introduction: Apolipoprotein E4 (*APOE4*), the major genetic risk factor for Alzheimer's Disease (AD), yet increasing evidence suggest *APOE4* may detrimentally alter neurophysiology independent of classical AD hallmarks⁽¹⁾. Whilst hippocampal synaptic dysregulation caused by *APOE4* is well-studied, the impact of *APOE4* on intrinsic neuronal membrane properties is poorly studied.

Aims/Objectives: This study then looks to functionally characterise the impact of Apolipoprotein E genotype (*APOE*) on intrinsic neuronal excitability.

Methods: *APOE*-targeted replacement⁽²⁾ mice were housed in 12/hr light/dark cycles with *ad libitum* water and food. Organotypic hippocampal slices were prepared as previously described⁽³⁾ before patch-clamp electrophysiology was performed at DIV21. A current-step protocol from -200 pA to +400 pA allowed visualisation and analysis of intrinsic membrane properties⁽⁴⁾. Modulation of the NMDAR was made separately with the following drugs (in μ M): 20 ketamine, 10 memantine hydrochloride, 5 D-APV, 5 GNE-9278. Analysis of the relationship between *APOE* genotype and drug condition was inferred through multilevel linear modelling and bootstrap resampling (10,000 resamples). Post-hoc ANOVA permutation testing then analysed the interaction term. 12 animals per genotype were included, with a minimum of four slices per animal being produced. Only one recording per cell was then included in the analysis.

Results: Depolarizing current injection into CA1 neurons of *APOE3* slice cultures caused neurons to fire at frequencies up to 11.00 Hz (95% *CI* [9.31, 12.31]). However, in *APOE4* neurons, the firing rate was -2.94 Hz (95% *CI* [-5.06, -0.78], $p = .007$) lower. While acute application of ketamine had little effect in *APOE3* neurons (+0.08 Hz, 95% *CI* [-2.94, +2.72], $p = .95$), ketamine increased firing rates more in *APOE4* (than in *APOE3*) neurons by +3.53 Hz (95% *CI* [+0.15, +7.18], $p = .043$). Similarly to ketamine, acute application of memantine had little effect in *APOE3* neurons (+0.71 Hz, 95% *CI* [-0.98, +2.65], $p = .44$) and increased firing rates more in *APOE4* (than in *APOE3*) neurons by +4.27 Hz (95% *CI* [+1.00, +7.24], $p = .021$). A two-way ANOVA permutation test confirmed a significant interaction: the effect of the drugs (ketamine or memantine) on maximum firing rate depended on the *APOE* genotype ($p = .023$). To then confirm whether these described effects were mediated by the NMDAR a more specific NMDAR antagonist was applied, D-APV. While acute application of D-APV had little effect in *APOE3* neurons (+1.88 Hz, 95% *CI* [-1.16, 5.29], $p = .216$), D-APV increased firing rates more in *APOE4* (than in *APOE3*) neurons by +8.15 Hz (95% *CI* [3.35, 12.87], $p < .001$). Further confirming the involvement of the NMDAR, acute application of the positive allosteric modulator, GNE-9278 significantly decreased firing rates in *APOE3* neurons (-

5.51 Hz, 95% CI [-8.06, -2.66], $p = < .001$) and decreased firing rates more in *APOE3* (than in *APOE4*) neurons by -5.89 Hz (95% CI [-1.16, -10.56], $p = .016$).

Conclusion: Not only does *APOE4* perturb action potential firing, but the rescue of this phenotype is also dependent on the NMDAR hinting at a conserved pathway that could act as a future therapeutic target.

1. Steele and Stuart OG and AC, Minkley L, Shaw K, Bonnar O, Anderle S, Penn AC, et al. A multi-hit hypothesis for an *APOE4*-dependent pathophysiological state. *Eur J Neurosci* [Internet]. 2022 [cited 2022 May 31];n/a(n/a). Available from: <https://onlinelibrary.wiley.com/doi/abs/10.1111/ejn.15685>
2. Sullivan PM, Mezdour H, Aratani Y, Knouff C, Najib J, Reddick RL, et al. Targeted Replacement of the Mouse Apolipoprotein E Gene with the Common Human *APOE3* Allele Enhances Diet-induced Hypercholesterolemia and Atherosclerosis. *J Biol Chem*. 1997 Jul 18;272(29):17972–80.
3. Elmasri M, Lotti JS, Aziz W, Steele OG, Karachaliou E, Sakimura K, et al. Synaptic Dysfunction by Mutations in *GRIN2B*: Influence of Triheteromeric NMDA Receptors on Gain-of-Function and Loss-of-Function Mutant Classification. *Brain Sci*. 2022 Jun 15;12(6):789.
4. Telezhkin V, Schnell C, Yarova P, Yung S, Cope E, Hughes A, et al. Forced cell cycle exit and modulation of GABAA, CREB, and GSK3 β signaling promote functional maturation of induced pluripotent stem cell-derived neurons. *Am J Physiol-Cell Physiol*. 2015 Dec 30;310(7):C520–41.

C59

Assessment of olfactory response to social and non-social cues in valproic acid induced rat model of autism

Süeda Tunçak², Sevgi Ece Koç², Ceren Oy³, Şule Mergen⁴, Gökhan Göktalay⁴, Zehra Minbay³, Bülent Gören²

¹Bursa Uludağ University, Bursa, Turkey, ²Department of Physiology, Faculty of Medicine, Bursa Uludağ University, Bursa, Turkey, ³Department of Histology and Embryology, Faculty of Medicine, Bursa Uludağ University, Bursa, Turkey, ⁴Department of Pharmacology, Faculty of Medicine, Bursa Uludağ University, Bursa, Turkey

Autism Spectrum Disorders (ASD), are characterized with impairments in communication, lack of interest in social interactions and repetitive behaviours. Prenatal valproic acid (VPA) exposure, is used for modelling ASD like symptoms in rodents (1). Olfactory bonding with mother is crucial for a healthy social development and this is often tested with olfactory discrimination test (2). However, this test contains social cues only and therefore lacks the ability to distinguish whether observed differences occur due to social impairments or olfactory problems. This study aims to investigate olfactory response to social and non-social cues in prenatal VPA exposed rats.

Pregnant Wistar Albino rats received either 400mg/kg VPA ($n_{\text{Mother}}: 3; n_{\text{Pup}}: 8$) or saline ($n_{\text{Mother}}: 3; n_{\text{Pup}}: 8$) on embryonic day 12.5 *intraperitoneally*. Female pups were tested for olfactory discrimination (OD) on postnatal day 9 (P9), anxiety on P30 and olfaction without social cues on P40. OD test was performed for 3 minutes in plexiglass container with clean bedding on one side and bedding from mother cage on the other. Latency to reach either bedding was measured and rats were immediately returned to mothers. Anxiety was measured in open field. Total distance moved, velocity and frequency to enter border and centre zones were measured. Olfaction without social cues was tested for 5 minutes in a hole-board apparatus that consisted 16 holes with 2cm diameter. Rats were habituated to hole-board for 3 days prior testing to reduce stress. Food was removed from cages 8 hours prior testing. The test included a strawberry milk jar as a non-social olfactory cue under one of the centre holes. Latency of head digging into any holes was measured. Statistical analysis was performed with Student's-t test on Sigma-Plot. The study was approved by Bursa Uludağ University's ethics committee (numbered: 2023-13/02).

Prenatal exposure to VPA impaired OD of mother/clean bedding. Latency to reach mother bedding was significantly increased in VPA group ($p < 0.022$) whereas latency to reach any bedding showed no statistical difference between groups. In open field, VPA group showed decreased velocity ($P < 0.003$) and frequency to enter both border ($p < 0.001$) and centre zones ($p = 0.002$). Control group had increased distance moved ($p < 0.001$) and spent more time in centre areas compared to VPA group. In olfactory hole-board test, VPA group showed increased latency to dig their head into strawberry milk ($p = 0.003$) whereas there was no significant difference between groups for latency of head digging into holes.

Olfaction is crucial in rodent survival. Inability to discriminate mother bedding from clean bedding suggests impairments in social communication. Results of open field test suggest increased anxiety in VPA group as expected from literature. For that reason, rats were habituated to hole-

board. Insignificant difference in latency of head-digging shows that anxiety was eliminated. Within these results, this study suggests an impaired response to olfactory cues, whether social or non-social. This new set of information should be taken into account especially when sociability is assessed in models of ASD as inability to discriminate novel conspecific may occur merely as a result of a problem in olfaction.

(1) Schneider T, & Przewłocki R. (2005). *Neuropsychopharmacology*, 30(1), 80-89. (2) Favre MR et al. (2013). *Frontiers in behavioral neuroscience*, 7, 88.

PCA001

Effect of Bradykinin on Renal Hemodynamics of Anesthetized Wister Rats

Ahmad Ahmeda¹

¹*Ajman University, College of Medicine, Ajman, United Arab Emirates*

Background:

Bradykinin (BK) is an endogenously produced active peptide that causes vasodilation. However, its effect on the renal microvasculature is not well described when introduced as an exogenous compound. This study evaluated the effects of BK on renal cortical and medullary blood perfusion and investigated whether the effect of BK is similar when given locally into the renal medulla or systematically with the intravenous route (IV).

Materials and Methods:

Four groups (n=7) of male Wistar rats (250-300 g) were anaesthetised with an I.P injection of 1 ml chloralose/urethane, 16.5/250 mg/ml. The right femoral vein was cannulated for infusion of saline (154mM NaCl), BK (50µg/kg/min) at 3ml/h and supplemental doses of anaesthetic. The right femoral artery was cannulated to measure blood pressure (BP). The left kidney was exposed via a flank incision, and a small cannula was inserted 4.5mm into the kidney for intramedullary (i.m) infusion of saline or BK at 0.6-1.0 ml/h. Two Laser-Doppler microprobes (each 0.5 mm diameter) were inserted 1.5 and 4.0 mm into the kidney to measure cortical and medullary blood perfusion, respectively (100 perfusion units (PU) = 1 V). After 90 min, baseline measurements were taken, and then either vehicle or BK were infused i.m or IV for 60 min. At the end of the experiments, the animals were killed with an anaesthetic overdose. Data \pm SEM were subjected to the Student's t-test, and significance was taken at $P < 0.05$.

Results:

The baseline levels of BP were 95 ± 8 mmHg, Heart Rates (HR) were 335 ± 10 BPM, CP was 138 ± 7 PU, and MP was 57 ± 5 PU. Administration of bradykinin i.m significantly increased MP and CP ($18 \pm 6\%$ and $33 \pm 9\%$, respectively, $P < 0.05$). BK had no effect on BP and HR when given locally. IV Infusion of BK resulted in a significant increase in CP ($23 \pm 6\%$, $P < 0.05$) and a decrease in MAP ($15 \pm 6\%$, $P < 0.05$), but had no effect on MP and HR.

Conclusion:

BK, when given locally, dilates renal blood vessels, mediating an increase in CP and MP. When given systematically, the effect of bradykinin was less on the renal microvasculature and had no impact on the MP. These data indicate that the BK has a more significant effect on the medullary microvasculature when given locally. Further research is suggested to understand the action of BK on renal microvasculature and the involvement of the free radicals such as superoxide anion and nitric oxide.

PCA002

The effects of NS1643 on two disease causing hERG channel variants

Majid Khamis Al Salmani¹

¹*Department of Physiology, College of Medicine, Sultan Qaboos University, Muscat, Oman*

The human ether-a-go-go gene (hERG) encodes a voltage-dependent K⁺ ion channel (KCNH2) largely responsible for the rapid component of the delayed rectifier currents in the heart. Loss of function mutations in hERG cause type-2 long QT syndrome (LQTS-2) and predispose affected individuals to cardiac arrhythmias. Several classes of hERG channel variants have been described, including variants that affect channel gating, conductance and/or expression. T1019PfsX38- and Q1070X-hERG are LQTS-2 causing variants reported in Oman and Saudi Arabia (Bhuiyan et al. 2008; Al Senaidi et al. 2014). When expressed as cDNA in heterologous expression systems, these variants exhibited functional ion channels on the cell surface (Bhuiyan et al. 2008; Al Salmani et al. 2022).. However, T1019PfsX38-hERG displayed characteristics of defective channel gating (Al Salmani et al. 2022). In this study we try to test the responsiveness of T1019PfsX38- and Q1070X-hERG channels to the hERG channel activator N,N'-Bis[2-hydroxy-5-(trifluoromethyl)phenyl]urea (NS1643). We expressed wild-type and the mutant channel variants in HEK293 cells and studied their electrophysiology using the whole-cell patch clamp technique. We used paired and non-paired Student's t-test where appropriate to assess the statistical significance of difference, n is the number of cells. A 400 ms ventricular action potential (VAP) clamp revealed that T1019PfsX38- (p = 0.04) but not Q1070X-hERG (p = 0.774) exhibits reduced potassium currents at the repolarisation phase of the action potential (AP) (75-95 % of the AP duration) when compared with WT-hERG ($I_{(integral)}$: WT = 2.63 ± 0.29 pA.s/pF (n = 6), T1019PfsX38 = 1.43 ± 0.42 pA.s/pF (n=4), Q1070X = 2.94 ± 1.23 pA.s/pF (n = 4)). The application of NS1643 (10 μ M) to the bath solution increased these $I_{(integral)}$ values by 53%, 80.3% and 78% in cells expressing WT- (p = 0.031, n=6), T1019PfsX38- (p = 0.001, n = 4) and Q1070X-hERG (p = 0.036, n = 4), respectively. To understand these effects further, we measured the voltage and time dependences of channel activation in response to NS1643. NS1643 shifted the half-maximum voltage (V_{mid}) of activation to more negative values (p < 0.01) compared to control but did not increase the maximal current amplitudes (control V_{mid} : WT = 2.90 ± 3.25 mV (n = 5), T1019PfsX38 = 6.96 ± 4.94 mV (n = 3), Q1070X = 10.40 ± 2.40 mV (n = 5); NS1643 V_{mid} : WT = -16.70 ± 3.60 mV (n = 5), T1019PfsX38 = -13.57 ± 4.37 mV (n = 3), Q1070X = -15.38 ± 3.69 mV (n = 5)). In addition, NS1643 accelerated the activation process of the three variants at multiple test potentials (p < 0.05, n = 4 – 9). Moreover, NS1643 stabilised the open configuration of the channel and slowed the deactivation process when measured at -40 mV. When applied to untransfected HEK293 cells, NS1643 (10 μ M) inhibited endogenous currents that display fast activation and fast inactivation kinetics at potentials ≥ 0 mV (p < 0.01, n = 5). Overall, NS1643 enhances the activities of WT-, T1019PfsX38- and Q1070X-hERG channels but its therapeutic potential require testing for undesired side effects.

Al Salmani MK, Tavakoli R, Zaman W, Al Harrasi A (2022) Multiple mechanisms underlie reduced potassium conductance in the p.T1019PfsX38 variant of hERG. *Physiol Rep* 10:e15341. <https://doi.org/10.14814/PHY2.15341> Al Senaidi KS, Wang G, Zhang L, et al (2014) Long QT syndrome, cardiovascular anomaly and findings in ECG-guided genetic testing. *IJC Hear Vessel* 4:122–128. <https://doi.org/10.1016/j.ijchv.2014.06.001> Bhuiyan ZA, Momenah TS, Gong Q, et al (2008) Recurrent intrauterine fetal loss due to near absence of HERG: Clinical and functional

Physiology in Focus 2024

Northumbria University, Newcastle, UK | 2 – 4 July 2024

characterization of a homozygous nonsense HERG Q1070X mutation. *Hear Rhythm* 5:553–561.
<https://doi.org/10.1016/J.HRTHM.2008.01.020>

PCA003

Effect of Sodium Fluoride on Lipid Profile in Male Wistar rats

Olusola Ayegboyin⁴, Abayomi Ige³, Elsie Adewoye²

¹University of Ibadan,, Ibadan, Nigeria, ²University of Ibadan, Ibadan, Nigeria, ³University of Ibadan, Ibadan, Nigeria, ⁴University of Ibadan, Ibadan, Nigeria

This study investigated the effect of sodium fluoride (NaF) on lipid profile in the serum and aorta of male Wistar rats. Sodium fluoride has garnered increased attention due to its potential detrimental effects on human health. Excessive ingestion and accumulation of sodium fluoride from sources like water, toothpaste, and pesticides can trigger dyslipidemia in rats. These heightened disturbances in the lipid profile, pose a significant risk and may predispose individuals to severe vascular and cardiovascular-related diseases, which are the leading causes of global mortality. The study involved ten male Wistar rats weighing 150-180 grams. The rats were divided into two groups (n=5) Group 1 (Control), received distilled water, and Group 2 received an oral dose of 10 mg/kg of sodium fluoride daily for 21 days. Lipid profiles [Total Cholesterol (TC), Triglycerides (TG), High-Density Lipoprotein Cholesterol (HDL-C), Low-Density Lipoprotein Cholesterol (LDL-C), Very Low-Density Lipoprotein Cholesterol (VLDL-C)] were determined in the serum of male Wistar rats using UV/VIS spectrophotometer. Ethical consideration was obtained for this work from the University of Ibadan Animal Care and use research ethical committee. Data analysis was conducted using descriptive statistics and a student t-test with a significance level set at $\alpha=0.05$. Total cholesterol (116.10 ± 7.84 vs 82.37 ± 2.27 mg/dL), triglyceride (161.90 ± 4.06 vs 105.80 ± 4.26 mg/dL), VLDL-C (32.38 ± 0.81 vs 21.16 ± 2.85 mg/dL), and LDL-C (46.37 ± 4.17 vs 25.82 ± 2.40 mg/dL) levels significantly increased ($p < 0.05$), while HDL-C (20.57 ± 0.86 vs 40.80 ± 6.44 mg/dL) level reduced significantly ($p < 0.05$) in NaF compared with control. There was moderate congestion of the lumen in the aortic vessel in NaF, which was absent in control. These findings suggest that sodium fluoride exposure causes dyslipidemia. Hypertension and dyslipidemia are major risk factors for cardiovascular disease, responsible for global morbidity and mortality. Given these results, continuous fluoride exposure in populations residing in regions with endemic fluoride levels should be a matter of significant concern given the potential health risks associated with sodium fluoride exposure, emphasizing the need for vigilance in affected regions.

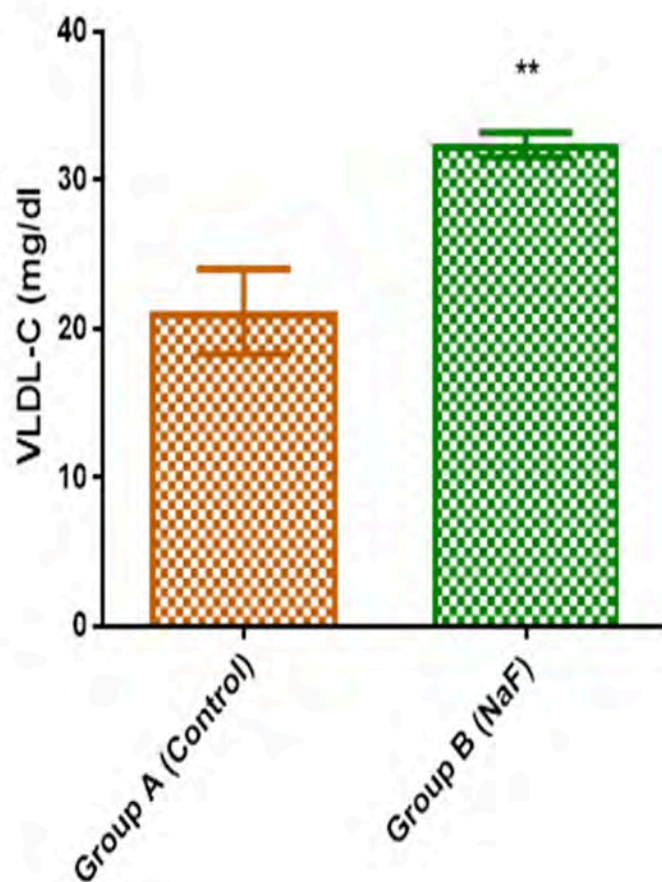


Figure 5. Sodium Fluoride (10mg/kg) effect on very low-density lipoprotein-cholesterol. Values are expressed as Mean \pm SEM. (N=5) (** P <0.01)

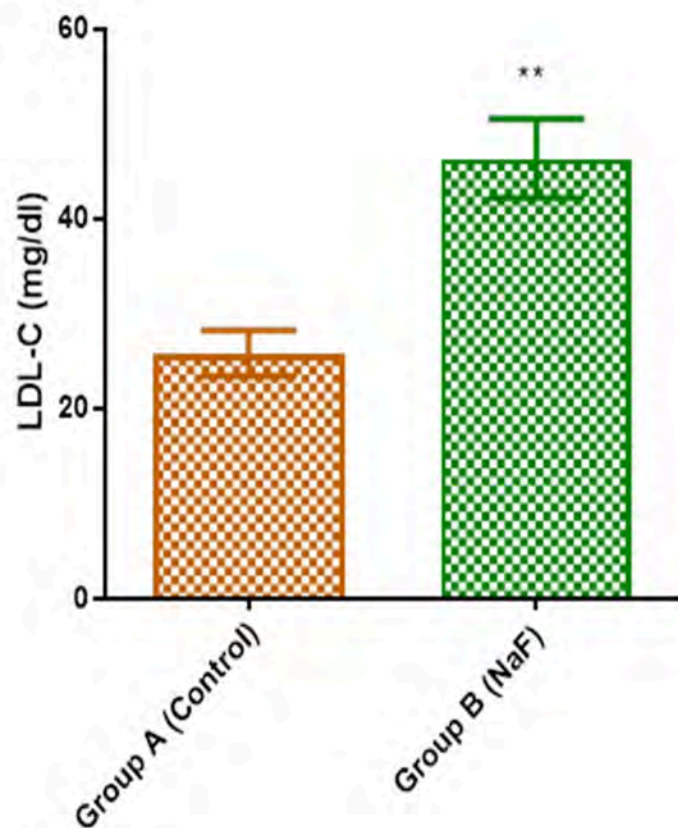


Figure 4. Sodium Fluoride (10mg/kg) effect on low-density lipoprotein cholesterol. Values are expressed as Mean \pm SEM. (N=5) (** P <0.01)

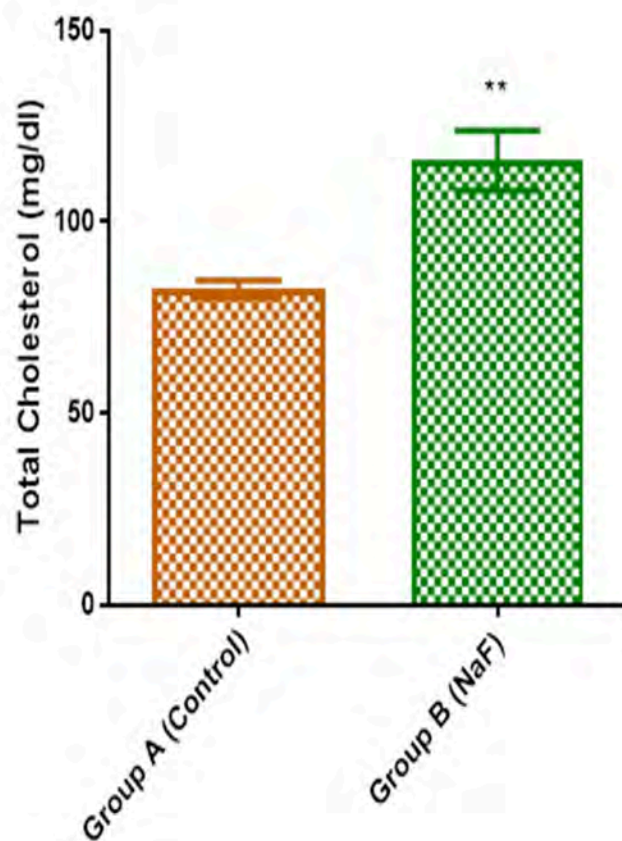


Figure 1. Sodium Fluoride (10mg/kg) effect on Total Cholesterol. Values are expressed as Mean \pm SEM. (N=5) (** $P<0.01$)

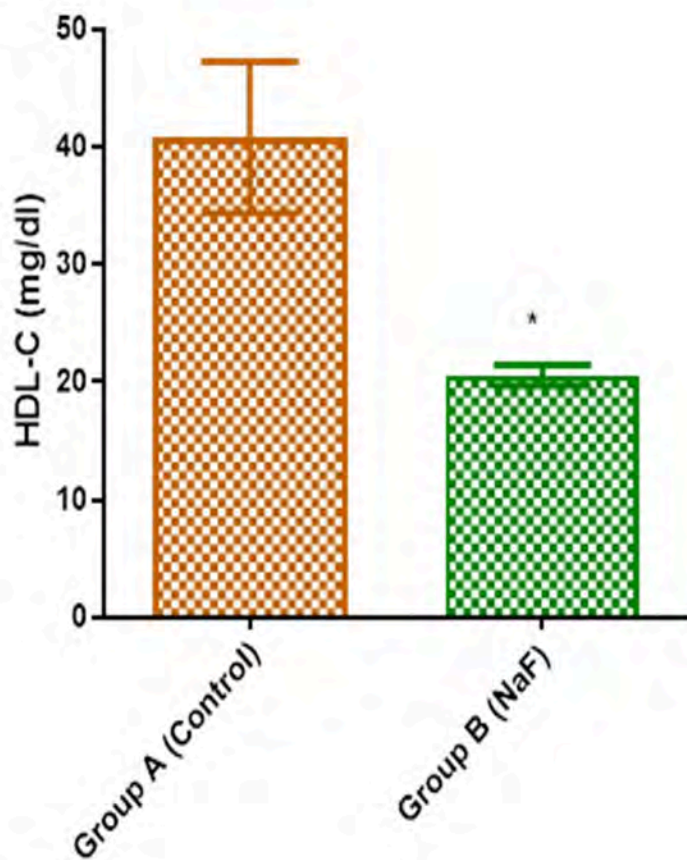


Figure 3. Sodium Fluoride (10mg/kg) effect on high-density lipoprotein cholesterol. Values are expressed as Mean \pm SEM. (N=5) (* $P<0.05$)

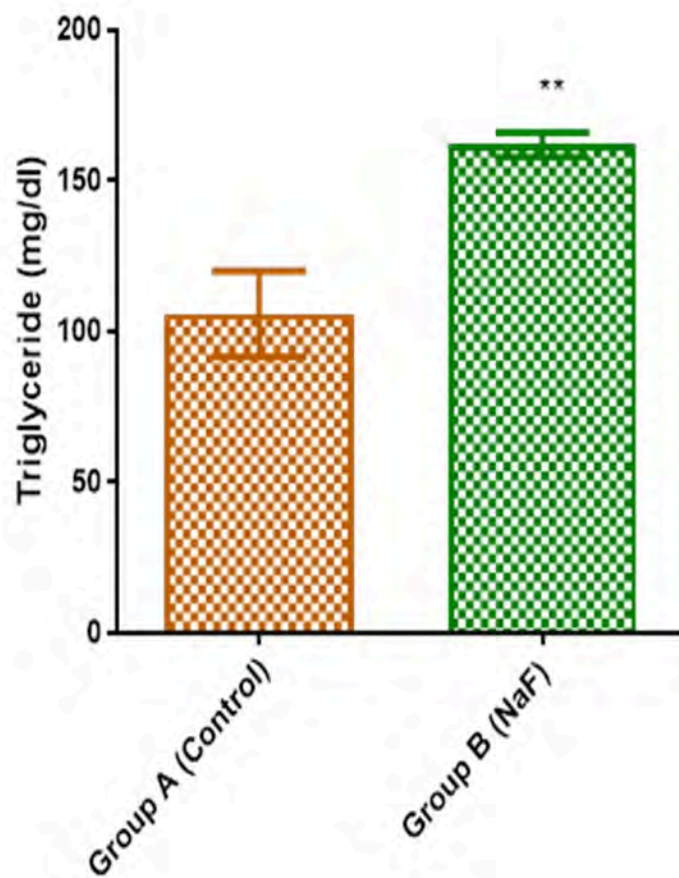


Figure 2. Sodium Fluoride (10mg/kg) effect on Triglyceride. Values are expressed as Mean \pm SEM. (N=5) (** $P<0.01$)

PCA004

Improving Maturity of iPSC-derived Cardiomyocyte Models for Cardiac Disease, Cardiotoxicity and Drug Screening

Steven Broadbent¹, Jamie Bhagwan¹, George Buchanan¹, Ashley Barnes¹

¹*Axol Bioscience Ltd., Edinburgh, United Kingdom*

Despite decades of effort, there is a pressing need for better *in vitro* cardiac and cardiotoxicity models. Cardiovascular diseases (CVD) remain the leading global cause of death and cardiotoxicity is responsible for a third of all pre-clinical pharmaceutical regulatory failures. While traditional models (*ex vivo* and *in vivo* animal models, primary human tissue and immortalised cell lines) have provided valuable insights, there remains a translational gap between the “bench and bedside” due to issues with human-relevance, alongside well-characterized challenges with availability, throughput and cost.

Researchers have therefore been turning to human iPSC-derived cardiomyocytes for their potential to provide a limitless source of consistent, human-relevant cardiac cells. By taking donor cells, reprogramming them to an iPSC state and then differentiating them into cardiomyocytes, researchers can mimic human physiology in a scalable format, using these cells to power advanced *in vitro* cardiac disease and cardiotoxicity models.

However, standard differentiation protocols can lead to less mature cardiomyocyte phenotypes, impairing functional performance and therefore the utility of human iPSC-based models. Key measures of immature phenotype include the following six parameters; their sarcomere alignment, cardiac maturity marker expression, lower levels of spontaneous beating, longer Field Potential Duration (FPD), slower Conduction Velocity (CV) and a switch from glycolysis to fatty acid metabolism.

Axol Bioscience, in collaboration with partner organizations, have developed a new metabolic maturation media to enhance the maturity of human iPSC-derived cardiomyocytes, enabling better models for cardiac research, disease and cardiotoxicity.

This new metabolic maturation media has been validated on two healthy control-derived ventricular cardiomyocyte lines: a newborn male line (ax2508) and a middle-aged female line (ax5858). This media drives more mature cardiac morphology as measured by ICC, with improved sarcomere alignment and increased expression of the key cardiac maturity markers Troponin T and Connexin-43 by DIV8. Transcriptomics analysis demonstrates improvement in the expression of cardiac maturity markers including PLN, SCN1B, KCNJ2, KCNJ3 and KCNQ1, with a Log2fold change from 2.6 to 3.8 for KCNJ2 and corresponding decreases in the expression of immaturity markers including HCN2. Functionally, the maturation media drives more mature electrical activity measured via cardiac electrophysiology, with a reduction in beat rate from 44 ± 1 bpm to 23 ± 2 bpm, increases in CV from 0.40 ± 0.04 mm/ms to 0.70 ± 0.04 mm/ms and a shortening of FPD from 491 ± 55 ms to 312 ± 14 ms (all $n=7-8$, $p<0.05-0.0001$, unpaired t-test with Welch’s correction) by DIV14. The maturation media also incorporates a factor which selects against cells utilising glycolysis in favour of cells utilising fatty acid metabolism causing the die-back of any remaining

immature cardiomyocytes as detected by microscopy and confluence measurements. These improvements represent a more mature cardiomyocyte phenotype across the six parameters described previously.

With these improvements, human iPSC-derived cardiomyocytes can be produced with enhanced structural and functional maturity to power advanced *in vitro* models of cardiac disease and cardiotoxicity. This addresses a key challenge to the wider adoption of iPSC-derived cardiomyocytes for cardiac research, drug testing and cardiotoxicity.

PCA005

The acute effect of maximal sprint exercise on cerebrovascular reactivity in healthy young adults

Philip Buys¹, Emma Curtin¹, Conor Brady¹, Cillian Rooney¹, Ahmed Alshahrabally¹, Paul McConkey¹, Shane Donohoe¹, Hoda Darwish¹, Shane Spring¹, Gustav Hagon¹, Cara Gallagher¹, Aidan Mahon¹, Norita Gildea¹, Mikel Egana¹, Max Weston¹

¹*Department of Physiology, School of Medicine, Trinity College Dublin, Dublin, Ireland*

Background and Purpose Exercise training is known to have positive effects on cerebrovascular health, and in particular there is a growing interest surrounding high-intensity exercise and cerebrovascular function. Cerebrovascular reactivity (CVR) is one measure of cerebrovascular function, and refers to the ability of the cerebral blood vessels to dilate and constrict in response to acute changes in the partial pressure of arterial CO₂. However, little is known about the acute effect of sprint exercise on CVR. Therefore, the purpose of this study was to investigate the acute effect of maximal sprint exercise on CVR in healthy young adults.

Methods Twenty-one healthy adults (mean \pm SD age, height and weight: 22.7 \pm 3.1 years, 173.4 \pm 8.4 cm and 70.3 \pm 10.1 kg, respectively, 13 males, 8 females) volunteered to participate in this study. Participants visited the laboratory for one experimental visit, having refrained from caffeine, alcohol and vigorous physical activity for 24 hours, and arrived at the laboratory >2 hours postprandial. CVR of the middle cerebral artery to hypocapnia was determined through one minute of voluntary hyperventilation, performed at 25 breaths.min⁻¹. Middle cerebral artery blood velocity (MCAv) was measured using transcranial Doppler ultrasonography, and the partial pressure of end-tidal carbon dioxide (P_{ET}CO₂) was measured breath-by-breath using a gas analyser. Participants completed the CVR protocol at baseline, and 30 minutes following a maximal, 30 second Wingate test completed on a cycle ergometer. CVR was quantified as both the absolute (cm.s⁻¹) and relative (%) change in MCAv from baseline per 1 mmHg change in P_{ET}CO₂, taken from the final 10 s of hyperventilation. The effect of the Wingate test on MCAv, P_{ET}CO₂ and CVR was explored using paired samples t-tests.

Results Baseline MCAv was significantly lower following the Wingate test (60.8 \pm 11.0 vs 66.2 \pm 11.5 cm.s⁻¹, P<0.01), as was baseline P_{ET}CO₂ (32.4 \pm 4.3 vs 36.8 \pm 4.2 mmHg, P<0.01). During the hyperventilation protocol, both MCAv and P_{ET}CO₂ fell by a significantly smaller magnitude following the Wingate test, compared to baseline (20.6 \pm 8.9 vs 26.0 \pm 9.7 cm.s⁻¹ and 12.3 \pm 5.1 vs 14.5 \pm 5.7 mmHg, respectively, P<0.01). However, CVR remained unaltered following the Wingate test, when expressed in both absolute (1.7 \pm 0.4 vs 1.9 \pm 0.4 cm.s⁻¹.mmHg⁻¹, P=0.16) and relative (2.9 \pm 0.6 vs 2.8 \pm 0.6 %.mmHg⁻¹, P=0.70) terms.

Conclusion These findings indicate that both resting MCAv and P_{ET}CO₂ are not fully recovered 30 minutes following maximal sprint exercise in healthy young adults. However, despite these marked changes in baseline values, the reactivity of MCAv to hypocapnia remained unaltered 30 minutes following a Wingate test. Future research investigating the time-course of CVR responses following sprint exercise is warranted to further our understanding of high-intensity exercise on cerebrovascular function.

PCA006

Skin vasoconstriction during negative pressure is not mediated exclusively by the myogenic response, but also by the venoarteriolar reflex

Nigel A. Callender^{1,2,3}, Samuel J. Oliver⁴, Lars Øivind Høiseth⁵, Jamie H. MacDonald⁴, Justin S. Lawley^{7,8}, Jonny Hisdal^{1,2}

¹Faculty of Medicine, University of Oslo, Oslo, Norway, ²Department of Vascular Surgery, Oslo University Hospital, Oslo, Norway, ³Otivio AS, Oslo, Norway, ⁴Institute for Applied Human Physiology, Bangor University, Bangor, United Kingdom, ⁵Department of Anaesthesiology, Oslo University Hospital, Oslo, Norway, ⁶Faculty of Medicine, University of Oslo, Oslo, Norway, ⁷Department of Sports Science, University of Innsbruck, Innsbruck, Austria, ⁸Institute of Mountain Emergency Medicine, EURAC Research, Bolzano, Italy

The non-baroreceptor mediated reduction in limb blood flow during local negative pressure has been attributed to the myogenic response (Lott *et al.*, 2002). However, local negative pressure influences vascular transmural pressure, which is the stimulus underlying both the myogenic response and the venoarteriolar reflex (VAR). Venoarteriolar reflex and myogenic response mechanisms can be differentially manipulated using either venous congestion, which engages only the VAR but reduces regional perfusion pressure, or limb dependency, which engages both the VAR and myogenic response while preserving perfusion pressure (Okazaki *et al.*, 2005). Although there may be some neural mediation of the myogenic response (Scotland *et al.*, 2004), the VAR is entirely axon dependent, therefore topical anaesthetic block combined with the experimental manipulations described previously can separate the relative contributions of the two responses (Okazaki *et al.*, 2005). By combining these experimental manipulations, we aimed to investigate whether the VAR contributes to vasoconstriction during negative pressure and if so, what proportion it may account for.

Following ethical approval and provision of informed consent, 25 healthy participants were recruited (14 males, 11 females; age: 32±8 y; height: 1.75±0.09 m; weight: 70.8±13.6 kg). First ($n=17$), we investigated the change in skin blood flux (Laser doppler fluxometry; Periflux 4001; Perimed, Järfälla, Sweden) during -40 mmHg negative pressure (180-sec), in a region of anaesthetised skin upon one lower leg (EMLA cream; Aspen pharma, Dublin, Ireland). The contralateral leg underwent the same interventions without anaesthetic block. Among a subset of participants ($n=11$), using methods based on Okazaki *et al.* (2005), the responses in skin blood flux following venous congestion (40 mmHg thigh cuff) were compared to limb dependency (45cm below horizontal), and negative pressure (-40 mmHg). The difference between the reduction in skin flux under control and blocked conditions was calculated and assumed to represent the VAR alone during venous congestion (DeltaC), and a combination of the VAR and myogenic response during limb dependency (DeltaD) or negative pressure (DeltaNP). Thereafter, assuming similar transmural stresses during each manipulation, the relative contribution of the VAR during limb dependency was estimated as $[\text{DeltaC}/\text{DD}] \times 100$, and during negative pressure as $[\text{DeltaC}/\text{DNP}] \times 100$. Data were analysed using repeated measures ANOVA, or Wilcoxon signed rank tests (mean ± SD or median [IQR]; $p<0.05$).

Topical anaesthetic block attenuated the reduction in skin blood flux during negative pressure (control: -53 [16], blocked: -6 [38]%, $p<0.001$; Figure 1). Negative pressure and limb dependency

elicited similar reductions in skin blood flux (Figure 2). Results comparing the proportions of differences between skin sites (Figure 3) and between the interventions suggest the VAR is responsible for ~57% of the local vasoconstriction observed during negative pressure or limb dependency, with the remaining ~43% contributed by myogenic mechanisms.

These data suggest that the VAR *does* contribute to reduced skin blood flux during negative pressure, accounting for over half of local vasoconstriction. Negative pressure and limb dependency elicited comparable vasoconstriction, indicating that without baroreceptor-mediated input, local vascular responses are similar whether transmural stress is induced by gravity or external negative pressure.

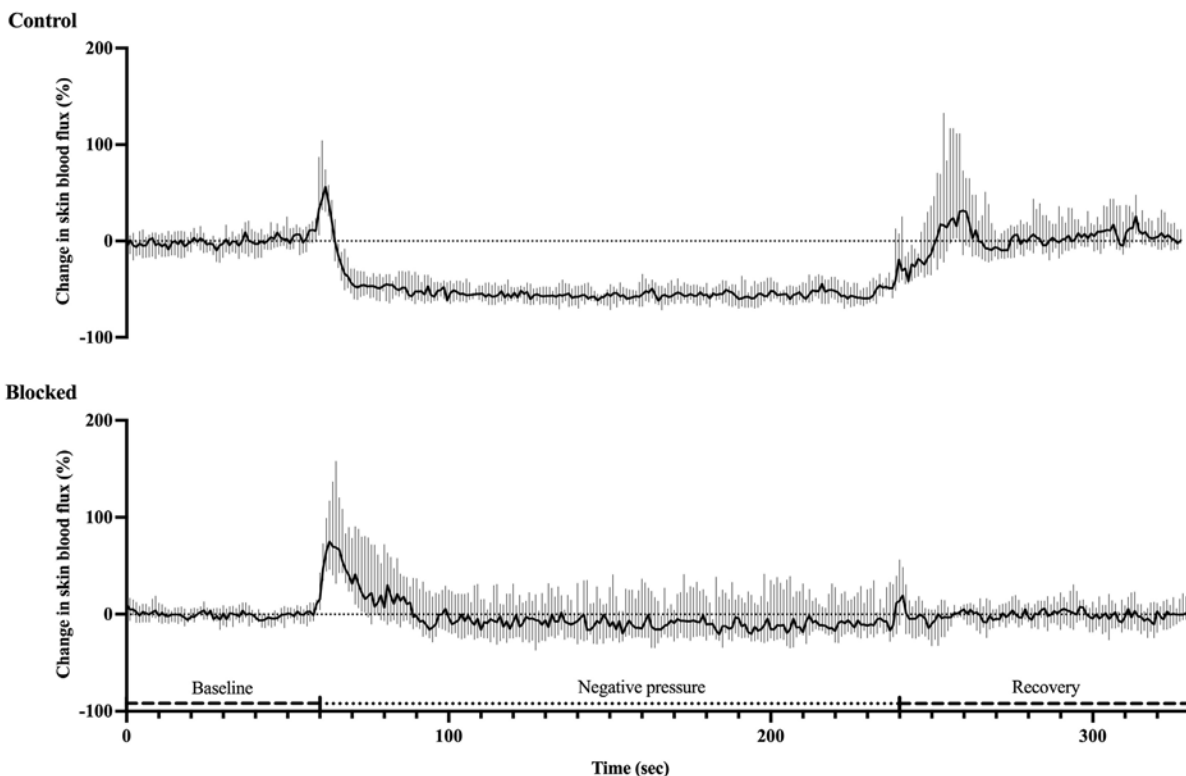


Figure 1: Time course of the changes to skin blood flux during sustained negative pressure (-40 mmHg)

Data ($n=17$) represent the **median [IQR]** percent change in skin blood flux per-second relative to the 60-sec baseline period, in control (upper panel) and blocked skin (lower panel).

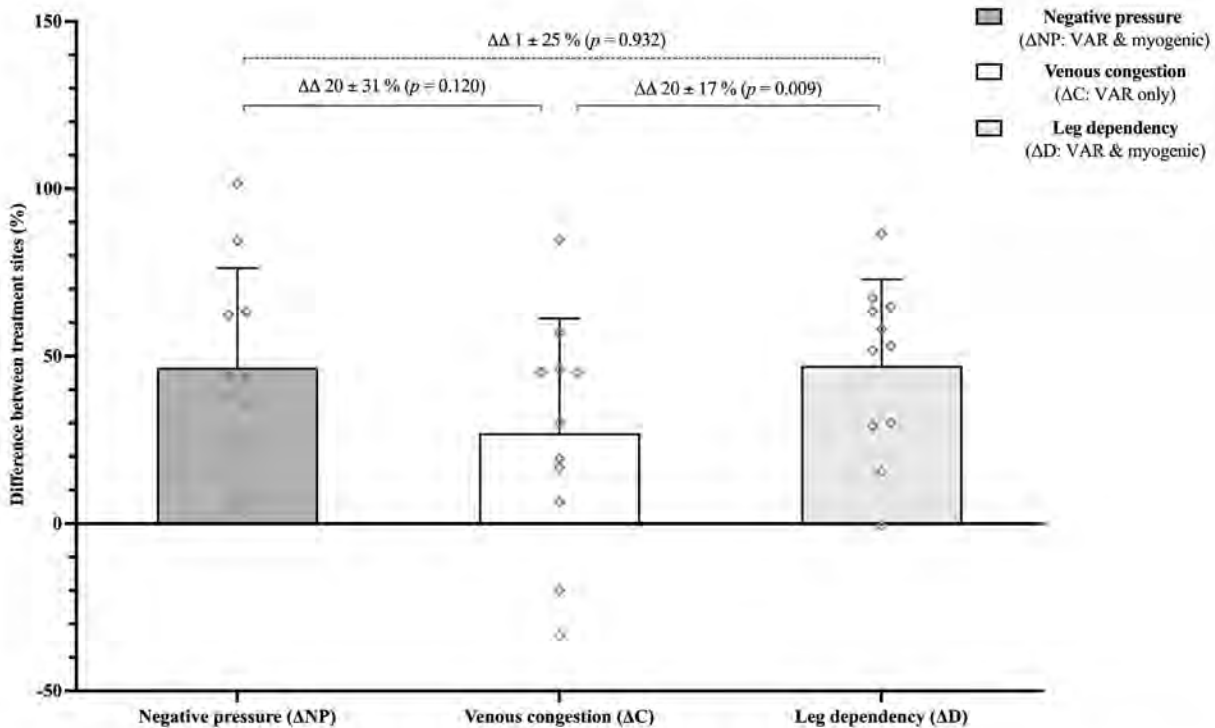


Figure 3: Differences in skin blood flux responses between treatment conditions during negative pressure (-40 mmHg), venous congestion (40 mmHg) and leg dependency (45 cm).

Data ($n = 11$) represent the **mean \pm SD** difference between the percentage reductions in control and blocked skin found in Figure 2. Individual participants are indicated as diamonds. $\Delta\Delta$ indicates between-intervention differences. P -values relate to comparisons between interventions using one-way repeated measures ANOVA and *post hoc* pairwise t -tests with Holm-Bonferroni correction.

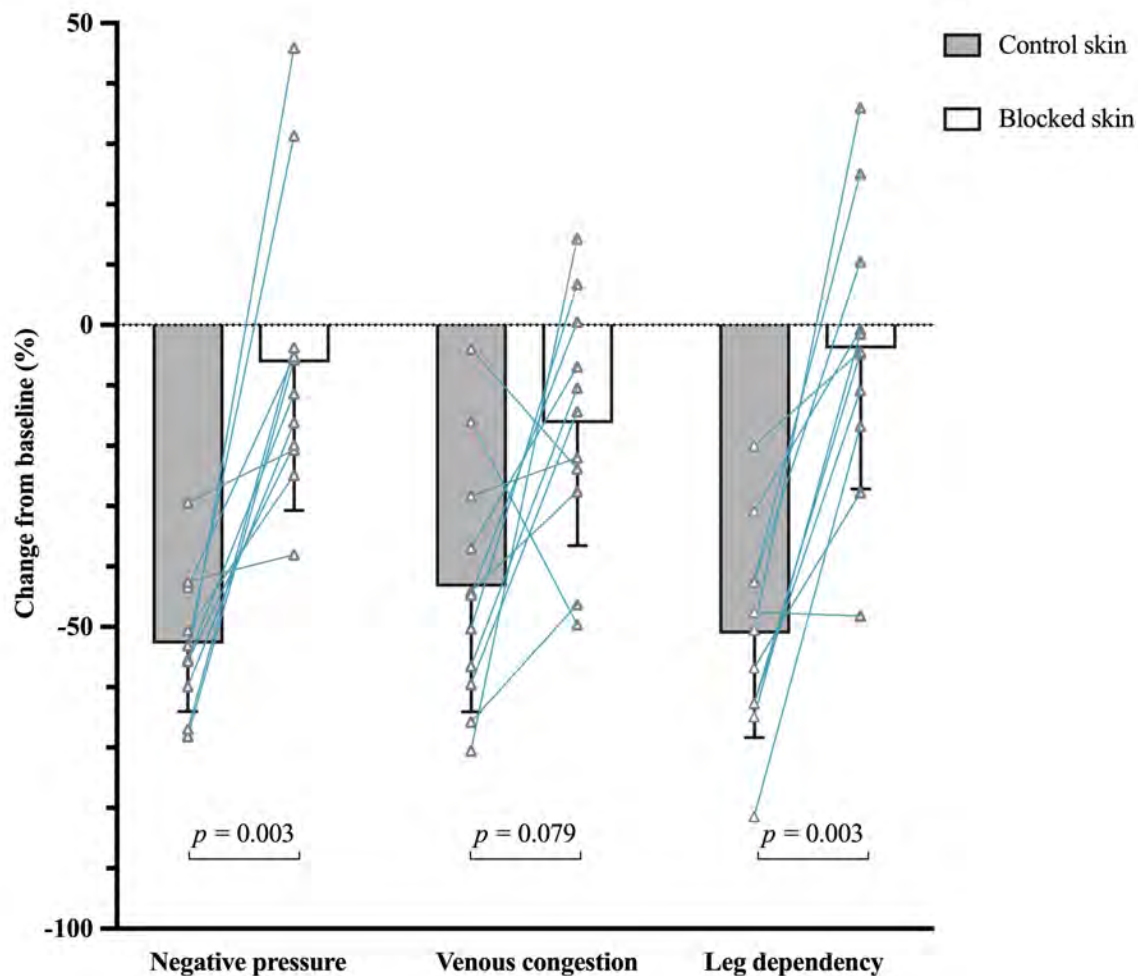


Figure 2: Changes in skin blood flux during negative pressure (-40 mmHg), venous congestion (40 mmHg) and leg dependency (45 cm).

Data ($n = 11$) represent the **mean \pm SD** percentage reduction in skin blood flux relative to baseline during the final 60-sec of each intervention, in control (grey bars) and blocked skin (white bars). Individual participants indicated by triangles. *P*-values relate to comparisons between conditions using two-way repeated measures ANOVA and *post hoc* pairwise *t*-tests with Holm-Bonferroni correction.

Lott ME, Herr MD, Sinoway LI. Effects of transmural pressure on brachial artery mean blood velocity dynamics in humans. *J Appl Physiol* (1985). 2002 Dec;93(6):2137-46. doi: 10.1152/jappphysiol.00443.2002. Okazaki K, Fu Q, Martini ER, Shook R, Conner C, Zhang R, Crandall CG, Levine BD. Vasoconstriction during venous congestion: effects of venoarteriolar response, myogenic reflexes, and hemodynamics of changing perfusion pressure. *Am J Physiol Regul Integr Comp Physiol*. 2005 Nov;289(5):R1354-9. doi: 10.1152/ajpregu.00804.2004. Scotland RS, Chauhan S, Davis C, De Felipe C, Hunt S, Kabir J, Kotsonis P, Oh U, Ahluwalia A. Vanilloid receptor TRPV1, sensory C-fibers, and vascular autoregulation: a novel mechanism involved in

Physiology in Focus 2024

Northumbria University, Newcastle, UK | 2 – 4 July 2024

myogenic constriction. *Circ Res.* 2004 Nov 12;95(10):1027-34. doi:
10.1161/01.RES.0000148633.93110.24

PCA007

The effects of sex and fitness on cerebrovascular reactivity and cerebral autoregulation in healthy young adults

Emma Curtin¹, Max Weston¹, Philip Buys¹, Thayumaan Bissoonauth¹, Hassan Al-Shammary¹, Olamide Ojelabi¹, Ahmed Osman¹, Jason Li¹, Tihara Wickramasinghe¹, Ying Lim¹, Zhi Ching¹, Muireann Carey¹, Enda Rooney¹, Mikel Egana¹, Norita Gildea¹

¹*Department of Physiology, School of Medicine, Trinity College Dublin, Dublin, Ireland*

Background and Purpose Sex and fitness have been suggested to influence cerebrovascular function across the lifespan, but the effects of sex and fitness in healthy young adults remains debated. The purpose of this study was to investigate the effects of sex, cardiorespiratory fitness and anaerobic capacity on cerebrovascular reactivity (CVR) and dynamic cerebral autoregulation (dCA) in healthy young adults.

Methods 13 males (mean \pm SD age, height and weight: 23.1 \pm 2.5 years, 178.0 \pm 5.3 cm and 73.7 \pm 9.4 kg, respectively) and 11 females (22.1 \pm 2.1 years, 165.2 \pm 6.5 cm and 61.6 \pm 9.5 kg) volunteered to take part in this study. Participants visited the laboratory on two occasions. During the first visit, participants completed a ramp incremental and verification test to determine maximal oxygen uptake ($\dot{V}O_{2max}$). In the second visit, dCA was assessed using a single sit-to-stand manoeuvre, and CVR to hypocapnia was determined during 60 seconds of voluntary hyperventilation. Middle cerebral artery blood velocity (MCAv) was measured via transcranial Doppler ultrasound, mean arterial pressure (MAP) via finger plethysmography and breath-by-breath end-tidal carbon dioxide ($P_{ET}CO_2$) through a gas analyser. dCA was quantified as the percentage fall in MCAv relative to the percentage fall in MAP upon standing ($\Delta\%MCAv/\Delta\%MAP$). CVR was calculated as both the absolute ($cm.s^{-1}$) and relative (%) change in MCAv from baseline per 1 mmHg change in $P_{ET}CO_2$, taken from the final 10 seconds of hyperventilation. Participants then completed a maximal, 30 second Wingate test on a cycle ergometer. Peak power output (PPO) and mean power output (MPO) from the Wingate test were recorded and expressed relative to body weight ($.kg^{-1}$). Independent samples t-tests explored differences in MCAv, dCA and CVR responses between males and females, and Pearson's correlation explored relationships between $\dot{V}O_{2max}$ and Wingate performance with dCA and CVR responses.

Results Males had a significantly greater $\dot{V}O_{2max}$ (49.5 \pm 8.0 vs 39.1 \pm 8.5 $ml.kg^{-1}.min^{-1}$, $P=0.01$), PPO (12.6 \pm 2.7 vs 9.5 \pm 2.0 $W.kg^{-1}$, $P<0.01$) and MPO (8.1 \pm 1.0 vs 6.3 \pm 1.1 $W.kg^{-1}$, $P<0.01$), compared to females. There were no significant differences between males and females in resting MCAv (62.5 \pm 10.9 vs 70.4 \pm 9.7 $cm.s^{-1}$, respectively, $P=0.08$), dCA (0.9 \pm 0.7 vs 0.8 \pm 0.4, $P=0.76$), absolute CVR (1.8 \pm 0.3 vs 2.1 \pm 0.5 $cm.s^{-1}.mmHg^{-1}$, $P=0.08$) nor relative CVR (2.8 \pm 0.5 vs 3.0 \pm 0.8% $.mmHg^{-1}$, $P=0.53$). $\dot{V}O_{2max}$ was not significantly correlated with dCA, relative CVR or absolute CVR across the whole sample ($r=-0.12$ to 0.34 , $P\geq 0.12$), in males ($r=-0.19$ to 0.50 , $P\geq 0.10$) or in females ($r=0.07$ to 0.33 , $P\geq 0.32$). MPO was also not significantly associated with dCA or CVR across the whole sample ($r=-0.16$ to 0.07 , $P\geq 0.45$), in males ($r=-0.16$ to 0.25 , $P\geq 0.41$) or in females ($r=-0.27$ to 0.35 , $P\geq 0.30$).

Conclusion These findings indicate that, in healthy young adults, dCA and CVR are not different in males and females. Furthermore, cardiorespiratory fitness and anaerobic capacity were not associated with dCA or CVR in healthy young adults.

PCA008

Chronic Exposure to Global Pollutant Phenanthrene is Cardiotoxic in Mice

Ellie England¹, Holly Shiels¹, Alicia D'Souza²

¹Division of Cardiovascular Sciences, Faculty of Biology, Medicine and Health, The University of Manchester, Manchester, United Kingdom, ²National Heart and Lung Institute, Imperial College London, London, United Kingdom

Phenanthrene (Phe) is a polycyclic aromatic hydrocarbon found predominantly in fossil fuel and petroleum-based pollution. Previous research has shown that acute exposure to high concentrations of Phe is pro-arrhythmic in mice. To determine the arrhythmic potential of chronic low-level exposure to Phe 16 5-week-old mice and 16 20-month-old mice were fed 6µg/kg Phe daily for 10 weeks. Repeat ECG and echocardiography measurements were collected during the exposure period. All animal work was carried out in accordance with the UK animals (scientific procedures) act 1986. Following the 10-week exposure hearts were subjected to an ex-vivo arrhythmia challenge and tissue was collected for gas-chromatography mass-spectrometry and histological analysis. Preliminary analysis has revealed an increased susceptibility to arrhythmia in aged mice. 63% of aged mice exposed to Phe showed spontaneous arrhythmic activity ex vivo versus none of the control or young mice (n=8, t test- p<0.05). Phe exposure significantly increased arrhythmia induction following pacing, from 17% to 75% (n=8, t test- p<0.05). This difference was not present when hearts were treated with isoprenaline before pacing, suggesting bradycardia as an underlying mechanism for Phe induced arrhythmia.

S. Yaar, et al. Global air pollutant phenanthrene and arrhythmic outcomes in a mouse model
Environmental Health Perspectives, 131 (11) (2023), Article 117002:
<https://www.ncbi.nlm.nih.gov/pmc/articles/PMC10619431/>

PCA009

Mechanistically complex effects of variant calmodulin on ryanodine receptor 2 in CPVT

Aisha Gendra¹, Ewan D. Fowler³, Nordine Helassa⁴, N Lowri Thomas¹

¹*School of Pharmacy and Pharmaceutical Sciences, Cardiff University, Cardiff, United Kingdom,*

²*School of Pharmacy & Pharmaceutical Sciences, Cardiff University, Cardiff, United Kingdom,*

³*School of Biosciences, Cardiff University, Cardiff, United Kingdom,* ⁴*Faculty of Health and Life Sciences, University of Liverpool, Liverpool, United Kingdom*

The cardiac ryanodine receptor (RyR2) is a Ca²⁺ channel located on the sarcoplasmic reticulum of cardiomyocytes. In regulating Ca²⁺ release, it maintains both electrical and contractile function, and in these tasks its normal function is modulated by the Ca²⁺-binding accessory protein calmodulin (CaM)^{1,2}. Several CaM mutations have been linked to cardiac arrhythmias, such as Catecholaminergic Polymorphic Ventricular Tachycardia (CPVT), but their arrhythmogenic mechanisms are not fully resolved. This research investigates the effects of two arrhythmia-linked CaM mutations (D132E and Q136P) on RyR2 function (either directly, or by virtue of CaM's regulation of its associated kinase: CaMKII) and how this might lead to aberrant Ca²⁺ signalling³.

RyR2 and CaM were recombinantly co-expressed in HEK293 cells and live-cell confocal Ca²⁺ imaging was used to assess recursive Ca²⁺ release dynamics. The effect of wild type (WT) CaM co-expression on RyR2 is inhibitory - decreasing the duration of Ca²⁺ release events (thereby affecting the frequency of release). Co-expression of D132E and Q136P CaM was shown to reverse this phenomenon by increasing the duration of Ca²⁺ release events (WT 9.79±0.54 vs D132E 12.62±0.52 vs Q136P 13.20±1.02 seconds (mean±SEM), $p<0.05$, one-way ANOVA test, $n=11, 19$ and 10 field of view containing approximately 15 cells each, for WT, D132E and Q136P CaM respectively). This finding suggests a decrease in direct regulation of RyR2 by these mutant CaMs. Additionally, in line with HEK293 data, D132E CaM significantly reduced the endoplasmic reticulum Ca²⁺ store load in HEK293 cells compared to WT CaM ($\Delta F/F_0$ = WT 0.47, 95% CI [0.42, 0.55] vs D132E 0.24, [0.22, 0.28], $p<0.05$, Kruskal-Wallis test, $n=150$ cells for each construct, values are shown as median, 95% CI [lower confidence limit, upper confidence limit]), as determined by the addition of 10mM caffeine. It is, therefore, likely that D132E variant CaM is causing Ca²⁺ leakage from the channel which results in smaller Ca²⁺ stores.

Line-scans were used to detect Ca²⁺ sparks in permeabilised C57BL/6 mouse ventricular myocytes in the presence of WT or mutant CaMs. D132E variant CaM was shown to significantly increase spark duration (WT 51.25, 95% CI [45, 57.5] vs D132E 58.75, 95% CI [52.5, 67.5] ms) and time to peak (WT 10, 95% CI [8, 11] vs D132E 12, 95% CI [10, 13.5] ms) in cardiac myocytes compared to WT CaM ($p<0.05$, Kruskal-Wallis test, $n=39$ and 37 cells isolated from 3 mice for WT and D132E CaM respectively, values are shown as median, 95% CI [lower confidence limit, upper confidence limit]).

The time course of CaMKII autophosphorylation showed significantly reduced autophosphorylation in the presence of Q136P CaM compared to WT ($p<0.05$ at each timepoint, one sample Wilcoxon signed rank test, $n=5$). Western analysis also revealed that Q136P CaM significantly reduced RyR2 phosphorylation at the S2814 CaMKII phosphorylation site compared to WT CaM ($p<0.05$, one

sample Wilcoxon signed rank test, $n=6$). These results show that D132E and Q136P exert their dysfunction in different ways, suggesting that calmodulinopathy in CPVT is likely mechanistically complex.

(1) W. Peng et al., “Structural basis for the gating mechanism of the type 2 ryanodine receptor RyR2,” *Science*, vol. 354, no. 6310, Oct. 2016, doi: 10.1126/SCIENCE.AAH5324. (2) A. B. Sorensen, M. T. Søndergaard, and M. T. Overgaard, “Calmodulin in a Heartbeat,” *FEBS Journal*, vol. 280, no. 21, pp. 5511–5532, Nov. 2013, doi: 10.1111/FEBS.12337. (3) N. Makita et al., “Novel calmodulin mutations associated with congenital arrhythmia susceptibility,” *Circulation: Cardiovascular Genetics*, vol. 7, no. 4, pp. 466–474, Aug. 2014, doi: 10.1161/CIRCGENETICS.113.000459/-/DC1.

PCA010

Long-term impact of high-intensity interval-training on cardiac structure and function after COVID-19: an investigator-blinded randomised controlled trial

Iben Elmerdahl Rasmussen^{1,2}, Mathilde Løk², Cody Garrett Durrer¹, Anna Agnes Lytzen¹, Frederik Foged¹, Vera Graungaard Schelde¹, Josephine Bjørn Budde¹, Rasmus Syberg Rasmussen¹, Emma Fredskild Høvighoff¹, Villads Rasmussen¹, Mark Lyngbæk¹, Simon Jønck¹, Rikke Krogh-Madsen^{1,3}, Birgitte Lindegaard^{1,4}, Peter Godsk Jørgensen⁵, Lars Køber⁵, Niels Vejlstrup⁵, Bente Klarlund Pedersen¹, Mathias Ried-Larsen^{1,6}, Morten Asp Vonsild Lund^{2,5}, Ronan M.G. Berg^{1,2,7,8}, Regitse Højgaard Christensen^{1,9}

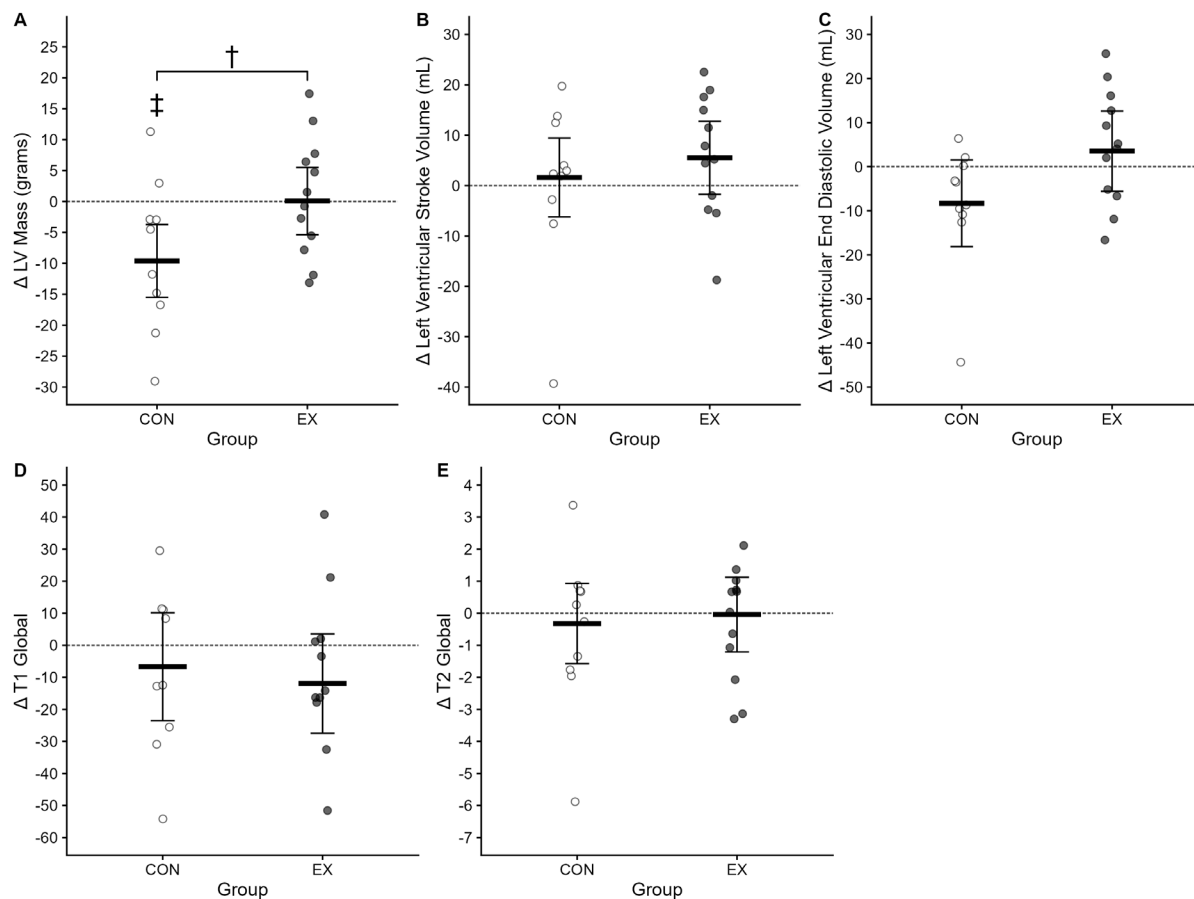
¹Centre for Physical Activity Research, University Hospital Copenhagen – Rigshospitalet, Copenhagen, Denmark, ²Department of Biomedical Sciences, Faculty of Health and Medical Sciences, University of Copenhagen, Copenhagen, Denmark, ³Department of Infectious Diseases, University Hospital Copenhagen – Hvidovre Hospital, Hvidovre, Denmark, ⁴Department of Pulmonary Medicine and Infectious Diseases – North Zealand Hospital, Hillerød, Denmark, ⁵Department of Cardiology, University Hospital Copenhagen – Rigshospitalet, Copenhagen, Denmark, ⁶Research Unit for Exercise Epidemiology, Department of Sports Science and Clinical Biomechanics, University of Southern Denmark, Odense, Denmark, ⁷Department of Clinical Physiology and Nuclear Medicine, Rigshospitalet, University Hospital Copenhagen – Rigshospitalet, Copenhagen, Denmark, ⁸Neurovascular Research Laboratory, Faculty of Life Sciences and Education, University of South Wales, Pontypridd, United Kingdom, ⁹University Hospital Copenhagen – Herlev Hospital, Herlev, Denmark

Introduction: Following the acute phase of SARS-CoV-2 infection, more than a quarter of individuals suffer from persistent exercise intolerance. In a recent study, we observed that a supervised 12w high-intensity interval training (HIIT) scheme resulted in a ~4 g/m² increase in left ventricular mass (LVM) with a corresponding improvement of functional limitations immediately after the intervention. However, there was no effect on pulmonary diffusing capacity or other lung function metrics [14]. Yet, it is unknown whether these changes persist at the long-term. We aim to investigate whether HIIT has long-term effects on cardiopulmonary function in individuals previously hospitalised for COVID-19.

Methods: We enrolled 28 patients (57 ± 11 years; 64% male) previously hospitalised for COVID-19 for this investigator-blinded randomized study with a 12-week (3 sessions/week) supervised HIIT intervention (4x4 HIIT scheme). Outcomes were assessed as the between-group change from baseline to 12mo follow-up. The primary outcome was change in LVM in grams measured by cMRI. The secondary outcomes were between-group change in pulmonary diffusing capacity for carbon monoxide corrected for haemoglobin (D_{L,COc}), V̇O₂peak, as well as the post-COVID-19 function scale (PCFS) and King's Brief Interstitial Lung Disease (KBLID) questionnaire scores. A constrained baseline longitudinal data analysis was used to compare cardiopulmonary changes within and between groups. The study was approved by The Research Ethics Committee of the Capital Region of Denmark (H-20033733 with amendment 75068). The study conformed with the Declaration of Helsinki, and all participants provided oral and written informed consent prior to participation.

Results: Of the 28 patients invited from the main study, 23 consented to participate in the 12mo follow-up, which was completed on average 12.4 ± 0.6 mo after enrollment in the study. Ultimately, 28 participants were included in the final analysis at 12mo (HIIT: $n=14$, control: $n=14$). LVM was maintained between 3mo and 12mo follow-up in the HIIT group, whereas it decreased in the control group with a between-group difference of 9.7 [1.7 ; 17.6] g ($p=0.018$). LVEDV and LVESV showed a similar pattern, but without a significant between-group difference (Figure 1). $D_{L,COc}\%pred$, $FEV_1\%pred$, $FVC\%pred$, $TLC\%pred$ and increased similarly in both groups, while $RV\%pred$ only increased in the control group.

Conclusion: In individuals previously hospitalised for COVID-19, a 12w supervised HIIT scheme leads to a persistently increased LVM reflecting physiological hypertrophy at 12mo follow-up.



Rasmussen, I. E., Løk, M., Durrer, C. G., Foged, F., Schelde, V. G., Budde, J. B., Rasmussen, R. S., Høvighoff, E. F., Rasmussen, V., Lyngbæk, M., Jønck, S., Krogh-Madsen, R., Lindegaard, B., Jørgensen, P. G., Køber, L., Vejlstrup, N., Pedersen, B. K., Ried-Larsen, M., Lund, M. A. V., ... Berg, R. M. G. (2023). Impact of high-intensity interval training on cardiac structure and function after

Physiology in Focus 2024

Northumbria University, Newcastle, UK | 2 – 4 July 2024

COVID-19: an investigator-blinded randomized controlled trial. *Journal of Applied Physiology*, 135(2), 421–435. <https://doi.org/10.1152/JAPPLPHYSIOL.00078.2023>

PCA011

Investigation of RyR2 Arg1051 arrhythmia and cardiomyopathy-linked mutations: functional effects at the single channel, population and whole cell level.

Tessa Harris¹, Lowri Thomas¹

¹*School of Pharmacy and Pharmaceutical Sciences, Cardiff University, Cardiff, United Kingdom*

The human cardiac ryanodine receptor (hRyR2) is a Ca^{2+} ion channel found on the sarcoplasmic reticulum of cardiomyocytes that plays a central role in excitation-contraction coupling. This channel is tightly regulated to prevent dysfunction, though mutation of hRyR2 is associated with arrhythmia and cardiomyopathy. Inter-channel clustering of hRyR2 is proposed to regulate its function¹, preventing uncontrolled Ca^{2+} release and possibly promoting concerted gating². This research aims to functionally characterise arrhythmia / cardiomyopathy-linked mutations (R1051P, R1051C, and R1051H) found in the P1 domain – a region likely involved in inter-channel clustering³ - to determine whether any Ca^{2+} release dysfunction is influenced by functional changes at the clustering level.

HEK293 cells recombinantly expressing either wild-type (WT) or mutant hRyR2 were loaded with Calbryte 520 AM Ca^{2+} sensitive dye and imaged using confocal microscopy to assess whole cell Ca^{2+} release. Ca^{2+} release from populations of human recombinant RyR2 channels incorporated into droplet interface bilayers (DIBs)⁴ was analysed optically (with Cal590) using total internal reflection fluorescence microscopy (TIRF). Purified hRyR2 was incorporated into artificial bilayers for single channel recording and analysis of gating mechanisms⁵.

Spontaneous whole cell Ca^{2+} release from R1051-mutants was significantly different from WT hRyR2 ($p < 0.05$, one-way ANOVA with Tukey post-hoc tests) and displayed longer duration of oscillations (WT = 17.7 ± 0.18 , R1051P = 21.4 ± 0.51 , R1051C = 21.3 ± 0.34 , R1051H = 20.5 ± 0.30 , seconds), and lower amplitude (WT = 1.15 ± 0.2 , R1051P = 0.88 ± 0.03 , R1051C = 0.76 ± 0.02 , R1051H = 0.71 ± 0.02 , $\Delta F/F_0$) (n = number of cells, WT $n=645$, R1051P $n=204$, R1051C $n=357$, R1051H $n=447$, results expressed as mean \pm SEM), indicating Ca^{2+} release dysfunction. Populations of R1051P hRyR2 exhibited additional Ca^{2+} flux behaviours not observed for the WT indicative of rapid switching between stable periods of low and high Ca^{2+} flux ($n=42-63$ channel populations). Preliminary analysis estimating cluster size did not indicate any difference in cluster size between R1051P and WT hRyR2, although results suggested these behaviours manifested more frequently in larger populations. Single channel experiments showed comparable open probabilities (P_o) for mutant and WT channels ($n=3-4$ channels), although mathematical modelling of higher P_o traces indicated R1051P visited longer open states more frequently (WT $\tau = 36.5\text{ms}$, amp = 54%, R1051P $\tau = 60.4\text{ms}$, amp = 68%) with fewer flicker closings than WT hRyR2.

This research demonstrates that mutation of R1051 affects hRyR2 function at multiple organisational levels. Effects at the single channel level seem of minor impact, with dysfunction becoming more pronounced and distinct from the WT in populations of channels, suggesting that the mutational effect largely manifests at the cluster level. This has downstream effects on global Ca^{2+} release dynamics that may act as a substrate for arrhythmia. Future work aims to better quantify cluster size and correlate this to Ca^{2+} release behaviour from populations, and

consideration of hRyR2 distribution within clusters will be important in consolidating the mechanism of dysfunction.

1. Baddeley D et al. (2009). *Proc Natl Acad Sci USA* 106, 22275-22280. 2. Marx SO et al. (2001). *Circ Res* 88, 1151-1158. 3. Cabra V et al. (2016). *Biophys Journal* 110 12, 2651-2662. 4. Leptihn S et al. (2013). *Nature Protocols* 8, 1048-1057. 5. Mukherjee S et al. (2012). *JGP* 140(2), 139–158.

PCA012

Developing p21-activated kinase 1 (PAK1) activators to treat hypertrophic cardiomyopathy (HCM)

YU HE², James. S. H. Bae¹, Ming Lei³

¹Department of Pharmacology, University of Oxford, Oxford, United Kingdom, ²Department of Pharmacology, University of Oxford, Oxford, United Kingdom, ³Department of Pharmacology, University of Oxford, Oxford, United Kingdom

Research rationale: Despite significant progress in comprehending the genetic and metabolic underpinnings of cardiomyocyte dysfunction, there is still a pressing need for targeted treatments to address hypertrophy and progressive remodelling (e.g., fibrosis), seen in HCM [1]. PAK1, a regulator of ion channels and myofilaments in cardiomyocytes, has shown promise in curbing pathological hypertrophy [2]. Our hypothesis centres on the potential therapeutic benefits of pharmacologically activating PAK1 in managing hypertrophy and adverse remodelling in HCM.

Methods: Molecular docking and high-throughput kinase assays using RapidFire-mass spectrometry were employed for virtual and physical screening to develop PAK1 activators. The effect of these activators on cellular hypertrophy was assessed using hypertrophic neonatal rat cardiomyocytes (n=200-300) induced by isoprenaline (ISO, 40 μ M). Subsequently, the small molecule PAK1 activator JB2020A was evaluated in a well-characterized transgenic mouse model expressing the hypertrophic cardiomyopathy-causing mutation Actc1^{E99K}, known for its rapid disease progression [3]. A six-week oral treatment regime (10 mg/kg/day of JB2020A, Vehicle, and WT, N=5 in each group) was initiated at 4 weeks of age. The therapeutic efficacy of these pharmacological interventions and the endpoints were assessed using echocardiography, histology including Sirius red staining and H&E staining, and biomarker assessment using western blot. Data were analysed as mean \pm SEM, ****p < 0.0001, ***p < 0.001, **p < 0.01, *p < 0.05, ns, not significantly different according to one-way ANOVA with Tukey's posthoc test.

Results: We have identified potent and effective small molecule PAK1 activators that significantly increased PAK1 activity by 3 to 5-fold, with an EC₅₀ range between 0.5 and 2.5 μ M. Through the evaluation of PAK1 activators on cellular hypertrophy, JB2020A not only prevented ISO-induced hypertrophy but also reversed pre-existing cellular hypertrophy induced by ISO 24 hours earlier. Moreover, after 6 weeks of JB2020A treatment, we observed a significant reduction in cardiomyocyte hypertrophy and cardiac fibrosis, accompanied by preserved cardiac function in Actc1^{E99K} HCM mice compared to vehicle treatment. These cardio-protective effects were associated with increases in phosphorylated PAK1 observed after activator treatment. Furthermore, JB2020A treatment resulted in a reduction in pro-apoptotic CHOP expression and an upregulation of protective endoplasmic reticulum (ER) response molecules (such as ATF4 and Xbp1), suggesting an amelioration of ER stress in HCM.

Conclusions: Collectively, these findings underscore the therapeutic potential of small molecule PAK1 activators as a novel approach for addressing hypertrophy and progressive remodelling in HCM.

1Watkins, Hugh, et al. "Inherited cardiomyopathies." *New England Journal of Medicine* 364.17 (2011): 1643-1656. 2. Wang, Yanwen, et al. "The p21-activated kinase 1 (Pak1) signalling pathway in cardiac disease: from mechanistic study to therapeutic exploration." *British journal of pharmacology* 175.8 (2018): 1362-1374. 3. Song, Weihua, et al. "Molecular mechanism of the E99K mutation in cardiac actin (ACTC Gene) that causes apical hypertrophy in man and mouse." *Journal of Biological Chemistry* 286.31 (2011): 27582-27593.

PCA013

Evaluation of the skin microcirculation response by wavelet analysis: the impact of the cone of influence

Lana Kralj¹, Helena Lenasi¹

¹*Institute of Physiology, Faculty of Medicine, Ljubljana, Slovenia*, ²*Institute of Physiology, Faculty of Medicine, Ljubljana, Slovenia*

Introduction

Wavelet analysis (WA) is a perspective method for performing spectral analysis of laser Doppler (LD) microcirculatory signals. WA decomposes LD signals into wavelet spectra consisting of six frequency intervals related to physiological influences (endothelial nitric oxide (NO)-independent, endothelial NO-dependent, neurogenic, myogenic, respiratory, and cardiac) that modulate the microcirculatory response and range from 0.005-2 Hz [1].

As WA is applied to finite length signals, the analysis results inevitably suffer from edge effects that lead to distortions of the spectral amplitude. The cone of influence (COI), defined as the e-folding time for the autocorrelation of wavelet transform at each scale, delineates the regions of the wavelet spectrum where such edge effects become important [2,3]. Since the cone of influence reduces the available data, these regions can affect the relevance of the results provided [4]. However, the extent to which performing WA by considering the values outside the COI affects the analysis results has not yet been fully investigated.

Aims

We aimed to determine whether accounting for COI leads to significant differences in the results obtained by WA. We observed two typical patterns of LD signal: a stationary signal represented by the baseline LD signal and a complex transient signal represented by the post-occlusive phase of transient arterial occlusion.

Method

Following ethical approval by the National Ethics Committee of the Republic of Slovenia (no. 87/06/13), eighteen healthy young volunteers were recruited.

LD signals were acquired at the volar forearm during a five-minute baseline recording, a transient three-minute occlusion of the brachial artery, and a recovery phase lasting an additional five minutes.

WA was performed on the signals acquired during the baseline and recovery phases. The time-averaged wavelet spectra were constructed in two ways: with and without the data affected by edge effects (i.e. without and with COI correction).

To compare the contribution of different physiological mechanisms to the regulation of microcirculatory responses during these phases, the relative power (RP = median power of each frequency interval / median power of the total spectrum) was determined for each frequency interval of the corresponding phase.

A non-parametric Wilcoxon signed-rank test was used to compare the differences between the RP of the spectral components obtained without and with COI correction, respectively. The results are presented as group medians and the interquartile range.

Results

No statistically significant differences were found between the RPs of the baseline phase determined without and with COI correction. Statistically significant differences were observed in the RPs of the frequency bands associated with endothelial NO-independent (9.72 [6.76-11.76] without vs. 2.47 [1.27-4.44] with correction, $p < 0.001$), endothelial NO-dependent (4.33 [2.58-7.61] without vs. 1.15 [0.76-2.47] with correction, $p < 0.001$), neurogenic (1.89 [1.25-2.62] without vs. 1.12 [0.81-1.19] with correction, $p < 0.05$), myogenic (0.84 [0.51-0.93] without vs. 1.06 [0.97-1.41] with correction, $p < 0.001$), respiratory (0.33 [0.22-0.42] without vs. 0.51 [0.44-0.77] with correction, $p < 0.001$) and cardiac (0.25 [0.16-0.59] without vs. 0.54 [0.31-0.95] with correction, $p < 0.001$) influence.

Conclusion

Our results suggest that it may be crucial to adjust WA results for COI correction in case of transient LD signals, especially for low-frequency endothelial intervals that are questionable to evaluate in practice.

[1] Kralj, L., & Lenasi, H. (2023). Wavelet analysis of laser Doppler microcirculatory signals: Current applications and limitations. *Frontiers in Physiology*, 13.
<https://doi.org/10.3389/fphys.2022.1076445> [2] Chen, X., Gupta, R. S., & Gupta, L. (2023). Exploiting the Cone of Influence for Improving the Performance of Wavelet Transform-Based Models for ERP/EEG Classification. *Brain Sciences*, 13(1).
<https://doi.org/10.3390/brainsci13010021> [3] Torrence, C., & Compo, G. P. (1998.). A Practical Guide to Wavelet Analysis. *Bulletin of the American Meteorological Society*, 79 (1).
[https://doi.org/10.1175/1520-0477\(1998\)0792.0.CO;2](https://doi.org/10.1175/1520-0477(1998)0792.0.CO;2) [4] Reynès, C., Vinet, A., Maltinti, O., & Knapp, Y. (2020). Minimizing the duration of laser Doppler flowmetry recordings while maintaining wavelet analysis quality: A methodological study. *Microvascular Research*, 131.
<https://doi.org/10.1016/j.mvr.2020.104034>

PCA014

Does exercise training and estradiol affect wound healing in microvascular smooth muscle cells of post-menopausal women?

Sophie Møller¹

¹*University of Copenhagen, Copenhagen, Denmark*

Introduction: Menopause is linked to decreased vascular function and increased cardiovascular risk (1). Although exercise is cardioprotective, improving vascular health, post-menopausal women have shown a blunted response due to lower estrogen levels (2). Research has solely focused on endothelial cells, neglecting the role of smooth muscle cells (SMCs) in vascular function. While literature on the direct effects of estrogen on SMCs are conflicting, what is clear is the existence of estrogen receptors on SMCs (3). Additionally, estrogen appears to inhibit SMC proliferation (4,5).

Objective: This study investigated if exercise training and/or estradiol treatment improved wound healing in microvascular SMCs from early and late post-menopausal women.

Methods: The study was approved by the ethics committee of Copenhagen (H-20037633) and conducted according to the Declaration of Helsinki. All participants were informed about the procedures and potential risks, both orally and in writing, with written informed consent obtained before enrollment.

Early (1-5 years) and late (≥ 10 years) post-menopausal women not on hormone replacement therapy participated. Microvascular SMCs were isolated from muscle biopsies of both early (n=7) and late (n=7) post-menopausal women, before and after an 8-week exercise regimen (aerobic interval training 3 times/week). Wound healing was assessed by scratching cultured SMCs and measuring wound closure at set time points (t=0, 4, and 24 post-wound infliction). An additional group were pre-incubated with 3.67 μ M estradiol for 2 days prior to the wound healing assay.

Results: Basal wound healing was similar across groups. Estradiol pre-incubation had no independent effect. Exercise training improved wound healing profiles in both early and late post-menopausal groups. This improvement was significant in the late post-menopausal group with estradiol pre-treatment (P = 0.034).

Conclusion: Preliminary data suggests exercise training improves the wound healing profile of SMCs, potentially indicating improved cellular health. This effect might be amplified when combined with estrogen therapy in late post-menopause.

References: (1) Nyberg M, Egelund J, Mandrup CM, Nielsen MB, Mogensen AS, Stallknecht BM, Bangsbo J & Hellsten Y (2016). Early postmenopausal phase is associated with reduced prostacyclin-induced vasodilation that is reversed by exercise training. The Copenhagen Women Study. *Hypertens* 68, 1011-20. (2) Nyberg M, Egelund J, Mandrup CM, Anderson CB, Hansen KMBE, Hergel IMF, Valbak-Andersen N, Frikke-Schmidt R, Stallknecht B, Bangsbo J & Hellsten Y (2017). Leg vascular and skeletal muscle mitochondrial adaptations to aerobic high-intensity exercise training are enhanced in early postmenopausal phase. *J Physiol* 595, 2696-83. (3) Karas RH,

Patterson BL & Mendelsohn ME (1994). Human vascular smooth muscle cells contact functional estrogen receptor. *Circ* 89, 1943-50. (4) Li QY, Chen L, Zhu QH, Zhang M, Wang YP & Wang WM (2011). Involvement of estrogen receptor- β in ferrolol inhibition of rat thoracic aorta vascular smooth muscle cell proliferation. *Acta Pharmacol Sinica* 32, 433-40. (5) Ortmann J, Veit M, Zingg S, Di Santo S, Traupe T, Yang Z, Völzmann J, Dubey RK, Christen S & Baumgartner I (2011). Estrogen receptor- α but not - β or GPER inhibits high glucose-induced human VSMC proliferation: Potential role of ROS and ERK. *J Clin Endocrinol Metab* 96, 220-8.

PCA015

The Role of Sortillin-Related VPS10P Containing Receptor, SorCS2 in Endothelial and Smooth Muscle Cell Function.

Rashika Sivakumar, Elizaveta Melnikova, Christian Stæhr, Vladimir Matchkov

undefined

Introduction. Sortillin-related VPS10P containing receptor (SorCS2) is expressed in neurons and other tissues during development where it mediates trafficking of target proteins between cell membrane and intracellular compartments. It has also been suggested that SorCS2 modulates signal transduction (Malik et al., 2020; Salasova et al., 2022). Moreover, SorCS2 is upregulated in the vascular wall under pathological conditions, e.g., atherosclerosis (Amadio et al., 2017). The aim of this study was to elucidate the contribution of endothelial and smooth muscle SorCS2 to the vascular function.

Method. We compared mesenteric small arteries (MSA) from endothelium- and smooth-muscle-specific knockouts (KO) for SorCS2 with matching controls in isometric myograph. For the endothelium-specific KO study, mice of two genotypes were used as controls: mice with floxed SorCS2 gene but without any Cre-recombinase expression, and mice with Cre-recombinase expression without any SorCS2-floxed gene. The endothelium-specific SorCS2 KO was constitutive KO with Cre expression controlled by Tie2 promoter. For this knockout, the mice were grouped into homozygote and heterozygote sub-groups, respectively. Cre expression was controlled by estrogen receptor type 2 under smooth-muscle-myosin-heavy-chain promoter and the smooth-muscle-specific knockout was induced by tamoxifen treatment. Vascular compliance, inner arterial diameters, noradrenaline-induced contraction, acetylcholine-induced relaxation, and relaxation to NO donor, sodium nitroprusside were compared between KOs and matching wild types.

Results. The MSA from endothelial-specific SorCS2 homozygote KO mice (n= 5-6) showed reduced compliance and reduced contractility to noradrenaline in comparison with the matching controls (n = 3-6). Furthermore, the MSA from endothelial-specific SorCS2 homozygote KO (n=5-6) demonstrated an increased sensitivity to acetylcholine-induced relaxation, which seemed to be NO-dependent. The MSA from smooth-muscle-specific SorCS2 KO (n = 3) had no changes in both acetylcholine- and sodium-nitroprusside-induced relaxations but showed decreased noradrenaline-induced contraction and compliance in comparison with the control arteries.

Conclusion. Our findings from the cell-specific vascular KO models indicate that SorCS2 contributes to endothelial- and smooth muscle-cell functions in murine mesenteric arteries.

References: Amadio, P., Colombo, G. I., Tarantino, E., Gianellini, S., Ieraci, A., Brioschi, M., Banfi, C., Werba, J. P., Parolari, A., Lee, F. S., Tremoli, E., & Barbieri, S. S. (2017). BDNFVal66met polymorphism: a potential bridge between depression and thrombosis. *Eur Heart J*, 38(18), 1426-1435. <https://doi.org/10.1093/eurheartj/ehv655> Malik, A. R., Lips, J., Gorniak-Walas, M., Broekaart, D. W. M., Asaro, A., Kuffner, M. T. C., Hoffmann, C. J., Kikhia, M., Dopatka, M., Boehm-Sturm, P., Mueller, S., Dirnagl, U., Aronica, E., Harms, C., & Willnow, T. E. (2020). SorCS2 facilitates release of endostatin from astrocytes and controls post-stroke angiogenesis. *Glia*, 68(6), 1304-1316. <https://doi.org/10.1002/glia.23778> Salasova, A., Monti, G., Andersen, O. M., & Nykjaer, A. (2022). Finding memo: versatile interactions of the VPS10p-Domain receptors in Alzheimer's disease. *Mol Neurodegener*, 17(1), 74. <https://doi.org/10.1186/s13024-022-00576-2>

PCA016

Effects of maternal obesity on cardiac metabolism and mitochondrial respiratory function in young adult mice born to obese dams.

Benjamin Thackray¹, Denise Fernandez-Twinn², Alice Knapton¹, Susan Ozanne², Andrew Murray¹

¹*Department of Physiology, Development and Neuroscience, University of Cambridge, Cambridge, United Kingdom,* ²*Wellcome-MRC Institute of Metabolic Science, University of Cambridge, Cambridge, United Kingdom*

Introduction: In a well-established model of murine diet-induced maternal obesity, offspring of obese dams show age-dependent and sex-specific cardiac hypertrophy and contractile dysfunction. While alterations in energy metabolism and myocardial substrate preference are associated with pathophysiological changes in cardiac function, programmed changes in offspring cardiac metabolism in response to maternal obesity remain incompletely defined. Recent studies have highlighted altered metabolic gene expression in the hearts of offspring of obese pregnancy, both in late fetal life and adulthood, however the impact on mitochondrial respiratory function in the developing and adult heart is unclear.

Objective: To evaluate myocardial mitochondrial respiratory capacity and metabolic substrate preference in young adult offspring born to obese dams in a well-established murine model of diet-induced maternal obesity.

Methods: Animal work received ethical approval from the University of Cambridge Animal Welfare and Ethical Review Board and was performed in accordance with UK Home Office guidelines under the Animals (Scientific Procedures) Act 1986. Cardiac tissue was collected from 8 week old C57BL/6J mice of both sexes born to dams fed either a control or obesogenic diet for 10 weeks prior to mating and throughout gestation and lactation, with all offspring subsequently weaned onto control diet. Mitochondrial electron transfer system (ETS) capacity was assessed using a protocol optimised for frozen samples. Respiratory complex subunit levels were measured by immunoblotting, and gene expression by RT-qPCR. Data was analysed by two-way ANOVA for sex and maternal diet, with Tukey *post-hoc* testing where $p(\text{Interaction}) < 0.05$ ($n = 8$).

Results: In the hearts of 8 week old offspring of obese pregnancy, myocardial mitochondrial complex I-supported respiration (relative to maximal ETS capacity) was greater than in the offspring of dams fed a control diet (control: 0.37 ± 0.038 vs. obese: 0.41 ± 0.065 , $p(\text{Diet}) = 0.041$). This change in complex I-supported respiration was accompanied by an increase in NDUF9 subunit protein levels which did not reach statistical significance (control: 0.31 ± 0.002 vs. obese: 0.35 ± 0.002 , $p(\text{Diet}) = 0.063$). In the hearts of the offspring of obese dams, there was differential expression of genes encoding fatty acid oxidation associated proteins by maternal diet. *Hadh*

expression was 1.4-fold higher in the offspring of obese pregnancy compared with controls ($p(\text{Diet}) = 0.0096$). Expression of *Cpt1b* and *Ucp3* were altered by maternal diet in a sex-specific manner, being lower in the hearts of female offspring of obese pregnancy, compared with female offspring of control pregnancy. These findings suggest sex-specific alterations in myocardial fatty acid oxidation as a result of maternal diet.

Conclusions and further work: The hearts of young adult offspring of obese dams are characterised by metabolic alterations including changes in mitochondrial respiration and fatty acid oxidation (in a sex-specific manner). Further work is underway to profile mitochondrial respiration and substrate metabolism in the cardiac tissue of neonatal offspring of obesogenic diet- and control-fed dams, in order to understand the time course of metabolic alterations in relation to cardiac development.

PCA017

Spatiotemporal electrical excitations during spontaneous contraction in isolated uterine tissues of pregnant guinea pig

Wing Chiu Tong¹, Michael Taggart¹

¹*Biosciences Institute, Newcastle University, Newcastle upon Tyne, United Kingdom*, ²*Biosciences Institute, Newcastle University, Newcastle upon Tyne, United Kingdom*

Regulation of the contractile activities of uterine smooth muscle underpins the fundamental physiological processes of parturition. It is accepted that contractions in uterine smooth muscle cells are determined by episodic, spontaneous electrical potentials. However, the mechanisms that spread the electrical excitations and thus contractions throughout the uterus are still in debate [1]. Optical mapping techniques enable the visualisation and quantification of the spatiotemporal spread of electrical excitations with high spatial and temporal resolutions, and at the same time, also allow simultaneous observations of both electrical activities and the corresponding contractions. We, therefore, have undertaken optical mapping experiments to examine the spatiotemporal characteristics of excitation propagation in isolated uterine tissues from pregnant guinea pigs at term.

Optical imaging was performed according to well-established methods described for the heart [2] with some modifications. Uterine tissues marked with position markers were mounted and stretched to its in vivo dimensions then superfused in Krebs (with 95% O₂ and 5% CO₂) at 37°C. After a period of stabilization, the tissues were stained with the voltage-sensing fluorescent dye di-4-ANEPPS. Fluorescence was excited by light-emitting diodes at 470 nm, and two ranges of emission signals (515 to 565 nm and >590 nm) were projected onto the same image frame and collected simultaneously by a highspeed camera at 250 Hz. A viewing area of 2 cm x 4 cm of uterine tissue was projected onto half of the image frame of 64x128 pixels, resulting in spatial resolutions of 312.5 x 312.5 µm². Uterine movements were separated from the electrical excitation signals by taking the ratio of the two emission signals [3]. The electrical excitation signals were then subjected to spatial and temporal filtering to reduce noise. Excitation wavefronts and conduction velocity vectors were computed using a modified method based on fitting a polynomial surface at each pixel along the wavefronts [4].

All isolated uterine tissues contracted spontaneously. The underlying electrical activities often originated from all around the edges of the tissue. The propagations consisted of mostly repetitive plane waves with occasional re-entrants that rotated around portions of contracted tissues. Multiple initiations might coexist and these excitations would collide, merge or dissipate, complicating the organisation. However, we never observed chaotic excitation patterns such as those of ventricular fibrillation in the heart. The average conduction velocity of 354 excitations is 4.29±1.56 cm/s (mean±SD). However, instantaneous speeds of the wavefronts can reach >52 cm/s momentarily, especially when multiple waves merged. The uterine contractions of the whole

tissue area did not require complete synchronised excitations, and it can be sustained by excitations originated from multiple directions. Further investigations would advance our understanding of the physiological processes of uterine electrical excitation at tissue and organ levels of organisation.

[1] Young RC. (2016). *Reproduction* 152, R51-R61. [2] Matiukas A et al. (2007). *Heart Rhythm* 4, 1441-1451. [3] Holcomb MR et al. (2009). *Exp Biol Med* 234, 1355-1373. [4] Tong WC & Taggart MJ. (2018). *Proc Physiol Soc* 41, PCB038.

PCA018

Liraglutide reduced the dark period core body temperature and curtailed cardiac sympathetic activity during the restraint stress.

Marian Turcani¹, Elham Ghadhanfar¹

¹*Department of Physiology, Faculty of Medicine, Kuwait University, Kuwait, Kuwait*

Glucagon-like peptide 1 (GLP-1) receptor agonists are proposed as a treatment option in patients with heart failure. However, the recommendation remains controversial because several clinical trials did not effectively improve cardiovascular outcomes in heart failure patients (1). One of the problems not settled is the concern about the positive chronotropic and sympathomimetic effect of GLP-1 receptor agonists (2).

We experimented to discover the potentially hazardous effects of chronic treatment with long-acting GLP-1 receptor agonist liraglutide on the hemodynamics and autonomic nervous system (ANS).

During general anesthesia (120 mg.kg⁻¹ ketamine & 6 mg.kg⁻¹ xylazine i.p.), we implanted 10-month-old male Sprague-Dawley rats (n = 14, randomly assigned to the control or treated groups, n = 7) with telemetric transmitters (HD-S11, Data Sciences, USA). Implants allowed simultaneous monitoring of aortic pressure, ECG, core body temperature, and locomotor activity. After baseline 24-hour (12 h light-dark cycles, dark started at 7.00 a.m.) recording of telemetric signals, we used pharmacological tests and 30-minute restraints to estimate ANS activity (3, 4). We applied (i.p.) liraglutide daily, gradually increasing the dose. We started with 0.1 mg/kg of liraglutide for 18 days, continued with 0.3 mg/kg for 55 days, and 1mg/kg for 59 days. We injected (i.p.) saline to control rats. Telemetric signals were recorded weekly for 24 hours. We performed pharmacological and restraint stress ANS tests one month after injecting liraglutide 0.3 mg.kg⁻¹ or 1 mg.kg⁻¹. In addition, we calculated time and frequency domain indices of cardiovascular variability (3, 4). Data were analyzed with the multivariate (Wilks) repeated measure ANOVA. The post hoc Tukey HSD test was used if the interaction between the main effects (treatment & time) was significant.

While body weight remained steady in control rats (645 (SD 80) g), liraglutide-treated rats lost 17 % (p < 0.001) of their body weight at the end of the experiment. We found no significant change in mean arterial pressure, but liraglutide accelerated the heart rate by 10% (p < 0.001) during the light period, increasing it from 278 (SD 10) bpm to 305 (SD 14) bpm. We recorded a significant (p < 0.001) reduction in the core body temperature (-0.4 (SD 0.2)°C) associated with liraglutide treatment during the dark period. No pharmacological tests or any heart rate variability or systolic pressure variability indices pointed to possible alterations in autonomic regulation of the hemodynamics. However, during the restraint stress test, liraglutide-treated rats showed a significantly (p = 0.013) lower elevation of mean arterial pressure by 30% and longer pre-ejection time by 28% (p = 0.011) than control rats.

In conclusion, chronic treatment with liraglutide did not affect the mean arterial pressure but accelerated heart rate during the light period. Surprisingly, we found signs of the sympatholytic

effect of liraglutide, i.e., reducing the core body temperature during the dark period and prolonging pre-ejection time during the restraint stress.

Reference 1: Merza N, et al. (2023). *Curr Probl Cardiol* 48, 101602 Reference 2: Heuvelman VD, et al. (2020). *Cardiovasc Res* 116, 916-930 Reference 3: Ghadhanfar E, et al. (2014). *PloS One* 9, e108909 Reference 4: Turcani M & Ghadhanfar E. (2019). *Sci Rep* 9, 2586

PCA019

Vascular pulsatility in the ageing brain and confounding effects of isoflurane and ketamine/xylazine.

Mia Viuf Skøtt¹, Eugenio Gutiérrez¹, Vladimir Matchkov¹, Leif Østergaard¹, Dmitry Postnov¹

¹*Aarhus University, Aarhus, Denmark*

Increased vascular stiffness and, consequently, pulsatility increase the risk of developing Alzheimer's disease and several cardiovascular diseases, but the exact pathways are still a mystery. Most of our knowledge on the *in-vivo* effects of increased stiffness comes from the large vessels, while capillaries are expected to play the most significant role in cognitive decline. Using Laser Speckle Contrast Imaging (LSCI), we investigated how the microvascular pulsatility changes with age in wild-type mice (C57BL/6) and how it is affected by two of the most commonly used anaesthetics: isoflurane and ketamine/xylazine (k/x).

Twelve mice aged 18 (n=5), 43 (n=3), and 65 (n=4) weeks, respectively, were imaged at 5 separate time points, 4 weeks apart. To access the cortical microvessels, we used LSCI in awake-restrained mice with a chronic cranial window over the left middle cerebral artery (MCA) and its branches. Without changing the field of view, the animals were also imaged under isoflurane anaesthesia followed by k/x anaesthesia. After finishing *in-vivo* experiments, the MCA was isolated and mounted on a wire myograph and tone was recorded to assess the physiological changes of ageing in the vasculature.

The blood flow and pulsatility index in veins, arteries and parenchyma did not change with age and remained constant throughout the experiment. The pulse-associated relative diameter dilation remained constant in veins, but in arteries, it began to increase after 65 weeks of age, from 0.0986 arb. unit at 65 weeks to 0.1580 a.u. at 81 weeks (60.2 %, $p = 0.0521$). These results are supported by the myograph results, indicating an age-related increase in compliance of the MCA. Both anaesthesia caused significant changes to the pulsatility of blood flow velocity in arteries ($p = 8.5 \times 10^{-10}$ under isoflurane and $p = 1.4 \times 10^{-11}$ under k/x using a paired t-test) veins (9.4×10^{-9} under isoflurane and 1.3×10^{-12} under k/x using a paired t-test) and parenchyma (9.2×10^{-9} under isoflurane and 5.5×10^{-12} under k/x using a paired t-test). However, because isoflurane causes a strong vasodilation, the pulse-associated diameter change did not change in arteries ($p = 0.69$, paired t-test) but did in veins (5.4×10^{-7} , paired t-test). But k/x caused a significant response in both arteries ($p = 1.1 \times 10^{-7}$, paired t-test) and veins (1.8×10^{-8} , paired t-test). These results clearly show that while more time-consuming, awake imaging is better when assessing physiological changes in the vasculature and blood flow.

All experimental protocols were approved by the Danish National Animals Experiments Inspectorate and conducted according to their guidelines.

PCA020

Dynamic cerebral autoregulation is unchanged following maximal sprint exercise in healthy young adults

Max Weston¹, Philip Buys¹, Emma Curtin¹, Delphine Guichard¹, Ellen Harbison¹, Alberto Croce¹, Evan Ng¹, Carlo Delle Monache¹, Alberto Maero¹, Gabriel Tan Tan¹, Tobias Khoo¹, Abhinav Sreekanth¹, Norita Gildea¹, Mikel Egana¹

¹*Department of Physiology, School of Medicine, Trinity College Dublin, Dublin, Ireland*

Background and Purpose Maximal sprint exercise is known to exert marked and dynamic changes in cerebral blood flow and blood pressure both during and following exercise. However, the effect of maximal sprint exercise on cerebral autoregulation has not been investigated, which forms an important area of investigation given the growing interest surrounding high-intensity exercise and cerebrovascular function. Therefore, the purpose of this study was to investigate the acute effect of maximal sprint exercise on dynamic cerebral autoregulation (dCA) in healthy young adults.

Methods Twenty-one healthy adults (mean \pm SD age, height and weight: 22.7 ± 3.1 years, 173.4 ± 8.4 cm and 70.3 ± 10.1 kg, respectively, 13 males, 8 females) volunteered to participate in this study, which involved a single experimental visit. Participants visited the laboratory >2 hours postprandial, having refrained from caffeine, alcohol and vigorous physical activity for 24 hours prior to the visit. dCA was determined using a single sit-to-stand manoeuvre. Following >10 min of seated baseline, participants rapidly (< 3 seconds) stood up and remained standing for 3 minutes. Middle cerebral artery blood velocity (MCAv) was measured using transcranial Doppler ultrasonography, and beat-to-beat blood pressure was measured using finger plethysmography. Participants then completed a maximal, 30 second Wingate test on a cycle ergometer, before repeating the dCA assessment after 25 minutes of seated recovery. Baseline measurements were taken as the last 60 seconds of seated measurements, and the nadir in both MCAv and mean arterial pressure (MAP) were identified as the minimum value during the initial 20 seconds following standing. The fall in MCAv and MAP were expressed in both absolute and relative terms, and dCA was quantified as the percentage fall in MCAv relative to the percentage fall in MAP upon standing ($\Delta\% \text{MCAv} / \Delta\% \text{MAP}$). Paired samples t-tests explored the effect of the Wingate test on MCAv, MAP and dCA responses.

Results Baseline MCAv was significantly lower following the Wingate test (59.4 ± 10.4 vs 65.5 ± 11.3 cm.s⁻¹, $P < 0.01$), whilst baseline MAP was unaltered (81.2 ± 10.3 vs 78.7 ± 11.1 mmHg, $P = 0.44$). Upon standing, the fall in MAP was significantly greater following the Wingate test, expressed in both absolute (23.9 ± 6.4 vs 18.4 ± 8.5 mmHg, $P = 0.01$) and relative (29.8 ± 8.3 vs $23.7 \pm 11.1\%$, $P = 0.01$) terms. The relative fall in MCAv from baseline during the sit-to-stand manoeuvre was significantly greater following the Wingate test (23.7 ± 6.2 vs $18.2 \pm 8.1\%$, $P = 0.02$), but not in absolute terms (14.1 ± 4.6 vs 12.0 ± 5.5 cm.s⁻¹, $P = 0.16$). When expressed relative to each other, dCA was unaltered following exercise (0.9 ± 0.3 vs 0.9 ± 0.6 , $P = 0.75$).

Conclusion These findings indicate that maximal sprint exercise significantly impacts the MCAv and MAP responses during a single sit-to-stand manoeuvre. Specifically, the standing-induced fall

in both MAP and MCAv are augmented 25 minutes following sprint exercise. Despite this, dynamic cerebral autoregulation remained unaltered in healthy young adults following a Wingate test.

PCA021

Mitochondria-IP₃Rs coupling is a key regulator of vascular tone in smooth muscle cells

Xun Zhang¹, Matthew Lee¹, Charlotte Buckley¹, Calum Wilson¹, John McCarron¹

¹University of Strathclyde, Glasgow, United Kingdom, ²University of Strathclyde, Glasgow, United Kingdom

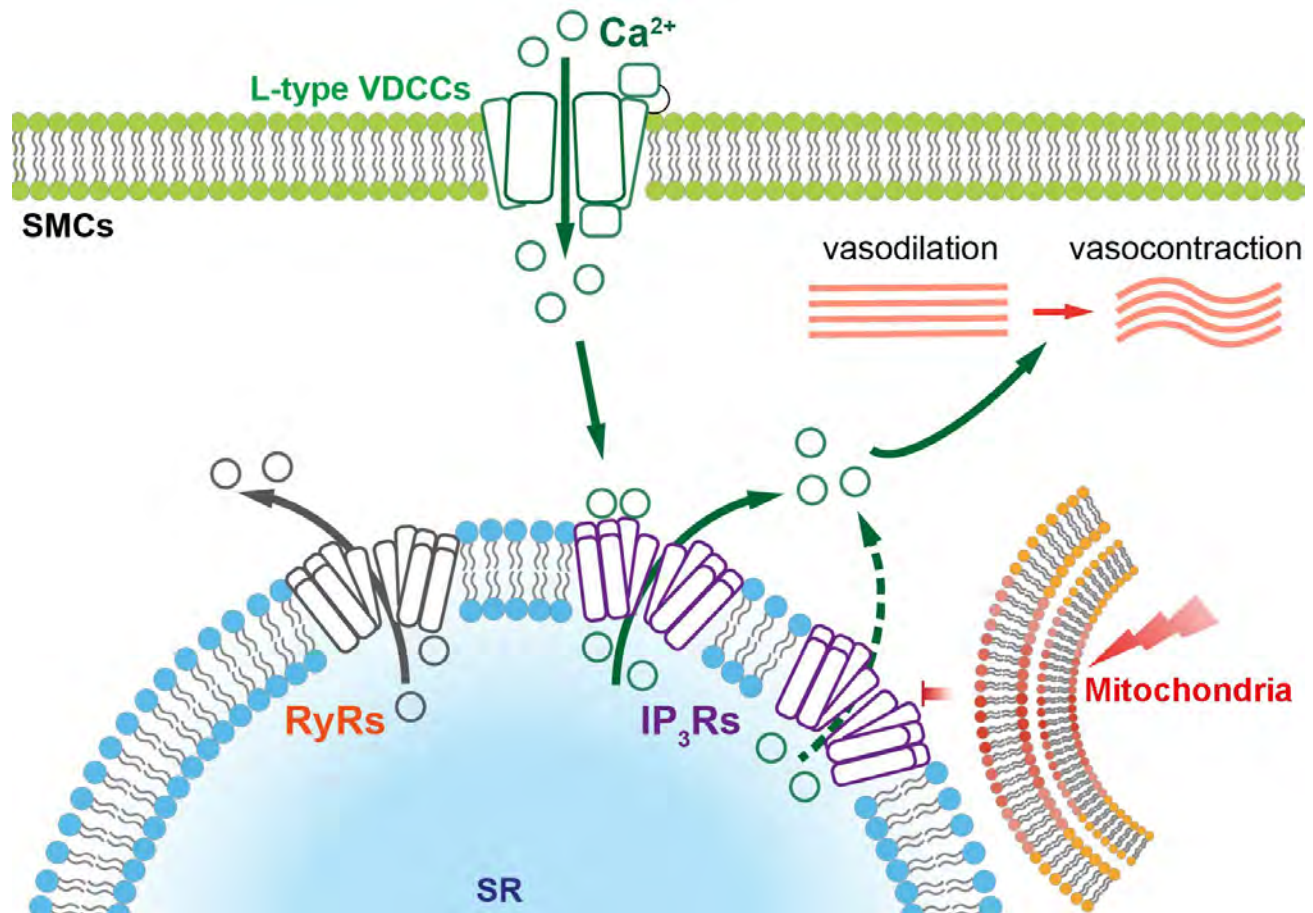
The contractility of vascular smooth muscle cells (VSMCs) in resistance arteries is the major contributor of vascular tone and blood pressure. In VSMCs, increase of intracellular Ca²⁺ level directly generates the force to contract arteries. A major source of intracellular Ca²⁺ is entry through voltage dependent Ca²⁺ channels (VDCCs) on plasma membrane. While mitochondria are now recognised as key regulators of intracellular Ca²⁺ homeostasis by modulating internal Ca²⁺ store in several cell types including smooth muscle cells and endothelial cells, their role in modulating Ca²⁺ signalling generated by VDCC in intact VSMCs is still under studied. Given the potential interaction between mitochondria and VDCCs in VSMCs, we hypothesize that mitochondria can directly regulate Ca²⁺ release from sarcoplasmic reticulum in VSMCs, hence regulate Ca²⁺ signalling and vascular tone generated mediated by VDCCs.

The interplay between mitochondria and VDCCs was investigated by imaging and analysing intracellular Ca²⁺ signals in smooth muscle cells in intact arteries from rat mesentery (n = 5). Summarized data were analyzed and presented as mean ± SD of n biological replicates. When the data extracted from same preparations under different treatment, data were analyzed by using paired t-test.

Depolarization of the plasma membrane potential, by high potassium (30 mM) physiological saline solution, triggered Ca²⁺ entry through VDCCs and a sustained increase in intracellular Ca²⁺ on which repetitive Ca²⁺ oscillations occurred. All Ca²⁺ signals were abolished by removal of external Ca²⁺ and by dihydropyridine inhibitors of VDCCs. Significantly, the repetitive Ca²⁺ oscillations, but not the sustained Ca²⁺ signals, were blocked by the IP₃ receptor inhibitor 2-APB and SERCA inhibitor cyclopiazonic acid. Neither the repetitive Ca²⁺ oscillations or the sustained Ca²⁺ signals were altered by the ryanodine receptor inhibitors ryanodine and dantrolene (paired t-test). These results suggest that Ca²⁺ entry via VDCC triggers Ca²⁺-induced Ca²⁺ release via IP₃ receptors in intact mesenteric arteries.

Depolarization of the mitochondrial membrane potential (ψ_m , indicated by a membrane sensitive dye, TMRE), by the uncoupler CCCP (1 μ M), but not ATP deprivation with the ATP synthesis blocker oligomycin (1 μ M), inhibited VDCCs evoked IP₃ mediated Ca²⁺ oscillations but not the sustained Ca²⁺ signals. Furthermore, in intact arteries, depolarization of ψ_m directly suppressed inositol triphosphate receptors (IP₃Rs) mediated Ca²⁺ release from the internal Ca²⁺ store evoked by photolysis of caged IP₃. These results suggest that mitochondria regulate Ca²⁺ release via IP₃Rs triggered by voltage dependent Ca²⁺ entry. In return, Ca²⁺ entry via VDCCs did not alter ψ_m . In addition, depolarization of ψ_m suppressed sustained vasocontraction that was mediated by voltage dependent Ca²⁺ entry.

Together, these results suggest that mitochondria regulate Ca^{2+} -induced Ca^{2+} release at IP_3 receptors triggered by Ca^{2+} entry via VDCCs but do not directly regulate VDCCs activity.



Chalmers, S., and McCarron, J.G. (2008). The mitochondrial membrane potential and Ca^{2+} oscillations in smooth muscle. *Journal of Cell Science* 121: 75–85. Poburko, D., Liao, C.-H., Breemen, C. van, and Demaurex, N. (2009). Mitochondrial Regulation of Sarcoplasmic Reticulum Ca^{2+} Content in Vascular Smooth Muscle Cells. *Circulation Research* 104: 104–112. Wilson, C., Lee, M.D., Heathcote, H.R., Zhang, X., Buckley, C., Girkin, J.M., et al. (2019). Mitochondrial ATP production provides long-range control of endothelial inositol trisphosphate-evoked calcium signaling. *Journal of Biological Chemistry* 294: 737–758.

PCA022

Development of a digital escape room to raise awareness of the effects of climate change on human health

André Justin Carpio¹, Catriona Jane Cunningham¹, Silvia Mazzotta²

¹School of Medicine, Medical Sciences & Nutrition, University of Aberdeen, Aberdeen, United Kingdom, ²School of Pharmacy & Life Sciences, Robert Gordon University, Aberdeen, United Kingdom

Climate change presents an increasing threat to human life and health. The World Health Organisation has predicted that malnutrition, malaria, diarrhoea and heat stress alone will cause around 250,000 additional deaths annually between 2030 and 2050. However, the health impacts of climate change are currently sparsely taught in medical curricula. The aim of this study was therefore to develop a digital escape room to raise awareness of the effects of climate change on human health.

The escape room was hosted on a WordPress website and H5P (HTML5 Package) was used to create interactive puzzles including a crossword and jigsaw. Solving each puzzle, revealed a code to “unlock” the door. Additionally, a countdown timer set to 40 mins was coded in to simulate the physical escape room experience. During summer 2023, all current medical students were invited to play the digital escape room via email. Anonymous pre- and post-activity questionnaires were used to explore existing knowledge and interest levels in the effects of climate change on health. A second iteration of the escape room with a standalone questionnaire was ran as a face-to-face activity during induction week for incoming year 1 medical students.

Both current (n=23) and new medical students (n=66) reported an increase in self-assessed knowledge of the effects of climate change on human health after participating in the activity. The majority agreed escape rooms could effectively teach new content (91.3%, 78.8%) and should be used in medical education (91.3%, 91%). Over 80% of year 1 medical students agreed the escape room was an excellent icebreaker activity.

In conclusion, this digital escape room was an engaging and enjoyable method of teaching medical students about the impact of climate change on health.

PCA024

A review of palliative and end-of-life care physiology education in Scottish paramedic undergraduate courses

Ross MacInnes¹, Laura Ginesi², Derek Scott¹

¹University of Aberdeen, UK, Aberdeen, United Kingdom, ²University of East Anglia, Norwich, United Kingdom

Introduction: Paramedics are being increasingly dispatched to community palliative and end-of-life care (EoLC) patients (Kirk et al., 2017). Despite this, paramedics consistently report a lack of confidence in treating these patient populations (Blackmore, 2022). Sufficient education in these areas has been identified as a key enabler to the provision of adequate care for these patients by paramedics (Pentaris & Mehmet, 2019). Scotland has recently moved to a degree-based training programme for paramedics, and it has yet to be assessed whether or not paramedics qualifying in Scotland are being educated adequately in the physiology underpinning palliative and EoLC topics. We have previously reported that paramedic curriculum guidance had more reference to these topics than that for many other healthcare professions (Scott et al., 2023).

Aims: To review and analyse palliative and EoLC physiology education within the five Scottish undergraduate paramedic degrees and compare it to the recommendations made by the relevant educational guidance.

Methods: Information gathered from publicly accessible online curriculum documents and data collected by contacting course representatives from each university was screened for information regarding the following: (1) Content delivered in modules relating to palliative and EoLC; (2) Teaching techniques used to deliver palliative and EoLC teaching content; (3) Number of hours dedicated to the delivery of palliative and EoLC material. A thematic analysis was carried out on the data collected regarding course content to gain a comprehensive summary of the educational framework in Scotland. This was compared to the educational recommendations identified.

Results: When compared to the educational guidance, 5 of the identified recommendations were met by ≥ 2 universities, 3 were only met by 1 university each, and 1 recommendation did not appear to be met by any of the courses studied. Teaching techniques used included lectures, tutorials/workshops, seminars, simulations and self-directed study. The mean teaching time dedicated to this content was 12.9 ± 8.47 hours.

Conclusion: Scottish undergraduate paramedic courses largely met the education guidance for palliative and EoLC physiology teaching, however there is scope for implementing further interactive teaching sessions focussing on these topics to address the gaps in the existing framework and further develop student confidence in these areas of practice. This work has led to the design of a potential high-fidelity simulation session in an attempt to address these issues. We hope to deliver such simulations in the near future to continue this work.

Blackmore TA (2022). What is the role of paramedics in palliative and end of life care? Palliative Medicine 36(3), 402–404 <https://doi.org/10.1177/02692163211073263> Kirk A, Crompton PP,

Knighting K, Kirton J, & Jack B (2017). Paramedics and their role in end-of-life care: perceptions and confidence. *Journal of Paramedic Practice* 9(2), 71–79 Pentaris P & Mehmet N (2019). Attitudes and perceptions of paramedics about end-of-life care: a literature review. *Journal of Paramedic Practice* 11(5), 206–215. <https://doi.org/10.12968/jpar.2019.11.5.206> Scott D, Anderson J, Ginesi L & Naczek S (2023) Education about the physiology of death and dying in the training of healthcare practitioners - do we need to do more? *Proc Physiol Soc* 54, C23

PCA025

Comparison of Biomedical Science students' perceptions of online versus paper-based examinations

Mirza Subhan¹, Elizabeth Winters², William Mitchell¹, Kris Jeremy¹

¹School of Biomedical Sciences, Faculty of Health, University of Plymouth,, Plymouth, United Kingdom, ²School of Biomedical Sciences, Faculty of Health, University of Plymouth,, Plymouth, United Kingdom

Online examinations are becoming increasingly incorporated into higher education. However, Biomedical Science students' perspectives on exam format preferences remains unexplored. This study aims to investigate exam format preferences and attitudes of these students. A secondary aim was to also determine any differences between responses regarding age, gender, and programme.

146 participants were sampled across six different programmes. The study was approved by the University of Plymouth Science and Engineering Human Ethics Committee. Questionnaire participants were asked to give their consent as a preliminary question and to confirm they were over the age of 18.

A self-reported survey of 31 questions on online exam perceptions was utilised and composed of six dimensions: affective factors, validity, practicality, reliability, security, and pedagogy. Median scores using a Likert scale measured student attitudes around online exams. Additionally, categorical questions examined attitudes around open-book online exams (OBOEs), closed-book online exams (CBOEs), and paper-based exams (PBEs). Qualitative analysis was conducted via the use of open-ended questions and a focus group on five participants. The results were statistically analysed in SPSS Version 25. Internal validation using Cronbach alpha test results were reported for each dimension. Descriptive statistics were used to report student demographics, examination preference, and responses to questions. A Mann-Whitney U test was used to assess differences in dimension perception with regard to gender and student programme. Multiple linear regression was conducted to look for associations between age and dimensions. $p < 0.05$ was considered as significant.

The findings revealed that 57.5% of students preferred OBOEs while only 19.9% preferred PBEs. OBOEs were perceived as more favourable in all six dimensions and superior in terms of reducing stress, ensuring fairness, allowing demonstration of understanding, and retaining information. Gender had no statistically significant influence on perception. However, programme showed significant difference in to dimensions. Qualitative data supported the main statistical analysis and identified a trade-off between the ability to retain information with PBEs, despite the stress and better demonstration of understanding with OBOEs.

Overall, OBOEs were viewed positively and were well accepted by most participants. Institutions wishing to implement online exams should consider the perceived benefits they have over traditional exams. These findings contribute to the understanding of students' perceptions of exam formats, which can inform their design and application in higher education. Further research

Physiology in Focus 2024

Northumbria University, Newcastle, UK | 2 – 4 July 2024

should explore the perceptions of other disciplines and identify ways to address any challenges associated with online exams.

PCA026

From Movie Theatre to Lecture Theatre: Using Films to Engage Students in Expanded Physiological Cases

Grace Hogan¹, Christopher Torrens¹

¹*Royal College of Surgeons in Ireland, Dublin, Ireland*

Introduction

It is widely appreciated that a considerable understanding of physiology is fundamental to medical practice and a solid factual knowledge is essential for developing clinical skills (Finnerty *et al.*, 2010). However, time allocated to early years basic science teaching only ever decreases (Weston, 2018). This reduction limits sufficient exploration or application of concepts in the traditional manner. Fictional characters and events have been used by others to engage students in the application of concepts they have been taught (Berg & Polvsing, 2016; Scott *et al.*, 2022), and we have utilised films during an elective module to encourage students to think about physiology in the extremes.

Methods

The medical programme at RCSI offers a student choice week in the middle of term, consisting of four taught sessions (Mon-Thu) and an assessment (Fri). We ran an optional Extreme Physiology course, with each of the four days being dedicated to one topic. The four topics were temperature (hypo/hyperthermia), pressure (altitude/depth), space and physiology in the intensive care unit. On the four didactic days, students were given presentations on content with examples linked to films and readily available clips. For the assessment, groups of students had to select a film depicting a relevant extreme situation and discuss the physiological challenges faced by the characters.

Results

All student groups chose highly appropriate scenes to discuss with no duplications. This gave a range of examples portraying situations relating to hypo- and hyperthermia, altitude, depth and/or microgravity. The students were able to discuss key physiological challenges faced by the characters and, in places, were able to critique the accuracy of the depiction portrayed. Feedback from the anonymised centralised student survey had students rating the session as very good (67%) or good (33%). There were also strongly positive comments in the free text sections, all of which indicated that the course had deepened their understanding of physiology.

Conclusions

Student engagement and discussion was good in the sessions and the positive feedback suggests that they found the content and delivery useful. In choosing appropriate scenes and then discussing them, the students were able to demonstrate their problem solving capacity by conducting a thought experiment on the physiological processes triggered by environmental change. As such, we think these fictional scenarios can be used to facilitate students thinking more deeply about physiology.

Berg RMG & Polvsing RR (2016). *Advances in Physiological Education* 40, 234-236 Finnerty EP et al. (2010). *Academic Medicine* 85, 349–355. Scott DA et al. (2022). *Acta Physiologica* 236 (s725), 263-264 Weston WW (2018). *Canadian Medical Education Journal* 9, e109-e114

PCA028

Mineralocorticoid receptor activation induced by hypoxia modulates hepatocyte lipid and glucose metabolism, implicating a role in liver cirrhosis progression.

Mohammad Mohabbulla Mohib¹, Sindy Rabe¹, Alexander Nolze¹, Alexander Zipprich², Michael Gekle¹, Barbara Schreier¹

¹Julius Bernstein Institute of Physiology, Medical School, Martin Luther University of Halle-Wittenberg, Halle, Germany, ²Clinic for Internal Medicine IV, Universitätsklinikum Jena, Jena, Germany

Introduction:

The mineralocorticoid receptor (MR) is a pivotal regulator of water and electrolyte balance and has been implicated in various physiological processes, including blood pressure regulation and renal function. However, aberrant MR activation has been associated with detrimental effects such as promoting fibrosis in the cardiovascular system. Recent studies have indicated a potential role of MR activation in the progression of liver cirrhosis, particularly under conditions of hypoxia commonly observed in cirrhotic livers. Nevertheless, the precise impact of non-physiological MR activation in hepatocytes remains poorly understood.

Objective:

This study aimed to elucidate the consequences of hypoxia-induced MR activation in hepatocytes.

Methods:

We conducted RNA sequencing analysis on rat livers from control animals, cirrhotic animals, and those treated with eplerenone, an MR antagonist (N= 5 animals per group). Animal experiments complied with German law (Tierschutzgesetz, 42502-2-1123 MLU, Landesverwaltungsamt Sachsen-Anhalt), directive 2010/63/EU, and ethical guidelines (ARRIVE guidelines and NIH standards). With respect to the results of the Gene ontology (GO) term enrichment analysis from rat livers, we investigated the impact of MR activation on metabolic processes in HepG2 cells. To induce non-physiological MR activation, we exposed the cells to hypoxia, using an oxygen concentration of 0.2% for at least 24h. mRNA and protein levels of key metabolic genes were determined using quantitative RT-PCR and Western blotting. Glucose consumption, lactate production, and lipid accumulation were assessed as well with or without eplerenone treatment. The data are presented as mean ± standard error of the mean (SEM) % of control. Statistical significance was determined using a two-tailed t-test, with a significance threshold set at $p < 0.05$. Each experiment was conducted with N = 5-10 replicates, and there were n = 15-24 petri dishes per group.

Results:

GO term enrichment analysis revealed that in a rat model for liver cirrhosis (CCl₄ treatment) eplerenone, an MR antagonist, reverses the downregulation of genes annotated to the GO term

“Monocarboxylic acid metabolic process”. We already demonstrated that under hypoxic conditions that the MR-induced transcriptional activity shifts to other response elements on the DNA (Schreier, 2018). Therefore, we incubated HepG2 cells with or without hypoxia in the presence of eplerenone. We have demonstrated that hypoxia reduced the mRNA levels of PPAR α ($46.3 \pm 8.4\%$), PDK4 ($11.4 \pm 3.3\%$), AMACR ($39.2 \pm 6.6\%$), ABCC2 ($67.4 \pm 10.5\%$), and Lipin 1 ($49.1 \pm 15.8\%$); as well as the protein. This downregulation can be partially attenuated by eplerenone treatment for PPAR α ($73.7 \pm 12.7\%$), PDK4 ($66.3 \pm 17.9\%$), and ABCC2 ($99.3 \pm 12.2\%$), suggesting a mineralocorticoid receptor (MR)-dependent mechanism. Hypoxia augments glucose uptake ($282.7 \pm 33.2\%$), and lactate production ($202.7 \pm 11.8\%$) in HepG2 cells. This effect was partially reversed upon eplerenone administration (glucose: $169.2 \pm 10.2\%$ and lactate: 153.5 ± 10.2 ; $p < 0.05$, two-tailed t-test) respectively. Additionally, hypoxia-associated lipid accumulation ($257.9 \pm 26.7\%$) in hepatocytes is partially mitigated by MR blocker ($120.3 \pm 9.8\%$).

Conclusion

Our findings suggest role of MR in dysregulating glucose and lipid metabolism in hepatocytes, potentially contributing to liver cirrhosis development. Therefore, MR antagonism may hold therapeutic promise in the management of liver cirrhosis.

Schreier B, Wolf A, Hammer S, Pohl S, Mildenerberger S, Rabe S, Gekle M, Zipprich A. The selective mineralocorticoid receptor antagonist eplerenone prevents decompensation of the liver in cirrhosis. *Br J Pharmacol*. 2018 Jul;175(14):2956-2967. doi: 10.1111/bph.14341. Epub 2018 Jun 7. PMID: 29682743; PMCID: PMC6016674.

PCA030

Regular practice of 12 weeks of Yoga Therapy attenuates worsening of lipid profile in Early Indian Postmenopausal Women

Praveena Sinha¹, Asha Gandhi², Sunita Mondal³, Anju Jain⁴, Ratna Biswas⁵

¹Assistant Professor, Department of Physiology, Amrita School of Medicine, Faridabad, India, ²Ex-Director Professor & HOD, Department of Physiology, Lady Hardinge Medical College, New Delhi, India, ³Director Professor & HOD, Department of Physiology, Lady Hardinge Medical College, New Delhi, India, ⁴Ex-Director Professor & HOD, Department of Biochemistry, Lady Hardinge Medical College, New Delhi, India, ⁵Director Professor, Department of Obstetrics and Gynaecology, Lady Hardinge Medical College, New Delhi, India

Introduction: Postmenopause is an estrogen deficient state associated with increased incidence of deranged lipid profile, an important marker for cardiovascular diseases. CVD is projected to be the cause of 45% of deaths in Indian postmenopausal women by 2020. Yoga has been described as having beneficial effect on lipid profile in many studies and populations.

Aims: The aim of our research was to study the effect of 3-month long Yoga practice on lipid profile in early postmenopausal women within five years of their menopause.

Methods and Material : A prospective interventional study of 67 women within five years of menopause between 45 and 60 years of age attending the menopause clinic of a tertiary care hospital fulfilling inclusion and exclusion criteria and consenting were enrolled for study. Institutional Ethical Clearance (IEC- Lady Hardinge Medical College & SKH, New Delhi) was sought and obtained before conducting the study. The group was divided into two groups on the basis of their willingness to join the Yoga intervention - Group 1 (n=37)- Postmenopausal patients receiving routine management along with Yogic intervention and Group 2 (n=30)- Postmenopausal patients receiving routine gynaecological management. Yoga group participants received intervention of Integrated Yoga module comprising asanas, pranayama, savasana, and OM chanting for a period of 12 weeks under a trained Yoga teacher from Department of Yoga, Naturopathy and Lifestyle Intervention, Department of AYUSH, Ministry of Health and Family Welfare, India in addition to routine gynaecological management. Lipid profile of 37 cases (Yoga group) and 30 controls (non-Yoga group) was measured pre and postintervention. Statistical Analysis was done by GraphPad Prism Version 5 software. Values are a mean and standard error of mean. Mean and standard error of mean (Mean \pm SEM) of all the variables for both groups were calculated according to accepted statistical methods. Intergroup comparison for parametric data was done using Unpaired 't' test to compare the different parameters in Group 1 and Group 2. Intergroup comparison for non-parametric data was done using Mann-Whitney U test. Intragroup comparison within Group 1 and Group 2 for normally distributed data was done using Paired 't' test. Intragroup comparison within Group 1 and Group 2 for non-parametric data was done using Wilcoxon matched pair test. Statistical significance was set up at $P < 0.05$.

Result: A definite decrease was observed in S. Total Cholesterol (mg/dl) [189.3 \pm 6.03(post) vs 188.5 \pm 5.72 (pre)], S.Triglycerides (mg/dl) [(129.0 \pm 7.51(post) vs 122.3 \pm 8.77(pre)], T.VLDL (mg/dl) [(25.8 \pm 1.50 (post) vs 24.46 \pm 1.75(pre)] in the Yoga Group post intervention but it failed to achieve

statistical significance. In the Non-Yoga Group, S. Total Cholesterol (mg/dl) [(187.6±6.36 (post) vs 196.4±5.58 (pre)], T.LDL(mg/dl) [(113.8±4.82 (post) vs 121.2±4.69 (pre)] worsened after 3 months while S.Triglycerides (mg/dl) [(153.2±14.93 (post) vs 152.8±10.66 (pre)] and T.VLDL (mg/dl) (30.65±2.98 (post) vs 30.56±2.13 (pre)] remained relatively unchanged. S.HDL(mg/dl) remained predominantly unchanged in both groups.

Conclusion: Three-month long Yoga practice attenuated worsening of lipid profile in early postmenopausal women and has the potential to prevent early onset of atherosclerosis and consequent cardiovascular diseases in our population if instated early in menopause.

1. Lopez AD, Murray CCJL. The global burden of disease, 1990–2020. *Nat Med*. 1998 Nov;4(11):1241–3. 2. Mehra P, Anand A, Nagarathna R, Kaur N, Malik N, Singh A, Pannu V, Avti P, Patil S, Nagendra HR. Role of Mind-Body Intervention on Lipid Profile: A Cross-sectional Study. *Int J Yoga*. 2021 May-Aug;14(2):168-172. 3. Nagarathna, R., Usharani, M.R., Rao, A.R. et al. Efficacy of yoga based life style modification program on medication score and lipid profile in type 2 diabetes—a randomized control study. *Int J Diabetes Dev Ctries* 32 (2012);122–130. 4. Ghazvineh D, Daneshvar M, Basirat V, Daneshzad E. The Effect of Yoga on the Lipid Profile: A Systematic Review and Meta-Analysis of Randomized Clinical Trials. *Front Nutr*. 2022 Jul 14;9:942702. 5. Innes KE, Selfe TK, Vishnu A. Mind-body therapies for menopausal symptoms: a systematic review. *Maturitas*. 2010 Jun;66(2):135–49.

PCA031

Are the effects of increased dietary potassium on blood pressure salt dependent?

Adrienne Assmus¹, Louise Nystrup Odgaard¹, Vladimir Matchkov¹, Robert Fenton¹

¹*Department of Biomedicine, Aarhus University, Aarhus, Denmark*

Hypertension is a primary risk factor for cardiovascular disease and a major driver of disability and premature death. High dietary sodium (Na⁺) intake contributes to high blood pressure (BP), but evidence is mounting that dietary potassium (K⁺), typically low in the western diet, also modulates BP. In some studies, greater K⁺ intake lowers BP (1), an effect partially explained by a higher plasma K⁺ being associated to lower activity of the sodium chloride cotransporter NCC in the distal convoluted tubule of the kidney (2). However, other studies do not always see a beneficial effect of greater K⁺ intake on BP (3). The aim of this study is to investigate the mechanisms and potential of increasing dietary K⁺ intake to lower BP, the effects of combining it with higher salt intake and the limitations of such an approach.

Methods: Initially, two cohorts of male mice were fed diets containing 0.74% NaCl and increasing percentages of K⁺ (0.75% K⁺, 1%, 1.25%, 1.5%, 1.75%, 2%, 2.5% and 5%) each for 5 sequential days. Cohort 1 had BP recorded using telemetry for 24 h on the last day of each diet. Cohort 2 had blood and 24 h urine collected at the same time points for assessment of renal function and electrolyte balance. In another cohort, mice were switched directly from a 0.75% K⁺ to a 2% K⁺ diet. Mice were then fed either a high salt diet (4% NaCl) combined with a 0.75% or 2% K⁺ intake for 15 days.

Results: Incremental increases in K⁺ intake led to a linear ($R^2=0.98$) increase in 24 h urinary K⁺ excretion, which plateaued at 2.5% K⁺ (0.35 ± 0.05 to 1.19 ± 0.28 mmol/24h, mean \pm SD). Natriuresis was not significantly different across the diets, with the exception of the 5% K⁺ diet where Na⁺ excretion was $33.8 \pm 10.6\%$ lower ($p=0.014$). 24 h urine volume was significantly increased for all dietary K⁺ intakes $> 1.75\%$ K⁺. Systolic BP (SBP, active period) for all dietary K⁺ intakes was not significantly different to control ($n=7$ vs. $n=5$), with the exception of the 5% K⁺ where SBP increased by 7.16 ± 1.72 mmHg ($p=0.014$). Plasma K⁺ was not significantly different across the diets relative to 0.75% K⁺, until an intake of 2.5% K⁺, after which plasma K⁺ was significantly higher. A direct switch from a 0.75% to 2% K⁺ diet on normal Na⁺ intake led to an increase in SBP of 5.10 ± 2.5 mmHg after 5 days (active period, $p=0.027$). This increase in SBP was not apparent in mice concomitantly receiving a high Na⁺ diet.

Conclusion: This study shows that progressively increasing K⁺ intake on a normal salt diet leads to increased urinary K⁺ excretion, but no changes in plasma K⁺ or BP, until K⁺ intake exceeds 2.5% K⁺. However, a direct jump to a higher dietary K⁺ intake increases BP on normal salt intake, but this effect is attenuated during high salt intake. The molecular mechanisms underlying these responses are under investigation.

(1) Mente, A. et al., *N Engl J Med* 371, 601- 611 (2014) (2) Poulsen, S et al., *J Physiol* 597, 4451-4464 (2019) (3) Chaudhary, P. & Wainford, R. D., *J Hum Hypertens* 35, 577-587 (2021)

PCA032

A novel urine pH-ammonium acid/base-score and progression of chronic kidney disease

Peder Berg¹, Samuel Levi Svendsen¹, Amalie Quist Rousing¹, Rasmus Kirkeskov Carlsen², Dinah Khatir², Danny Jensen², Nikita Misella Hansen³, Louise Salomo³, Henrik Birn², Niels Henrik Buus², Jens Leipziger¹, Mads Vaarby Sørensen¹

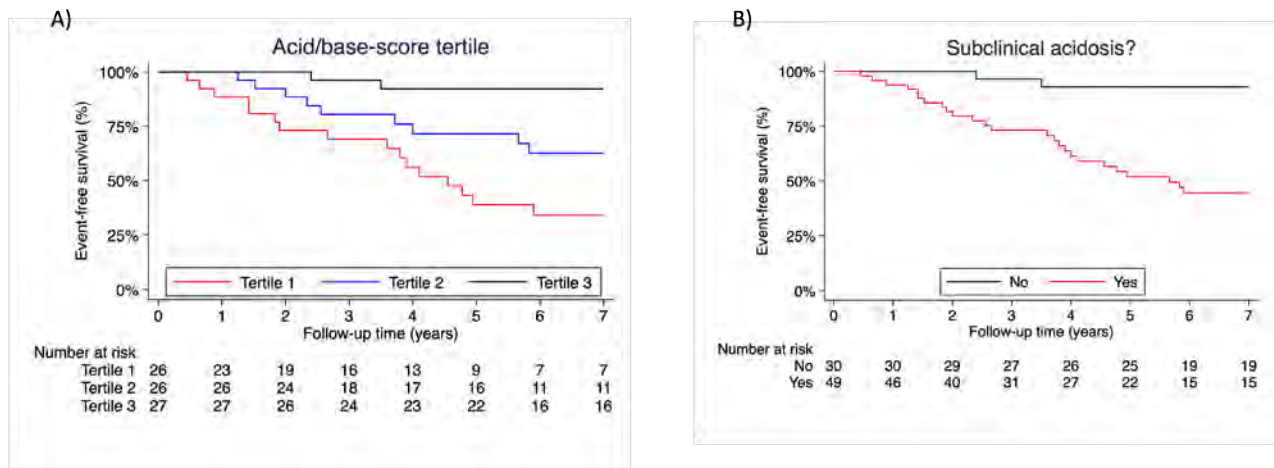
¹Department of Biomedicine, Aarhus University, Aarhus, Denmark, ²Department of Renal Medicine, Aarhus University Hospital, Aarhus, Denmark, ³Department of Nephrology, Copenhagen University Hospital, Copenhagen, Copenhagen, Denmark

Introduction: Acidosis is associated with exacerbated loss of kidney function in chronic kidney disease (CKD). Currently, acid/base status is assessed by plasma measures, although organ-damaging covert acidosis, subclinical acidosis, may be present before reflected in plasma. Low urine NH_4^+ excretion associates with poor renal outcomes in CKD and has been proposed as a marker for subclinical acidosis. However, a low NH_4^+ excretion could result from either a low capacity or a low demand for acid excretion. We hypothesized that a urine acid/base-score reflecting both the demand and capacity for acid excretion would better predict CKD progression.

Methods: 24-hour urine collections were included from three clinical studies of patients with CKD stage 3 and 4: A development cohort (n=82), a variation cohort (n=59), and a validation cohort (n=73). A urine acid/base-score was derived and calculated from urinary pH and $[\text{NH}_4^+]$. Subclinical acidosis was defined as an acid/base-score below the lower limit of the 95% prediction interval of healthy controls. Main outcomes were percentage change in measured GFR after 18 months and CKD progression (defined as $\geq 50\%$ decline in eGFR, initiation of long-term dialysis or kidney transplantation) during up to 10 years of follow-up. To assess percentage change in measured GFR as a function of acid/base-score and subclinical acidosis status, log-transformed measured GFR values was analyzed as outcome variable using a mixed-effects models for repeated measures. Models included visit (baseline vs. 18 months follow-up), acid/base-score or subclinical acidosis and visit-by-acid/base-score or subclinical acidosis interaction as fixed effects. The risk for CKD progression as a function of acid/base-score and subclinical acidosis status was assessed by cox proportional hazards models. All estimates were assessed with and without adjustment for important clinical risk factors for GFR decline and CKD progression (sex, age, baseline GFR, proteinuria, systolic blood pressure, and plasma bicarbonate).

Results: Subclinical acidosis was prevalent (development cohort: n=51/82, 62%, validation cohort: n=47/73, 65%). Subclinical acidosis was associated with an 18% (95% CI: 2-32) larger percentage decrease of measured GFR after 18 months. During a median follow-up of 6 years, subclinical acidosis was associated with a markedly higher risk for CKD progression. Adjusted hazard ratios were 5.1 (95% CI 1.1-23.3) in the development cohort and 11 in the validation cohort (95% CI: 2.9-42.4). The adjusted hazard ratio in the pooled cohorts was 5.7 (95% CI: 2.3 to 14.4) for patients with subclinical acidosis. Kaplan-Meier plots for event-free survival stratified for acid/base-score tertile and subclinical acidosis are shown in figure 1. The acid/base-score had a higher predictive value for CKD progression than NH_4^+ excretion alone (C-score of 0.73 vs. 0.55, difference: 0.18, 95% CI: 0.05 to 0.30).

Conclusion: Subclinical acidosis, defined by a new urine acid/base-score, is associated with a higher risk of CKD progression in patients with CKD stage 3 and 4.



PCA033

Electrophysiological studies of TRPV4-mediated transepithelial electrolyte flux in relation to potassium channels involved in cerebrospinal fluid production

Cameryn Davis¹, Verayna Newland¹, Bonnie Blazer-Yost¹

¹*Indiana University Indianapolis, Indianapolis, United States*

Introduction: Hydrocephalus is a neurological disorder characterized by accumulation of cerebrospinal fluid (CSF) within the brain caused by an overproduction of CSF, blockage of flow, or decreased reabsorption. The CSF accumulation causes pathologies including ventriculomegaly, increased intracranial pressure, and cell damage. CSF is secreted by the choroid plexus, a fenestrated capillary network surrounded by an epithelial monolayer in the ventricles. This epithelium is composed of polarized choroid plexus epithelial cells (CPE) in which ion channels are located on either the apical (CSF-facing) or basolateral (blood-facing) membrane. The production and amount of CSF is regulated by a complex interaction between these channels including transient receptor potential vanilloid 4 (TRPV4), calcium-activated potassium channel (KCa3.1), K⁺-Cl⁻ cotransporter (KCC) and the sodium, potassium 2 chloride channel (NKCC1). TRPV4 is an osmo-, shear-, temperature- and pressure-sensitive nonselective cation channel. TRPV4 activation causes an influx of Ca²⁺ and Na⁺ which can secondarily activate KCa3.1. TRPV4 activation also involves the Ste20/SPS1-related proline-alanine-rich kinase (SPAK) pathway which inhibits KCC and regulates NKCC1. Altering the extracellular K⁺ concentration within physiological parameters also has the potential to affect transport via electrochemical gradients.

Aim: Our goal was to identify a relationship between activation of TRPV4 and potassium channels within the CPE. Identifying the regulation of these channels, will provide further understanding of CSF production in normal and pathophysiological states and provide a basis for identifying potential targets for future drug development for a variety of diseases including hydrocephalus.

Methods: The human choroid plexus papilloma (HIBCPP) cell line was cultured in media supplemented with 10% fetal bovine serum, 1% penicillin and streptomycin, 5 ng/L insulin, and sodium bicarbonate. Cells were seeded onto permeable supports until they formed a monolayer with resistances <400 ohm.cm². Ussing-chamber electrophysiology was used to measure net ion flux and changes in cellular permeability. The relationship between ion channels were investigated using treatments including increasing extracellular K⁺ to 10 mM, 50 μM (Dihydroindenyl)oxy alcanoic acid (DIOA, KCC inhibitor), and 5 μM TRAM-34 (Triaryl methane-34, KCa3.1 inhibitor). Compounds were added to either the apical, basolateral, or bilateral sides to determine polarity. After a short (10 min) drug pre-treatment, 15 nM GSK1016790A (TRPV4 agonist) was added to the cells thereby stimulating a complex ion and fluid transepithelial flux. Each treatment had a minimum of six trials. Statistical significance was determined using a paired multiple T-test.

Results: When KCa3.1 was inhibited on the apical side, both a decrease in net transepithelial ion flux and membrane permeability occurred. Inhibition on the basolateral side resulted in an increased membrane permeability, while inhibition on both sides led to decreased transepithelial ion flux. When KCC was inhibited on the basolateral side, a decrease in both transepithelial ion flux and membrane permeability was observed while inhibition on both sides only showed a decrease

in transepithelial ion flux. Increasing the concentration of extracellular K^+ showed no significant change.

Conclusion: Our results show that there is a relationship between TRPV4 and the potassium channels KCC and KCa3.1, but no significant relationship with physiologically relevant changes in extracellular K^+ .

PCA034

Identifying a binding site for voltage-independent CFTR blockade by GlyH-101

Tzyh-Chang Hwang¹, Zhiwei Ma², Shiting Ho¹

¹National Yang Ming Chiao Tung University, Taipei, Taiwan, Province of China, ²University of Missouri, Columbia, United States

Cystic Fibrosis Transmembrane conductance Regulator (CFTR) is a chloride channel with characteristic structural similarities to ABC Transporters. Recent cryo-EM studies (Zhang et al., 2018) have revealed a large internal vestibule in the ion permeation pathway of activated CFTR proteins (i.e., phosphorylated, ATP-bound state). We and others lately identified a binding site at the external end of this vestibule for CFTR_{inh}-172 (Young et al., 2024; Gao et al., 2024), a known voltage-independent CFTR inhibitor. These cryo-EM data also suggest that the binding of CFTR_{inh}-172 induces conformational changes in CFTR's two transmembrane segments TM8 and TM12 to obstruct the external end of the pore. Interestingly, our patch-clamp electrophysiological studies show that GlyH-101, another membrane-permeant CFTR blocker, not only blocks CFTR from the external side of the membrane in a voltage-dependent manner ($z_d = 0.37 \pm 0.02$; $K_d(0) = 3.2 \pm 0.8$ μ M, $n = 3$) as reported previously (Muanprasat et al., 2004) but also inhibits CFTR currents from the cytoplasmic end with little voltage dependence, suggesting the presence of two distinct binding sites for GlyH-101. Despite structural differences between CFTR_{inh}-172 and GlyH-101, they are similar in size and polarized charge. We thus hypothesize that GlyH-101 and CFTR_{inh}-172 may share the same binding pocket—or at least their binding sites may overlap with each other. Indeed, molecular docking shows that GlyH-101 can be accommodated in the same area where CFTR_{inh}-172 binds. A poorly membrane-permeant GlyH-101 analog (GlyH-101-1) was synthesized by adding a hydrophilic polyethylene glycol tail to the C6 position of the naphthalene ring in GlyH-101. External GlyH-101-1 blocks whole-cell CFTR current in a voltage-dependent manner ($z_d = 0.30 \pm 0.01$, $K_d(0) = 134 \pm 18$ μ M, $n = 5$); however, when applied to the cytoplasmic side of an excised inside-out membrane patch, it blocks CFTR in a voltage-independent manner ($z_d = 0.04 \pm 0.001$, $K_d(0) = 45 \pm 17$ μ M, $n = 4$). Single-channel data suggest two steps of inhibition: a binding step leading to a short-lived blocked state and a stabler blocked state likely reflecting binding-induced conformational changes. Examining the effects of mutations at the residues involved in the binding of CFTR_{inh}-172 on the GlyH-101 blockade is underway to further test our hypothesis.

Zhang et al., (2018). Molecular structure of the ATP-bound, phosphorylated human CFTR. *Proc. Natl. Acad. Sci. USA*, 115 (50) :12757-12762. Young et al., (2024). Structural basis for CFTR inhibition by CFTR_{inh}-172. *Proc. Natl. Acad. Sci. USA*, 121(10): e2316675121. Gao et al., (2024). Allosteric inhibition of CFTR gating by CFTR_{inh}-172 binding in the pore. Submitted. Muanprasat et al., (2004). Discovery of glycine hydrazide pore-occluding CFTR inhibitors: mechanism, structure-activity analysis, and in vivo efficacy. *J. Gen. Physiol.* 124(2):125-137.

PCA035

Investigation of human UT-B urea transporter regulation in various cell lines

Lauren McKeever¹, Kate Duffy¹, Gavin Stewart¹

¹School of Biology and Environmental Science, University College Dublin, Dublin, Ireland

Facilitative UT-B urea transporters play a pivotal role in maintaining urea homeostasis by regulating levels of urea in various tissues of the human body. However, the precise regulatory mechanisms governing UT-B expression and activity in different tissues remain to be elucidated. Dysregulation of UT-B transporters has also been implicated in numerous pathological conditions including renal disorders, metabolic diseases, and certain cancers, underscoring the significance of understanding their regulatory mechanisms. This current study therefore compared the levels of both UT-B RNA and UT-B protein in various human cell lines - namely PC-3 (prostate adenocarcinoma), PWR-1E (prostatic epithelia), HT-29 (colorectal adenocarcinoma), and RT-4 (urinary bladder epithelia) - to investigate the regulatory mechanisms governing human UT-B expression. Initially endpoint RT-PCR experiments revealed detectable levels of UT-B RNA in PC-3, HT-29, and RT-4 cells. However, despite the presence of RNA, western blotting experiments detected no significant UT-B protein abundance in either the PC-3 or HT-29 cell lines (All NS, N = 3-4, unpaired T-test). In contrast to these findings, our analysis demonstrated a high UT-B protein abundance level in RT-4 cells and a moderate protein abundance level in the PWR-1E cell line (N = 4), with a 30-35 kDa UT-B1 signal/protein. Experiments were then carried out to assess if urea treatment could regulate UT-B abundance in the PWR-1E cell line, however, no significant changes were observed with either 24 or 48 hour exposure to 5mM urea (NS, N = 4, unpaired T-test). This disparity between the cell lines emphasises potential differences in cellular pathways governing protein synthesis and confirmed variances between UT-B1 protein abundance in 'normal' and cancerous prostate. Elucidating the intricate mechanisms governing UT-B abundance and its functional implications within prostate cells holds promise for advancing our understanding of prostate physiology and pathology.

KEYWORDS

Urea; UT-B transporter; protein

PCA036

Pathophysiological mechanisms of afatinib-induced epithelial barrier disruption in human colonoid models

Chatchai Muanprasat², Saravut Satitsri¹, Nichakorn Worakajit¹

¹*Faculty of Medicine, Ramathibodi Hospital, Mahidol University, Bangkok, Thailand,* ²*Faculty of Medicine Ramathibodi Hospital, Mahidol University, Bangkok, Thailand*

As a severe adverse effects of afatinib, a tyrosine kinase inhibitor (TKI), diarrheas lead to mortality and morbidity in cancer patients. This study was designed to investigate the effect of afatinib on intestinal epithelial barrier integrity using a human colonoid model. Afatinib at 0.5 μ M significantly decreased the transepithelial electrical resistance (TEER) in human colonoids (Mean \pm S.D.= 100 \pm 12.2% vs 32 \pm 5.4%; p -value = 0.0003, n =5, one-way ANOVA followed by Tukey test). Delocalization of zonular occluding-1 (ZO-1) and a decrease in mRNA and protein expression of claudin-4 and ZO-1 were observed in the afatinib-treated human colonoids (n =5). Nuclear translocation of nuclear factor kappa B (NF- κ B) and mRNA expression of tumor necrosis factor (TNF)-alpha and inducible nitric oxide synthase (iNOS) were also found after afatinib treatment (n =5). Importantly, mRNA and protein expression of myosin light chain (MLC) kinase (MLCK) and MLC phosphorylation, a known inducer of intestinal epithelial barrier disruption, were observed (n =5). Treatment with iNOS inhibitor or MLCK inhibitor suppressed the effect of afatinib on TEER (Mean \pm S.D. = 22 \pm 1.2 % vs 36 \pm 3.5 % relative to non-treated group, p -value = 0.004, n = 5, one-way ANOVA followed by Tukey test). Collectively, our results indicate that afatinib induces intestinal epithelial barrier dysfunction via NF- κ B-iNOS-MLCK-dependent mechanisms. These findings provide insight into pathophysiology of afatinib-induced diarrheas.

PCA037

A Reporter System to Study Adipocyte-Derived Extracellular Vesicles in vivo

Didde Riisager Hansen¹

¹*Institute of Molecular Medicine, Odense, Denmark*

Introduction

Adipocytes secrete extracellular vesicles (EVs), but how they affect whole-body metabolism remains unexplored. This is due to technical limitations of tracking and isolating adipocyte-derived EVs *in vivo*¹. To address this, we have developed two Cre-dependent EV reporter mouse models: 1) The EGFP-EV reporter that labels EVs by CD9 fused to enhanced green fluorescent protein (EGFP), and 2) The NanoLuc-EV reporter labeling EVs by CD63 fused to Nanoluciferase (NanoLuc) and hemagglutinin (HA). We hypothesized that viral delivery of adiponectin-driven Cre to CD9-EGFP mice induces adipocyte-specific expression of EGFP. We also hypothesized that viral delivery of CD63-NanoLuc-HA to adiponectin-Cre mice induces adipocyte-specific expression of NanoLuc, creating a more sensitive reporter system.

Methods

To obtain our EGFP-EV reporter, we designed an adeno-associated viral (AAV) vector with adiponectin-driven Cre. CD9-EGFP mice (*Mus musculus*) were intraperitoneally injected with varying doses of AAV9 (5×10^{10} , 5×10^{11} , and 1×10^{12} viral genomes) to determine the optimal dose for efficient AAV delivery.

To obtain our NanoLuc-EV reporter, we designed an AAV vector harboring a CD63-NanoLuc-HA construct. As a control, we included a vector with an IgK signal peptide-NanoLuc-HA construct. Both vectors were packed in AAV9 capsid, and adiponectin-Cre mice (*Mus musculus*) were given a dose of 5×10^{11} viral genomes by intraperitoneal injection.

After two weeks, mice were humanly sacrificed by terminal anesthesia (10 mg/kg xylazine, 50 mg/kg ketamine).

Organs such as adipose tissues and liver, and plasma were harvested and evaluated for adipocyte-specific expression of CD9-EGFP or NanoLuc and HA by western blotting and luciferase assays.

Results

For the EGFP-EV reporter, CD9-EGFP was not detected in non-adipose tissues (n=20) or non-AAV-treated CD9-EGFP mice (n=4). CD9-EGFP expression in tissues was robust using a dose of at least 5×10^{11} viral genomes and was detected in brown adipose tissue (BAT) (n=16) and in white adipose tissue (WAT), including inguinal WAT (n=16), epididymal WAT (n=18) and mesenteric WAT (n=7). Unfortunately, CD9-EGFP was not detected in plasma (n=15). For the NanoLuc-EV reporter, a dose of 5×10^{11} viral genomes was tested. The HA-tag was not detected by western blotting of tissue homogenates (n=1). NanoLuc activity was detected in plasma (n=1) and tissues (n=1), with highest levels in liver, mesenteric and epididymal WAT. For control AAV, the NanoLuc levels were higher across tissues compared to the NanoLuc-EV reporter, having the highest levels in epididymal WAT, BAT, and plasma (n=1).

Conclusion

To obtain a proper adipocyte-specific EV reporter mouse model, the reporter system needs to be

sensitive enough to track circulating EVs. Using NanoLuc as a reporter instead of EGFP seems crucial in this context. The control AAV, reflecting normal cellular release, serves well as a baseline for comparison. Intriguingly, the highest NanoLuc levels were observed in the liver of the NanoLuc-EV reporter. This raises questions about the interplay between adipose tissue and the liver, and whether hepatocytes take up adipocyte-derived EVs. In conclusion, our NanoLuc-EV reporter enables adipocyte-specific Cre-dependent EV labeling, providing a tool to study adipocyte-derived EVs *in vivo* to unveil their role in normal physiology and during metabolic disturbances.

1. Welsh JA et al. (2024). J Extracell Vesicles, 13(2), e12404.

PCA038

Ubiquitylation of K890 in the thiazide sensitive sodium chloride cotransporter NCC is important for potassium-induced degradation of NCC

Lena Rosenbaek¹, Eric Delpire², Olivier Staub³, Robert Fenton¹

¹*Department of Biomedicine, Aarhus University, Aarhus, Denmark,* ²*Department of Anesthesiology, Vanderbilt University Medical Center, Nashville, United States,* ³*Department of Biomedical Sciences, University of Lausanne, Lausanne, Switzerland*

Background: Dietary potassium intake inversely associates with blood pressure, with low dietary potassium intake increasing blood pressure and a high dietary potassium intake often resulting in a lower blood pressure (1). NCC phosphorylation (pseudo-marker of activity) and abundance are lower during higher dietary potassium intake, with the lower total NCC levels linked to greater ubiquitin-dependent NCC degradation (2). We have previously found that ubiquitylation of K890 in mouse NCC is important for modulation of NCC function *in vitro* (3). The aim of this study was to investigate the role of K890 ubiquitylation in the potassium-induced reduction of NCC *in vivo*.

Methods: A novel mouse model with a K890R mutation in NCC was generated using CRISPR/Cas9 technology. Male and female K890R and wildtype (wt) mice were fed a control (2% KCl, 0.74% NaCl) or high potassium (10% KCl, 0.74% NaCl) diet for 4 days after which their blood pressure was measured using tail cuff plethysmography and their kidney function assessed by balance studies in metabolic cages. After euthanasia, kidneys were collected and levels of NCC were examined by western blotting. *Ex vivo* kidney tubule suspensions from K890R and wt mice were incubated in control (4.2 mM KCl) or high potassium (8.0 mM KCl) media for 24 h and levels of NCC examined by western blotting.

Results: No significant differences in systolic blood pressure were apparent in male or female K890R and wt mice fed control or high potassium diets (males n=5-16, females n=5-8). No significant differences were observed in plasma potassium, chloride, or sodium levels, nor their urinary excretion rates, between genotypes fed either diet. On control diet, no differences between genotypes were detected in NCC or phosphorylated NCC abundances. In both male and female wt and K890R mice, high dietary potassium intake decreased total and phosphorylated NCC levels. In male K890R mice, the decrease of total NCC was greater than in wt mice, whereas phosphorylated NCC levels did not decrease to the same extent in female K890R mice relative to wt mice. Incubation of tubule suspensions from male or female wt mice in high potassium media significantly decreased total and phosphorylated NCC abundances. Similar reductions in total NCC (male and female) and phosphorylated NCC (females) were not detected in tubules from K890R mice.

Conclusion: These preliminary data suggest that ubiquitylation of NCC at K890, particularly in females, plays a role in the potassium-induced degradation of NCC. Further studies are required to clarify the role of K890 NCC ubiquitylation in potassium balance or blood pressure, and whether compensatory mechanisms exist in the K890R mice.

1. Poulsen, S. B., and Fenton, R. A. (2019) K(+) and the renin-angiotensin-aldosterone system: new insights into their role in blood pressure control and hypertension treatment *The Journal of physiology* 597, 4451-4464 10.1113/JP276844
2. Kortenoeven, M. L. A., Esteva-Font, C., Dimke, H., Poulsen, S. B., Murali, S. K., and Fenton, R. A. (2021) High dietary potassium causes ubiquitin-dependent degradation of the kidney sodium-chloride cotransporter *The Journal of biological chemistry* 297, 100915 10.1016/j.jbc.2021.100915
3. Rosenbaek, L. L., Rizzo, F., Wu, Q., Rojas-Vega, L., Gamba, G., MacAulay, N. et al. (2017) The thiazide sensitive sodium chloride co-transporter NCC is modulated by site-specific ubiquitylation *Sci Rep* 7, 12981 10.1038/s41598-017-12819-0

PCA039

A pilot study on the role of potassium ion channel TRESK, in maintaining joint homeostasis in aged mice.

Annalise Bains¹, Humaira Ahmed¹, Oludayo Adeyemi¹, Joycelyn Boateng¹, Melisa Ceritli¹, Egezona Hyseni¹, Oluferanmi Oni¹, Sadaf Ashraf¹

¹*Medway School of Pharmacy, Universities of Kent and Greenwich, Chatham, United Kingdom*

Background: Potassium ion channels are implicated in aged-associated osteoarthritis and joint pain. The two-pore-domain potassium ion channel, TRESK, regulates neuronal excitability and governs resting cellular membrane potential. However, little is known about the role of TRESK in maintaining knee joint homeostasis. In a rat model of cancer-induced bone pain, over expression of TRESK, attenuated the bone pain [1]. Osteoarthritis affects all joint tissues, including the cartilage and subchondral bone, leading to joint pain. Bone sclerosis and cartilage calcification are key histopathological features of osteoarthritis. Chondrocytes, the main cell type in the cartilage, undergo a phenotypic shift, increasing calcification of the cartilage. Peripheral nerves can regulate bone remodelling, accelerating subchondral bone sclerosis.

Purpose: The aim of this pilot study was to determine whether TRESK influences joint homeostasis in aged-mice through regulating cartilage and bone health.

Methods: Paraffin-embedded, knee joint sections of aged (2 years and 6 months approximately) TRESK knockout (n=4) and wild-type control (n=3) C57BL/6 male mice were sectioned at 5µm thickness and at least 4 sections per knee joint were analysed for histopathological changes, by observers blinded to the groups. Thickness of the subchondral bone was analysed on haematoxylin and eosin stained sections. Osterix is a transcriptional factor which is expressed by osteoblasts (bone forming cells). Osterix-immunohistochemistry was performed to assess whether chondrocytes were adopting osteoblast-like phenotype. Trabecular bone area within the subchondral bone region and osterix-positive chondrocytes in the cartilage were quantified using Image-J (Fiji) software. Univariate comparisons were made using student's T-test. A two- tailed $P < 0.05$ was taken to indicate statistical significance. Data is shown as mean \pm standard deviation.

Ethical Considerations: All procedures complied with the UK Animals (Scientific Procedures) Act of 1986 and were performed under a UK Home Office Project Licence in accordance with the University of Kent Policy on the use of Animals in Scientific Research and the ARRIVE guidelines.

Results: Knee-joints of aged wildtype control mice showed osteoarthritis-like changes, these included cartilage damage and subchondral bone remodelling. Aged TRESK-knockout mice had thicker trabecular bone measured as percentage of trabecular bone within the subchondral bone region compared to wildtype control mice (knockout: $45\% \pm 4.5$, wildtype: $37\% \pm 2.5$, $p=0.04$). Increased percentage of osterix-positive chondrocytes were observed in the cartilage of TRESK-knockout ($62\% \pm 2.5$) compared to wildtype control ($46\% \pm 8.9$) mice, although this difference did not reach significance ($p=0.08$).

Conclusion: This proof-of-concept study highlights that TRESK is indeed an important ion channel that regulates joint homeostasis through maintaining cartilage and bone health. Loss of TRESK can exacerbate age-associated osteoarthritis-like changes observed in mice knee joints. Further studies are needed to elucidate its role in osteoarthritis and joint pain.

References: 1. Liu JP et al. Contribution of TRESK two-pore domain potassium channel to bone cancer-induced spontaneous pain and evoked cutaneous pain in rats (2021). *Molecular Pain*. 17:1-18

PCA041

Carotid and brachial artery changes after 12 weeks of upper-body rowing exercise in spinal cord-injured humans

Rasmus Kopp Hansen^{1,3}, Rasmus Bering¹, Afshin Samani¹, Ryan Godsk Larsen¹

¹ExerciseTech, Department of Health Science and Technology, Aalborg University, Aalborg, Denmark, ²Department of Research and Development, University College of Northern Jutland., Aalborg, Denmark, ³Respiratory and Critical Care Group, Department of Health Science and Technology, Aalborg, Denmark

Introduction: A spinal cord injury (SCI) results in deconditioning of the cardiovascular system, including changes in both vascular function and structure (1), leading to an elevated risk of cardiovascular diseases (2). While exercise training (arms-only) for persons with SCI has been shown to increase the diameter of the peripheral conduit artery feeding the active limb, little is known about the effects of arm exercise on central artery diameter and wall thickness. Our main hypothesis was that peripheral, but not central, conduit artery diameter would be increased following 12 weeks of upper-body rowing exercise (UBROW) in SCI individuals.

Methods: Seventeen male and female adults with chronic (>1 yr) motor-complete and incomplete SCI (level of injury: C4-L3) were randomized to control (CON, n=9) or exercise (UBROW, n=8). Participants in UBROW performed 12 weeks of 3 weekly sessions of 30-min moderate-to-vigorous-intensity rowing (arms-only) on an ergometer adapted to wheelchair users. In supine resting position, common carotid artery (CCA) and brachial artery (BA) lumen diameters (M-line to M-line) were determined using high-resolution ultrasound at baseline, after 6 weeks (6W), and after the intervention (12W). CCA wall thickness was measured by near and far-wall carotid intima-media thickness (CIMT). Recordings of resting arterial diameters and CIMT were analyzed off-line frame-by-frame using semi-automated edge-detecting and wall-tracking software. Intra-observer coefficient of variation for CIMT and CCA diameter analyses was 1.6% and 0.95%, respectively. Linear mixed-effects model was used to determine main effects of group and time, and their interaction, with Holm-Sidak Post hoc tests in case of significant interaction effects.

Results: For BA diameter, there was a group-by-time interaction ($P=0.016$). UBROW increased BA diameter from baseline (4.80 ± 0.72 mm) to 12W (5.08 ± 0.91 mm; $P<0.01$), with no changes at 6W (4.96 ± 0.91 mm), and no changes in CON.

For CCA diameter, there was no interaction ($P=0.478$) or main effects of time or group ($P \geq 0.102$). For CIMT near-wall, there was no interaction ($P=0.72$) or main effects of time or group ($P \geq 0.43$). UBROW vs. CON: Baseline (0.69 mm vs. 0.73 mm); 6-week (0.70 mm vs. 0.72 mm); and 12-week (0.71 mm vs. 0.71 mm). For CIMT far-wall, there was a main effect of group ($P \geq 0.02$) but no interaction ($P=0.06$). UBROW vs. CON: Baseline (0.56 mm vs. 0.65 mm); 6-week (0.59 mm vs. 0.61 mm); and 12-week (0.55 mm vs. 0.60 mm).

Conclusions: 12 weeks of arms-only rowing significantly increased peripheral conduit artery diameter (BA) but did not change central artery diameter (CCA) or wall thickness (CIMT) in individuals with SCI. These results demonstrate localized, but not systemic, arterial adaptations in response to 12 weeks of arm exercise. While structural enlargement of the BA seems likely, it is

possible that changes in sympathetic nervous system activity may have influenced BA resting diameter. Further research is needed to fully understand the underlying mechanism for the exercise-induced enlargement in peripheral arterial diameter and the possible influence of this adaptation on cardiovascular disease risk.

1) West CR et al. (2013). Spinal Cord 51, 10-19. 2) Cragg JJ et al. (2013). Neurology 81, 723-728.

PCA042

An investigation of the acute effects of dance on heart rate variability in patients with Parkinson's disease

Jaspreet Kaur¹, Sophia Hulbert², Ruth Way³, Mirza Subhan⁴

¹UCLan School of Medicine & Dentistry, Preston, United Kingdom, ²School of Health Professions, Faculty of Health, University of Plymouth,, Plymouth, United Kingdom, ³School of School of Art, Design and Architecture, Faculty of Arts, Humanities and Business, University of Plymouth, Plymouth, United Kingdom, ⁴School of Biomedical Sciences, University of Plymouth, Plymouth, United Kingdom

Parkinson's is a neurodegenerative movement disorder that has no cure. The most common motor symptoms observed are postural instability, rigidity, and bradykinesia. The role of therapies is well documented, however, there is now substantial evidence to support the use of alternative therapies to alter the progression of Parkinson's. Dance has shown improvements in mobility and balance. There is limited research currently available that investigates cardiovascular autonomic dysfunction in people with Parkinson's (PwP), especially in a dance community setting. Therefore, HRV could be used as a non-invasive marker during dance to detect autonomic dysfunction in PwP in its early stages and assess any autonomic benefits of dance. The main aim of this study was to investigate the effects of dance on heart rate variability in patients with Parkinson's.

Ten PwP were recruited from a Parkinson's dance class, situated at Pavilion Dance Southwest, Bournemouth with written informed consent. The study was approved by the Faculty of Health Research Ethics and Integrity Committee and procedures were in accordance with the Declaration of Helsinki. Inclusion criteria was mild-moderate Parkinson's diagnosis for more than 6 months. Exclusion criteria was previous surgeries that could alter their physiological response to dance. The classes took place once weekly for 90 minutes and consisted of the following sections in chronological order: rest 1, teach 1, dance 1, teach 2, dance 2 and rest 2. The first half was danced sitting while the latter half was standing. Wireless physiological monitoring measurements including breathing rate (BR), skin temperature and heart rate variability (HRV) were taken before, during and after the dance classes using LabChart software. HRV was assessed using time domain (heart rate - HR, standard deviation of the RR interval – SDRR, SD1 and SD2) and frequency domain (low and high frequency - LF and HF). Data was also normalised by considering the heart rate [1], prefixed by n. The results were statistically analysed in SPSS by repeated measures ANOVA. $p < 0.05$ was considered as significant.

Analysing all six sections together showed skin temperature ($p=0.00001$), HR ($p=0.029$), SD1 ($p=0.025$), nSDRR ($p=0.028$), and BR ($p=0.001$) were significantly different across all sections. LH and HF showed no significant difference.

The main finding of our study was that significant changes in HR, SD1, nSDRR, BR and skin temperature of PwP occurred during all six sections. Furthermore, it was noted that HR and HRV frequency domain variables altered, albeit non-significantly, for both the sitting and standing sections, with similar patterns, demonstrating internal consistency throughout dance classes. Our data showed dance improved autonomic function. However further work examining the long-term effects of HRV in a community setting with diverse groups is needed to fully understand the potential benefits of Parkinson's dance.

References Sacha J (2014). *Ann Noninvasive Electrocardiol* 19, 207-16

PCA043

How is regular swimming affecting micro- and macro-vascular physiology in older adults? The ACELA-II study findings.

Alexandros Mitropoulos¹, Markos Klonizakis¹

¹*Lifestyle, Exercise and Nutrition Improvement (LENI) Research Group, Sheffield Hallam University, Sheffield, United Kingdom*

Background: Cardiovascular disease (CVD) remains the number one death cause in the Western world, affecting also severely the quality of life (QoL) of those affected. Older people are of particular interest, as cardiovascular (CV) ageing affects pathophysiological pathways, which are also implicated in CVD development. Water-based, aerobic exercise such as swimming, may delay CV ageing, and consequently prevent the development of CVD in older adults.

Nevertheless, current literature presents conflicting evidence with some studies showing no improvement in CV parameters, while others suggest a positive effect on the intima-media thickness of carotid arteries, hemodynamic and biochemical markers. ACELA-II aimed to assess the micro- and macro-vascular function in older adults randomised to either regular (e.g., 2-3 times/week) swimming or no intervention for an 8-week period.

Methods: This was a single-centre, pragmatic, two-arm randomized controlled trial conducted in Sheffield, UK. The study was approved by the Ethics Committee of the Faculty of Health and Wellbeing of Sheffield Hallam University (ER5320861). Participants were invited at Sheffield Hallam University for two visits (i.e., baseline and 8-week follow up). Following baseline assessments, participants were randomised to either swimming (n=20) or control (n=17) groups. Assessments consisted of anthropometrics and demographics, smoking and clinical history, as well as micro- and macro-vascular function tests assessed by flow mediated dilation (using ultrasound) and laser Doppler flowmetry (using thermal hyperaemia), respectively. The swimming group followed an 8-week (2-3 sessions/week), self-managed exercise intervention, carried out in local public pools.

Results: Participant characteristics did not present any differences between groups both at baseline (Table 1) and follow up assessments. Following the exercise intervention, the exercise group significantly improved the macrovascular function ($9.8 \pm 4.2\%$, $p < 0.001$) compared to the control group ($4.6 \pm 2.5\%$) as shown in Figure 1. Statistically significant differences were also found between groups comparison for the microvascular function as presented in both raw and the percentages of cutaneous vascular conductance (Table 2).

Conclusions: Regular swimming seems to benefit both the macro- and micro-vascular function in older adults when compared to no exercise (i.e., sedentary lifestyle). Considering that certain vascular parameters did not show a statistically-significant difference, rather a tendency towards improvement for the swimming group, it may be recommended that a longer (i.e., ≥ 12 weeks) intervention may offer great vascular health benefits.

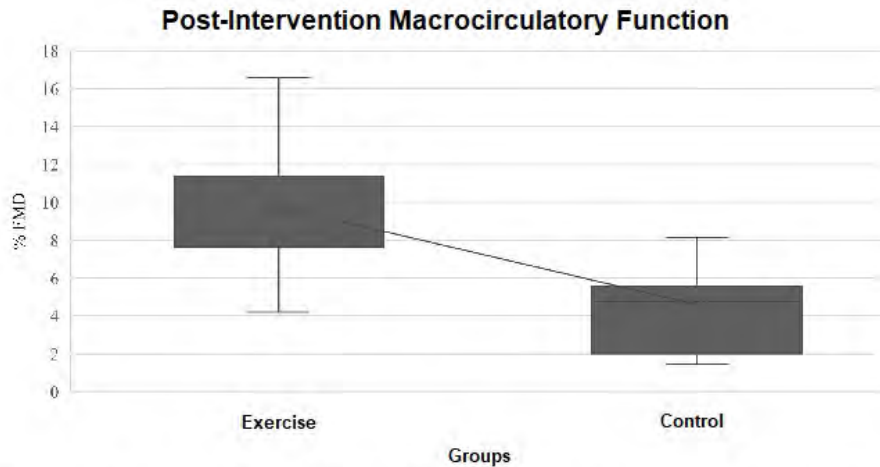


Figure 1. Comparison of brachial artery function post exercise intervention between the exercise and control groups.

Table 2. Between groups comparison of microvascular function pre- and post-intervention.

	Groups			
	Baseline		Follow up	
	Swimming	Control	Swimming	Control
CVC max (%)				
Baseline	8.73 ± 6.5	12.6 ± 9.1	10.7 ± 4.2*	7.9 ± 3.3
Initial peak	68.3 ± 8.7	74.1 ± 17.6	74.4 ± 18.1	66.6 ± 12.6
Plateau	87.3 ± 34.5	84.2 ± 21.0	85.3 ± 10.7	81.2 ± 10.1
RAW CVC (APU/mm Hg)				
Baseline	0.3 ± 0.2	0.4 ± 0.1	0.3 ± 0.1	0.2 ± 0.1
Initial peak	2.3 ± 0.8	2.3 ± 0.7	2.6 ± 0.8	2.2 ± 0.8
Plateau	2.7 ± 0.5	2.7 ± 1.1	3.1 ± 0.9	2.6 ± 1.1
Max	3.2 ± 1.0	3.1 ± 0.8	4.1 ± 0.9**	3.2 ± 1.1

Table 1. Subject characteristics at baseline assessments.

	Swimming (n=20)	Control (n=17)
Age (years)	61 ± 4	62 ± 5
Body mass (kg)	83 ± 15	75 ± 14
Body fat (%)	36.7 ± 9.0	36.2 ± 6.5
BMI (kg m⁻²)	27.7 ± 8.6	27.2 ± 4.2
Waist circumference (cm)	94 ± 15	92 ± 12
Hip circumference (cm)	109 ± 11	104 ± 9
WHR	0.9 ± 0.1	0.9 ± 0.1

Data is presented as means ± SD. BMI, body mass index; WHR, waist to hip ratio.

PCA044

Characterization of an inflammation-driven chronic kidney disease model using human precision-cut kidney slices

Camilla Merrild¹, Gitte Albinus Pedersen¹, Kristian Wiborg Antonsen¹, Sterre Bente Verwoerd¹, Mia Gebauer Madsen², Anna Krarup Keller², Holger Jon Møller¹, Lene Niemann Nejsum¹, Henricus Antonius Maria Mutsaers¹, Rikke Nørregaard¹

¹Department of Clinical Medicine, Aarhus University, Aarhus, Denmark, ²Department of Urology, Aarhus University Hospital, Aarhus, Denmark

Introduction

Chronic Kidney Disease (CKD) represents a substantial global health burden, affecting approximately 10% of the adult population. A major contributor to CKD progression is low-grade inflammation, which promotes fibrosis, leading to gradual loss of kidney function. To date, a need remains for reliable and translational human models of inflammation-driven CKD to enhance our understanding of the mechanisms linking inflammation and fibrosis driving CKD pathogenesis.

Aim

Our objective was to establish a novel model of inflammation-driven CKD using human precision-cut kidney slices (PCKS).

Methods

Human PCKS were prepared from macroscopically healthy kidney tissue obtained from tumor nephrectomies. The PCKS were cultured for 24h or 48h with or without Tumor Necrosis Factor α (TNF α) or Lipopolysaccharide (LPS) stimulation. The inflammatory response in the slices was assessed via qPCR by studying the expression of four different pro-inflammatory genes (*TNF*, *IL1B*, *CCL2*, and *IL6*) and a 42-target cytokine membrane array. Furthermore, the presence of tissue resident macrophages and their activation potential, were investigated using immunofluorescent staining of the macrophage markers: CD68 and CD163, along with ELISA measurements of soluble CD163 (sCD163) – a macrophage activation marker.

Results

Stimulation of the PCKS with TNF α , a key pro-inflammatory mediator, led to a more than 2.5-fold increase in the gene expression of *TNF*, *IL1B*, *CCL2*, and *IL6* compared with the 24h and 48h control (n=10, p<0.01 shown by a Wilcoxon signed rank test). In addition, the cytokine membrane array revealed that 17 out of the 42 targets could be detected in the culture media from the slices. The levels of these cytokines and chemokines varied depending on the incubation time and presence of TNF α stimulation.

Moreover, using immunofluorescence we observed clear staining of CD68+ and CD163+ cells in the tissue, indicating the presence of tissue resident macrophages in the PCKS model. As a

measure for macrophage activation, we detected a 1.5-fold increase in the amount of sCD163 in the culture media after 24h of stimulation with LPS, known to mediate CD163 shedding and macrophage activation, compared to the 24h control (n=4, $p < 0.05$ shown by a Mann-Whitney test). There was no significant change in sCD163 levels after TNF α stimulation.

Conclusion

In conclusion, this study presents a novel human model for investigating inflammation-driven CKD, paving the way for an improved understanding of the complex CKD pathophysiology. Furthermore, the PCKS model holds potential as a future platform for the screening of anti-inflammatory CKD therapeutics.

PCA046

Differences in Physiological Responses to submaximal graded exercise and its recovery in Adults With and Without Type 1 Diabetes

Ivana Potočnik², Eva Gabrovšek¹, Nejka Potočnik²

¹Department of Physiotherapy, Faculty of Health Sciences, University of Ljubljana, Ljubljana, Slovenia, ²Institute of Physiology, Medical Faculty, University of Ljubljana, Ljubljana, Slovenia

Introduction: Physical activity is an important part of the management of type 1 diabetes (T1D) and reduces the risk of associated complications. Many people with T1D exercise regularly. For safe exercise in T1D, in addition to glycemic control, it is important to recognise the differences in physiological response to exercise compared to healthy peers. **Aim:** We aimed to determine the changes in cardiovascular, respiratory and metabolic parameters in response to short-term submaximal exercise (SGSE) in recreational athletes with T1D compared to age- and sex-matched healthy controls. **Methods:** Eighteen recreational athletes, 9 per group, performed SGSE in the form of graded cycling on a cycloergometer until 85% of the maximal heart rate was reached, with 20 minutes recovery in a seated position. Cardiovascular (heart rate, mean arterial blood pressure (MAP)), respiratory (respiratory rate, ventilation) and metabolic (oxygen consumption, exhaled CO₂ (VCO₂)) parameters were measured non-invasively and averaged at three minutes before, one minute at the end and three minutes in recovery to SGSE. Cutaneous blood flow was measured using the laser Doppler method in the recovery phase after SGSE. Heart rate variability (HRV), heart rate recovery 30 and 60 seconds at the end of exercise, acral and forearm cutaneous vascular conductance (lnCVC), ventilatory equivalent for oxygen and carbon dioxide (VE/VCO₂), respiratory quotient and the slope of oxygen uptake efficiency (OUES) were calculated. Normality was tested using the Shapiro-Wilk test. Data before, at peak power and after SGSE were compared for differences over time and between groups using a two-way ANOVA for repeated measures with Sidak adjustment for multiple comparisons. Independent samples t-test was used to determine differences between groups. **Results:** The expected temporal dynamics during exercise and its recovery were comparable in both groups for all measured parameters except MAP. The effect of exercise on MAP varied between groups: at peak exercise, MAP was significantly higher in the T1D group than in the control group (146.7±8.6mmHg in T1D; 129.8±11.2mmHg in controls; p=0.002). There was a significant main effect of the group on VE/VCO₂. At peak exercise and in the recovery, VE/VCO₂ was significantly lower in T1D compared to control group (25.7±2.4 in T1D; 30.5±4.7 in controls; p=0.016 at peak exercise and 34.6±2.5 in T1D; 41±4.3 in controls; p=0.001 in the recovery phase). In addition, higher OUES (3833.8±1133.1 in T1D; 2761.0±576.4 in healthy subjects; p=0.0396) and lower forearm lnCVC (-2.4±0.4 in T1D; -1.1±1.2 in healthy subjects; p=0.009) were observed in T1D compared to controls. **Discussion and conclusion:** The response of recreational athletes with T1D to SGSE differed from healthy subjects primarily in MAP and ventilatory response, which may be attributed to the differences in baroreflex and chemoreflex described in T1D compared to healthy participants. Cutaneous forearm blood flow after exercise is decreased in T1D compared to control subjects, which confirms the previously described decreased ability to excrete heat in T1D and may be related to differences in autonomic nervous system activity on the vasculature in T1D. Further studies are needed to confirm these conclusions and possibly uncover the mechanisms underlying our findings.

PCA047

**Toward Efficient Musculoskeletal Function Rehabilitation via the use of Artificial Intelligence:
The MSC-AI Project at UoD**

Francesco V. Ferraro¹, Oluwarotimi W. Samuel²

¹*School of Sports and Exercises Science, University of Derby, Derby, United Kingdom*, ²*School of Computing, University of Derby, Derby, United Kingdom*

Introduction Conventional methods for analysing MSK characteristics of healthy individuals and pathological patients are limited by their inaccuracies and confounding factors that preclude proper assessment and treatment strategies. However, the recent research progress in the field of Artificial intelligence (AI) has re-iterated possibilities in healthcare applications (Rajpurkar et al., 2022; Volpp & Mohta, 2016), particularly in the domain of musculoskeletal (MSK) rehabilitation. Based on the current state of literature, this study proposes an AI-based approach for analysing MSK characteristics to provide accurate and robust assessment outcomes that will inform adequate and real-time therapeutic intervention for common MSK conditions. **Aim** This initiative is aimed at addressing the critical need for evidence-based practices and improved treatment outcomes, which are currently lacking in Sports Therapy and Rehabilitation (STR). **Ethical Considerations** While acknowledging ethical considerations raised by Kiani et al. (2020), the project will adhere to standardised protocols established by SPIRIT and CONSORT for rigorous evaluation of medical AI applications. The project would employ a collaborative effort between the University of Derby's AI research team and the STR clinics toward leveraging AI to enhance MSK assessment and treatment strategies. **Objectives** Additional expected contributions of the project include (a) the provision of an AI-powered platform that enables STR students to analyse various MSK conditions and make informed decisions, (b) the provisioning of real-world clinical datasets that can aid the advancement of research and development in the field of MSK analysis for researchers at the University and beyond. **Methods** The research team will initially create a database with anonymised pictures and no-personal information collected from the STR clinic; these will then be processed by AI, which will identify the MSK condition and provide the best treatments. The AI will be coded using objective-oriented program language. All code and user information are stored in server-secured databases, not in clouds (e.g., Github), to prevent data leaks. Additionally, to compare and test the validity of AI, the STR practitioner will complete a full parallel screening, and the results between AI and STR experts will be compared to report the level of agreement and accuracy of the results. **Conclusion** This proposed project has the potential to make significant contributions to the burgeoning field of AI-powered MSK rehabilitation. By developing a robust AI framework within the STR clinics, we can enhance the students' learning experience, promote evidence-based practices, and improve patient outcomes. This initiative aligns with our research commitment to cutting-edge projects and dedication to providing students with the skills and knowledge necessary to excel in a rapidly evolving healthcare landscape. The project (titled MSC-AI) has recently applied for funding, and the methodological approach will be discussed at the conference.

References Commins, J. (2010). Nurses say distractions cut bedside time by 25%. *Health Leaders*. Davenport, T., & Kalakota, R. (2019). The potential for artificial intelligence in healthcare. *Future healthcare journal*, 6(2), 94. Kiani, A., Uyumazturk, B., Rajpurkar, P., Wang, A., Gao, R., Jones, E., Yu, Y., Langlotz, C. P., Ball, R. L., & Montine, T. J. (2020). Impact of a deep learning assistant on the

histopathologic classification of liver cancer. NPJ digital medicine, 3(1), 23. Rajpurkar, P., Chen, E., Banerjee, O., & Topol, E. J. (2022). AI in health and medicine. Nature medicine, 28(1), 31-38. Volpp, K. G., & Mohta, N. S. (2016). Patient engagement survey: improved engagement leads to better outcomes, but better tools are needed. NEJM Catalyst, 2(3).

PCA048

The venoarteriolar reflex decreases skin flowmotion entropy

Henrique Silva^{1,2,3}, Carlota Rezendes²

¹Research Institute for Medicines (iMed.Ulisboa), Faculdade de Farmácia, Universidade de Lisboa, Av. Prof. Gama Pinto, 1649-003, Lisbon, Portugal, ²Department of Pharmacy, Pharmacology and Health Technologies, Faculdade de Farmácia, Universidade de Lisboa, Av. Prof. Gama Pinto, 1649-003, Lisbon, Portugal, ³Biophysics and Biomedical Engineering Institute (IBEB), Faculdade de Ciências, Universidade de Lisboa, Campo Grande, 1749-016, Lisbon, Portugal

The robustness of a given physiological effector can be assessed by exploring the complexity profile of the biological signals it generates. The complexity of a signal is typically assessed as “entropy”, a general measure of disorganization. Higher complexity level reflects a higher robustness of the respective physiological effector, i.e., a higher adaptation capability to changing internal and external conditions. Recent publications have reported that physiological signals from subjects in pathological and prepathological states show lower entropy than in healthy subjects. On an experimental level, provocation maneuvers (e.g. postural changes, limb occlusion, drug administration, etc.) that challenge certain physiological effectors are also able to highlight their robustness, even in healthy subjects. Our objective was to assess the robustness of the physiological effectors of skin perfusion during a classic maneuver to evoke the venoarteriolar reflex (VAR). Fifteen healthy subjects (22.4 ± 5.2 y.o.) participated in this study after giving informed consent. After acclimatization, subjects performed a protocol to evoke VAR on the upper limb while sitting upright – 7 min resting with both arms at heart level (phase I), 5 min with one random arm (i.e., test limb) placed 40 cm below heart level (VAR, phase II) and 7 min recovery in the initial position (phase III). Skin blood flow was assessed in the index finger of both limbs with photoplethysmography (PPG). Raw PPG signals were then decomposed into their respective spectral components (cardiac, respiratory, myogenic, sympathetic, endothelial NO-dependent and endothelial NO-independent) with the wavelet transform. Finally, the complexity index of the raw PPG signal and of its components was calculated using the multiscale entropy analysis (MSE) algorithm. The Wilcoxon signed rank test was used to compare skin blood flow and complexity index between the different phases of the protocol ($p < 0.05$). As expected, VAR induced a significant bilateral decrease in skin blood flow, more pronounced in the test limb. Similarly, during VAR the complexity index of the raw PPG signals and their components decreased significantly, again with higher magnitude in the test limb. These results suggest that a decrease in the competence of skin perfusion regulation effectors might be present during VAR, likely related to the magnitude of skin perfusion decrease.

Silva H, Ferreira HA, Rocha C, Monteiro Rodrigues L. Texture Analysis is a Useful Tool to Assess the Complexity Profile of Microcirculatory Blood Flow. *Applied Sciences*. 2020; 10(3):911. <https://doi.org/10.3390/app10030911>

PCA049

Assessing skin perfusion with USB digital microscopy – a pilot study

Henrique Silva^{1,2,3}, Carlota Rezendes²

¹Research Institute for Medicines (iMed.Ulisboa), Faculdade de Farmácia, Universidade de Lisboa, Av. Prof. Gama Pinto, 1649-003, Lisbon, Portugal, ²Department of Pharmacy, Pharmacology and Health Technologies, Faculdade de Farmácia, Universidade de Lisboa, Av. Prof. Gama Pinto, 1649-003, Lisbon, Portugal, ³Biophysics and Biomedical Engineering Institute (IBEB), Faculdade de Ciências, Universidade de Lisboa, Campo Grande, 1749-016, Lisbon, Portugal

Assessment of skin microcirculation can be noninvasively assessed with many different technologies, including laser Doppler flowmetry and imaging, photoplethysmography and capillaroscopy, among others. Capillaroscopy is an imaging technique employed for observation of skin microvasculature at nail cuticle level, particularly for the detection of the morphological abnormalities that accompany several diseases, including connective tissue diseases. In recent years several publications have demonstrated that universal serial bus (USB) digital microscopes provide high quality images with comparable diagnostic sensitivity to conventional devices at a lower cost. However, few studies have tested the usefulness of USB digital microscopes to assess skin perfusion in vivo. This pilot study aimed at assessing skin perfusion in healthy subjects during a classic upper limb occlusion maneuver to evoke reactive hyperemia using a USB digital microscope. Seven healthy subjects (21.2 ± 3.4 y.o.) participated in this study after giving informed consent. After acclimatization, subjects performed a standard suprasystolic limb occlusion (SLO) protocol in a random upper limb while sitting upright, as follows: 5 min resting with both arms at heart level (phase I), 3 min occlusion (200 mmHg, phase II) with a tourniquet cuff and 5 min recovery (phase III). The nailfold capillaries of the fourth finger were continuously visualized with a USB digital microscope throughout the protocol. Each video recording was decomposed into its individual frames and several regions of interest (ROI) were selected. For each ROI several image texture parameters were calculated (entropy, contrast, correlation, energy, homogeneity). Skin blood flow was quantified in the pulp of the second finger with photoplethysmography. These parameters were compared between the different phases of the protocol with the Wilcoxon test for related samples ($p < 0.05$). As expected, skin blood flow decreased significantly during occlusion and increased significantly upon release of the cuff. Most texture parameters also changed significantly in both phases of the protocol, although with opposite trends and with different magnitudes. These results suggest that skin perfusion could be easily assessed with low-cost USB digital microscopes, although further studies are needed to compare its performance with other optical technologies.

Chanprapaph K, Fakprapai W, Limtong P and Suchonwanit P (2021) Nailfold Capillaroscopy With USB Digital Microscopy in Connective Tissue Diseases: A Comparative Study of 245 Patients and Healthy Controls. *Front. Med.* 8:683900. doi: 10.3389/fmed.2021.683900

PCA050

Evaluating the suitability of precision-cut tissue slices to study bile acid-induced nephrotoxicity

Rianne van Dekken¹

¹*Aarhus University, Aarhus, Denmark*

Evaluating the suitability of precision-cut tissue slices to study bile acid-induced nephrotoxicity

Rianne van Dekken, Sandra M. Hansen, Rikke Nørregaard and Henricus A.M. Mutsaers

Department of Clinical Medicine, Aarhus University

Background: Chronic kidney disease (CKD) is characterized by progressive damage to the kidneys, leading to a gradual decline in kidney function over time. In 2017, 1.2 million deaths were caused by CKD, which is expected to rise to 2.2-4.0 million deaths by 2040. Currently, dialysis and kidney transplantation are the only treatment options for patients with end-stage renal disease, emphasizing the need for novel treatments. Recent studies suggest that elevated bile acid levels in the blood are a risk factor for CKD; however, the exact pathophysiological mechanism remains unclear. This study will evaluate the suitability of Precision-Cut Kidney Slices (PCKS) to study bile acid-induced nephrotoxicity. The PCKS model is a unique technique in the sense that each slice contains all cell types and components of the kidney in the original configuration, with intact cell-cell and cell-matrix interactions.

Methods: Using the Alabama R&D Tissue Slicer (formerly Krumdieck Tissue Slicer), mice PCKS (mPCKS) were prepared from kidneys harvested from C57BL/6 mice (n=5). Mice were anesthetized with 5% sevoflurane and sacrificed by cervical dislocation. mPCKS were cultured for 24H, 48H, and 72H. Afterwards, the gene expression of various bile acid receptors (FXR, PXR, VDR, CAR, TGR5, and S1PR2) was evaluated using RT-PCR. Gene levels were normalized and compared to the 0H control using one-way ANOVA.

Results: The results demonstrated that all tested bile acid receptors are expressed on gene level in mPCKS. The gene expression of FXR, PXR, VDR, and CAR significantly decreased more than 3,7-fold after 24H (P-value: <0.0011 for all receptors), after which expression levels remained stable up to 72H. The gene expression of TGR5 and S1PR2 significantly increased more than 5-fold after 24H, after which the expression levels increased consistently up to 72H (P-value: <0.0141). In addition, mPCKS remained viable during the whole incubation period, as illustrated by stable ATP levels.

Conclusion: These data indicate that the various components for bile acid signaling are present in mPCKS. Based on this we suggest that mPCKS can be used as a model for bile acid-induced nephrotoxicity.

PCA052

Unveiling the metabolic health landscape: a machine learning exploration of regional adiposity's influence on phenotypic variations among young adults

Shipra Das¹, Manjish Pal², Sanjay Kumar³

¹Bharat Ratna Late Shri Atal Bihari Vajpayee Memorial Medical College, Rajnandgaon, India, ²IIT Kharagpur, Kharagpur, India, ³Sikkim Manipal Institute of Medical Sciences, Gangtok, India

Introduction: Complex interface between adiposity and metabolic health heterogeneity has led to the detection of distinct phenotypes like metabolically healthy obese (MHO) and metabolically unhealthy normal weight (MUNW) individuals. Understanding the association between regional adiposity and metabolic disorder components of different young adult phenotypes is necessary to develop appropriate intervention strategy in early stage.

Aim and objectives: The present study aims to use advanced statistical methods including path analysis, random forest analysis, and support vector machine (SVM) to unwind the association of regional adiposity among MHO, metabolically unhealthy obese (MUO), and MUNW young adult population.

Methodology: On the basis of body mass index (BMI) and cardio-metabolic risk factor 400 young adults aged 18-25 years were categorized into metabolically healthy obese (MHO), metabolically unhealthy obese (MUO), and metabolically unhealthy normal weight (MUNW) groups. Regional adiposity was assessed by using predictive equations for Asian Indians (Goel K et al, 2008). Path analysis was used to explore direct and indirect effects of regional adiposity on metabolic health. Random forest analysis and SVM were employed to predict metabolic health status.

Results: Metabolically Healthy Obese (MHO): Path analysis shown that in the MHO group, Visceral adipose tissue (VAT) had a significant direct effect on metabolic health ($\beta = 0.34$, $p < 0.01$), while Subcutaneous adipose tissue (SAT) showed a weaker direct effect ($\beta = 0.17$, $p < 0.05$). Random forest analysis identified VAT (importance score = 0.41) as the most important predictor of metabolic health in this group, followed by SAT (importance score = 0.27). **Metabolically Unhealthy Obese (MUO):** In the MUO group, both VAT and SAT had significant direct effects on metabolic health (VAT: $\beta = 0.38$, $p < 0.01$; SAT: $\beta = 0.29$, $p < 0.05$). Random forest analysis indicated that VAT (importance score = 0.43) was the most important predictor of metabolic health in this group, followed by SAT (importance score = 0.39). **Metabolically Unhealthy Normal Weight (MUNW):** Path analysis showed that in the MUNW group, VAT had a significant direct effect on metabolic health ($\beta = 0.21$, $p < 0.05$), while SAT show a very weaker direct effect ($\beta = 0.09$, $p < 0.05$). Random forest analysis identified VAT (importance score = 0.39) as the most important predictor of metabolic health in this group.

Conclusion: This research provides important insights into the association between regional adiposity and cardio-metabolic risk factors among young adults across different obesity phenotypes. The results emphasize the differential effects of VAT and SAT on metabolic health in each phenotype, highlighting the significance of personalized approach to obesity management and prevention.

Physiology in Focus 2024

Northumbria University, Newcastle, UK | 2 – 4 July 2024

Keywords: metabolically healthy obese (MHO), metabolically unhealthy normal weight (MUNW), metabolically unhealthy obese (MUO), Visceral adipose tissue (VAT), Subcutaneous adipose tissue (SAT).

PCA053

Correlation of serum levels of nitric oxide metabolites with body mass index and arterial stiffness in young individuals

VIDYA GANJI¹

¹ASSISTANT PROFESSOR, ALL INDIA INSTITUTE OF MEDICAL SCIENCES, BIBINAGAR, HYDERABAD, India

Introduction: Obesity is a multi-factorial disorder defined as abnormally high levels of body fat accumulation. It is a major emerging pandemic of this century which can be attributed to alterations in eating habits, lifestyle choices and rise in sedentary behaviour. The activation of pro-inflammatory signalling pathways linked to obesity can result in vascular endothelial dysfunction and changed levels of Nitric oxide(NO). Hyperlipidaemia may exacerbate arterial stiffness which is a precursor to atherosclerosis. In this study, we tried to evaluate the changes in levels of nitric oxide in obese individuals and its association with arterial stiffness.

Objectives: To identify the association of serum levels of Nitric oxide metabolites with Body Mass Index(BMI) in apparently healthy subjects.

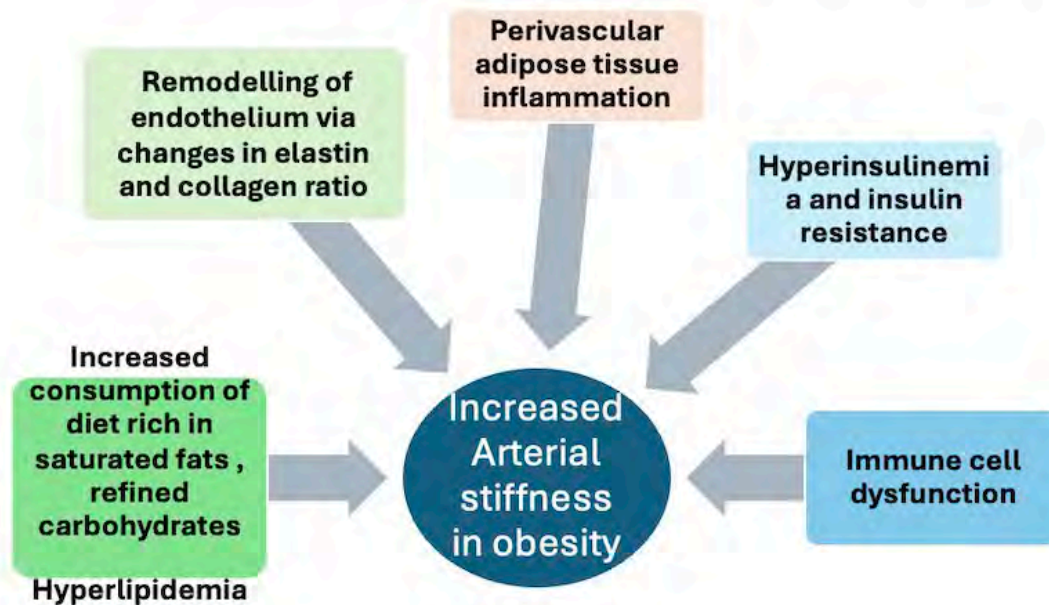
2. To evaluate any correlation between serum nitric oxide metabolites, BMI and arterial stiffness in obese individuals.

Methodology: The study was conducted after obtaining Institutional Ethical committee(IEC) approval on 120 adults in the age group of 20 -40 yrs, non-smokers having sedentary working habits who are apparently healthy. The weight and height of all the study participants were measured according to standard protocols. Body mass index (BMI) was calculated as weight divided by square of height(h²). The subjects were divided into three groups depending on their BMI as follows: **Group I: BMI 18.5 to 22.9 (controls)(n=40), GROUP II: BMI 23 to 29.9 (overweight and pre-obese subjects) (n=40) and Group III: BMI 30 and above (obese subjects) (n=40)(Asian classification of BMI).** Fasting venous blood samples were collected and Serum NOx concentration were measured by the nitrite, nitrate assay kit which determines the levels of NO metabolites (total nitrite and nitrate) using GREISS reaction method and absorbance read at 540nm. Serum lipids and triglycerides were measured using enzymatic colorimetric method with glycerol phosphate oxidase and serum cholesterol levels were estimated using standard kits. **Arterial stiffness** of the participants was measured using an oscillometric non-invasive arteriography for cardiovascular risk assessment.

Result: The results showed a significant increase in systolic blood pressure ($p < 0.001$) and no change in diastolic blood pressure and significant increase in pulse pressure ($p < 0.001$) with increase in visceral adiposity (Waist Circumference) more than BMI. Results of Pearson correlation indicated that there is a significant small negative relationship between BMI and Serum NO levels, ($r = -0.534, p < .001$). There was significant increase in Brachial ankle Pulse Wave Velocity (Ba PWV) ($p = 0.001$) and Carotid Femoral Pulse Wave Velocity (CF PWV) ($p = 0.01$) in obese subjects when compared to controls.

Conclusion: Our study results showed that abdominal obesity more than overall obesity is more strongly associated with decreased serum NO levels and Increased arterial stiffness. In obese individuals, increased arterial stiffness as reflected by increased pulse wave velocity may contribute to predicting cardiovascular disease in both genders in addition to development of hypertension.

Figure 1. The various mechanisms causing increased arterial stiffness in obesity



References: 1. NHMRC. Clinical practice guidelines for the management of overweight and obesity in adults. Treatment. Canberra, ACTNHMRC.2003;81-106. 2. Aroor AR, Jia G, Sowers JR. Cellular mechanisms underlying obesity-induced arterial stiffness. *Am J Physiol Regul Integr Comp Physiol.*2018;314(3):387-398. 3. Miranda K M, Espey MG, Wink DA. A rapid, simple spectrophotometric method for simultaneous detection of nitrate and nitrite. *Nitric oxide.* 2001;5(1):62-71. 4. Raddino R, Caretta G, Teli M, Bonadei I et al: Nitric oxide and cardiovascular risk factors: *Heart Int:*2007;3(1):18. 5. Ghasemi A, Zahediasl S, Azizi F. Elevated Nitric oxide metabolites are associated with obesity in women. *Arch Iran Med.* 2013; 16(9): 521-525. 6. Perreault M, Marette A. Targeted distribution of inducible nitric oxide synthase protects against obesity-linked insulin resistance in muscle. *Nat Med.*2001;7(10):1138-1143. 7. Dallaire P, Marette A. Obesity-linked insulin resistance. Is nitric oxide the missing link? *Can J Diabetes.*2004;28:59-66. 8. Gruber HJ, Mayer C, Mangge H, Fauler G et al. Obesity reduces the bioavailability of nitric oxide in juveniles: *Int J Obesity:* 2008;32(5),826-831. 9. Ahmed N, Adam SI, Nawi AM et al. Abdominal obesity indicators: Waist circumference or waist-to-hip ratio in Malaysian adult population. *Int J Prev Med.* 2016 Jun; 7:82. 10. Fisher E, Brzezinski RY, Ehrenwald M et al. Increase in Body mass

Physiology in Focus 2024

Northumbria University, Newcastle, UK | 2 – 4 July 2024

index and waist circumference predicts development of metabolic syndrome criteria in apparently healthy individuals with 2 and 5 yrs follow up. *Int J Obes.*2019;43(4):800-807.

PCA054

Intergenerational Impact of Parental Zinc Deficiency on Metabolic Outcomes in *Drosophila melanogaster*

Kasimu Ghandi Ibrahim², Kamaldeen Olalekan Sanusi^{3,4}, Murtala Bello Abubakar^{4,5}, Mustapha Umar Imam^{4,6}

¹Department of Human Physiology, Faculty of Health Sciences, Al-Hikmah University, P.M.B. 1601, Ilorin, Nigeria, Sokoto, Nigeria, ²Department of Basic Medical and Dental Sciences, Faculty of Dentistry, Zarqa University, P.O. Box 2000, Zarqa 13110, Jordan, ³Department of Human Physiology, Faculty of Health Sciences, Al-Hikmah University, P.M.B. 1601, Ilorin, Nigeria, ⁴Centre for Advanced Medical Research and Training (CAMRET), Usmanu Danfodiyo University, P.M.B. 2254, Sokoto, Nigeria, ⁵Department of Physiology, College of Medicine and Health Sciences, Sultan Qaboos University, Muscat, Oman, ⁶Department of Medical Biochemistry, Faculty of Basic Medical Sciences, College of Health Sciences, Usmanu Danfodiyo University, P.M.B. 2254, Sokoto, Nigeria

Background

Gene-environment interactions play a crucial role in shaping the health of the offspring, with environmental factors like dietary zinc deficiency exerting significant impacts. Yet, the effect of parental zinc deficiency on the health of the offspring demands a holistic approach beyond solely examining maternal zinc status.

Aim

In this study, we investigated the physiological and molecular basis of both maternal and paternal zinc deficiency on offspring metabolic health, using the *Drosophila melanogaster* model.

Methods

Dietary zinc deficiency was induced in flies by incorporating TPEN (N, N, N', N'-tetrakis (2-pyridylmethyl) ethylenediamine) into their diet, starting from the egg stage through adulthood. Offspring were subsequently raised on standard diets. Following adulthood, parents and offspring were assessed for various parameters after seven days of exposure. Male and female flies (n = 10) were weighed and their locomotion was analysed. After being anaesthetized with ice, haemolymph was extracted and used to measure levels of glucose, trehalose, triglycerides, malondialdehyde, catalase activity, and total antioxidant capacity using commercially available kits. Finally, RNA was extracted, and quantitative real-time PCR (qPCR) was used to assess the mRNA expression of genes involved in zinc transport (*dZIP1*, *dZnT1*, *dZIP71B*, and *dZnT53*), glucose regulation (*DILP2* and *PEPCK*), antioxidant defence (*SOD1* and *CAT*), and inflammatory pathways (*UPD2* and *Eiger*). Data were analysed using two-way ANOVA followed by Bonferroni multiple comparison *post hoc* test and expressed as mean ± standard deviation.

Results

While parental flies exhibited significantly reduced ($p < 0.05$) body weight, both male and female offspring showed increased body weight. Moreover, the offspring manifested disruptions in glucose metabolism, lipid homeostasis, and antioxidant enzyme activity. Gene expression analysis revealed significant ($p < 0.05$) alterations in zinc transport genes, with elevated *dZIP1* mRNA levels in females and increased *dZnT1* mRNA levels in males. Both sexes displayed reduced *dZnT35C* mRNA fold change. Additionally, *DILP2* and the pro-inflammatory markers *Eiger* and *UPD2* mRNA were upregulated.

Conclusion

This study reveals the lasting consequences of paternal zinc deficiency, impacting offspring health and highlighting the need to consider both parents when studying intergenerational health effects. Understanding these mechanisms could lead to preventative strategies against zinc deficiency-related metabolic disorders.

Keywords: Zinc deficiency, intergenerational, *Drosophila melanogaster*, metabolism, zinc transport

Not applicable

PCA056

Wars1 knockdown in hepatocytes regulates whole-body glucose homeostasis

Francesca Pontanari¹

¹EPFL, Lausanne, Switzerland

INTRODUCTION:

Aminoacyl tRNA synthetases (ARSs) are central and indispensable enzymes facilitating protein synthesis by shuttling amino acids to tRNA molecules. The vital importance of ARSs is exemplified by the embryonic lethality resulting from their knockout *in vivo*. We aimed to identify the metabolite transported by SLC25A47, a unique mitochondrial carrier specific to hepatocytes. To achieve this goal, we implemented a commercially available hepatocyte-specific knockout mouse model of *Slc25a47*. Unexpectedly, the genomic recombination of the *Slc25a47* locus, in this mouse model, induces a knockdown of the cytosolic tryptophanyl tRNA synthetase (*Wars1*), found in the same locus (hereafter referred to as the *Slc25a47-Wars1* locus).

METHODS:

To delineate the effects associated with *Wars1*, we employed a co-injection protocol wherein *Slc25a47-Wars1*^{lox/lox} mice were administered AAV8_*Cre* to induce gene locus recombination. Concomitantly, mice were injected with either *Slc25a47* or *Wars1* enabling us to segregate the phenotypic outcomes attributable to *Wars1*. The injected viruses were under the human alpha-1 anti-trypsin promoter, which made the expression hepatocyte-specific. C57BL/6J mice were fed either tryptophan-deficient, methionine-deficient, or amino acid-sufficient diets. Body weight was collected twice per week, and an oral glucose and an insulin tolerance test were performed. Significance was determined using Two-way ANOVA followed by Tukey's post-hoc correction, n=9 mice for the rescue experiment and n=10 mice for the special diet were tested. qPCR analysis of inflammation and fibrosis markers was performed on n=6 mice, and statistical significance was determined using One-way ANOVA followed by Tukey's post-hoc correction.

RESULTS:

The knockdown of *Wars1* in hepatocytes induced a hypermetabolic phenotype, reflected by reduced body weight, improved glucose tolerance, and insulin sensitivity. When we compared these phenotypes with tryptophan-deficient and methionine-deficient feeding, we found that *Wars1* knockdown in hepatocytes was sufficient to recapitulate the whole-body phenotypes of these amino acid-deprived diets. However, the better metabolic health came at a high cost for the liver, as inflammation and fibrosis were observed after *Wars1* knockdown.

CONCLUSIONS:

These findings underscore the significance of amino acid incorporation into protein, particularly within hepatocytes, in governing whole-body homeostasis. Further investigation is warranted to elucidate the central role of hepatocytes and amino acid metabolism in metabolic diseases.

PCA057

The safety and efficacy of free protein diet with ketoacid analogues in chronic kidney disease-affected diabetic rats

Ahmed Taha¹, Ahmed El-Sayed Nour El-Deen¹

¹*Department of Basic Medical and Dental Sciences, Faculty of Dentistry, Zarqa University, Zarqa, Jordan*

Background: Diabetic nephropathy (DN) is a common vascular complication of diabetes mellitus (DM) which needs weight control and caloric restriction, especially for protein. A protein-restricted diet with ketoacids reduces the intake of nitrogen while avoiding the harmful consequences of inadequate dietary protein intake.

Objective: This study examined the safety and effectiveness of a free-protein diet with ketoacid analogues (KAA) in diabetic rats with chronic kidney disease (CKD).

Material and methods: Adult male albino rats (n=60) were induced with diabetes mellitus using streptozotocin and grouped into six *vis*: (1) Control group rats received standard diet (2) Normal rats received low protein diet (3) Diabetic control rats received standard diet (4) Diabetic rats received low protein diet (5) Diabetic rats received α -keto amino acids with low protein diet (6) Diabetic rats received α -keto amino acids with free protein diet. The body weights of the rats were measured weekly, and the urine volume recorded for 24 hours. After 12 weeks of treatment, the rats were euthanized using halothane inhalation. Blood samples were collected via the carotid artery and used to assess blood glucose (mg/dl), insulin (pmol/L), urea (mg/dl), creatinine (mg/dl), total cholesterol (TC) (mg/dl), LDL (mg/dl), HDL (mg/dl), triglycerides (TG) (mg/dl), and albumin (mg/dl) levels were determined. Data were analyzed using a one-way analysis of variance followed by Tukey's *post hoc* test to compare between the groups.

Results: A significant decrease ($p < 0.05$) in blood glucose, serum total cholesterol, LDL, triglycerides, serum urea and creatinine were observed, while insulin level, albumin, GFR, urine volume and HDL were significantly increased ($p > 0.05$) in diabetic rats received α -keto amino acids with free protein diet, without significant changes in body weight.

Conclusion: A free-protein diet containing KAA improves renal function, lowers blood glucose levels, maintains body weight, and does not worsen nutritional status in CKD in diabetic rats over time.

Not applicable

PCA058

An investigation into the impact of functional mutations on the binding of leucine to Sestrin2 in the context of aging and age-related degenerative conditions using structural and molecular simulation approaches

Abbas Khan¹, Muhammad Ammar Zahid¹, Muhammad Shahab², Raed Al-Zoubi³, Mohanad Shkoor⁴, Tarek Benameur⁵, Abdelali Agouni¹

¹Department of Pharmaceutical Sciences, College of Pharmacy, QU Health, Qatar University, Doha, Qatar, ²Department of Chemistry, Beijing University of Chemical Technology (BUCT), Beijing, China, ³Surgical Research Section, Department of Surgery, Hamad Medical Corporation, Doha, Qatar, ⁴Department of Chemistry, College of Arts and Science, Qatar University, Doha, Qatar, ⁵College of Medicine, King Faisal University, PO Box 400, Al-Ahsa, Saudi Arabia

Leucine is the native known ligand of Sestrin2 (Sesn2) and its interaction with Sesn2 is particularly noteworthy, as it influences the activity of mTOR in aging and its associated pathologies. It is important to find out how leucine interacts with Sesn2 and how mutations in the binding pocket of leucine affect the binding of leucine. Therefore, this study was committed to investigating the impact of non-synonymous mutations by incorporating a broad spectrum of simulation techniques, from molecular dynamics to free energy calculations. Our study was designed to model the atomic-scale interactions between leucine and mutant forms of Sesn2 already described in the literature.

Due to the crucial role of hydrogen bonding in biological processes, we assessed hydrogen bonds in each trajectory over time. The wild-type displayed a higher average number of hydrogen bonds in comparison to the mutants, particularly evident in T374A, T386A, R390A, and E451Q mutants. Our results demonstrated that the interaction paradigm for the mutants has been altered thus showing a significant decline in the hydrogen bonding network. These mutations compromised dynamic stability by disrupting conformational flexibility, sampling time, and leucine-induced structural constraints, leading to variations in binding affinity and structural stability. The analysis of molecular dynamics-based flexibility highlighted an increased fluctuation in regions 217-339 and 371-380. These regions correspond to a linker and a loop that cover the leucine binding cavity. This cavity is critical for the "latch" mechanism in the N-terminal, which is essential for binding leucine. Specifically, mutations at three threonine residues that show a high degree of conservation, Thr374, Thr377, and Thr386, disrupted interaction with leucine, as these residues are critically located above the binding site. Mutations at these positions (T374A or T386A) lead to the disruption of the interaction with leucine. Further validation of reduced binding and modified internal motions caused by the mutants was obtained through binding free energy calculations, Principal Components Analysis (PCA), and Free Energy Landscape analysis (FEL). The MM/PBSA approach was used to calculate the total binding free energy for wild-type and mutants. The values obtained were as follows: -47.32 ± 0.71 kcal/mol for the wild-type, -31.93 ± 0.73 kcal/mol for T374A, -37.79 ± 0.76 kcal/mol for Y375F, -35.67 ± 0.82 kcal/mol for T386A, -38.13 ± 0.85 kcal/mol for R390A, -35.44 ± 0.84 kcal/mol for W444E, and -32.21 ± 0.77 kcal/mol for E451Q mutants. Similar patterns were noted in the total binding free energy determined by the MM/GBSA approach. The significant drop in total binding free energy in mutants reinforces previous observations suggesting the functional impairment of Sesn2 caused by these mutations.

Through studying the complex molecular interactions between Sesn2 and leucine, as well as their mutations, and identifying specific areas where mutations significantly affect leucine binding. These findings will aid in identifying potential targets for drugs that can control the mTOR pathway. These therapeutic compounds may play a crucial role in treating metabolic diseases, cancer, and neurological disorders, thereby extending the health span, and improving the quality of life for the aging population.

PCA059

Exploring the light adaptation effect of photopic electroretinogram components with the use of long duration stimuli in healthy participants

Harry Arbuthnott^{2,3}, Charlie Bosshard^{2,3}, Isabelle Chow^{4,5}, Shaun Leo^{3,6}, Xiaofan Jiang^{3,5}, Omar Mahroo^{2,3,4,5,6}

¹college, Harpenden, United Kingdom, ²Physiology, Development and Neuroscience, University of Cambridge, Cambridge, United Kingdom, ³Institute of Ophthalmology, University College London, London, United Kingdom, ⁴Department of Ophthalmology, St Thomas' Hospital, London, United Kingdom, ⁵Section of Ophthalmology, King's College London, St Thomas' Hospital Campus, London, United Kingdom, ⁶NIHR Biomedical Research Centre at Moorfields Eye Hospital and the UCL Institute of Ophthalmology, London, United Kingdom

Purpose

The electrical response of the human retina to light stimuli can be recorded non-invasively as the electroretinogram (ERG). The light adaptation effect (LAE) refers to the increase, over several minutes, in the amplitude of the ERG elicited in response to repeated flashes delivered superimposed on a light-adapting background, following a prior period of dark adaptation. Previous studies investigating the LAE measured the a-wave and b-wave elicited by brief flash stimuli. We used long duration stimuli to explore the LAE of the response to stimulus onset and offset.

Methods

Bilateral ERG recordings were made to 200ms flash stimuli over the course of light adaptation in 3 healthy adult male participants (6 eyes), aged 21, 21 and 32. Participants gave written informed consent, and the study had Research Ethics Committee approval and conformed to the tenets of the Declaration of Helsinki. Pupils were dilated pharmacologically and conductive fibre electrodes were placed in the lower conjunctival fornix. Participants were fully dark adapted for 20 minutes, and then exposed to a white rod-suppressing background (40 cd m⁻²), and 50 white 200 ms flashes (250 cd m⁻²) were delivered in quick succession. The train of flashes was repeated at 2-minute intervals for up to 20 minutes; responses to each series of 50 flashes were averaged. The amplitude and peak time of the response to stimulus onset (a-wave, b-wave) and offset (d-wave) were measured.

Results

In all participants, the a-wave, b-wave, and d-wave increased in amplitude during the course of light adaptation, reaching a plateau after 10-12 minutes following the onset of the background. The peak times were found to shorten during this period. A time point of 14 min following background onset was chosen for comparison: the amplitudes of all components were significantly larger ($p < 0.013$) and peak times significantly shorter ($p < 0.01$) compared with the corresponding values measured immediately following background onset (paired t test). The mean (SEM) proportional increases in amplitude were 43 (19)%, 38 (5.5)% and 73 (20)% for a-wave, b-wave and d-wave

respectively. Mean (SEM) advancements in peak time were 1.1 (0.2), 3.0 (0.6) and 2.8 (0.6) ms respectively.

Conclusions

We consistently found an increase in amplitude for all 3 components, indicating that the response to both stimulus onset and offset increases in amplitude over the course of light adaptation. Response kinetics also appear to become more rapid over this time period. The mechanisms underlying the LAE are still unknown, but our findings indicate that they apply to electrical activity elicited by both onset and offset of light stimuli.

PCA060

Measuring [O₂] in mouse brain slices reveals changes in modelled oxygen consumption kinetics following changes in bath [O₂]

Sam Atkinson¹

¹*University of Sussex, Brighton, United Kingdom*

The brain is disproportionately aerobic for its size, consuming 20% of inspired oxygen primarily to produce ATP via oxidative phosphorylation (1,2). However, this high oxygen demand leads to a vulnerability to hypoxia when oxygen supply drops below demand (3).

The structure of the hippocampal vascular network, alongside pericyte and endothelial function, results in reduced blood flow and neurovascular coupling compared to the neocortex, potentially underlying the particular vulnerability of this region to hypoxia (4). Hypoxia may occur in Alzheimer's disease (AD) development, as perturbed blood flow is observed prior to symptomatic AD (5) and a decline in hippocampal function is an early AD cognitive marker (6,7). To better understand the impact of mild hypoxia on hippocampal function we investigated how neuronal function and oxygen use was altered by a mild reduction in oxygen supply in mice in vivo and in mouse hippocampal brain slices.

Using haemoglobin spectrometry and laser doppler flowmetry to measure changes in blood oxygen saturation and blood flow, and 2-photon microscopy to measure neuronal calcium signals in Thy1/GCaMP6f mice, our preliminary data shows that mild acute hypoxia is associated with both increased oxygen consumption and frequency of calcium events.

We then tested whether we could recapitulate these findings in mouse hippocampal slices to provide a better model for studying underlying mechanisms.

Using a Unisense A/S oxygen microsensor, we measured depth profiles of [O₂] through the pyramidal layer of the hippocampus of acute sagittal forebrain slices (300µm thickness, 32 slices from 7 mice (5 C57BLJ/6 2 Thy1xDsRed, 3 males, 4 females)), while varying bath [O₂] gassing between 95% and 20%. Slice [O₂] was largely hyperoxic at 95% O₂, 5% CO₂, approached normoxia at 58% O₂, 5% CO₂ and became hypoxic at 20% O₂, 5% CO₂, though surface [O₂] in this condition was in the normoxic range (4,9).

We then compared these profiles to theoretical [O₂] profiles generated by an oxygen diffusion and Michaelis-Menten consumption model, adapted from our previous work (10). The kinetic parameters that best fit experimental data varied depending on bath [O₂] (Median: 95%:K_m: 1e-5mM, V_{max}: 1.2mM/min; 58%:K_m: 0.0025mM, V_{max}: 4mM/min; 20%:K_m: 7.5e-4mM, V_{max}: 0.55mM/min), predicting highly variable rates of oxygen consumption.

Our data suggest a deviation in the O₂-dependence of oxidative phosphorylation (which accounts for the bulk of oxygen consumption in the brain (1)) from simple Michaelis-Menten kinetics, which could contribute to increased oxygen consumption rates in hypoxic brain tissue. Previous work on isolated mitochondria and cytochrome c oxidase suggest that alterations in pH and cellular energy balance, such as likely occur during hypoxia, can cause such kinetic changes (11).

Here we show that in vivo [O₂] can be recapitulated in acute mouse brain slices, and that modelled oxygen consumption kinetics are altered as bath [O₂] is changed.

In summary, our data show a counter-productive increase in hippocampal neuronal activity and oxygen use in mild hypoxia in vivo and altered O₂ consumption kinetics across different [O₂] in brain slices. Improving understanding of hypoxia as a potential early AD mechanism will help

enable clinical translation.

1. Silver I, Erecińska M. Oxygen and Ion Concentrations in Normoxic and Hypoxic Brain Cells. In: Hudetz AG, Bruley DF, editors. *Oxygen Transport to Tissue XX* [Internet]. Boston, MA: Springer US; 1998. p. 7–16. Available from: https://doi.org/10.1007/978-1-4615-4863-8_2
2. Erecińska M, Silver IA. Tissue oxygen tension and brain sensitivity to hypoxia. *Respir Physiol*. 2001 Nov 15;128(3):263–76.
3. Mukandala G, Tynan R, Lanigan S, O'Connor JJ. The Effects of Hypoxia and Inflammation on Synaptic Signaling in the CNS. *Brain Sci*. 2016 Feb 17;6(1).
4. Shaw K, Bell L, Boyd K, Grijseels DM, Clarke D, Bonnar O, et al. Neurovascular coupling and oxygenation are decreased in hippocampus compared to neocortex because of microvascular differences. *Nat Commun*. 20210527th ed. 2021 May 27;12(1):3190.
5. Badimon A, Torrente D, Norris EH. Vascular Dysfunction in Alzheimer's Disease: Alterations in the Plasma Contact and Fibrinolytic Systems. *Int J Mol Sci*. 2023 Apr 11;24(8).
6. Swinford CG, Risacher SL, Wu YC, Apostolova LG, Gao S, Bice PJ, et al. Altered cerebral blood flow in older adults with Alzheimer's disease: a systematic review. *Brain Imaging Behav*. 2023 Apr;17(2):223–56.
7. Rao YL, Ganaraja B, Murlimanju BV, Joy T, Krishnamurthy A, Agrawal A. Hippocampus and its involvement in Alzheimer's disease: a review. *3 Biotech*. 2022 Feb;12(2):55.
8. Setti SE, Hunsberger HC, Reed MN. Alterations in Hippocampal Activity and Alzheimer's Disease. *Transl Issues Psychol Sci*. 2017 Dec;3(4):348–56.
9. Lyons DG, Parpaleix A, Roche M, Charpak S. Mapping oxygen concentration in the awake mouse brain. Kleinfeld D, editor. *eLife*. 2016 Feb;5:e12024.
10. Hall CN, Klein-Flügge MC, Howarth C, Attwell D. Oxidative phosphorylation, not glycolysis, powers presynaptic and postsynaptic mechanisms underlying brain information processing. *J Neurosci*. 2012 Jun 27;32(26):8940–51.
11. Wilson DF, Owen CS, Erecińska M. Quantitative dependence of mitochondrial oxidative phosphorylation on oxygen concentration: A mathematical model. *Arch Biochem Biophys*. 1979;195(2):494–504.

PCA061

Change of voltage-gated sodium channel repertoire in skeletal muscle of a MuSK myasthenia gravis mouse model

Olena Butenko¹

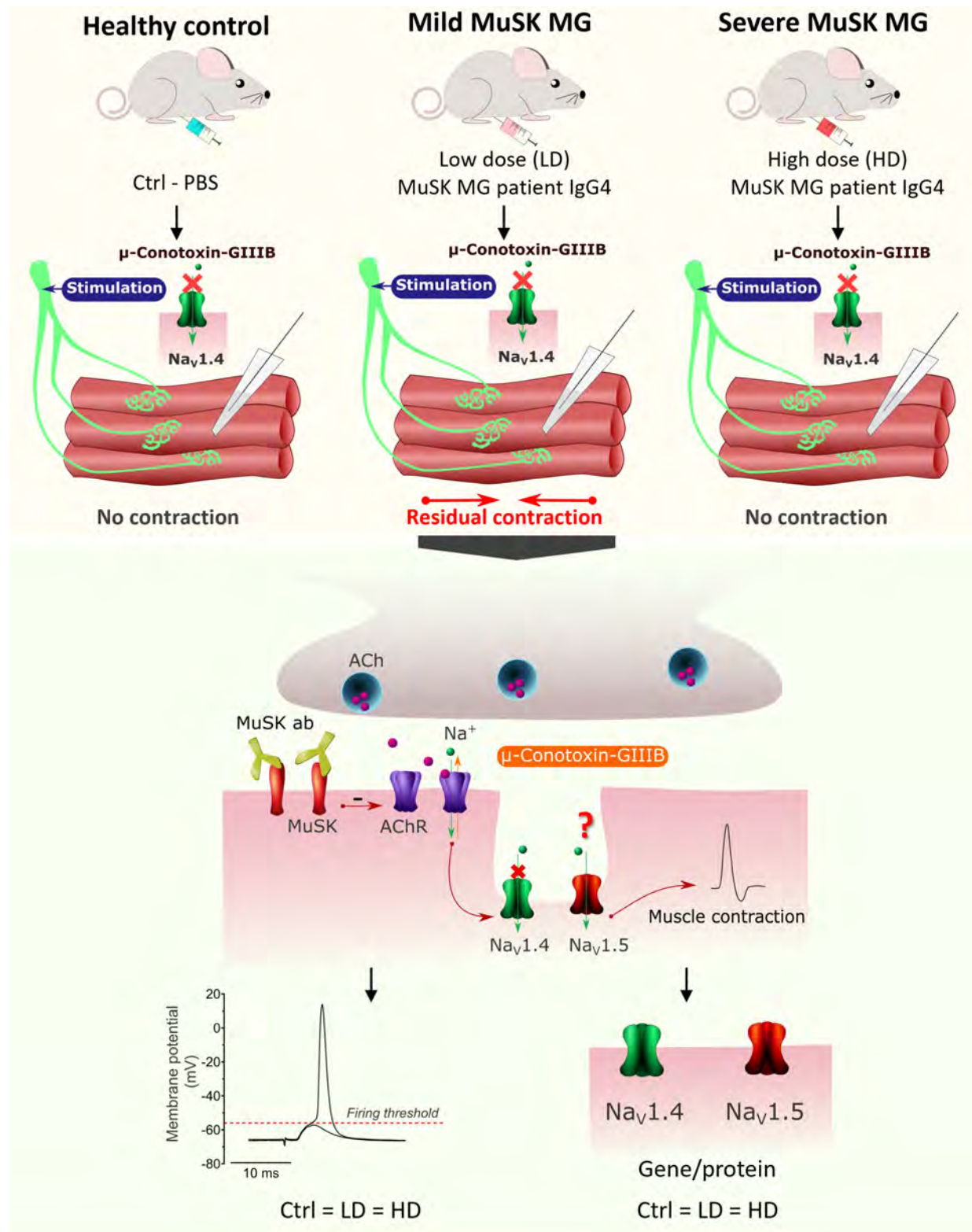
¹*Department of Human Genetics, Leiden University Medical Center, Leiden, Netherlands*

Muscle-specific kinase myasthenia gravis (MuSK MG) is an autoimmune neuromuscular disorder. It is caused by autoantibodies against MuSK, a key postsynaptic membrane molecule involved in acetylcholine receptor clustering at the neuromuscular junction (NMJ). MuSK MG patients have fluctuating, fatigable weakness. The disease severity can vary greatly between patients, in spite of comparable autoantibody levels. One explanation for inter-patient and inter-muscle variability in sensitivity might be variations in compensatory muscle responses. Previously, we developed a passive transfer mouse model for MuSK MG, using purified patient IgG4. In our *ex vivo* experiments we observed that nerve stimulation-evoked contraction of muscles from mild MuSK MG mice appeared partly insensitive to μ -Conotoxin-GIIIB. This blocker of Na_v1.4 voltage-gated sodium channels normally completely eliminates muscle contraction. We hypothesized that changes in Na_v channel expression profile, possibly compensatory expression of (μ -Conotoxin-GIIIB insensitive) Na_v1.5 cardiac-type channels, might lower the muscle fibre's firing threshold and improve neuromuscular synaptic transmission in mild MuSK MG.

We performed passive transfer in immuno-deficient NOD.CB17-Prkdcscid/J (Nod/scid) mice, using 'high' (n=12), 'intermediate' (n=3) and 'low' (n=12) dosing regimens of purified MuSK MG patient IgG4. Next, we assessed myasthenia levels, μ -Conotoxin-GIIIB resistance and firing thresholds. *Ex vivo* analysis of myasthenic NMJs was performed by evaluation of miniature endplate potentials and endplate potentials in the presence of μ -Conotoxin-GIIIB in diaphragm-nerve preparations. To detect changes in Na_v1.4 and Na_v1.5 channels expression profile we performed qPCR and immunostaining in muscle tissue. Data is presented as mean \pm S.E.M., with n representing the number of animals per group. Statistical analysis was performed using multiple unpaired t-tests or one-way ANOVA with Tukey's post hoc tests. All procedures involving the use of laboratory animals were performed in accordance with Dutch law and Leiden University guidelines.

High- and intermediate-dosed mice showed severe, progressive myasthenia, not detected in low-dosed animals. However, during electrophysiological analysis of diaphragm NMJs we found equally reduced amplitudes and frequencies of miniature endplate-potentials (MEPPs), and equal reductions of endplate potentials (EPPs) amplitudes (all by ~40-50%, as compared to the PBS-control), probably associated with direct exposure to MuSK MG patient IgG4 via the intraperitoneal injection route. Notably, the diaphragms from low-dosed mice (n=12) showed a much higher degree of μ -Conotoxin-GIIIB resistance according to the scale for contraction responses when compared with PBS mice (n=7) or high-dosed mice (n=12). However, *Scn5a*, the gene encoding Na_v1.5, was not upregulated in muscle tissue of these mice (PBS mice: n=4, low-dosed mice n=6, high-dosed mice n=6; $p > 0.05$). Furthermore, no reduction of firing thresholds or expression of histologically detectable Na_v1.5 channels was found (PBS mice: 8.61 ± 0.11 mV (n=4); low-dosed mice: 8.60 ± 0.28 mV (n=6); high-dosed mice 8.69 ± 0.22 mV (n=6)). Thus, we observed Na_v1.4-independent muscle contraction *ex vivo*, preferentially in mice experiencing subclinical MuSK MG,

which is unlikely associated with upregulation of $\text{Na}_v1.5$. It remains to be established which other Na_v channels or factors are responsible for the observed μ -Conotoxin-GIIIB insensitivity and if the change in Na_v repertoire is compensatory beneficial.



PCA062

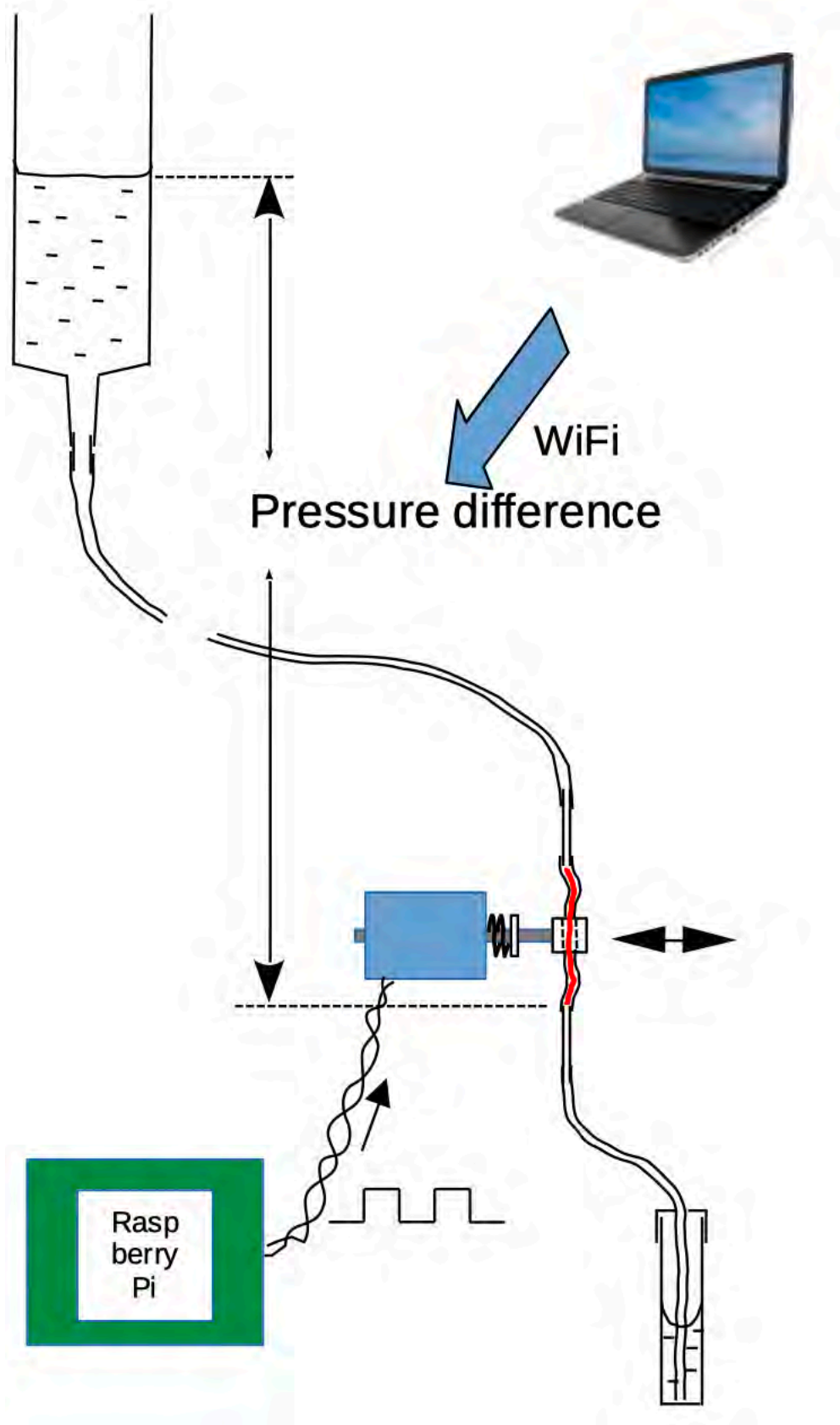
Does cerebrospinal fluid flow along the basement membranes of brain capillaries? In a new in vitro model, oscillating lateral displacement of a porous medium increased flow by a factor of at least 3.6.

Jonathan Coles, Michael Hale¹

¹*School of Physical Sciences, The Open University, Walton Hall,, Milton Keynes, United Kingdom*

Cerebrospinal fluid (CSF) delivers molecules, such as vitamin E, to the vicinity of brain cells and may carry away others, such as amyloid-beta. CSF enters the brain parenchyma by flowing from the brain surface down peri-arteriolar spaces: its subsequent pathway is uncertain (see Hladky & Barrand, 2022). Protein marker molecules in CSF are observed to accumulate in the pericapillary basement membranes of brain capillaries (e.g., Rennels et al. 1985; Fig. 3C in Iliff et al. 2012) but it is improbable that a constant physiological pressure gradient could drive adequate CSF along a pericapillary pathway. Brain tissue moves at the cardiac frequency (Sloots et al., 2020) and accumulation of CSF marker in the pericapillary space is slower if blood pulsation is reduced (e.g., Rennels et al. 1985). We had previously tested the effect of a pulsating pressure gradient on flow through a medium mimicking a basement membrane in various configurations but observed at most only a small enhancement. We have now tested the effect of oscillating lateral movement on flow of 0.15 M NaCl through a vertical silicone tube (i.d. 1.0 mm, o.d. 2.0 mm) filled with a porous medium (a thread of wool, 30 mm long; Fig. 1). With a longitudinal pressure difference of 125 mm H₂O, moving the centre of the tube by 3.5 mm at 5 Hz increased flow by a mean factor of 3.62, SEM = 0.10, n = 5. When the pressure difference was increased to 225 mm H₂O, the enhancement was 1.87, SEM = 0.26, n = 5, which is significantly less (P = 0.0002). Menisci at air/liquid interfaces are susceptible to oscillating pressures, so we took care to avoid them.

We have found no previous report of the effect of experimental movement on flow through a porous medium, apart from that of McMaster & Parsons, 1938, on transport of Evans Blue in a rabbit ear.



Hladky SB & Barrand MA (2022). *Fluids Barriers CNS* 19.9. Iliff JJ et al. (2012). *Sci Transl Med* 4,147ra111 McMaster PD & Parsons RJ (1938). *J Exp Med* 68, 377-400. Rennels ML et al. (1985). *Brain Res* 326, 47-63 Sloots JJ, Biessels G, Zwanenburg JM (2020). *Neuroimage* 210, 116581

PCA063

Comparison of Cx45 and Cx36 expression in retinal organoids and mice retinas

Hannah Kendall², Mingaile Jackson², Simon Rutter², Birthe Dorgau³, Evelyne Sernagor³, Majlinda Lako³, Gerrit Hilgen^{2,3}

¹*Applied Sciences, Faculty of Health and Life Sciences, Northumbria University, Newcastle-upon-Tyne, United Kingdom,* ²*Applied Sciences, Faculty of Health and Life Sciences, Northumbria University, Newcastle upon Tyne, United Kingdom,* ³*Biosciences Institute, Faculty of Medical Sciences, Newcastle University, Newcastle upon Tyne, United Kingdom*

Gap junctions, direct cell-cell connections deemed crucial in facilitating the synchronisation and collection of electrical signals, are widely prevalent in the nervous system. In vertebrates, gap junctions are comprised of two adjacent hemichannels, which in turn, are made up of six connexins (Cx). During neural development, connexins and their gap junctions emerge before chemical synapse formation and are thought to be involved in establishing distinct neural circuits. Despite being the most abundant in mouse retinas, it is unclear to what extent Cx45 and Cx36 are involved in retinal circuit creation, or indeed, how much they contribute to this process in human induced pluripotent stem cell derived retinal organoids (ROs).

To assess whether developmental parallels can be found in both systems, we quantified the expression patterns of Cx45 and Cx36 in mice retina (postnatal day 8-16) (Hilgen *et al*, 2022) and ROs at varying differentiation stages (days 40, 90, 150 and 200, respectively). In order to do this, we developed a custom software enabling automatic analysis of multiple anatomical parameters (e.g. size, overlap and near-by location) of all channels within a confocal microscopy stack. Our results show that numerous soma-somatic Cx45 and Cx36 gap junctions exist in ROs, and, both connexins are localised on and near synaptic terminals in both tissues (shown by synaptophysin and vesicular glutamate transporter 1 staining). Expression levels of Cx45 and Cx36 in both plexiform layers of the mouse retina increased until eye opening, which then reduced slightly from this stage. Within ROs, expression patterns of Cx45 showed increasing densities at the latter stages of differentiation (number of analysed sections for d20 = 125, d45 = 67, d90 = 133, d>150 = 214), whereas Cx36 expression was less pronounced than in mice (number of analysed sections for d20 = 112, d45 = 21, d90 = 73, d>150 = 119)

Heterotypic Cx45/Cx36 gap junctions, which can be found in the rod pathway between ON cone bipolar cells and all amacrine cells, were similarly expressed in both mice and ROs. Within mice, the percentage of Cx45/Cx36 gap junctions was found to be higher before eye opening (number of analysed sections for P8 = 54, P10 = 50, P12 = 51, P16 = 66), whereas, in ROs, it steadily increased (number of analysed sections for d20 = 24, d45 = 54, d90 = 78, d>150 = 216). In addition to this, our multielectrode array recordings from ROs revealed gap-junction-coupled retinal ganglion cells (RGCs) which is consistent with our findings from both connexins between RGCs in mice (not yet quantified).

In conclusion, our data suggests that both mice and ROs have very comparable Cx45 and Cx36 expression patterns. In addition to this, we have shown for the first time, ROs have both heterotypic Cx45/Cx36 gap junctions, and functional gap junctions between RGCs. Together, these findings

imply that both connexins play a pivotal role during the development of both mouse retina and ROs.

Hilgen, G (2022) Connexin45 colocalization patterns in the plexiform layers of the developing mouse retina. *Journal of Anatomy*, 243 (2), 258-264. doi: 10.1111/joa.13651

PCA064

Tracking of tibialis anterior motor units reveals no detrimental effects of intramuscular needle electrode insertion .

Mollie O'Hanlon¹, Elisa Nédélec², Tom Inns², Caroline Sunderland¹, Angus Hunter¹, Mathew Piasecki³, Jessica Piasecki¹

¹*Sport Health and Performance Enhancement (SHAPE) Research Centre, Nottingham Trent university, Department of Sport Science., Nottingham, United Kingdom,* ²*Sport Health and Performance Enhancement (SHAPE) Research Centre, Nottingham Trent university, Department of Sport Science., Nottingham, United Kingdom,* ³*Centre of Metabolism, Ageing and Physiology (COMAP), University of Nottingham, Nottingham, United Kingdom*

Introduction. Exploration of human motor unit (MU) characteristics in clinical and research settings is commonly applied using intramuscular electromyography (iEMG) [1]. This typically involves the insertion of a concentric needle electrode into the muscle during voluntary contractions, and although minimally invasive, may cause discomfort and/or intramuscular damage. Afferent feedback from the muscle as a direct cause of needle insertion may influence MU characteristics such as firing rate (FR) and recruitment [2], thereby influencing the parameters it is designed to investigate. However, this has not yet been fully explored. Methodological advances in non-invasive high-density (HD) EMG allow the direct tracking of MUs across successive contractions in humans, inclusive of simultaneous recording with intramuscular needles, and presents an opportunity to investigate the true effects of needle insertion.

Aim. The aim of this study was to track the function of individual MU characteristics across subsequent contractions, with and without intramuscular needle insertion.

Method. Following familiarisation, six individuals (females n = 3) performed two dorsiflexor trapezoid contractions at 25% of maximum force (3s ascent, 12s hold, 3s descent). HD-EMG was recorded from the tibialis anterior (TA) with a 64ch surface electrode, and signals were decomposed into individual MU potentials and their corresponding spike trains [3]. Prior to the second contraction, a 26-gauge iEMG needle electrode was inserted into the TA, and individual MUs from HD-EMG were tracked with and without needle insertion. Multi-level regression models were used to determine the effect of needle insertion on MUFR at recruitment, derecruitment and during the sustained phase, MU recruitment threshold ratio (recruitment:derecruitment), and the coefficient of variation in force. Statistical significance was accepted at $p < 0.05$.

Results. The mean number of recorded and tracked across MUs contractions was 27 ± 13 . MUFR at recruitment was 11.33 Hz without the needle and did not differ with needle insertion (9.96 Hz, $p = 0.259$). During the steady phase at 25% MVC, MUFR was 15.40Hz without needle and did not differ significantly with needle insertion (13.02 Hz, $p = 0.175$). MUFR at de-recruitment was 7.90 Hz without the needle and did not change significantly with the needle inserted (7.24 Hz, $p = 0.198$). The recruitment ratio was not altered between the contraction types ($p = 0.627$). The coefficient of variation in force was not impaired with needle insertion ($p = .895$).

Conclusion. The current pilot data reveal minimal effects of intramuscular needle insertion on a range of TA MU characteristics at 25% of maximum force and highlight the applicability of combining EMG techniques. However, further exploration is required in a variety of muscle sizes and locations, at different contraction intensities to allow definitive conclusions to be determined.

1. Piasecki M, Garnés-Camarena O, Stashuk, DW. Near-fiber electromyography. *Clinical Neurophysiology*. 2021;132(5):1089-1104. [Accessed 10 April 2024]. Available from: <https://doi.org/10.1016/j.clinph.2021.02.008>
2. Cabral HV, Inglis JG, Cudicio A, Cogliati M, Orizio C, Yavuz U, Negro F. 2023. Muscle contractile properties directly influence shared synaptic inputs to spinal motor neurons. *bioRxiv*. 2023:2023-11. [Accessed 10 April 2024]. Available from: <https://doi.org/10.1101/2023.11.30.569389>
3. Guo Y, Jones EJ, Škarabot J, Inns TB, Phillips BE, Atherton PJ, Piasecki M. 2024. Common synaptic inputs and persistent inward currents of vastus lateralis motor units are reduced in older male adults. *GeroScience*. 2024:1-13. [Accessed 10 April 2024]. Available from: <https://doi.org/10.1007/s11357-024-01063-w>

PCA065

Muscle spindles, motor control and mitochondrial superabundance - what is the connection?

Maria Roxana¹, Amy Vincent², Robert W Banks³, Guy S Bewick⁴

¹Institute of Medical Sciences, University of Aberdeen, Aberdeen, United Kingdom, ²Translational and Clinical Research Institute, Faculty of Medical Sciences, Newcastle University, Newcastle Upon Tyne, United Kingdom, ³Department of Biosciences, Durham University, Durham, United Kingdom, ⁴Institute of Medical Sciences, University of Aberdeen, Aberdeen, United Kingdom

Mitochondrial dysfunction represents the most prevalent inherited metabolic disorder, affecting 1 in 5,000 individuals. Sensory ataxia, a disruption in motor control, is frequently an early symptom of mitochondria dysfunction, leading to an increased risk of falling and associated injury and fears. Mutations causing mitochondrial dysfunction may arise within the mitochondrial genome or nuclear-encoded mitochondrial genes (1). Mitochondria occupy approximately 55% of the volume of sensory terminals in the mouse muscle spindle, making them extraordinarily abundant (2). To investigate their function within muscle spindle primary sensory terminals, we have examined the effects of drugs that interfere with different aspects of mitochondrial activity on the firing of the primary afferents in response to muscle stretching.

Trapezoidal stretch-hold-release extensions (+10% of resting muscle length) were administered every 20 minutes to isolated adult C57/Bl6 mouse soleus muscles *ex vivo*. Whole nerve responses were recorded, for control, drug and drug washout from the same preparation. We investigated the effects of NH₄Cl (0.5-50 mM), which neutralizes pH in intracellular compartments and regulates mitochondrial biogenesis (3), caffeine (0.1-10 mM), which releases Ca²⁺ from intracellular stores (4), and thapsigargin (0.1-1 µM), which also releases Ca²⁺ from intracellularly stores and, in mitochondria, induces the permeability transition (5).

NH₄Cl (50 mM) abolished stretch-evoked firing in all preparations (n = 5; *P* < 0.05, paired *t*-test) within 20 min, indicating great importance of pH in some functional aspect. Caffeine resulted in a substantial inhibition in firing (1 mM, 63.5 ± 9.5 %, *P* < 0.05; & 10 mM, 42.9 ± 18.8 %, *P* < 0.05; n = 11. All data expressed as mean ± SEM). Finally, thapsigargin (0.1, 0.5 & 1.0 µM) tended to produce a dose-dependent decrease (to 48.8 ± 12.5 % at 1 µM) in firing but did not reach significance (n = 7; *P* = 0.09). All effects were at least partially reversible on drug washout.

In summary, these findings suggest that mitochondrial function significantly influences the capacity of primary afferent mechanosensory terminals to respond to physiological stimuli.

References 1. Zhang Q et al.(2021). Front Hum Neurosci. 15, 639871. 2. Banks RW et al. (2023). Proc Physiol Soc. 54, PCA082 3. Genders AJ et al. (2021). Physiol Rep. 9 e14797. 4. Usachev YM & Thayer SA. (1999) J Physiol. 519, 115–130. 5. Korge P & Weiss JN. (1999) Eur J Biochem. 265, 273–280.

PCA066

Suppressed Triose-phosphate isomerase activity affects synaptic vesicle dynamics and reduces *Drosophila* life span

Ælfrin Stone¹, Joern. R Steinert¹

¹*University of Nottingham, Nottingham, United Kingdom*

Neurodegeneration has been extensively linked to aberrant production of redox active molecules, e.g. nitric oxide (NO). One target of NO-mediated post-translational modifications, specifically 3-Nitrotyrosination, is the glycolytic enzyme triose-phosphate isomerase (TPI) which catalyses the conversion of dihydroxyacetone phosphate and glyceraldehyde-3-phosphate. In parallel, reported mutations within the TPI protein render it inactive and are also associated with neurodegenerative human disease, such as in TPI deficiency which is caused by a point mutation in the TPI gene.

In this work *Drosophila melanogaster* expressing mutant TPI (wstd¹, M80T, and I170V point mutations) were used as disease models vs wild-type controls (w¹¹¹⁸ and Canton.S), to identify impacts of aberrant TPI function on neuronal physiology at excitatory glutamatergic neuromuscular junctions (NMJ).

Two-electrode voltage-clamp recordings were taken from third instar larvae fillets. Confocal images of larval NMJs and adult brains, labelled with HRP/BRP, and caspase/anti-AGE, were taken on a Zeiss LSM 880 confocal microscope to characterise active zones (BRP), bouton morphology (HRP), apoptosis (caspase), and advanced glycation end-products (AGE). Western blots were run as standard, longevity assays assessed daily survival.

Data is expressed as mean±SEM (n=no. of muscles/flyes). Student's t-test and Log-rank (Mantel-Cox test) were used for comparisons with p<0.05 being significant.

Longevity was seen to be reduced in TPI mutants, median lifespans of 40 and 42 days in wstd¹ and M80T vs 60 and 68 days in w¹¹¹⁸ and Canton.S respectively (p<0.005, N=145,165,146,139).

M80T showed slightly increased evoked amplitudes and Wstd1 showed significantly increased evoked amplitudes compared to Canton.S (88.12nA and 99.07nA vs 69.8nA). I170V showed significantly reduced amplitudes compared to w1118 (72.2nA vs 108.6nA).

None of the TPI mutants showed altered amplitudes of spontaneous events; 0.6787nA, 0.9194nA, 1.235nA for wstd¹, M80T, and I170V, 0.8132nA and 0.8656 for w1118 and Canton. S respectively. For evoked and spontaneous events n≥9, N≥3, p<0.05.

Quantal content was seen to be reduced in I170V in comparison to w1118 (68.2 vs 183), M80T showed no significant difference and in wstd1 quantal content was seen to be increased in comparison to Canton.S (80.26, and 167.3 vs 83.93).

Synaptic depletion following 50Hz train stimulations varied between lines, amplitudes were suppressed to $67\pm4\%$, $47\pm6\%$, $52\pm8\%$, and $54\pm9\%$ for w^{1118} , $wstd^1$, M80T, and I170V respectively ($n=11,11,5,4$ $N\geq 3$ $p<0.0001$).

Wstdt1 and M80T lines show significantly reduced expression of TPI protein, however the I170V line does not show this reduction in comparison to controls. Preliminary confocal data suggests higher levels of AGE and apoptosis in $wstd^1$ cf w^{1118} . The data suggests that the TPI-mutant phenotype is in part due to altered synaptic vesicle dynamics, possibly associated with vesicle pool organisation or endo/exocytosis. Suppressed TPI activity also enhances protein glycation and redox stress, possibly contributing to the observed phenotypes. Both of these possibilities offer potential therapeutic routes to manage or treat disease.

Gnerer J., Kreber R., & Ganetzky B. (2006). PNAS, 103(41), 14987–14993. Hrizo S., Fisher I., Long D., Hutton J., Liu Z., & Palladino M. (2013). 54, 289–296. Roland B., Amrich C., Kammerer C., Stuchul K., Larsen S., Rode S., Aslam A., Heroux A., Wetzel R., VanDemark A., & Palladino M. (2015). 1852(1), 61–69. Stone Æ., Cujic O., Rowlett A., Aderhold S., Savage E., Graham B., & Steinert J. (2023). Front. Synaptic Neurosci., 15.

PCB001

Role of sex hormones in modulating cardiovascular responses to fructose and high salt diet: insights from Dahl salt-sensitive rats.

Muhammad Asad Akhtar¹, Stian Ludvigsen², Costantino Mancusi³, ANNE DRAGØY HAFSTAD¹, Eva Gerds⁴, KIRSTI YTREHUS¹

¹Cardiovascular Research Group, UiT-The Arctic University of Norway, Tromsø., Tromsø, Norway,

²Cardiovascular Research Group, UiT-The Arctic University of Norway, Tromsø, Norway, ³Dept of Advanced Biomedical Science, University of Naples Federico II, Naples, Italy, ⁴Dept of Clinical Science, University of Berge, Bergen, Norway, Bergen, Norway

Background: The prevalence of hypertension is rising alongside obesity rates. High-fructose corn syrup and high sodium intake are linked to metabolic disorders, cardiovascular morbidity, hypertension, aortic stiffness, and diastolic dysfunction. The sex-specific responses to these dietary factors and the role of sex hormones in salt-sensitive hypertension and fructose-induced cardiovascular dysfunction remain unclear.

Aim: The study aims to examine the impact of a fructose-rich diet, with or without high salt, on blood pressure regulation, cardiac function, and molecular remodelling in Dahl salt-sensitive (DSS) rats. Additionally, we explored the influence of sex hormones by comparing male, females with intact ovaries and ovariectomized (OVX) Dahl salt sensitive (DSS) rats.

Methods: The study utilized 60 female and 30 male DSS rats, aged 10 weeks, where 15 females underwent OVX before the diet intervention. The diet intervention groups were given chow with 6% NaCl and 10% fructose in drinking water for 9 weeks: male-NaCl (DSSM-NaCl), female-NaCl (DSSF-NaCl), and female OVX-NaCl (DSS-OVX-NaCl). Control groups received regular chow with 10% fructose water: male (DSSM), female (DSSF), ovariectomized female (DSS-OVX). LV assessment was conducted using echocardiography at baseline and at endpoint, using a short axis view (SAX) and M-mode imaging. Rats were euthanized for LV biopsies, and gene expression was analyzed using RT-qPCR. Echocardiography and gene data were analyzed using two-way ANOVA multiple comparison test. For ovariectomy and echocardiography, we used gaseous anaesthesia with isoflurane, (4% induction and 1.8 % maintenance).

Results. Ovariectomized rats gained more weight than intact females, but echocardiography showed no significant LV functional differences. However, LV mass and wall thickness increased in ovariectomized groups, especially with salt treatment. Males differed significantly in LV functional and morphological parameters from females.

When analyzing genes related to heart function in LV tissue, we found that beta myosin heavy chain mRNA expression levels were significantly upregulated in both OVX female groups (DSS-OVX and DSS-OVX-NaCl) compared to the DSSF group. Atrial natriuretic factor mRNA expression was upregulated in the DSS-OVX, DSS-OVX-NaCl and DSS-M-NaCl group compared to the DSSF group. Notably, brain natriuretic peptide mRNA expression level was significantly higher only in DSS-OVX-NaCl group.

In terms of genes related to fibrosis and inflammation, monocyte chemoattractant protein-1 mRNA expression was slightly elevated in salt treated female groups. Additionally, TIMP metalloproteinase inhibitor 1 mRNA expression were upregulated in the DSS-OVX-NaCl and DSS-M-NaCl group as compared to DSSF group. Interestingly, transforming growth factor β 2 mRNA expression was significantly higher in DSS-OVX, DSS-OVX-NaCl and DSSM-NaCl groups.

Furthermore, genes encoded by the mitochondrial genome, such as mitochondrially encoded cytochrome C oxidase I and cytochrome b (subunit of complex III) MT-CYB exhibited changes in expression across all salt-treated groups compared to intact females. Peroxisome proliferator activated receptor coactivator 1 beta mRNA expression was significantly higher only in DSS-OVX-NaCl group.

Conclusion. Ovariectomy in female DSS rats leads to gene expression and cardiac morphology changes, intensified by salt. Males exhibit distinct cardiac responses, indicating sex hormones' role in cardiovascular outcomes. The study underscores the complex relationship between diet, sex hormones, and cardiovascular health in hypertension.

PCB002

The truth of air pollution. Does woodsmoke induce cardiac hypertrophy?

Raghad Al-Dulaymi¹, Andrew Trafford¹, Katharine Dibb¹, Aristeidis Voliotis¹, Gordon Mcfiggans¹

¹University of Manchester, Manchester, United Kingdom, ²University of Manchester, Manchester, United Kingdom

The Truth of Air Pollution. Does Woodsmoke Induce Cardiac Hypertrophy?

Authors: Raghad Al-Dulaymi, Prof. Andrew Trafford, Dr. Katharine Dibb, Dr. Aristeidis Voliotis, Prof. Gordon Mcfiggans

Background:

Air pollution from indoor and outdoor sources is a global health problem and is predicted to cause millions of deaths annually. Previous studies demonstrated that short- and long-term exposure to woodsmoke emissions was associated with an increased risk of respiratory diseases. However, the evidence on the association between air pollution from woodsmoke and cardiovascular diseases is not conclusive. Cardiac hypertrophy has been recognised as an independent risk factor for adverse cardiovascular outcomes such as heart failure and sudden cardiac death. Previous evidence suggested the role of tadalafil, a phosphodiesterase 5 (PDE5) inhibitor, in protecting against cardiac hypertrophy in various animal studies.

Objectives:

For this stage of the project, our objective was to measure the effect of woodsmoke particles on the surface area of neonatal rat ventricular myocytes (NRVM) cells to detect any signs of hypertrophy.

Methods:

All experiments and procedures were conducted in accordance with the University of Manchester guidelines for animal care under the Animal (Scientific Procedures) Act 1986 (ASPA). Ethical approval for the work was obtained from the University of Manchester Animal Welfare and Ethical Review Board. Samples of woodsmoke were collected from a modern wood-burner based at the University of Manchester. Woodsmoke was collected from 2 phases of combustion: flaming and smouldering. Emission particles were immersed in cell maintenance media before cell exposure. NRVM were harvested from 1-2 days old Wistar rats (Charles River). The effect of pollutants on the cell surface area (hypertrophy) was measured using fluorescent microscopic techniques and software analysis.

Results

Our results showed an increase in cell surface area in response to increasing pollutant concentrations. Incubation of cells with pollutants (from either the flaming or smouldering phases)

and a cardioprotective agent (tadalafil 50nM) was associated with a significantly smaller surface area compared to incubation with pollutants alone ($P < 0.0001$). Moreover, incubation of the cells with pollutants first then with a combination of pollutants and PDE5 inhibitor reversed the hypertrophy for both the flaming and smouldering phase groups.

Conclusions:

Our data showed that woodsmoke-derived pollutants induced cardiac hypertrophy in NRVM in a dose-dependent manner. The cardiac hypertrophy could be prevented and reversed by an antihypertrophic agent 'tadalafil'. The next phase of the project will be dedicated to exploring the mechanism by which woodsmoke pollutants induce cardiac hypertrophy.

PCB003

DNA damage accumulation causes dystrophin deficiency in heart muscle

Daniel Brayson¹, Ehsan Ataei Ataabadi², Keivan Golshiri³, Anton Roks⁴

¹School of Life Sciences, University of Westminster, London, United Kingdom, ²Department of Internal Medicine, Erasmus Medical Center, Rotterdam, Netherlands, ³Department of Internal Medicine, Erasmus Medical Center, Rotterdam, Netherlands, ⁴Department of Internal Medicine, Erasmus Medical Center, Rotterdam, Netherlands

Introduction: DNA damage accumulation is a classical hallmark of ageing often culminating in replicative senescence. In cells such as cardiac myocytes, which do not replicate, downstream mechanisms resulting in functional decline are less well understood. The stochastic model of DNA damage accumulation states that long genes are more susceptible to DNA damage induced lesions than shorter genes. Dystrophin is large structural protein encoded by one of the longest genes in the genome, DMD. Loss of function mutations result in profound skeletal and cardiac muscle disease and age-related reductions in protein have been observed. Therefore, we hypothesised that DNA damage would confer a loss of dystrophin in cardiac muscle.

Methods: In line with local regulations regarding the use of animals in research we dissected cardiac tissues from 3 male and 3 female 17-week old *Ercc1Δ/-* mice, a well-established model to investigate the pathophysiological effects of DNA damage *in vivo*. We used an antibody directed to the C-terminus of the dystrophin protein to perform Western blotting on these tissues and compared abundance with a panel of proteins from cardiac genes of short and medium lengths known to play an important role in cardiac physiology and health.

Results: We discovered that *Ercc1Δ/-* mouse hearts exhibited a substantial decline in protein abundance of the 427kDa isoform of dystrophin in both male and females when compared with wildtype littermate controls ($P < 0.05$, Mann-Whitney U test). Modest reductions were also observed in proteins of cardiac genes, these however, were not found to be statistically significant.

Conclusion: Our preliminary investigation supports the hypothesis that dystrophin abundance is highly susceptible to DNA damage. Future research will seek to understand the precise DNA/RNA signatures leading to dystrophin deficiency, how these can be measured in humans and how important this mechanism is to functional outcomes in ageing.

PCB004

Disturbed cardiac circadian rhythm in diabetes: autonomic contributions

Connor J Leadley², Shivani Sethi², Roseanna A Smither², Grace W Belworthy², Colin H Brown², Regis R Lamberts², Carol T Bussey^{2,3}

¹Manaaki Manawa Centre for Heart Research, Department of Physiology, Faculty of Medical and Health Sciences, University of Auckland, Auckland, New Zealand, ²Department of Physiology and HeartOtago, School of Biomedical Sciences, University of Otago, Dunedin, New Zealand, ³Manaaki Manawa Centre for Heart Research, Department of Physiology, Faculty of Medical and Health Sciences, University of Auckland, Auckland, New Zealand

Introduction: The healthy heart displays a circadian rhythm in which heart rate and blood pressure decrease overnight. However, this rhythm is blunted, absent or even reversed in the diabetic heart, which is a crucial risk factor for the development of cardiovascular disease. The origin of the circadian rhythm in the heart and its dysregulation, has not yet been fully elucidated, but changes in autonomic neural control have been implicated.

Objective: Determine changes in circadian cardiac autonomic responsiveness in diabetes.

Methods: We investigated autonomic regulation in 20-week old male Zucker type 2 Diabetic Fatty rats (DM) and their non-diabetic littermates (ND) at two timepoints, the start of the inactive and the active period (Zeitgeber times 3 and 15, respectively). Autonomic responsiveness (noradrenaline 0.5µM, acetylcholine 1µM) was assessed in the Langendorff-perfused isolated heart preparation, following pentobarbital anaesthesia (80mg/kg i.p.) (2-way RM ANOVA). Sinoatrial node (SAN) and left ventricle were dissected from naïve ND and DM ZDF for assessment of protein expression via Western Blot (2-way ANOVA). Brains, post-fixed in paraformaldehyde (4%), were immunostained for quantification of activated sympathetic cells (c-fos and tyrosine-hydroxylase co-expression) (2-way ANOVA). Data are presented as mean±SEM.

Results: We observed diurnal variation in cardiac sympathetic responsiveness (noradrenaline; ΔDevP ND: ZT3 25.7±13.4, ZT15 32.6±11.9; DM: ZT3 6.3±10.1, ZT15 32.5±7.9 ΔmmHg , n=8-9, p<0.05). Conversely, lower parasympathetic responsiveness was associated with diabetes (acetylcholine; ΔHR ND: ZT3 -93.5±21.6, ZT15 -88.0±15.4; DM: ZT3 -66.4±11.5, ZT15 -72.3±13.5 Δbpm , n=4-10, p<0.05). While no significant difference in the expression of cardiac beta-adrenergic (β_1 , β_2) or muscarinic (M_2) autonomic receptors was found, circadian rhythms were observed in the expression of calcium handling proteins (SERCA2a, PLB), which were higher during the active period (ZT15). CLOCK protein levels were also lower in the SAN in DM (ND: ZT3 0.5±0.1, ZT15 0.6±0.1; DM: ZT3 0.4±0.1, ZT15 0.3±0.02, n=5-6, p<0.05). Activation of sympathetic cells was higher in DM in the nucleus tractus solitarius (p<0.001), and significantly higher both in DM and during the active period (ZT15) in the rostral ventrolateral medulla (p<0.001).

Conclusions: Physiological circadian signalling was primarily associated with sympathetic regulation, while we uncover changes in parasympathetic responsiveness in diabetes that might signal an underestimated therapeutic target. Increased activation of sympathoregulatory brain

regions might contribute to sympathetic overactivation as well as disrupted circadian rhythms in diabetes.

PCB005

Systolic and diastolic shear stress and endothelial cell orientation and polarity in mouse common carotid artery

Nabil Nicolas¹, Clémence Caillaud¹, Alexandre de Tilly³, Etienne Roux¹

¹Univ. Bordeaux, INSERM, Biologie des maladies cardiovasculaires, U1034, Pessac, France, ²Univ. Bordeaux, INSERM, Biologie des maladies cardiovasculaires, U1034, Pessac, France, ³Hemovis, Fontenay-sous-Bois, France

Blood flow produces fluid shear stress (SS), a frictional force parallel to the blood flow, on the endothelial cell (EC) layer of the lumen of the vessels. ECs themselves are sensitive to this SS in terms of directionality and intensity. The aim of this study was to determine the physiological SS value during the cardiac cycle and EC polarity and orientation from blood flow in healthy male and female mouse carotid artery. All procedures were done according to current national and European legislation, and agreed upon by the local ethical committee. Experiments were performed on 8 male and 8 female 8-week-old C5BL/6J mice. Measurements of maximum blood velocity and vessel diameter in diastole and systole of the right common carotid artery were performed in vivo by Doppler ultrasound imaging on isoflurane-anesthetized mice. Blood samples were then collected for determination of plasmatic and total blood viscosity and hematocrit, using a newly developed device [1]. After animal euthanasia, the right common carotid was dissected for confocal imaging after labeling the EC nucleus and Golgi apparatus. Diastolic and systolic SS values were calculated from maximal velocity, vessel diameter, and viscosity values applying a newly developed method assuming heterogeneous blood flow, i.e., a red cell central plug flow surrounded by a peripheral plasma sheath flow, initially evidenced by Fahraeus [2] (F-method), compared with the classical method considering total blood as a “Newtonian” homogenous fluid with constant viscosity (N-method) [3]. F- and N-methods differed in blood velocity profile (including hematocrit in the F-method) and viscosity values, plasmatic and total, respectively. EC orientation was defined as the angle of the nucleus-Golgi apparatus vector to the blood flow direction, classified as dromic [0;60°], antidromic [120°;180°], and lateral [60°;120°], and compared to random distribution. EC polarity was defined by the length of this vector and nucleus elongation (long/short axis ratio). Statistical comparisons were done using Mann-Whitney and Chi² tests when appropriate and considered significant for P<0.05. Total blood and plasmatic viscosity were 4±0.5 cP and 1.27 cP, respectively. Diastolic and systolic SS, calculated by F-method, were 6±2.5 Pa and 30±6.5 Pa, respectively. Diastolic and systolic SS, calculated by the N-method, were, respectively, 6% and 14% higher than by the F-method. Total blood and plasmatic viscosity were 4±0.5 cP and 1.27 cP, respectively (table 1). ECs were significantly oriented against blood flow but not polarized. No sex difference was identified, whatever the parameters. Our results showed that both methods, though based on different theoretical assumptions, were convergent in their SS calculated values. However, the F-method seems more accurate since it considers the hematocrit value whereas the N-method does not. The cardiac cycle is characterized by high rate and amplitude changes in WSS values and ECs are sensitive to the direction of the blood flow, without sex difference.



1. de Tilly A et al. (2023). Measurement system for a liquid (WO2023111614A1). Available at : [https://patents.google.com/patent/WO2023111614A1/en?q=\(tilly+jouenne\)&oq=tilly+jouenne](https://patents.google.com/patent/WO2023111614A1/en?q=(tilly+jouenne)&oq=tilly+jouenne).
2. Fåhræus R (1929). *Physiological Reviews* 9, 241–274.
3. Roux E et al. (2020). *Front Physiol* 11, 861.

PCB006

Associations between accelerometry and echocardiographic measurements in individuals with hypertrophic cardiomyopathy

Katie Cooper², Christopher Eggett^{1,2}, Peter Luke^{1,2}, Alasdair Blain², Nduka Okwose^{1,2,3}, Amy Fuller^{1,2,3}, Alaa Alyahya^{1,2}, Kristian Bailey¹, Guy MacGowan^{1,4}, Djordje Jakovljevic^{1,2,3}, Sarah Charman^{1,2}

¹Newcastle upon Tyne Hospitals NHS Foundation Trust, Newcastle Upon Tyne, United Kingdom,

²Translational and Clinical Research Institute, Faculty of Medical Sciences, Newcastle University, Newcastle Upon Tyne, United Kingdom, ³Faculty of Health and Life Sciences, Coventry University, and University Hospitals Coventry and Warwickshire NHS Trust, Coventry, United Kingdom,

⁴Biosciences Institute, Newcastle University, Newcastle Upon Tyne, United Kingdom

Background: Physical activity is recommended to individuals with hypertrophic cardiomyopathy (HCM) as a management option to reduce disease burden. However, over 50% of individuals with HCM are not meeting the recommended physical activity guidelines. Beta-blockers (BB) are prescribed to individuals with HCM to aid symptom management, but the effects on physical activity are relatively unknown. The aim of this study was to investigate the associations between accelerometry and echocardiographic measurements in individuals with HCM. Data described as median unless otherwise stated.

Methods: Twenty-one individuals with HCM (males, n=15, age (mean±SD) 52±15 years old, body mass index (BMI) 29 (25-31) kg/m², prescribed BB, n=11, left atrial volume index (LAVI) 32 (30-35) mL/m² and stroke volume (SV) 55 (44-65) mL) had accelerometry and echocardiographic measurements recorded. Accelerometry categories were measured over 7 days using wrist-worn accelerometers (GENEActiv, ActivInsights Ltd., United Kingdom). Echocardiographic measures were taken in the rest-supine position and included LAVI and SV.

Results: In individuals with HCM, time spent in 1 to 5 minute bouts of light intensity physical activity was positively correlated with LAVI ($r=0.55$, $p<0.01$). However, time spent in 1 to 5 minute bouts of light physical activity was negatively correlated with SV ($r=-0.50$, $p<0.05$). A positive trend was found between time spent in 10 minute bouts of moderate to vigorous physical activity and SV ($r=0.20$, $p=0.44$). The same trends applied for those prescribed BB versus those who were not.

Conclusion: In individuals with HCM, our findings highlight that there are associations between light and moderate to vigorous physical activity and cardiac structure and function that requires further explorations.

PCB007

Hypoxia Inducible Factor Signalling Pathway in a Neuronal PC12 Cell-Line Deprived from Oxygen (1% O₂) and Glucose

Rebecca Edwards¹

¹*Keele University, Newcastle-under-Lyme, United Kingdom*

Introduction: Vascular cognitive impairment (VCI) is the second most prevalent form of dementia and is associated with reduced cerebral blood flow. We know this causes hypoxia inducible factor (HIF) expression and harnessing this could represent a new therapeutic target for VCI. Prolyl-hydroxylase domains (PHD) increase HIF expression; DMOG and FG4592 are PHD inhibitors. We aim to characterise additional mechanisms of action.

Methods: Neuronal cell-line rat pheochromocytoma (PC12 cells) were cultured with DMEM media at 37 ° C with 21% O₂ and 5% CO₂. DMOG, FG4592 (100uM) or 1% DMSO (vehicle) was added across four oxygenation conditions: 21% O₂, 21% O₂ and glucose deprivation (GD), 1% O₂, and 1% O₂ glucose deprivation (OGD) for a duration of 6 or 24-hours. Each experiment consisted of three biological and three technical replicates. 3-(4, 5-dimethylthiazolyl-2)-2,5-diphenyltetrazolium bromide (MTT) and lactate-dehydrogenase (LDH) assays were carried out to determine energy production and cytotoxicity. HIF-1α and HIF-2α protein levels were examined by Western immunoblotting while HIF-1α and PHD2 RNA expression was also analysed via q-PCR.

Results: Relative HIF1α RNA expression was increased following oxygen deprivation, and this was exacerbated with OGD at 6-hours but was not observed at 24-hours (Figure 1A). Interestingly, PHD2 RNA expression was only increased with OGD exposure at 6-hours, but the inverse was observed at 24-hours exposure (Figure 1B), though high variability was observed with the OGD group.

As expected, under typical oxygenation conditions at 24-hours HIF-1α protein expression was low, but it only slightly increased when oxygen was withdrawn. Expression levels increased dramatically during OGD and the same was true under vehicle conditions and with DMOG. However, there was an increase in expression when oxygen was withdrawn and FG4592 was provided (Figure 2A).

Decreased metabolic activity is presented across all OGD exposures when compared to 1% O₂, thus highlighting the role of glucose in cellular metabolism (Figure 3). Paired with LDH release to assess cytotoxicity, an increase in cytotoxicity is observed in GD exposed cells with FG4592 administration (Figure 4).

Conclusions: HIF signalling increases following OGD exposure due to PHD inactivation, thus limiting HIF degradation and increasing its abundance. With the inhibition of PHD by DMOG administration, we see a further increase in OGD HIF abundance, thus supporting the role of DMOG in HIF therapeutics. Regarding PHD2 expression at an RNA level, it is possible that a negative feedback-loop is in play by which increased HIF-1α expression causes a further increase in PHD2 expression to counteract this signalling alteration. The pathway by which DMSO causes increased HIF signalling remains unclear but poses useful insights for future research.

Deoxygenation causes PHD expression downregulation to therefore allow the activation of HIF, which aligns with these results. When paired with FG4592, we see further increase in HIF signalling as this increases the deregulatory effects of PHD inactivation to form a summative HIF abundance response. Further research is required to understand the precise mechanisms at play for the signalling pathways of DMOG and FG4592. Furthermore, western immunoblotting for HIF 6-hour exposures and PHD2 will be carried out and paired with q-PCR data for HIF-2 α .

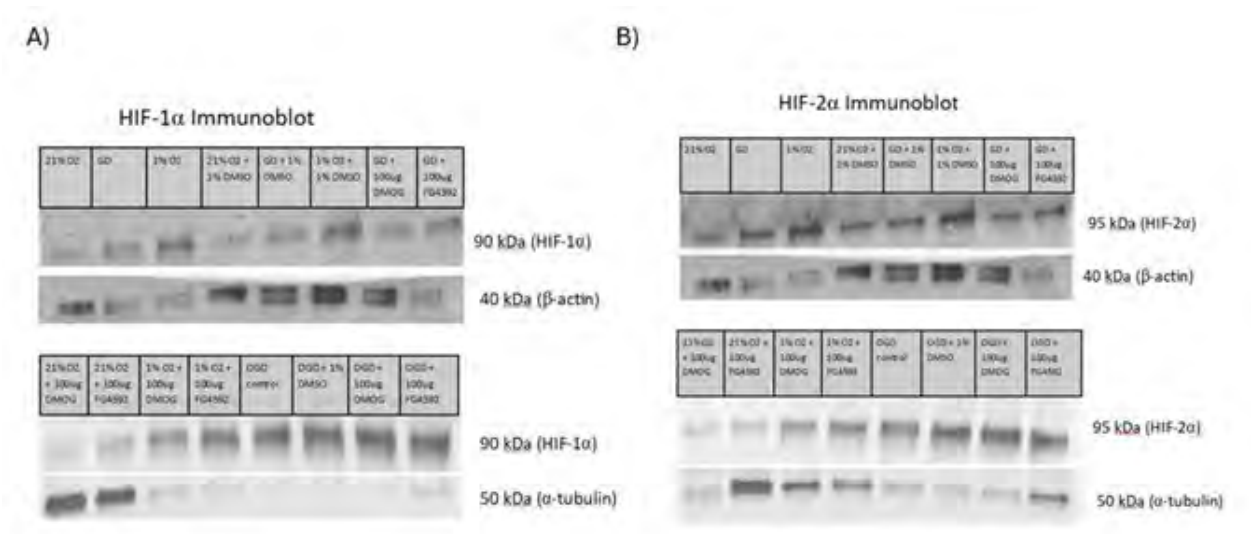


Figure 5: Western immunoblotting layout and raw data for HIF-1 α and HIF-2 α proteins.

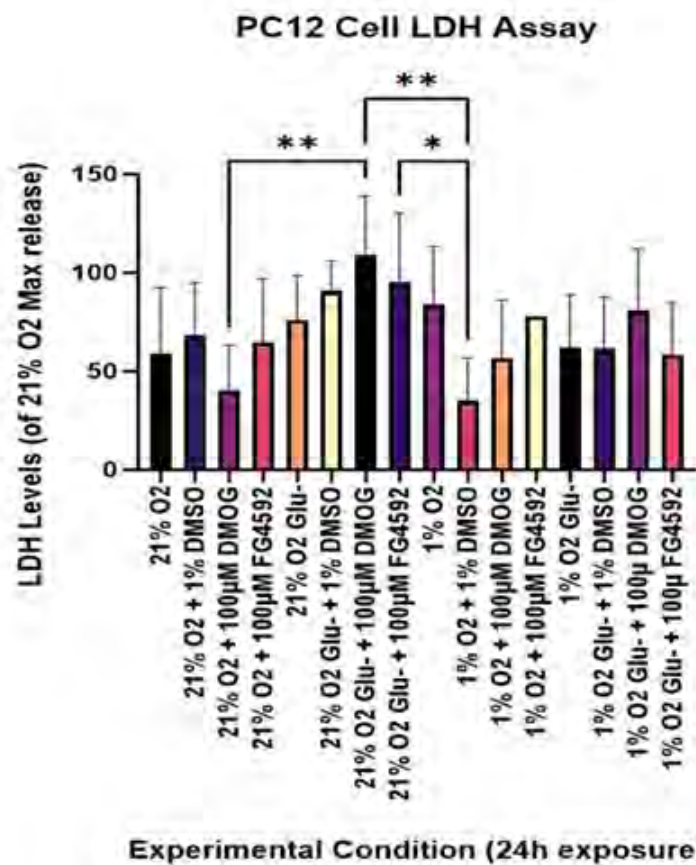


Figure 4: LDH Assay of PC12 cells across 4 oxygenation states and drug/vehicle exposures for 24 hours. Statistical analysis was conducted using a one-way ANOVA where * indicates $p < 0.05$ and ** indicates $p < 0.01$, lack of * suggests no significance.

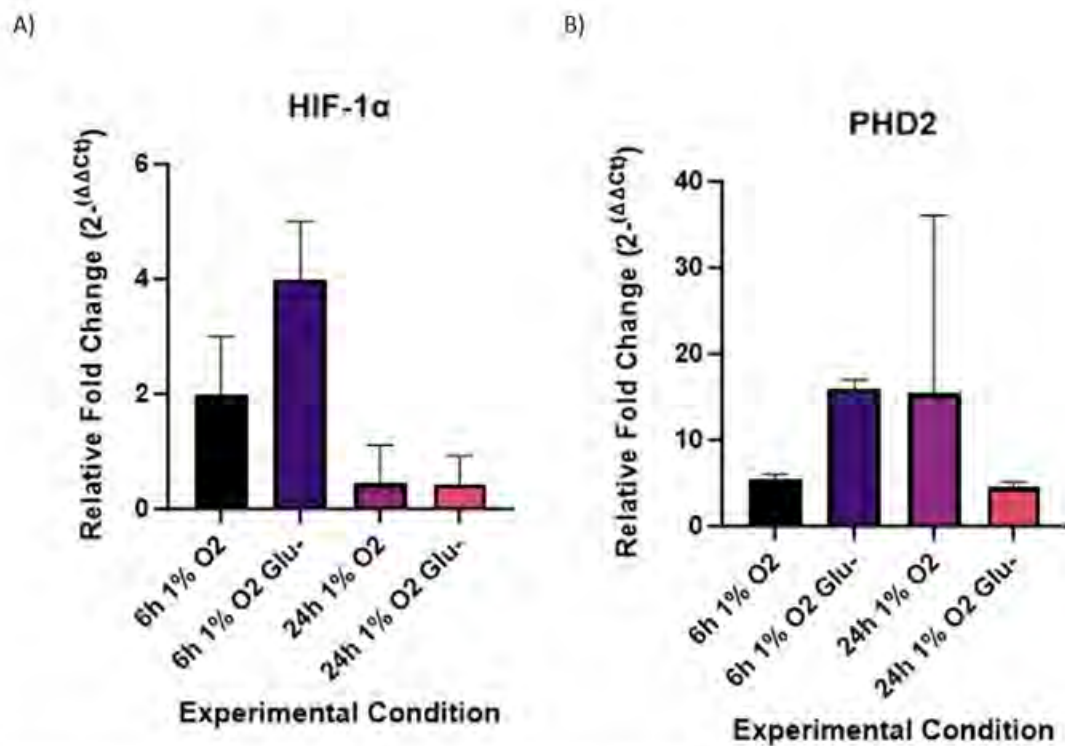


Figure 1: q-PCR analysis of HIF-1 α (A) and PHD2 (B) following differential durations of oxygen deprivation and oxygen-glucose deprivation (n=3 each).

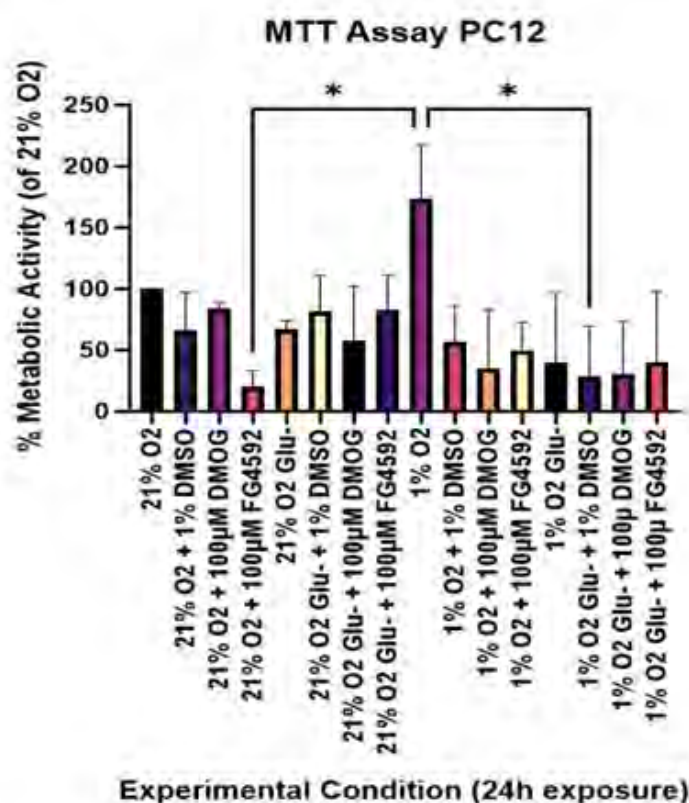


Figure 3: MTT Assay of PC12 cells across 4 oxygenation states and drug/vehicle exposures for 24 hours. Statistical analysis was conducted using a one-way ANOVA where * indicates $p < 0.05$, lack of * suggests no significance.

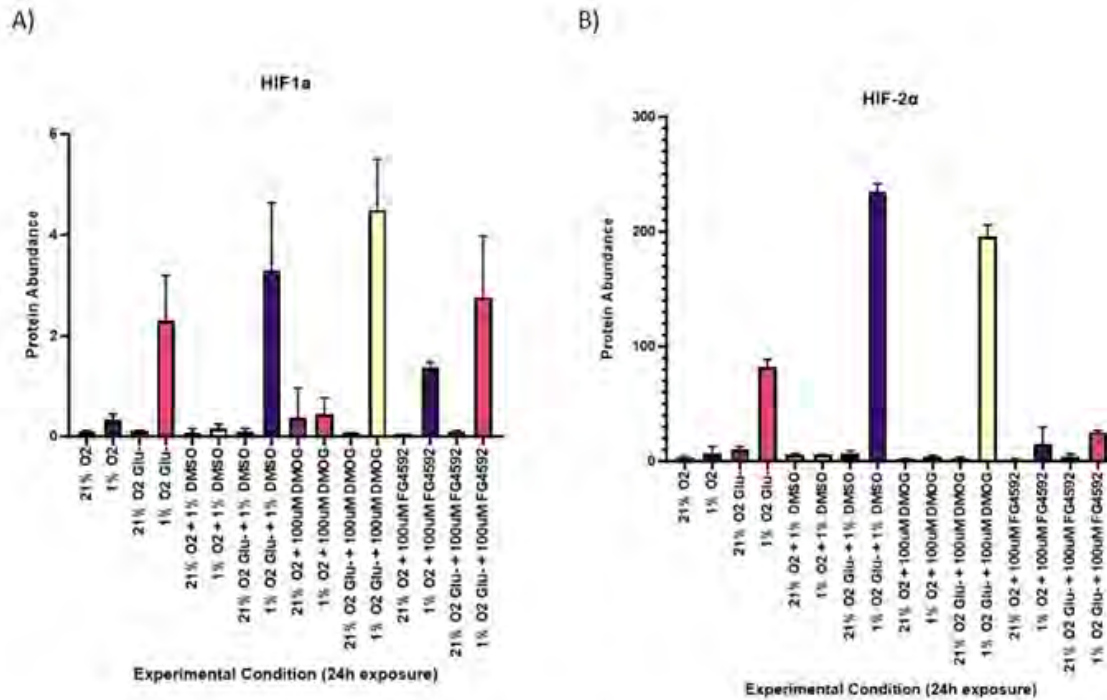


Figure 2: Western blot analysis of HIF-1α (A) and HIF-2α (B) following 24-hours of exposure with PHD inhibitors, DMOG, FG4592 or vehicle (n=3 each). Analysis was conducted on PC12 cells following 24 hour exposures.

1) Linton, A.E., Weekman, E.M. and Wilcock, D.M. (2021) 'Pathologic sequelae of vascular cognitive impairment and dementia sheds light on potential targets for intervention', *Cerebral Circulation - Cognition and Behavior*, 2 Available at: <https://doi.org/10.1016/j.cccb.2021.100030>. 2) Zhou, M., Hou, J., Li, Y., Mou, S., Wang, Z., Horch, R.E., Sun, J. and Yuan, Q. (2019) 'The pro-angiogenic role of hypoxia inducible factor stabilizer FG-4592 and its application in an in vivo tissue engineering chamber model', *Scientific reports*, 9(1), pp. 6035-5 Available at: <https://doi.org/10.1038/s41598-019-41924-5>.

PCB008

Hypoxia increases blood pressure variability and impairs arterial baroreflex sensitivity in middle-aged hypertensive men

Ojikutu Qudus¹, Jeann Sabino-Carvalho², Katherine Latham¹, Igor A Fernandes¹

¹Purdue University, West Lafayette, United States, ²Emory University, Atlanta, United States

Introduction: Sleep apnea-induced acute hypoxia and arterial oxygen desaturation are common phenotypes in arterial hypertension. While the transient hypoxic insult alone does not consistently elevate blood pressure, it does trigger exaggerated increases in muscle sympathetic activity (MSNA) among hypertensive individuals. Elevated resting MSNA levels correlate with greater blood pressure variability (BPV), an index associated with an increased likelihood of target organ damage regardless of absolute blood pressure levels. **Hypothesis:** We hypothesized that transient hypoxic insults would provoke exaggerated increases in BPV among hypertensive individuals. Additionally, hypoxia is known to reset the arterial baroreflex operating point to higher pressures. We also theorize that exaggerated increases in BPV will be followed by reduced sensitivity of the spontaneous cardiac and sympathetic arms of the baroreflex. **Methods:** Eight 1-2 stage naive hypertensive (HT– 43 ± 12 yrs.) and normotensive (NT – 40 ± 11 yrs.) men were exposed to 5-minute bouts of (1) normoxia (21% O₂) and (2) isocapnic-hypoxia (10% O₂). Oxygen saturation (pulse oximetry), beat-to-beat BP (photoplethysmography), MSNA (Microneurography), and partial pressure of end-tidal carbon dioxide (PETCO₂) were monitored throughout the study. PETCO₂ clamp was performed through a rebreathing system. We calculated the standard deviation (SD), average real variability (ARV), and other indices of BPV. Spontaneous cardiac baroreflex was assessed via the sequence technique and cardiac autonomic modulation through time- and frequency-domain HR variability. The sensitivity (gain) of the sympathetic baroreflex was determined via weighted linear regression analysis between MSNA and diastolic BP. **Results:** Independent T-tests indicated that both experimental groups showed similar reductions in oxygen saturation in response to isocapnic-hypoxia (NT –25.7 ± 3.3 vs. HT –21.2 ± 4.0%, $p > 0.05$). There were no substantial changes in BP absolute levels and PETCO₂ during isocapnic hypoxia. MSNA recordings revealed greater increases in sympathetic activation of hypertensive individuals (HT +12.7 ± 6.7 vs. NT +3.6 ± 1.6 bursts/min, $p = 0.012$). Isocapnic-hypoxia similarly increased BPV (HT SD: +4.7 ± 1.6 versus NT +7.6 ± 4.4 mmHg, $P = 0.006$; HT +2.9 ± 1.0 versus NT +4.7 ± 1.9 mmHg, $P = 0.001$; HT +3.3 ± 1.1 versus NT +5.4 ± 2.7 mmHg, $P = 0.002$, for systolic, diastolic and mean BP, respectively) in both hypertensive and normotensive individuals. Other traditional measures of variability showed similar results. Isocapnic-hypoxia provoked similar reductions in cardiac and sympathetic baroreflex gain in both groups. **Conclusion:** In summary, isocapnic hypoxia increases blood pressure variability and reduces both cardiac and sympathetic baroreflex sensitivity in normotensive and hypertensive men.

PCB009

The effects of fetal hypoxia on arrhythmia sensitivity in catecholaminergic polymorphic ventricular tachycardia mouse model

Zarin Tasnim Gias¹, Luigi Venetucci¹, Gina Galli¹

¹*Division of Cardiovascular Sciences, School of Medical Sciences, University of Manchester, Manchester, M13 9NT, United Kingdom*

INTRODUCTION: Catecholaminergic polymorphic ventricular tachycardia (CPVT) is an inherited arrhythmic condition defined by episodic syncope that occurs during intense emotion or exercise. CPVT is usually caused by mutations in the cardiac ryanodine receptor (RyR2) gene, and while some patients remain asymptomatic into adulthood, others develop the disease during childhood, which suggests environmental factors can influence disease progression. However, to our knowledge, no one has considered the role of the maternal environment in programming CPVT outcomes. Recent data from our laboratory suggests that ventricular arrhythmia sensitivity can be programmed during fetal development by exposure to hypoxia. Therefore, we hypothesised that fetal hypoxia increases disease severity in individuals with a CPVT mutation.

METHOD: RyR2-R2474S knock-in male mice were bred with wild-type C57BL/6NRj female mice. Pregnant mice were either subjected to normoxic (21% O₂, n = 10) or hypoxic (13% O₂, n = 5) conditions from gestational day (GD) 6-18. From this experimental design, four groups were established - (1) Wild Type Normoxia (WT-N), (2) RyR2 normoxia (RyR2-N), (3) Wild Type Hypoxia (WT-H) and (4) RyR2 Hypoxia (RyR2-H). Maternal weight, food and water intake were monitored during the incubations, as well as offspring litter size, sex split and body weight from birth to 16 weeks. Ventricular electrical mapping was used to investigate offspring arrhythmia sensitivity at 16 weeks using programmed electrical stimulation.

RESULT: There were no significant differences in maternal body weight, food intake or water intake between the normoxic and hypoxic offspring. Furthermore, no significant relationship was found between litter size, sex split, individual offspring body weight, and litter weight between the experimental groups. The initial data suggests that fetal hypoxia and CPVT mutation both increase the likelihood of arrhythmia under programmed electrical stimulation, but there was no significant interaction between these factors.

CONCLUSION: At this preliminary stage, we show that hypoxia had no significant effect on maternal and fetal parameters in either wild-type or CPVT mutants, suggesting no overt morphological effects of either treatment. The electrical mapping showed that arrhythmia sensitivity is increased by fetal hypoxia or CPVT mutation, but no interaction was observed between these factors. However, data should be interpreted cautiously because of a low sample size (n = 4-7 offspring). Therefore, future work will increase the sample size to fully ascertain whether exposure to fetal hypoxia can influence cardiovascular outcomes in CPVT mutants.

PCB011

Peripheral vascular adaptations to high-intensity interval training in patients with COPD

Jacob Peter Hartmann^{1,2,3}, Stine Nymand¹, Helene Louise Hartmeyer¹, Camilla Ryrso^{1,2}, Milan Mohammad¹, Iben Rasmussen¹, Amalie Bach Andersen¹, Rie Skovly Thomsen¹, Jann Mortensen³, Ronan Martin Griffin Berg^{1,2,3,4}, Ulrik Winning Iepsen^{1,5}

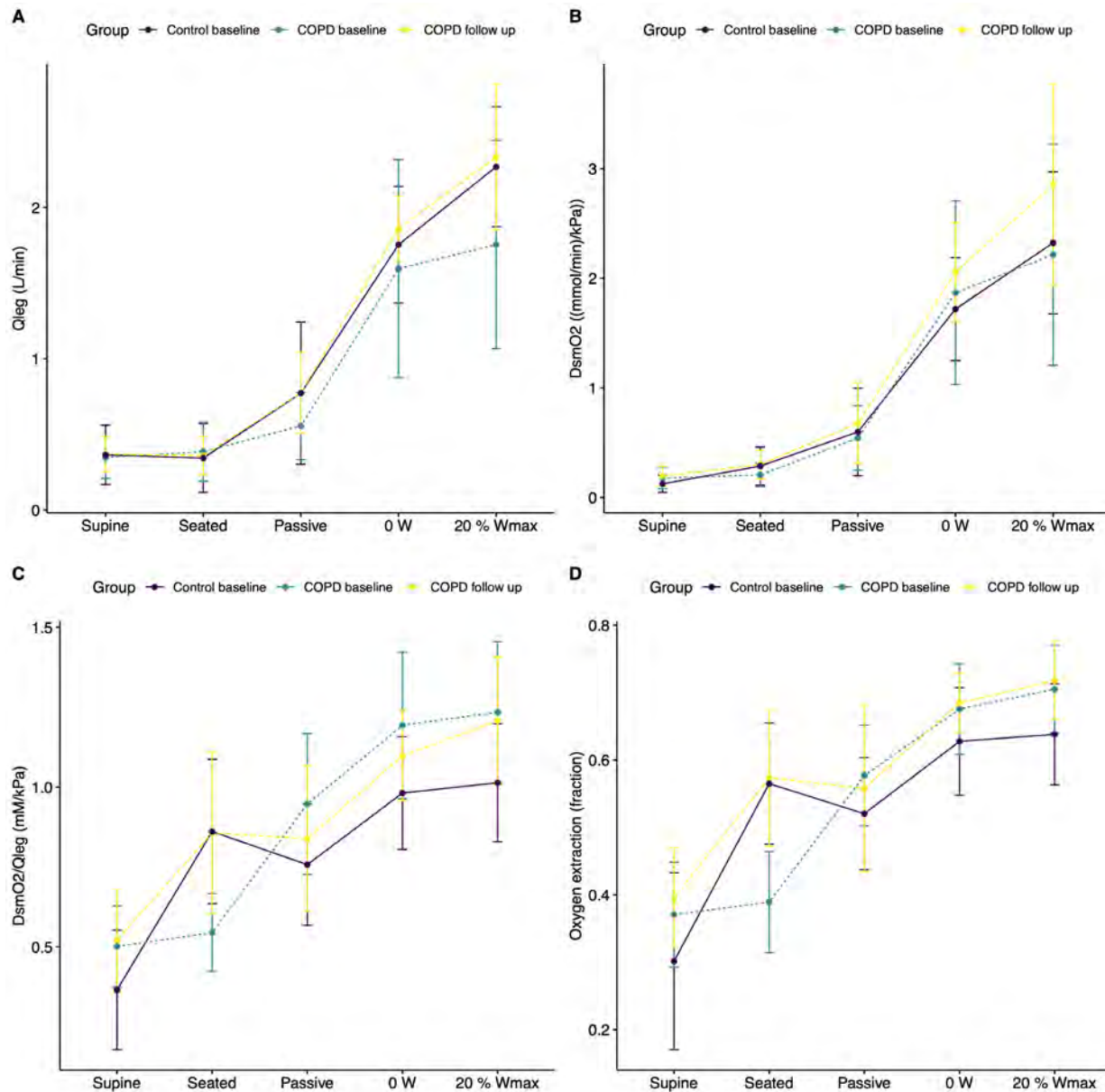
¹Centre for Physical Activity Research, Copenhagen University Hospital – Rigshospitalet, Copenhagen, Denmark, ²Department of Biomedical Sciences, Faculty of Health and Medical Sciences, University of Copenhagen, Copenhagen, Denmark, ³Department of Clinical Physiology and Nuclear Medicine, Copenhagen University Hospital – Rigshospitalet, Copenhagen, Denmark, ⁴Neurovascular Research Laboratory, Faculty of Life Sciences and Education, University of South Wales, Pontypridd, United Kingdom, ⁵Department of Anaesthesiology and Intensive Care, Copenhagen University Hospital, Hvidovre Hospital, Copenhagen, Denmark

Aim: Patients with chronic obstructive pulmonary disease (COPD) exhibit markedly diminished exercise capacity, particularly in advanced stages, hindering their ability to perform routine activities of daily living. Previous studies have shown that skeletal muscle convective and diffusive O₂ transport mechanisms play pivotal roles as peripheral determinants of exercise capacity in COPD (1, 2). This study aims to investigate whether a 12w high-intensity interval training (HIIT) intervention could reverse some of the peripheral alterations observed in patients with COPD when compared to healthy, matched controls.

Methods: Eight patients diagnosed with mild to severe COPD and eight healthy controls, untrained, matched for age, sex, and BMI, participated in this study. Baseline assessments were conducted, and the COPD patients followed by a 12-week HIIT intervention, which consisted of three weekly sessions, each comprising a 40-minute 4x4 HIIT protocol on a bicycle ergometer. Leg blood flow (\dot{Q}_{leg}) was assessed using Doppler ultrasound during submaximal single-leg knee-extensor exercise (KEE), with arterio-venous variables sampled across the leg. Reconstruction of the capillary oxyhaemoglobin dissociation curve was performed utilizing paired femoral arterial-venous O₂ tensions and saturations for the assessment of microvascular oxygenation, including skeletal muscle O₂ conductance ($D_{sm}O_2$) and its correction for flow ($D_{sm}O_2/\dot{Q}_{leg}$) to differentiate convective from diffusive O₂ transport.

Results: The COPD and control group were similar in height, sex, and BMI, but the COPD group had more pack years ($p=0.0001$) as well as a lower FEV₁ ($p=0.002$) and diffusion capacity ($p=0.008$). While resting values were similar, COPD patients had a higher $D_{sm}O_2/\dot{Q}_{leg}$, but a lower \dot{Q}_{leg} during KEE (**Figure 1**). After the HIIT intervention in COPD patients, the \dot{Q}_{leg} increase to KEE became more pronounced (428; 156 to 811 mL/min, $p=0.01$), but with similar O₂ extraction and arterio-venous difference levels compared to pre-intervention ($p=0.43$). This led to a significantly higher $D_{sm}O_2$ to KEE compared to pre-intervention (0.65; 0.16 to 1.12 (mmol/min)/kPa, $p=0.01$), but with a similar change in $D_{sm}O_2/\dot{Q}_{leg}$ (0.02; -0.18 to 0.13 (mM/kPa), $p=0.7$) (**Figure 1**).

Conclusion: The diminished convective O_2 transport response observed in working muscle of COPD patients can be enhanced by a 12-week HIIT intervention, so that it becomes similar to that of healthy untrained individuals without COPD. In contrast, the skeletal muscle diffusive O_2 transport response in working muscle appears to be unaffected by the intervention, indicating limited skeletal muscle microvascular adaptations in COPD.



1. Hartmann JP, Dahl RH, Nymand S, Munch GW, Ryrsø CK, Pedersen BK, Thaning P, Mortensen SP, Berg RMG, Iepsen UW. Regulation of the microvasculature during small muscle mass exercise in chronic obstructive pulmonary disease vs. chronic heart failure. *Front Physiol* 13, 2022. doi: 10.3389/fphys.2022.979359. 2. Broxterman RM, Wagner PD, Richardson RS. Exercise training in COPD: Muscle O_2 transport plasticity. *European Respiratory Journal* 58, 2021. doi: 10.1183/13993003.04146-2020.

PCB012

Circadian rhythms in the electrophysiology and pro-arrhythmic activity of pulmonary vein cardiomyocytes

Andrew F. James¹, Laura M.K. Pannell¹, Alexander Carpenter¹, Francisca Segers², Yi Zhe Koh¹, Stephen C. Harmer¹, Hugh D. Piggins¹, Jules C. Hancox¹

¹*School of Physiology, Pharmacology & Neuroscience, University of Bristol, Bristol, BS8 1TD, United Kingdom,* ²*Bristol Genomics Facility, School of Biological Sciences, University of Bristol, Bristol, BS8 1TQ, United Kingdom*

Episodes of atrial fibrillation (AF) in patients are more prevalent at night, and cardiomyocytes in the pulmonary vein (PV) sleeves are a major source of ectopic activity driving AF. While it is known that circadian clocks within heart muscle cells contribute to the control of pacemaking and ventricular repolarisation, the mechanisms underlying the nighttime preponderance in AF are unknown. We aimed to address the hypothesis that circadian clocks exist within PV cardiomyocytes, controlling their electrophysiology and susceptibility to pro-arrhythmic activity. Animal procedures were approved by the University of Bristol Animal Welfare and Ethics Review Board and conducted in accordance with UK law. Male Wistar rats were maintained in a 24-hour cycle of 12-hr light/dark (lights-on at Zeitgeber time, ZT=0; lights-off, ZT12) and hearts were removed at ZT=0, 6, 12 or 18 hr under terminal general anaesthesia (140 mg/kg Na pentobarbital i.p.). RNA was extracted from left atrial (LA) appendage (LAA) and proximal PV at the LA/PV junction (3 rats per ZT) and RNA sequencing conducted. Reads were mapped to the rat genome, counts normalised and models in which ZT was or was not included as a factor compared (Likelihood Ratio Test, adjusted- $P < 0.01$). Whole-cell current clamp recordings were made from cardiomyocytes isolated from the proximal PV ($n=308$) and the LAA ($n=264$) ($N=74$ rats). The effects of noradrenaline (NA, 1 μ M) and acetylcholine (ACh, 1 μ M) were examined. Data were plotted against the ZT of the time of recording and fitted to a sine wave to establish circadian rhythmicity ($P < 0.05$, extra-sum-of-squares F-test). The effect of ≥ 24 hr constant dark in the period immediately before experiment was examined. Data are reported as mean \pm standard error. The expression of 1368 genes varied significantly with ZT, including circadian clock components (e.g. *Bmal1*). PV cells were larger than LAA cells (73 ± 1.6 pF vs 53 ± 1.3 pF, $P < 0.0001$) and had more depolarised resting membrane potential (-69 ± 0.2 mV vs -72 ± 0.1 mV, $P < 0.0001$). Both cell types showed circadian variation in action potential duration at 90% repolarisation (APD₉₀) and frequency of pro-arrhythmic activity. Pro-arrhythmic activity was greatest in PV cells and the frequency was greater during the rest phase (ZT0-12) in both cell types. In contrast, the circadian rhythm in APD₉₀ differed between cell type, with the longest APD₉₀ recorded during the resting phase in PV cells (ZT12-24) but during the active phase in LAA cells. Pro-arrhythmic activity was increased by NA and decreased by ACh in both cell types, with the maximal effect of either neurotransmitter during the rest phase. Circadian variation in APD₉₀ and proarrhythmic-activity has been demonstrated in isolated proximal PV and LAA cardiomyocytes, with differences in rhythm between the two cell types. RNA sequencing suggests the presence of peripheral clocks in LAA and PV cardiomyocytes. Understanding circadian rhythms in the pro-arrhythmic activity of PV cardiomyocytes is likely to be valuable in the development of future therapeutic options for AF.

PCB013

Doppler ultrasound-based leg blood flow assessments during single-leg knee-extensor exercise in patients with chronic obstructive pulmonary disease vs. healthy controls: a test-retest reliability study

Milan Mohammad^{1,2,3}, Jacob Hartmann^{3,4}, Amalie Andersen⁴, Helene Hartmeyer¹, Ulrik Iepsen^{1,5}

¹Centre for Physical Activity Research, Copenhagen University Hospital – Rigshospitalet., Copenhagen, Denmark, ²Department of Biomedical Sciences, Faculty of Health and Medical Sciences, University of Copenhagen., Copenhagen, Denmark, ³Department of Clinical Physiology and Nuclear Medicine, Copenhagen University Hospital – Rigshospitalet., Copenhagen, Denmark, ⁴Centre for Physical Activity Research, Copenhagen University Hospital – Rigshospitalet, Copenhagen, Denmark, Copenhagen, Denmark, ⁵Department of Anaesthesiology and Intensive Care, Copenhagen University Hospital, Hvidovre Hospital, Copenhagen, Denmark

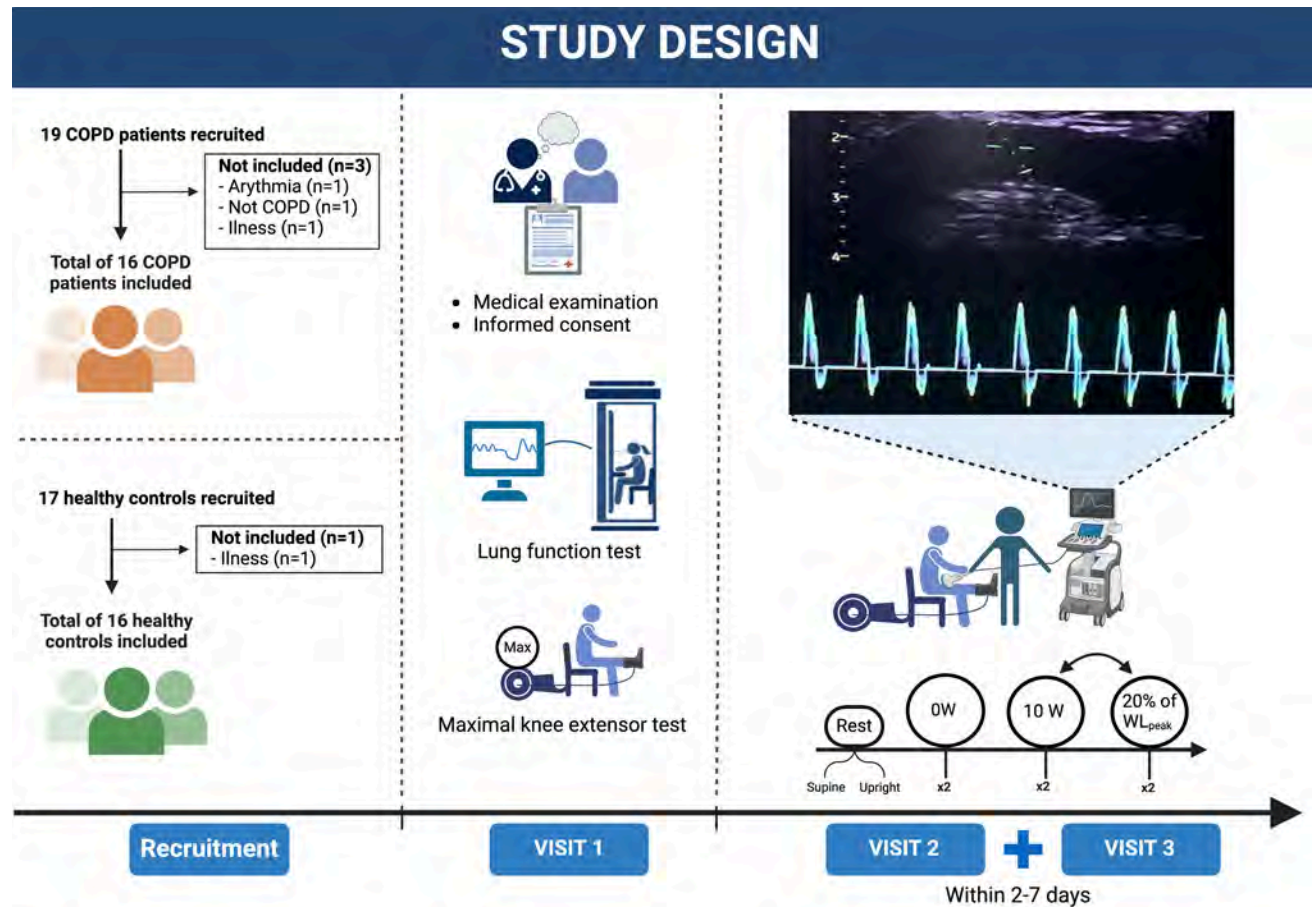
Introduction: Patients with chronic obstructive pulmonary disease (COPD) exhibit markedly diminished exercise capacity. Studies have shown that skeletal muscle leg blood flow (\dot{Q}_{leg}) plays an important role as a peripheral determinant of exercise capacity (1, 2). Doppler ultrasound may be used to assess \dot{Q}_{leg} both at rest and during exercise. However, the reliability of this method remains unknown when applied to patients with chronic obstructive pulmonary disease (COPD).

Objectives: This study aimed to investigate the within-day and between-day reliability of Doppler ultrasound in quantifying \dot{Q}_{leg} during single-leg knee-extensor exercise in COPD patients and compare these measurements with those obtained from healthy matched controls.

Methods: In this case-control study, 16 participants with COPD were matched based on sex and age with 16 healthy controls. All participants underwent measurement of \dot{Q}_{leg} using Doppler ultrasound in a single-leg knee-extensor setup at various intensities on two separate visits (Figure 1). Influential factors on \dot{Q}_{leg} were controlled for, and the ultrasound scans were consistently performed by the same sonographer. The study was approved by the Regional Ethical Committee of the Capital Region of Denmark (file no. H-23049997) and performed according to the most recent guidelines of the Declaration of Helsinki. All participants provided oral and written informed consent prior to enrolment. The study was registered on ClinicalTrials.gov (ID: NCT06135701).

Results: Results indicated a high within-day and acceptable to high between-day reliability for Doppler ultrasound measurements in both COPD patients and controls. Coefficient of variance ranged from 2.9 % to 10 % for within-day and 7.9 % to 20.4 % for between-day with small between-group differences in reliability estimates favouring the healthy control group. \dot{Q}_{leg} was similar between group at rest, but significantly lower in COPD during single-leg knee-extensor exercise.

Conclusion: Doppler ultrasound is a reliable tool for evaluating \dot{Q}_{leg} in both COPD patients and healthy individuals. Furthermore, the findings of this study offer novel insights into the peripheral circulatory constraints experienced by COPD patients during exercise, as evidenced by consistently diminished leg blood flow when compared to their healthy control.



1. Hartmann JP, Dahl RH, Nymand S, Munch GW, Rysø CK, Pedersen BK, Thaning P, Mortensen SP, Berg RMG, Iepsen UW. Regulation of the microvasculature during small muscle mass exercise in chronic obstructive pulmonary disease vs. chronic heart failure. *Front Physiol* 13, 2022. doi: 10.3389/fphys.2022.979359. 2. Broxterman RM, Wagner PD, Richardson RS. Exercise training in COPD: Muscle O₂ transport plasticity. *European Respiratory Journal* 58, 2021. doi: 10.1183/13993003.04146-2020.

PCB014

Impact of Air Pollution on the Cardiohepatic Transcriptome and Inflammation

Joseph Morris¹, Holly Shiels¹

¹*University of Manchester, Manchester, United Kingdom*

Air pollution is responsible for around 7 million deaths per year, with around half of these attributable to cardiovascular conditions. Pollution modelling in Greater Manchester identified a 1.4% increased incidence of ischaemic heart disease per 1 ug/m³ increase in PM_{2.5} concentration. Cardiotoxic polyaromatic hydrocarbons like phenanthrene are frequently found adsorbed to the surface of this inhalable fraction of PM. However, the source and impact of phenanthrene-induced inflammation on this cardiovascular dysfunction is unknown. Mice were exposed to environmentally relevant concentrations (3 ug/kg or 30 ug/kg) of phenanthrene by intraperitoneal injection every day for 6 weeks. Single nucleus RNA sequencing was carried out on liver samples of 12 (n=4) male mice to identify changes in expression of pro/anti-inflammatory genes. Thirteen distinct cell populations were identified via UMAP clustering, including a population subset seen only in mice exposed to the high dose of phenanthrene. In this subset, pro-inflammatory genes like LCN, Syt12, TERC, CYP4a31 and APCS were significantly overexpressed by scores of 51.2, 28.8, 17.0, 15.8 and 15.7 respectively. Further RNA velocity analysis in the high dose phenanthrene group suggests rapid differentiation of 'neutral' cell types into inflammatory subsets. Initial cytokine panel analysis identified dose-dependent increases in plasma and liver of potent Th2-related cytokines like IL-16 and IL-33, although not significant. Together, these findings demonstrate the range of effects phenanthrene has on the immune system, and subsequently, the cardiovascular system.

PCB015

Capillary dysfunction is associated with impaired neurovascular coupling after ischemic stroke

Christian Staehr^{1,2}, John T. Giblin¹, Eugenio Gutiérrez-Jiménez³, Halvor Ø. Guldbrandsen², Shaun L. Sandow⁴, David A. Boas¹, Vladimir V. Matchkov²

¹Neurophotonics Center, Dept. Biomedical Engineering, Boston University, Boston, United States,

²Dept. Biomedicine, Aarhus University, Aarhus, Denmark, ³CFIN, Aarhus University, Aarhus,

Denmark, ⁴Biomedical Science, School of Health, University of the Sunshine Coast, Sippy Downs, Australia

Introduction: Neurovascular coupling, as the local hyperemic response to neuronal activity, is impaired in peri-ischemic brain regions after stroke, with the mechanism being poorly understood. The mechanism is important for the control of brain blood flow, and its dysfunction after stroke, where reduced neurovascular coupling may contribute to futile reperfusion, as poor neurological outcome despite successful recanalization. Understanding these mechanisms is therefore critical for the development of targeted therapy.

Objective: The study aimed to assess neurovascular responses and capillary perfusion in the peri-ischemic area before stroke and after ischemia reperfusion. It was hypothesized that impaired neurovascular coupling in the peri-ischemic area is associated with disrupted capillary microcirculation.

Methods: Mice implanted with chronic cranial windows were trained for awake head-fixation prior to experiments. One-hour occlusion of the anterior middle cerebral artery branch was induced using single vessel photothrombosis. Cerebral perfusion and neurovascular coupling were assessed by optical coherence tomography and laser speckle contrast imaging. Capillaries and pericytes were studied in perfusion-fixed tissue by labelling lectin and platelet-derived growth factor receptor β .

Results: Arterial occlusion induced on average 11 spreading depressions over one hour associated with substantially reduced blood flow in the peri-ischemic cortex. Approximately half of the capillaries in the peri-ischemic area were no longer perfused after reperfusion (45% [95% CI, 33%, 58%] and 53% [95% CI, 39%, 66%] reduction in number of perfused capillaries at 3- and 24-hour follow-up, respectively; $P < 0.0001$, $n = 6$), which was associated with a reduced diameter of capillaries surrounded by pericytes. The capillaries in the peri-ischemic cortex that remained perfused showed an increased prevalence of flow stalling (0.5% [95% CI, 0.2%, 0.7%] at baseline, 5.1% [95% CI, 3.2%, 6.5%] and 3.2% [95% CI, 1.1%, 5.3%] at 3- and 24-hour follow-up, respectively; $P < 0.001$, $n = 6$). Blood flow velocity in the capillaries that remained perfused was similar to baseline at the 3-hour follow-up but increased at the 24-hour follow-up compared with baseline (1.16 mm/sec [95% CI, 1.08, 1.24 mm/sec] at baseline, and 1.29 mm/sec [95% CI, 0.97, 1.63 mm/sec] and 1.62 mm/sec [95% CI, 1.44, 1.79 mm/sec] at 3- and 24-hour follow-up, respectively; $P < 0.05$, $n = 6$). Whisker stimulation led to reduced neurovascular coupling responses in the sensory cortex corresponding to the peri-ischemic region 3 and 24 hours after reperfusion compared with baseline (19.2% [95% CI, 16.3%, 22.5%] blood flow increase at baseline, 13.4%

[95% CI, 10.0%, 16.8%] at 3-hour follow-up, and 12% [95% CI, 9%, 15%] at 24-hour follow-up, $P < 0.001$, $n = 6$).

Conclusion. Arterial occlusion led to a reduced diameter of pericyte-surrounded capillaries in the peri-ischemic cortex associated with microcirculatory failure. This reduced capillary capacity may, at least in part, underlie impaired neurovascular coupling in peri-ischemic brain regions after reperfusion. Control and correction of capillary capacity may reduce the neurological dysfunction after stroke as a target for therapy.

Staeher, Christian et al. “Neurovascular Uncoupling Is Linked to Microcirculatory Dysfunction in Regions Outside the Ischemic Core Following Ischemic Stroke.” *Journal of the American Heart Association* vol. 12,11 (2023): e029527. doi:10.1161/JAHA.123.029527

PCB016

The Long-Term Impact of Vaping on Brachial Artery Blood Flow Responses to Exercise

Mared Tomkinson¹, Maddie Roscoe¹, Rhiannon Price-Wickenden¹, Cory Richards², Thomas Griffiths², Zoe Adams², Lydia Simpson¹, Rachel Lord², Ben Chant¹, Emma Hart¹

¹University of Bristol, Bristol, United Kingdom, ²Cardiff Metropolitan University, Cardiff, United Kingdom

Electronic cigarette use (e-cigarettes) has surged in popularity over the last decade particularly among young adults. Despite perceptions of reduced harm compared to traditional tobacco cigarettes, studies suggest that e-cigarette use may have adverse impacts on cardiovascular health, comparable to those of tobacco smoking. Understanding the impact of vaping on brachial artery blood flow responses to exercise is crucial for evaluating its impact on endothelial function, a biomarker for cardiovascular disease. This study aims to investigate brachial artery blood flow and diameter responses to dynamic handgrip exercise (DHG) in a vaping group compared to a non-vaping control group. This study had ethical approval from the University of Bristol (17598) and conformed to the Declaration of Helsinki. Fourteen healthy, non-tobacco smokers were recruited. Six participants (4 males) were regular e-cigarette users (vaping group; defined as ≥ 5 days per week > 6 months) and 8 (5 males) were non-users who have never used e-cigarettes or tobacco products (non-vaping control group). The vaping group were asked not to vape before attending the study visit. After a 2-min baseline, DHG was performed at 40% maximal voluntary contraction (MVC) for 4 minutes, at 20 contractions/minute, followed by a 2-min recovery period. Brachial artery blood flow and diameter were measured continuously using vascular ultrasound via a (12-Hz Doppler probe with an insonation angle of 60° over the brachial artery). Blood pressure (Finapres) and heart rate (3-lead ECG) were measured continuously throughout the protocol. Brachial artery diameter and mean blood flow were calculated via synchronised Doppler waveform envelope analysis, edge detection, and wall-tracking of high-resolution B-mode arterial ultrasound images. Absolute and change from baseline values were analysed over 30s increments. Brachial vascular conductance was calculated as flow (mL/min) / mean arterial pressure (mmHg). The change in brachial blood flow and conductance from rest to the final 30 seconds of handgrip exercise were compared using an unpaired t-test. Data are mean \pm SD. There were no differences in age (controls; 22 ± 1.5 years vs. vapers; 22 ± 1.4 years, $P=0.4467$) or body mass index (23.3 ± 2.1 kg/m² vs. 22.6 ± 3.8 kg/m², $P=0.6284$). There was no difference in the change in blood flow from rest to exercise between controls and vapers ($\Delta 359 \pm 176$ mL/min vs. 291 ± 201 mL/min, $P=0.2448$). However, there was a large effect of vaping on brachial vascular conductance, where controls had a larger change from rest to exercise vs. vapers ($\Delta 4.0 \pm 1.6$ mL/min/mmHg vs 2.6 ± 1.5 mL/min/mmHg, $P=0.0544$, Cohen's d (effect size)=0.90). Vaping potentially impacts vasodilator response to exercise but needs further research.

PCB017

The cardioselective beta1-adrenergic receptor antagonist, bisoprolol, inhibits isoprenaline-induced relaxation of human chorionic plate arteries

Teresa Tropea^{1,2}, Paul Brownbill^{1,2}, Anthony M. Heagerty³, Jenny E. Myers^{1,2}

¹Maternal & Fetal Health Research Centre, University of Manchester, Manchester, United Kingdom,

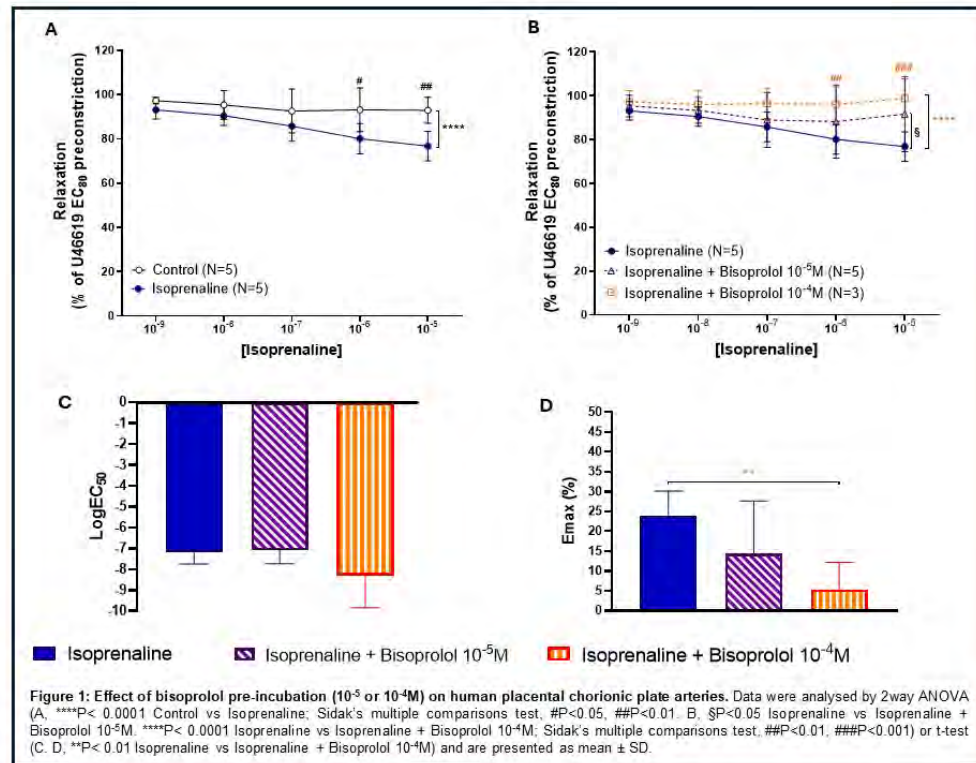
²St Mary's Hospital, Manchester University Hospital NHS Foundation Trust, Manchester, United Kingdom, ³Division of Cardiovascular Sciences, University of Manchester, Manchester, United Kingdom

Introduction: The placenta is a low-resistance vascular organ that provides an efficient maternal-fetal exchange system for oxygen and nutrients. The cardioselective beta1-adrenergic receptor antagonist, bisoprolol, is commonly prescribed to women with pre-existing cardiac disease to improve maternal stroke volume and cardiac output during pregnancy. Clinical evidence of decreased umbilical blood flow velocity and increased rate of low-birth-weight babies in women exposed to bisoprolol [1] raises safety concerns. Although the placenta is devoid of innervation, we hypothesised that bisoprolol may alter placental perfusion via a direct effect on beta-adrenergic receptors in isolated human placental chorionic plate arteries (CPAs).

Methods: CPAs (<500µm diameter) were dissected from biopsies of uncomplicated term placentas (N=3-5). Using wire myography, concentration-dependent effects of the non-selective beta-adrenergic receptor agonist isoprenaline (10^{-9} - 10^{-5} M) were tested on CPAs pre-incubated with bisoprolol (10^{-5} M and 10^{-4} M) and pre-constricted with an EC₈₀ dose of U-46619. Sensitivity was evaluated as the molar concentration of isoprenaline causing 50% of the maximal effect (Emax) and expressed as logarithm.

Results: Isoprenaline caused significant relaxation of CPAs in a dose-dependent manner ($P<0.0001$, Figure 1A). The relaxant effect of isoprenaline was significantly reduced after pre-incubation with bisoprolol 10^{-5} M ($P<0.05$, Figure 1B) and was abolished by blockade with bisoprolol 10^{-4} M ($P<0.0001$, Figure 1B). Maximum relaxation to isoprenaline was significantly reduced by bisoprolol 10^{-4} M (Emax, $P<0.01$; 24.01 ± 6.09 vs $5.21 \pm 6.94\%$, Figure 1C), whereas the sensitivity was not different between the two groups ($P=0.800$, -7.178 ± 0.56 vs -8.316 ± 1.53 LogEC₅₀; isoprenaline vs isoprenaline + bisoprolol 10^{-4} M).

Conclusions: These data show non-selective functional activation and inhibition of beta-adrenergic receptors on CPAs. The increased inhibitory effect of bisoprolol at supraphysiological concentration (10^{-4} M) tested on isoprenaline-induced relaxation may suggest potential off target beta1 blockade effects. Further study is needed to determine the functional role of beta-adrenergic receptors on the fetoplacental vasculature and to identify the relationship between actions mediated by maternal plasma levels of bisoprolol on CPAs and placental perfusion.



[1] Ormesher, L., et al., Prevalence of pre-eclampsia and adverse pregnancy outcomes in women with pre-existing cardiomyopathy: a multi-centre retrospective cohort study. Sci Rep, 2023. 13(1): p. 153.

PCB018

Sodium-Glucose Cotransporter-2 Inhibition Prevents Development of Left Ventricular Hypertrophy

Anna Vingborg¹, Vladimir Matchkov¹, Markus Rinschen^{1,2,3,4}, Tina Pedersen¹, Elina Kovalenko¹

¹Department of Biomedicine, Aarhus University, Aarhus, Denmark, ²III Department of Medicine and Hamburg Center for Kidney Health, University Medical Center Hamburg-Eppendorf, Hamburg, Germany, ³Scripps Research, Center for Metabolomics, San Diego, California, United States, ⁴Aarhus Institute of Advanced Studies, Aarhus University, Aarhus, Denmark

Introduction

More than 64 million people suffered from heart failure worldwide in 2017, and this number is expected to be growing (1). Originally, sodium-glucose cotransporter-2 (SGLT2) inhibitors were used to treat type 2 diabetes, but several clinical studies have demonstrated their significant beneficial effects in patients with heart failure independent of their diabetic status (2). The underlying mechanisms are unknown, but intensively investigated. A recent study proposes that a part of the cardioprotective mechanism is a result of SGLT2 inhibition-related improvements in metabolic communication reflecting in the kidney (3). However, heart morphology and function were not investigated. Nevertheless, changes in cardiac metabolism are suggested to promote heart failure development, including left ventricular hypertrophy (4).

We hypothesized that SGLT2 inhibitors may reduce severity of heart failure by preventing cardiac remodeling due to an improved cardiometabolic state.

Methods

33 BL57c6j male mice were randomly divided into the following 5 subgroups; I) mice on a normal diet, II) vehicle-treated mice on High Fat Diet (HFD); III) vehicle treated mice on HFD receiving N-nitro-1-arginine methyl ester (L-NAME, 600 mg/kg/day) in drinking water; IV) SGLT2 inhibitor-treated (dapagliflozin; 10 mg/kg diet (DAPA)) mice on HFD; and V) SGLT2 inhibitor-treated mice on HFD and L-NAME with all interventions lasting for 6-8 weeks. This combination of HFD and L-NAME was used to induce heart failure with preserved ejection fraction (5).

Blood pressure measurements and echocardiography were conducted before intervention and every 2nd week during the intervention period.

The protocol was conducted in accordance with the animal experiment permissions from the Danish Ministry of Food, Agriculture and Fisheries.

Data were analyzed using mixed-effects model followed by Tukey post-test for multiple comparison (GraphPad Prism 10.2.1). Data are presented as means ± standard errors of the means, P<0.05 is considered statistically significant.

Results

L-NAME increased mean arterial pressure in both groups receiving HFD and HFD+DAPA. Six weeks after intervention, mean arterial pressure was 91 ± 4 , 118 ± 6 , 89 ± 2 and 122 ± 6 mmHg ($n=4-5$, $P=0.0004$) in HFD, HFD+L-NAME, HFD+DAPA and HFD+DAPA+L-NAME, respectively. An increased heart rate by L-NAME was also observed in the group receiving HFD (588 ± 9 BPM), but the effect was absent in the HFD+DAPA-group (545 ± 16 BPM).

No difference was observed between the groups in stroke volume, ejection fraction, fractional shortening and cardiac output. However, the left ventricular mass was increased in the groups receiving HFD and HFD+L-NAME but this was prevented in both groups receiving DAPA (Figure 1).

Conclusion

Our results suggest that one of the mechanisms underlying SGLT2-inhibitor-related cardiac protection is its ability to reduce the development of left ventricular hypertrophy, which is a known part in the pathogenesis of heart failure.

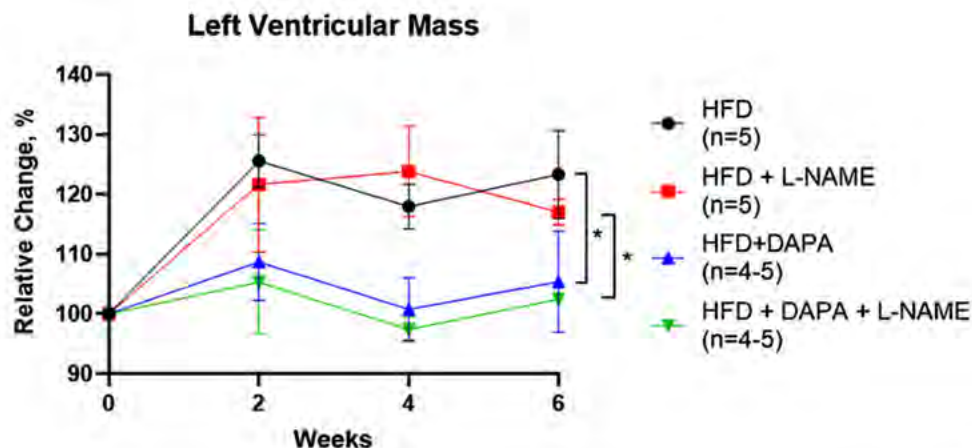


Figure 1: Left ventricular mass presented as relative changes over weeks of interventions ($n=4-5$). *, $P < 0.05$

1. Savarese G, Becher PM, Lund LH, Seferovic P, Rosano GMC, Coats AJS. Global burden of heart failure: a comprehensive and updated review of epidemiology. *Cardiovasc Res.* 2023;118(17):3272-87.
2. Zou X, Shi Q, Vandvik PO, Guyatt G, Lang CC, Parpia S, et al. Sodium-Glucose Cotransporter-2 Inhibitors in Patients With Heart Failure : A Systematic Review and Meta-analysis. *Ann Intern Med.* 2022;175(6):851-61.
3. Billing AM, Kim YC, Gullaksen S, Schrage B, Raabe J, Hutzfeldt A, et al. Metabolic Communication by SGLT2 Inhibition. *Circulation.* 2024;149(11):860-84.
4. Nakamura M, Sadoshima J. Mechanisms of physiological and pathological cardiac hypertrophy. *Nat Rev Cardiol.* 2018;15(7):387-407.
5. Schiattarella GG, Altamirano F, Tong D, French KM, Villalobos E, Kim SY, et al. Nitrosative stress drives heart failure with preserved ejection fraction. *Nature.* 2019;568(7752):351-6.

PCB019

A Single Session of Combined 4-7-8, Box and Pursed Lip Breathing Patterns Reduces Blood pressure and Heart Rate at Rest and After Exercise

Basheer Waziri¹, Fatima Saleh Barau², Nafisa Y. Wali³

¹Cardiovascular & Molecular Unit, Department of Human Physiology, Bayero University, Kano, Nigeria, ²Department of Human Physiology, Bayero University, Kano, Nigeria, ³Endocrine Physiology Unit, Department of Human Physiology, Bayero University, Kano, Nigeria

Introduction: Various breathing exercises promote relaxation, reduce blood pressure and heart rate. However, findings from existing literature indicated that some of these exercises have more effect on systolic blood pressure (SBP), some on diastolic blood pressure (DBP) and some lower blood pressure only but not heart rate (HR). Some studies reported no immediate effect on SBP, DBP and Heart rate following breathing exercise. It is unclear whether combining different breathing exercises at a time have an immediate positive effect on SBP, DBP, HR and peripheral oxygen saturation (SPO2) at rest and after exercise and whether the combination has more effect than individual techniques. **Aim:** The purpose of this study was to investigate immediate effect of combining 4-7-8, Box and Pursed lip breathing patterns at a time on SBP, DBP, HR and SPO2 at rest and after exercise. **Method:** Following ethical approval (ref: SHREC/2024/4721) by the Health Research Ethics Committee, Kano State Ministry of Health, Kano Nigeria, eighty healthy young adults (18 – 25 years) with normal BMI (Mean \pm SE: 20.72 ± 0.19) were recruited into the study. HR, SBP, DBP and SPO2 of the participants were recorded at rest and after one session of combined 4-7-8, box and pursed lip breathing patterns. The participants were then divided into two groups, intervention and control groups, both performed five minutes of fast walking (using a treadmill speed of 4-mph). At the end of this exercise, the intervention group performed the same pattern of combined breathing exercise as described above. HR, SBP, DBP and SPO2 of the participants from the two groups were recorded at exactly one-minute after fast walking. IBM SPSS version 26 was used for data analysis, paired t-test was used to compare the baseline variables recorded before and after breathing exercise while independent t-test was used to compare variables between the two groups recorded after exercise. **Results:** A significant decrease in resting HR, SBP and DBP was recorded after one session of combined 4-7-8, box and pursed lip breathing patterns (Mean \pm SE: HR $82.26 \pm 1.33 - 79.05 \pm 1.40$, $p=0.001$; SBP $114.42 \pm 1.24 - 109.94 \pm 1.14$, $p=0.001$; DBP $80.44 \pm 1.06 - 76.51 \pm 1.03$, $p=0.01$). No significant change in SPO2 was observed ($p=0.35$). Independent t-test revealed significantly lower HR, SBP and DBP (82.04 ± 1.39 , 117.18 ± 1.36 and 80.11 ± 1.16) in the intervention group than in the control group (89.61 ± 1.38 , 124.21 ± 1.35 and 84.07 ± 1.28). The decline in HR was significantly higher with the combine pattern than with individual technique (Mean \pm SE: Combine, 7.58 ± 1.08 ; individual, 4.90 ± 0.83 ; $p=0.02$). **Conclusion:** One session of combined 4-7-8, box and Pursed lip breathing caused immediate decrease in HR, SBP and DBP at rest and after exercise. Furthermore, the combine pattern was more effective in lowering heart rate after exercise than individual technique.

PCB020

Effect of short-term culture on t-tubule structure and L-type Ca current in adult cardiac ventricular myocytes.

Kester EJ Young¹, Stephen C Harmer¹, Cherrie HT Kong¹, Laura MK Pannell¹, Andrew F James¹

¹*University of Bristol, Bristol, United Kingdom*

Introduction:

T-tubules (TTs) are invaginations of sarcolemma in cardiomyocytes important in excitation-contraction coupling. Mechanisms underlying the genesis and maintenance of TTs are poorly understood, but their loss in disease states contributes to the pathogenesis of heart failure and arrhythmia. Short-term culture of cardiac myocytes may provide a model system to study mechanisms underlying the maintenance of TT function.

Aims:

To examine changes in TTs and L-type calcium current (ICa) in adult rabbit ventricular myocytes (ARVMs) in short-term culture.

Method:

ARVMs were isolated from hearts of adult male rabbits and cultured on laminin-treated borosilicate glass coverslips for up to four days. TTs were identified by confocal imaging using Alexa-680-conjugated wheat germ agglutinin (WGA) and quantified by fast Fourier transform analysis ('TT-power'). Juncophilin-2 (JPH2) staining was examined by immunofluorescence on the day of isolation (day 0) and following 4 days in culture (day 4). ICa was recorded from ARVMs at 37 °C using the whole-cell patch clamp technique on days 0, 1, 2 and 4. Response to 100 nM of the β -adrenoceptor agonist, isoprenaline (ISO), was examined in currents activated by depolarisation to 0 mV. Current densities were calculated as currents normalised to whole-cell capacitance, as an index of cell surface area. Data are reported as mean \pm standard error and sample sizes as n cells/N animals. ICa density-voltage relations were plotted and fitted with Equation 1:

$$ICa = (Gmax(Vm - Vrev)/(1 + e^{(Vm - Vhalf)/k})),$$

where *Gmax* = maximal conductance density for ICa, *Vm* = command potential, *Vrev* = effective reversal potential for the current, *Vhalf* = voltage of half-maximal activation and *k* = slope factor. Fits to ICa density-voltage relations on days in culture were compared by extra sum-of-squares F test (GraphPad Prism 10.2). Responses to ISO were quantified as percentage increases relative to control and compared across days in culture by Welch's one-way ANOVA).

Results:

Cultured ARVMs became more rounded and whole-cell capacitance decreased exponentially with a time constant of 1.68 days ($n/N = 16/3, 11/3, 18/5, 6/2$ for days 0,1,2 and 4). TT-power showed a threefold-reduction from day 0 to day 4 ($p = 0.001$, unpaired t-test, $n/N = 6/1$ and $4/1$). JPH2 staining intensity (AU) was significantly less at day 4 (25.5 ± 2.29 ; $n/N = 5/1$) compared to day 0 (36.1 ± 1.74 ; $n/N = 6/1$) of culture ($p = 0.0045$). At culture day 1, G_{max} fell from 0.36 ± 0.03 nS/pF to 0.21 ± 0.02 nS/pF, but then recovered to 0.25 ± 0.02 nS/pF at day 2 and by day 4 had recovered to 0.33 ± 0.05 nS/pF ($p < 0.0001$, $n/N = 11/3, 10/3, 13/5, 6/2$ for days 0,1,2 and 4). The response to 100 nM ISO was preserved across days in culture ($p = 0.91$, $n/N = 8/3, 6/3, 6/4, 3/2$ for days 0,1,2 and 4).

Conclusions:

Short-term culture of ARVMs was associated with loss of membrane surface area, loss of TT-power, reduced I_{Ca} density and reduced JPH2 staining, although responses to β -adrenoceptor stimulation were preserved. In future studies, we will use this experimental model to investigate mechanisms underlying loss of TTs and I_{Ca}.

PCB021

Diversifying laboratory assessment modes broadens engagement with practical competencies in life science students

Bernard Drumm¹, Ronan Bree¹, Caoimhin Griffin¹, Niall O'Leary²

¹Dundalk Institute of Technology, Dundalk, Ireland, ²University College Cork, Cork, Ireland

Laboratory practicals in life science subjects at many undergraduate institutions are traditionally assessed by written reports which reflect disciplinary norms of documenting experimental activities. Over the last 20 years, assessment of scientific laboratory classes has continued to diversify, with the sole use of report or research paper writing style assessments becoming increasingly less ubiquitous. Such alternative assessments include but are not limited to student reflections on skills obtained, poster presentation sessions on laboratory experiments and skills, drafting of grant proposals based on data obtained in laboratory practicals and various survey instruments designed to evaluate experimental design capability. However, over-reliance on reports can potentially promote rote learning and evaluate a narrow set of competencies. A commonly reported drawback of report writing is students struggle with placing experimental data in a wider context and find writing introductions and discussions tedious and challenging, to the point that students often revert to copy and paste exercises to fill out their reports. In this study, we explored how multiple modes of laboratory assessments (a group presentation, an online quiz and a written report) might affect student perceptions of learned skills in a life science module at Dundalk Institute of Technology, Ireland.

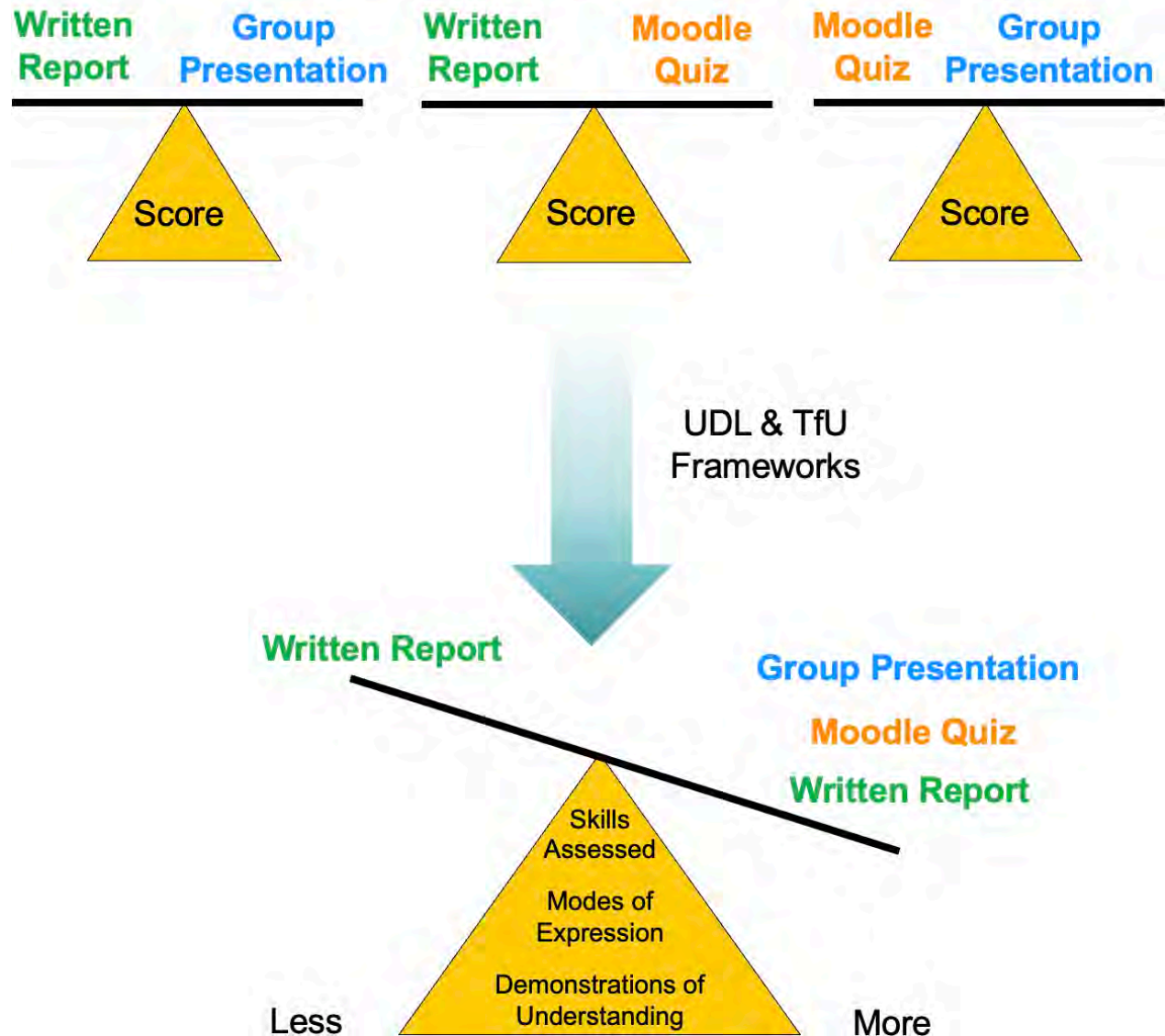
For this study, we aimed to address the following specific research questions:

1. In an undergraduate life science module that uses 3 different assessments (reports, online quizzes, group presentations), on average across a class, do students score higher in any of these assessment modes over another?
2. Do students perceive that different assessments (reports, online quizzes, group presentations) promote awareness of, and engagement with, a broad range of practical competencies?

This was informed by universal design for learning (UDL) and teaching for understanding (TfU) frameworks. Anonymous surveys collected over 3 consecutive years (2020-2022) with 66 total students, evaluated whether this expanded portfolio of assessments promoted awareness of, and engagement with, a broader range of practical competencies. Interestingly, when student scores were compared across the assessments, there was no significant difference between any comparisons in any year ($P > 0.05$, unpaired one-way ANOVA, Tukey test, $n=29$ for 2020, $n=13$ for 2021, $n=24$ for 2022). Survey data showed that aspects that influenced student preferences in assessment mode included time limitations, time investment, ability to practice new skills, links with lecture material and experience of assessment anxiety. In particular, presentations were highlighted as promoting collaboration and communication and the quiz as an effective means of diversifying assessment schedules. A key takeaway from students was that while reports were important, an over reliance on them was detrimental, as exemplified by one student *"I think that the three of these modes work well together. They provide different ways of learning that is not just*

the usual lab report”, also summarized in Figure 1. This study suggests that undergraduate life science students can benefit significantly from a holistic assessment strategy that complements reports with performance-based approaches that incorporate broader competencies and allow for greater student engagement and expression in undergraduate modules.

Effect of Diversifying Laboratory Assessment on Student Performance And Skills



"I think that the three of these modes work well together. They provide different ways of learning that is not just the usual lab report."

"The assessments worked well together, makes student take different approaches to learning."

"This module had great engagement out of all the other modules of third year. I found it kept me on my toes and I had to work hard but it was completely worth the effort. The different methods of assessment were good as they varied and were not boring. "

**Student
Voice**

Neurodiversity and the Physical Environment of the University - An undergraduate research project

Dawn Davies¹

¹University of Bristol, Bristol, United Kingdom

Neurodiversity can manifest in many different ways. One issue that many neurodivergent individuals face is hypersensitivity to sensory stimuli, for example auditory stimuli where decreased sound tolerance can lead to disabling features, including inability to concentrate. There is an increasing interest in designing spaces for a neurodiverse population with the understanding that a good environment for the neurodivergent will be good for all. Within the University, teaching spaces are often being refurbished. However, how much does the sensory environment and its effect on members of our community impact on the design criteria of these spaces? In this undergraduate project, third year life sciences students ran focus groups to understand the student experience of University spaces, with a particular focus on the sensory environment. This information was incorporated into a presentation to members of staff who are involved in decision making regarding building design. The aim was to increase awareness of criteria that should be included in those decisions. Data, gathered through pre- and post-presentation questionnaires, showed that the participants had gained knowledge of the issues and, importantly, that they would be interested in finding out more. In their dissertations, students combined this research with a review of the current understanding of the neural pathways involved in sensory hypersensitivity, appropriate to their degree programme. Student agency was key to the development of this project as they decided who to consult with to gather information. The resulting presentation highlighted the importance of design for inclusion, addressing a key challenge for higher education.

PCB024

Microscopy for Teaching Physiology: An Online Perspective

Katja Rietdorf¹, Mark Hintze¹, Francesco Crea¹, Martin Bootman¹

¹*The Open University, Milton Keynes, United Kingdom*

The Open University (OU) is a distance learning university that offering several STEM subjects as part of its curriculum. Within those courses, various aspects of physiology are taught through explanation and interactive content via the OU's virtual learning environment. This includes presenting numerous techniques as interactive screen experiments (ISEs) to around 400-500 students per course, allowing our students to gain experience of these techniques and explore the underlying theoretical concepts. The ISEs are primed with images and data that enable students to collect individualised data and generate independent reports and interpretations. Here, we present examples how we teach microscopy online at the OU.

In both Biology and Health Sciences modules, we use three digital microscopes: a digital light microscope for presenting micrographs after histological staining, a digital fluorescence microscope for immunofluorescence staining micrographs, and a digital transmission electron microscope to showcase ultrastructure images. These microscopes aid student learning by featuring a unified interface. Storing images within a database allows easy interchange of images, facilitating the use of the digital microscopes across different levels or subject areas.

The digital light microscope serves, for example, to teach cancer biology concepts by counting Ki67-positive cells and grading prostate cancers in patient-derived tissue samples. These examples highlight the impact of cancer on cell and tissue physiology and enhance the students' ability to visualise and understand core concepts around tissue structure-function relationships and gain an understanding in diagnostics. Similarly, the digital fluorescence microscope provides insights into the structure of organelles and alterations induced by diseases. Students can visualise, for instance, the changes in the Golgi apparatus due to spinal muscular atrophy or the variances in CFTR expression in cells with *CFTR* mutations. This interactive approach significantly enhances students' understanding of tissue structure-function relationships and diagnostic skills.

In another ISE students learn how to collect and analyse data from imaging experiments using the fluorescent mitochondrial membrane potential indicator TMRE. The images used within this ISE were obtained from fibroblasts of healthy individuals and patients with a lysosomal storage disorder. Students quantitate fluorescence intensity from mitochondria in regions of interest they choose and students learn about experimental design, application of statistics, as well as the broad changes in cell physiology caused by lysosomal dysfunction.

Using ISE means that our students can study asynchronously and remotely. In one such remote experiment, students measure cell proliferation or cell migration after pharmacological treatments they decide on. The experiment is running live at the OU campus in Milton Keynes, and students access the instrument remotely for their data collection.

Presentation of work carried out using these ISEs is integral to assessment in teaching modules, allowing for authentic assessment. The individualised data enables the re-use of assessment in successive presentations of a module with reduced concerns about plagiarism.

Although online microscopy does not replace the hands-on experience of using a microscope, our students appreciate that the ISEs are based on real data and allow them to participate as researchers in a laboratory through designing experiments, collecting information and producing reports.

PCB025

Remote STEM outreach improves STEM engagement.

Jamie Young¹, Sharon Parkinson¹, Etain Tansey¹

¹*Centre for Biomedical Sciences Education, Queen's University Belfast, Belfast, United Kingdom*

Background

STEM outreach initiatives aim to address the consistent decline of student interest in STEM which becomes increasingly apparent as students transition from primary to secondary school (1). Typically, outreach programmes are delivered in-person and require volunteers to travel to schools or students to travel to outreach sites. This takes time out of an already busy curriculum and can place students in less accessible locations at a disadvantage, e.g., rural students are already underperforming within STEM education when compared to their metropolitan counterparts (2). Remote/on-line delivery presents a possible alternative for STEM outreach programmes. The main advantage is greater accessibility and flexibility, enabling its use for a greater number of audiences. The aim of this study was to determine if remote delivery of STEM activities is a viable outreach alternative to in-person events.

Methods

As part of the STEM Ambassador Programme (<https://www.stem.org.uk>) and during the COVID-19 pandemic, secondary schools in Northern Ireland were approached to participate in an on-line STEM outreach activity suitable for students in Years 10-12 (ages 14-17). The activity consisted of an interactive presentation (40 minutes) covering the importance of a STEM education and then specifically the topics of genetics and inheritance. Pre-and post-presentation questionnaires were sent in advance to teachers. The anonymous questionnaires assessed students' understanding of STEM, knowledge of genetics and inheritance and opinions on remote delivery. A Likert scale was used to quantitatively analyse data related to student perceptions and aspirations (5 - strongly agree to 1 - strongly disagree). Data are presented as means \pm SEM. A Student's unpaired *t*-test assessed statistical significance ($p < 0.05$). Ethical approval was obtained through the Queen's University Belfast Research Ethics Committee.

Results

Four student groups completed the outreach activity from three different schools, completing both a pre-presentation questionnaire ($n=126$) and a post-questionnaire ($n=95$). Results from the pre- and post-questionnaires highlight that the STEM event produced a significant increase in student 1) knowledge of genetics and inheritance ($p \leq 0.0001$), 2) STEM awareness ($p \leq 0.001$) and 3) positive association with on-line learning ($p=0.01$). In one school with 2 separate cohorts, significant differences between year 10 and year 12 post-presentation responses were found with the older cohort more positively affected by the outreach than the younger cohort. This was evident in the categories of STEM awareness (4.3 ± 0.2 year 10 vs. 4.8 ± 0.2 year 12, $p=0.02$), perception of online learning (3.7 ± 0.2 year 10 vs. 4.1 ± 0.2 year 12, $p=0.03$) and student acquisition of knowledge (4.3 ± 0.5 year 10 vs. 5.3 ± 0.5 year 12, average correct answers, $p=0.03$).

Discussion

One of the ultimate goals of STEM outreach is to drive student aspirations towards STEM fields. Remote delivery of STEM outreach increased student knowledge of a STEM-related subject, raised STEM awareness and increased students' positive perceptions of on-line learning. The increase was greater for year 12 students than year 10 which may relate to prior learning experiences. Overall, the results suggest that remote delivery of STEM outreach activities is a viable alternative to in-person events and may assist with encouraging STEM awareness particularly in otherwise difficult to access students.

(1) Fadzil HM, Saat RM. (2014). Enhancing STEM education during school transition: Bridging the gap in science manipulative skills. *Eurasia J Math Sci Technol Educ*; 10: 209–21 (2) Morris J, Slater E, Fitzgerald MT, et al. (2019). Using Local Rural Knowledge to Enhance STEM Learning for Gifted and Talented Students in Australia. *Research in Science Education*; 1–19.

PCB026

Enhancing Physiology Learning Through Gamification

Marta Woloszynowska-Fraser¹, Jenny Moran¹

¹Keele Univeristy, Newcastle-under-Lyme, United Kingdom

Mastering physiology requires not only knowledge of individual organ systems, but also appreciation for their intricate interconnectedness. This work explores two novel game-based activities designed to enhance student understanding of complex physiological concepts.

The first activity, a collaborative card game, was inspired by the human body as a complex ecosystem. Students were involved in co-design of the game where players are tasked with creating functioning human body by strategically selecting and passing cards representing anatomical structures and physiological processes. Points are awarded for correctly placing cards, reinforcing connections between components like red blood cells and veins or gas exchange in the lungs. This adaptable game can target specific systems like the heart, liver, or brain, ensuring knowledge acquisition while highlighting interdependencies and core functions.

The second activity utilises a family quiz format. Divided into teams, students research and develop questions related to a provided prompt, varying in difficulty and point value. A designated quiz master then poses these questions to other groups, awarding points based on answer complexity. This approach fosters teamwork, research skills, and reinforces understanding of key physiological concepts. Additionally, its quick implementation maintains high student engagement.

By implementing these interactive and collaborative games, lecturers can create dynamic learning experiences that not only solidify physiological knowledge, but also cultivate a sense of ownership and relevance among students. Gamification and teamwork provide lecturers with powerful tools to enhance learning efficacy without sacrificing student engagement or instructional efficiency.

PCB027

Investigating Toll-like receptor expression in the adrenal gland of a male and female rat pup model of physiological stress.

Maria L. Dias Casacao¹, Anna O'Connell¹, Ken D. O'Halloran^{1,3}, Fiona B McDonald^{1,3}

¹Department of Physiology, School of Medicine, College of Medicine and Health, University College Cork, Cork, Ireland, ²University College Cork, Cork, Ireland, ³INFANT Research Centre, Cork, Ireland

Introduction: Newborn neonatal infants that require intensive care often exhibit unstable patterns of breathing and require oxygen support for several weeks. These infants are at risk of late onset, nosocomial, infection. Toll-like receptors (TLR) and their downstream signalling pathways are important mediators of the innate immune system and upon activation by, damage associated molecular patterns or pathogen associated molecular patterns, promote inflammation. TLRs have a critical role in facilitating immune-adrenal crosstalk during inflammation and may modulate adrenal physiology under common clinical conditions of oxygen dysregulation and infection.

Objective: To quantify TLR expression in the adrenal gland of male and female rat pups which have been exposed to chronic oxygen dysregulation and acute gram-positive protein challenge.

Methods: Ethical approval was obtained locally by University College Cork and project authorisation was issued by Health Products Regulatory Authority Ireland AE19130/P100, P163 and experiments performed under authorisation in accordance with Irish and European directive 2010/63/EU. Sprague Dawley rat pups and their dam were exposed either to room air or intermittent hypoxia (FiO₂ 8%)-hyperoxia (FiO₂ 30%)—normoxia (FiO₂ 21%)- (IHH) 24-hour protocol from postnatal day (PND) 3-12 and acutely challenged the animals with either sterile saline i.p. or mixture of 3mg/kg of lipoteichoic acid and 5mg/kg peptidoglycan i.p. on PND 13. Adrenal glands were dissected following rapid decapitation and either snap frozen in dry ice and stored at -80C and later used for TLR mRNA analysis of TLR-1, -2, -4, -9, MYD88, NOD2 and NFκB or cryoprotected and frozen in cooled isopentane and later used for histological assessment.

Results: TLR-4, TLR-9, MYD88, NOD2 and NFκB mRNA expression were increased in IHH exposed animals compared to Sham animals (P≤0.02; n=8 per group). IHH exposure interacted with LTA&PGN administration to reveal a higher expression of TLR-2 mRNA (gas x drug, P=0.01) and NFκB mRNA (gas x drug, P=0.05), (n=8 per group). GAPDH mRNA was utilised as the housekeeper for the mRNA analysis performed on the adrenal gland.

Discussion and Conclusions: We have previously reported that in PND13 rat pups LTA&PGN administration increased plasma cytokine and cortisol concentrations. Interestingly, ILβ, IL-10, Leptin and Gro/KC were increased many fold when animals were pre-exposed to oxygen dysregulation. In this further analysis we sought to investigate the expression of TLR expression and some of its downstream signalling molecules. We found that TLR-2 was robustly increased with gram- positive bacterial proteins only when the animals were pre-exposed to oxygen dysregulation. This indicates that in early life pre-exposure to oxygen dysregulation may act to prime the body to generate a heightened inflammatory response upon infection.

PCB028

Preadipocytes as drivers of inflammation in white adipose tissue – A pilot study

Adrian O'Hara¹, Paul Trayhurn²

¹*School of Pharmacy and Biomolecular Sciences, Liverpool John Moores University, Liverpool, United Kingdom*, ²*Institute of Ageing and Chronic Disease, University of Liverpool, Liverpool, United Kingdom*

Obesity can be characterised as a mild chronic inflammatory condition. Observed inflammation can be driven by different factors, including infiltration of macrophages into adipose tissue and by hypoxia. As white adipose tissue is heterogenous at the cellular level, it provides an ideal environment for cell-to-cell communication, and in particular for crosstalk between adipocytes, preadipocytes and macrophages. Over the past two decades there have been several studies that have examined the role of macrophage-driven inflammation in adipose tissue and how this impacts the inflammatory state of both adipocytes and preadipocytes. An area that has yet to be fully explored involves the crosstalk between adipocytes and preadipocytes, as well as their influence on macrophages. This pilot study seeks to investigate this area of crosstalk through a candidate gene approach.

SGBS (human) preadipocytes were cultured (20,000 cells/well) and maintained at 37°C in a humidified atmosphere of 5% CO₂/ 95% air. Once confluent, the media was collected to be used as preadipocyte conditioned medium (PACM). The preadipocytes were then differentiated into adipocytes, and 10 days post differentiation media was collected to be used as adipocyte conditioned media (ACM). U937 monocytes were plated at 2 x 10⁵ cells/ml at 37°C in a humidified atmosphere of 5% CO₂/95% air, differentiation was induced by the addition of 30 nM phorbol myristic acid. Cells were treated with 150 µl of the relevant conditioned media for 24 h, after which mRNA was extracted and reverse transcribed. Expression of candidate genes was carried out using qPCR (n = 6) and fold-changes determined using the 2^{-ΔΔCT} method, results expressed as ± standard error of the mean and a Student's t-test applied to the results to determine statistical significance (p<0.05).

Treating adipocytes with PACM led to changes in mRNA expression of key adipokines. A 16-fold increase in IL-6 mRNA was observed (p<0.001 compared to control), and an 8-fold increase was seen in MCP-1 mRNA level (p<0.001 compared to control). When it came to adiponectin expression, the treatment led to no significant changes in mRNA level. Macrophages treated with PACM demonstrated a 1.8-fold increase in IL-6 expression (p<0.05 compared to control), 2.1-fold increase in TNFα (p<0.01 compared to control), and a 3.2-fold increase in MCP-1 mRNA levels (p<0.05 compared to control). When treated with ACM, preadipocytes demonstrated no measurable changes in IL-6, MCP-1 and adiponectin mRNA levels. However, when U937 cells were treated with ACM, no significant change in TNFα expression was seen, but a statistically significant decrease in IL-6 (1.7-fold) and MCP-1 (2.5-fold) mRNA level (p<0.05 compared to control) was evident.

These experiments show that preadipocytes can exert an inflammatory response in adipocytes, and a very mild effect on macrophages. In contrast, adipocytes do not appear to induce a

significant change in inflammation-related genes in preadipocytes but a slight decrease in inflammation related genes in macrophages is apparent. These data suggest a possible pro-inflammatory role for preadipocytes in adipose tissue, with adipocytes possibly exerting an anti-inflammatory effect on macrophages.

PCB029

Outcomes of Variable Stress and Vitamin C Supplements on Ovarian Cycle in Wistar Rats

Odunayo Olumide¹, Aaron Alale-Yusuf¹, Olawale Aina¹, Ibiyemi Olatunji-Bello¹

¹*Department of Physiology, Faculty of Basic Medical Sciences, Lagos State University College of Medicine, Ikeja, Lagos, Nigeria*

The influence of stress on female fertility is multifaceted with intricate mechanisms that are not fully elucidated. Nonetheless, it is certain that free radicals play a role.

This study was therefore aimed at investigating the effects of vitamin C supplement and stress on the ovarian functions in Wistar rats.

Twenty female Wistar rats with regular estrus cycle of 4 to 5 days were divided into four groups (n=5). Group A (Control); 10ml/kg BW/day distilled water, group B (VitC); 10mg/kg BW/day vitamin C, group C (Stress); exposed to varying stress models alongside 10ml/kg distilled water, group D (stress/vitC); exposed to varying stress alongside 10ml/kg BW/day vitamin C. Animals were exposed to dark cycles stress models; overnight saturated beddings and strange objects. Light cycles: Multiple cage changes, immobility and noise. The animals were exposed to varying stress every other day for 3 weeks. Vagina secretion was taken from each rat between 8 and 9am for daily monitoring of estrus cycle. After 3 weeks, each rat was placed in diethylether fume chamber, blood samples were taken from the heart after cervical dislocation. Blood samples were centrifuged to assay estradiol, progesterone, follicle stimulating hormone (FSH), luteinizing hormone (LH) and cortisol using enzyme linked immunosorbent assay (ELISA) (AccuBind, USA). The activities of superoxide dismutase (SOD), catalase (CAT), and malondialdehyde (MDA) were assayed in the ovaries with randox kit (Sigma Chemicals Ltd, USA). Histology of the ovaries were done. Procedures were done at estrus phase. Graphed pad prism 8.0 was used to analyze data, ANOVA was used to compare the means, Newman keuls was posthoc test and P values \leq was considered significant.

Results showed a significant decrease ($P<0.05$) in the number of complete estrus cycle in stress (3.0 ± 0.05 days) compared with vitC (4.87 ± 0.03 days) and control (4.9 ± 0.21 days). Stress (5.80 ± 0.66 days), (3.40 ± 0.40 days) significantly reduced ($P<0.05$) diestrus and estrus compared with VitC (8.40 ± 0.40 days), (5.00 ± 0.48 days) and control (6.40 ± 0.51 days), (5.20 ± 0.37 days). Occurrence of metestrus was significantly increased ($P<0.05$) in stress (8.00 ± 0.63 days) compared with VitC (3.80 ± 0.37 days) and control (4.80 ± 0.37 days). Progesterone and estradiol were significantly higher ($P<0.05$) in Vitamin C (15.8 ± 1.19 ng/dl), (22.24 ± 1.31 ng/dl) than stress (11.58 ± 0.80 ng/dl), (19.38 ± 1.16 ng/dl) and control (13.70 ± 0.66 ng/ml), (20.13 ± 0.74 ng/dl). Progesterone was also higher ($P<0.05$) in stress/vitC (13.21 ± 0.70 ng/dl) than in stress (11.58 ± 0.80 ng/dl). Cortisol was significantly higher ($P<0.05$) in Stress (1.14 ± 0.12 μ g/dl) than stress/vitC (0.78 ± 0.09 μ g/dl), vitC (0.32 ± 0.07 μ g/dl) and control (0.34 ± 0.24 μ g/dl). Serum MDA was higher ($P<0.01$) in stress (2.30 ± 0.14 mol/ml) than in stress/vitC (1.64 ± 0.25 mol/ml), vitC (1.0 ± 0.24 mol/ml) and control (1.46 ± 0.20 mol/ml). Activities of SOD and CAT were lower ($P<0.05$) in stress (4.38 ± 0.27 mg/dl), (3.08 ± 0.48 mg/dl) compared with stress/vitC (5.10 ± 0.42 mg/dl), (3.70 ± 0.25 mg/dl), vitC (7.36 ± 0.43 mg/dl), (5.14 ± 0.68 mg/dl) and control (6.48 ± 0.40 mg/dl), (4.2 ± 0.27 mg/dl). Histology of the ovary

showed reduced follicular development with degenerating corpus luteum in stress group compared with control and VitC

In conclusion, despite the disruption of the estrus cycle and ovarian follicle distortion induced by stress, the supplementation of vitamin C facilitated follicular development and regulated the cycle.

Casillas F, Flores-González A, Juárez-Rojas L, López A, Betancourt M, Casas E, Bahena I, Bonilla E, Retana-Márquez S. (2023). Chronic stress decreases fertility parameters in female rats. *Syst Biol Reprod Med*. 69(3):234-244. Vašková, J., Klepcová, Z., Špaková, I., Urdzík, P., Štofilová, J., Bertková, I., Křoc, M., & Rabajdová, M. (2023). The Importance of Natural Antioxidants in Female Reproduction. *Antioxidants* (Basel, Switzerland), 12(4): 907.

PCB031

Male sex and age do not associate with higher kidney tissue protein abundance of ACE2 and TMPRSS2 while ACE2 is shedded into the urine in patients with COVID-19

Marie Lykke Bach¹, Sara Latif¹, Jesper Kingo Andresen¹, Rune Micha Pedersen^{1,2}, Lone W Madsen², Kirsten Madsen^{1,2}, Gitte Rye Hinrichs^{1,2}, Rikke Zachar², Per Svenningsen¹, Lars Lund², Isik Somuncu², Lennart Friis Hansen³, Yaseelan Palarasah¹, Boye L. Jensen¹

¹University of Southern Denmark, Odense, Denmark, ²Odense University Hospital, Odense, Denmark, ³Hillerød Hospital, Hillerød, Denmark

Background: The SARS-CoV-2 virus infects cells in a TMPRSS2-dependent mechanism by engaging with ACE2. ACE2 display high levels in kidneys, and risk factors for severe disease are high age and male sex. We hypothesized that in human kidneys, ACE2 and TMPRSS2 are 1) more abundant in male and with increasing age; 2) co-localize; 3) more abundant in urine and extracellular vesicles (EVs) from male patients with acute SARS-CoV-2 and 4) SARS-CoV-2 antigen is present in urine and EVs.

Methods: Kidney cortex tissue from cancer nephrectomy patients (male >75y n=6, female >75y, male <50y n=6, female <50y n=6) was analyzed for ACE2 and TMPRSS2 protein level. Urine collected from hospitalized patients with SARS-CoV-2 (male=7, female n=11) was analyzed for ACE2 and albumin and compared with healthy control (n=3) and patients with albuminuria with COVID (n=12). Urine EVs from patients with COVID-19 were used to detect ACE2, TMPRSS2 and SARS-CoV-2 antigen. Studies were approved by the Ethics Committee of the Region of Southern Denmark and the Danish Data Protection Agency and carried out in accordance with the Declaration of Helsinki. Data were tested for normal distribution, and log transformed if this yielded normal distribution. The 2-variables dataset and 1-variable dataset were analyzed by two-way-ANOVA or Student's t-test, respectively. Correlation between parameters was assessed by linear regression with 95% confidence intervals. For all data, a p-value < 0.05 was considered significant. Normally distributed data are displayed as mean ± standard error of mean (SEM), and non-normally distributed as mean ±interquartile range. Analyses were carried out using GraphPad Prism 9.5.0

Results: Immunoblot analyses (n=6) of ACE2 and TMPRSS2 protein levels were not different with age. ACE2 was more abundant in female kidneys across ages. Immunohistochemistry (n=6) showed that ACE2 protein was associated with proximal tubule apical membranes in the cortex, while TMPRSS2 was observed predominantly in the medulla. ACE2 was elevated significantly in uEVs (immunoblot n=4) and urine from patients with severe SARS-CoV-2 with no sex difference compared with urine from controls w/wo albumin (ELISA). TMPRSS2 was elevated in EVs from male patients compared to female (immunoblot n=4). ACE2 and TMPRSS2 did not co-immunoprecipitate in EVs/apical membranes (immunoblot n=6). SARS-CoV-2 antigen and mRNA were not detected in urine and EVs (PCR).

Conclusion: Higher kidney ACE2 protein abundance is unlikely to explain higher susceptibility to SARS-CoV-2 in male or elderly. Higher TMPRSS2 in male tissues could contribute. Loss of ACE2 into urine in COVID-19 could impact susceptibility and angiotensin metabolism with systemic consequences.

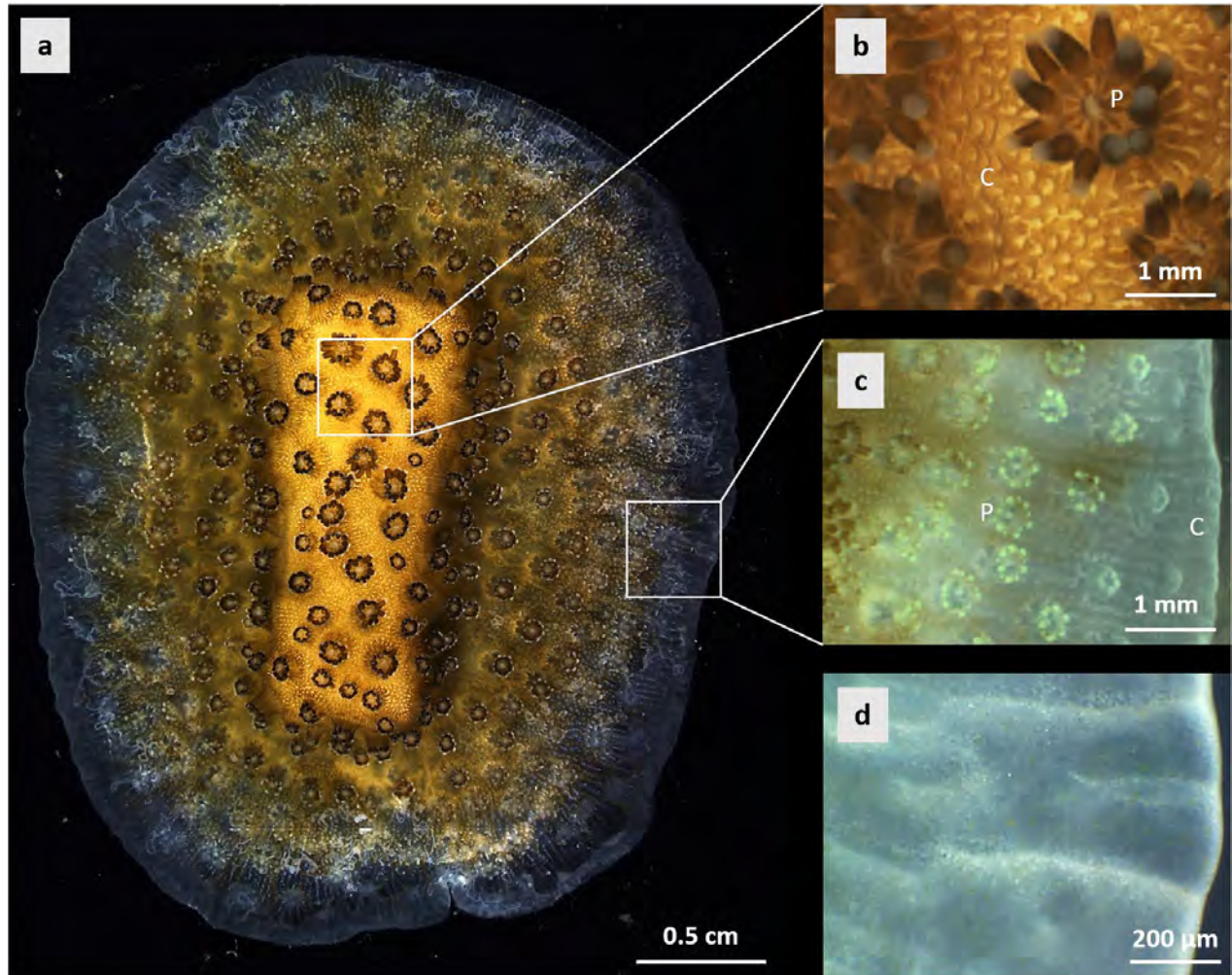
PCB032

Characterization of the coelenteron pH in a reef coral with microsensors: spatial variability, effect of environmental parameters and relationship with calcification

Lucas Crovetto^{1,2}, Alexander Venn¹, Duygu Sevilgen¹, Sylvie Tambutté¹, Eric Tambutté¹

¹Marine Biology Department, Centre Scientifique de Monaco, Monaco, Monaco, ²Sorbonne Université - ED 515 Complexité du Vivant, Paris, France

Coral reefs, the largest bioconstruction on Earth, are formed by calcium carbonate skeletons of corals through a process commonly referred to as calcification. As increasing anthropogenic carbon dioxide dissolves in the world's oceans, the pH of seawater decreases (a phenomenon known as ocean acidification), leading to a reduction in the rate of coral calcification. Calcification models often assume a direct relationship between the surrounding seawater and the extracellular calcifying medium (ECM), which is located between the aboral calcifying ectoderm and the skeleton. However, the ECM is separated from the seawater by several tissue layers and the coelenteron, which contains the coelenteric fluid. Symbiotic dinoflagellate-containing cells line the coelenteron and their photosynthetic activity contributes to changes in the chemistry of the coelenteric fluid, particularly with respect to pH. Therefore, to understand the pH gradients in the different compartments of corals (both cellular and extracellular), the pH values in all compartments, including the coelenteron, need to be determined. The coelenteron may indeed play an important role in mediating the transport of molecules/ions between the external environment and the compartment where calcification occurs (i.e. the ECM). The aim of our study was to determine whether dinoflagellate density (based on tissue coloration), light/dark conditions, and decreasing seawater pH could affect coelenteron pH and potentially influence pH in the ECM in a single coral species, *Stylophora pistillata*. To accomplish this, we worked with liquid ion exchange (LIX) pH microsensors to measure pH in the coelenteron under different environmental conditions. Seven samples of *S. pistillata* grown in long-term coral culture facilities on glass slides at the Centre Scientifique de Monaco were used for this study. For each sample, at least three replicate measurements were performed under all conditions to allow statistical analysis. Our results show that pH of the coelenteron differs between tissues with high and low dinoflagellate density (HDD and LDD respectively). In HDD tissues, pH of the coelenteron indeed exhibits light-dark fluctuations due to the photosynthetic activity of the symbiotic dinoflagellates. No such fluctuations are observed in LDD tissues, as the combined photosynthetic activity of the few dinoflagellates present in these tissues is not sufficient to increase the pH of the coelenteron in the light. We interpret our results in terms of what light and dark exposure means for the proton gradients between the ECM and the coelenteron and how this might affect calcification.



PCB033

Elevated blood pressure in aged male mice with hyperaldosteronism is associated with reduced blood vessel compliance.

Debra Fong¹, Robert Little¹, Mariavittoria D'acierno¹, Tina Myhre Pedersen¹, Michael Stowasser², Eric Delpire³, Vladimir Matchkov¹, Robert Andrew Fenton¹

¹Aarhus University, Aarhus, Denmark, ²The University of Queensland, Brisbane, Australia,

³Vanderbilt University Medical Center, Tennessee, United States

Introduction

Primary aldosteronism (PA) is a common cause of secondary hypertension and is characterized by excessive production of aldosterone despite lower renin activity (1). Mutations in the chloride channel 2 (*Clcn2*) gene cause Familial Primary Aldosteronism Type II (FH-II), which is a milder form of hyperaldosteronism associated with high blood pressure (BP) (2). However, the mechanisms behind the association of high levels of aldosterone and the elevation in BP are poorly understood. Volume regulation by the kidney and vascular function are well established regulators of BP (3). Thus, in this study we aimed to examine BP, renal function, and vessel compliance in a novel mouse model of FH-II due to a R180Q *Clcn2* mutation.

Methods

The mouse model with a R180Q *Clcn2* mutation was generated using CRISPR/Cas9 gene editing. Young and aged male wildtype (WT), heterozygote (Hz) and homozygote mutant (Mut) mice were characterized for BP, vessel compliance (wire myography), and kidney function (metabolic cage studies). BP in 8-11-week-old mice (WT, n=5; Mut, n=5; Hz, n=5) were measured via tail cuff plethysmography, whereas BP in older 16-20-week-old mice (WT, n=3; Mut, n=3; Hz, n=5) were measured via gold standard radio-telemetry. 24-hour urine samples were collected via metabolic cage studies, and blood samples were collected via submandibular vein for plasma. Mesentery arteries were collected from a separate cohort of similarly aged mice and vessel compliance studies were performed *ex vivo* using wire myography. Data are presented as mean \pm standard error mean (SEM) and were analyzed using 2-way ANOVA with Tukey's multiple comparisons test. P-value of ≤ 0.05 is considered statistically significant.

Results

In the older cohort of animals, systolic BP was found to be significantly higher in the Mut and Hz groups compared to their age-matched WT controls ($P < 0.05$). Furthermore, this increase in BP was associated with a decrease in vessel compliance ($P < 0.05$). However, in the younger animals, there was no significant difference in BP and/or vessel compliance between the genotypes, suggesting that there could be a time-dependent increase in BP due to increase in aldosterone, which could be a potential driving factor for the development of disease in this model. The urine and plasma analyses for this study are still to be determined.

Conclusion

We have shown that BP increases with age in the Mut in our model of hyperaldosteronism, and that this elevation in BP with age is associated with reductions in vessel compliance. This suggests that the increase in aldosterone levels could be a potential driving factor behind the development of

higher blood pressure with age in this model. Further studies are still required to determine whether the development of disease in this model is also associated with any changes in renal function. This would help to determine potential developmental origins and further our understanding of the physiological mechanisms behind the development of this disease.

References 1. Funder JW, Carey RM, Mantero F, Murad MH, Reincke M, Shibata H, et al. The Management of Primary Aldosteronism: Case Detection, Diagnosis, and Treatment: An Endocrine Society Clinical Practice Guideline. *J Clin Endocrinol Metab*. 2016;101(5):1889-916. 2. Schewe J, Seidel E, Forslund S, Marko L, Peters J, Muller DN, et al. Elevated aldosterone and blood pressure in a mouse model of familial hyperaldosteronism with CLC-2 mutation. *Nat Commun*. 2019;10(1):5155. 3. Guyton AC. Roles of the kidneys and fluid volumes in arterial pressure regulation and hypertension. *Chin J Physiol*. 1989;32(2):49-57.

PCB034

Assessing the role of glucocorticoid signalling in the development/maintenance of resistive, transporting epithelia in the renal collecting duct.

Taksaporn Tangwanchai¹, Struan Loughlin¹, Etang Collins Etang¹, Morag Milne¹, Morag Mansley¹

¹University of St Andrews, St Andrews, United Kingdom

Background: Tight junctions (TJs) are the most apical intercellular junctional complexes in epithelia. These demarcate apical and basolateral aspects of the plasma membrane, enabling vectorial transport of molecules. Within the epithelial monolayer lining the collecting duct (CD) of the kidney, the tightly regulated transcellular transport of Na⁺ and H₂O critically maintains both the volume and osmolality of our circulating volume. Here, corticosteroid hormones modulate Na⁺ transport, signalling *via* mineralocorticoid (MR) and glucocorticoid (GR) receptors. In a model of CD epithelia with deletion of the GR, preliminary electrophysiological measurements demonstrated attenuated transepithelial voltage (V_t) and resistance (R_t). This suggests a role of glucocorticoid signalling in the development and/or maintenance of TJs in the CD, though the specific TJ proteins involved remains unclear.

Aim: To assess the role of glucocorticoid signalling in the development of polarised and electrically resistive CD epithelia and determine which TJ proteins are involved.

Methods: Two experimental models were employed. Firstly, comparison of mCCD_{cl1} murine CD cells [1] with *Nr3c1* deletion (GR knockout, GR-KO) with non-targeting controls (SHAM). Secondly, parental mCCD_{cl1} cells grown in culture media with (DEX) or without (NO-DEX) the glucocorticoid dexamethasone. All cells were cultured on permeable supports for 9-11d, V_t and R_t were measured by epithelial volt-ohm-meter. RNA was extracted and expression of genes encoding TJ protein families: Zona occludens, Occludin, Claudins, Tricellulin and Angulins were quantified by qRT-PCR. SHAM and GR-KO cells on filters were labelled with antibodies against: GR, ZO-1, Claudin7 and Claudin8, and imaged using a Zeiss AxioScanZ1 slidescanner. Data are shown as mean±SD and statistical significance determined by Mann-Whitney or unpaired t-test, where appropriate.

Results: In GR-KO cells, R_t was negligible compared to SHAM cells after 9d, measuring 0.3±0.1 kΩ·cm² and 5.6±0.4 kΩ·cm², respectively ($n=8$, $p<0.001$). Similarly, V_t was greatly reduced compared to SHAM cells at 9d, measuring -0.9±0.6 mV and -28.0±11.1 mV, respectively ($n=8$, $p<0.001$). Interestingly, R_t remained unaltered in NO-DEX cells compared to DEX cells after 9d, measuring 2.5±0.5 kΩ·cm² and 2.3±0.3 kΩ·cm², respectively ($n=6$). V_t , however, was greatly reduced in NO-DEX cells compared to DEX cells after 9d, measuring -14.9±3.4 mV and -50.3±7.2 mV, respectively ($n=6$, $p<0.01$).

Across the panel of genes assessed, GR-KO cells had decreased *Tjp3*, *Cldn3*, *Cldn7*, *Cldn8* and *Ildr1* ($n=8$, $p<0.05$), but increased *Cldn1*, *Cldn2* and *Cldnd1* ($n=8$, $p<0.01$). NO-DEX cells exhibited decreased expression of *Tjp1*, *Tjp2*, *Tjp3*, *Cldn8*, *Cldn12* and *Ildr1* ($n=8$, $p<0.05$), but increased expression of *Ocln*, *Cldn2* and *Cldnd1* ($n=8$, $p<0.01$), compared to DEX cells.

Qualitative assessment of immunolabelled cells confirmed loss of nuclear GR but no change to lateral ZO-1 labelling in GR-KO cells ($n=6$). Furthermore, initial studies revealed lateral labelling of Claudin7 and 8 in SHAM cells was greatly reduced in GR-KO cells ($n=2$).

Conclusions: Together these data provide evidence that glucocorticoid signalling plays an important role in the development of polarised, transporting CD epithelia. Whilst a number of TJ genes were modified by loss of receptor or removal of ligand, Claudin7 and Claudin8 protein expression was modified, indicating their possible role in development/maintenance of V_t and R_t .

[1] Gaeggeler, H.P., et al. (2005) JASN 16: 878-891.

PCB035

Investigating novel transport mechanisms for aldosterone and the identification of putative corticosteroid transporters in the collecting duct of the kidney.

Morag Milne¹, Morag Mansley¹, Natalie Homer²

¹University of St Andrews, St Andrews, United Kingdom, ²The University of Edinburgh, Edinburgh, United Kingdom

Background: The kidney is responsible for the long-term control of blood pressure (BP) and this is achieved by maintaining total body Na⁺ balance. The kidneys match Na⁺ excretion with Na⁺ intake with fine-tuning of Na⁺ balance occurring in the collecting duct (CD). In response to decreased BP, the key volume-regulating corticosteroid aldosterone (ALDO) increases Na⁺ reabsorption *via* the epithelial sodium channel (ENaC) by upregulating its expression and activity, driving fluid reabsorption and thus normalising BP. ALDO exerts its effects specifically in principal cells (PC) of the CD due to expression of the enzyme 11 β HSD2 which inactivates the related hormone cortisol (CORT). Corticosteroids are typically thought to passively diffuse into target cells owing to their lipophilicity. However, preliminary studies in the lab have provided the first evidence that CORT may be actively transported in the CD. This study aimed to determine if ALDO is also actively transported in PCs and to identify which transporters may be responsible.

Methods: Murine cortical collecting duct cells (mCCD_{cl1}) were cultured on permeable supports for 9 days [1]. Cells were treated with ALDO (3nM, 3h) in the basolateral bath. Amiloride-sensitive ENaC-mediated Na⁺ transport was assessed by measuring the equivalent short-circuit current. Samples of media were collected from the apical and basolateral baths and the monolayer lysed in 0.1% SDS. ALDO concentration was determined by solid-liquid phase (SLE) extraction and targeted LC-MS/MS analysis using an assay optimised to detect physiological concentrations of ALDO. The apical membrane was isolated from polarised mCCD_{cl1} cells by biotin labelling and streptavidin pulldown. Isolation was validated by western blot using antibodies against streptavidin and α -ENaC. Unbiased proteomic analysis of the apical fraction was carried out by LC-MS/MS enabling assessment of changes in protein expression in response to ALDO.

Results:

The stimulatory effect of ALDO on ENaC activity was confirmed where ALDO increased I_{eq} by $-3.0 \pm 1.3 \mu A \cdot cm^{-2}$ after 3h compared to control, where the change in I_{eq} was $0.1 \pm 0.2 \mu A \cdot cm^{-2}$. Interestingly, after 3h, ALDO was unevenly distributed across the monolayer of cells. $16.5 \pm 2.8\%$ was detected in the apical bath, $72.3 \pm 10.2\%$ detected in the basolateral bath, and a small proportion $2.7 \pm 1.1\%$ in cell lysates ($n=6-9$).

Following separation of the apical membrane from the remaining protein lysate (supernatant) in vehicle or ALDO-treated cells, streptavidin was detected in the apical fraction but not the

supernatant, confirming successful isolation ($n=2$). α -ENaC was also detected in both fractions, the presence in the apical fraction correlating with functional channel activity. Subsequent proteomic analysis of the apical membrane detected a total of 3188 proteins. Changes in expression of 9 members of the ABC and SLC transporter superfamilies was seen in response to ALDO treatment; 6 up-regulated and 3 down-regulated.

Conclusions: Together these data suggest an active mechanism contributes to ALDO transport into and/or out of PCs of the CD. This has important implications for the control of ALDO bioavailability within target PCs, and may present a possible therapeutic target. Ongoing work is being carried out to interrogate which transporter(s) are responsible.

PCB036

TRPV4 and chloride channels: Ion movement in relation cerebrospinal fluid production

Verayna Newland¹, Bonnie Blazer-Yost¹, Cameryn Davis¹

¹*Indiana University Indianapolis, Indianapolis, United States*

Introduction: Hydrocephalus is a disease caused by an overproduction of cerebrospinal fluid (CSF), blockage of flow, or decreased reabsorption. When CSF accumulates in the brain it causes ventriculomegaly, increased intracranial pressure, inflammation, and cell damage. The choroid plexus within the brain's ventricles consists of a fenestrated capillary network surrounded by an epithelial monolayer. This tissue produces CSF. Choroid plexus epithelial cells (CPE) are polarized, meaning that the ion channels are located apically (CSF-facing) or basolaterally (blood-facing) and regulation of these channels is responsible for the composition and production of CSF. Some notable channels include transient receptor potential vanilloid 4 (TRPV4), calcium-activated chloride channel (TMEM16A), cystic fibrosis transmembrane conductance regulator (CFTR), and Na⁺/Cl⁻ co-transporter (NCC). Activation of TRPV4, a nonselective cation channel that is osmo-, shear-, temperature-, and pressure-sensitive, allows Ca²⁺ and Na⁺ influx into the CPE which, secondarily, causes transepithelial electrolyte flux that involves multiple electrolyte transporters. In *Tmem67*^{-/-} rats, a genetic form of hydrocephalus was reversed with TRPV4 antagonist treatment [1]. TMEM16A and CFTR are located basolaterally on the CPE while NCC is apical. Interestingly, patients with posthemorrhagic hydrocephalus (PHH) have elevated Cl⁻ levels in their CSF [2]. This could be caused by an interaction of blood components with chloride channels. We investigated hemoglobin, a major protein found in red blood cells.

Aims: The goal of this study was to determine if there was intercellular signaling between activated TRPV4, TMEM16A, CFTR, and NCC. By investigating the role of these channels in the CPE, we aim to understand the regulation of CSF production in normal and pathophysiological states. Additionally, we investigated the role of hemoglobin as a potential pathological factor in hydrocephalus development.

Methods: Human choroid plexus papilloma (HIBCPP) cells were grown in Dulbecco's modified eagle media (DMEM) with sodium bicarbonate, 10% fetal bovine serum, 1% penicillin/streptomycin, and 5 ng/L insulin. Ussing-style electrophysiology was used to measure net transepithelial electrolyte flux and transepithelial permeability in the cultures. To determine the relationship between the ion channels, cells were pre-treated with the following compounds and concentrations: Anil 10 μ M (TMEM16A inhibitor), FeCl₃ 10 nM (TMEM16A activator), CFTR Inhibitor 172 5 μ M, metolazone 0.2 mM (NCC inhibitor), and bovine hemoglobin 140 mg/mL. Compounds were added apically, basolaterally, or bilaterally to determine polarity. 10 minutes after effector treatments, TRPV4 agonist GSK1016790A (GSK) was used to stimulate the influx of Ca²⁺ and Na⁺ into the cells. Each drug treatment group (n=6) was analyzed for statistical significance with a multiple T-test.

Results: TMEM16A activation or inhibition substantially altered the complex, multiphase transepithelial ion flux that is activated in response to TRPV4 agonist stimulation. When CFTR was inhibited basolaterally, the membrane permeability increased. NCC inhibition had no significant

effect. Hemoglobin treatment potentiated the agonist-stimulated transepithelial ion flux and increased conductance.

Conclusion: There is a relationship between TRPV4 and chloride channels. By investigating these interactions, we hope to understand PHH pathophysiology and identify drug targets for non-invasive hydrocephalus treatments.

1. Hochstetler, A.E. et al. (2020). Jci Insight 5, 1-14. 2. Otun A. et al (2021). Fluids and Barriers of the CNS 18, 1-14.

PCB037

Functional analysis of gene-edited CF variant G542X.

Isabelle Rose¹, Lucia Nicosia², Miriam Greenwood³, Kader Doran-Cavusoglu², Mathew Biggart⁴, Patrick Harrison², Stephen Hart³, Robert Tarran⁴, Deborah Baines¹

¹St George's University of London, London, United Kingdom, ²University College Cork, Cork, Ireland, ³UCL Great Ormond Street Institute of Child Health, London, United Kingdom, ⁴Kansas City University Medical Centre, Kansas City, United States

The Cystic Fibrosis (CF) causing variant G542X (GGA>TGA) results in premature termination of translation of the cystic fibrosis transmembrane regulator (CFTR) protein, and nonsense-mediated decay of the CFTR mRNA resulting in almost complete loss of functional CFTR protein expression. This leads to defective anion transport and the development of CF disease pathology. Currently available CF modulator therapies cannot be used to treat this variant, but an Adenine Base Editor (ABE) and guide RNA combination can convert the G542X stop codon to G542R, a variant which retains about 30% of WT activity^[1] and is amenable to CFTR triple modulator therapy (Elexacaftor-Tezacaftor-Ivacaftor ETI).

Plasmid DNA encoding this ABE and guide RNA with GFP were encapsulated in lipid-based nanocomplexes, which have reduced immunogenicity and high cellular uptake, and were delivered to human airway epithelial cells (HAECs) harboring the G542X CFTR variant. Transfected cells were identified by analysing GFP fluorescence. Ion transport was measured as short circuit current (Isc) across resistive epithelial monolayers. Cultures were equilibrated using standard physiological salt solution before addition of pharmacological drugs, forskolin, 10 µM (bilateral) to activate CFTR; CFTRInh-172, 10 µM (apical) to inhibit CFTR; and ouabain, 100 µM (basolateral) to inhibit Na⁺K⁺ATPase activity. Airway Surface Liquid (ASL) height was visualised using Texas-red dextran as a soluble fluorescent label of volume, and perfluorocarbon-77 to prevent fluid evaporation. CFTR was activated using vasoactive intestinal peptide (VIP)(100 nM, basolateral), and changes were calculated from XZ scans taken at regular intervals. ASL pH was measured using pHrodo-dextran pH-sensitive fluorescent labelling normalised to a pH-insensitive (pHins) *in situ* control.

48 hours post transfection, next-generation sequencing showed 17% of alleles had been edited from G542X to G542R. Isc measurements showed that even as little as 17% of editing restored CFTR activity to ~ 60 % that of normal levels when in combination with modulators. CFTRInh-172 inhibitable current was ~ four-fold greater in ETI treated G542R compared to G542X samples (Table 1; p=0.015, n = 6). Transfected cells were sorted using fluorescence-activated cell sorting (FACS) to concentrate the population of edited cells (henceforth called edited and sorted). CFTRInh-172 inhibitable Isc was not significantly different to that of wild-type samples (p = 0.97; n = 6, N = 2). VIP stimulated changes in ASL height indicated that edited and sorted cell monolayers displayed wild-type like airway hydration (Table 1). Additionally, VIP stimulated changes in ASL pH were positively correlated to the proportion of G542R cells, suggesting that bicarbonate transport was also being restored by correction of G542X to G542R CFTR protein.

This data provides proof-of-concept for restoration of anion transport by gene editing of G542X.

Physiology in Focus 2024

Northumbria University, Newcastle, UK | 2 – 4 July 2024

[1] Xue, X. et al. Hum Molec Gen. 2017; 26 (16), 3116–3129.

PCB038

Altered voltage-gated ion channel expression around drusen accumulations in induced pluripotent stem cell model of age-related macular degeneration.

Molly Rowland², Majlinda Lako¹, Marzena Kurzawa-Akanbi¹, Gerrit Hilgen^{1,2}

¹*Biosciences Institute, Faculty of Medical Sciences, Newcastle University, Newcastle, United Kingdom*, ²*Applied Sciences, Faculty of Health and Life Sciences, Northumbria University, Newcastle, United Kingdom*

Age-related macular degeneration (AMD) is one of the leading causes of irreversible blindness globally and is associated with increasing prevalence and socioeconomic burden. As a result, additional treatment avenues are under constant investigation. AMD can be characterised into a wet or dry form; wet AMD involves the formation of a pathological neovascular membrane that results in the accumulation of subretinal fluid and/or haemorrhaging and dry AMD is characterised by the presence of protein and lipid deposits, known as drusen, that form beneath the retinal pigment epithelium (RPE). Although wet AMD results in a sudden, severe loss of vision, treatment options are available. Dry AMD is slow progressing and has a high conversion rate into wet AMD before reaching end stage disease. The exact cause of AMD is unknown, although it is thought to originate within the RPE and is multi-factorial with both genetic and environmental factors playing a role. An overlooked potential contributing mechanism to AMD is the dysfunction of ion channels, or channelopathies, with their involvement in AMD pathophysiology being poorly understood.

Induced pluripotent stem cell (iPSC) derived RPE can be used to model AMD, both low (control) and high-risk lines were stained for pan markers of voltage-gated sodium channels (Nav) alongside key RPE cell markers such as CRALBP and ZO1. Early experiments show that Nav is expressed in the cell membrane of iPSC RPE, aligned with ZO-1, a tight junction protein (data obtained from three 24-well inserts). Additionally, drusen were identified using antibodies against complement proteins C3b and C5b-9. Initial data has shown altered Nav localisation relative to drusen formations, with less homogenous and more numerous Nav staining in the high-risk lines (data obtained from six low-risk and six high-risk 12-well inserts). Further experiments will confirm and quantify these findings, including a physiological characterisation of these ion channels in AMD. Funding for this project has been received from the Academy of Medical Sciences (GH) and the ECR support Northumbria University. Acknowledgement goes to Northumbria Microscopy Lab for their exceptional service and support during the project.

PCB039

Exploring the metabolic fate of adenine in adenine-induced chronic kidney disease in mice

Jasmine Atay¹, Søren Elsborg¹, Johan Palmfeldt¹, Rikke Nørregaard¹

¹*Department of Clinical Medicine, Aarhus University, Aarhus, Denmark*

Animal models of chronic kidney disease (CKD) are crucial for understanding the disease, its pathogenesis, and for developing new treatments. The adenine-induced CKD model offers a non-surgical approach to studying CKD pathogenesis. At physiological concentrations, adenine is metabolised to AMP through adenine phosphoribosyl transferase, serving as a precursor for several adenine derivatives, and is ultimately metabolised to uric acid and excreted by the kidneys. However, at supraphysiological doses, adenine follows an alternative pathway, resulting in the formation of 2,8-dihydroxyadenine (2,8-DHA). Due to its limited solubility in urine, 2,8-DHA precipitates as crystals and deposits within the renal tubules, leading to tubulointerstitial injury. This study investigates kidney injury and fibrosis at 2 and 4 weeks of adenine-feeding, while also measuring plasma and urine levels of adenine metabolites to investigate the molecular fate of adenine.

To induce CKD, 8-week-old C57BL/6J mice were fed a diet enriched with 0.2% adenine. Mice were grouped randomly into three categories: control (n=11), 2-week adenine diet (n=8) and 4-week adenine diet (n=8). At sacrifice, anaesthesia was induced with 5% sevoflurane and maintained at 3–4%. Blood was collected and immediately after both kidneys were excised and cortical tissue was isolated for subsequent RNA analysis. Mice were euthanised by cervical dislocation. Plasma and urinary metabolites were analysed by LC-MS and compound identification was performed using the mzLogic Data Analysis Algorithm (Compound Discoverer Software, Thermo Scientific). Statistical analyses were performed using a one-way ANOVA, followed by Tukey's multiple comparisons test. $p < 0.05$ was considered significant.

Following 2 weeks of adenine feeding, kidney injury, as measured by plasma creatinine, blood urea nitrogen and cortical hepatitis A virus cellular receptor 1 (*Havcr1*) mRNA expression, was significantly increased compared with the control group. Additionally, fibrosis markers, fibronectin (*Fn1*), collagen type 1 (*Col1a1*) and transforming growth factor- β (*Tgfb1*) mRNA expressions were significantly increased compared with control. Unexpectedly, extending adenine feeding to 4 weeks resulted in significant reduction of both kidney injury and fibrosis markers compared to 2 weeks. These markers remained significantly elevated compared to control, except for *Havcr1* expression, which had returned to control levels at 4 weeks.

Following 2 weeks of adenine feeding, plasma levels of adenine and 2,8-DHA were elevated compared to the control group, but at 4 weeks, these levels had returned to control levels. Interestingly, plasma concentrations of other adenine metabolites, such as inosine, hypoxanthine, guanine, and uric acid, were higher at 4 weeks compared to 2 weeks. In contrast, urinary levels of adenine and 2,8-DHA increased following 2 weeks of adenine feeding and remained elevated at 4 weeks compared to control levels.

The adenine-enriched diet resulted in significant increase in markers of renal injury and fibrosis within 2 weeks, which showed a noteworthy decrease at 4 weeks. Analysis of plasma metabolites revealed that adenine and 2,8-DHA levels were reduced at 4 weeks, suggesting an adaptive response in adenine metabolism over time, which could explain the less severe kidney injury and fibrosis observed at 4 weeks. We are currently further exploring these mechanisms by investigating the expression levels of enzymes involved in adenine metabolism.

PCB040

Physiological network mapping predicts survival in critically ill patients with sepsis

Emily Ito¹, Tope Oyelade¹, Alireza Mani¹

¹*Network Physiology Lab, Division of Medicine, University College London (UCL), London, United Kingdom*

Introduction: Sepsis is a life-threatening condition in which dysregulated host response to infection leads to multiorgan failure. Early detection of deterioration in sepsis is key to improving overall patient outcomes. Studies investigating complex disorders using a network physiology approach have shown a distinct pattern of organ system connectivity between different patient populations with positive and negative disease outcomes. Physiological network mapping is not currently used in intensive care units. This study used a parenclitic network approach to compute organ connectivity for individual patients with sepsis using records of routine laboratory test results.

Aims/objectives: The goal of this study was to investigate whether analysing organ connectivity in individual patients with sepsis using a parenclitic network could predict the deterioration and mortality of sepsis patients.

Method: Electronic patient records from 162 patients with sepsis were obtained from the MIMIC-III database (Ethics IRB protocol nos. 2001P001699). Patients were studied retrospectively, and clinical data on 48-hour deterioration and 30-day survival were obtained. Fifteen physiological variables (serum phosphate, arterial pH, urea, haemoglobin, lactate, white blood cell count, serum sodium, international normalized ratio, platelets, total bilirubin, blood glucose, serum creatinine, alanine transaminase, bicarbonate, and serum potassium) representing different organ systems were extracted from the laboratory data. Correlation analysis of physiological variables was performed to study the pattern of interaction between patient groups with different outcomes (i.e., survivors versus non-survivors). The parenclitic network investigated organ connectivity in individual patients by examining how individual patient data deviated from the characteristics of organ relationships established in a reference population (survivors). Parenclitic deviations were computed for everyone, and Cox regression was used to investigate if parenclitic deviations could predict 48-hour deterioration and 24-hour survival in sepsis patients.

Results: Correlation analysis identified 7 and 9 pairs of unique correlations in physiological variables that were significantly different between survivors and non-survivors for 30-day survival and between deteriorated and non-deteriorated patients for 48-hour deterioration, respectively. Parenclitic deviations for the pH-bicarbonate axis (hazard ratio = 2.081, $p < 0.001$) and pH-lactate axis (hazard ratio = 2.773, $p = 0.024$) were able to significantly predict 30-day mortality in sepsis patients independent of the measures of organ dysfunction severity, SOFA, and ventilation status. None of the parenclitic deviations were able to predict 48-hour deterioration.

Conclusions: Investigating organ connectivity in individual patients using parenclitic network analysis significantly predicted 30-day mortality in sepsis population. Parenclitic deviation may

Physiology in Focus 2024

Northumbria University, Newcastle, UK | 2 – 4 July 2024

potentially offer useful insight into pathophysiology of sepsis and give useful insight into different physiological response towards sepsis between survivors and non-survivors.

PCB042

Comparative study of systemic and local delivery of mesenchymal stromal cells for the treatment of chronic kidney disease

Jean-Claude Kresse¹, Emil Gregersen¹, Anders Toftegaard Boysen¹, Peter Nejsum¹, Rikke Nørregaard¹

¹*Department of Clinical Medicine, Aarhus University, Aarhus, Denmark*

Introduction:

Renal fibrosis is a hallmark of chronic kidney disease (CKD), characterized by excessive inflammation and fibrosis, and contributes significantly to progressive renal dysfunction. There is a pressing need for effective anti-fibrotic interventions, an area where options are lacking. One such promising treatment method is the employment of cell therapy with mesenchymal stromal cells (MSCs). MSCs have shown promise as anti-inflammatory and immunomodulatory agents, making them a promising opportunity for intervention. This study investigates two critical factors influencing treatment specificity 1) delivery methods as well as 2) preconditioning of adipose tissue derived MSCs, for the treatment of CKD-associated renal fibrosis.

Methods:

We investigated the effects of proinflammatory preconditioning on MSCs and their derived secretome using an *in vitro* fibrosis model. To this end, conditioned medium (CM) was collected from either preconditioned MSCs (Pr-MSCs) treated with TNF- α and IFN- γ or vehicle, or naïve MSCs. Furthermore, CM was processed using size exclusion chromatography, a soluble protein (SP) fraction and an extracellular vesicle (EV) fraction collected and employed in TGF- β stimulated HKC-8 cells. Analysis of gene expression of inflammatory and fibrotic markers was carried out using qPCR.

Additionally, *in vivo* experiments were conducted using a murine unilateral ureteral obstruction (UUO) model of CKD to evaluate the therapeutic efficacy of systemic versus local administration of preconditioned MSCs and their EVs. For this, C57BL/6j mice were anesthetized with isoflurane by inhalation and the left kidneys surgically obstructed with silk ligature or SHAM operated. Mice were concurrently treated with either local (subcapsular) or systemic (tail vein) delivered Pr-MSCs. Mice were sacrificed by collecting blood through the heart under anesthesia after five days. Analysis on gene expression levels with qPCR as well as immunohistochemical analyses and cytokine multiplex (V-PLEX Mouse Cytokine 19-plex, Meso Scale Diagnostics) screening of inflammatory cytokines were carried out.

Results:

Pr-MSC derived CM and SP demonstrated significant antifibrotic effects *in vitro*, reducing expression of fibrotic markers fibronectin (n=6, p<0.05) and collagen type 1 α 1 in TGF- β -stimulated HKC-8 cells (n=6, p<0.05) compared to vehicle-treated cells. EVs did not replicate these effects when compared to vehicle-treated cells (n=6, p>0.05), suggesting that SPs secreted by Pr-MSCs may be the primary mediators of antifibrotic effects. *In vivo*, both systemic and local delivery of Pr-MSCs were explored in a murine UUO model. Local administration of Pr-MSCs showed a more pronounced impact on the cytokine profile of UUO compared to systemic administration.

Particularly, local administration resulted in the upregulation of the mRNA of the inflammatory cytokine IL-10 ($n=6$, $p<0.05$) indicating anti-inflammatory properties of locally delivered Pr-MSCs *in vivo*. Additionally, local delivery, but not systemic delivery, showed a reduction in the number of myofibroblasts, as shown by decreased staining of the myofibroblast marker α -smooth muscle actin, compared to vehicle-treated UUO mice ($n=5$, $p=0.059$).

Conclusion:

This study provides critical insights into the therapeutic efficacy of MSCs and emphasizes the importance of delivery methods and preconditioning strategies in enhancing MSC-based therapies for renal fibrosis. Further optimization of MSC delivery strategies and mechanistic elucidation is warranted to fully exploit their potential in treating CKD.

PCB043

Physiologic responses during exertional heat strain following 34-39h complete caloric restriction.

Toby Mundel¹, Huixin Zheng², Chung-Yu Chen³, Claire Badenhorst⁴

¹*Brock University, St. Catharines, Canada,* ²*University of Otago, Wellington, New Zealand,*

³*University of Taipei, Taipei, Taiwan, Province of China,* ⁴*Massey University, Auckland, New Zealand*

Complete caloric restriction is common to most humans. Whether characterised by regular religious practise, a surgical patient's perioperative period or the trend of intermittent fasting for health (e.g., periodic fasting, time-restricted feeding) a large proportion of the global population experiences caloric restriction. These examples often accompany physical activity for sport, exercise, or occupation. Whilst the separate and combined effects of caloric restriction and exercise have been studied for several physiological consequences, few investigations have investigated the thermoregulatory outcomes. Previous research demonstrated that 48h of caloric restriction in both men and women increased metabolic rate and peripheral blood flow such that core temperature was reduced when subjected to cold stress. To our knowledge, no study has determined this for heat stress, the purpose of the current study.

Eight healthy and recreationally active adults (4 female, age: 31 ± 8 y, weight: 69 ± 15 kg, body fat: $15 \pm 8\%$, VO_2max : 3.8 ± 1.1 L·min⁻¹) performed two treadmill trials in a heat chamber (30°C, 40% RH) that consisted of consecutive 20 min bouts at 40% (5.7 ± 0.6 km·h⁻¹) and 70% (10.0 ± 1.0 km·h⁻¹) of their individually-determined ventilatory threshold. Both trials were scheduled at ~10am and followed either 34-39h of complete caloric restriction or their usual diet. Measures of gastro-intestinal temperature (T_{gi}), heart rate (HR), blood pressure (MAP), skin blood flow (SkBF, laser Doppler flowmetry), fluid loss (body weight change) and sweat rate (technical absorbent), expired gases, urine specific gravity (USG) and blood biochemical markers were taken. Descriptive data are provided as mean \pm SD, with all analyses conducted using SPSS software for Windows and significance accepted at $p < 0.05$. Data were analysed using either a paired samples t-test or ANOVA for repeated measures.

Baseline resting data for T_{gi} , HR, MAP, SkBF, USG and body weight were not different between trials ($p \geq 0.22$), whilst caloric restriction decreased blood glucose (4.7 ± 0.3 vs. 5.4 ± 0.3 mmol·L⁻¹, $p < 0.01$) and insulin (28 ± 15 vs. 89 ± 53 pmol·L⁻¹, $p < 0.01$) and increased free fatty acids (0.6 ± 0.2 vs. 0.3 ± 0.2 mEq·L⁻¹, $p < 0.01$). Participants were exercising at 34 ± 4 and 78 ± 10 % VO_2max respectively, with no difference between trials ($p = 0.60$); although caloric restriction reduced the respiratory exchange ratio (0.77 ± 0.04 vs. 0.81 ± 0.03 a.u., $p = 0.02$). Exercise increased T_{gi} ($\Delta 1.2 \pm 0.3$ °C, $p < 0.01$) reaching 38.5 ± 0.4 °C with no difference between trials ($p = 0.56$). Water consumed (0.35 ± 0.43 L·h⁻¹, $p = 0.62$), whole-body sweat loss (0.66 ± 0.35 kg·h⁻¹, $p = 0.32$) and local sweat rate (0.60 ± 0.28 mg·min⁻¹·cm⁻¹, $p = 0.16$) were not different between trials. Exercise increased SkBF and decreased MAP (both $p < 0.01$) with no difference between trials (both $p > 0.60$). Exercising HR continued to increase ($p < 0.01$) and was higher with caloric restriction ($\Delta 3 \pm 3$ beats·min⁻¹), reaching $90 \pm 8\%$ VO_2max .

Complete caloric restriction lasting 34-39h had minimal physiologic impact during 40 min of exertional heat strain, with only heart rate mildly increased.

PCB044

Application of physiological network mapping in the prediction of survival in critically ill patients with acute liver failure

Tope Oyelade^{1,4}, Kevin Moore², Ali R. Mani^{3,4}

¹*Institute for Liver and Digestive Health, Division of Medicine, UCL, London, United Kingdom,*

²*Institute for Liver and Digestive Health, Division of Medicine, UCL, London, United Kingdom,*

³*Institute for Liver and Digestive Health, Division of Medicine, UCL, London, United Kingdom,*

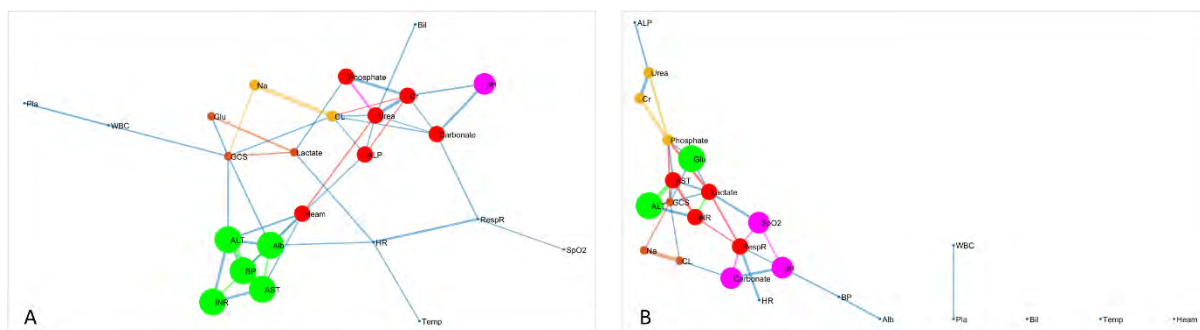
⁴*Network Physiology Laboratory, UCL Division of Medicine, London, United Kingdom*

Background: Reduced functional connectivity of physiological systems is associated with poor prognosis in critically ill patients. However, physiological network analysis is not commonly used in clinical practice and needs further validation. Acute liver failure (ALF) is associated with multiorgan failure and mortality. Prognostication in ALF is highly important for clinical management but is currently dependent on models that do not consider the interaction between organ systems. This study aims to examine the impact of physiological network analysis in prognostication of patients with ALF.

Methods: Data from 640 adult patients admitted to the intensive care unit (ICU) for paracetamol-induced ALF between 2001 and 2012 were extracted from the MIMIC-III database. Parenclitic network analysis was performed on patients' routine biomarkers and network clusters were identified using the k-clique percolation method. Statistical analysis was performed to predict the 28-day survival of patients independent of their sequential organ failure assessment (SOFA) score and King's College Criteria.

Results: There is higher organ system disconnection in non-survivals compared with survivals with a shift toward acidosis. pH regulation was respectively directed toward renal function and respiratory functions in survivors and nonsurvivors (Figure 1). Parenclitic deviation along the blood pH and serum creatinine (HR(hazard ratio) = 187.08, $p = 0.001$), blood pH and bicarbonate (HR = 78.94, $p < 0.001$), lactate and glucose level (HR = 1.10, $p < 0.001$), lactate and heart rate (HR = 1.09, $p < 0.001$), as well as oxygen saturation (SpO₂) and respiratory rate (HR = 1.13, $p = 0.018$) axes, predicted ICU mortality independent of SOFA. The addition of the parenclitic network indices significantly improved the prognostic value of SOFA.

Conclusion: These results demonstrate that network analysis can provide pathophysiologic insight and predict survival in critically ill patients with paracetamol-induced ALF



PCB045

Intra- and inter-session reliability and repeatability of proton magnetic resonance spectroscopy for quantifying total creatine levels in multiple human brain regions

Jedd Pratt¹, James McStravick¹, Aneurin Kennerley¹, Craig Sale¹

¹*Department of Sport and Exercise Sciences, Manchester Metropolitan University Institute of Sport, Manchester, United Kingdom*

Introduction: Creatine (Cr) dynamics within the human brain is a research area with promising clinical value, particularly for cohorts exposed to metabolically demanding periods (e.g., ageing, neurological diseases, sleep deprivation). Consequently, increasing reliance will be placed upon proton magnetic resonance spectroscopy (¹H-MRS) for determining total creatine (tCr) concentrations in the brain. Importantly, however, before data from experimental studies can be accurately interpreted, more consideration should be given to the inherent sources of error in ¹H-MRS, and their effect on the reliability of repeated measurements. This need is underscored by weaknesses in the design of existing studies, and ultimately, by large margins of error in repeated ¹H-MRS reported to date. Herein, we examined the intra- and inter-session reliability and repeatability of ¹H-MRS for quantifying tCr concentrations in multiple brain regions (midbrain: MB; visual cortex: VC; frontal cortex FC).

Methods: Eighteen healthy adults aged between 20-32 years were recruited for this study [mean age=25.8±3.0years; 50% female; n=14 intra-session analysis; n=15 inter-session analysis (n=11 both)]. MR imaging and ¹H-MRS (PRESS) were performed on a 3T Siemens scanner using a 20-channel head coil. Intra-session analyses involved repeated measurements of the MB, VC and FC without removing the participant from the scanner, while inter-session analyses involved repeated measurements from the same regions, but with a brief break between measurements (involving repositioning of the participant and voxels). TARQUIN was used to analyse ¹H-MRS data, and water unsuppressed data were used to determine absolute tCr concentrations. Paired t-tests, minimum detectable change (MDC), Pearson's correlation coefficient (r), coefficient of variation (CV), intra-class correlation coefficient (ICC) were calculated. Bland-Altman plots were generated to visually assess the data.

Results: A total of 174 spectra were acquired, including 84 for intra-session analyses and 90 for inter-session analyses. No significant differences in absolute tCr concentrations between repeated intra- or inter-session measurements were shown in any region (mean differences=0.1-1.2%). Intra- and inter-session r values were between 0.909-0.985 and 0.836-0.858 (all p<0.001), depending upon region, and no trends in measurement bias were found. For the MB, VC and FC, intra-session CVs were 1.7%, 0.8% and 2.1%, ICCs were 0.903 (95%CI=0.727-0.968), 0.979 (95%CI=0.935-0.993) and 0.921 (95%CI=0.772-0.974) (all p<0.001), and MDCs were 1.2%, 0.6% and 1.5%, while inter-session CVs were 2.7%, 1.7% and 2.7%, ICCs were 0.835 (95%CI=0.578-0.941), 0.854 (95%CI=0.619-0.948) and 0.847 (95%CI=0.603-0.946) (all p<0.001), and MDCs were 1.9%, 1.2% and 1.9%. Inter-region differences in tCr concentration of up to 20.7% were shown.

Conclusions: Our findings indicate that ¹H-MRS at 3T can reliably and repeatably quantify absolute tCr concentrations in multiple human brain regions, when appropriate consideration is given to

potential sources of error. Changes in tCr concentration as small as 2% may be discernible from measurement error, however, centre-specific margins of error should be established prior to experimental investigation. More studies are required to determine whether similar findings are shown in other populations of interest, such as people suffering from neurological diseases or movement disorders.

Ethical statement: Manchester Metropolitan University's research ethics committee granted ethical approval and all participants provided written informed consent.

PCB046

Verification of the effectiveness and safety of serpentine-containing arm supports

Yoshinori Sato¹, Jun Hirayama⁴, Naotoshi Sugimoto³

¹Komatsu University, Komatsu, Japan, ²Kanazawa University, Kanazawa, Japan, ³Kanazawa University, Kanazawa, Japan, ⁴Komatsu University, Komatsu, Japan

Research Background and Objectives

In ancient Japan, warm stones ("*onjaku*") were used to warm the body during cold weather. *Onjaku* retains heat well and is considered the prototype of modern portable heat pads. Talc, pagodite, serpentinite, and hornblende were suitable for this purpose. We created arm supporters from serpentine-containing fibers and examined their effectiveness and safety.

Participants and Methods

Participants were young, healthy Japanese adults who were asked to enter a 25 °C room and stay there for approximately 30 min. The arm support was worn for 30 min, and we measured forearm temperature and the median venous vessel diameter of the forearm before and after wearing the arm support. Data are presented as means ± standard errors. A $p < 0.05$ indicated statistical significance. All research experiments were approved by the Ethics Committee of Komatsu University (approval number IRIN2219-2).

Results

We recruited ten Japanese female undergraduate students (age: 20.3 ± 0.2 years, body mass index: 20.4 ± 0.6 kg/m²). No adverse events, such as burning, redness, and swelling, or complaints of discomfort occurred during or after the 30-min period where the arm support was worn. We observed significant increases in forearm temperature (32.47 ± 0.29 °C to 34.59 ± 0.32 °C) and in median venous vessel diameter (2.65 ± 0.2 mm to 3.56 ± 0.14 mm) while the arm supporter was worn.

Discussion

Warming devices, such as modern disposable heat pads, often lead to burns and dermatitis. In this study, we used non-self-heating arm supports, which are considered extremely safe. Wearing the serpentine-containing arm supports for 30 min did not cause any adverse events, thus demonstrating their safety.

Moreover, we observed an increase in skin temperature and dilation of the median vein owing to the use of arm supports. Because the median vein is usually targeted during blood collection and infusion, increasing venous dilation might be beneficial for collecting blood or placing an intravenous line. Our novel, serpentine-containing arm supports have the potential for implementation in clinical practice.

Conclusion

Our results confirm the heat retention properties and safety of serpentine-containing arm supports.

Sato Y, Hirayama J, Sugimoto N (2023): Safety and heat retention of arm warmers made of serpentine-containing fibers. *J Well Health Care* 47, 9-14.

PCB047

Exploring skin blood flow signals with the wavelet transform

Henrique Silva^{1,2,3}, Carlota Rezendes²

¹Research Institute for Medicines (iMed.Ulisboa), Faculdade de Farmácia, Universidade de Lisboa, Av. Prof. Gama Pinto, 1649-003, Lisbon, Portugal, ²Department of Pharmacy, Pharmacology and Health Technologies, Faculdade de Farmácia, Universidade de Lisboa, Av. Prof. Gama Pinto, 1649-003, Lisbon, Portugal, ³Biophysics and Biomedical Engineering Institute (IBEB), Faculdade de Ciências, Universidade de Lisboa, Campo Grande, 1749-016, Lisbon, Portugal

The wavelet transform (WT) is an analytical tool that allows the decomposition of complex physiological signals into their respective spectral components, showing better performance than the fast Fourier transform. WT has been extensively applied to many physiological time series, including perfusion signals, where it has contributed to a deeper understanding of the underlying mechanisms of flowmotion regulation. However, there is a considerable heterogeneity in terms of application of the WT among different authors, which often leads to highly different conclusions regarding the same physiological mechanism. Our objective was to test different approaches regarding the application of WT to skin blood flow signals during a classic maneuver to evoke the venoarteriolar reflex (VAR). In particular, we aimed to clarify whether the characteristics of the original signal influenced the WT output and its interpretation. Fifteen healthy subjects (22.4 ± 5.2 y.o.) participated in this study after giving informed consent. After acclimatization, subjects performed a protocol to evoke VAR on the upper limb while sitting upright – 7 min resting with both arms at heart level (phase I), 5 min with one random arm (i.e., test limb) placed 40 cm below heart level (VAR, phase II) and 7 min recovery in the initial position (phase III). Skin blood flow was assessed in the index finger of the test limb with photoplethysmography (PPG). From the raw PPG signals (PPGr), two new time series were created – (1) PPG amplitude over time (PPGa) and (2) pulse over time (PPGp). All three signals were then processed with the wavelet transform (WT) and decomposed into their respective spectral components. For all WT spectra the dominant frequency and amplitude ratio of each major component were assessed. Both parameters were statistically compared between phases and between signals with the Wilcoxon test for related samples ($p < 0.05$). The PPGr and PPGa spectra showed the same components (cardiac, respiratory, myogenic, endothelial NO-dependent and endothelial NO-independent) in regions with similar dominant frequencies. In contrast, the PPGp spectra only showed components in regions consistent with the cardiac, respiratory and sympathetic activity. The amplitude ratios of the low frequency components (myogenic, sympathetic, endothelial) were significantly different between the PPGr and PPGa spectra during all phases of the protocol. Our results show that although highly valuable as an analytical tool, the WT shows considerable different outputs to different signals, especially in the low frequency components. This suggest that different WT analytical approaches could be considered to extract different information from the same physiological signal.

PCB048

Assessing superficial vein topography with a near-infrared vein finder – a pilot study

Henrique Silva^{1,2,3}, Carlota Rezendes²

¹Research Institute for Medicines (iMed.Ulisboa), Faculdade de Farmácia, Universidade de Lisboa, Av. Prof. Gama Pinto, 1649-003, Lisbon, Portugal, ²Department of Pharmacy, Pharmacology and Health Technologies, Faculdade de Farmácia, Universidade de Lisboa, Av. Prof. Gama Pinto, 1649-003, Lisbon, Portugal, ³Biophysics and Biomedical Engineering Institute (IBEB), Faculdade de Ciências, Universidade de Lisboa, Campo Grande, 1749-016, Lisbon, Portugal

The study of vessel topography is highly relevant in vascular physiology since it can have a considerable effect in hemodynamics. Furthermore, vascular abnormalities or dysmorphic features are present in several cardiovascular disorders. Branching regions of vascular trees are common sites for dysfunctional blood flow patterns due to well-known biophysical factors. Several imaging technologies are useful to assess vascular topography, although their high cost limits their use in experimental physiology. In the last decade the so-called portable “vein finders” were introduced and their popularity has been considerably increasing. These devices use near-infrared or visible light to improve the contrast of superficial veins and facilitate their detection for venipuncture. However, their potential has been underexplored in vascular physiology. This pilot study aimed at quantitatively describing the branching topography of the superficial veins of the hand dorsum using a low-cost near-infrared vein finder. Five healthy subjects (25.5 ± 5.2 y.o.) participated in this study after giving informed consent. While sitting upright and with both hands at heart level, an image of each hand dorsum was obtained from each subject. From these images 30 bifurcating superficial veins were assessed using ImageJ®, which allowed the calculation of several branching parameters (branching angle, branching coefficient, angular asymmetry, area ratio, optimality ratios, length-to-diameter ratio, junctional exponent deviation). Linear correlations between these parameters were tested with the Spearman coefficient ($p < 0.05$). Significant positive correlations were detected between the branching coefficient and area ratio, branching coefficient and optimality ratios and between the branching vessel diameter and the junctional exponent deviation. These results suggest that portable vein finders are useful tools for characterizing venous superficial vein topography. Further studies are needed to test their usefulness to assess venous perfusion in vivo.

Francisco MD, Chen W-F, Pan C-T, Lin M-C, Wen Z-H, Liao C-F, Shiue Y-L. Competitive Real-Time Near Infrared (NIR) Vein Finder Imaging Device to Improve Peripheral Subcutaneous Vein Selection in Venipuncture for Clinical Laboratory Testing. *Micromachines*. 2021; 12(4):373.
<https://doi.org/10.3390/mi12040373> Ikram MK, Cheung CY, Lorenzi M, Klein R, Jones TL, Wong TY. Retinal vascular caliber as a biomarker for diabetes microvascular complications. *Diabetes care* 2013, 36(3), 750.

PCB049

Investigating the acute effect of transcutaneous vagal stimulation on respiration and heart rate variability in healthy subjects

Heba Mohamed², Jenifer Gunaseelan¹, Sereene Ghariani¹, Richard Struthers³, Mirza Subhan¹

¹*School of Biomedical Sciences, University of Plymouth, Plymouth, United Kingdom*, ²*School of Biomedical Sciences, University of Plymouth, Plymouth, United Kingdom*, ³*Anaesthetic Department, University Hospitals Plymouth NHS Trust, Plymouth, United Kingdom*

Previous work has suggested that transcutaneous vagus nerve stimulation (tVNS) of the auricular branch of the vagus nerves might be associated with symptom relief pre-operatively and fewer complications after surgery. Recent studies have also shown improvements in heart rate variability (HRV) after tVNS in healthy subjects, but there is limited published data. The aim of this study was to compare the acute effects of tVNS with sham stimulation on respiration and HRV.

Thirty healthy subjects were recruited and gave written informed consent. The study was approved by the Science and Engineering Ethical Committee and was in accordance with the Declaration of Helsinki. Inclusion criteria was 18-65 year old healthy adults. Exclusion criteria was previous history of neuromuscular, autonomic, cardiorespiratory or ear skin conditions. Subjects completed a questionnaire, anthropometry and resting blood pressure, heart rate, and oxygen saturation measurements. Each participant completed three randomized interventions, each having a rest (10 minutes), stimulation (15 minutes), and recovery period (10 minutes), therefore, they completed nine consecutive experiments supine.

Electrical stimulation was delivered by placing an electrode clip to the auricular branch of the vagus nerve on the tragus of the external ear, earlobe, or thenar web space (the space between the thumb and index finger), using a commercial non-invasive transcutaneous electrical nerve stimulation (TENS) device. Electrodes were applied bilaterally, with the amplitude gradually adjusted until just below participants' level of sensory perception. The earlobe and the web space simulated sham stimulation, occurring at two different anatomical locations, relative to the tragus. During the stimulation, the electrocardiogram, heart rate variability, breathing rate (BR) and skin temperature were measured with Equivital wireless physiological monitoring equipment using LabChart software. HRV was assessed using time domain (heart rate - HR, standard deviation of the RR interval - SDRR) and frequency domain (low and high frequency - LF and HF). Data were statistically analysed for the complete time, the first and last five minutes, by repeated measures ANOVA, using SPSS. $P < 0.05$ was considered as significant.

Results were analyzed over all nine experiments. SDRR showed a significant increase ($P < 0.05$) for the first five minutes. Over the complete time, skin temperature ($P < 0.0001$) significantly increased. HR, LF, HF, LF/HF ratio, BR ($P > 0.05$) were not significantly different.

The primary findings of our investigation showed that tVNS & other sham site stimulation largely did not have a significant effect on the HRV, HR or BR, demonstrating that tVNS is not effective in modifying these aspects of autonomic function in our subjects. One reason our subjects did not show a marked vagal cardiorespiratory effect of tVNS could be due to their younger age (mean SD = 27.8 (12.1) years), relative to previous work. A steady increase in temperature across the interventions could have been due to a cold couch the subjects were lying on. This investigation includes limitations such as the small population size and a varied TENS neuro-sensitivity threshold. In conclusion, these findings provide a potential foundation for further research into the effects of tVNS and possible clinical applications.

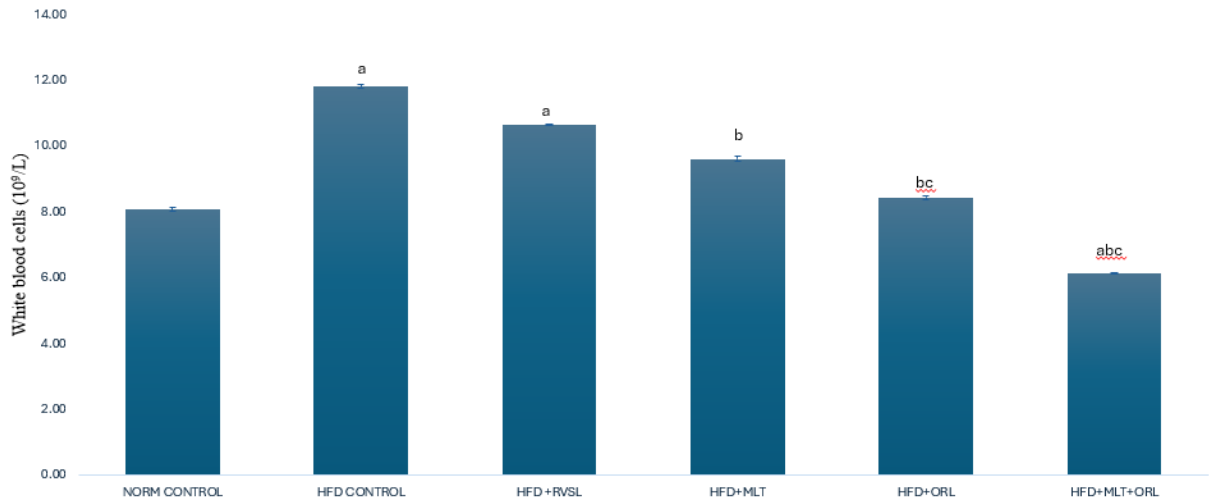
HAEMATOLOGICAL EFFECTS OF MELATONIN ADMINISTRATION ON OBESE WISTAR RATS: A COMPARATIVE ANALYSIS

Tahir Abdussalam², Luqman Olayaki¹

¹University of Ilorin, Ilorin, Nigeria, ²University of Ilorin, Ilorin, Nigeria

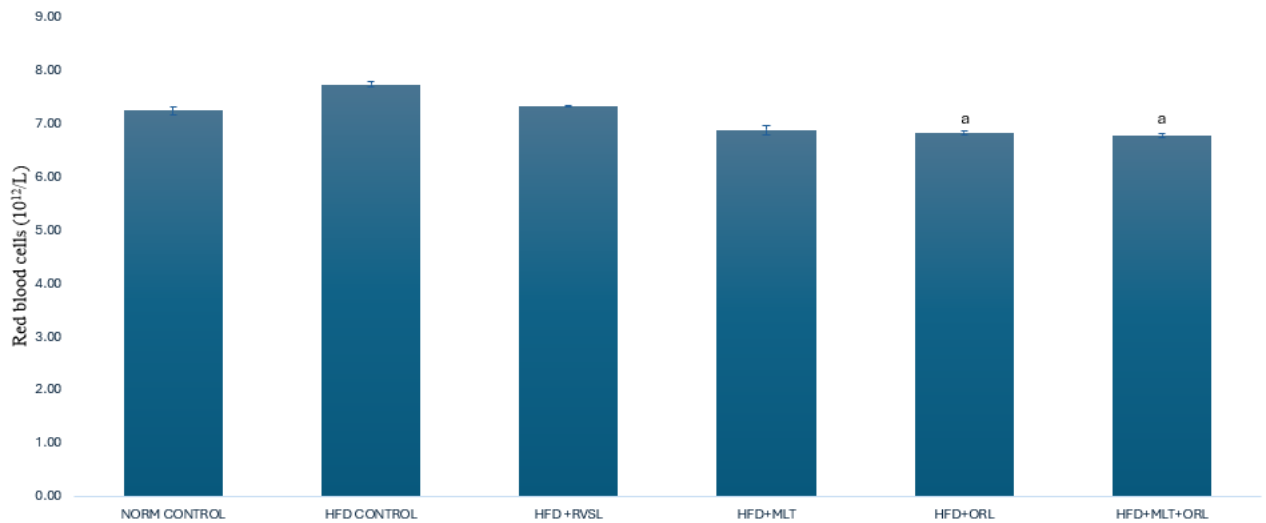
The prevalence of obesity, characterized as a metabolic disorder, has escalated to epidemic levels, posing significant public health challenges. Studies have demonstrated a direct correlation between increased body weight, altered haematological indices and elevated mortality rates. Despite concerted efforts, the persistent struggle against these conditions has prompted the exploration for innovative therapeutic interventions. For the treatment of obesity, the gastrointestinal lipase inhibitor orlistat has been suggested. Nonetheless, the majority of patients have been dissuaded from continuing to use it due to the gastrointestinal adverse effects. Therefore, a stronger medication with fewer adverse effects is required. It has been observed that melatonin, a commonly used alternative medication, effectively lowers body weight with very little negative effects. Therefore, the present study investigated the haematological effects of melatonin administration in obesity model of male Wistar rats weighing between 120 – 140 g. It was hypothesized that combined administration of melatonin and orlistat are not anti-obesitogenic therapy on obese rat model. Sixty (60) rats of ten (10) animals per group were divided into the following: control (untreated); high fat diet (HFD); high fat diet recovery (hfd); HFD + melatonin (4 mg/kg); hfd + orlistat (30 mg/kg); and HFD + melatonin (4 mg/kg) + orlistat (30 mg/kg). Obesity was induced by exposing the rats to high fat diet for 16 weeks and confirmation was done using Lee index, which was determined by the formula: $4\sqrt{\text{body weight (g)} / \text{nose-anal length (cm)}}$ (Adeyemi et al., 2020). Rats with an index higher than 0.30 were considered obese and were used for the study. Diagnostic kits for the determination of the biomarkers were obtained from Abcam PLC, Cambridge, UK and the assays were performed according to the manufacturer's instruction. Data were analyzed using analysis of variance and LSD *post hoc* test at 0.05 level of significance. The results showed that the induced obesity was accompanied with significant increases in plasma glucose, plasma insulin, packed cell volume (PCV), haemoglobin (HB), red blood cells (RBC) and white blood cells (WBC). Relative to the obese control, treatments with melatonin, orlistat and combined administration of both agents caused significant decrease in those parameters with the combined administration having a more potent effect. Hence, it was concluded that combined administration of melatonin and orlistat could be a better candidate in the management of haematological parameters in obese conditions.

Figure 5: Effects of combined administration of melatonin and orlistat on white blood cells



Values are expressed as MEAN \pm SEM. ^a $p < 0.05$ vs control, ^b $p < 0.05$ vs high fat diet (HFD) control, ^c $p < 0.05$ vs HFD reversal group.

Figure 4: Effects of combined administration of melatonin and orlistat on red blood cells



Values are expressed as MEAN \pm SEM. ^a $p < 0.05$ vs high fat diet (HFD) control.

Figure 1: Effects of combined administration of melatonin and orlistat on plasma glucose

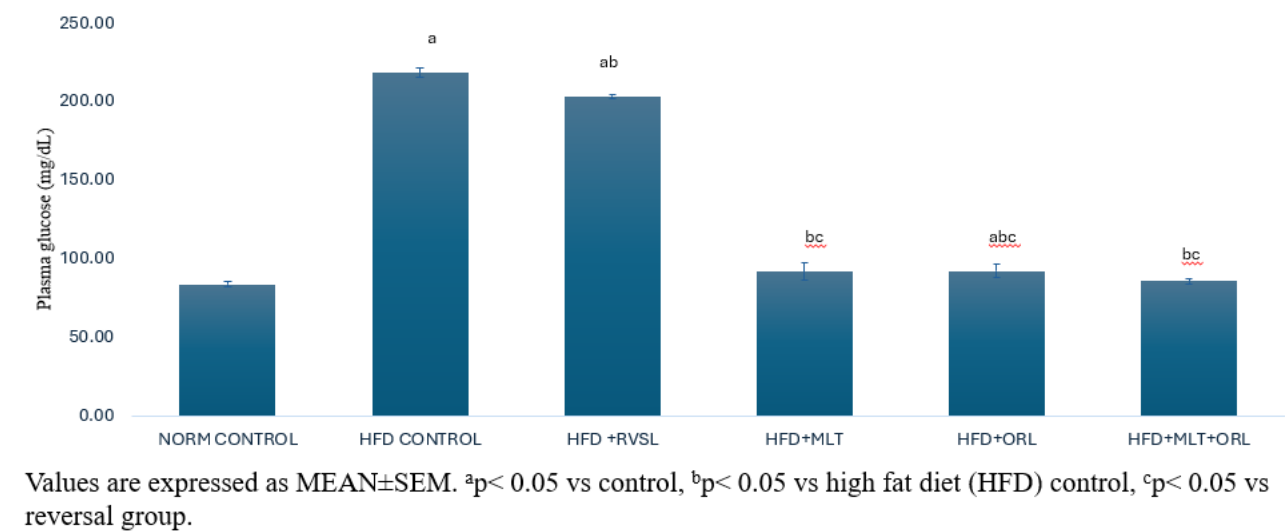


Figure 3: Effects of combined administration of melatonin and orlistat on packed cell volume

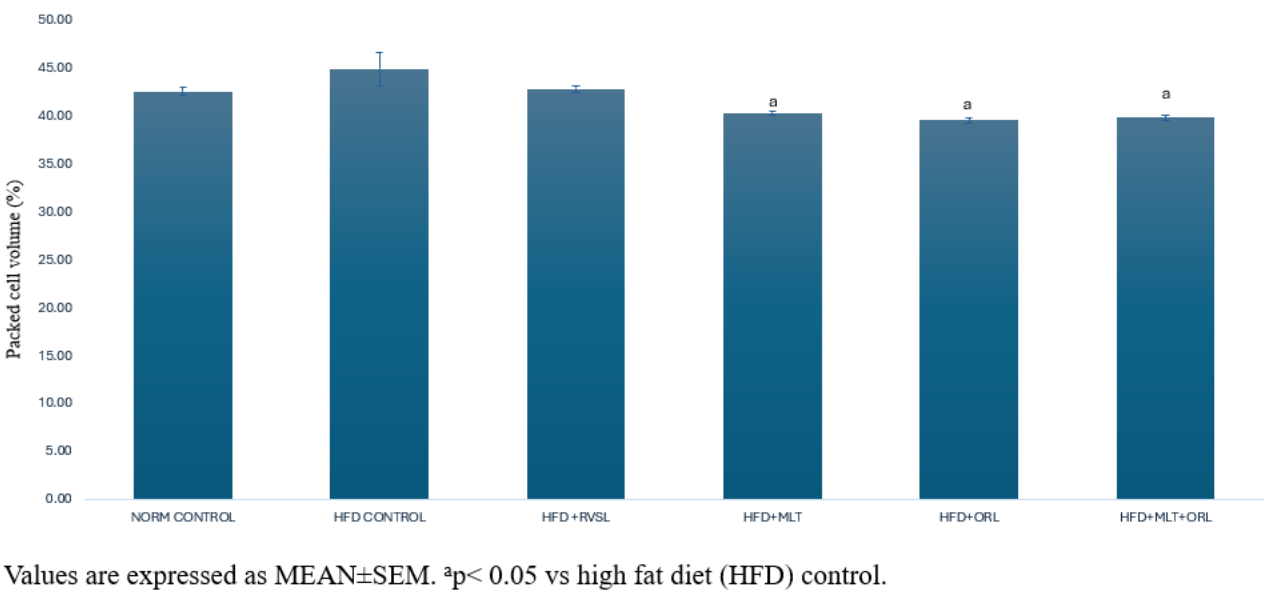
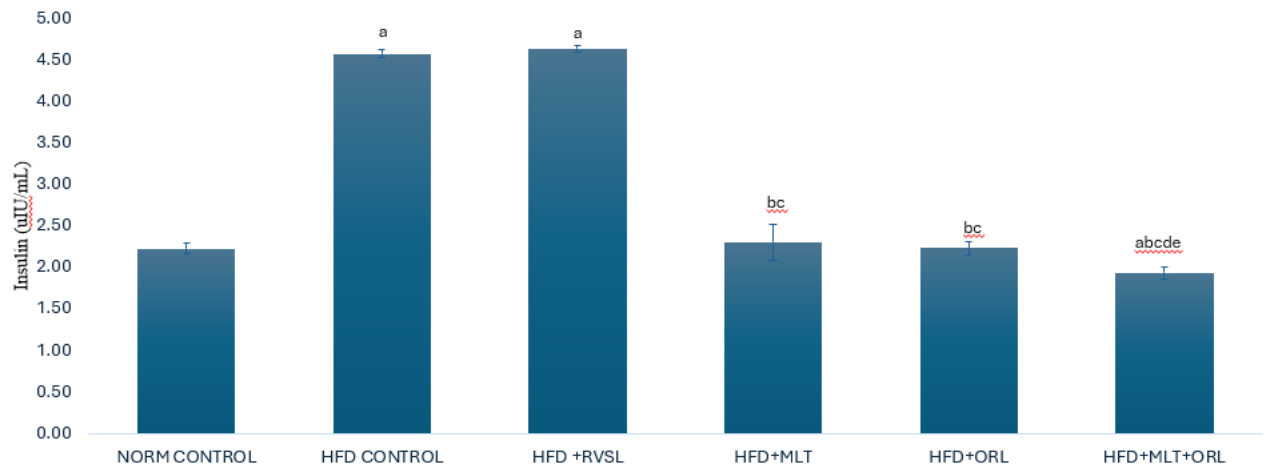


Figure 2: Effects of combined administration of melatonin and orlistat on plasma insulin



Values are expressed as MEAN \pm SEM. ^a p < 0.05 vs control, ^b p < 0.05 vs high fat diet (HFD) control, ^c p < 0.05 vs reversal group, ^d p < 0.05 vs HFD+MLT group, ^e p < 0.05 vs HFD+ORL group.

Adeyemi et al. (2020). PharmaNutrition 13, 100192.

PCB051

Mechanistic insights into plasma glucose lowering action of whey protein: role of glucoregulatory hormones on glucose flux

Giang Dao^{1,2}, Chris Shaw², Andrew Betik², Vicky Kuriel², Clinton Bruce², Greg Kowalski^{1,2}

¹*Metabolic Research Unit, School of Medicine, Deakin University, Geelong, Australia,* ²*Institute for Physical Activity and Nutrition, School of Exercise and Nutrition Sciences, Deakin University, Geelong, Australia*

Introduction: It is generally regarded that insulin and glucagon exert opposing actions on plasma glucose: insulin lowers glucose by suppressing endogenous glucose production (EGP) and stimulating glucose uptake, while glucagon increases glucose by stimulating EGP. Protein and glucose co-ingestion stimulates both insulin and glucagon secretion, however glucose excursions are typically reduced compared to ingestion of a matched amount of glucose alone. Despite stimulating glucagon secretion, it is unclear how protein lowers glucose excursions. Therefore, this study addressed this by measuring postprandial glucose fluxes via the triple stable isotope glucose tracer technique following ingestion of either glucose (alone), or glucose and whey protein combined.

Methods: The study was approved by Deakin University Human Research Ethics Committee (2022-181). Eleven adults (5M/6F, 27±1.5 years, BMI: 23.4±0.6 kg/m²) underwent three trials in random order, ingesting either 25g glucose (25G;~100 kcal), 50g glucose (50G;~200kcal) or 25g glucose plus 25g whey protein (WG;~200kcal). This allowed group comparisons where both glucose (WG vs 25G) and calories (WG vs 50G) were matched. Each trial utilised three stable isotope glucose tracers: [6,6-²H] and [U-¹³C] for variable infusions, and [1-²H] for ingestion. Arterialised blood samples were obtained for 4h post-meal, to determine tracer enrichments (gas chromatography-mass spectrometry), insulin, glucagon, GLP-1, GIP, and C-peptide (ELISA). Glucose fluxes (EGP and rates of exogenous glucose appearance (meal Ra) and glucose disappearance (Rd)) were calculated using Steele's non-steady-state model. Data were reported as mean±SEM. One-way or two-way ANOVA were used for analyses where appropriate, followed by a Holm-Sidak's post hoc test (Graphpad Prism), with statistical significance set at p<0.05.

Results: The integrated postprandial glucose response (incremental area under the curve; iAUC) was markedly lower for WG (78±13 mmol.240min/L) compared to both 25G (182±27 mmol.240min/L, p<0.001) and 50G (310±45 mmol.240min/L, p<0.001). As expected, WG increased glucagon concentrations (~3-fold basal), while both 25G and 50G reduced glucagon levels. Insulin total iAUC was higher for WG vs 25G (p=0.01). Comparing WG vs 50G (calories matched), WG produced higher peak insulin concentrations (630±131 pmol/L vs 442±82 pmol/L, p=0.04) and tended to produce a higher insulin response over the initial 30min postprandial period (iAUC_{0-30min}, p=0.07). Despite the enhanced early insulin response, WG and 50G produced comparable GIP and GLP-1 responses (p>0.05). EGP suppression was less pronounced for WG (~48% suppressed) compared to 25G (~70% suppressed) or 50G (79% suppressed), p<0.001. WG vs 25G resulted in comparable Rd iAUC_{0-60min} (p>0.05) but tended to lower meal Ra iAUC_{0-60min} (254±35 mg.60min/kg vs 294±36 mg.60min/kg, p=0.07).

Conclusion: The findings confirm that whey/glucose co-ingestion, compared to the same glucose dose alone, reduces postprandial glucose excursions, enhances the insulin response, and induces a robust glucagon response. Additionally, we show that for the same caloric content but half glucose amount, whey/glucose co-ingestion enhances the early insulin response compared to glucose alone, which could be driven by amino acids and/or glucagon but not GLP-1 or GIP. We also provide novel mechanistic data, revealing that the addition of whey protein lowers glycaemic excursions despite less EGP suppression, with the net glycaemic benefit coming from reduced glucose absorption rates, not enhanced Rd.

PCB052

Effect of Vitamin B12 on leucine-induced anabolic signaling in C2C12 myotubes

Naoki Fukao¹, Mito Watanabe¹, Satoshi Fujita²

¹Graduate School of Sport and Health Science, Ritsumeikan University, Kusatsu, Shiga, Japan,

²Faculty of Sport and Health Science, Ritsumeikan University, Kusatsu, Shiga, Japan

Introduction

Skeletal muscle mass is regulated by the balance between protein synthesis and degradation. Leucine, an essential amino acid, is known to activate mechanistic/mammalian target of complex1 (mTORC1) activity and enhance muscle anabolic response (Atherton et al. 2010). Recently, lower serum level of vitamin B12 (VB12) (<350pg/ml) has been reported to be associated with the incidence of sarcopenia (Choi et al. 2023). One of the factors contributing to sarcopenia is believed to be blunted skeletal muscle anabolic response to protein and amino acids intake (Cuthbertson et al. 2005, Aragon et al. 2023). However, effect of VB12 on leucine-induced anabolic signaling has not been investigated. Therefore, this study aimed to investigate the effect of VB12 on leucine-induced responses on anabolic signaling pathways.

Methods

Mouse C2C12 cells were seeded at 0.5×10^5 cells/ml in 12-well plates and cultured in DMEM containing 2% horse serum for 6 days to form myotubes. After differentiation, myotubes were cultured in serum-free medium for 1 hour, followed by incubation in amino acids and serum-free medium for 1 hour. Cells were then cultured in (1) Control (Con), (2) Leucine 1.5mM (Leu), (3) Leucine 1.5mM + VB12 10 μ M (Leu + Low-VB12), (4) Leucine 1.5mM + VB12 100 μ M (Leu + High-VB12) for 30 minutes and collected (n=4/group). Western blotting was performed to evaluate the expression levels of proteins involved in muscle protein synthesis. For statistical analysis, SPSS Statistics ver.28 was used. One-way ANOVA was performed, and multiple comparisons were conducted by Tukey only when significant differences were found. Significance level was set at $p < 0.05$.

Results

There was a significant difference in phosphorylation / total-p70S6K expression, a downstream factor of mTORC1, between groups ($p < 0.001$). Multiple comparisons showed that Leu + Low-VB12 group showed significantly lower phosphorylation / total-p70S6K expression than Leu group (Leu + Low-VB12: 1.02 ± 0.08 vs Leu: 1.46 ± 0.10 , $p = 0.016$) and there is no significant difference between Leu + Low-VB12 group and Con group (Leu + Low-VB12: 1.02 ± 0.08 vs Con: 1.00 ± 0.06 , $p = 0.998$). On the other hand, Leu + High-VB12 group showed significantly higher phosphorylation / total-p70S6K expression compared to Con and Leu group (Leu + High-VB12: 2.02 ± 0.10 vs Con: $1.00 \pm$

0.06 / Leu: 1.46 ± 0.10 , $p < 0.001$, $p = 0.003$, respectively). Moreover, there was a significant difference in t-4E-BP1 γ form ratio between groups ($p = 0.002$). Multiple comparisons showed that Leu and Leu + High-VB12 group showed significantly higher t-4E-BP1 γ form ratio than Con group (Leu: 1.20 ± 0.02 / Leu + High-VB12 1.18 ± 0.03 vs Con: 1.00 ± 0.02 , $p = 0.002$, $p = 0.006$, respectively).

Conclusion

These results suggest that low-level VB12 blunt anabolic signaling but high-level VB12 enhanced leucine-induced anabolic signaling in C2C12 cells.

Atherton et al. (2010). Amino Acids, 38(5). Choi et al. (2023). Nutrients, 15(4). Aragon et al. (2023). Nutrition Reviews, 81(4). Cuthbertson et al. (2005). FASEB J, 19(3)

PCB053

Identifying microbial protein metabolites that regulate Glut4 translocation in skeletal muscle

Sati Gurel¹, Rashmi Sivasengh², Madalina Neacsu², Brendan M. Gabriel²

¹*Department of Nutrition and Dietetics, Faculty of Health Sciences, Trakya University, Edirne, Turkey,* ²*University of Aberdeen, Aberdeen, United Kingdom*

The intake of plant-based foods has been shown to lead to a reduction in plasma levels of branched-chain amino acids, phenylalanine, and tyrosine, which are amino acids linked to insulin resistance (Neacsu et al., 2022). Hemp is a high protein crop and stands out due to its quality nutritional profile among gluten-free plant species that provide valuable industrial outputs with less impact on the environment (Yano & Fu, 2023). After consuming isoproteic meals rich in hemp or meat, certain plasma microbial metabolites were significantly elevated following the hemp meal and linked to lower levels of insulin and ghrelin. It is important to investigate the impact of plant-based foods on altering plasma amino acid profiles and gut hormone levels, given that diets rich in high-protein crops have been shown to be inversely related to the risk of metabolic syndrome and Type 2 Diabetes (T2D) (Neacsu et al., 2022). Several metabolomics studies have explored the relationship between systemic and microbial metabolites and metabolic diseases, underscoring the importance of comprehending their diverse roles in insulin resistance development for identifying novel therapeutic targets against metabolic disorders.

Skeletal muscle, which is considered a central organ in T2D pathology, has an important role in glucose homeostasis in the body. In insulin resistant skeletal muscle, proximal insulin signalling events are impaired and this blocks the insulin-dependent GLUT4 translocation to the plasma membrane. Thus, impaired glucose uptake in skeletal muscle is often considered a primary defect in T2D and is therefore targeted as a therapeutic strategy against insulin resistance (Abdelmoez et al., 2020). In this study we have conducted a scoping review of human studies that investigated protein microbial metabolites and insulin sensitivity. For our scoping review, Pubmed, Scopus, ScienceDirect databases were searched to determine studies examining the effects of protein microbial metabolites on glucose metabolism. From a total 203 articles initially identified, 17 were included in this review. 11 were epidemiological studies, 6 were clinical studies (including dietary intervention studies). The majority of the identified studies (14 articles) report an inverse relationship of indole-3-propionic acid with T2D development and/or its effect on glucose metabolism. Furthermore, the hippuric acid, benzoic acid and phenylalanine were reported to have a beneficial effect on glucose metabolism (fasting glucose, fasting insulin, HOMA-IR, insulin sensitivity) (Neacsu et al. 2022; Koistinen et al. 2024; Vangipurapu et al. 2020). In summary, our scoping review has identified several promising protein microbial metabolites that may affect peripheral tissue insulin sensitivity and could be used as nutritional therapies for T2D.

Abdelmoez, A. M., Sardón Puig, L., Smith, J. A., Gabriel, B. M., Savikj, M., Dollet, L., ... & Pillon, N. J. (2020). Comparative profiling of skeletal muscle models reveals heterogeneity of transcriptome and metabolism. *American Journal of Physiology-Cell Physiology*, 318(3), C615-C626. Koistinen, V. M., Haldar, S., Tuomainen, M., Lehtonen, M., Klåvus, A., Draper, J., ... & Hanhineva, K. (2024). Metabolic changes in response to varying whole-grain wheat and rye intake. *npj Science of Food*, 8(1), 8. Neacsu, M., Vaughan, N. J., Multari, S., Haljas, E., Scobbie, L., Duncan, G. J., ... & Russell,

W. R. (2022). Hemp and buckwheat are valuable sources of dietary amino acids, beneficially modulating gastrointestinal hormones and promoting satiety in healthy volunteers. *European journal of nutrition*, 1-16. Vangipurapu, J., Fernandes Silva, L., Kuulasmaa, T., Smith, U., & Laakso, M. (2020). Microbiota-related metabolites and the risk of type 2 diabetes. *Diabetes care*, 43(6), 1319-1325. Yano, H., & Fu, W. (2023). Hemp: A sustainable plant with high industrial value in food processing. *Foods*, 12(3), 651.

PCB054

Investigating the inter-organ crosstalk between liver and heart in a model of metabolic disease

Joanna Konieczny¹, John Martin Fredriksen¹, Cecilie Ness¹, Julija Lazarevic¹, Manar Kalaaji¹, Trine Lund¹, Kirsti Ytrehus¹, Neoma Boardman¹

¹*University of Tromsø-The Arctic University of Norway, Tromsø, Norway*

Fatty liver is a silent manifestation of the metabolic syndrome that affects millions worldwide leading to metabolic-associated fatty liver disease (MAFLD) with both a lean and overweight phenotype. There is a high risk of cardiovascular complications and mortality associated with the disease, that is more prevalent than liver pathology-related deaths. To study changes occurring in early stages of the disease can shed a light on the extend of those associations related to inter-organ crosstalk.

We hypothesized that chronic fructose intake leads to liver steatosis and can induce liver mitochondrial stress and an alarm response in the heart. In this project, we have investigated the consequences of fructose intake in the liver and heart, with a focus on mitochondrial stress and its drivers in liver-heart crosstalk under these conditions.

Methods

Animal experiments were designed according to European guidelines (FELASA; EU animal research directive 86/609/EEC and 2010/63/ EU) and approved by the local authority of the National Animal Research Authority in Norway. Male rats (Sprague-Dawley, 250 g) were given normal chow and tap water ad libitum (CON, n=12) or a 15% fructose drink (FRU, n=12) for 16 weeks. Body composition was measured throughout the intervention (EchoMRI) as well as tail-cuff measurement of blood pressure (CODA) and tail-vein blood samples. Serum cytokines (Bioplex) were analyzed. Tissue from liver and heart was obtained postmortem following 16-weeks fructose intake. Liver triglycerides (TG) were assessed by a colorimetric assay. Cardiac and liver mitochondrial respiratory capacity was determined in tissue homogenate (O2K, Oroboros) and mitochondrial H₂O₂ production was determined in the heart. Histology and Reverse Transcription quantitative PCR were used to assess changes in liver and heart, including hematoxylin and eosin (H&E), PicroSirius Red (PSR), Oil Red O (ORO) and dihydroethidium (DHE) stainings.

Results

16-week fructose intake increased body weight, percentage of fat mass and induced liver steatosis. Histological analysis determined increased ORO staining of lipid droplets in liver and TG in tissue homogenate was increased. H&E staining did not reveal macrovesicular steatosis, nor was increased liver collagen deposition observed with PSR. Mean arterial pressure as well as serum levels of interleukin-6 and tumour necrosis factor-alpha were elevated in fructose (FRU) rats. The heart weights were elevated in FRU however histological analysis did not reveal changes in cardiomyocyte size by H&E staining, collagen deposition, lipid droplet and reactive oxygen species formation in the nuclei measured by DHE. Complex I-linked mitochondrial oxidative

phosphorylation (CI-OXPHOS) and mitochondrial respiratory capacity was lower in liver homogenate from FRU and mRNA expression indicated metabolic changes, mitochondrial stress and elevated Fibroblast Growth Factor 21 (FGF21). CI-OXPHOS was also lower in heart homogenates from FRU along with altered mitochondrial H₂O₂ production.

Conclusion

Liver steatosis is associated with cardiac adaptations that may contribute to the development of heart failure. Increased FGF21 expression levels in the liver indicate potential driver of detrimental liver-heart crosstalk, a role that is of interest for further investigation.

PCB055

The effects of cysteamine on visceral adipose tissue remodelling in an LDL receptor knockout model after a high-fat diet

Chiemelum Okagbue¹, Feroz Ahmed², David Leake¹, Sam Boateng¹, Dyan Selleyah¹

¹University of Reading, Reading, United Kingdom, ²Race Oncology, Sydney, Australia

Obesity contributes to the pathological remodelling of adipose tissue due to accommodating the caloric imbalance. Obesity can lead to several associated risk factors such as elevated cholesterol (specifically low-density lipoproteins (LDLs)) which can result in an increased risk of cardiovascular disease. However, the administration of anti-oxidizing agents and switching to a balanced diet have been shown to ameliorate the pathological effects of obesity on adipose tissue. For example, cysteamine has been previously shown to reduce the size of atherosclerotic lesions in the aorta in an LDL receptor knockout (*Ldlr*^{-/-}) model fed a high-fat diet (HFD) as well as inhibit the oxidation of LDLs by iron at optimal lysosomal pH (4.5). (Wen et al., 2019).

Therefore, this study explored whether cysteamine can enhance the benefits of switching from a high-fat diet (HFD) to a balanced chow diet. This was done by investigating the extent of the remodelling of visceral adipose tissue (VAT) in an LDL receptor knockout model fed an HFD.

Nine-week-old female *Ldlr*^{-/-} mice were separated into an HFD group, a regular chow diet-only (RCD) group, and a regular chow diet + cysteamine (RCD/C) group. The VAT cellularity was studied using haematoxylin and eosin staining. The extent of VAT fibrosis and VAT oxidative stress were measured using picro sirius red and dihydroethidium staining respectively. Lastly, the gene expression in the VAT was studied using RNA-Seq Analysis. All procedures complied with the Animals (Scientific Procedures) Act 1986 and were approved by the Ethical Review Process Committee of the University of Reading.

The VAT cellularity analysis showed that switching to a balanced chow diet alone resulted in a significant decrease in the adipocyte diameter of the VAT ($960.36 \pm 62.45\mu\text{m}$; $n=5$) in comparison to the RCD/C group ($1889.49 \pm 298.20\mu\text{m}$; $n=5$). This implies the possible inhibition of lipolysis by cysteamine because the VAT larger adipocytes were a similar size to the HFD control group ($1363.19 \pm 179.40\mu\text{m}$; $n=5$). Markers of both fibrosis and oxidative stress showed no marked difference in any of the treatment groups suggesting cysteamine did not affect the VAT phenotype in terms of fibrosis and oxidative stress.

The gene ontology (GO) enrichment analysis highlighted GO terms associated with glucose homeostasis and the negative regulation of cell growth/signalling in the sole downregulated gene between the RCD group and the RCD/C group (*Bmal1*). The GO enrichment analysis for the differentially spliced genes also revealed GO terms associated with cell growth/signalling such as “anatomical structure morphogenesis” between the RCD group and the RCD/C group. Additionally, the GO term “regulation of cold-induced thermogenesis” was also enriched during the analysis that is specific to adipose tissue function. This possibly corroborates the inhibition of the reduction in the VAT adipocyte diameter with cysteamine treatment due to the role of thermogenesis in the lipolysis of white adipose tissue.

Overall, this suggests that cysteamine can influence adipocyte remodelling during the switch from an HFD to an RCD by preventing the lipolysis of the VAT lipid stores required for lipid homeostasis under normal conditions and obesity.

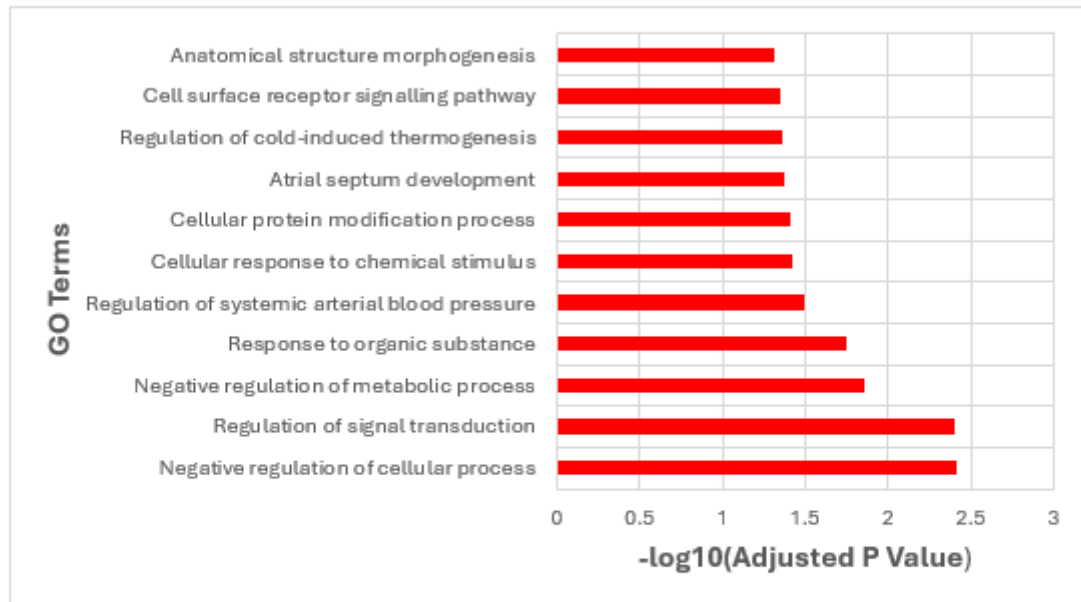


Figure 4: The gene ontology of the genes that were differentially spliced between the RCD/C and RCD groups showing the biological processes that spliced variants are involved in determined by the Fisher exact test with $n=4$ from the RNA-Seq Analysis by Genewiz ($p \leq 0.05$).

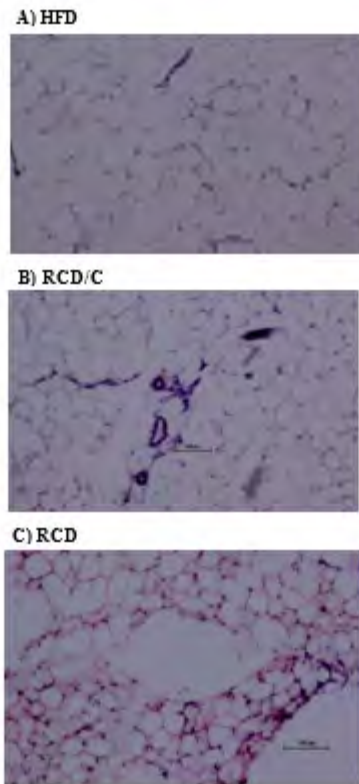


Figure 1: H&E staining showing the adipocyte morphology of VAT at a magnification of 100x in (A) The HFD control, (B) The cysteamine treatment group and (C) The regression diet only group after 8 weeks of a HFD and a further 8 weeks of a normal chow diet and cysteamine treatment (B and C); bar = 100µm.

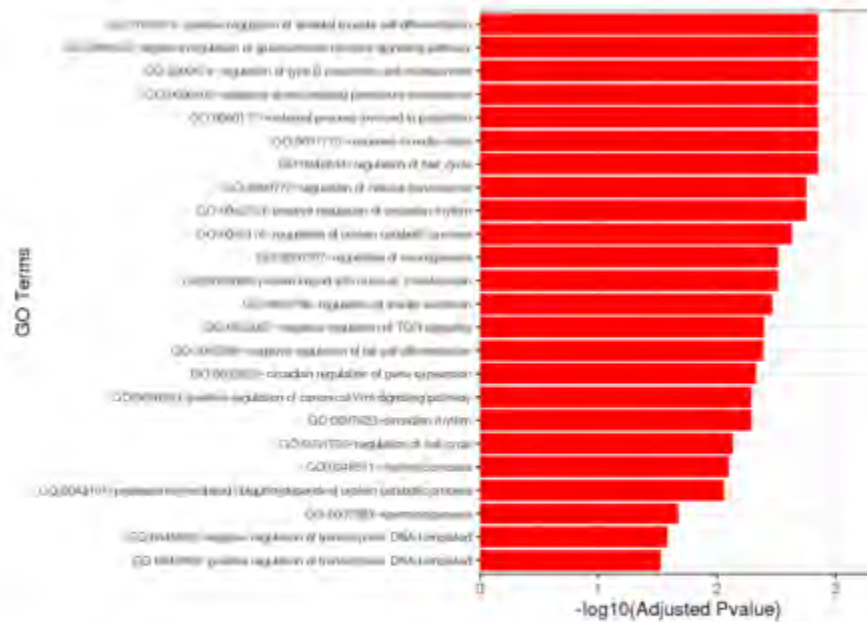


Figure 3: The gene ontology of the genes that were differentially expressed between the RCD/C and RCD groups showing the biological processes that the genes are involved in determined by the Fisher exact test with $n=4$ from the RNA-Seq Analysis by Genewiz ($p \leq 0.05$).

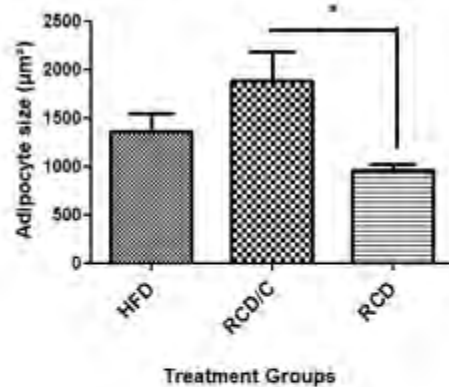
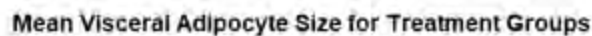


Figure 2: A regression diet alone can reduce the diameter of visceral adipocytes after the administration of an HFD. The addition of cysteamine has no marked effect on the diameter of visceral adipocytes. All values represent the mean \pm the standard error of the mean with $n = 5$. In comparison across the experimental groups, the statistical significance is denoted as * $p < 0.05$ using the Kruskal-Wallis test and post hoc Dunn's correction.

Physiology in Focus 2024

Northumbria University, Newcastle, UK | 2 – 4 July 2024

WEN, Y., ET AL. (2019). "Cysteamine inhibits lysosomal oxidation of low-density lipoprotein in human macrophages and reduces atherosclerosis in mice." *Atherosclerosis* 291: 9-18.

PCB056

The impact of acute exercise before and after a simulated nightshift on metabolic health markers in healthy adults: an interim analysis of a randomised controlled trial

Cian Sweeney¹, David Clayton¹, Fran Pilkington-Cheney¹, Angus Hunter¹, Emma Sweeney¹

¹*Nottingham Trent University, Nottingham, United Kingdom*

Introduction

Shift work is associated with an increased risk of developing cardiometabolic diseases (Ho et al., 2022). Experimental research has demonstrated decreased insulin sensitivity after simulated nightshifts (Morris et al., 2016). Despite these well-documented consequences of shift work, feasible mitigation strategies are lacking. Exercise is beneficial for cardiometabolic health, with moderate-intensity exercise improving insulin sensitivity (Bird and Hawley, 2016). Therefore, exercise may alleviate the effect of shift work on cardiometabolic health. Hence, this study aimed to investigate the impact of exercise before or after a simulated nightshift on metabolic health in adults.

Methods

Seven healthy participants completed a familiarisation and three experimental trials in a randomised, counterbalanced, crossover design, separated by at least seven days. The experimental protocol involved a simulated 12-hour nightshift, with exercise (30 minutes cycling at 60% of $\text{VO}_{2\text{max}}$ peak power) either immediately before (PRE) or immediately after (POST) the shift, or no exercise (CON). Each trial started at 07:00, with a nap opportunity from 15:00-17:00. The simulated nightshift then started at 20:00. During the shift, participants completed cognitive assessments, appetite and fatigue questionnaires, light physical activity, and consumed a standardised diet. Participants were then in bed from 10:00-16:00. Wrist actigraphy was used to ensure compliance. At 17:00, an oral glucose tolerance test (OGTT) was conducted, with blood samples collected for measurement of insulin and glucose, followed by an ad-libitum evening meal to assess energy intake. Linear mixed models were used to compare outcomes between trials. Data are presented as mean \pm SD, with significance set at $p < 0.05$.

Results

No significant differences were present between the PRE, POST and CON trials for glucose AUC (675.3 ± 131.1 AU, 700.1 ± 134.7 AU and 726.3 ± 140.8 AU, respectively; $p = 0.761$), insulin AUC (2862.1 ± 1307.3 AU, 3376.0 ± 1350.3 AU, and 3054.1 ± 617.2 AU, respectively; $p = 0.470$), Matsuda index (13.20 ± 3.44 , 11.08 ± 2.34 and 11.72 ± 2.81 respectively; $p = 0.381$) and HOMA-IR (0.66 ± 0.06 , 0.80 ± 0.25 , and 0.77 ± 0.67 , respectively; $p = 0.151$). No significant differences were observed for substrate utilisation (CHO oxidation PRE: 106.4 ± 25.8 g vs POST: 105.4 ± 20.0 g; $p = 0.516$ and fat oxidation PRE: -1.1 ± 3.4 g vs POST: -2.3 ± 3.0 g; $p = 0.263$), rate of perceived exertion ($p = 0.216$) or heart rate ($p = 0.106$) during exercise before compared to after the simulated nightshift. Ad-libitum energy intake was not significantly different between trials (1021 ± 500 Kcal, 1137 ± 454 Kcal, and 1108 ± 677 Kcal for PRE, POST and CON, respectively; $p = 0.106$).

Discussion

This interim analysis demonstrated no significant impact of exercise before or after a simulated nightshift on metabolic health markers during an OGTT, or changes in physiological variables during exercise before compared to after a shift. The findings suggest that acute exercise is not sufficient to induce meaningful improvements in metabolic markers. However, due to the sample size in the current interim analysis, further research is warranted to fully understand the efficacy of exercise in mitigating the consequences of shift work on metabolic health.

1. Bird, S.R., & Hawley, J.A. (2017). Update on the effects of physical activity on insulin sensitivity in humans. *BMJ Open Sport & Exercise Medicine*, 2(1), e000143. 2. Ho, F.K., Celis-Morales, C., Gray, S.R., Demou, E., Mackay, D., Welsh, P., Katikireddi, S.V., Sattar, N., & Pell, J.P. (2022). Association and pathways between shift work and cardiovascular disease: a prospective cohort study of 238,661 participants from UK Biobank. *International Journal of Epidemiology*, 51(2), 579–590. <https://doi.org/10.1093/ije/dyab144> 3. Morris, C.J., Purvis, T.E., Mistretta, J., & Scheer, F.A.J.L. (2016). Effects of the Internal Circadian System and Circadian Misalignment on Glucose Tolerance in Chronic Shift Workers. *The Journal of Clinical Endocrinology & Metabolism*, 101(3), 1066–1074. <https://doi.org/10.1210/jc.2015-3924>

PCB057

Effects of β -hydroxybutyrate on muscle protein synthesis and anabolic signaling in C2C12 myotubes

Mito Watanabe¹, Fukao Naoki¹, Ryo Takagi³, Jonathan Little⁴, Satoshi Fujita⁵

¹Graduate School of sports and health science, Ritsumeikan University, Kusatsu, Japan, ²Graduate School Sports and Health Science, Ritsumeikan University, Kusatsu, Japan, ³Ritsumeikan Global Innovation Research Organization, Ritsumeikan University, Kusatsu, Japan, ⁴School of Health and Exercise Sciences, University of British Columbia Okanagan, Kelowna, Canada, ⁵Faculty of Sport and Health Science, Ritsumeikan University, Kusatsu, Japan

Introduction:

Ketone bodies are small molecules consisting of β -hydroxybutyrate, acetoacetate, and acetone that serve as an alternative energy source when carbohydrates are depleted ¹⁾. In particular, β -hydroxybutyrate, which accounts for approximately 80% of ketone bodies in the blood, has been shown to have potent physiological effects. It has been reported that β -hydroxybutyrate improves mitochondrial function and may suppress muscle catabolism caused by inflammation in skeletal muscle ²⁾³⁾. However, the effect on skeletal muscle protein synthesis response is not clear. Therefore, the purpose of this study was to examine the direct effects of β -hydroxybutyrate on muscle protein synthesis and anabolic signaling in C2C12 myotubes.

Methods:

C2C12 myoblasts were cultured in DMEM containing 2% horse serum for 5 days to induce differentiation into myotubes. After differentiation, the myotubes were incubated with DMEM containing different concentrations of β -hydroxybutyrate (0, 0.25, 0.5, 1, 2, 5mM) for 30 minutes. For assessment of protein synthesis, myotubes were treated with 1 μ M puromycin 30 min prior to cell collection. Protein synthesis and mTORC1 related proteins were quantified using Western blotting. Data were analyzed using one-way ANOVA.

Results:

A significant increase in puromycin-labeled protein expression was observed after stimulation with 1mM β -hydroxybutyrate (1.20 ± 0.06 arbitrary units) compared to 0mM (1.00 ± 0.05 , $p < 0.05$). However, phosphorylation of mTORC1 related proteins (p70S6K^{Thr389}, rpS6^{Ser240/244}, 4E-BP1^{Thr37/46}) was not changed by any concentrations of β -hydroxybutyrate.

Conclusion:

These results suggest that β -hydroxybutyrate might enhance muscle protein synthesis in C2C12 myotubes. In contrast, mTORC1-related signaling did not change with short-term exposure to β -hydroxybutyrate. It appears that β -hydroxybutyrate may activate muscle protein synthesis through mTORC1-independent pathways.

1) Evans M et al., J Physiol, 2017 2) Thomsen HH et al., Am J Clin Nutr, 2018 3) Parker BA et al., Int J Mol Sci, 2018

PCB058

Exploring the Link Between Microglial Morphology and Beta-Amyloid Accumulation in an Alzheimer's Disease Mouse Model

AlBeshr AlMasri¹, Harry Trewhitt¹, Kira Shaw¹, Catherine Hall¹

¹*University of Sussex, Brighton, United Kingdom*

Introduction: Microglia, central nervous system resident immune cells, play a pivotal role in the neuroinflammatory response associated with Alzheimer's disease (AD). Their dysregulation and morphological changes contribute to AD pathogenesis, activating in response to beta amyloid plaques (Doens and Fernández, 2014). However, the timing of microglial activation in relation to early Alzheimer's pathology remains unclear. This study aims to elucidate whether microglial morphological changes occur in the early stages of amyloid-beta (A β) accumulation, using a mouse model to selectively induce amyloid precursor protein expression (thus A β -production).

Methods: We bred transgenic mice with human APOE3/APOE4 alleles, using a Tet-off system and dietary doxycycline to modulate APP expression and control A β production. The study assessed the impact of APOE genotypes, entorhinal cortex and hippocampus regions, and A β production on Alzheimer's pathology. Microglia visualization was through IBA1 immunohistochemistry, A β quantification via the MSD 6E10 A β panel (protein-normalized), and amyloid aggregation detected with MethoxyX04 staining. We assessed microglial morphology in 150 cells from 28 animals using ImageJ's Moti-Q plugin, following Hansen et al., 2022. Statistical analysis involved principal component analysis (PCA) for morphological data dimensionality reduction and a targeted approach focusing on neuroinflammation-related metrics, as per Olabiyi et al., 2023.

Results: Without doxycycline for 18 weeks, APPSwe/Ind mice exhibited increased A β levels (38, 40, 42 isoforms; $p = 0.012$) without amyloid aggregation. Neither A β levels nor microglial morphology were affected by APOE genotype. Unbiased PCA revealed nine principal components, explaining 80% of the variance in microglial morphology, with the primary component explaining 46%, largely reflecting cell size and branching complexity. However, multi-way ANOVA found no significant morphological differences between control mice and those accumulating A β .

Targeted analysis on key microglial activation markers—Iba1 intensity, tree length, branching, and ramification — did however reveal significant inflammation-linked changes in A β -producing mice: heightened intensity (100.52 ± 5.69 vs. 68.48 ± 2.90 ; $p < 0.0001$), fewer branches (98.27 ± 9.23 vs. 162.72 ± 13.67 ; $p = 0.0038$), lower ramification index (7.05 ± 0.26 vs. 10.37 ± 0.36 ; $p < 0.00001$), and reduced tree lengths ($615.08 \pm 47.89 \mu\text{m}$ vs. $935.32 \pm 65.32 \mu\text{m}$; $p = 0.00282$). However, cell volume remained unchanged ($4304.56 \pm 312.92 \mu\text{m}^3$ vs. $4699.72 \pm 290.89 \mu\text{m}^3$; $p = 0.424$), despite its previous association with microglial activation (Olabiyi et al., 2023). Post-hoc analysis revealed marked intensity and ramification differences in A β mice in the assessed regions (intensity: cortex $p=0.00086$, hippocampus $p=0.00218$; ramification: cortex $p=0.00005$, hippocampus $p=0.007$) and significant cross-regional variations (intensity: cortex vs. control hippocampus $p<0.00001$; ramification: hippocampus vs. control cortex $p=0.0081$, cortex vs. control hippocampus $p=0.00006$). These results indicate early, albeit incomplete, microglial activation in early Alzheimer's disease pathology, prior to beta amyloid plaque formation.

Conclusion: Our results demonstrated elevated neuroinflammation and A β levels in early AD mouse model, irrespective of APOE genotype. Initial PCA and multi-way ANOVA showed no significant microglial morphology changes due to A β . Yet, targeted analysis of microglial activation markers—like increased intensity, reduced branches, shorter tree length, and lower ramification index—indicates early microglial activation signs during initial A β accumulation, before plaque formation.

Doens, D. and Fernández, P.L., 2014. Microglia receptors and their implications in the response to amyloid β for Alzheimer's disease pathogenesis. *Journal of Neuroinflammation*, 11(1), p.48. Available at: <https://doi.org/10.1186/1742-2094-11-48>. Hansen, J.N., et al., 2022. MotiQ: an open-source toolbox to quantify the cell motility and morphology of microglia. *Molecular Biology of the Cell*, 33(11), ar99. doi: 10.1091/mbc.E21-11-0585. Olabiyi, B.F., et al., 2023. Pharmacological blockade of cannabinoid receptor 2 signaling does not affect LPS/IFN- γ -induced microglial activation. *Scientific Reports*, 13(1), 11105. doi: 10.1038/s41598-023-37702-z.

PCB059

Central and peripheral serotonin levels and its ovarian mRNA receptors interplay at diestrus in perimenopausal rats following exercise

Adesina Arikawe¹, Adetoke Adekitan², Okikiade Oghene³, Adedunni Olusanya⁴, Abimbola Ogunsola⁵, Naomi Ojedokun¹, Daniel Adebayo¹, Valentine Nwachukwu¹, Folashade Ofere¹

¹Department of Physiology, Faculty of Basic Medical Sciences, College of Medicine, University of Lagos, Idi-Araba, Lagos, Nigeria, ²Department of Physiology, Faculty of Basic Medical Sciences, College of Medicine, University of Lagos, Idi-Araba, Lagos, Nigeria, ³Department of Physiology, Faculty of Basic Medical Sciences, College of Medicine, University of Lagos, Idi-Araba, Lagos, Nigeria, ⁴Department of Pharmacology, Therapeutics & Toxicology, Faculty of Basic Medical Sciences, College of Medicine, University of Lagos, Idi-Araba, Lagos, Nigeria, ⁵Department of Physiology, Babcock University, Ilishan-Remo, Ilishan, Nigeria

Reproductive aging in females is characterized by a progressive decline in fertility that begins at birth and extends through the perimenopausal transition. A decline in estrogen concentrations during this transitory period lowers the activity of serotonin; a known neurotransmitter which has been well established to ultimately improve mental health status. Thus, this study aimed to assess ovarian serotonin mRNA receptors; its central and peripheral levels interplay at diestrus phase of the estrous cycle in perimenopausal rats subjected to standard exercise regimen.

Female immature Wistar rats (postnatal day [PND] 21) were housed in groups of seven per cage (n = 7) and randomly divided into three major groups (Control, VCD, and Aging). At PND 28, Control rats were injected with Corn oil (2.5uL/kg BW) for 15 days; VCD rats were injected with 4-Vinylcyclohexene diepoxide (160mg/kg BW) diluted in Corn oil (2.5uL/kg BW) for 15 days; naturally Aging rats 180 days old (no injection of VCD or Corn oil) were used as aged rats. Fifty (50) days after corn oil/VCD injection and 230 days in Aging rats, animals were further sub-divided into 2 groups; exercise (subjected to exercise regimen of 1 hour duration 3 times weekly on a treadmill for 3 weeks) and non-exercise group. On diestrus morning after the exercise regimen, animals were humanely sacrificed, prefrontal cortex (PFC) and hippocampus (HIPPO) were removed on ice and homogenized; and cardiac puncture was carried out to collect blood (serum) for measurement of peripheral serotonin levels using specialized ELISA kits. Both ovaries were quickly removed and placed in RNA later fluid for storage until serotonin mRNA analysis using standard mRNA extraction and RT-qPCR techniques. Data was analyzed using One-way ANOVA followed by a Bonferroni post hoc test using GraphPad Prism 7 software.

Serum serotonin (ng/ml) was significantly higher ($p < 0.05$) in Aging rats (45.61 ± 6.72) compared to Control (19.45 ± 2.80) and VCD (20.90 ± 2.30). Exercise significantly reduced ($p < 0.05$) serum serotonin in VCD (14.62 ± 1.13 ng/ml) and Aging rats (26.72 ± 5.71) compared to Control (23.52 ± 1.83). In PFC, serotonin (ng/ml) in Aging rats (3.41 ± 0.31) was significantly lower ($p < 0.05$) compared to Control (5.91 ± 0.60) and VCD (6.90 ± 0.90) rats. Exercise significantly increased ($p < 0.05$) serotonin in Aging rats (6.99 ± 1.04) compared to Control (5.79 ± 0.83) and VCD (8.01 ± 0.71). In HIPPO, there were no significant changes observed across the groups. In the ovaries, 5-HT₁ receptors were significantly reduced ($p < 0.05$) in Aging rats (4.33 ± 0.43) compared to VCD (9.63 ± 0.82) rats only [Control was (4.60 ± 1.58)]. Exercise significantly reduced ($p < 0.05$) 5-HT₁ receptors (6.41 ± 0.95) in

VCD rats; while significantly increasing it ($p < 0.05$) in Aging rats (8.04 ± 1.69), and no significant difference in Control rats (5.97 ± 1.33). The 5-HT₂ receptors in ovaries, were significantly lowered ($p < 0.05$) in VCD (2.27 ± 0.49) and Aging (2.81 ± 0.56) compared to Control (5.20 ± 1.23). Exercise significantly increased ($p < 0.05$) 5-HT₂ receptors in Aging (5.91 ± 1.57), Control (8.32 ± 1.37) and VCD (4.23 ± 1.41) rats.

Exercise seems beneficial in improving mental health during perimenopausal transitory period by enhancing central, peripheral and ovarian serotonin interplay.

PCB060

Investigating the luminance-response function of human retinal cone-driven responses to 30 Hz flickering stimuli presented on different backgrounds

Charlie Bosshard^{1,2}, Harry Arbuthnott^{1,2}, Isabelle Chow^{3,4}, Shaun Leo^{2,5}, Xiaofan Jiang^{2,4}, Omar Mahroo^{1,2,3,4,5}

¹Physiology, Development and Neuroscience, University of Cambridge, Cambridge, United Kingdom, ²Institute of Ophthalmology, University College London, London, United Kingdom, ³Department of Ophthalmology, St Thomas' Hospital, London, United Kingdom, ⁴Section of Ophthalmology, King's College London, St Thomas' Hospital Campus, London, United Kingdom, ⁵NIHR Biomedical Research Centre at Moorfields Eye Hospital and the UCL Institute of Ophthalmology, London, United Kingdom

Purpose

The electroretinogram (ERG) reflects changes in electrical activity across the entire retina, in response to light stimulation, and can be recorded non-invasively from the human eye. The amplitude of cone-driven ERG responses to flashes increases with flash luminance up to a maximum and then declines with further increases in flash luminance, termed the “photopic hill”. In this study we investigated the cone-driven response to 30 Hz flickering stimuli of increasing luminance as well as the effect of changes in background luminance on the response.

Methods

Extended recordings were conducted in 2 healthy adults, both male, aged 20-21. The study had Research Ethics Committee approval and conformed to the tenets of the Declaration of Helsinki. Subjects' pupils were dilated pharmacologically with 1% tropicamide, and conductive fibre electrodes were placed into the lower conjunctival fornix of only one eye for recording, whilst the other eye was patched. Participants were exposed to a standard white light-adapting, rod-saturating background (30 photopic cd.m⁻²; 86 scotopic cd.m⁻²) and ERGs were recorded in response to white 30 Hz flicker stimuli of increasing luminance (ranging from 0.5 to 50 cd.s.m⁻²). The same flicker stimuli were also delivered on other background luminances (50 and 100 photopic cd.m⁻²; approximate scotopic luminances, 143 and 287 cd.m⁻² respectively) following initial adaptation to each background for one minute.

Results

Each participant underwent five repetitions of the same experiment over several days, with recordings made from right and left eyes (yielding a total of 20 experiments for analysis). Findings were broadly consistent for both subjects. For the 30 cd.m⁻² background, a photopic hill effect was observed with maximal amplitudes to a stimulus c.5-10 cd.s.m⁻². With increasing background

luminance, the hill effect was also observed, such that response amplitudes to the strongest stimuli for each background were lower than responses to weaker stimuli; the response elicited by the 50 cd.s.m⁻² stimulus was smaller than that elicited by the 10 cd.s.m⁻² stimulus on each background ($p < 0.0002$, paired t test). Also, as background strength increased, a rightward shift was seen in the luminance-response relation. For the 1 cd.s.m⁻² stimulus (consistently on the ascending limb of the photopic hill in each background), the response-amplitude was significantly smaller on backgrounds of greater luminance ($p < 0.01$ for all pair-wise comparisons between backgrounds, paired t test).

Conclusion

Our findings show a photopic hill effect can be observed in responses to 30 Hz flicker stimuli. The decline in response amplitudes to a fixed stimulus strength delivered on brighter backgrounds is consistent with a reduction in sensitivity with greater background luminance, reflecting retinal light adaptation. The flicker ERG arises largely from signals in cone-driven ON and OFF bipolar cells, and concurrent changes in amplitude and response kinetics of the two pathways are likely to underlie the trends observed.

PCB061

Alcohol triggers the accumulation of oxidatively damaged proteins in neuronal cells and tissues.

Anusha Mudyanselage¹, Wayne Carter²

¹Clinical Toxicology Research Group, School of Medicine, University of Nottingham, Royal Derby Hospital Centre, Derby, United Kingdom, ²Clinical Toxicology Research Group, School of Medicine, University of Nottingham, Royal Derby Hospital Centre,, Derby, United Kingdom

Alcohol is toxic to neurons and can trigger alcohol-related brain damage, neuronal loss, and cognitive decline. Neuronal cells may be vulnerable to alcohol toxicity and damage from oxidative stress after differentiation. To consider this further, the toxicity of alcohol to undifferentiated SH-SY5Y cells was compared with that of cells that had been acutely differentiated. Cells were exposed to alcohol over a concentration range of 0-200 mM for up to 24 hours and alcohol effects on cell viability were evaluated by MTT and LDH assays. Effects on mitochondrial morphology were examined via transmission electron microscopy, and mitochondrial functionality was examined using measurements of ATP and the production of reactive oxygen species (ROS). Alcohol reduced cell viability and depleted ATP levels in a concentration and exposure duration-dependent manner, with undifferentiated cells more vulnerable to toxicity (viability threshold concentration of ≥ 20 mM for 6 h, $p < 0.001$ for undifferentiated cells and $p < 0.0001$ for differentiated cells). Alcohol exposure resulted in significant neurite retraction (from ≥ 50 mM for 6 h, $p < 0.001$), altered mitochondrial morphology, and increased the levels of ROS in proportion to alcohol concentration from 10 mM ($p < 0.0001$); these peaked after 3 and 6 h exposures and were significantly higher in differentiated cells. Protein carbonyl content (PCC) lagged ROS production and peaked after 12 and 24 h, increasing in proportion to alcohol concentration (from 10 mM, $p < 0.0001$), with higher levels in differentiated cells. Carbonylated proteins were characterised by their denatured molecular weights and overlapped with those from adult post-mortem brain tissue, with levels of PCC higher in alcoholic subjects than matched controls ($p < 0.01$). Hence, alcohol can potentially trigger cell and tissue damage from oxidative stress and the accumulation of oxidatively damaged proteins.

PCB062

Folate binding protein-1 localisation in the plexiform layers of the mouse retina

Emily Flood¹, Bernadett Gnotek¹, Gerrit Hilgen¹

¹*Northumbria University, Newcastle Upon Tyne, United Kingdom*

Folate (vitamin B9) is the naturally occurring form of folic acid. Folate cannot be synthesised by the human body so must be acquired through diet/supplementation. Folate carries one-carbon groups for methylation reactions and nucleotide base synthesis making it fundamental for DNA replication, repair, and RNA synthesis. Folate deficiency has been implicated in retinal diseases, including nutritional amblyopia, diabetic retinopathy, exfoliation glaucoma and age-related macular degeneration. In most cases, the exact mechanism of how this contributes to disease is still unknown. There are 3 cellular mechanisms for folate transport: folate receptors, reduced folate carrier and the proton-coupled folate transporter. Folate receptors are attached to the surface of the cell plasma membrane via glycosylphosphatidylinositol. In mice, there are 3 isoforms referred to as the folate binding protein which are analogous to the -a, -b, and -d human forms. RT-PCR, immunohistochemistry and confocal imaging have been used to identify folate binding protein-1 expression in mouse RPE cells, retinal Müller cells and in several layers of retinal tissues, with particularly prominent staining in the outer plexiform layer (Bozard et al. 2010; Smith et al. 1999). To the best of our knowledge, no study has tried to localise any of these folate receptors at the subcellular level in the retina. Such cellular knowledge of folate receptor expression in the retina is critical for understanding their involvement in retinal physiology in health, disease onset and ageing, as well as cell-type specific drug development. Our research will reveal not only whether and which folate receptors are expressed in the retina, but also where they are expressed. Immunohistochemistry analysis (methods previously stated by (Hilgen 2023)) of adult mouse retinal tissue was used to establish localisation of folate binding protein-1 on key retinal cell types, particularly those with dendritic structures extending into the inner plexiform layer (bipolar, amacrine and ganglion cells). Preliminary data shows colocalization of folate binding protein-1 with SMI-32 (alpha retinal ganglion cells), PKCα (bipolar cells) and Calretinin (retinal ganglion cells) at the inner nuclear at plexiform layers of the retina. Experimental procedures were granted ethical approval by Northumbria University and all procedures accorded with current UK legislation.

Bozard, B. R., P. S. Ganapathy, J. Duplantier, B. Mysona, Y. Ha, P. Roon, R. Smith, I. D. Goldman, P. Prasad, P. M. Martin, V. Ganapathy, and S. B. Smith. 2010. 'Molecular and biochemical characterization of folate transport proteins in retinal Müller cells', *Invest Ophthalmol Vis Sci*, 51: 3226-35. Hilgen, G. 2023. 'Connexin45 colocalization patterns in the plexiform layers of the developing mouse retina', *J Anat*, 243: 258-64. Smith, S B, R Kekuda, X Gu, C Chancy, S J Conway, and V Ganapathy. 1999. 'Expression of folate receptor alpha in the mammalian retinol pigmented epithelium and retina', *Investigative Ophthalmology & Visual Science*, 40: 840-48.

PCB063

Homocysteine and Post-Stroke Cognitive Decline: Unravelling the Neurovascular nexus

Rahul Kumar¹

¹*Assistant Professor, Department of Biotechnology, GITAM School of Sciences, GITAM (Deemed to be) University, Visakhapatnam, Visakhapatnam, India*

Introduction: A significant proportion of stroke patients exhibits impaired reperfusion (1), which manifests in different clinical outcomes including cognitive impairment. Although effective treatments to reverse cognitive decline following stroke are still not available, interventions to control risk factors implicated in the disease onset may help to reduce the burden of dementia (2). One such modifiable risk factor is hyperhomocysteinemia (HHcy) or elevation in plasma total homocysteine (tHcy), which has been extensively studied for its cerebrovascular effects (3). HHcy is independently associated with increased incidence of stroke as well as dementia (4-7).

Objective: We wanted to determine if Hcy exacerbates post-stroke memory impairment through a NMDAr dependent mechanism.

Methods: From 4 weeks of age, mice were fed either a control diet or a high methionine/low folate (HM/LF) diet that increases the blood plasma level of Hcy leading to HHcy. Inhibition of NMDAr was achieved using memantine. The stroke was modelled using middle cerebral artery occlusion, followed by the assessment of learning and memory impairment using a battery of behavioral tests. Blood brain barrier (BBB) leakage was assessed using Evans Blue extravasation. We performed repeated measures for time dependent assays and the analysis of variance (ANOVA) with Tukey's post-hoc analysis for multiple comparisons within several groups. For unpaired comparisons, with a standard deviation of 30% and a minimum expected difference between groups of 40%, 10 mice were included in each group to achieve 80% likelihood of detecting significance at the 0.05% level. Values presented as Mean

Results: In fear conditioning, I observed that overall freezing time was significantly less ($p < 0.05$) in mice after stroke (84.75 ± 5.99) compared to naive mice (111.75 ± 11). Next, I observed significantly less freezing in HHcy (Control (84.75 ± 5.99); HHcy 61.75 ± 5.69 , $p < 0.05$), suggesting that it can exacerbates loss of memory post-stroke. Next, we assessed if HHcy can promote learning and memory impairment in novel object recognition. Mice acquired a memory of the familiar object by exploring two identical objects. 24 hours after acquisition, we assessed NOR by replacing one of the familiar objects with a novel object and assessing the amount of time that mice spent interacting with the novel and familiar objects. Surprisingly, when NOR was assessed 24 h later, we found that mice with HHcy failed to discriminate between the novel and familiar objects lower discrimination index s compared to controls (Control 71.35 ± 3.63 ; HHcy 54.25 ± 6.27 ; $p < 0.05$). We further made an interesting observation that HHcy leads to BBB leakage that was reversed by the administration of memantine (Control; 2.65 ± 0.36 $\mu\text{g/g}$; HHcy 4.2 ± 0.38 ; HHcy with memantine 2.57 ± 0.53 ; p value for HHcy vs Control < 0.05 ; p value for HHcy vs HHcy with memantine < 0.05).

Conclusion: Altogether, the findings from the project suggests that HHcy exacerbates cognitive and BBB leakage following stroke. The findings from the project will allow us to initiate clinical

trials to determine if stroke patients with higher level of Hcy are more vulnerable to the development of cognitive dysfunction and need a memantine or Vitamin B12 supplementation as prophylactic treatment.

The Use and Effectiveness of Traditional Turmeric-Based Preparations and Vitamin Products as Antioxidants in Combating Oxidative Stress in Various Neuropathologies

Krishma Parwana¹, Marta Wołoszynowska-Fraser¹, Jenny Moran¹

¹Keele University, Keele, United Kingdom

Turmeric has been a key player in Ayurvedic medicine for thousands of years, mentioning its antioxidant and anti-inflammatory properties which have gained increasing popularity in modern medicine (Hewlings and Kalman, 2017). As of present, the use of turmeric or its main polyphenol compound curcumin has been investigated as a therapy in conditions such as Alzheimer's Disease, Osteoarthritis and Schizophrenia to either improve symptoms or the condition itself (Hewlings and Kalman, 2017). Although the antioxidant properties of turmeric have been studied to combat oxidative stress within these conditions, there is a lack of studies which implement traditional turmeric-based products as a treatment and little supporting evidence of how effective turmeric-based vitamin products are as antioxidants. This study aimed to investigate the antioxidant properties of various traditional fresh (FT) and powdered (PT) turmeric-based preparations with or without black pepper (BP) which were boiled in either milk or water and three different turmeric-based vitamin products. Their antioxidant properties were tested using a superoxide scavenging assay in a Nicotinamide Adenine Dinucleotide + Hydrogen-Phenazine Methosulfate system, where the percentage inhibition of Nitro Blue Tetrazolium Chloride was calculated using absorbance values from a spectrophotometer to determine the amount of superoxide scavenging from the assay. ANOVA results showed a significant difference between all milk-based assays ($F_{(5, 18)}=10.99$, $p<0.0001$) (Figure 1) and water-based assays ($F_{(5, 18)}=384.1$, $p<0.0001$) (Figure 2). Within milk, powdered turmeric showed the highest percentage inhibition (44.19%) (Figure 1) and powdered turmeric and black pepper showed the highest percentage inhibition in water (49.65%) (Figure 2). Within our data, all assays showed percentage inhibition besides water as a control and fresh turmeric in water, which was deemed an unexpected result. All three vitamin products exhibited antioxidant properties ($F_{(3, 12)} = 218.7$, $p<0.0001$) (Figure 3), with Holland & Barratt (H&B) having a significantly higher percentage inhibition compared to the other two products ($p<0.0001$) (Figure 3), suggesting it displays the highest efficacy. These findings quantify the antioxidant properties of both traditional turmeric-based preparations and turmeric-based vitamin products and reveal the efficacy of their free radical scavenging properties. Evidence from these results suggests that traditional turmeric-based assays are effective as antioxidants in certain combinations, particularly when extracted in milk overall. Furthermore, Holland & Barrett displayed the highest percentage inhibition, which suggests that it may be the most effective therapy and that not all turmeric-based vitamin products display high free radical scavenging properties despite their claims. These results provide preliminary data which suggests that using turmeric-based preparations or vitamin products could be as an antioxidant to combat oxidative stress which has been suggested to be present in multiple neuropathologies. Findings from this study could be translated into further studies, such as *in vitro* cell work to test the efficacy of turmeric-based preparations and vitamin products to determine their effectiveness in combatting oxidative stress or potentially long-term *in vivo* studies to observe how they may improve various neuropathologies and their symptoms which may be induced or worsen by oxidative stress.

Physiology in Focus 2024

Northumbria University, Newcastle, UK | 2 – 4 July 2024

Hewlings, S. and Kalman, D. (2017). Curcumin: A Review of Its' Effects on Human Health. *Foods*, [online] 6(10), p.92. doi:<https://doi.org/10.3390/foods6100092>.

PCB065

Late Maternal Separation provides resilience to stress-induced behavioral disorder

Padmasana Singh, Rajesh Kumar Ojha, Shweta Dongre, Raj Kamal Srivastava

undefined

Introduction: Maternal separation (MS) is a widely recognized paradigm that can be employed to investigate the physiological effects of stress experienced during early life. During the first two weeks of life, daily maternal separation plays a crucial role in the development of the hypothalamic–pituitary–adrenocortical (HPA) axis, a significant neuroendocrine system that responds to environmental stressors. Prior research has indicated that MS has demonstrated that the plasticity of the central nervous system in childhood renders it vulnerable to stress in adulthood. Early maternal separation in adult mice leads to increased stress responsiveness, resulting in elevated glucocorticoid levels after acute or chronic stress. However, the effects of late MS (LMS) on HPA axis during adolescence have not been studied. Hence, aim of the current investigation was to examine the effects of late maternal separation (LMS) on neurobehavioral changes and stress responsiveness during adolescence.

Methodology: Swiss Albino male and female pups from LMS group were daily removed from their home cage for 3 hours from PND 10 to PND 21 between 14:00 h - 17:00 h. After 3 hours of maternal separation, the pups were returned to their home cage. At PND 22, both non-maternal separation group (NMS) and LMS mice were separated and housed together with littermates of the same sex. At PND 56, each mouse from NMS and LMS group were subjected to one chronic variable stress (CVS) randomly for 21 days - (a) overnight fasting; (b) 30 min of restraint stress; (c) shaking for 30 min at 80-100 rpm; (d) placed in ice cold water for 15 min (only paws); (e) placed on a hot surface for 30 min at 400C; (f) isolated and kept in a separate cage; (g) swimming for 5 min. After this period, each mouse was subjected to a series of behavioural tests for five consecutive days that comprised of sucrose preference test, open field test, light-dark box test, elevated plus maze test, and tail suspension test (TST).

Results: Behavioral tests suggested that male LMS mice are more resilient to chronic variable stress (CVS)-induced anxiety and depressive-like behavior, as confirmed by the open field, light dark field, elevated plus maze, sucrose preference, and tail suspension tests. In contrast, female LMS mice were equally resilient as mice without maternal separation. We found an increased expression of Npy, Npy1r, Npy2r, Npffr1, and Npffr2 in the hypothalamus of male LMS mice, whereas the opposite effect was observed in the hippocampus. LMS in male and female mice did not affect circulating corticosterone levels in response to psychological or physiological stressors. Thus, LMS makes male mice resilient to CVS-induced neurobehavioral disorders in adulthood.

Conclusion: LMS from PND10-PND21 provides resilience to anxiety and depression in male mice, while there were no significant changes in female mice. Our study indicated the role of two neuropeptides, Npy and Npvf, and their receptors in stress resilience to CVS-induced anxiety- and depression-like behavior in male LMS mice.

PCB066

Using a mouse model of Alzheimer's disease to unravel early pathological neurovascular changes preceding cognitive decline.

Harry Trewwhitt, Kira Shaw, Silvia Anderle, Letitia McMullan, Catherine N. Hall

undefined

Accumulating evidence suggests a link between amyloid beta (A β) accumulation and neurovascular dysfunction in early stages of Alzheimer's disease (AD) (Iadecola, 2004). The 'two-hit' vascular model proposes that age and cardiovascular risk-factor related neurovascular deterioration, such as a reduction in neurovascular coupling and the breakdown of the blood brain barrier, may act synergistically with initial A β deposition creating a feedforward cycle of progressive change, ultimately promoting neuronal dysfunction and loss (Zlokovic, 2011). However, the factors that first establish such a vicious cycle have not yet been determined. We hypothesised that early A β -induced hyperactivity of excitatory neurons (Busche et al., 2012), combined with a reduced capacity of the neurovasculature to support this (Korte et al., 2020), emerge early in disease, which could subsequently create repeated transient hypoxic areas throughout the brain, promoting further A β deposition (Chen & Hassan, 2021).

To interrogate this we have used a novel mouse model combining humanised APOE and doxycycline-inducible APPSwe/Ind transgenes as well as the CaMKII driven GCaMP6f neuronal calcium reporter. *In vivo* 2Photon imaging and combined haemoglobin spectrometry/ laser doppler flowmetry allowed us to investigate neuron and vessel function over a time-course of A β accumulation. A surgically implanted cranial window placed over the visual cortex allowed us to record baseline measurements before APP expression is 'switched on' and at subsequent timepoints up to four months after.

A behavioural testing regime, on the same mice we imaged *in vivo*, indicates that four-months of A β accumulation represents an early AD model, with mild cognitive symptoms starting to appear. After four months of APP expression (and A β accumulation) mice performed around 35% worse than non-APP expressing controls during the acquisition trials of a simple, non-appetitive Barnes Maze paradigm (LMM interaction between APP expression and time, **p = 0.005**). Although these mice are still able to learn, this indicates a mild deficit in spatial working memory. Preliminary *in vivo* data from the visual cortex reveals an increase in neuronal calcium peak size (LMM interaction between APP expression and time, **p = 0.04**) and duration (LMM main effect of APP expression, **p = 0.002**) after four months of A β accumulation. Such an increase in neuronal activity should be met by a requisite increase in oxygen supply via neurovascular coupling, however oxygen saturation measurements from the same cortical region indicate a significant drop in tissue oxygenation from baseline in APP expressing mice (one-sided T-Test, **p = 0.01**).

Further data is being collected and analysed which will hopefully help inform our understanding of how neuronal and neurovascular changes induced by A β accumulation contribute to early AD pathological changes, preceding significant cognitive decline.

References Iadecola, C. (2004) 'Neurovascular regulation in the normal brain and in alzheimer's disease', *Nature Reviews Neuroscience*, 5(5), pp. 347–360. doi:10.1038/nrn1387. Zlokovic, B.V. (2011) 'Neurovascular Pathways to neurodegeneration in alzheimer's disease and other disorders', *Nature Reviews Neuroscience*, 12(12), pp. 723–738. doi:10.1038/nrn3114. Busche, M.A. et al. (2012) 'Critical role of soluble amyloid- β for early hippocampal hyperactivity in a mouse model of alzheimer's disease', *Proceedings of the National Academy of Sciences*, 109(22), pp. 8740–8745. doi:10.1073/pnas.1206171109. Korte, N., Nortley, R. and Attwell, D. (2020) 'Cerebral blood flow decrease as an early pathological mechanism in alzheimer's disease', *Acta Neuropathologica*, 140(6), pp. 793–810. doi:10.1007/s00401-020-02215-w. Chen, R. and Hassan, H. (2021) 'Hypoxia in alzheimer's disease: Effects of hypoxia inducible factors', *Neural Regeneration Research*, 16(2), p. 310. doi:10.4103/1673-5374.290898.

PCB067

Differences in Thoracic Fluid Content and Cardiac contractility in Individuals with Myasthenia Gravis are Associated with the Severity of Autonomic Dysfunction

Monika Zawadka-Kunikowska¹, Mirosława Cieśllicka¹, Wieńczystawa Adamczyk¹, Monika Bejtka¹, Joanna Fanslau¹, Wojciech Kaźmierczak^{1,3}, Łukasz Rzepiński^{4,5}

¹Department of Human Physiology, Nicolaus Copernicus University Ludwik Rydygier Collegium Medicum in Bydgoszcz, Bydgoszcz, Poland, ²Department of Human Physiology, Nicolaus Copernicus University Ludwik Rydygier Collegium Medicum in Bydgoszcz, Bydgoszcz, Poland, ³The Institute of Physiology and Pathology of Hearing, Warszawa, Poland, ⁴Sanitas - Neurology Outpatient Clinic, Bydgoszcz, Poland, ⁵Department of Neurology, 10th Military Research Hospital and Polyclinic, Bydgoszcz, Poland

Introduction: Myasthenia gravis (MG), a rare autoimmune disorder, poses diagnostic and management challenges, with significant impacts on patients' quality of life. Cardiac autonomic dysfunction has been identified in patients with MG, often with limited comprehensive assessments integrating impedance cardiography (ICG).

Aims: We assessed cardiac function, including thoracic fluid content and myocardial contractility, in both MG patients and healthy controls (HCs), and its correlation with the severity of autonomic impairment using cardiovascular autonomic function tests (AFTs).

Methods: Fifty-three patients with MG (median age 41, interquartile range 36-45) and 30 HCs (median age 38, interquartile range 25-42) underwent standardized AFTs. Patients were categorized into Non-CAN (n=33) and CAN (n=20) groups based on their Cardiovascular Autonomic Neuropathy (CAN) status, as evaluated using the Composite Autonomic Scoring Scale (CASS). We continuously measured cardiovascular parameters using ICG, including thoracic fluid content (TFC), stroke volume (SV), cardiac output (CO), and myocardial contractility indices such as left ventricle ejection time (LVET), left ventricular work index (LVWI), index of contractility (IC), Heather Index (HI), and mean systolic ejection rate (MSER). Preload was assessed as end-diastolic index (EDI), and afterload as total peripheral vascular resistance (TPR). Heart rate and blood pressure (BP) were calculated from electrocardiography and plethysmography.

Results: At baseline before VM, the CAN-MG group exhibited significantly higher HR, diastolic BP, TPR, and lower values of EDI ($p < 0.001$), IC ($p < 0.001$), ACI ($p = 0.005$), LVET ($p = 0.003$), MSER ($p < 0.001$) than the HCs. Both MG groups (CAN, Non-CAN) had significantly lower values of SV, TFC than HCs ($p < 0.001$). In contrast, the CAN MG group showed significantly lower cardiac inotropy (HI) compared to the Non-CAN MG and HCs groups. Total CASS score correlated with lower resting thoracic fluid content ($R = -0.36$, $p=0.009$) and myocardial contractility parameters: IC ($R=-0.36$, $p=0.007$), HI ($R = -0.40$, $p=0.003$), EDI ($R = -0.36$, $p=0.009$), MSER ($R = -0.33$, $p=0.016$), LVWI ($R=-0.32$, $p=0.019$), ACI ($R = -0.31$, $p=0.024$). At baseline, decreased preload (EDV), TFC, myocardial contractility (MSER, LVWI, ACI), and cardiac inotropy (HI) parameters were associated with higher TPR at rest.

Conclusions: These findings underscore the significance of subclinical cardiac impairment associated with decreased thoracic fluid content and myocardial contractility in MG patients, as well as their relationship with the severity of autonomic abnormalities.

